

*INSTITUTE OF SEISMOLOGICAL RESEARCH*  
*Gandhinagar*  
*Department of Science and Technology*  
*Government of Gujarat*

*Annual Report*  
*2012-13*



# PREFACE



**D**uring the year 2012 an important project “Seismic Hazard Assessment for the proposed 13-story VS Hospital building at Paldi, Ahmedabad” was completed. Satisfactory progress has been made on Seismic Microzonation of Dholera Special Investment Region, Gandhinagar and Ahmedabad as well as on the project “Assessment of Seismic and tsunami Hazard on Installations in Coastal Gujarat”. With the induction of 9 regular positions some of the sections got much needed manpower support and the work improved. However, still much greater number of regular positions is required to carry out the work efficiently and also to take up new projects. Fixed salaries being meagre in ad hoc positions of scientists and the research scholars, attrition is high and many experienced persons are leaving every year. At the end of 2012 some 28 Scientists and JRF out of a total 48 are recruited in 2012 only.

Nevertheless the scientists who stayed back worked doubly hard and increased the number of SCI research papers and external cash flow. About 25 research papers in SCI Journals and 4 research papers in non-SCI Journals, 10 Technical Reports and 62 abstracts were published and papers were presented by ISR Scientists in Seminars/Symposia during 2012. The new projects undertaken include three from ISRO, one from MoES and a few small projects from NPCIL and Assam State Disaster Management Authority.

The Institute pursued varied studies on earthquake science which can be categorized into five areas: (i) Study of Physics of the Earthquake Processes, (ii) Crustal Structure, (iii) Earthquake Hazard Assessment and Seismic Microzonation and (iv) Earthquake Prediction Research. For initial few years, ISR is concentrating over the Gujarat region. Several new studies were started during last year and I am confident that significant findings from these studies will help in understanding physical processes of earthquake phenomenon and seismic hazard assessment in Gujarat.

Gujarat seismic network of 60 Broadband Seismographs and 50 Strong Motion Accelerographs has operated smoothly during 2012. Data of 36 broadband stations connected by VSAT to ISR were processed in real-time round the clock. Information of epicenter and magnitude of earthquakes was processed and disseminated within minutes of arrival of the seismic waves with the help of auto-location program.

Aftershock activity of the 2001 Bhuj earthquake continued and some other faults in Kachchh experienced low level activity. An earthquake of magnitude 5.0 occurred about 40km north of Bhachau on June 20, 2012 along a NE trending Khadir transverse fault.

Seismic, gravity, magnetotelluric, resistivity, GPR and other geophysical surveys were carried out for study of crustal structure and faults. Detection of active faults and pre-historic earthquakes in Kachchh continued through paleoseismological studies. ISR has pioneered a technique of 3D fault mapping by magnetotelluric investigation.

Crustal deformation study is being carried out through GPS measurements in seismically active belts of Gujarat. Twenty-two permanent GPS stations were setup in Gujarat and eleven campaign mode GPS stations were deployed in the Kachchh region. InSAR studies indicate significant uplift around the Kachchh Mainland Fault.

Earthquake Research Center at Bhachau and three multi-parametric geophysical observatories for earthquake prediction research in Kachchh were run smoothly. Precursory signals were observed in radon, gravity and magnetic fields.

As per our OUTREACH PROGRAM we helped a number of Universities in Gujarat in many ways like training their students in geology, geophysics, geotechnical investigations in our rich labs and field surveys, delivering lectures in their special courses. We train some 50 students annually for dissertation work for durations of months to a year and in summer / winter training programs for which students come from all corners of the country.

Many investigations were undertaken for matters of societal importance like: (i) Pilot Project on Extraction of Uranium from Nuclear Waste for BARC using the magnetic separator in the OSL lab and (ii) Investigation of the reporting of Cracks in houses in Faradi Village of Mandvi taluka in Kachchh by means of Rapid Visual Screening with Geological & GPS Survey.

ISR buildings (20,000 sq.m built up area in 12 hectares land) were constructed and most of the instruments were procured with World Bank Loan through GSDMA in 2008. MoES grants were made available for a few projects for which ISR thanks its Secretary as well as Head and Scientists of its Seismology Section. ISR is indebted to the Gujarat Chief Minister, Sc. & Tech. Dep't., GSDMA, GIDB, GSPC, SSNNL and various other Departments of GoG, like Finance and General Administration as well as ISRO, NPCIL and National Geophysical Research Institute for their contribution towards the development of ISR.

***Dr. B. K. Rastogi,***  
Director General



## **CONTENTS OF ISR ACTIVITIES DURING 2012**

<b>CHAPTER 1</b>	<b>: EARTHQUAKE MONITORING AND SEISMICITY PATTERNS IN GUJARAT</b>
1.1	SEISMIC NETWORK
1.2	EARTHQUAKES IN GUJARAT DURING 2012
<b>CHAPTER 2</b>	<b>: PHYSICS OF THE EARTHQUAKE PROCESS</b>
2.1	MECHANISM OF THE 20 JUNE (19 JUNE UT) 2012 M5 EARTHQUAKE AND ITS AFTERSHOCKS
2.2	CMT SOLUTION FOR 2010 M4.4 EARTHQUAKE USING REGIONAL STATIONS DATA
2.3	COULOMB STRESS CHANGES IN KACHCHH AND NORTH SAURASHTRA REGION SURROUNDING THE 2001BHUIJ MW7.7 EARTHQUAKE
2.4	GLOBAL SEISMIC CYCLICITY AND POSSIBLE ENHANCED SEISMICITY SINCE 2001
2.5	CRUSTAL HETEROGENEITIES BENEATH THE 2011 TALALA, SAURASHTRA EARTHQUAKE, GUJARAT, INDIA SOURCE ZONE AND ITS SEISMOTECTONIC IMPLICATIONS
<b>CHAPTER 3</b>	<b>: LITHOSPHERIC STRUCTURE</b>
3.1	ELECTROMAGNETIC, MAGNETO-TELLURIC AND RESISTIVITY IMAGING
3.2	GRAVITY STUDIES
<b>CHAPTER 4</b>	<b>: LONG-TERM EARTHQUAKE PROGNOSIS FROM CRUSTAL DEFORMATION STUDIES BY GPS AND INSAR MEASUREMENTS AS WELL AS ACTIVE FAULT STUDIES</b>
4.1	CRUSTAL DEFORMATION STUDIES BY GPS MEASUREMENTS
4.2	POST-SEISMIC DEFORMATION IN THE BHUIJ EARTHQUAKE ZONE AS OBSERVED IN GPS STATIONS
4.3	CRUSTAL STRAIN ANALYSIS DERIVED FROM GPS
4.4	COULOMB STRESS CHANGES IN KACHCHH AND NORTH SAURASHTRA REGION SURROUNDING THE 2001BHUIJ M <sub>w</sub> 7.7 EARTHQUAKE
4.5	INTERFEROMETRIC SYNTHETIC APERTURE RADAR (INSAR) STUDIES BY ISRO AND ISR
4.6	TRIGGERED SEISMICITY IN KACHCHH AND SAURASHTRA
4.7	PALEOSEISMOLOGY AND ACTIVE FAULT INVESTIGATION IN KACHCHH BASIN
<b>CHAPTER 5</b>	<b>: EARTHQUAKE HAZARD ASSESSMENT</b>
5.1	FREQUENCY CHARACTERIZATION MAP OF KACHCHH, GUJARAT
5.2	ASSESSMENT OF VULNERABILITY OF INSTALLATIONS NEAR GUJARAT COAST VIS-À-VIS SEISMIC DISTURBANCES
5.3	SHEAR-WAVE VELOCITY ESTIMATES IN DIFFERENT PARTS OF GUJARAT FROM MASW AND PS LOGGING PGA AND SA MAPS FROM PSHA ANALYSIS CONSIDERING SITE CONDITIONS AT 2% PROBABILITY OF EXCEEDANCE IN 50 YEARS FOR THE GUJARAT REGION
5.4	SEISMIC HAZARD ASSESSMENT OF NUCLEAR POWER PLANT SITES
5.5	GENERATION OF SITE SPECIFIC GROUND MOTION (SPECTRA) WITH DUE CONSIDERATIONS OF SHEAR WAVE VELOCITIES AND SOIL CONDITIONS FOR INDUSTRIAL SITES OF THE BHUIJ REGION
5.6	DEFINITION OF SEISMIC AND TSUNAMI HAZARD SCENARIOS BY MEANS OF INDO-EUROPEAN E-INFRASTRUCTURES
5.7	A REVIEW OF STRONG MOTION STUDIES IN GUJARAT STATE OF WESTERN INDIA
5.8	PROBABILISTIC SEISMIC HAZARD MAP OF INDIA
<b>CHAPTER 6</b>	<b>: SEISMIC MICROZONATION</b>
6.1	INVESTIGATIONS OF SEISMIC MICROZONATION OF AHMEDABAD CITY
6.1.1	GEOTECHNICAL INVESTIGATIONS IN AHMEDABAD
6.1.2	SHEAR-WAVE ESTIMATES BY MASW AND PS-LOGGING METHODS IN AHMEDABAD CITY, GUJARAT
6.2	INVESTIGATIONS FOR SEISMIC MICROZONATION AT GANDHINAGAR
6.2.1	GEOTECHNICAL INVESTIGATIONS IN GANDHINAGAR:

<b>CHAPTER 7</b>	<b>: EARTHQUAKE PREDICTION RESEARCH</b>
7.1	SHORT TERM PREDICTION OF KACHCHH EARTHQUAKE THROUGH CLUSTER ANALYSIS
7.2	OPERATION OF MULTI-PARAMETRIC GEOPHYSICAL OBSERVATORIES FOR EARTHQUAKE PREDICTION RESEARCH
7.2.1	PROCESSING OF DATA OF SUPER CONDUCTING GRAVIMETER
7.2.2	OBSERVATION OF SOIL RADON GAS EMISSIONS AS EARTHQUAKE PRECURSORS
7.2.3	SEISMO-MAGNETIC OBSERVATIONS IN THE KUTCH REGION
7.2.4	WATER LEVEL OBSERVATIONS
<b>CHAPTER 8</b>	<b>: PROJECTS OF SOCIETAL IMPORTANCE AND ADVICE TO IMPORTANT DEVELOPMENT ACTIVITIES</b>
8.1	PILOT PROJECT ON EXTRACTION OF URANIUM FROM NUCLEAR WASTE
8.2	INVESTIGATION FOR REPORTING OF CRACKS IN HOUSES OF MANDVI, KACHCHH
<b>CHAPTER 9</b>	<b>: NATIONAL AND INTERNATIONAL SCIENTIFIC COLLABORATION</b>
9.1	INDO-ITALIAN PROJECT
<b>CHAPTER 10</b>	<b>: SOCIETAL OUTREACH</b>
10.1	DISSEMINATION OF INFORMATION ABOUT EARTHQUAKES
10.2	HELP TO THE UNIVERSITIES
10.3	TRAINING TO STUDENTS
<b>CHAPTER 11</b>	<b>: PUBLICATIONS</b>
11.1	BOOKS/CHAPTERS:
11.2	PAPERS PUBLISHED IN SCIENTIFIC CITATION INDEX (SCI) JOURNALS DURING 2006 TO 2012
11.3	PAPERS PUBLISHED IN NON-SCI BUT REFERRED JOURNALS 2012
11.4	PAPERS PUBLISHED IN SYMPOSIUM PROCEEDINGS DURING 2012
11.5	ARTICLES / LECTURE NOTES 2012
11.6	TECHNICAL REPORTS 2012
11.7	ABSTRACTS FOR 2012
11.8	SEMINARS ATTENDED
11.9	INVITED LECTURES BY ISR SCIENTISTS
11.10	LECTURES IN TRAINING COURSES
<b>CHAPTER 12</b>	<b>: HUMAN RESOURCE AND DEVELOPMENT</b>
12.1	HONORS/ RECOGNITIONS/AWARDS TO ISR SCIENTISTS FROM OTHER AGENCIES
12.2	PHD AWARDED
12.3	DEPUTATIONS ABROAD
12.4	TRAINING OF ISR STAFF OUTSIDE
12.5	SEMINAR TALKS BY ISR SCIENTIFIC STAFF
12.6	LIST OF STAFF THAT JOINED DURING 2012
12.7	LIST OF STAFF THAT RESIGNED FROM ISR DURING 2012
<b>CHAPTER 13</b>	<b>: BUDGET, PROJECTS AND FUNDS</b>
<b>CHAPTER 14</b>	<b>: INSTRUMENTS / COMPUTERS/ ACCESSORIES AND SOFTWARE PROCURED</b>
<b>CHAPTER 15</b>	<b>: SEMINARS, SYMPOSIA, SPECIAL EVENTS ORGANISED</b>
15.1	ISR FOUNDATION DAY CELEBRATIONS
15.2	CULTURAL PROGRAM AND DINNER FOR THE SUMMER EXPERIENCE OF APPLIED GEOPHYSICS / GEOLOGY
15.3	SEMINARS ORGANIZED
15.3.1	INDO-US WORKSHOP ON INTRAPLATE SEISMICITY
15.3.2	IGU 49TH CONVENTION, OCTOBER 29-31, 2012
15.3.3	INDO-GERMAN WORKSHOP ON MAGNETOTELLURICS, NOVEMBER 1-3, 2012
15.3.4	2 <sup>ND</sup> INTERNATIONAL SYMP ADVANCES IN EARTHQUAKE SCIENCE, FEBRUARY 1- 2, 2013
15.3.5	INDO-ITALIAN TRAINING COURSE ON EARTHQUAKE HAZARD ASSESSMENT, FEB 3-4,'13

# CHAPTER 1

## 1. EARTHQUAKE MONITORING AND SEISMICITY PATTERNS IN GUJARAT

(Santosh Kumar, A.P. Singh, P. Mahesh and K. S. Roy)

### 1.1 Seismic Network

Gujarat State Seismic Network being maintained by Institute of Seismological Research, Gandhinagar since July 2006 (Fig. 1.1) functioned well with 60 Broadband Seismograph Stations (BBS) spread throughout the state and neighboring areas. Total 39 of which (including two very broadband seismographs) are connected via VSAT to ISR and the rest are offline. Some 54 Strong Motion Accelerographs (SMA) are also deployed. The network has detectibility of M2.0 in the Kachchh active area and M2.5 in other areas of Gujarat.

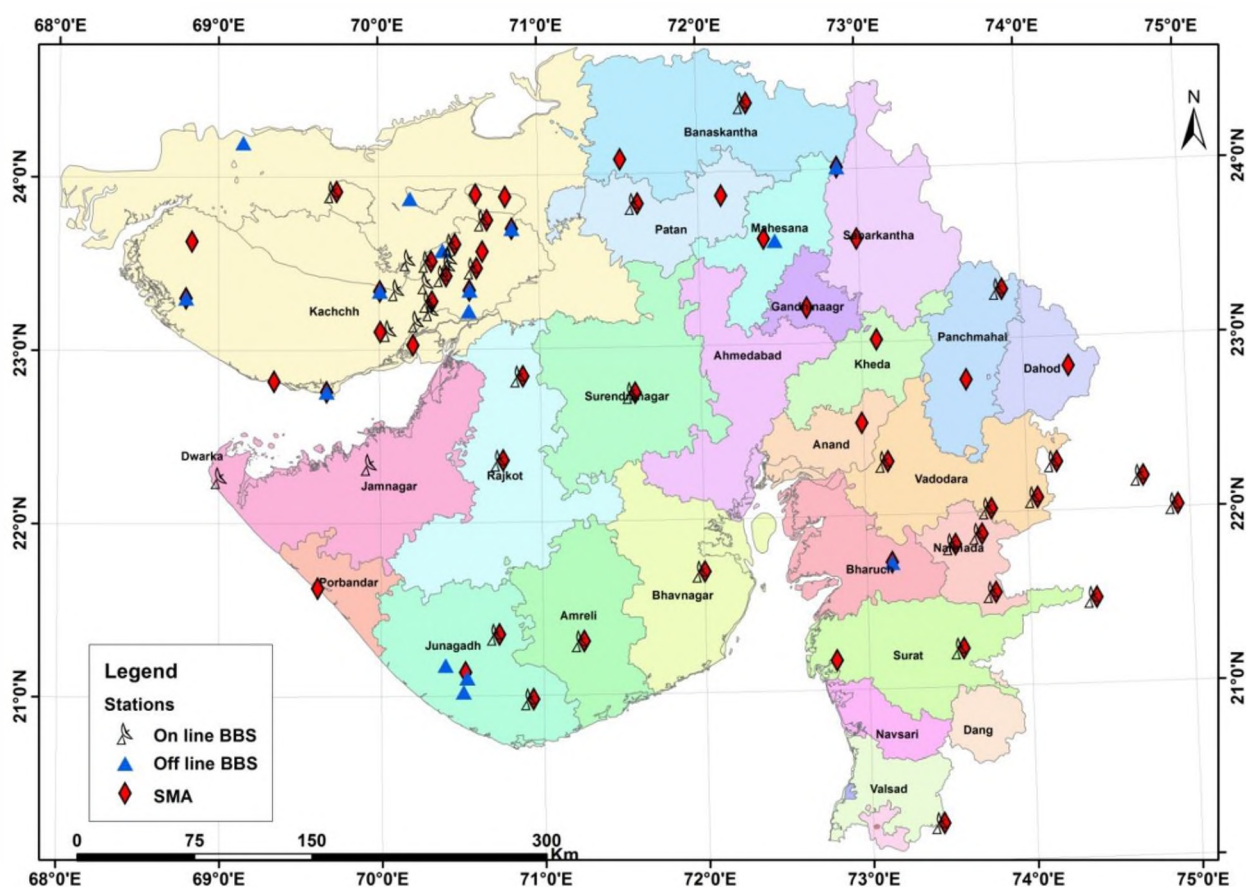


Fig. 1.1: Seismograph stations in Gujarat Net including 39 online Broad Band Seismographs (includes 2 Very Broad Band Seismographs), 10 offline Broad Band Seismographs and 54 Accelerographs.

Planning of installation of 10 no. Strong Motion Accelerographs at Navagam dam, Kevadia colony, SSNNL is being done presently. In the year 2012 new VSAT systems were installed at 8 seismic stations namely Kanthkot, Chadpada, Shivilakha, Dhamkada, Chobari, Bandhadi, Bhimasar and Radhanpur in Kachchh to receive seismic data online in near real time. Out of these 8 seismic stations, 4 were running in offline mode in Kachchh region. Also 2 new offline stations were installed in Saurashtra at Babra (Amreli) and Jamkandorana (Rajkot) and soon new VSAT systems will be installed at these stations.

Data at CRS, ISR was coming using ku-band and Xc-band VSAT systems. During monsoon and cloudy season data from ku-band was not being received. To receive data during rain and clouds, and to make the whole ISR seismic network homogeneous, the ku band VSAT systems were replaced with new Xc-

band VSAT systems in year 2012. Now data from all the seismic stations comes via Xc- band VSAT systems.

## 1.2 Earthquakes In Gujarat

Epicenters of earthquakes of  $M \geq 2$  from 1668 to 2012 in Gujarat excluding foreshocks and aftershocks are shown in Fig. 1.2 and listed in Appendix-1. The Gujarat region is at the tri-junction of three failed rifts: Kachchh, Cambay and Narmada, with several active faults (Biswas 1987). These rifts were formed by rifting along major Precambrian trends. The rifting occurred at successive stages during the northward movement of the Indian plate after the breakup from Gondwanaland in the Late Triassic or Early Jurassic (Mesozoic era at about 184 Ma). The Kachchh rifting took place in the Late Triassic-Early Jurassic, Cambay rifting in Early Cretaceous, and Narmada rifting in the Late Cretaceous. The rifting ceased in the Late Cretaceous era during the pre-collision stage of Indian plate. Post-collision, the Kachchh and Narmada rifts became zones of compression giving strike-slip and thrusting. Kachchh and Narmada rifts have E-W trending major faults which are active, while, the Cambay basin has N to NNW trending marginal faults which are less active. Kachchh has two major faults viz. Kachchh Mainland Fault and Island Belt Fault with its westward extension as Allahbund fault. Medium grade faults are South Wagad and Katrol Hill Fault while minor ones are Gedi, Banni and Gora Dungar Faults. There are some smaller transverse strike-slip faults in Kachchh. South of Kachchh, in the Deccan volcanics of Saurashtra, the NW and NE trending smaller strike-slip faults are also activated in the form of moderate earthquakes in response to the plate-tectonics stress. Magnitude distribution of the mainshocks in Gujarat is listed below:

Magnitude	7.7, 7.8	6, 6.3	5 – 5.9	4 – 4.9	3 -3.9	2-2.9	Total
No.	2	2	27	68	89	18	206

### STRONG MOTION ACCELEROGRAPH DATA

In the year 2012, some 47 shocks of  $M_{0.5-5.0}$  were recorded on strong motion accelerographs. Out of which 3 shocks (in Kachchh) were recorded on 2 or more stations (Table 1.1 & Figure 1.3). Remaining shocks were recorded on only 1 SMA station (Appendix 2). Out of these 32 aftershocks of Talala region having  $M_{0.5-2.2}$  were recorded on Hirenvel SMA Station. In Kachchh 15 shocks were recorded in one of the accelerographs. In Kachchh a tremor on 14<sup>th</sup> April 2012 of  $M_{4.1}$  which occurred 8km NW of Bhachau in Wagad area was recorded on 6 SMA stations. A moderate earthquake of  $M_{5.0}$  which occurred, 20 km SSE of Dholavira on 20<sup>th</sup> June, 2012 at 00:44 IST was recorded at 16 SMA stations (BDR, BHA, CHO, DESH, LOD, KHA, RAP, VAM, KAN, ANJ, DAY, MAN, RAD, RAJ, SUR, MOR). Tremor on 8<sup>th</sup> Dec. 2012 of  $M_{4.1}$  which occurred 28km NW of Bhachau was recorded at 2 SMA stations.

**Table 1.1: List of earthquakes of  $M \geq 4$  or more and no. of SMA stations triggered**

DD	HR	MM	Sec	Lat	Long	Dep	M	NST (SMA)	Area
14:04:12	3	22	59.1	23.391	70.537	18.9	4.1	6	20 km NE of Bhachau
19:06:12	20	14	0.4	23.645	70.283	11.1	5.0	16	20 km SSE of Dholavira
08:12:12	7	6	9.1	23.134	70.422	21	4.5	2	19 km SSE of Bhachau



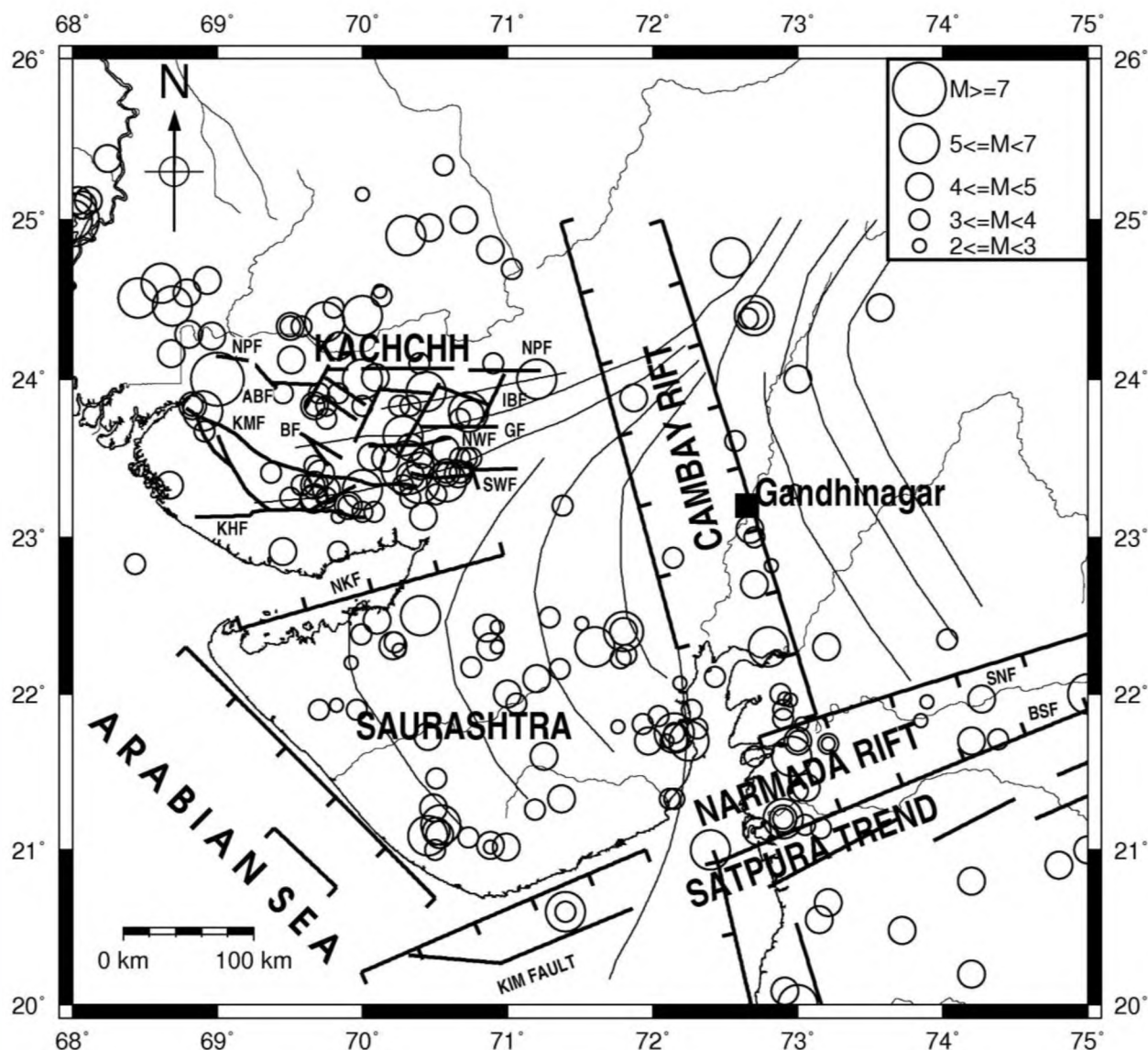


Fig.1.2: Significant faults and epicenters of earthquakes of M2 or greater from 1684 to 2012 excluding aftershocks. The Proterozoic age Aravali trend branches off in three directions. In Kachchh it becomes E-W along which faults might have been formed

### Earthquakes during 2012

Maishocks of  $M \geq 2$  during 2012 are listed in Table 1.2 and distinctly shown in Fig. 1.4 along with historical seismicity. All the recorded shocks during 2012 of  $M \geq 0.5$  are shown in Fig. 1.5. During 2012 three  $M > 4$  earthquakes occurred in Kachchh: M4.1 on 14.4.2012 along SWF, M5.0 on 30.6.2012 along KTF and M4.5 on 8.12.2012 in Kandla. Kachchh experienced 62 shocks of  $M \geq 3$  and 1359 shocks of  $M < 3$ . In Saurashtra the seismicity was subdued compared to heightened period of 2006 to 2011. In Jamnagar during 2012 seismicity was negligible with one M3 shock and only a few other small shocks. Seismicity in Talala was also much less during 2012. The area experienced shocks of M3.2 on 26.1.2012 and 25.2.2012 and 18 shocks of M2-2.9. Surendranagar cluster had 537 shocks of  $M \geq 0.5$  with  $M_{max}$  2.7.

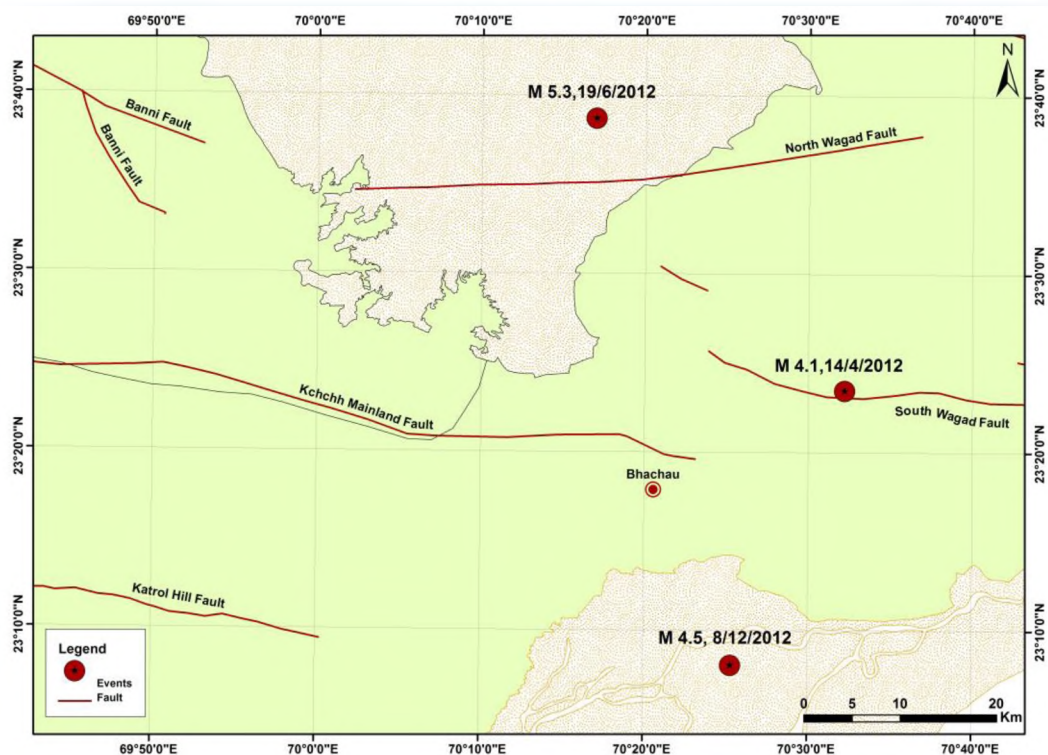


Fig. 1.3: Earthquakes of M-4 or more which occurred in Kachchh and recorded on SMA at two or more stations

Table 1.2: List of minshocks recorded in Gujarat during 2012

Year	MN	DD	HR	MN	Sec	Lat	Long	Dep	M	Reg.
2012	1	26	14	1	43.5	21.109	70.518	8	3.2	Talala
2012	2	19	11	13	1.1	21.118	72.29	22.1	3.2	
2012	3	21	14	50	29.1	21.716	72.405	15	3	Bhavnagar
2012	4	11	13	23	36.8	21.684	72.05	7	2.6	Surat
2012	4	14				23.39	70.54	19	4.1	SWF
2012	5	10	13	47	30	22.487	71.549	3.1	2.4	
2012	5	26	21	23	5.5	21.854	74.16	23.2	3.3	
2012	6	8	3	25	52	22.259	69.93	10.4	3.7	
2012	6	19	20	14	0.4	23.645	70.283	11.1	5.0	W of chobari
2012	7	30	8	3	49.1	21.213	72.826	9.8	3.6	
2012	7	30	8	3	49.1	21.213	72.826	9.8	3.6	
2012	8	24	21	17	2	25.336	70.561	27.5	3.3	
2012	8	28	14	26	13.5	20.629	70.457	9.5	3	
2012	9	1	14	36	3.8	22.074	70.103	8.2	2.7	
2012	10	9	22	7	20.2	21.127	70.57	3.1	2.3	
2012	11	15	18	43	54.7	21.598	72.796	9.6	2.4	
2012	11	16	0	23	12	22.201	72.537	9.8	2.4	
2012	12	8	7	6	9.1	23.134	70.422	21	4.5	Kandla
2012	12	16	4	13	42.3	24.474	71.887	3.2	2.8	

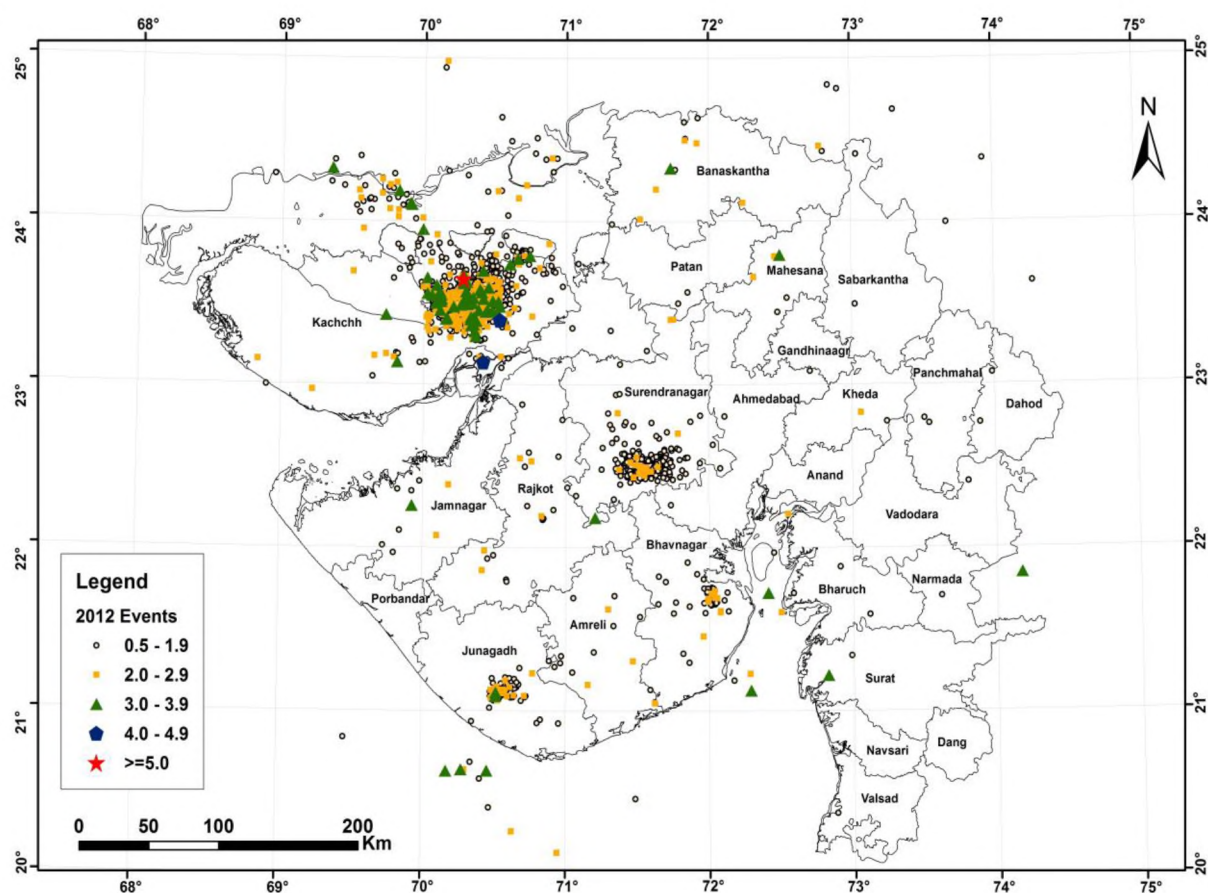


Fig. 1.5: Epicenters of earthquakes in magnitude range 0.5 to 5.0 in Gujarat during 2012

### Description of Earthquakes in Different Parts of Gujarat During 2012

Magnitude-wise distribution of earthquakes in the three regions of Gujarat during 2012 is given in Table 1.3. In the Kachchh region 1424 shocks were located of M0.5- 5.0 (65% of total in Gujarat). In the Saurashtra region 718 shocks were located of M1.0- 3.4 (33% of total in Gujarat). In the mainland 39 shocks were located of M1.0 – 3.2 (2% of total in Gujarat).

Table 1.3: Regional Distribution of Earthquakes Located in Gujarat during 2012

Region	<2.0	2-2.9	3-3.9	4-4.9	5-5.9	Total
Kachchh	1058	301	62	2	1	1424
Saurashtra	650	62	6	-	-	718
Mainland	26	9	4	-	-	39
Total	1734	372	72	2	1	2181

(Kindly note that due to the detectability in Kachchh being better, the % age of the earthquakes of this region will be a little less in real sense).

During 2012, the network recorded nearly 2337 shocks of magnitude 0.5 to 5.0 out of which hypocentral parameters of 2181 shocks were located (Fig. 1.5). Additional 64 regional earthquakes were recorded from Madhya Pradesh, Maharashtra, Rajasthan, Delhi and Himalaya with a significant shock of M5.0 near Delhi on 5<sup>th</sup> march 2012. Some 172 distant earthquakes of M4.0 or greater were recorded including M8.6 Sumatra earthquake on 11<sup>th</sup> April 2012.



**Table 1.4: Monthly number of located shocks in three regions namely Kachchh, Saurashtra and Mainland of Gujarat in year 2012.**

Month Region	Jan	Feb	Mar	Apr	May	Jun	Jul	Aug	Sep	Oct	Nov	Dec	Total
Kachchh	102	101	93	100	145	156	144	160	65	121	119	118	1424
Saurashtra	68	77	83	75	71	67	58	34	27	50	60	48	718
Mainland	2	5	1	3	3	3	5	6	4	3	3	1	39

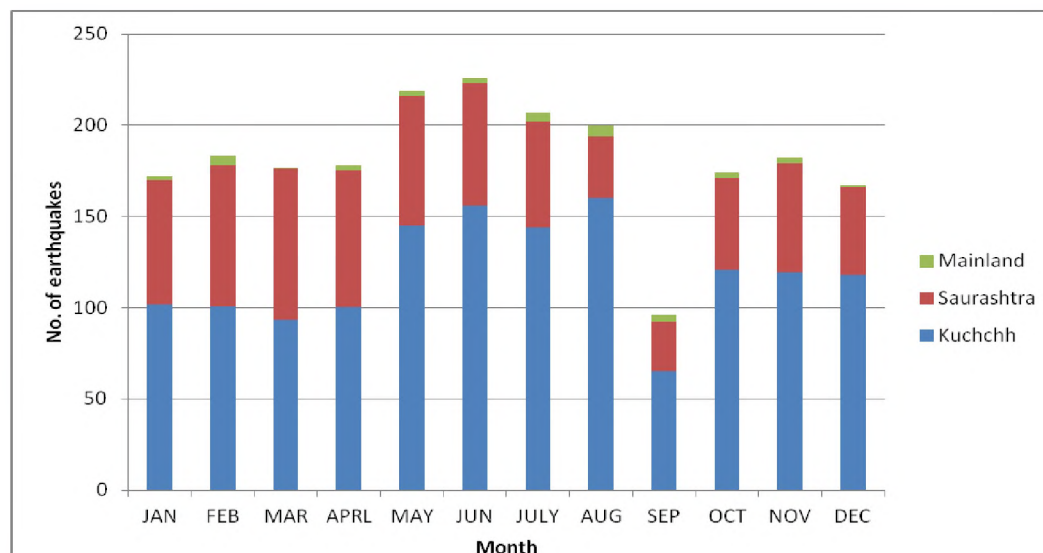


**Fig. 1.6: Histogram showing monthly no. of located shocks in three regions namely Kachchh, Saurashtra and Mainland of Gujarat during 2012**

### Seismicity in Kachchh

This year there were 1058 shocks of  $M_{0.5-1.9}$ , 301 shocks of  $M_{2.0-2.9}$ , 62 shocks of  $M_{3.0-3.9}$ , 2 shocks of  $M_{\geq 4.0}$ , and 1 shock of  $M_{5.0}$  was recorded. Shock of  $M_{5.0}$  occurred on 19<sup>th</sup> June 2012, 20 km SSE of Dholavira. Total 912 aftershocks were recorded from the same area of  $M_{0.7-3.8}$  till Dec. 2012 (Appendix 3).

**Table 1.5: Magnitude wise distribution of Dholavira aftershocks from 19<sup>th</sup> June 2012 to 31<sup>st</sup> December 2012.**

Magnitude Range	No. of earthquakes
0.5-1.9	696
2.0-2.9	168
3.0-3.9	48
5.0-5.9	1
Total	913

Focal depths of Kachchh earthquakes for  $M_{\geq 3.0}$  which occurred in the year 2012 are depicted in Fig. 1.7.

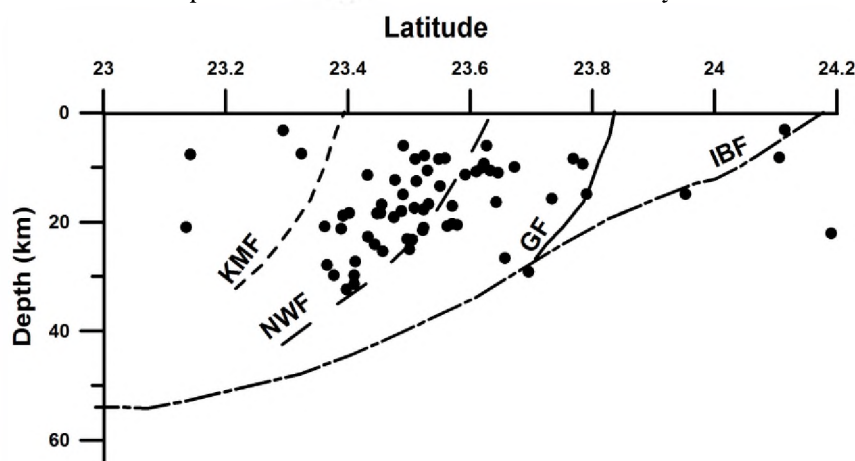


**Fig. 1.7: Focal depths of the earthquakes of  $M_{\geq 3}$  in Kachchh during 2012.**



### The Seismicity in Kachchh:

Seismicity in Kachchh has consistently been lower since 2008 (Fig. 1.8 and Table 1.6) with about 60 shocks of  $M \geq 3/y$ . However, one  $M5$  earthquake in 2012 has reminded its continuance to moderate level.

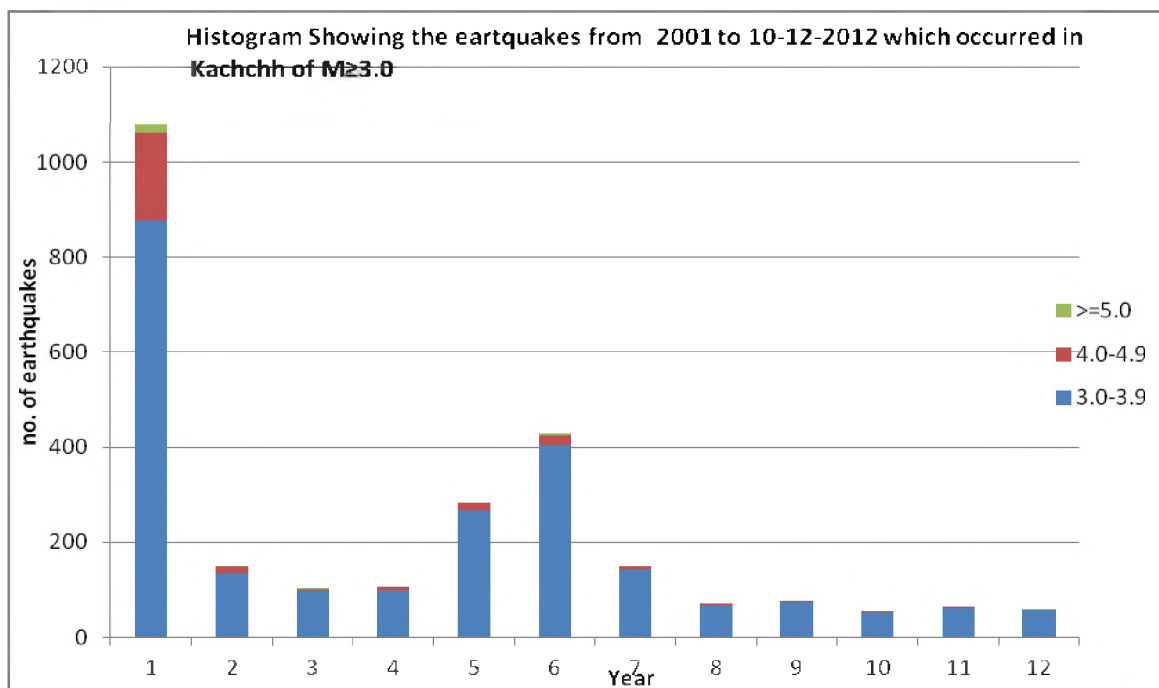


Fig. 1.8: Annual no. of shocks in Kachchh during 2001 to 2012. The green colour does not represent actual no. of shocks for  $M \geq 5.0$  in Kachchh. Total no. of shocks ( $M \geq 5.0$ ) in year 2001, 2006 and 2012 are 20, 4 and 1, respectively. Shock of  $Mw5.6$  in GEDI in the year 2006 caused slight damage

Table 1.6: Showing the no. of earthquakes of  $M \geq 3.0$  which occurred in Kachchh between 2001 to 2012

Year	2001	2002	2003	2004	2005	2006	2007	2008	2009	2010	2011	2012
M												
3.0-3.9	877	135	98	99	267	405	143	66	73	52	62	56
4.0-4.9	186	15	3	6	16	20	6	5	4	1	3	2
$\geq 5.0$	15	0	1	0	0	4	0	0	0	0	0	1

### Seismicity in Saurashtra

Epicenters of earthquakes of magnitude 0.5 to 3.4 in Saurashtra during 2012 are shown in Fig. 1.9. A shock of  $M_{max}3.4$  was recorded on 19<sup>th</sup> Sept. 2012, 44km ESE of Rajkot near Kamalpur. During August 2006 to December 2012, 120 earthquakes have occurred of  $M3-3.9$ , 7 earthquakes of  $M4-4.9$  and 2 earthquakes of  $M5.0$  &  $M5.1$  in Saurashtra (Tables 1.7, 1.8, 1.9 & Figure 1.10). Tremors were recorded from previously active areas such as Talala ( $M \geq 5.0$  on 6<sup>th</sup> November 2007 and on 20<sup>th</sup> Oct. 2011), near Surendranagar ( $M_{max}3.9$ ) and near Rajkot ( $M_{max}3.4$  on 19<sup>th</sup> Sept. 2012). Seismicity near Jamnagar was negligible and this year shocks were not noticed in Bhanvad- Adwana area. Focal depths of shocks in Saurashtra are from near surface to about 10km. Surendra Nagar area showed a large no. of microearthquakes,  $M < 2$  are 512 and  $M2-2.9$  are 21.

Table 1.10 lists earthquakes of  $M1-3$  (in three magnitude ranges) during 2012 in different parts of the Saurashtra region. Table 1.11 lists Monthly no. of located shocks in different parts of Saurashtra region during 2012.

### Seismic Activity in Talala of Junagadh District:

In the year 2012, some 77 shocks of  $M0.6-3.2$  were recorded from Talala area. Earthquake of  $M_{max}3.2$  occurred on 26<sup>th</sup> Jan and 25<sup>th</sup> Feb. 2012, 4 and 6 km, respectively, NNW of Talala.

In year 2011, an earthquake of Mw5.1 occurred, 12 km WNW of Talala in Gir on 20<sup>th</sup> Oct. An aftershock of M4.1 that occurred about 9 hours after the mainshock on 21<sup>st</sup> Oct. and another of M4.0 on 12<sup>th</sup> November were also strongly felt.

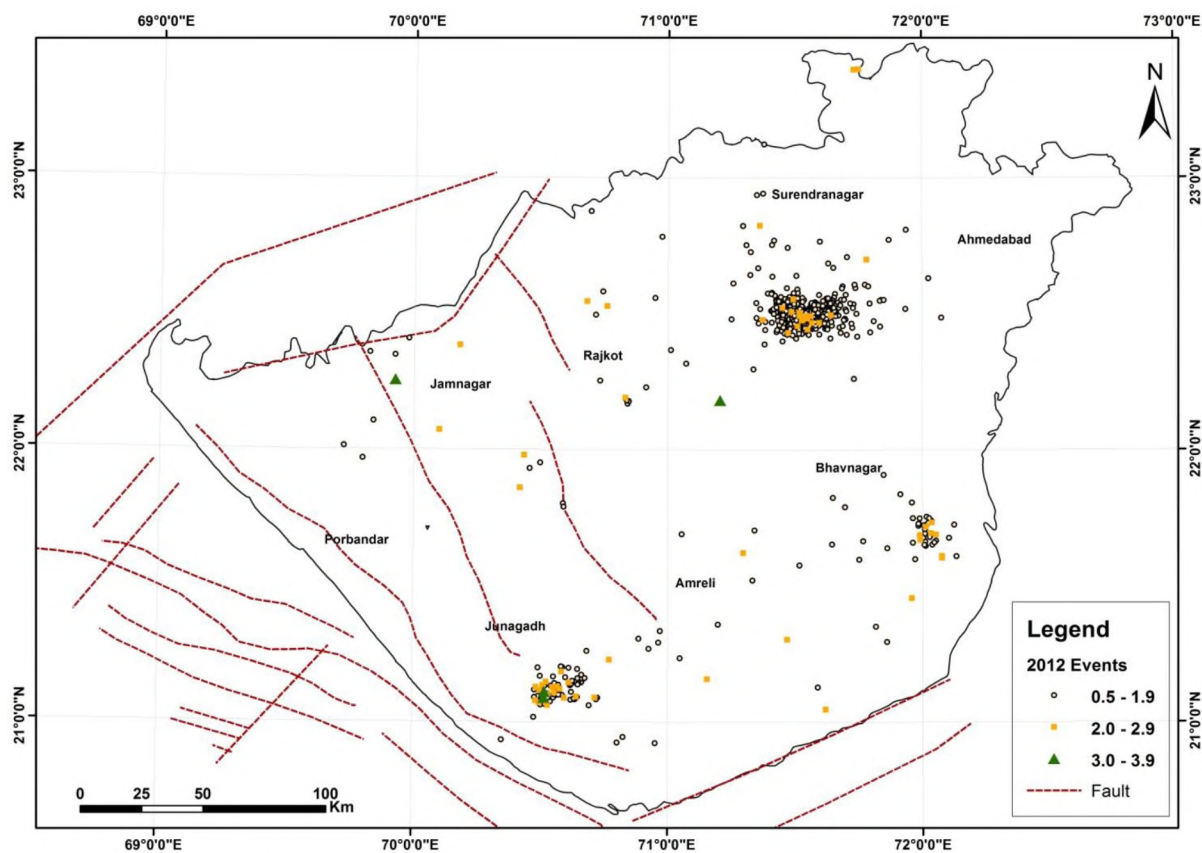


Fig. 1.9: Epicenters of earthquakes in magnitude range 0.5 to 3.4 in Saurashtra during 2012

Table 1.7: Seismicity of  $M \geq 3.0$  from Aug. 2006 to December 2012 in the Saurashtra region

Magnitude Range	No. of earthquakes
3.0-3.9	120
4.0-4.9	7
$\geq 5.0$	2

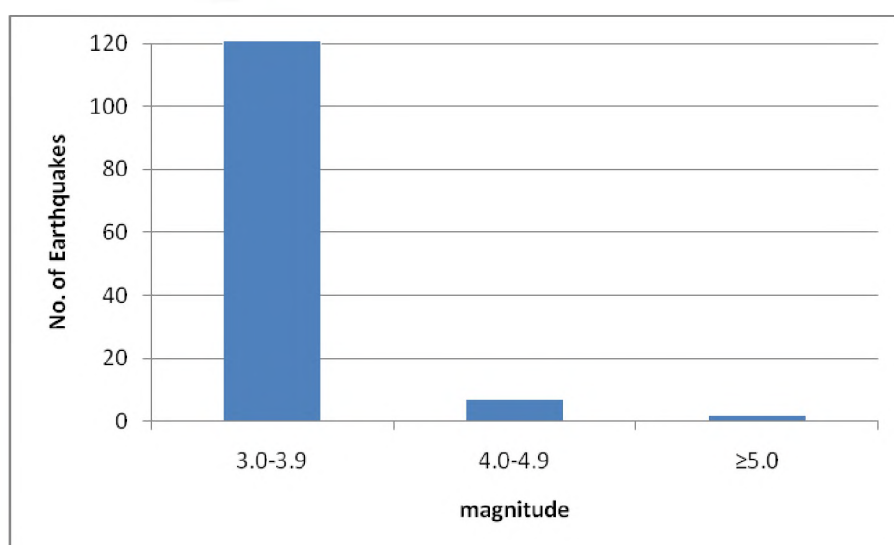


Fig. 1.10: Number of earthquakes in Saurashtra during Aug. 2006-Dec. 2012 in three magnitude categories.

**Table 1.8: List of earthquakes with magnitude  $M \geq 4.0$  in the Saurashtra region during August 2006 and December 2012.**

S. No.	YY:MN:DD	HR:MIN	Lat	Long	Dep.	M	Reg.
1	2006:09:30	00:16	22.30	70.20	5	4.0	Jamnagar
2	2007:11:06	00:27	21.11	70.51	8.5	4.8	Talala
3	2007:11:06	09:38	21.16	70.54	6	5.0	Talala
4	2008:10:05	11:33	21.16	70.54	12	4.3	Talala
5	2008:03:31	21:23	21.13	70.59	9.2	4.0	Talala
6	2011:05:23	23:43	21.10	70.53	3.9	4.0	Talala
7	2011:10:20	17:18	21.10	70.45	5.0	5.1	Talala
8	2011:10:21	03:07	21.11	70.50	6.1	4.1	Talala
9	2011:11:12	07:01	21.14	70.57	9.7	4.0	Talala

(After 2007, an earthquake of  $M \geq 5.0$  was recorded on October 20, 2011 in the Saurashtra region)

**Table 1.9: Annual number of earthquakes of M 0.5 to 5.1 in different areas of the Saurashtra region during 2007 to 2012.**

Year	2007	2008	2009	2010	2011	2012
Rajkot	7	12	20	33	21	12
Surendranagar	39	174	325	314	311	533
Talala	361	375	67	113	465	77
Jamnagar	87	25	29	182	24	8
Total	494	586	441	642	821	630

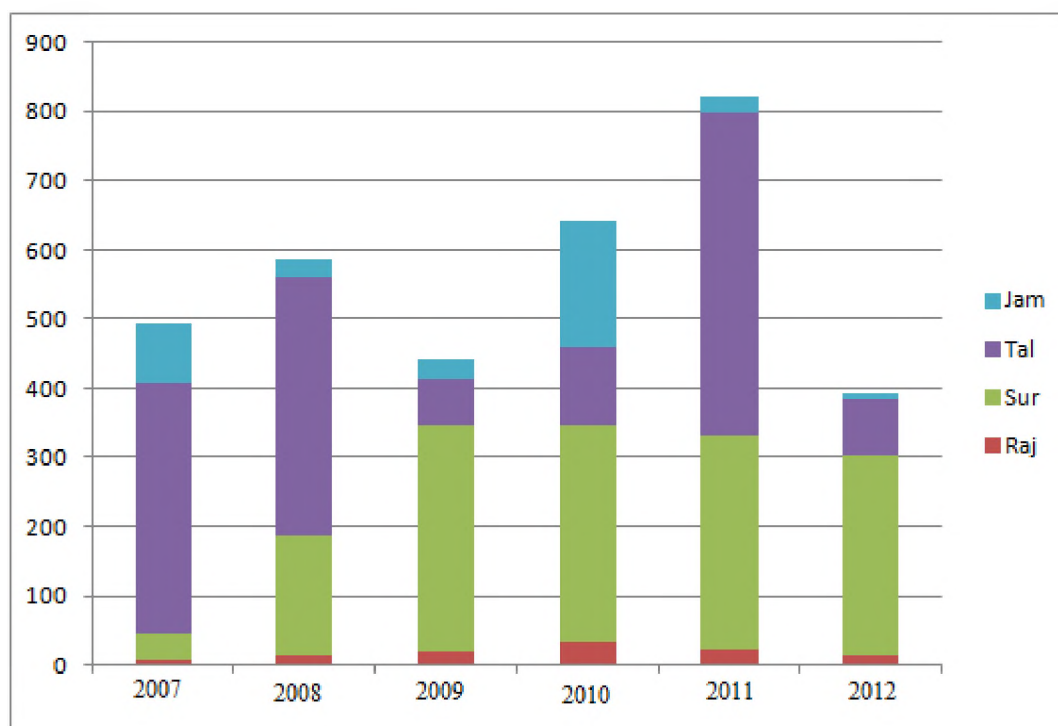


**Fig 1.11: Histogram showing the year wise seismicity variation in Jamnagar, Talala (Junagarh), Surendranagar and Rajkot district of Saurashtra.**

**Table 1.10: List of earthquakes region wise with magnitude  $M_{1.0-3.0}$  in the Saurashtra region in 2012.**

Region	< 2.0	2.0-2.9	3.0-3.9	Total
Lalpur	5	2	1	8
Adwana (Porbandhar)	1	0	0	1
Talala (Junagadh)	58	17	2	77
Bhavnagar	32	8	0	40
Rajkot	10	2	0	12
Surendranagar	512	21	0	533

**Table 1.11: Monthly number of earthquakes in different parts of Saurashtra during 2012.**

Region	No. of earthquakes in the month of											
	Jan	Feb	Mar	Apr	May	Jun	Jul	Aug	Sep	Oct	Nov	Dec
Lalpur	2	0	0	0	2	1	0	1	1	0	1	0
Adwana (Porbandhar)	0	0	0	0	0	0	1	0	0	0	0	0
Talala	10	20	12	7	2	8	9	1	3	3	3	5
Bhavagar	7	3	6	8	7	2	1	0	3	0	2	1
Rajkot	1	4	0	1	3	1	0	1	0	1	1	0

Seismic activity around Rajkot: In the year 2012, 13 shocks were recorded with M0.9-3.4. Shock of Mmax.3.4 was recorded on 19<sup>th</sup> Sept. 2012, 44km ESW of Rajkot district.

**Seismic activity around Surendranagar:**

In the year 2012, 533 shocks of M0.9-2.7 were recorded. Shock of Mmax.2.7 was recorded on 24<sup>th</sup> June 2012, 30 km SSW of Surendranagar.

**Earthquakes in Mainland Gujarat**

In the year 2012, 76 shocks of M1.0-3.2 were recorded from mainland region. Out of these 2 shocks are of  $M \geq 3.0$ . Shock of Mmax.3.2 occurred on 3<sup>rd</sup> July 2011, 35 km SW of Surat in South Gujarat. 2<sup>nd</sup> shock of M3.1 was located 73 km NNE from Palanpur in North Gujarat on 30<sup>th</sup> Nov. 2011.

# CHAPTER 2

## PHYSICS OF EARTHQUAKE PROCESS

### 2.1 Mechanism of the 20 June (19 June Ut) 2012 Mw5.1 Earthquake and its Aftershocks

The  $M_w$ 5.1 earthquake of 19 June 2012 occurred about 30km north of Bhachau and 20 km south of Dholavira (Figs. 2.1.1, 2.1.2a,b) along the NE trending Khadir (Ekal – Amrapar) Transverse Fault. The fault displaces the Island Belt Fault east of Dholavira (eastern side of Khadir Is.) and extends south to west of Chobari. The transverse faults are generally not expected to give major earthquakes. The location of mainshock (70.288 E 23.654E, focal depth 8.2km) is about 15 km north of the aftershock zone of 2001 earthquake. A few shocks had occurred in this area in 2011. More than 100 aftershocks of  $M_1$ -3.5 were recorded from the same area until June 2013 (Tables 2.1.1, 2.1.2). Depth section (Fig.2.1.2c) indicates nearly vertical fault with dip towards east.

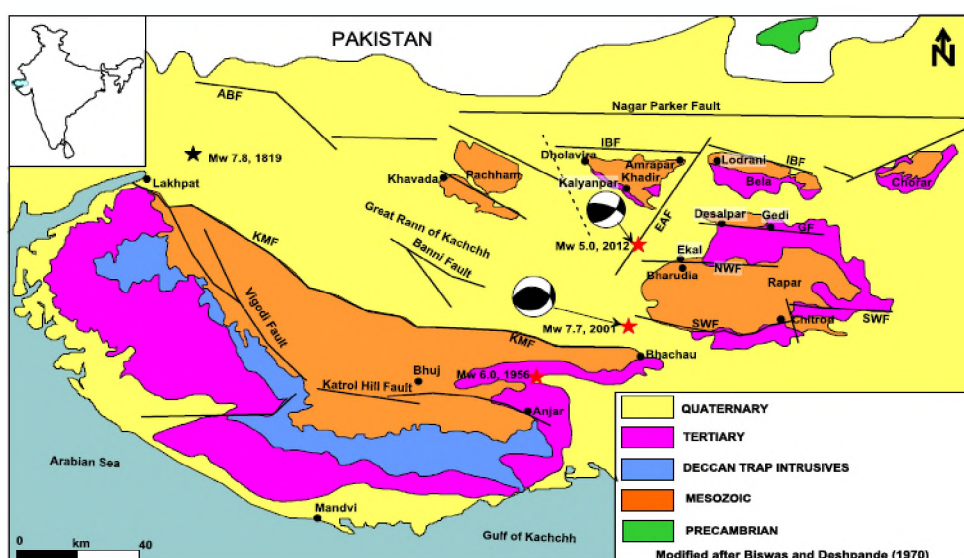


Fig. 2.1.1: Location of the 20 June 2012 Mw5.1 earthquake w.r.t. 2001 mainshock on the Geological map of the Kachchh region

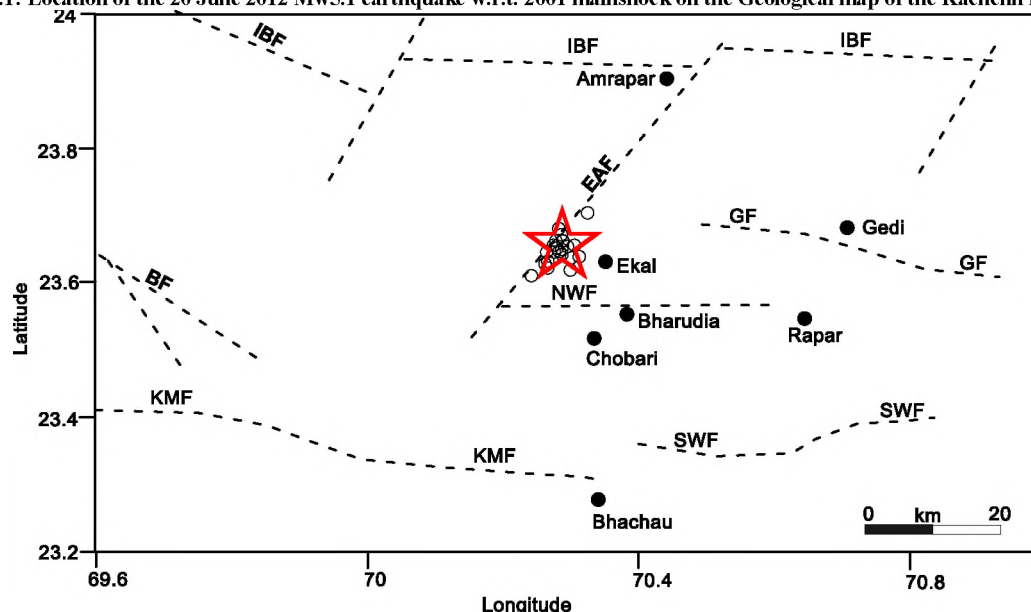


Fig. 2.1.2a: Epicenters of the mainshock of June 19, 2012 (IST June 20) (Mw5.1) and aftershocks which have occurred along the Khadir (Ekal-Amrapar) Transverse fault

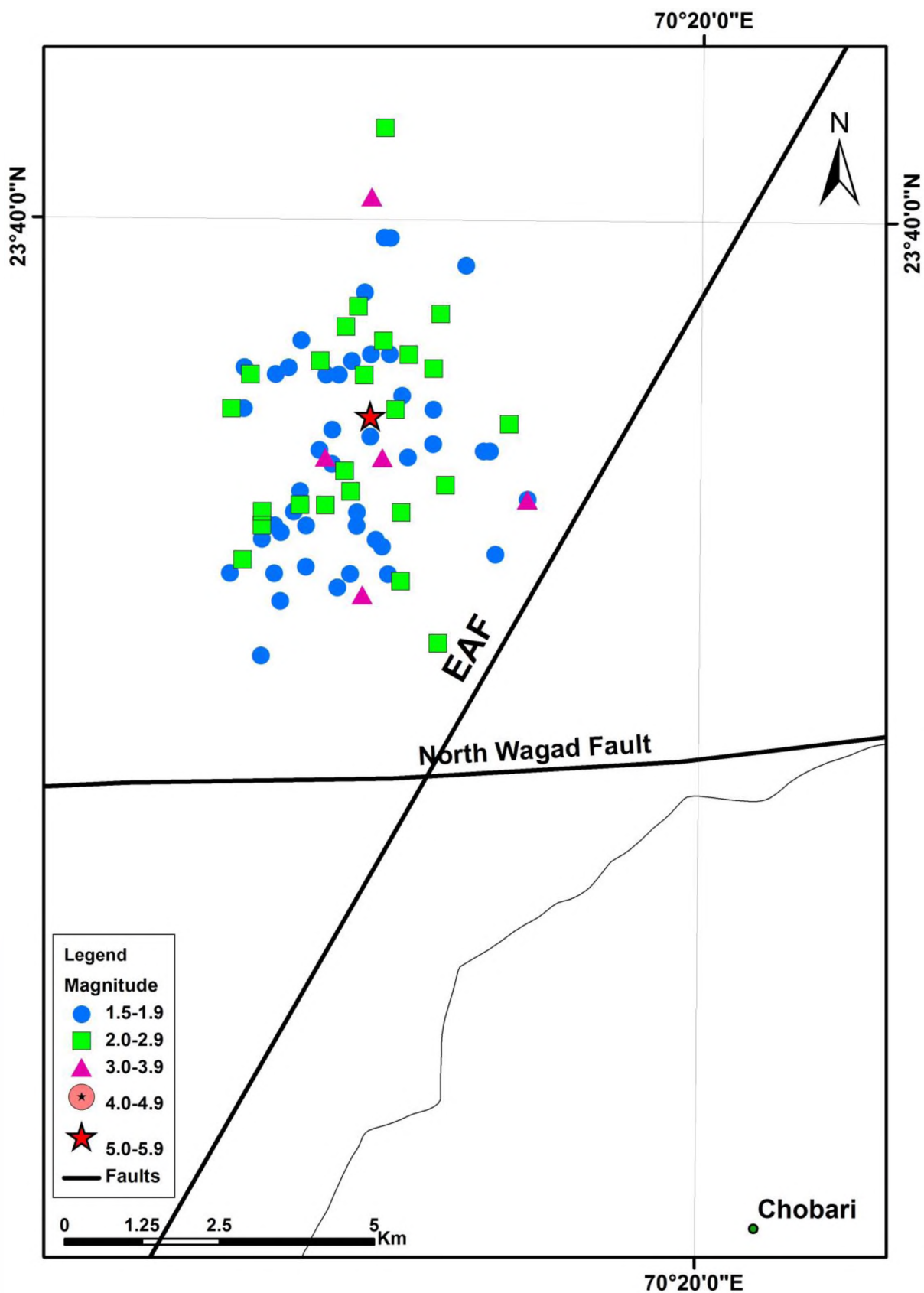


Fig.2.1.2b: Epicentral map of June 19, 2012 Mw5.1 epicentre and aftershocks of M1.5- 3.8. Wagad area is in SE whose boundary is shown. EAF: Ekal-Amrapar Fault



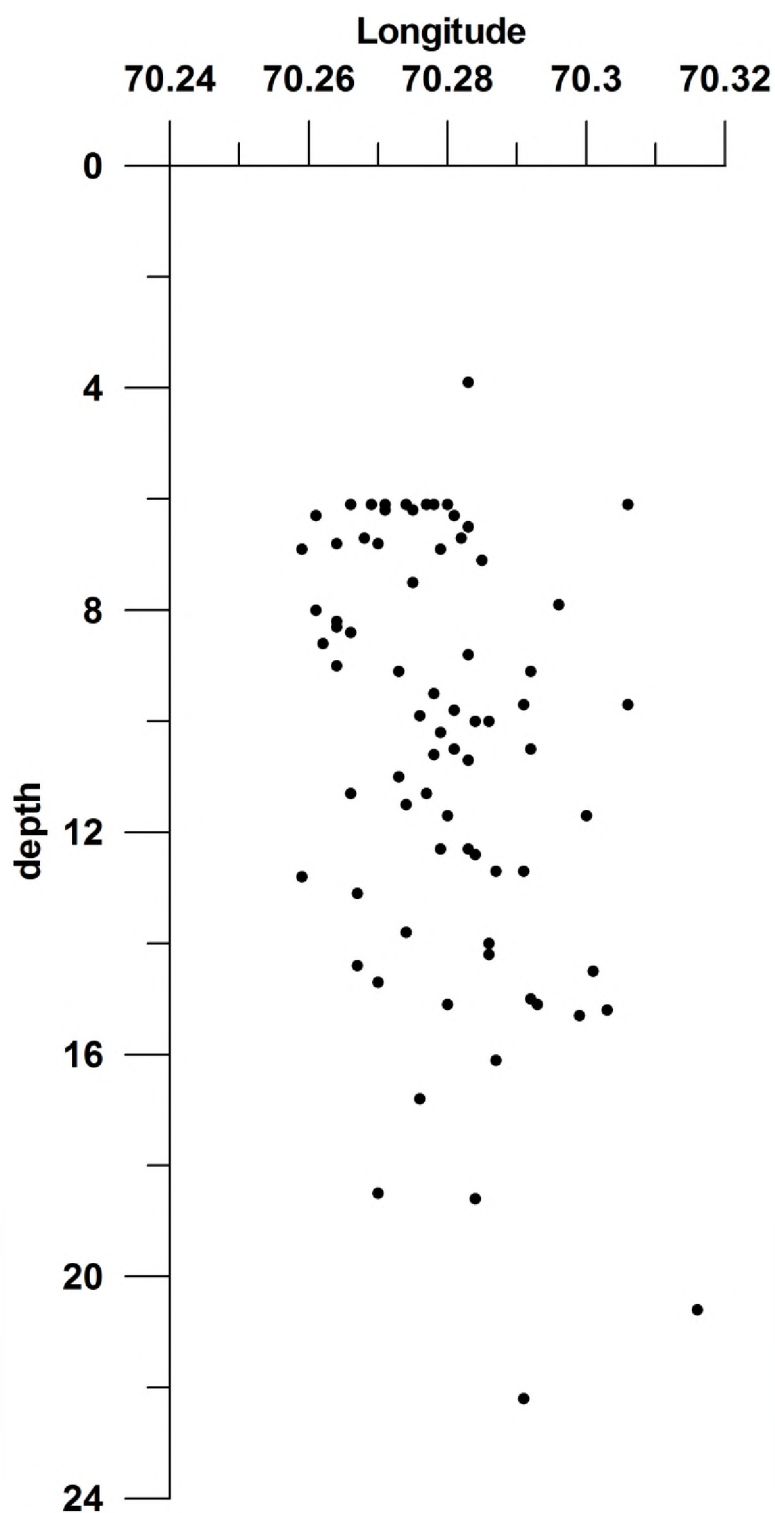


Fig. 2.1.2c: E-W Depth plot for the aftershocks of M1.5-3.8 of Dholavira earthquake of 19th June 2012 of  $M_w$  5.1

Table 2.1.1: List of earthquake showing no. of shocks which occurred in Dholavira region from 19-06-2012 to 17-06-2013.

M	No. of shocks
<2.0	74
2-2.9	25
3-3.9	8
4-4.9	Nil
5-5.9	1

**Table 2.1.2: List of earthquake which occurred in Dholavira region from 19-06-2012 to 17-06-2013.**

S.No.	YEAR	MN	DD	HR	MM	SEC	LAT	LONG	M
1	2012	6	19	20	14	0.4	23.645	70.283	5.1
2	2012	6	19	20	19	55.6	23.651	70.278	2.5
3	2012	6	19	20	26	47.6	23.667	70.282	2.9
4	2012	6	19	20	32	38.5	23.661	70.287	2.9
5	2012	6	19	20	37	40.5	23.647	70.273	1.7
6	2012	6	19	20	42	12.7	23.642	70.283	3.1
7	2012	6	19	20	45	37.1	23.653	70.276	2.9
8	2012	6	19	21	3	2.1	23.654	70.277	2.5
9	2012	6	19	21	8	51.9	23.65	70.282	1.5
10	2012	6	19	21	11	8	23.654	70.275	2.9
11	2012	6	19	21	15	56.7	23.665	70.282	2.8
12	2012	6	19	21	26	1.2	23.645	70.287	1.8
13	2012	6	19	21	44	17.2	23.644	70.277	1.9
14	2012	6	19	21	46	22.8	23.65	70.265	2
15	2012	6	19	22	20	51.2	23.678	70.29	1
16	2012	6	19	23	26	39.7	23.65	70.279	1.7
17	2012	6	19	23	32	47.5	23.641	70.277	1.3
18	2012	6	19	23	35	21.6	23.667	70.291	1.3
19	2012	6	19	23	39	33.9	23.676	70.289	1
20	2012	6	19	23	47	3.7	23.658	70.288	2.5
21	2012	6	20	0	11	53.1	23.675	70.286	1.7
22	2012	6	20	0	28	57.9	23.665	70.275	2.3
23	2012	6	20	1	27	55.6	23.66	70.278	1.7
24	2012	6	20	2	28	27	23.663	70.302	2.3
25	2012	6	20	4	26	44	23.662	70.286	1.5
26	2012	6	20	7	20	50.4	23.644	70.286	2.8
27	2012	6	20	8	15	32.8	23.659	70.283	1.7
28	2012	6	20	8	40	45	23.646	70.29	2.3
29	2012	6	20	14	8	22.8	23.631	70.27	2.2
30	2012	6	20	14	39	58.9	23.676	70.298	1.8
31	2012	6	20	15	33	49.9	23.679	70.284	1.3
32	2012	6	20	16	15	24.8	23.66	70.297	1.2
33	2012	6	20	18	3	53.2	23.644	70.277	1.7
34	2012	6	20	20	1	57.7	23.639	70.269	1.7
35	2012	6	20	20	5	15.4	23.64	70.296	1.4
36	2012	6	20	20	12	30	23.664	70.274	0.9
37	2012	6	20	20	48	31.7	23.655	70.274	1.6
38	2012	6	20	21	57	56	23.638	70.264	1.3
39	2012	6	21	4	53	57.4	23.64	70.269	2.7
40	2012	6	21	11	33	2.6	23.652	70.279	1.8
41	2012	6	21	16	44	13.7	23.642	70.285	1.3
42	2012	6	21	20	5	20.5	23.649	70.287	2.7
43	2012	6	21	22	18	59.6	23.68	70.298	1.1
44	2012	6	23	16	4	39.1	23.657	70.271	1.9
45	2012	6	23	21	38	13.5	23.652	70.288	1.8
46	2012	6	24	18	53	33.9	23.68	70.29	1.4
47	2012	6	24	19	24	37.1	23.644	70.277	1.8
48	2012	6	25	9	17	50.7	23.623	70.27	1.5
49	2012	6	25	10	24	21.6	23.643	70.291	2
50	2012	6	25	11	30	33.7	23.655	70.272	1.9
51	2012	6	25	12	31	17.5	23.657	70.272	1.7



S.No.	YEAR	MN	DD	HR	MM	SEC	LAT	LONG	M
52	2012	6	25	21	1	33.1	23.672	70.283	3.1
53	2012	6	27	7	56	22	23.658	70.276	2.5
54	2012	6	27	22	42	24.5	23.652	70.27	1.4
55	2012	6	27	22	52	51.3	23.66	70.279	1.2
56	2012	6	28	23	6	1.1	23.644	70.298	1.5
57	2012	6	29	14	5	20.7	23.632	70.294	1.9
58	2012	6	29	15	29	53.2	23.635	70.272	1.9
59	2012	6	29	23	7	47.3	23.678	70.292	0.9
60	2012	7	1	6	26	0.5	23.633	70.273	1.9
61	2012	7	1	14	49	34.9	23.625	70.274	2.5
62	2012	7	1	18	7	58.8	23.653	70.292	1.9
63	2012	7	2	12	0	44.1	23.615	70.284	1.5
64	2012	7	2	12	19	21.8	23.627	70.278	2.5
65	2012	7	2	13	56	33	23.634	70.291	1.7
66	2012	7	3	8	28	19.3	23.631	70.275	1.7
67	2012	7	6	8	41	16.4	23.615	70.259	1.5
68	2012	7	8	8	58	25.4	23.632	70.283	3.5
69	2012	7	9	16	42	50.1	23.635	70.281	1.9
70	2012	7	10	0	45	41.7	23.619	70.283	1.5
71	2012	7	11	11	41	30.8	23.615	70.278	1.9
72	2012	7	15	16	1	36	23.622	70.267	1.1
73	2012	7	16	10	55	11.8	23.63	70.277	2.8
74	2012	7	17	0	8	52.2	23.62	70.279	1.3
75	2012	7	20	5	32	14.8	23.613	70.276	1.9
76	2012	7	21	5	9	51.8	23.632	70.287	1.5
77	2012	7	25	8	23	35.3	23.611	70.267	1.9
78	2012	7	26	6	9	6.5	23.614	70.286	2.8
79	2012	7	26	12	26	49.5	23.603	70.264	1.6
80	2012	7	27	7	50	33.5	23.633	70.3	1.5
81	2012	7	29	5	40	10.6	23.617	70.278	1.2
82	2012	8	2	23	2	12.4	23.616	70.317	2.3
83	2012	8	7	15	38	34.1	23.61	70.272	1.7
84	2012	8	11	10	38	12.2	23.618	70.275	1.3
85	2012	9	2	23	29	20.4	23.622	70.286	3.3
86	2012	9	4	0	36	54.6	23.619	70.283	3
87	2012	9	10	8	0	57	23.62	70.282	1.7
88	2012	10	2	3	39	29.8	23.622	70.271	1.7
89	2012	10	18	8	6	6.1	23.62	70.264	1.5
90	2012	10	30	14	38	49.3	23.626	70.306	3.1
91	2012	11	4	14	52	0.4	23.626	70.306	1.8
92	2012	11	8	18	30	60	23.611	70.303	1
93	2012	11	9	23	49	29.7	23.622	70.279	1.5
94	2012	11	13	7	11	56.5	23.605	70.292	2
95	2012	11	18	2	21	34.1	23.621	70.282	1.3
96	2012	11	20	23	12	27.1	23.618	70.301	1.6
97	2012	11	25	0	8	54.6	23.616	70.271	1.6
98	2013	2	27	4	31	12	23.623	70.29	1.8
99	2013	3	9	0	38	34.6	23.607	70.289	1
100	2013	5	18	20	40	56.6	23.622	70.285	1.5
101	2013	1	18	16	42	12.2	23.666	70.251	2
102	2013	2	27	4	31	12	23.623	70.29	1.3
103	2013	3	9	0	38	34.6	23.607	70.289	1.6

S.No.	YEAR	MN	DD	HR	MM	SEC	LAT	LONG	M
104	2013	5	18	20	40	56.6	23.622	70.285	1.6
105	2013	5	29	12	25	36.9	23.598	70.281	1.6
106	2013	6	7	21	46	6.5	23.595	70.263	1.7
107	2013	6	9	9	31	4.4	23.596	70.25	3.5
108	2013	6	17	3	35	56	23.591	70.302	3.1

The fault plane solution from first motion directions indicates a NE trending and east dipping fault with combination of strike-slip and thrust movement (Fig. 2.1.3 and 2.1.4). A similar mechanism is obtained with worldwide data (Fig. 2.1.5).

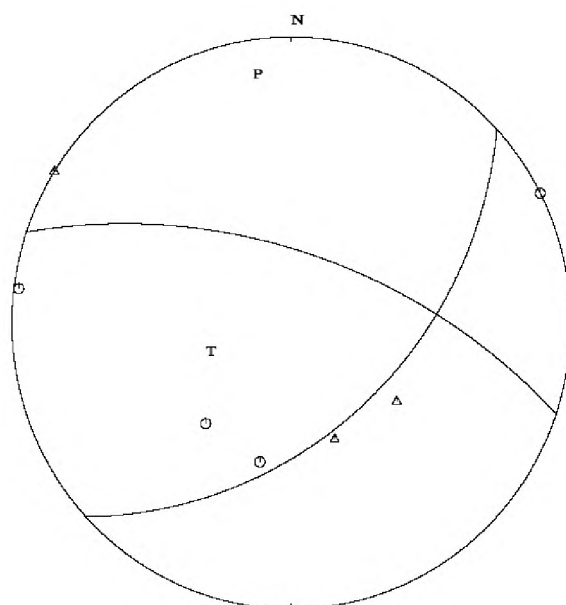


Fig. 2.1.3: The first motion focal mechanism solution of the 20 June 2012  $M_w$  5.1 earthquake using seven-station network around the epicenter

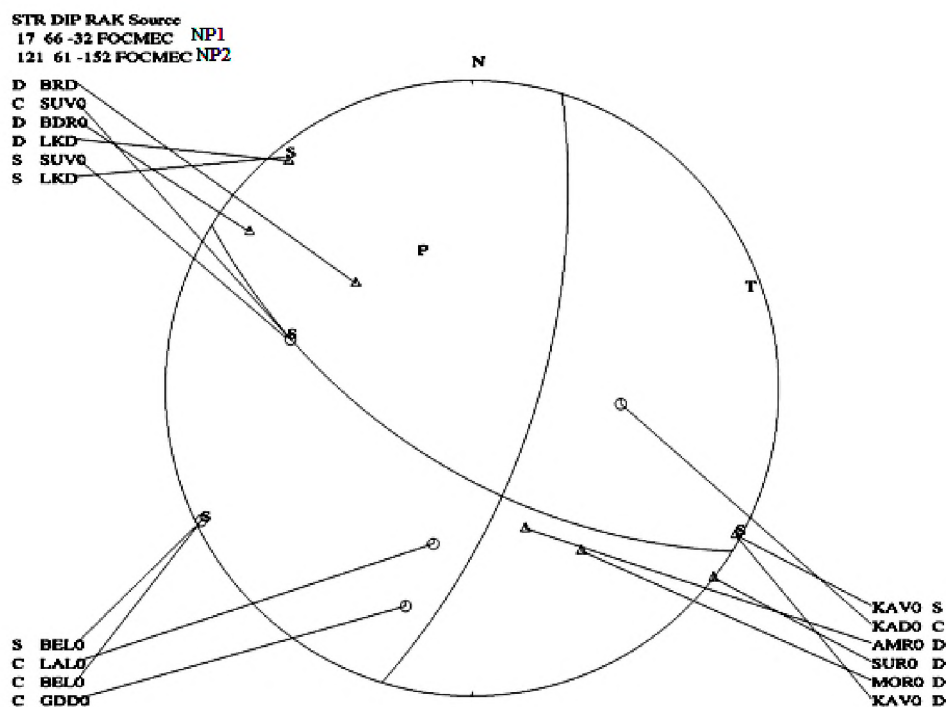


Fig 2.1.4: Focal mechanism obtained by first motion for the Dholavira earthquake of 19<sup>th</sup> June 2012,  $M_w$  5.1 using local and regional data sets.

### Moment Tensor Solution by Geo Forshung Centrum, Postdam, Germany

The focal mechanism is obtained to be nearly same by GFZ (Fig. 2.1.5) as given by first motion directions. Focal depth is estimated to be 11 km and moment magnitude  $M_w$  5.1.

GFZ MOMENT TENSOR SOLUTION, 12/06/19 20:14:03.55, Southern India

Epicenter: 23.67 70.30,  $M_w$  5.1, Depth 11      No. of sta: 24

Moment Tensor;      Scale  $10^{16}$  Nm

$M_{rr}$ = 0.12       $M_{tt}$ =-2.80

$M_{pp}$ = 2.69       $M_{rt}$ =-1.16

$M_{rp}$ = 0.07       $M_{tp}$ =-3.75

Principal axes:

T Val= 4.66      Plg= 7      Azm=242

N      0.24      76      120

P      -4.91      11      334

Best Double Couple:  $M_0=4.8 \times 10^{16}$

NP1: Strike=108      Dip=87      Slip=-166

NP2:      18      77      -2

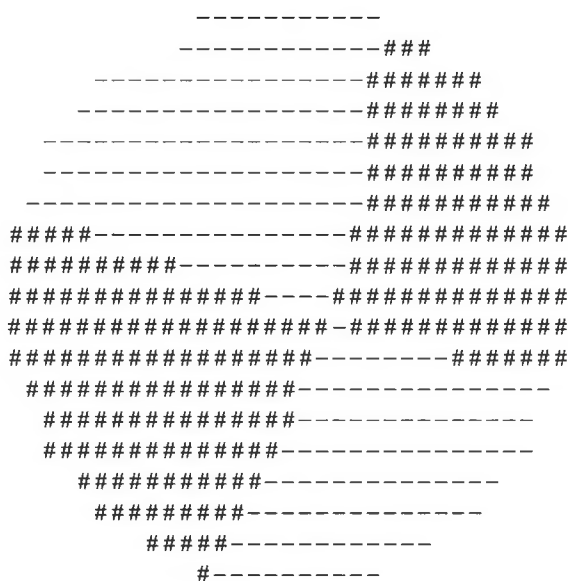


Fig. 2.1.5 Moment-Tensor Focal Mechanism Solution from GFZ, Potsdam

### Moment-Tensor Focal Mechanism Solution Using Local Data:

Moment tensor analysis has been carried out for Dholavira earthquake ( $M_L$  5.0), Kachchh region, that occurred on 19<sup>th</sup> June 2012 at 20:14:0.1 (GMT). For present analysis, good signal to noise ratio velocity data of ten 3-component stations with epicentral distance ranging from 33.8 to 365.8 km and azimuth varying from 63° to 301° have been used. Full waveforms containing the body waves and surface waves, amounting to several seconds of each trace are low-pass filtered by a 2-pole butterworth filter in the frequency range of 0.03 – 0.08 Hz, to remove the high frequency noise. After that, cut waveforms are rotated, integrated and re-sampled at 1 Hz to obtain the displacement seismograms.

The Green's functions are then computed using the approach of Takeo (1987), which uses a combination of the generalized reflection-transmission matrix method (Kennett, 1974, 1980) and the discrete wave number summation method (Bouchon, 1981). Synthetic seismograms are then generated and matched with observed waveform by using moment tensor inversion method of Kikuchi and Kanamori (1991), slightly modified for the near field earthquakes by Kosuga (1996). A simple triangular pulse is approximated for the source time function. The observed and synthetic waveforms are then matched using the cross-correlation approach with the criterion of obtaining minimum mismatch error. Waveform matching obtained in the study is depicted in Fig.1. Similar fault trend is indicated by fault-plane solution by first motion directions (Fig. 2.1.6). Also, the results are validated by MTS solution given by GFZ agency.

#### EQ 19 JUNE 2012

23.632N, 70.287E, 6.1km, M=5.0  
 $M_0 = 0.501E+17Nm$  ( $M_w=5.1$ )  
 $t_1=1.30s$ ,  $t_2=5.00s$ ,  $start=5.04s$   
 strike=114.8, dip=89.7, rake=-171.4  
 error=0.797  
 sampling=1.4Hz

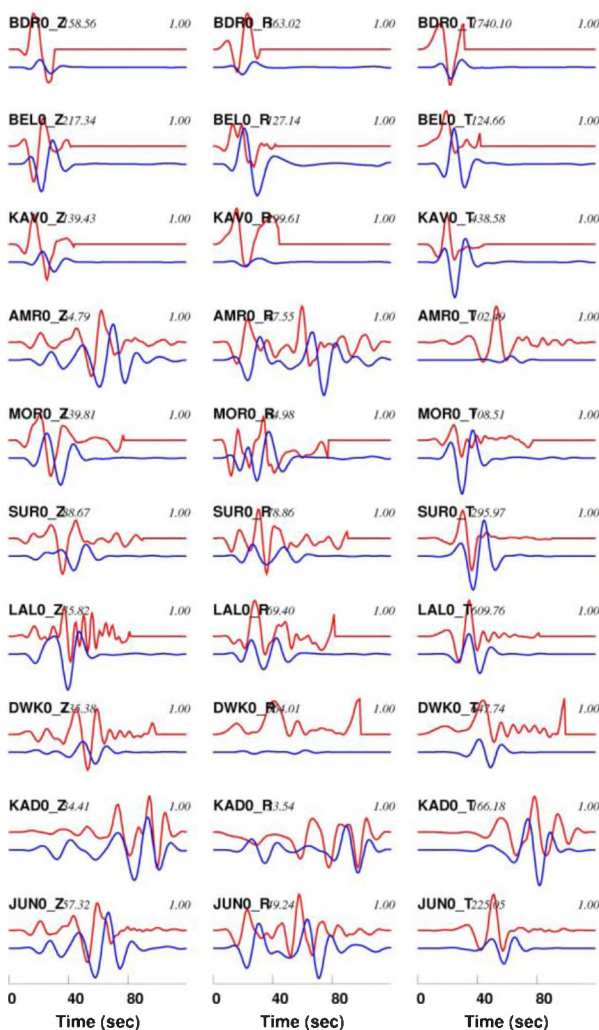
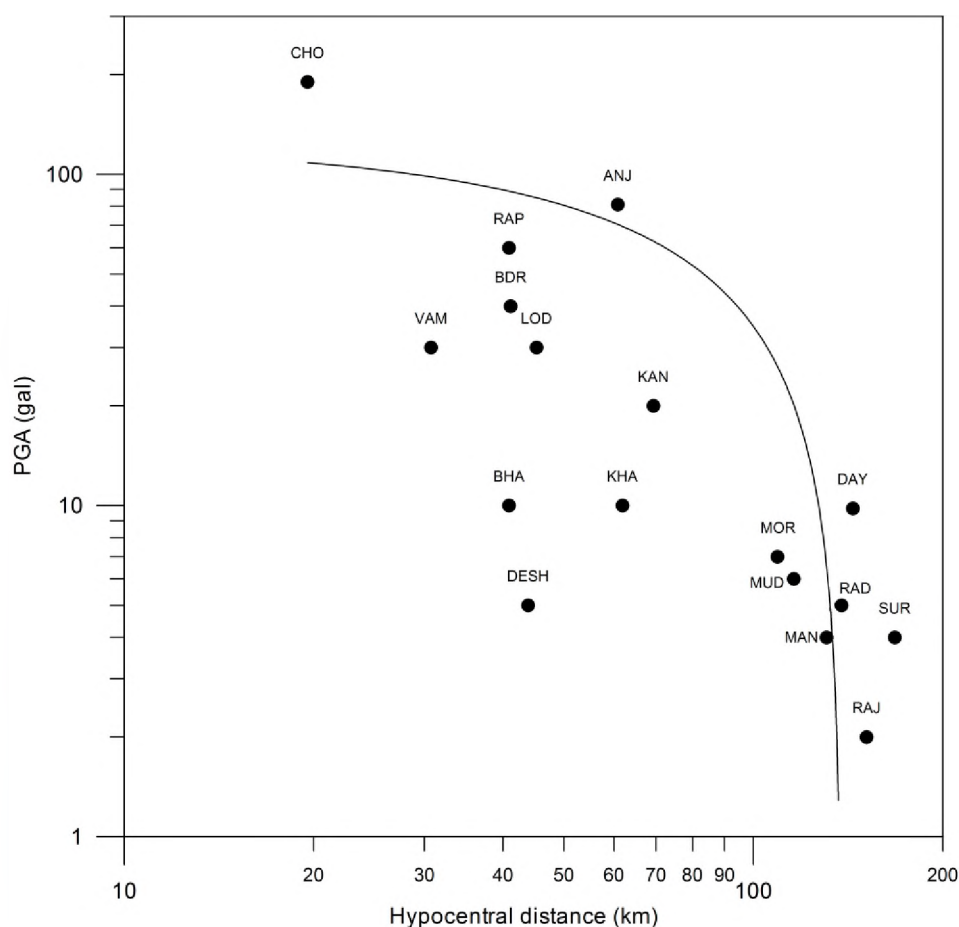


Fig. 2.1.6: Waveform inversion result for the Dholavira earthquake of 19th June 2012, ML 5.0, using the inversion approach of Kikuchi & Kanamori (1991). The waveform match between the observed (red) and synthetic (blue) filtered displacement seismograms is shown along with the source time function and focal mechanism obtained.

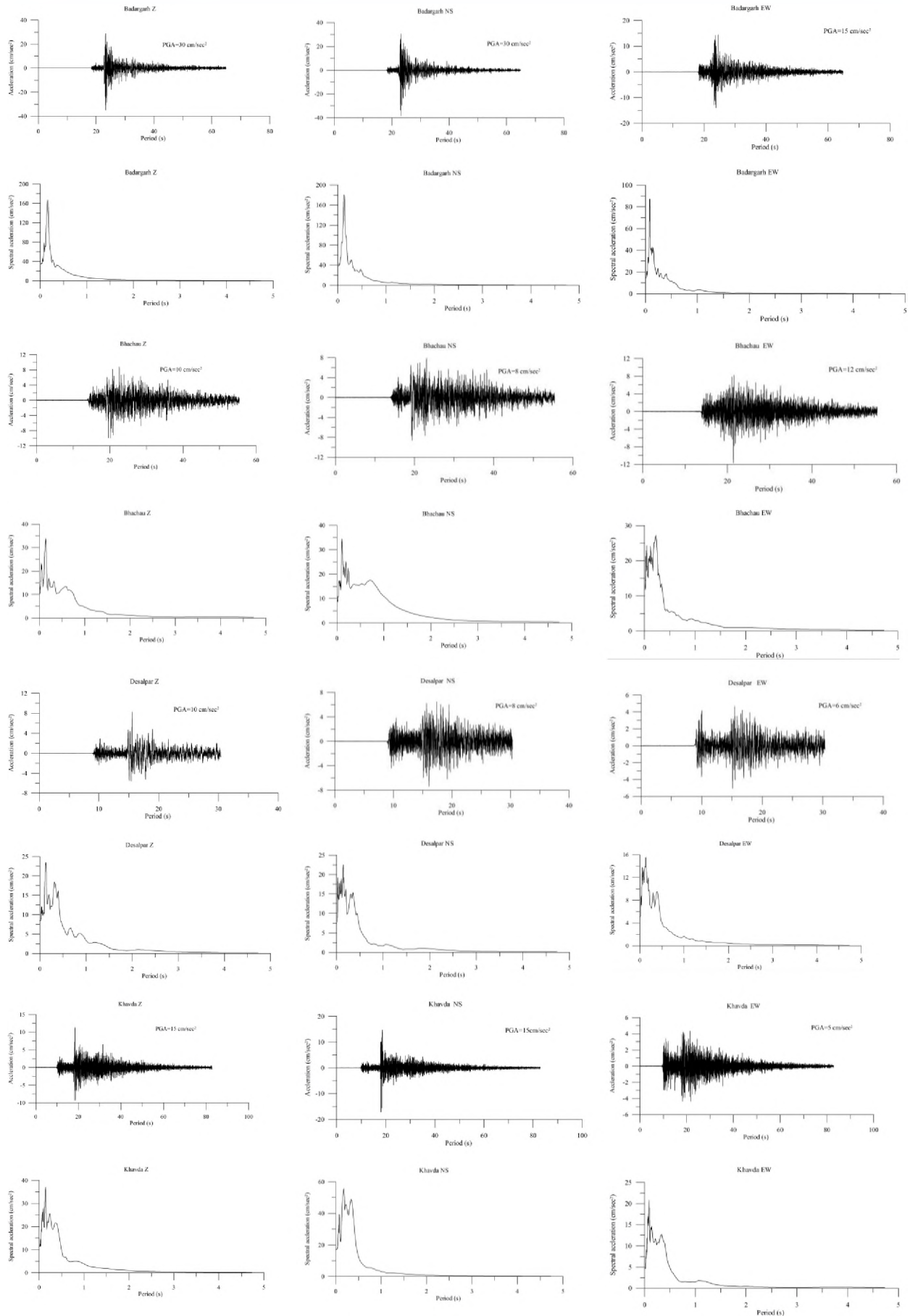
Recorded PGA at various SMA stations for 19-06-2012 Dholavira shock of M5.0 are listed in Table 2.1.3 and their decay with distance is shown in Fig. 2.1.7. Fig. 2.1.8 shows the recorded strong motion time histories and their response spectra for Dholavira M5 earthquake.

**Table 2.1.3: Recorded PGA at various SMA stations for 19-06-2012 Dholavira shock of M5.0**

STN	Epi-D	Hypo-D	PGA	Local subsurface
CHO	16.175	19.561	0.19	Soil
VAM	28.699	30.734	0.03	Hard Rock
BHA	39.37	40.882	0.01	Hard Rock
RAP	39.37	40.882	0.06	Soil
BDR	39.619	41.118	0.04	Hard Rock
DESH	42.72	43.853	0.005	Hard Rock
LOD	43.856	45.214	0.03	Hard Rock
ANJ	59.856	60.879	0.081	Soil
KHA	60.958	61.943	0.01	Hard Rock
KAN	68.48	69.36	0.02	Soil
MOR	108.839	109.394	0.007	Soil
MUD	115.45	115.97	0.006	Soil
MAN	130.16	130.63	0.004	Soil
RAD	137.3	138	0.005	Soil
DAY	143.512	143.933	0.0098	Soil
RAJ	150.4	151.32	0.002	Hard Rock
SUR	167.37	167.74	0.004	Hard Rock



**Fig. 2.1.7: for the Dholavira earthquake of 19th June'2012, M<sub>L</sub> 5.0**





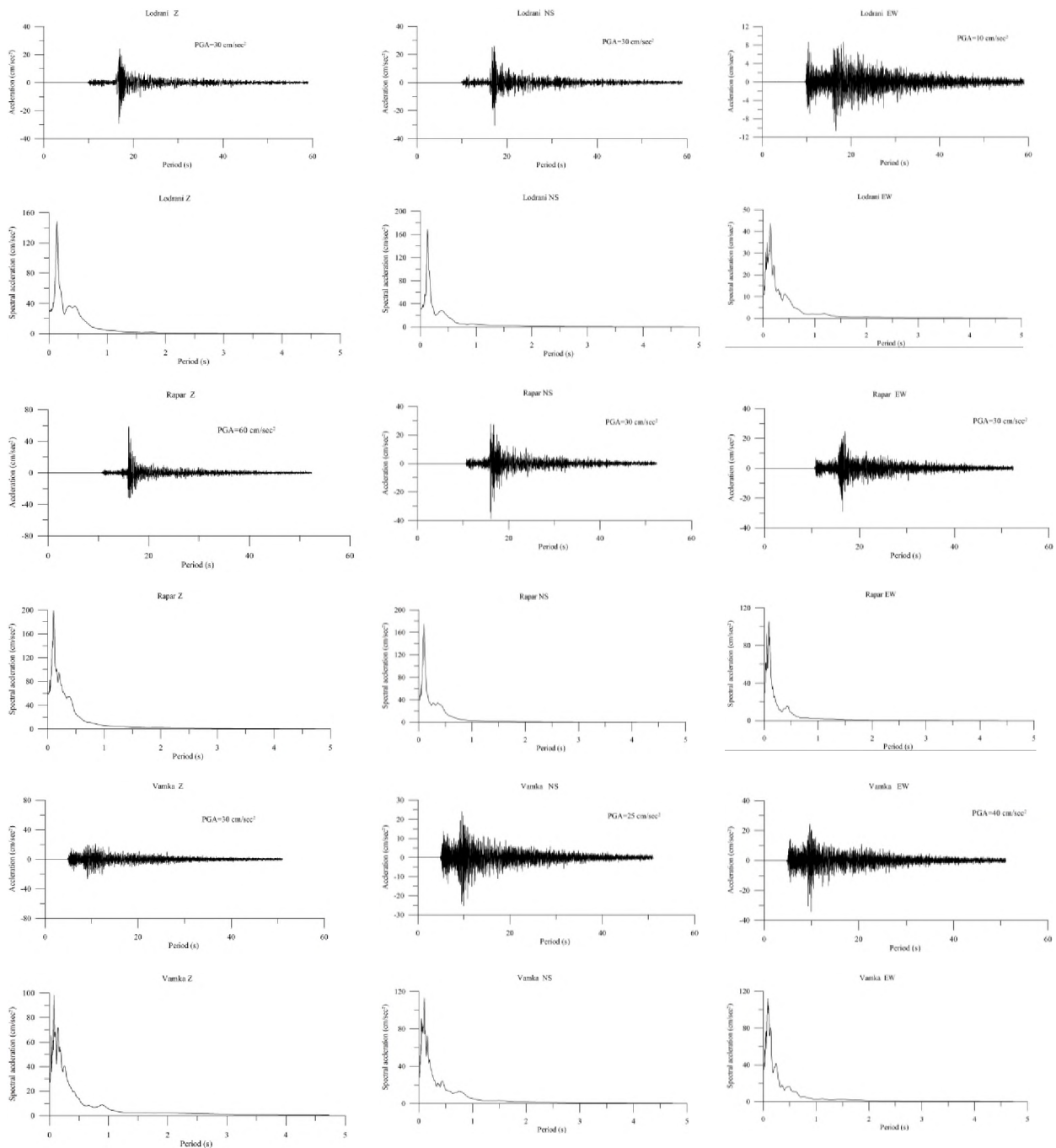


Fig. 2.1.8: Recorded strong motion time histories and their response spectra for Dholavira M5 earthquake

### References:

1. Bouchon, M., 1981. A simple method to calculate Green's functions for elastic layered media, Bull. seism. Soc. Am., 71, 959–971.
2. Kennett, B.L.N., 1974. Reflections, rays and reverberations, Bull. seism. Soc. Am., 64, 1685–1969.
3. Kennett, B.L.N., 1980. Seismic waves in a stratified half space—II. Theoretical seismograms, Geophys. J. R. astr. Soc., 61, 1–10.
4. Kikuchi, M., Kanamori, H., 1991. Inversion of complex body waves-III. Bull. seism. Soc. Am., 81, 2335–2350.
5. Kosuga, M., 1996. Near-field moment tensor inversion and stress field in northeastern Japan. Ph.D. thesis, Tohoku University, Sendai, Japan.
6. Takeo, M., 1987. An inversion method to analyse the rupture process of earthquakes using near-field seismograms, Bull. seism. Soc. Am., 77, 490–513.

## 2.2 Cmt Solution for 2010 M4.4 Earthquake Using Regional Stations Data

(Nagabhushana Rao, B.K. Rastogi and Purnachandra Rao)

An earthquake of M 4.4 occurred on September 2, 2010 along a EW fault, near Patan in Cambay Basin (Fig. 2.2.1 and 2.2.2). CMT shows thrust movement along a EW trending plane (Fig. 2.2). The pressure axis is oriented in N direction. The source time function indicates half source duration of 4.5 sec and maximum slip of 10 cm. The focal depth is indicated to be 12km.

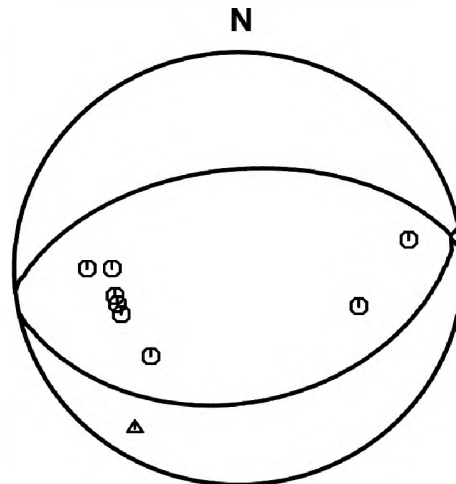


Fig. 2.2.2: CMT solution for September 2, 2010 Patan, Cambay Basin earthquake of M 4.4 that occurred along a EW fault shows thrust faulting. The first motion Data also matches with the mechanism. Circle represents compression while Triangle represents Dilatation

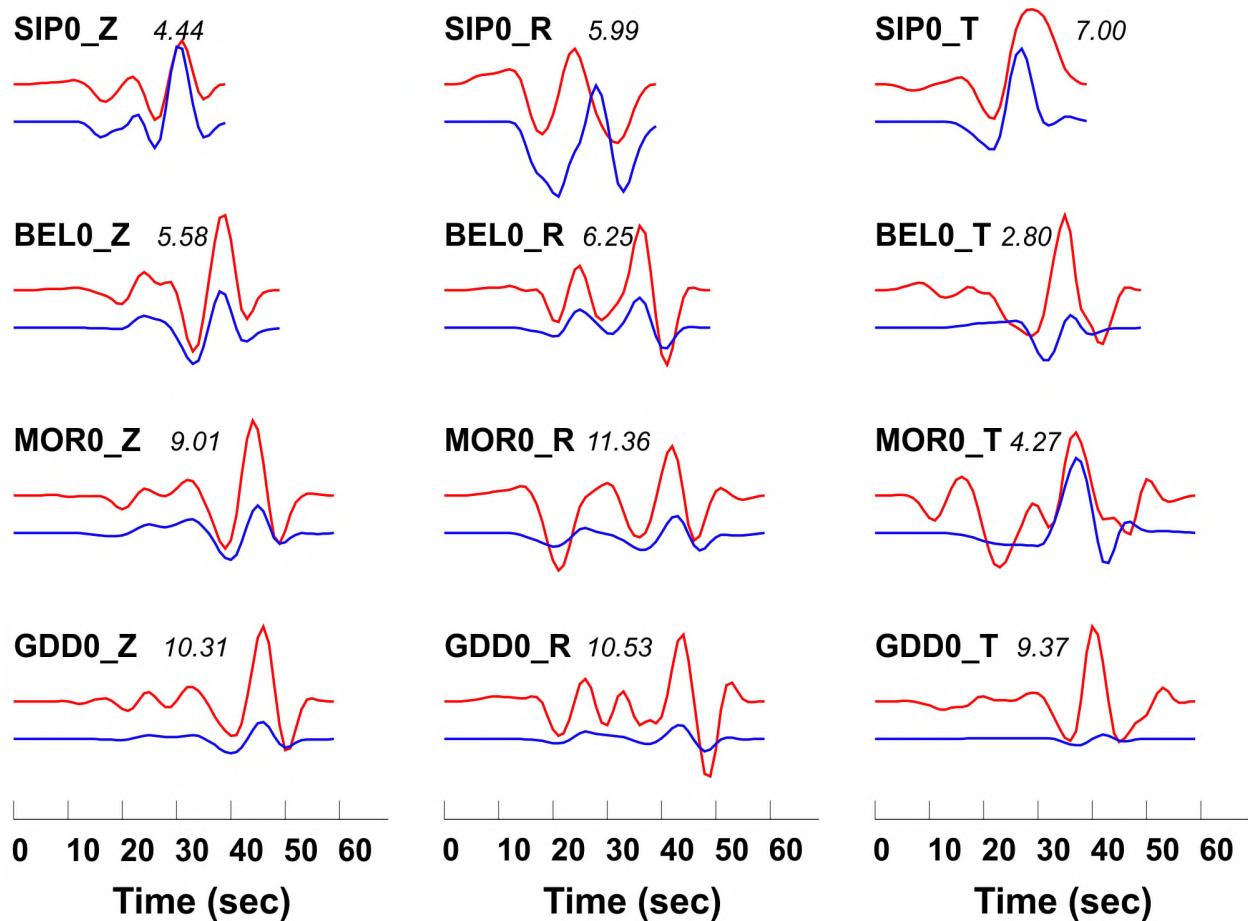


Fig. 2.2.1: Wave form matching for an earthquake of M 4.4 that occurred on September 2, 2010 along a EW fault, near Patan in Cambay Basin



### 2.3 Global Seismic Cyclicality and Possible Enhanced Seismicity Since 2001

(B. K. Rastogi and Jyoti Sharma)

Over the years global seismicity and seismic moment release patterns have been studied by various researchers including Benioff (1951, 1954), Davies and Brune (1971), Mogi (1974, 1979), Kagan and Jackson (1991), Pacheco and Sykes (1992), Bufe (1997). On the basis of previous studies, it has been observed that the temporal clustering of the large earthquakes followed by relative quiescence (stress shadow), is a characteristic seismic cycle's pattern along the plate boundaries. For the present study, Pacheco–Sykes catalog is used for the period 1900–1989 and from 1989 onwards Global Centroid Moment Tensor (GCMT) catalog is used, except for the magnitudes of 1960 Chile and 2004 Sumatra earthquakes. Pacheco and Sykes (1992) have provided a high quality homogeneous seismic-moment catalog for large shallow earthquakes (1990–1989). Moreover, Pacheco and Sykes (1992) have described the pattern of global seismic moment release for  $M \geq 7.0$  shallow ( $z < 70$  km) earthquakes. Earthquakes of  $M \geq 7.0$  have been considered to produce homogenous (1900–1989) catalog based on the assumption that the worldwide rate of occurrence of smaller ( $M < 7$ ) earthquakes does not change systematically over time. Dziewonski and others at Harvard (Dziewonski et al., 2001) have provided Centroid Moment Tensor solutions and Seismic Moment Release for worldwide earthquakes since 1977. In the present study, for 1960 Chile earthquake a lower value of  $2000 \times 10^{20}$  Nm and  $M_w$  9.5 (Kanamori and Anderson, 1975a, Bufe and Perkins, 2005) is used. The Pacheco and Sykes have reported the seismic moment  $3200 \times 10^{20}$  Nm,  $M$  9.6 (Cifuentes and Silver, 1989). The Sumatra earthquake is considered of  $M_w$  9.3 with seismic release of  $1200 \times 10^{20}$  Nm (Tsai et al., 2005, Stein and Okal, 2007) as compared to estimate of  $M_w$  9.0 by GCMT and USGS. Here, our main focus is on the larger events of  $M_w \geq 8.2$  as tabulated in Table 2.3.1 and represented in Figure 2.3.1, that dominate the history of the moment release. Further, from Table 2.3.1 and Figures 2.3.2 - 2.3.4, clustering of the larger earthquakes and high moment release is noticed during 1950s to 1960s followed by extended period of low-moment release until 2003. Subsequently, heightened moment release since 2004 has been observed, which represents one seismic cycle. Fig. 2.3.1 shows the locations of large earthquakes of the world. Fig. 2.3.2 shows the decadal moment release, Fig. 2.3.3 the decadal number of large earthquakes while Fig. 2.3.4 shows the Cumulative moment release for all the earthquakes. Fig. 2.3.5 demonstrates that 52% of the 10yr moment release was during the decades of 1950s and 1960s and 34% during the decades of 2000s and 2010s (there are still several years left in the last decade).

The seismic moment release of  $M_w \geq 8.2$  earthquakes for the past 11 decades is dominated in Pacific as compared to anti-Pacific region. During the decade of 1950s some energy was released in Assam-China region in anti-Pacific hemisphere, but the 2000 decade is exception. In the decade of 2000s, 92% of energy is released in anti-Pacific hemisphere. Till 2000 around 95% of the global moment release occurred in the Pacific hemisphere bounded by longitudes  $115^\circ\text{E}$  and  $65^\circ\text{W}$ . From the decade of 2000 the seismic moment release has increased tremendously, and with the start of 2010 decade globally seismic moment release rate has tremendously increased just like 1960 decade. Moreover, just in last 3.5 years globally seismic moment release has crossed half of the value of 2000 decade. This increase in global-moment release rate in both the Pacific and anti-Pacific hemispheres may be related to the recent change in moment of inertia and shape of the earth (Cox and Chao, 2002). Dickey *et al.* (2002) attribute the observed increase to subpolar glacial melting and mass shifts in the oceans. The observed global-moment release pattern (large event clustering, with acceleration before and deceleration after the mainshock) suggests that Earth, over many decades, may also respond as a coherent, nonrandom, nonlinear system of stress redistribution.

Table 2.3.2 and Fig. 2.3.6 show the earthquake cycle of Alpide-Himalaya-Andaman belt. Seismicity was high during 1897 to 1916, low during 1917 to 1933, high again during 1934 to 1951 and low during

1952-2000. It may be possible that since 2001 large earthquakes include 2001 Bhuj Mw 7.7, Andaman-Sumatra 2004 Mw9.3 and Iran 2012 Mw 7.8 indicate enhanced seismicity in Alpide-Himalayan Belt for  $M \geq 7.7$  earthquakes. It matches with global cycle of enhanced seismicity for  $M \geq 8.2$  earthquakes. It has been observed that during the periods when there are no great earthquakes in Himalaya, the Peninsular India has more number of  $M \geq 6$  earthquakes (Fig. 2.3.7). Since 1960s Peninsular India has unusually experienced a large number of  $M \geq 6$  earthquakes. Since 1960s Peninsular India has unusually experienced a large number of  $M \geq 6$  earthquakes when there are no M8 earthquakes in Himalaya.

**Table 2.3.1: Extended Pacheco-Sykes 2001 catalog (Bufe and Perkins, 2005) of events  $M_w \geq 8.2$ , 1900–2001 and subsequently from 2001 onwards by following GCMT catalog.**

Event Nos.	Date	Origin Time	Lat	Long	Depth (km)	$M_0 \times 10^{20}$ (Nm)	$M_w$	Location
	YYYY-MM-DD	Hr:Mn						
1	1905-07-09	09:40	49.0	99.0	35	55.0	8.5	Mangolia
2	1905-07-23	02:46	49.0	97.0	35	50.0	8.4	Mangolia
3	1906-01-31	15:36	01.0	-81.3	33	80.0	8.6	Colombia-Ecuador
4	1906-08-17	00:40	-33.0	-72.0	33	66.0	8.5	Chile
5	1917-06-26	05:49	-15.5	-173.0	33	70.0	8.5	Tonga Islands
6	1918-08-15	12:18	05.7	123.5	33	25.0	8.2	Philippines
7	1918-09-07	17:16	45.5	151.5	33	22.0	8.2	Kurile Islands
8	1919-04-30	07:17	-19.0	-172.5	33	27.1	8.3	Tonga Islands
9	1920-12-16	12:05	36.6	105.4	33	30.0	8.3	Kansu, China
10	1922-11-11	04:32	-28.5	-70.0	33	140.0	8.7	Chile
11	1923-02-03	16:01	54.0	161.0	33	70.0	8.5	Kamchatka
12	1924-06-26	01:37	-55.0	158.4	33	30.2	8.3	Macquarie Ridge
13	1933-03-02	17:30	39.3	144.5	30	43.0	8.4	Japan
14	1938-02-01	19:04	-05.5	131.5	40	52.0	8.4	Banda Sea
15	1943-04-06	00:00	-31.0	-71.3	20	25.0	8.2	Chile
16	1950-08-15	14:09	28.7	96.6	30	95.0	8.6	Assam
17	1952-11-04	16:58	52.8	159.5	33	350.0	9.0	Kamchatka
18	1957-03-09	14:22	51.6	-175.4	33	100.0	8.6	Aleutian Islands
19	1958-11-06	22:58	44.4	148.5	32	44.0	8.4	Kuril Islands
20	1960-05-21	10:02	-37.2	-73.0	33	20.0	8.2	Chile
21	1960-05-22	19:11	-38.2	-73.5	32	2000	9.5*	Chile
22	1963-10-13	05:17	44.9	149.6	40	75.0	8.6	Kuril Islands
23	1964-03-28	03:36	61.1	-147.6	30	750.0	9.2	Alaska
24	1965-01-24	00:11	-02.4	126.0	23	24.0	8.2	Banda Sea
25	1965-02-04	05:01	51.3	178.6	35	140.0	8.7	Aleutian Islands
26	1966-10-17	21:41	-10.9	-78.8	21	20.0	8.2	Peru
27	1968-05-16	00:48	40.9	143.4	35	28.0	8.3	Tokachi-oki, Japan
28	1969-08-11	21:27	43.6	147.2	30	22.0	8.2	Kurile Islands
29	1977-08-19	06:08	-11.1	118.5	23	24.0	8.2	Indonesia
30	1979-12-12	07:59	01.6	-79.4	24	29.0	8.3	Colombia-Ecuador
31	1989-05-23	10:54	-52.3	160.6	50	24.0	8.2	Macquarie Ridge
32	1994-10-04	13:23	43.6	147.6	68	30.0	8.3	Kuril Islands
33	1996-02-17	06:00	-0.7	136.6	15	24.0	8.2	Irian, Indonesia
34	2001-06-23	20:34	-17.3	-72.7	30	47.0	8.4	Peru
35	2003-09-25	19:50	41.8	143.9	27	30.5	8.3	Hokkaido, Japan

Event Nos.	Date	Origin Time	Lat	Long	Depth (km)	$M_0 \times 10^{20}$ (Nm)	$M_w$	Location
	YYYY-MM-DD	Hr:Mn						
36	2004-12-26	05:08	03.3	96.0	30	1200	9.3#	Sumatra
37	2005-03-28	16:09	2.1	97.1	30	105.0	8.6	Sumatra
38	2006-11-15	11:14	46.6	153.3	10	35.1	8.3	Kuril Islands
39	2007-09-12	11:10	-04.4	101.4	34	67.1	8.5	Sumatra
40	2010-02-27	06:34	-36.1	-72.9	22	186.0	8.8	Chile
41	2011-03-11	05:46	38.3	142.4	29	531.0	9.1	Honshu, Japan
42	2012-04-11	08:39	02.2	92.8	40	89.6	8.6	Sumatra
43	2012-04-11	10:43	0.8	92.3	53.7	25.3	8.2	Sumatra
44	2013-05-24	05:45	54.54	153.94	607.4	41.1	8.3	Sea of Okhotsk

\* Event no. 21 (1960 Chile earthquake)  $M_w$  is consider by following Kanamori and Anderson, 1975, Bufe and Perkins, 2005.

# Event no. 36 (2004 Sumatra earthquake)  $M_w$  is consider by following Tsai et al. (2005), Stein and Okal (2005, 2007).

**Table 2.3.2: Earthquakes of  $M_w \geq 7.7$  in Alpide-Himalaya-Andaman-Sumatra belt during 1991-2013. (Source:USGS)**

Event Nos.	Date	Origin Time	Lat.	Long.	Depth (Km)	$M_w$	Location
	YYYY-MM-DD	Hr:Mn:Sc					
1	1992-12-12	05:29:26	-8.48	121.90	27.7	7.8	Indonesia
2	1994-06-02	18:17:34	-10.48	112.84	18.4	7.8	Java,Indonesia
3	1996-01-01	08:05:11	0.73	119.93	24	7.9	Minahassa Peninsula, Sulawesi
4	1996-06-17	11:22:19	-7.14	122.59	587.3	7.9	Flores Sea
5	1998-11-29	14:10:32	-2.07	124.89	33	7.7	Ceram Sea
6	1999-09-20	17:47:18	23.77	120.98	33	7.7	Taiwan
7	2000-06-04	16:28:26	-4.72	102.09	33	7.9	Sumatra,Indonesia
8	2000-06-18	14:44:13	-13.80	97.45	10	7.9	South Indian Ocean
9	2001-01-26	03:16:41	23.42	70.23	16	7.7	Kachchh,Gujarat, India
10	2001-11-14	09:26:10	35.95	90.54	10	7.8	Qinghai,China
11	2004-12-26	00:58:53	3.30	95.98	30	9.3	Sumatra,Indonesia
12	2005-03-28	16:09:37	2.09	97.11	30	8.6	Sumatra,Indonesia
13	2006-07-17	08:19:27	-9.28	107.42	20	7.7	Java,Indonesia
14	2007-09-12	23:49:04	-2.63	100.84	35	7.9	Kepulauan Mentawai Region,Indonesia
15	2007-09-12	11:10:27	-4.44	101.37	34	8.5	Sumatra,Indonesia
16	2008-05-12	06:28:02	31.00	103.32	19	7.9	Sichuan,China
17	2010-04-06	22:15:02	2.38	97.05	31	7.8	Sumatra,Indonesia
18	2010-10-25	14:42:22	-3.49	100.08	20.1	7.8	Kepulauan Mentawai Region,Indonesia
19	2012-04-11	10:43:11	0.80	92.46	25.1	8.2	Sumatra,Indonesia
20	2012-04-11	08:38:37	2.33	93.06	20	8.6	Sumatra,Indonesia
21	2013-04-16	10:44:21	28.11	62.05	82	7.7	Iran -Pakistan Border Region

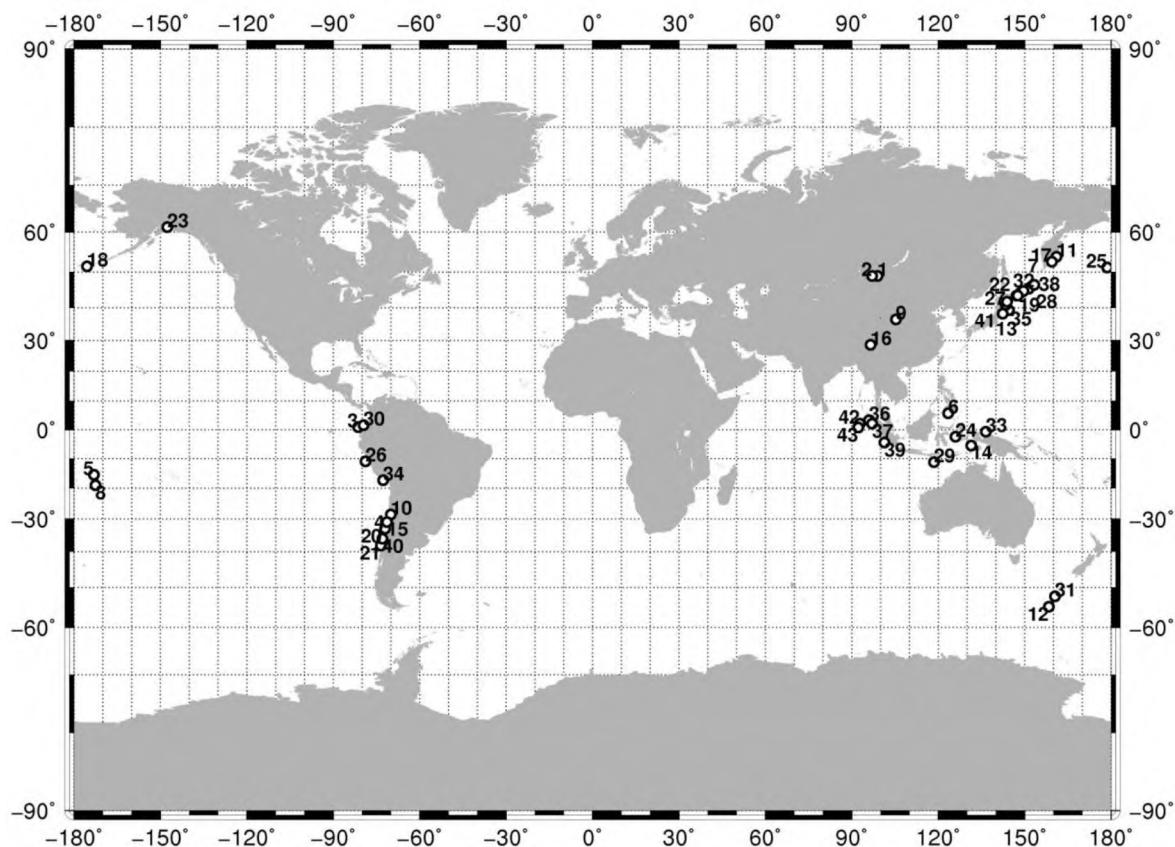


Fig. 2.3.1: Global distribution of  $M_w \geq 8.2$  earthquakes as a function of latitude and longitude by using catalog represented in Table 1.

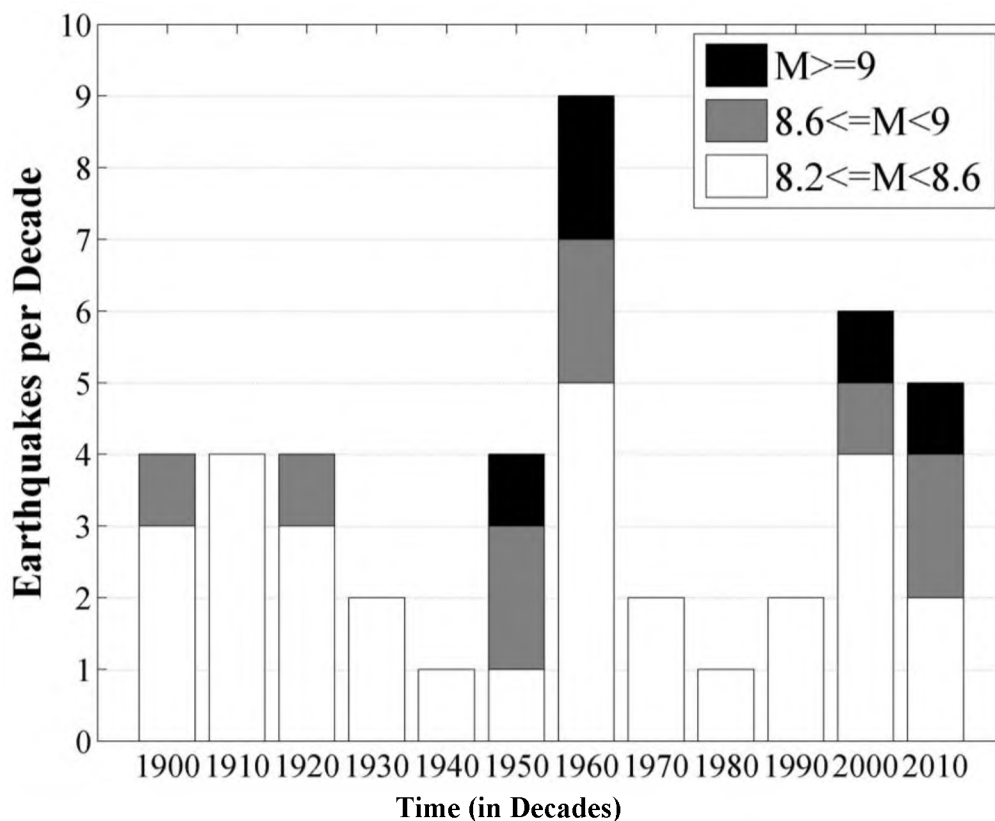


Fig. 2.3.2: Decadal histogram illustrating temporal clustering of global great earthquakes of  $M \geq 9.0$  (black),  $M \geq 8.6$  (black \_ gray), and  $M \geq 8.2$  (black\_gray \_ white). The bar for the 2010s is a lower bound, because only the first 3 yrs of the decade are represented.



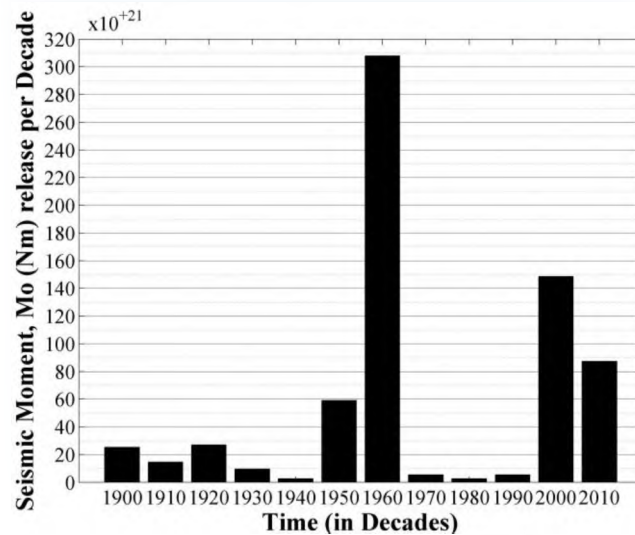


Fig. 2.3.3: Decadal histogram illustrating seismic moment, Mo (N-m) release of  $M_w \geq 8.2$  earthquakes by using catalog presented in Table 1.

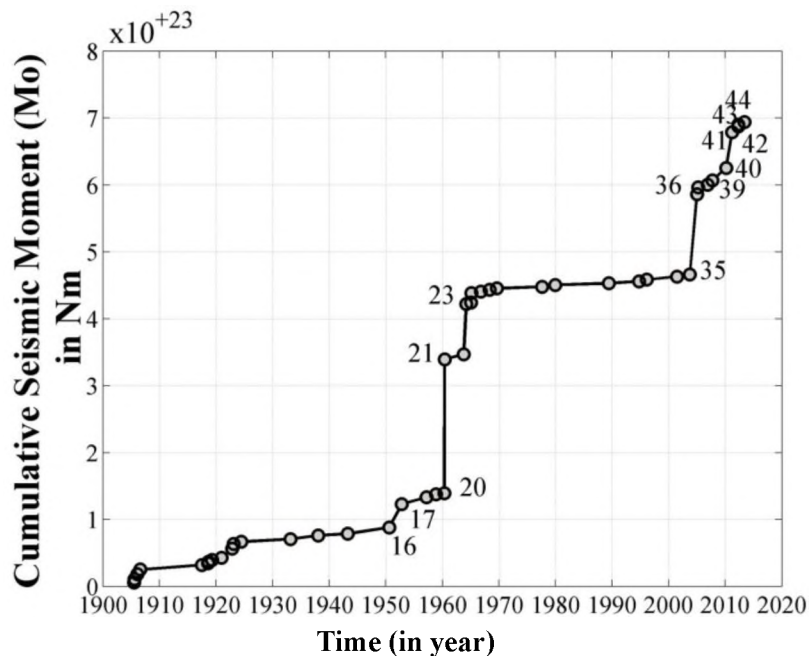


Fig. 2.3.4: Cumulative global seismic moment release, 1900–2013, for  $M_w \geq 8.2$  earthquakes by using catalog presented in Table 1.

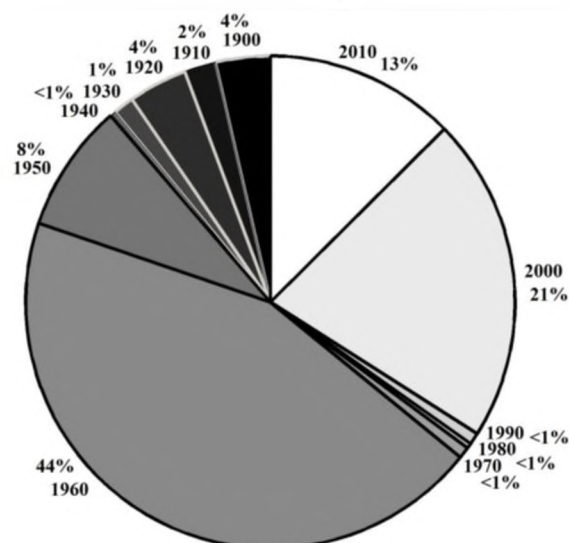


Fig. 2.3.5: Pictorial representation of the seismic moment release (in percentage of total moment release in 110yr) decade wise of earthquakes  $M_w \geq 8.2$ .

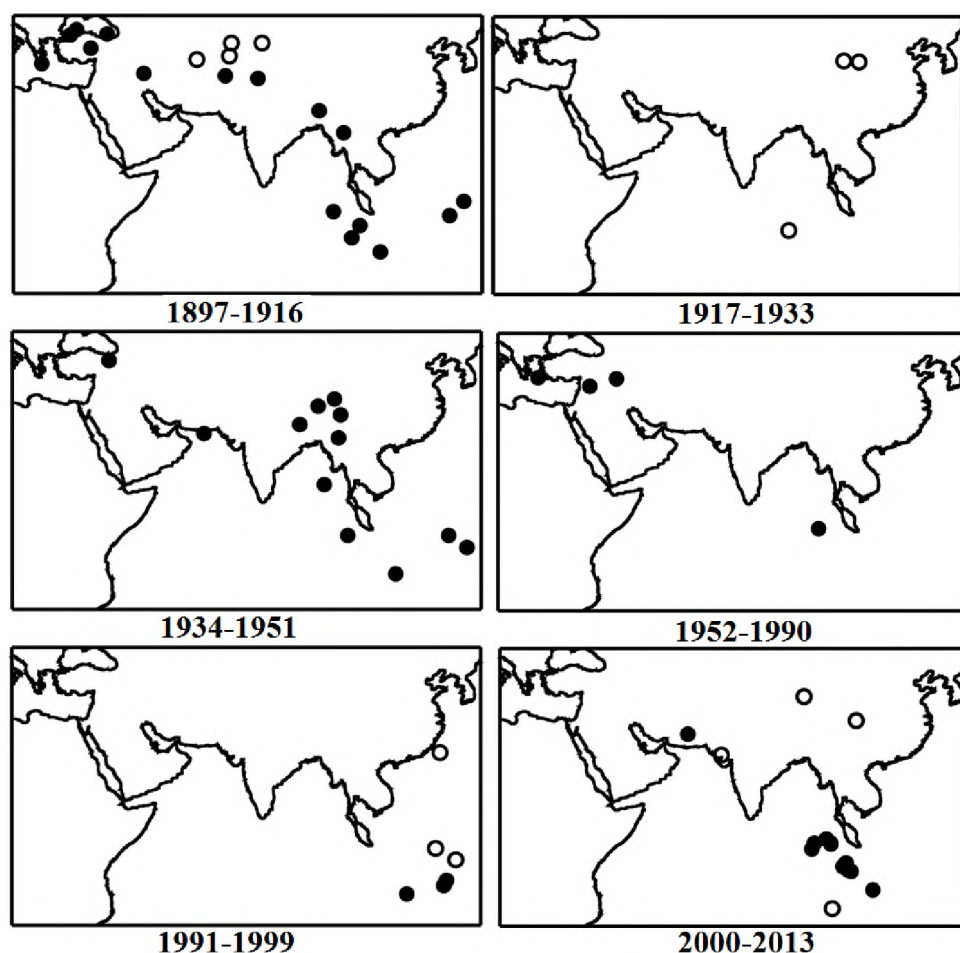


Figure 2.3.6: Seismicity cycles in Alpine-Himalaya-Andaman belt (up to 1981 after Hamada). Opn circles: epicenters away from the belt, earthquakes of  $M \geq 7.7$

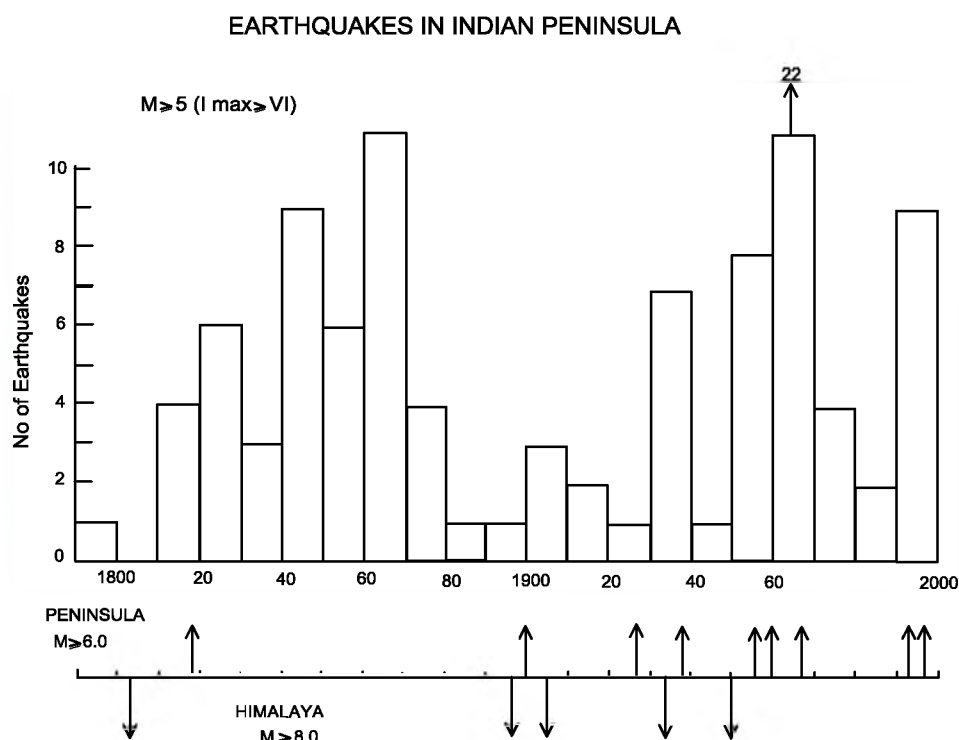


Fig. 2.3.7: During the shadow periods when  $M8$  earthquakes are absent in Himalaya (lowermost part), earthquakes are more in SCR India and vice-versa

## References:

1. Benioff, V. H., Global strain accumulation and release as revealed by great earthquakes. *Bull. Geol. Soc. Am.*, 1951, 62, 331–338.
2. Benioff, V. H., Evidence for world-strain readjustment following the Kamchatka earthquake of 4 November 1952. *Bull. Geol. Soc. Am.*, 1954, 65, 1332–1333.
3. Bufo, C. G., 1924–1994: evidence for a global moment release sequence, EOS Trans. *Am. Geoph. Un.*, 1997, 78, F476.
4. Bufo, C. G. and Perkins D. M., Evidence for a Global Seismic-Moment Release Sequence. *Bull. Seismol. Soc. Am.*, 2005, 95 (3), 833–843.
5. Cifuentes, I. and Silver, P., Low-frequency source characteristics of the Great 1960 Chilean earthquake. *J. Geophys. Res.*, 1989, 94, 643–663.
6. Cox, C., and Chao B. F., Detection of large-scale mass redistribution in the terrestrial system since 1998. *Science*, 2002, 297, 831–833.
7. Davies, G. and Brune, J., Regional and global fault slip rates from seismicity. *Nature Phys. Sci.*, 1971, 229, 101–107.
8. Dickey, J. O., Marcus, S. L., de Viron O., and Fukumori, I., Recent earth oblateness variations: unraveling climate and postglacial rebound effects. *Science*, 2002, 298, 1975–1977.
9. Gupta, Harsh K., *Indian J. Geol.*, 1987, 59, 1
10. Hamada, K. in Current research in Earthquake Prediction, Development in Earth and Planetary Sciences, Part 2, (Ed. T. Rikitake) Centre for Academic Publications, Japan, 1981, p.221.
11. Kagan, Y. Y. and Jackson, D. D., Long-term earthquake clustering. *Geophys. J. Int.*, 1991, 104, 117–133.
12. Kanamori, H. and Anderson D. L., Theoretical basis of some empirical relations in seismology. *Bull. Seismol. Soc. Am.*, 1975a, 65, 1073–1095.
13. Mogi, K., Active periods in the world's chief seismic belts. *Tectonophysics*, 1974, 22, 265–282.
14. Mogi, K., Global variation of seismic activity, *Tectonophysics*, 1979, 57, 43–50.
15. Pacheco, J. F. and Sykes, L. R., Seismic moment catalog of large shallow earthquakes, 1900 to 1989. *Bull. Seismol. Soc. Am.*, 1992, 82, 1306–1349.
16. Stein, S., and Okal E. A., Ultralong Period Seismic Study of the December 2004 Indian Ocean Earthquake and Implications for Regional Tectonics and the Subduction Process. *Bull. Seismol. Soc. Am.*, 2007, 97, January 2007, doi: 10.1785/0120050617.
17. Tsai, V. C., Nettles M., Ekström G., and Dziewonski A. M., Multiple CMT source analysis of the 2004 Sumatra earthquake. *Geophys. Res. Lett.*, 2005, 32, 17, L17304, doi: 10.1029/2005GL023813.

## 2.4 Crustal Heterogeneities beneath the 2011 Talala, Saurashtra Earthquake, Gujarat, India Source Zone and its Seismotectonic Implications

(A. P. Singh, P. Mahesh and O. P. Mishra of SAARC Disaster, New Delhi)

In the recent years, Talala area of Saurashtra, Gujarat has witnessed three damaging earthquakes of moderate magnitude, year 2007 (Mw 5.0; Mw 4.8) and in the year 2011 (Mw 5.1). A long series of aftershocks followed hereafter. The last damaging moderate earthquake of the 20th October 2011 in Talala region (21.090°N, 70.450°E), located at about 200 km south to the devastating 2001 Bhuj (23.412°N, 70.232°E) mainshock (Mw 7.6), jolted the entire Saurashtra region of Gujarat. Hypocenters of the aftershocks were relocated accurately using absolute and relative travel time (double-difference) method (Fig. 1). The fault plane solution of the mainshock of the 20th October 2011 Talala indicated left-lateral strike-slip rupture similar to that of the 2007 Talala earthquake (Rastogi et al., 2012). The b-value mapping has been done and the seismic velocities and Poisson's ratio structures of the upper crust beneath the 2011 Talala earthquake source zone are estimated. The 3D b-value distribution along with the later two estimates offer a reliable interpretation of crustal heterogeneities and their bearing on the genesis of moderate earthquakes and their aftershock sequences beneath the source zone. It is found that a high b-value region is sandwiched within the mainshock hypocenter at the depth of 6-9km and low b-value region above and below the 2011 Talala hypocenter. It is also found that the 2011 Talala

mainshock hypocenter depth (6km) is located near the boundary of the low and high velocity ( $V_p$ ,  $V_s$ ) and the source zone is associated with low- $\sigma$  anomalies flanked by the prominent high- $\sigma$  anomalies along the active fault zone having a strike-slip motion beneath the earthquake source zone (Fig. 2). The pattern of distribution of ( $V_p$ ,  $V_s$ ,  $\sigma$ ) and its association with occurrences of aftershocks provide seismological evidence of neo-tectonics in the region having a left lateral strike-slip motion of the fault (Fig. 2.4.1). Additionally, the overall b-value is estimated close to 1.05 which reveals that the seismogenesis is related to strong heterogeneities, that is supported by  $V_p$ ,  $V_s$  and  $\sigma$  structures (Fig. 2.4.2).

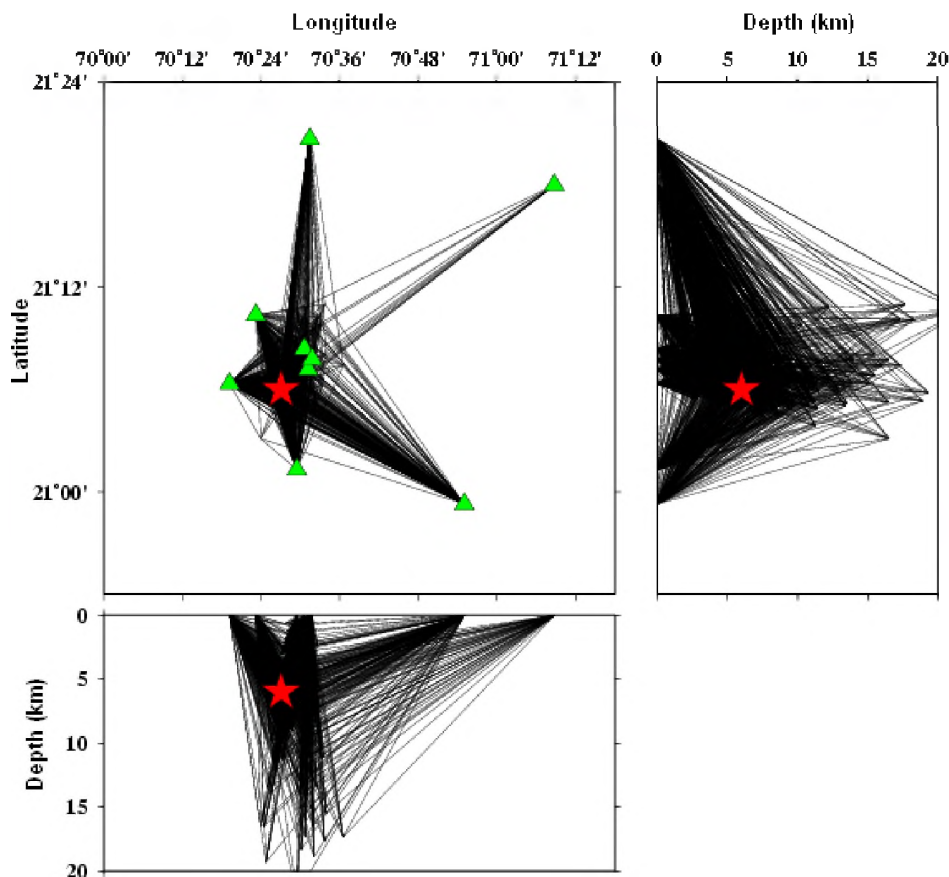


Fig. 2.4.1: The spatial distribution of seismic rays of 238 earthquakes in lateral and vertical directions. Every path between an epicenter and a station is drawn as a straight line. Green triangles show nine seismic stations that recorded the arrival times, while the red star denotes the 2011 Talala mainshock.

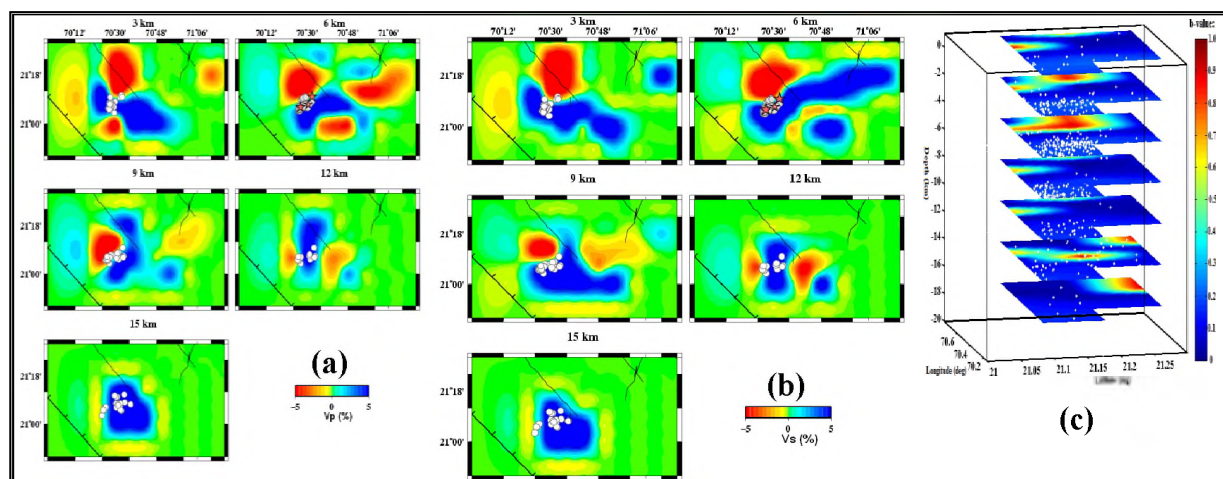


Fig. 2.4.2: (a) P-wave velocity (b) S-wave velocity perturbation from the average velocity model in (%) (c) b-values at different depth layers beneath the 2011 Talala epicentral region. The scale of the perturbation is shown in each of the figures. The figure also shows the identified faults and lineaments of the regions



## CHAPTER 3

## 3. LITHOSPHERIC STRUCTURE

## 3.1 ELECTROMAGNETIC, MAGNETO-TELLURIC AND RESISTIVITY IMAGING

3.1.1 The 3D Magnetotelluric Survey in Kachchh along with NGRI and Ukrain Geophysicists  
(Kapil Mohan, Sunita Raika and K. Veeraswamy as well as Md. Aziz of NGRI)

A 3D magnetotelluric survey was carried out in Kachchh for 2-months period during Nov.-Dec. 2011 to delineate the sub-surface nature of the South Wagad Fault, the hidden Samkhiali Fault that was detected by 2D MT survey and also the hidden North Wagad Fault which caused 2001 earthquake. This 3D survey at close grid for upper crustal structure is pioneering in the World. The work was done under a collaborative project between ISR, NGRI and Ukrain scientists under an MoES project. A total 37 long-period and short-period sites were occupied during 2011-2012 (Fig. 3.1). Instruments at different sites were deployed for 5 to 15 days each.

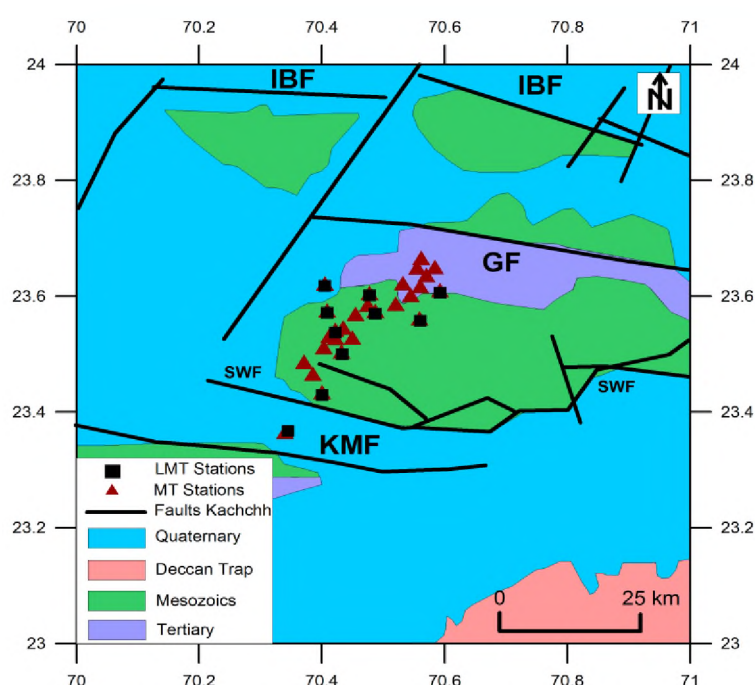


Fig. 3.1.1: Location map of the Magneto-Telluric stations

## 3.1.2 Identification of Kachchh Mainland Fault and South Wagad Fault from Magnetotellurics

The Kachchh region situated in the central-western part of the Indian subcontinent is a collage of uplifts (Wagad, Pachham, Khadir, Bela, Chorar and Nagar Parkar) and intervening basins bordered by E-W faults. The area is known for continuous seismicity, as several moderate to large magnitude intra-continental earthquakes (e.g. 1819 Kachchh and 2001 Bhuj of magnitude 7.8 and 7.7 respectively) have occurred. However, exact sub-surface location and orientation of these faults is not known. The Kachchh Mainland Fault is most active with known neotectonics and along western part of which Lakhpat 1845 M6.3 earthquake occurred. The South Wagad Fault is eastward step-over fault of KMF and which became active a few years after 2001 Bhuj earthquake. As described below signature of these two faults are observed in 2D Magnetotelluric (MT) profiles.

Two magnetotelluric profiles have been conducted east and west of the epicenter of 2001 Bhuj earthquake ( $23^{\circ}26.4'N$   $70^{\circ}18.6'$ , about 15km NW of Bhachau) with station spacing of 1-2 km (Fig.

3.1.2a). The western profile is 15 km long with Dudhai at its southern end. The eastern profile extends northeastward from Sikra and is 22km long. The two profiles are 20km apart. MT data has been acquired covering wide frequency range ( $10^{-4}$  to  $10^{-4}$  Hz) by using Broadband and Long period MT data acquisition units. Due to limitation of observation period and presence of wet soils the reliable information is obtained till to about 12 km depth in this area. The modeling results indicate considerable variation in thickness of the top conducting (<5 Ohm-m) sedimentary layer with maximum of ~3 km, followed by resistive (10-50 Ohm-m) and then high resistive (>1000 Ohm-m) basement.

From 1D analysis of the eastern profile of 19 MT stations, the sedimentary thickness is found to be varying from 1.5 km to 2.3 km, whereas along the western profile of 8 MT stations, the sedimentary thickness is found to be varying from 400m to 1.7km. The 2D inversion analysis of MT data of the eastern profile shows a resistive block in the north end corresponding to Wagad uplift. The resistive block of the Kachchh Mainland is not seen as it is further south of the profile. The KMF is seen shallow dipping towards south to about 4km depth in the western profile and to about 12km depth in the eastern profile. It is seen meeting the surface at about 2-3 km north of the uplifted area of the Kachchh Mainland. SWF is seen steeply dipping north in both the profiles. Its location corresponds to the geologically mapped location. The SWF seems to be confined to upper crust only as in the Eastern Profile the SWF is traced to 16km depth and to only 8km in the western profile.

Fig. 3.1.2 .a: Geology and Tectonic setting of the area (after Biswas, 2005). Locations of MT profiles: east and west of the epicenter of 2001 Bhuj earthquake ( $23^{\circ}26.4'N$   $70^{\circ}18.6'$  about 15km NW of Bhachau) are shown with solid green circles.

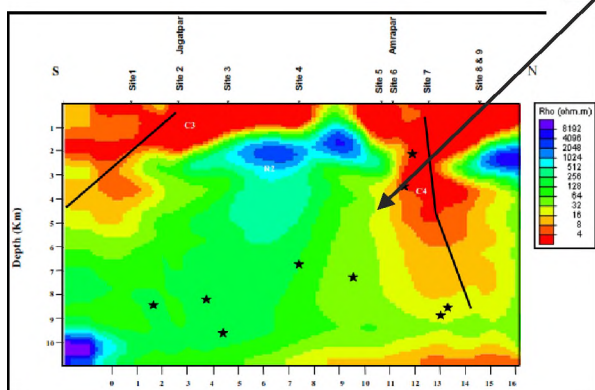
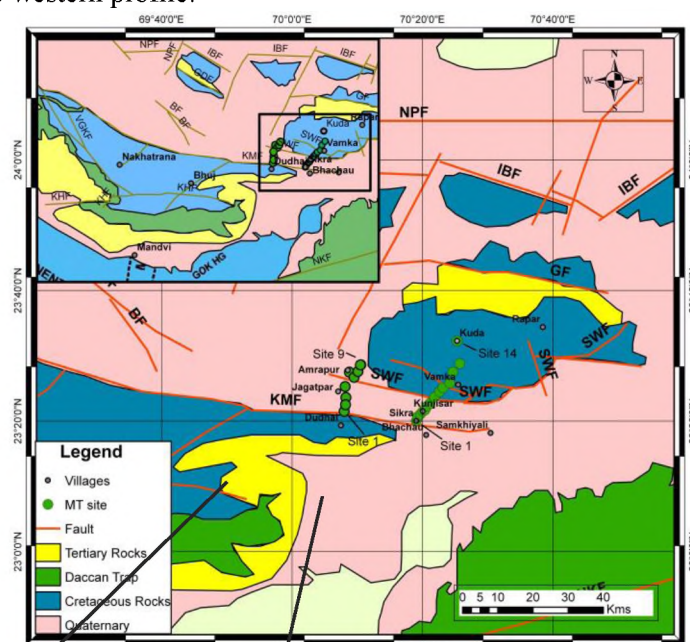


Fig. 3.1.2c: 2D Western Geoelectric depth section to 14km depth. The seismicity ( $M \geq 4$  from 2006 to 2012) is plotted, C3: KMF, C4: SWF

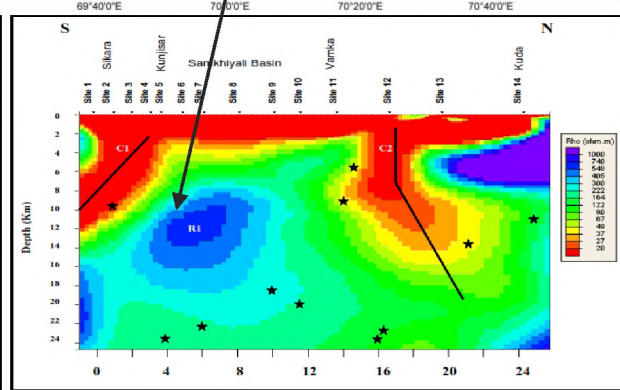


Fig. 3.1.2(b) 2D Geoelectric depth section (Eastern profile) down to 24km. The resistive block beneath site 1 (south end of the profile) is the Kachchh Mainland Block and resistive block beneath site 14 is the Wagad Block.  $M \geq 4$  hypocenters from 2006 to 2012 are plotted, C1: KMF and C2: SWF

### **3.1.3 Time Domain Electromagnetic Survey Shallow subsurface electrical resistivity mapping in central part of the Cambay basin, Ahmadabad using Transient Electromagnetic (TEM) method**

*(G. Pavan Kumar<sup>1</sup>, Peush Choudary<sup>1</sup>, A. Manglik<sup>2</sup>, Kapil Mohan<sup>1</sup>, A. Navaneeth<sup>1</sup>, A.P. Singh<sup>1</sup> and B.K. Rastogi<sup>1</sup>) <sup>1</sup>Institute of Seismological Research (ISR), Gandhinagar -382009; <sup>2</sup> CSIR-National Geophysical Research Institute, Hyderabad- 500606*

Shallow or near surface exploration techniques are being widely used to delineate mineral deposits, aquifers and also for mapping of stratigraphic sequence/lithology of an area. The Transient Electromagnetic (TEM) method is one of the near-surface exploration techniques through which we can get electrical resistivity of the subsurface up to 700-800m depth. TEM has been successfully applied to delineate stratified structures of geological interest, as well as, in the prospecting of groundwater, geothermal bodies, sulfide ores, deep graphite conductors, etc. In addition to the above objectives, the TEM data can also be useful for the treatment of “static shift” effects in magnetotelluric (MT) soundings. The obtained results from TEM survey can be integrated with other shallow geophysical and/or geotechnical data for characterizing the site response in microzonation studies.

TEM investigations have been carried out in and around the Ahmadabad region with the objective to map the stratigraphic sequence. This region is located in the central part of the Cambay basin comprising both Tertiary and Quaternary sediments. Ten fixed in-loop TEM soundings were made with 100m-sided transmitter loop to map the conductive and/or resistive zones in the subsurface, as the in-loop TEM method is well suited for a layered environment. Secondary magnetic fields produced by subsurface geological heterogeneities that result in a decline in voltage have been measured at every TEM sounding site. For each loop, the transmitter operated for a sequence of data repetition frequencies ranging from 32 Hz to 1 Hz. Using robust processing mode, data are accepted or rejected according to the coherency and outlier limit tests. The TEM data from some of the sites exhibit polarity reversals at early times (<1 msec). These cause spurious resistivities because of the apparent instantaneous change in the voltage gradient. Polarity reversals can be attributed to polarisation effects from local conductivity anomalies, such as 2D structure or shallow inhomogeneity near the receiver coil.

One dimensional (1D) modeling of all soundings was undertaken using an iterating best-fit algorithm to minimise the RMS residuals between the observed and calculated resistivities. Inverted resistivity section for all the TEM sounding data suggests in-general a three-layered structure (Fig. 1). The upper most layer is of 15-20 Ohm.m and 60 m average thickness. The intermediate layer has thickness of about 50 m and resistivity of ~10 Ohm.m. The lower most layer of resistivity less than 10 Ohm.m has average thickness of 70m. In addition, a vertical block of 20-30 ohm.m resistivity with 50-60m thickness at southern end of the profile is also obtained. An array microtremor survey carried out in the same area also suggested a three layered stratigraphic sequence. These layers are inferred to be of Holocene (0-60m), Pleistocene (60-90m) and Tertiary (100-200m) age from the estimated S-wave velocity structure. The obtained information from the TEM field survey may be further correlated with the data obtained from geo-technical observations like borehole data and detailed stratigraphic sequence of the region could be obtained in the form of resistivity distribution.

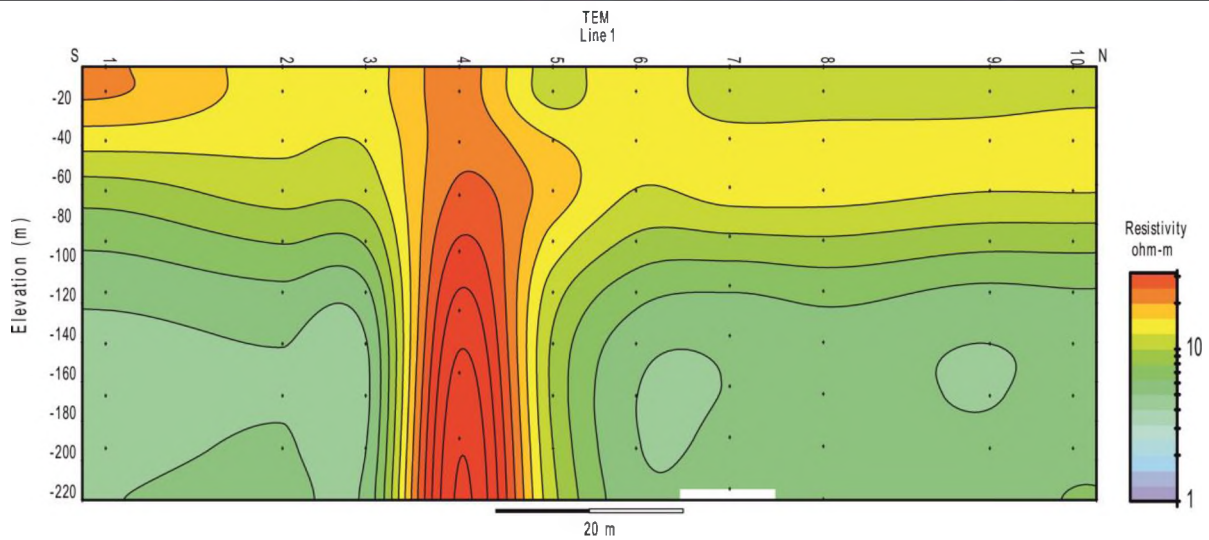


Fig. 3.1.3: One dimensional resistivity section obtained from the TEM field measurements at Doordarshan Bhavan grounds, Ahmadabad

Results from microtremor survey: Major Stratigraphic layers observed in microtremor survey, particularly at 40m, 80m and 140m depths are matched well with the electrical resistive layered pattern that has been observed in TEM measurements.

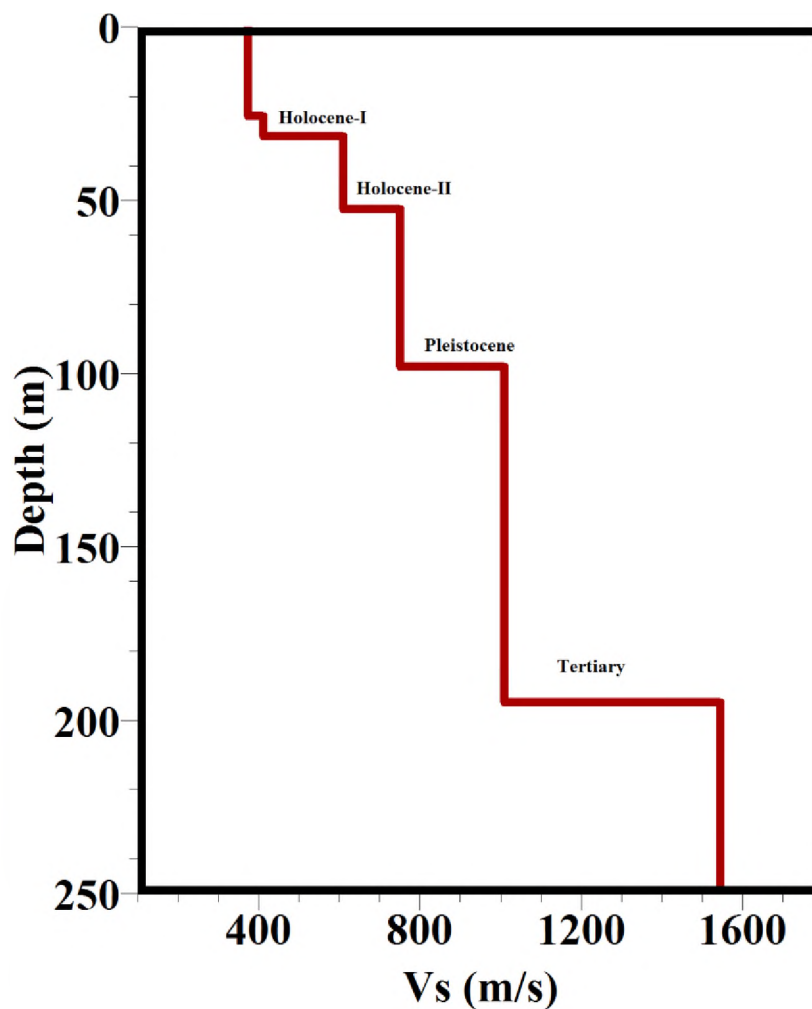


Fig. 3.1.4: Shear wave velocity ( $V_s$ ) profile as a function of depth derived from inverting Rayleigh wave phase velocity for the array size 100m at Doordarshan Bhavan



## 3.2 GRAVITY STUDIES

*(R.K. Singh, B.K. Rastogi, Rakesh Dumka, G Prasad, Sunita Sahoo, Meenakshi Rawat)*

### 3.2.1 Gravity Surveys in Kachchh

During 2012 Gravity observations were taken at about 400 locations in Kachchh (Bhuj-Nakhtarana-Nalia area and Loria-Khavda road) and western side of Cambay (near Dholera) and eastern side from Gandhinagar to Mehsana and Kalol. So far observations have been made at about 1500 locations. Usually observations are made at 1km interval but for detection of faults interval is kept 50 or 100m.

#### Gravity Studies in Kutch

**Delineation of Faults and Basement Structure in Kachchh Using High Resolution Gravity Survey:**

The regional gravity surveys were conducted at an interval of 1 km and gravity stations were fixed over permanent land marks available in the area. The locations of gravity survey points are shown in Fig. 3.1. The Bouguer Anomaly contour map was prepared at 1mgal interval for Kachchh rift basin (Fig. 3.2) and used to decipher the nature of known faults and some hidden faults. The leveling work of gravity stations were done by RTK (GPS) with excellent accuracy.

It is popularly believed that KMF is terminating very close to Bhachau and SWF is a displacement branch of KMF. The signature of bouguer gravity anomaly map (drawn at an interval of 1 mgal) shows that KMF is ending at Bhachau but it is meeting a NNE-SSW trending Ekal-Amrapar fault which extends possibly up to IBF and is responsible for separating two big islands of Bela and Khadir. The nearly E-W trending faults SWF and North Wagad fault (NWF) are abutting against the Ekal-Amrapar fault. The said transverse fault acts as a border line between Banni plane (gravity high) and Wagad upliftment (gravity low).

Another equally important feature is an intrusive body known as Fatehgadh high (27 mgals high) which is supported by Gedi fault in the north and NWF in the south. After visualizing the crowding nature of gravity contours, it can be said that the Gedi fault is associated with wide fracture zone. Kachchh and Wagad upliftments which are shown in Bouguer gravity map as “gravity low” may be occupied by thick sediments over the subsided basement. The Banni and Samkhiali areas are shown as gravity highs due to lesser thickness of sediments. The Bhuj fault which is seen as en-echelon fault on the ground surface has no gravity signature in Bouguer gravity map. So by gravity data, it is clear that Bhuj fault is of very shallow nature.



**Fig. 3.2.1: Gravity lines covered by ISR at intervals of 1km or less. Gravity Stations have been located over permanent landmarks available in Survey of India, degree sheet No 41 I & 41 E**



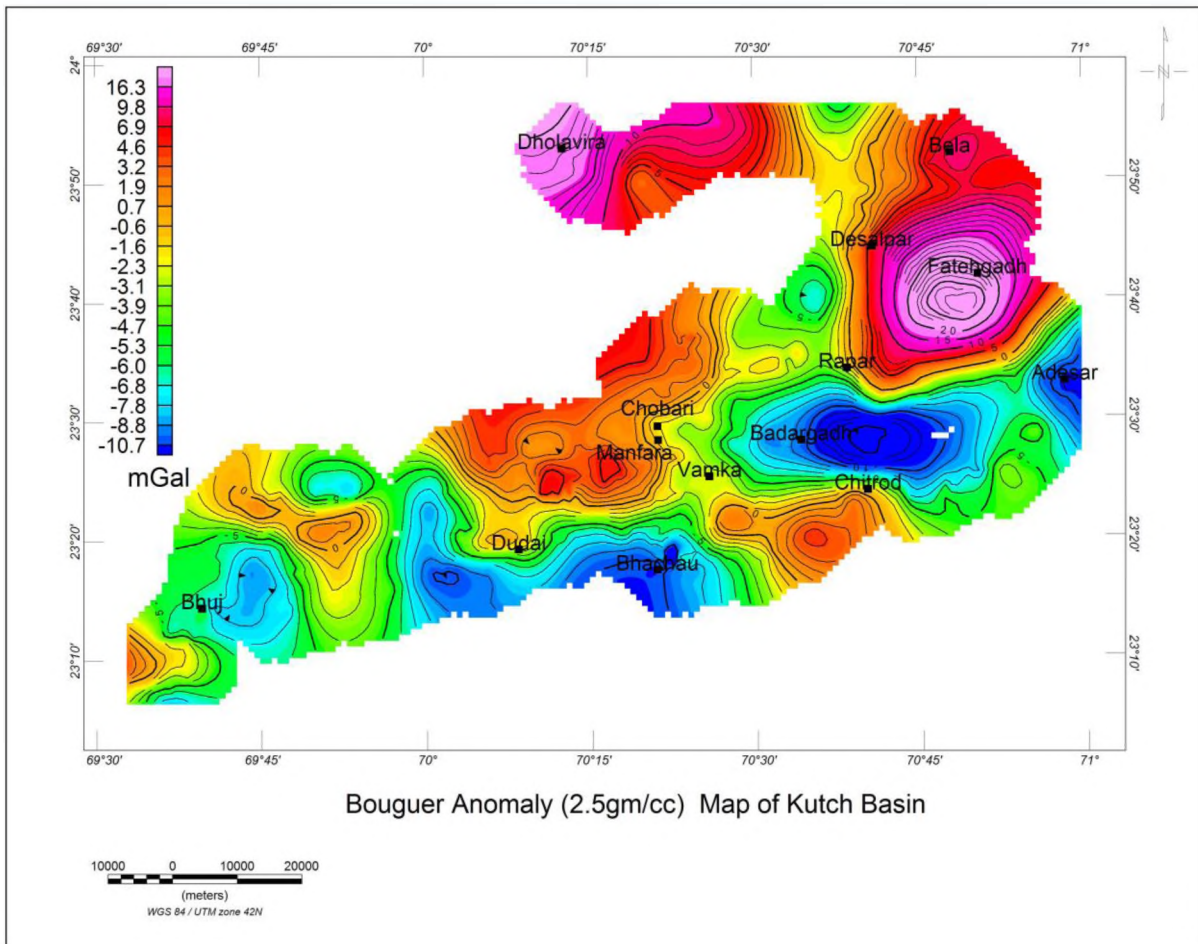


Fig. 3.2.2: Bouguer Gravity Contour Map of part of Kutch. Gravity Stations have been located over permanent landmarks available in Survey of India, degree sheet No 41 I & 41 E at 1km or less interval.

The Kachchh basin is dipping towards SE and basement is rising towards NW stepwise.

**The Bouguer Gravity Contour Map reflects the following features:**

- ⇒ Basement of the Kachchh basin is dipping towards SE stepwise.
- ⇒ An E-W trending Zero Contour from Dudhai to Bhachau is representative of KMF.
- ⇒ This Zero Contour meets a NW-SE trend from Vamka to Chobari, which may be the Manfara fault and has clustering of earthquakes.
- ⇒ Beyond Chobari the NNE trend of the Zero Contour matches with the Ekal- Amarapar Fault.
- ⇒ The South Wagad Fault is reflected from Chitrod to Vamka.
- ⇒ The North Wagad fault is reflected west of Rapar and south of Fatehghadh High. In the Banni plains it is not reflected may be due to its depth being deeper than 8km.
- ⇒ Wagad and Kachchh Mainland upliftments, reflected by gravity lows, may be due to thick sediments, and not with any kind of Basement upliftment.
- ⇒ The en-echelon Bhuj Fault exposed on the surface does not show any gravity anomaly. Hence, it is interpreted to be of very shallow nature, and as such may not become the source of a major earthquake.
- ⇒ The northern periphery of Fatehghadh high ( $27 \text{ mm/s}^2$ ) is associated with crowding of gravity contours and reflects presence of Gedi Fault.
- ⇒ The Vigodi fault in Kachchh Mainland (Fig. 3) indicates subsidence of the basement towards southwest.

## Gravity Observations in Kachchh Mainland

Profiles in Kachchh Mainland (Fig. 3.3) which cross the Vigodi fault indicate sudden change. The basement appears to have subsided on southwestern side (Fig. 3.4).

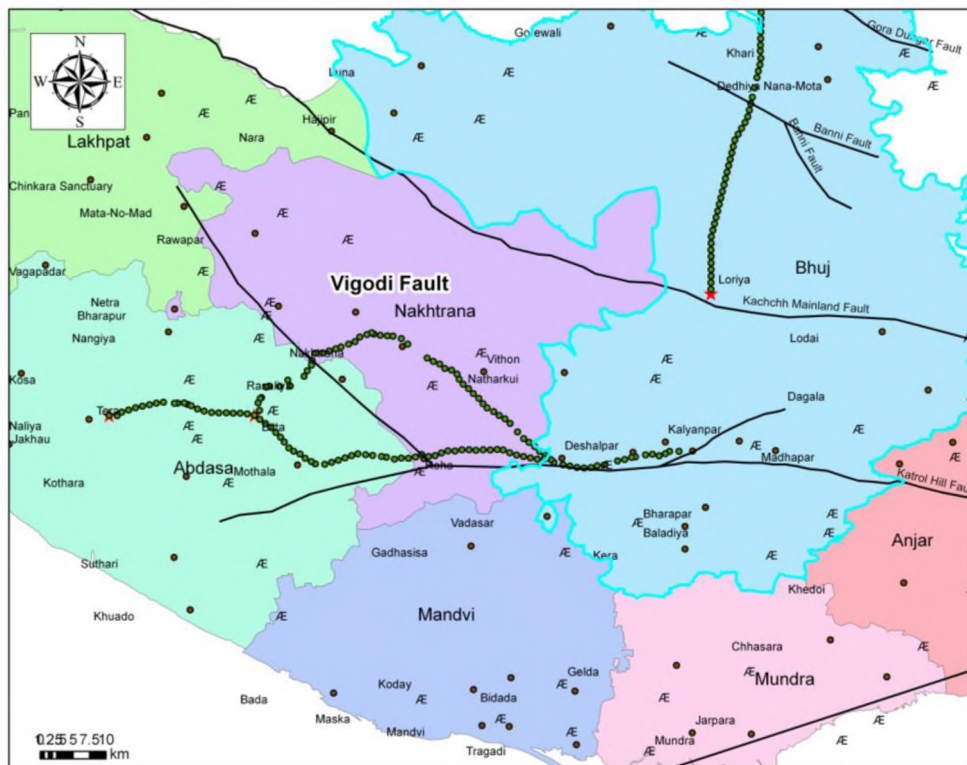


Fig. 3.2.3: Gravity lines covered by ISR in Kachchh during 2012 and faults on taluka map

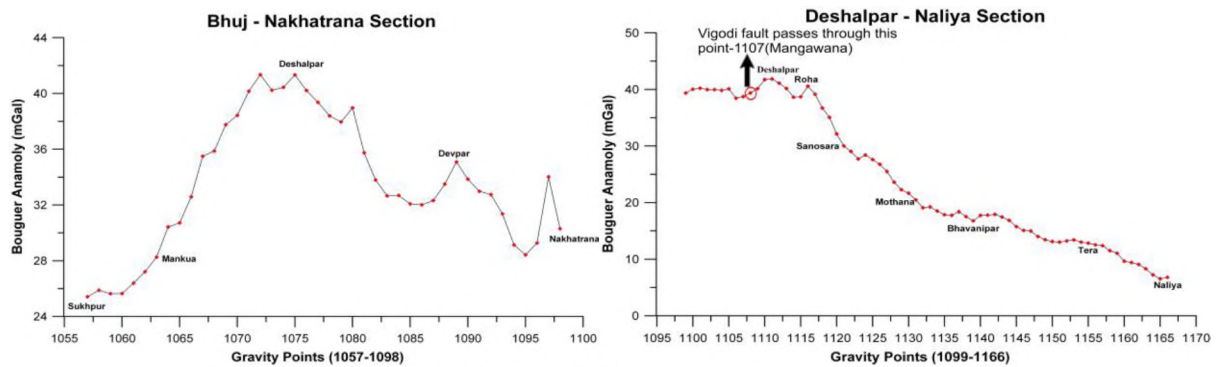


Fig. 3.2.4: Gravity profile across Vigodi fault indicate down throw towards southwest

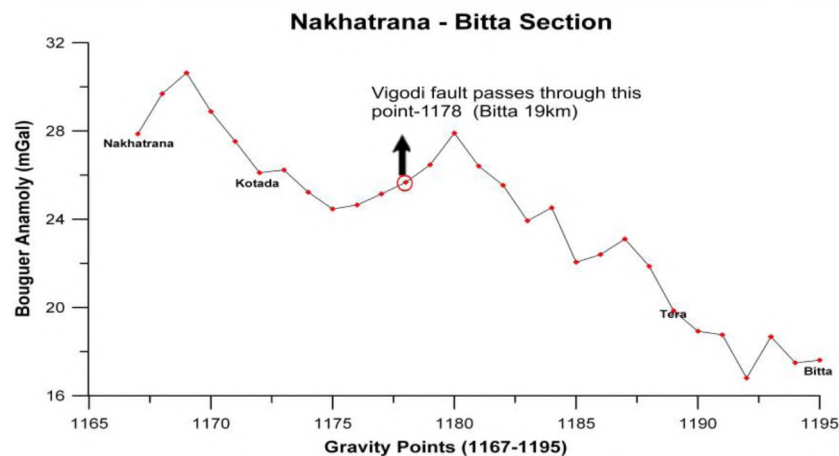


Fig. 3.2.5: Gravity profile in Kachchh Mainland

## Gravity Observations in Banni Area (Loriya to Khavda)

Profile Loriya to Khavda does not show any major fault

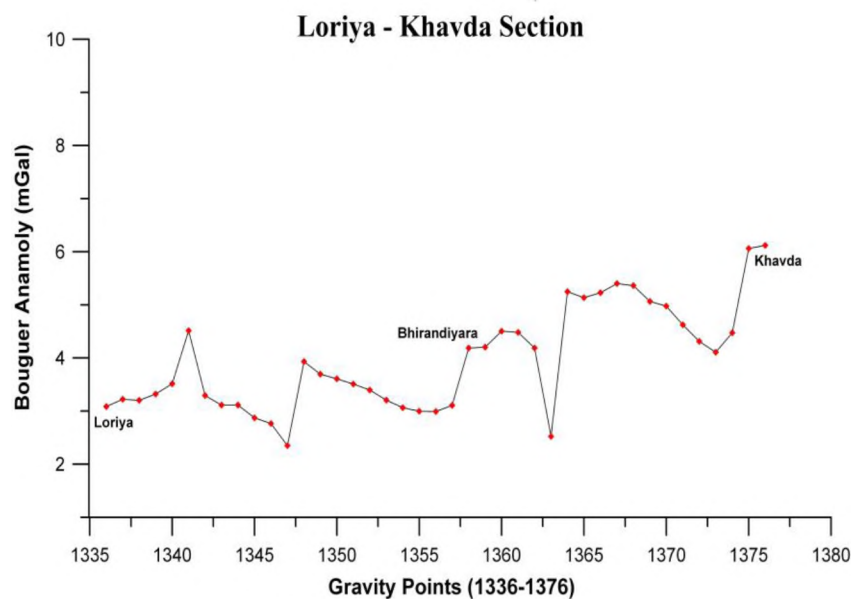


Fig. 3.2.6: Profile Loriya to Khavda

## 3.2.2 Gravity Observations in Cambay Area

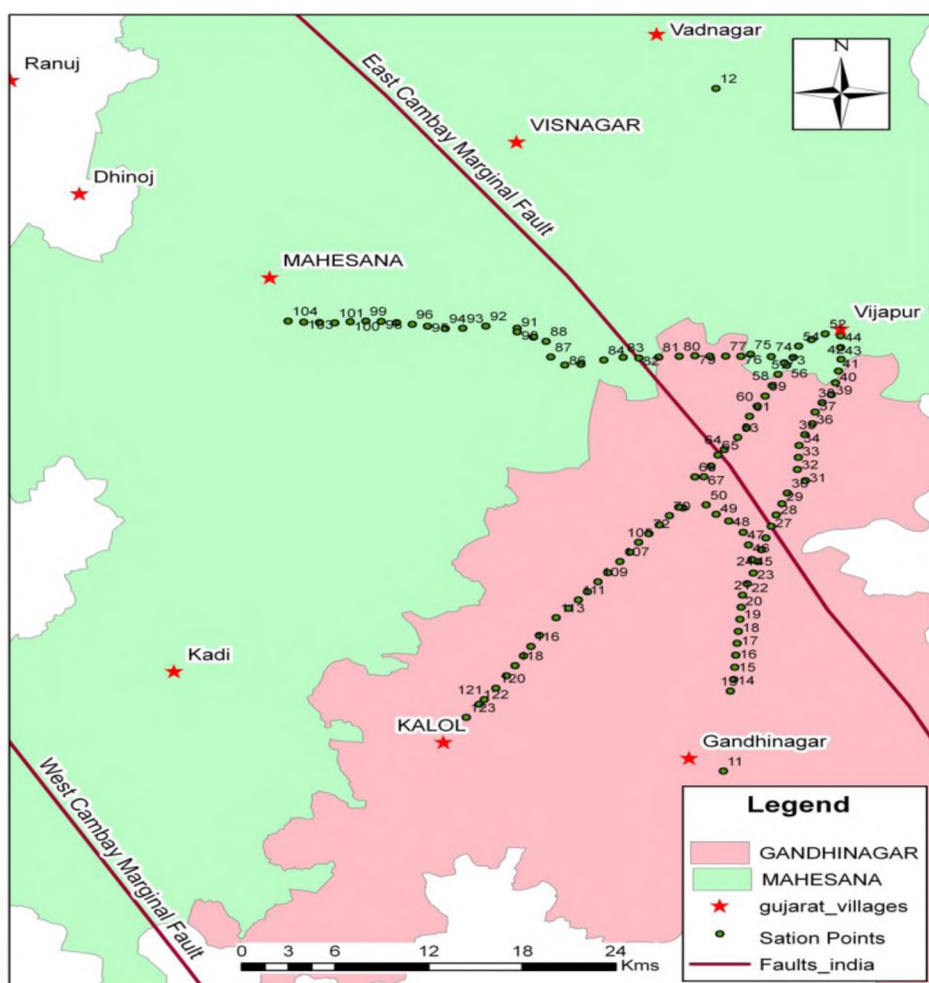


Fig. 3.2.7: Gravity observation points in Cambay basin on Gandhinagar & Mehsana Dit. map



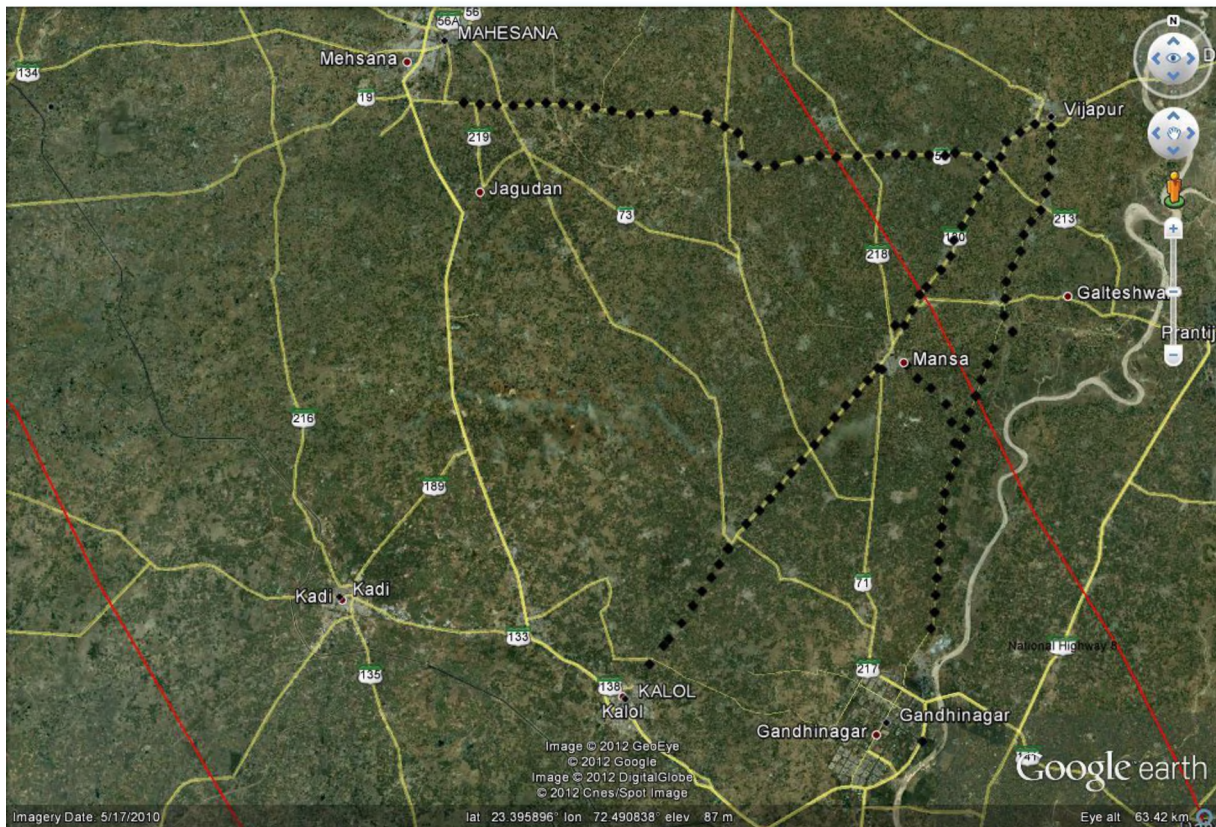


Fig.3.2.8: Gravity observation points shown on Google map in Cambay basin.

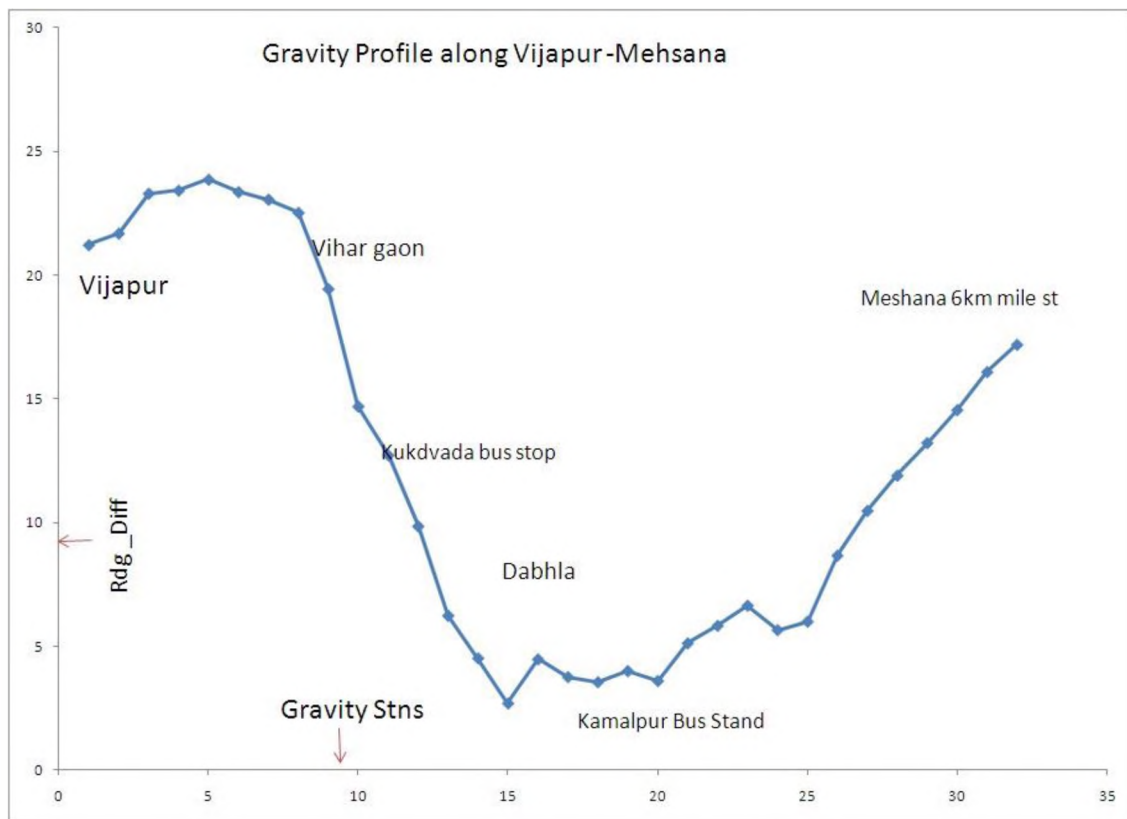


Fig. 3.2.9: Gravity profile east to west indicates presence of the East Cambay Fault. Central high is also indicated near Mehsana may be due to pillow lavas at depth formed at rift-shoulders during rifting.

# CHAPTER 4

## 4. LONG-TERM EARTHQUAKE PROGNOSIS FROM CRUSTAL DEFORMATION STUDIES BY GPS AND INSAR MEASUREMENTS

### 4.1 CRUSTAL DEFORMATION STUDIES BY GPS MEASUREMENTS

(Rakesh Dumka)

To understand the tectonic process from deformational pattern of different faults/thrust systems in the Gujarat region a long term GPS study is being carried out by ISR with 22 permanent GPS stations across different faults (Fig. 4.1.1).

For processing of the GPS data at first, the raw data were converted into the RINEX (Receiver Independent Exchange) format using the program TEQC (translation, editing and quality control) which is distributed on the Internet by UNAVCO (University NAVSTAR Consortium). This program is used for general data preprocessing and it offers a command line DOS or UNIX system interface. This program provides a summary that contains L1/L2 tracking status for each SV, session's start and end time, data logging interval, list of satellite observed and missing observations, clock drift rate/gaps, number of cycle slip and session length. This information is useful to decide or select the file for post – processing. The data were post-processed using GAMIT-GLOBK software, developed by MIT, USA (King and Bock, 2010) to create constrained solution (H-) files of parameter estimates and covariances. In GAMIT, Zenith tropospheric delay for each station was estimated by incorporating a linear model with stochastic constraints for the signal delay due to troposphere. The basic input for GAMIT are the observation files of permanent/IGS stations in the RINEX format, orbit file or g-files (sp3 /g-files) and the Global Navigation files (brdc). The orbit and IGS-RINEX files are available at Scripps Orbit and Permanent Array Centre (SOPAC) and brdc files are available at Continuously Operating Reference Stations. The IGS Stations used for present study are IISC (Bangalore, India), HYDE (Hyderabad-India), KIT3 (Kitab-Uzbekistan), LHAZ (Lhasa-China), DGAR (Diego Garcia Island- U.K.), TEHN (Tehran-Iran), KUNM (Kunming-China), URUM (Urumqi-China), POL2 (Bishkek - Kyrgyzstan), COCO (Cocos Island - Australia), DARW (Darwin- Australia), KARR (Karratha-Australia), SELE (Almaty-Kazakhstan), and MALI (Malindi-Kenya).

The velocities of all the twenty two stations were estimated in the ITRF08 reference frame after stabilizing IGS sites. The time series of each station were generated for all the years to provide the precision of measurements (Fig. 4.1.2) and after combination of daily solutions, the ITRF08 velocities of each site along with IGS sites were calculated. The ITRF08 velocities of 20 stations shows about  $46-50 \pm 0.19$  mm/yr with azimuth between  $33^{\circ} - 43^{\circ}$  (Table 4.1.1). The average ITRF08 velocity of Kachchh region is estimated  $48 \pm 0.18$  mm/yr,  $49 \pm 0.23$  mm/yr for mainland as well as for Saurashtra region. However the sites which are located in south Gujarat region show  $50 \pm 0.32$  mm/yr of motion, which may be the effect of Narmada rift zone. Internal deformation within Indian plate is very less and GPS site at Gandhinagar shows almost negligible amount of plate deformation.

Three campaign mode surveys for 11 temporary stations of Kachchh have been carried out in the months of October 2010, August 2012 and January 2013.



To estimate the local deformation pattern of the Kachchh region site ISRR was used as a local reference site, as this site is situated on seismically stable part as compared to the other parts of the Gujarat region and calculated residual velocities of all the campaign sites, which, indicate that at present horizontal deformation in this region is very less (2-3mm/y).

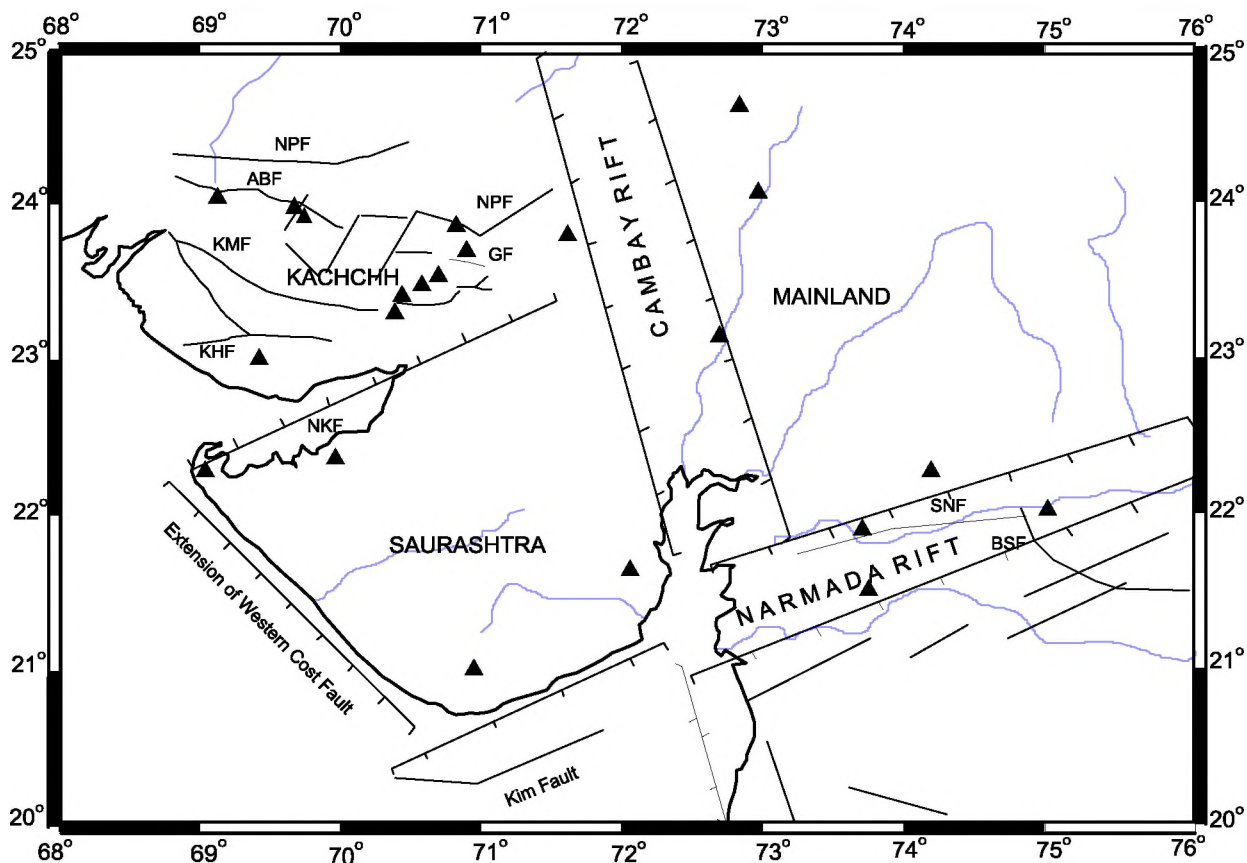
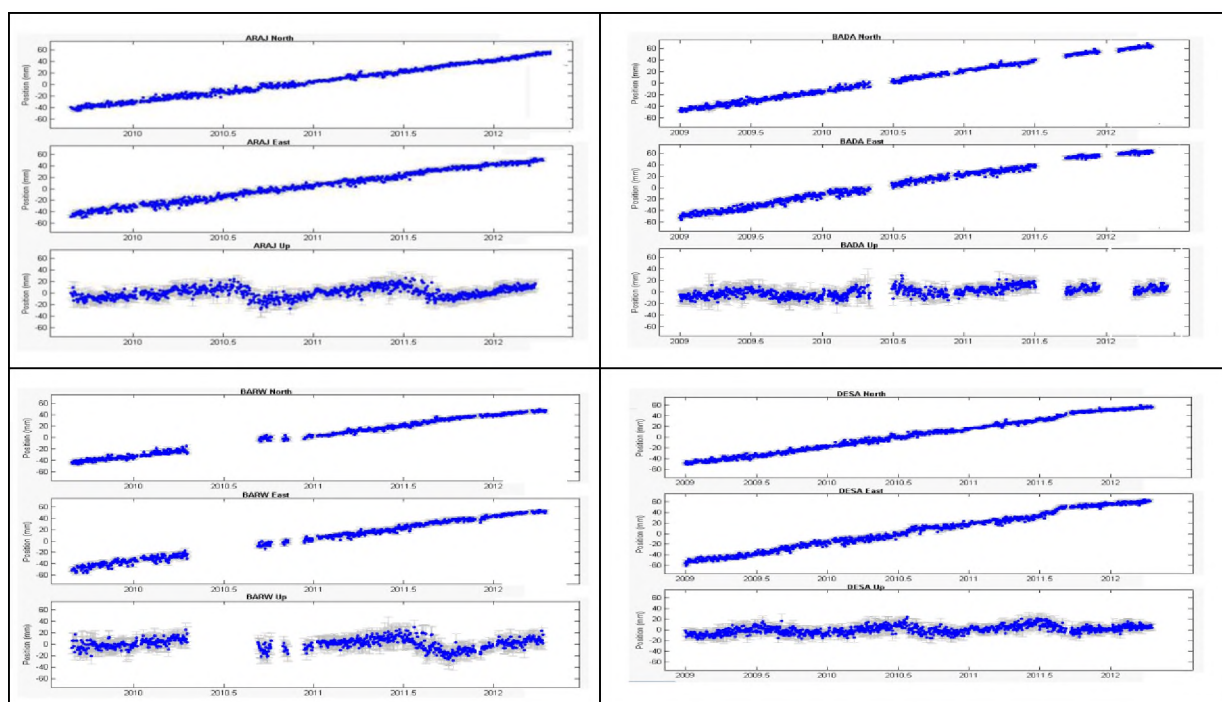
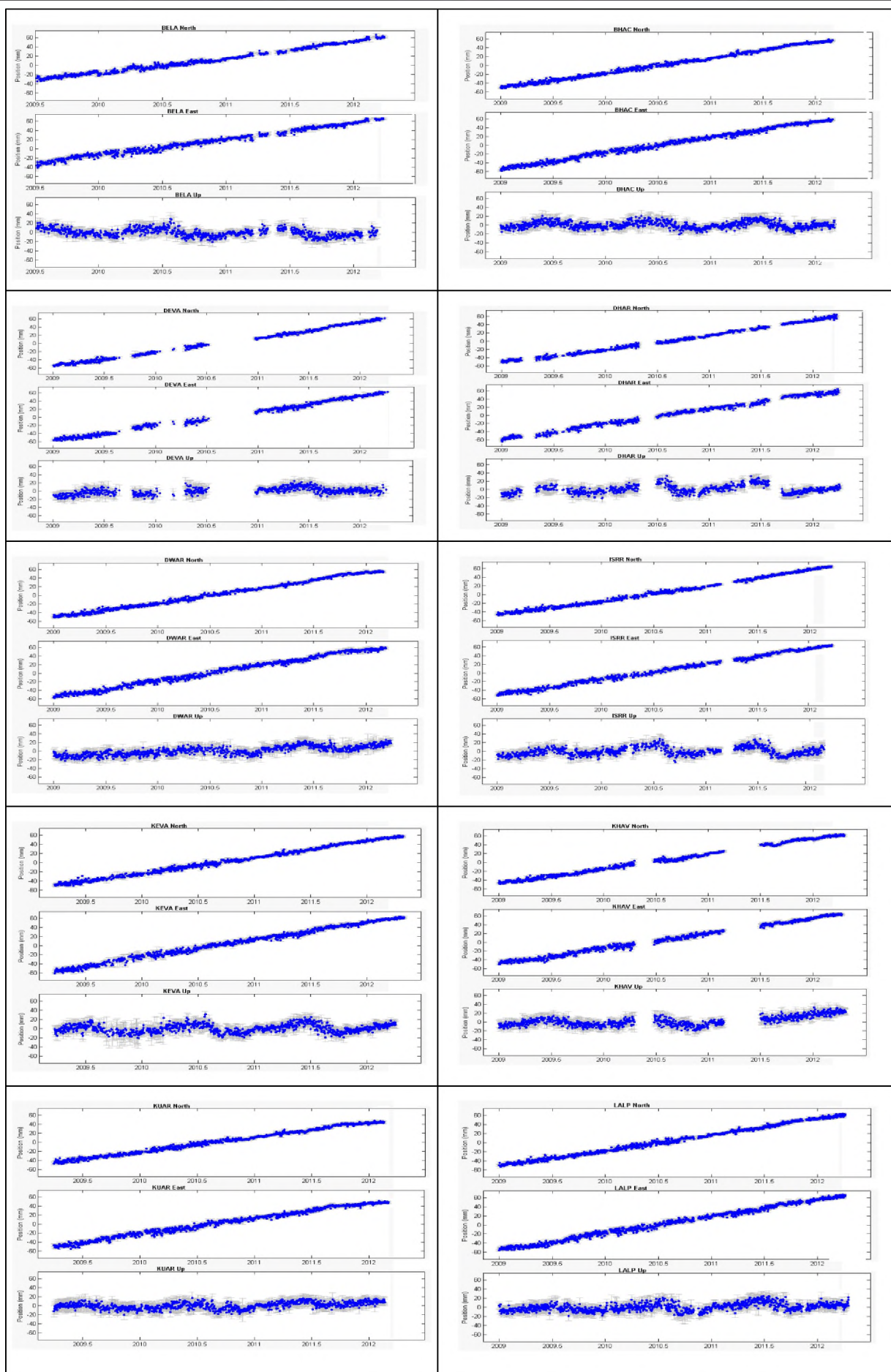


Fig. 4.1.1: Continuous Global Positioning System (CGPS) network of Gujarat, established by ISRR. Four stations in the NE corner around Cambay are connected to the National GPS monitoring program.







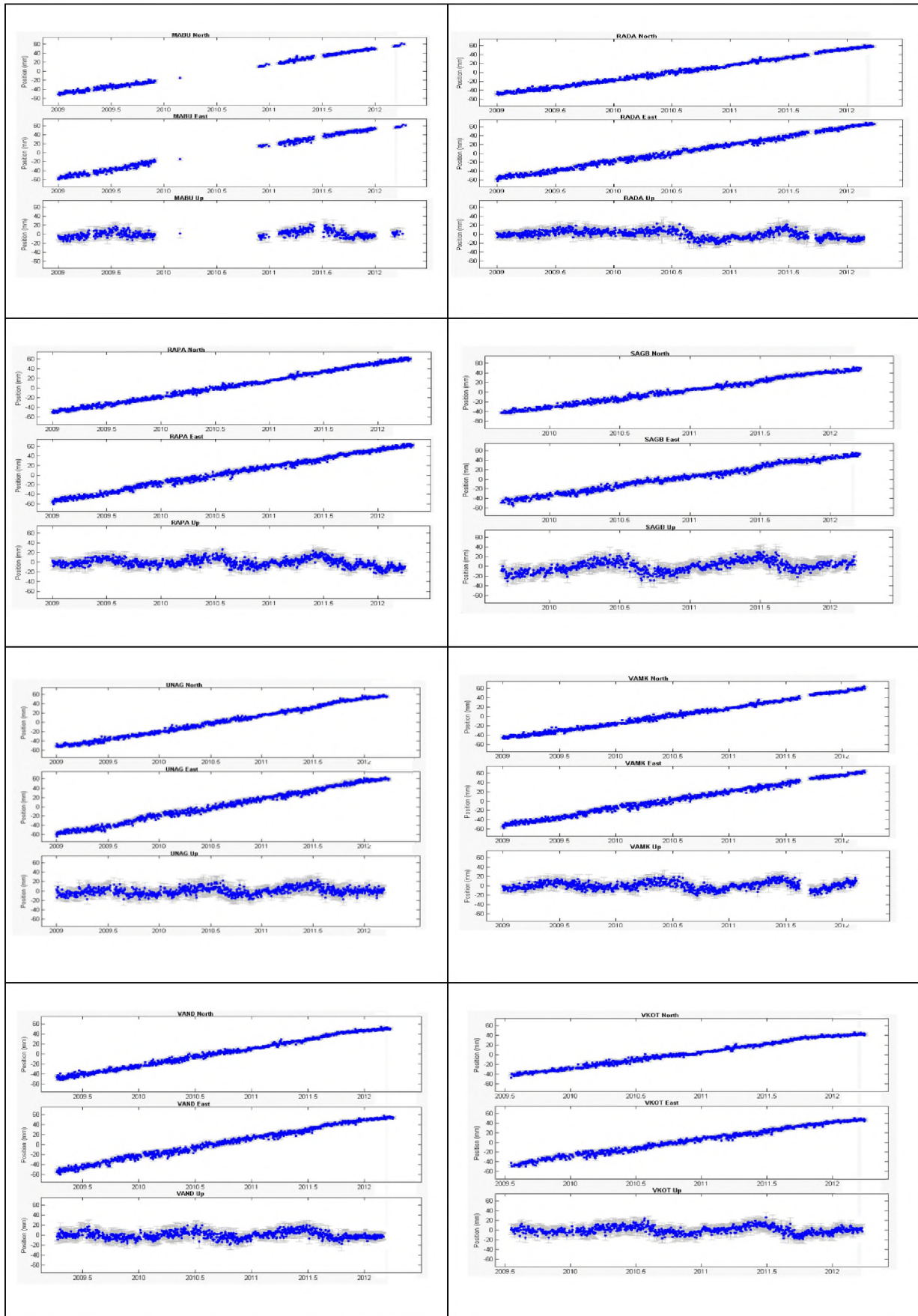


Fig. 4.1.2: ITRF08 velocities of all 22 permanent GPS stations, installed by ISR for three years period of 2009 to 2012. Seasonal variation has not been removed which is seen in vertical component

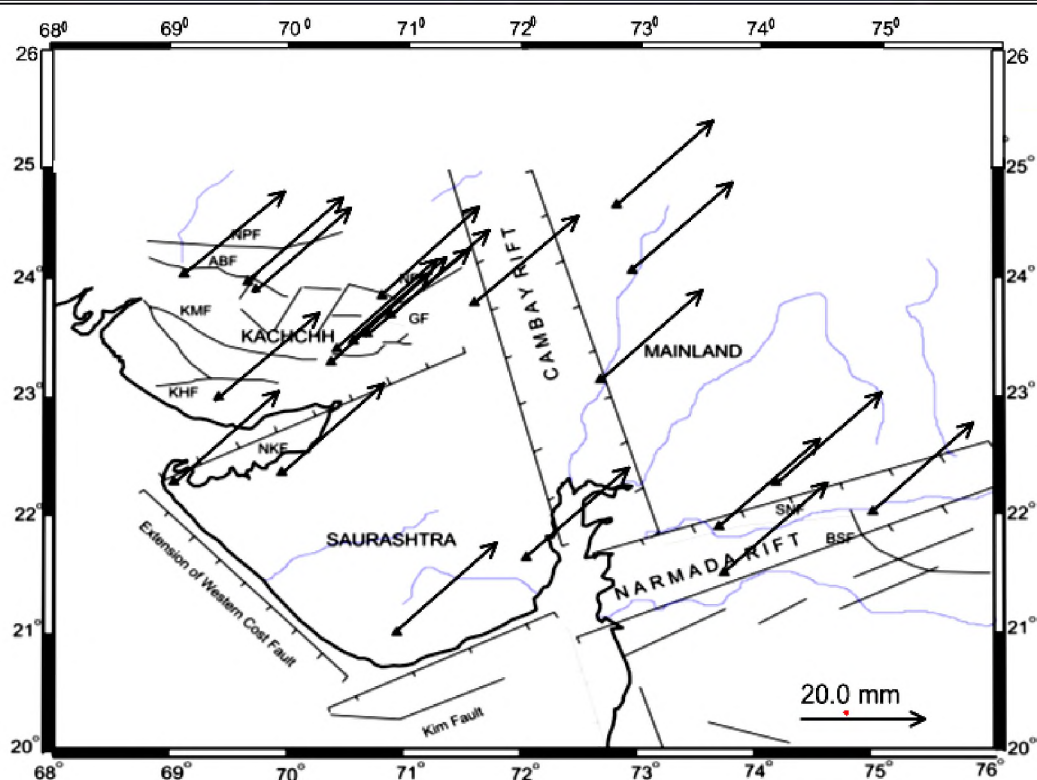


Fig. 4.1.2: Velocity, with reference to ITRF08, of GPS permanent sites of ISR

Table 4.1.1: velocity, ITRF08, of GPS permanent sites of Gujarat region, monitored by ISR

GPS_site	Velocity (ITRF08)	Sigma	Observation period	Region
BARW_GPS	51.18	0.26	2009.5 - 2012.5	South_Gujarat
ARAJ_GPS	49.35	0.21	2009.5 - 2012.5	South_Gujarat
SAGB_GPS	51.41	0.26	2009.5 - 2012.5	South_Gujarat
KEVA_GPS	50.72	0.19	2009-2012.5	South_Gujarat
DHAR_GPS	48.25	0.17	2009-2012.5	Mainland_Gujarat
MABU_GPS	47.96	0.17	2009-2012.5	Mainland_Gujarat
ISRR_GPS	47.56	0.16	2009-2012.5	Mainland_Gujarat
RADA_GPS	49.73	0.16	2009-2012.5	Mainland_Gujarat
BELA_GPS	46.13	0.17	2009.5 - 2012.5	Kachchh
DESA_GPS	47.34	0.17	2009-2012.5	Kachchh
RAPA_GPS	47.87	0.17	2009-2012.5	Kachchh
BADA_GPS	48.01	0.17	2009-2012.5	Kachchh
VAMK_GPS	47.98	0.17	2009-2012.5	Kachchh
BHAC_GPS	47.59	0.16	2009-2012.5	Kachchh
KHAV_GPS	46.95	0.19	2009-2012.5	Kachchh
KUAR_GPS	46.84	0.19	2009-2012.5	Kachchh
VAND_GPS	48.83	0.19	2009-2012.5	Kachchh
VKOT_GPS	46.85	0.24	2009.5-2012.5	Kachchh
DWAR_GPS	48.28	0.17	2009-2012.5	Saurashtra
DEVA_GPS	48.31	0.18	2009-2012.5	Saurashtra
LALP_GPS	48.84	0.17	2009-2012.5	Saurashtra
UNAG_GPS	49.12	0.19	2009-2012.5	Saurashtra

## 4.2 POST-SEISMIC DEFORMATION IN THE BHUJ EARTHQUAKE ZONE AS OBSERVED IN GPS STATIONS

Starting 2006, ISR is observing seismic deformation with 1 mm/yr accuracy across geological faults in Gujarat. Initially there were 4 permanent stations. From October 2008 the network of 22 permanent and 11 campaign DGPS stations is operating. Local deformation has been estimated with respect to Gandhinagar station operated more than 200 km east of the epicenter of the main earthquake of 2001. Indian Institute of Geomagnetism operated two GPS close to two of ISR stations during 2001 to 2005. Combining the two data sets the composite plot for the period 2001 to 2009 indicates that near the epicenter, initially the postseismic relaxation was large, being 12, 6, 4 and 3 mm for four consecutive 6 months periods of 2001 – 2002 but subsequently reduced exponentially (Fig. 4.2.1). Since 2007 all the ISR stations in Kachchh indicate the horizontal deformation to be very low, i.e., of the order of 2-5 mm/yr. However, vertical deformation is found to be quite large, i.e., 2 to 13 mm/yr as observed by GPS measurements near the epicenter of 2001 mainshock and up to 75km N and NE, being 13 mm/y at Dholavira (GDH, 75km N.), 10mm/yr at Dudhai (W. of 2001 mainshock epicenter), 6mm/y at Lilpar (NE of the 2001 mainshock epicenter), 6mm/y at Fatehgadh (further NE).

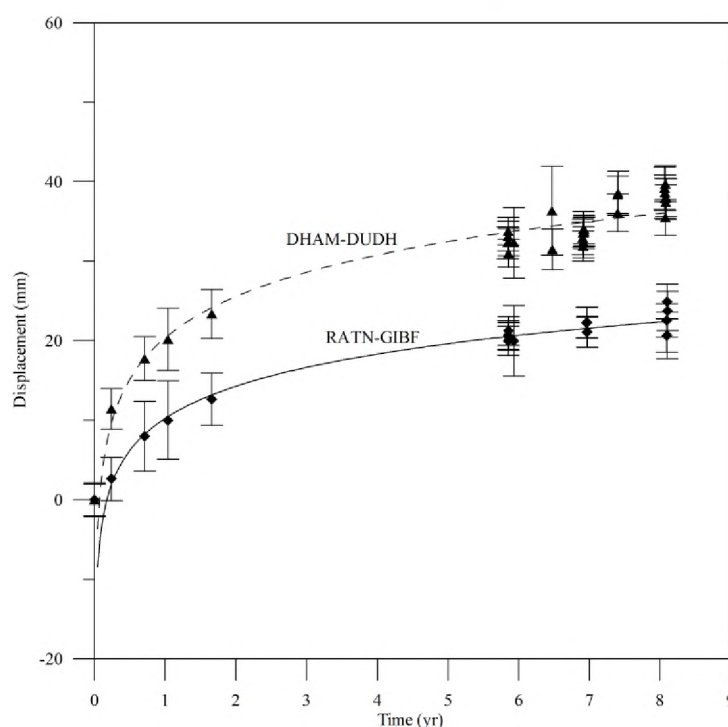


Fig. 4.2.1: Composite map of resultant displacement of 2 GPS sites (DHAM-DUDH (upper curve) and RATN-GIBF (lower curve) plotted with respect to ISRG from 14 days to 8 years after the 2001 Bhuj earthquake. DHAM and RATN are two GPS stations of Reddy and Sunil (2008) co-located with DUDH and GIBF of ISR stations, respectively. Displacement decay rate for upper curve is  $D = 7.6 \cdot \ln(t) + 20.36$ , for lower curve is  $D = 5.8 \cdot \ln(t) + 10.22$ .

## 4.3 CRUSTAL STRAIN ANALYSIS DERIVED FROM GPS

### 4.3.1 Crustal strain in the Rupture zone of 2001 Bhuj Earthquake

(Rakesh K Dumka and B.K. Rastogi)

Strain field of the Kachchh area along with the northern part of mainland Gujarat area was calculated using the International Terrestrial Reference Frame (ITRF08) velocities (Fig. 4.1.2) of 14 GPS stations operated during 2009 to 2011. Strain rate has been estimated in Kachchh, to calculate major and minor strain axes. The strain field was computed, based on rescaling of the covariance matrix of velocity data by means of a weighting function which takes into account the distances between the GPS stations. It indicates the direction of the estimated principal strain axes in the Kachchh region is changing from west



to east, being NNE-SSW in the west, N-S in the middle and NNW-SSW in the east (Fig. 4.3.1). Towards the eastern part of the study area after crossing the Cambay rift the strain rate is almost negligible. Presently, the maximum compressional strain of 0.05 micro-strain annually (Fig. 4.3.2) is observed near Wagad area, i.e. NE of the 2001 M 7.7 earthquake.

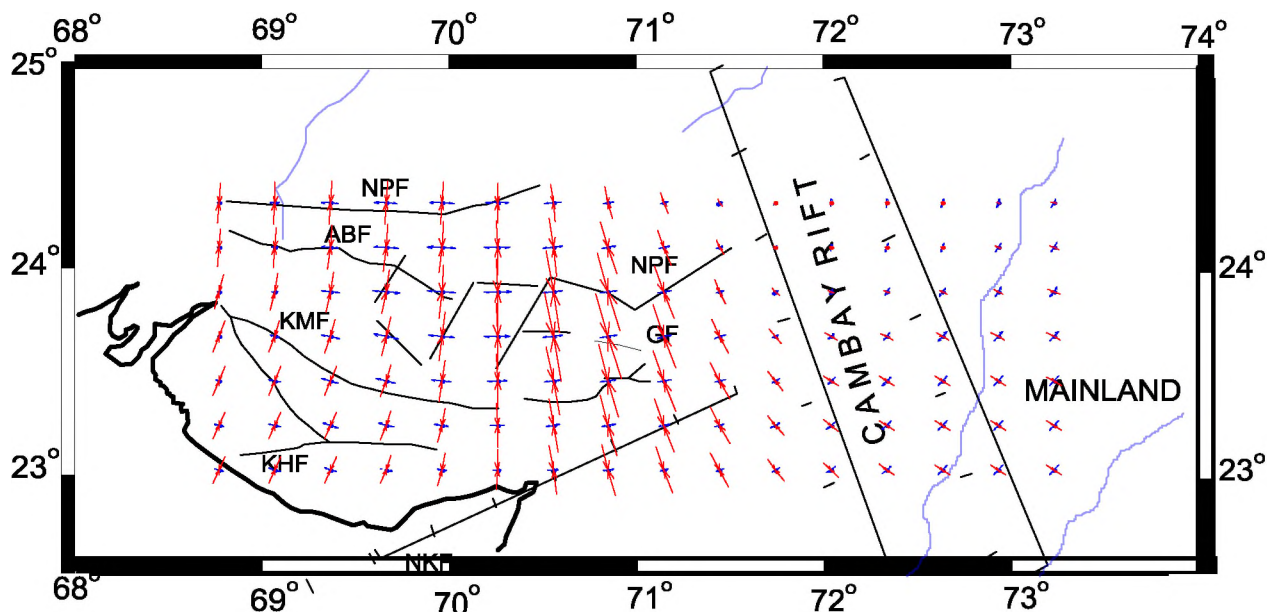


Fig. 4.3.1: Compressional (max 0.05 micro-strain annually) and negligible extension is estimated in Kachchh active area. East of Radhanpur Arch the strain is minimal as expected. The red lines indicate compression and blue lines indicate extension

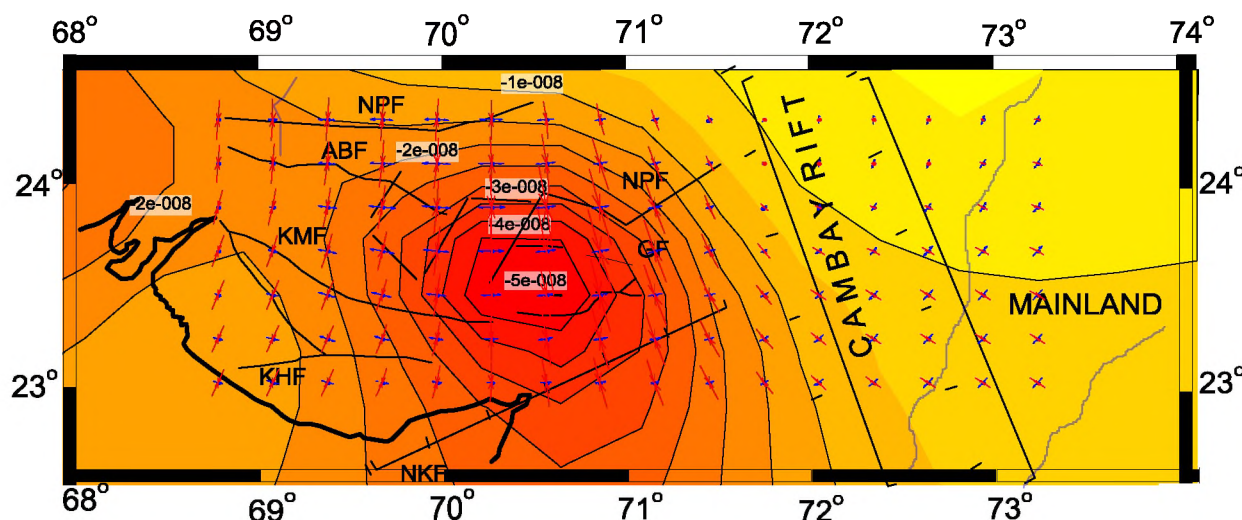


Fig. 4.3.2: Distributed strain rate in the Kachchh region, derived from the GPS network of ISR, maximum strain is observed in the Wagad area, i.e. NE of the 2001 M 7.7 earthquake. The negative sign of contours indicates compressional strain

#### 4.3.2 Strain analysis in Kachchh and Saurashtra region using GPS data

(Pallabee Choudhury, Ketan Singha Roy and B K Rastogi along with Sumer Chopra of Seismology Division, Ministry of Earth Sciences, Prithvi Bhawan, New Delhi)

As a result of tectonic plate movements, enormous forces are applied to the earth's crust. These forces when applied to rocks, results in the alteration of position and shape. In general, strain analysis is used for the determination of deformation pattern. The ratio of baselines is independent from the translation and rotation effect of the datum. Therefore, the baseline data was used for studying the strain variations. The strain was calculated in Kachchh and Saurashtra regions using the triangulation method.

In Kachchh region, horizontal strain was calculated for the year 2008-09 along South Wagad Fault located east of the Bhuj 2001 epicentre where as expected from Coulomb stress increase earthquakes have been triggered from 2005 (Fig. 4.3.3). The three permanent stations Khavda (KVD), Bhachau (BCH) and Radhanpur (RAD) make the triangle for the triangulation method. These three permanent stations were used as these we are running from 2008. For the year 2008-09, the strain was found to be  $0.02\mu\text{S}$ . The estimation is repeated for 2008-10 and 2008-11 and the strains were found to be  $0.03\mu\text{S}$  and  $0.06\mu\text{S}$  respectively. If we see Figs 4.3.4 and Table 4.3.1, we can find a correlation between seismicity and strain. Also, the strain in Saurashtra for 2008-11 is calculated. The three stations used are Dwarka (DWK), Una (UNA) and Lalpur (LAL). The strain is found to be  $0.02\mu\text{S}$  (Fig 4.3.3d) which is less than that in Kachchh as expected.

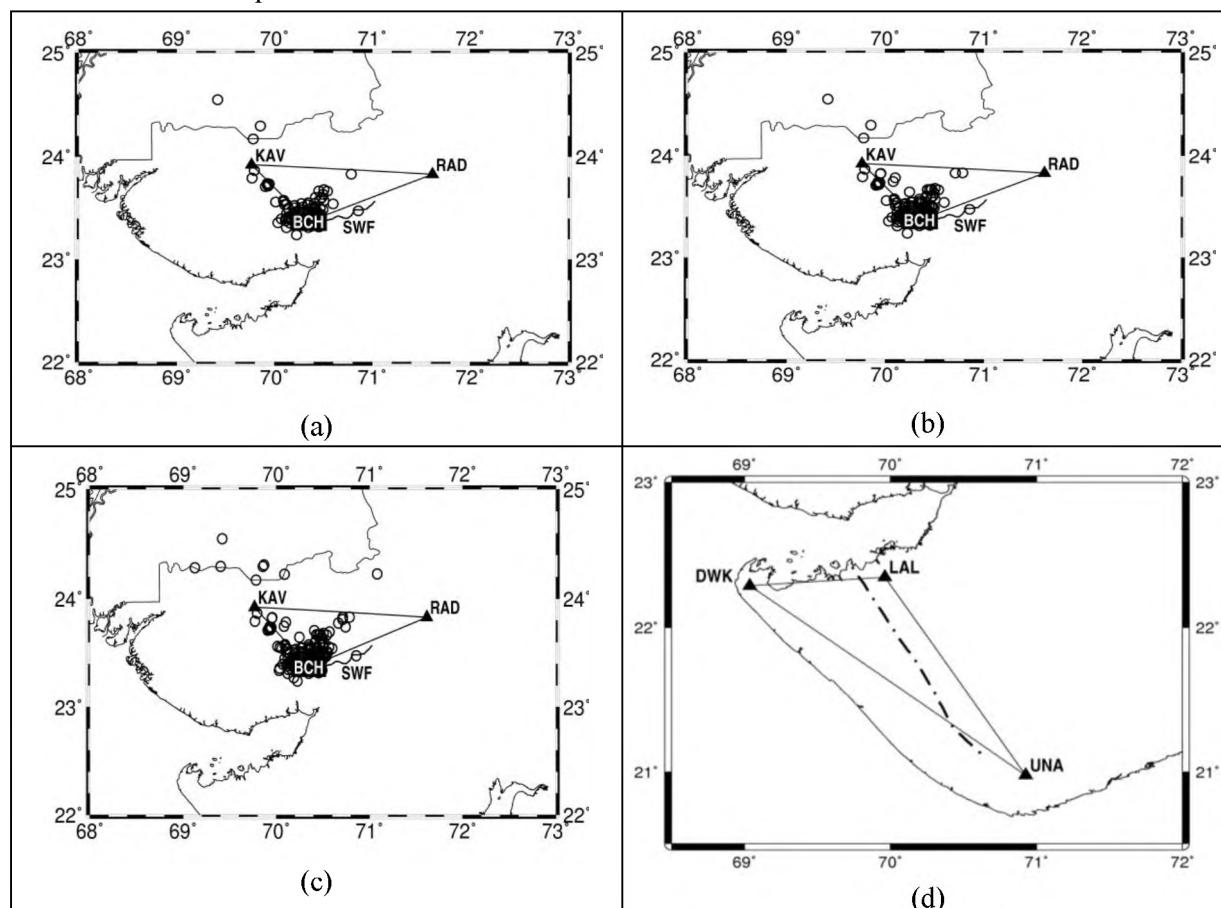


Fig. 4.3.3: Seismicity plot along SWF (a) during 2008-09 (b) 2008-10 (c) 2008-11 and the baselines used for strain calculation in Kachchh region (d) Baselines used for strain calculation in Saurashtra. The dot-dash line represents a lineament.

Table 4.3.1: No. of earthquakes around SWF during 2008-11.

Epoch	
t1	6/7/2008
t2	12/12/2009
t3	12/7/2010
t4	6/7/2011

Time interval	No of EQ			Time interval	No of EQ		
	M3.0-3.9	M4.0-4.9	E1		M3.0-3.9	M4.0-4.9	E1
t1-t2	92	5	2.01E-08	t1-t2	92	5	2.01E-08
t1-t3	121	5	3.44E-08	t2-t3	29	0	1.43E-08
t1-t4	172	7	6.72E-08	t3-t4	51	2	3.28E-08

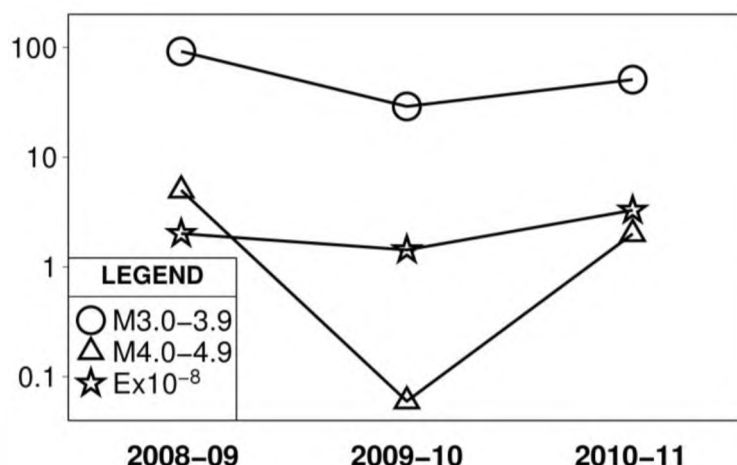


Fig 4.3.4: Number of shocks and the estimated strain in SWF area of Kachchh region during (i) 2008-09 (ii) 2009-10 (iii) 2010-11

#### 4.4 COULOMB STRESS CHANGES IN KACHCHH AND NORTH SAURASHTRA REGION SURROUNDING THE 2001 BHUJ MW7.7 EARTHQUAKE

We calculated the postseismic stress change in the Gujarat region due to the 2001 Bhuj earthquake considering viscoelastic mechanism using EDGRN/EDCMP code developed by Wang et al. (2003) which is based on the representation of a layered spherical earth with elastic-viscoelastic coupling. We adopted the earthquake source parameterization of Yagi and Kikuchi (2001). Strike, dip, rake, and seismic moment are  $78^\circ$ ,  $58^\circ$ ,  $81^\circ$ , and  $2.5 \times 10^{20}$  Nm, respectively. The model rupture is 75 km long and 35 km deep with hypocenter at 15km depth and rupture has variable slip distribution of Yagi and Kikuchi (2001). The velocity model of Kachchh was adopted from Mandal (2006).

Aftershocks or triggered earthquakes (during 2006-2012) have occurred in the zones of positive stress change up to 75km in Kachchh along KMF, SWF, Banni Fault, Gora Dungar Fault and Island Belt Fault. In the stress shadow zone along the Gedi Fault (GF) in the NE direction an earthquake of Mw 5.7 in 2006 was triggered. However, here also positive stress change is at depth of earthquakes of 5-10 km (Mandal et al. 2007). Seismicity in Saurashtra also can be triggered by small change of 1 bar or even 0.1 bar positive stress change in Jamnagar, Junagadh and Surendranagar of Saurashtra to 240km distance.

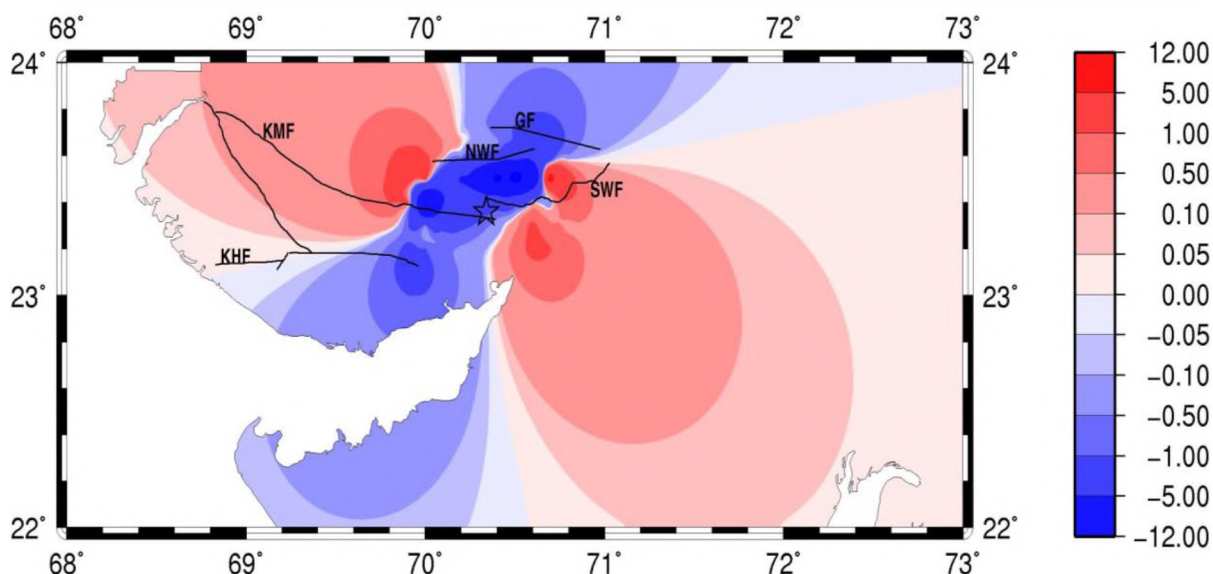


Fig. 4.4.1: Postseismic Coulomb stress changes (in bars) at surface due to Mw7.7 Bhuj 2001 earthquake (epicenter is marked as star) calculated assuming variable slip at 15 km depth. Max. Stress change is 12bars while 1 bar goes up to 100km. Aftershocks / triggered earthquakes (during 2006-2012) have occurred in the zones of positive stress change up to 75km in Kachchh and up to 240km south of 2001 epicenter in Saurashtra (prepared by Ketan Singha Roy and Pallabee Choudhury)



#### 4.5 INTERFEROMETRIC SYNTHETIC APERTURE RADAR (INSAR) STUDIES BY ISRO AND ISR

The interferogram generated with Differential Interferometry (DInSAR) aided with corner reflectors using ENVISAT ASAR data sets of June 22, 2008 and 25 October 2009 with a baseline separation of 125 m in and near the rupture zone of 2001 in Kachchh (Fig. 4.5.1) indicates vertical deformation rates of 10 to 40 mm in 1.5 yr or 10-27mm/yr vertical deformation (Fig. 4.5.2).

Vertical displacement of 10-20mm/yr have been observed 5-10km south of KMF (west of the 2001 epicenter) as well as along eastern portion of the Katrol Hill Fault (KHF) during 2007 to 2010 using ALOS PALSAR Data (ISR Annual Reports of 2011-12). The interferograms during 2004 to 2007 using ENVISAT ASAR data sets shown in this report indicate similar picture (Fig. 4.5.3). Year after year there is 10-20mm/yr vertical displacement along KMF and KHF.

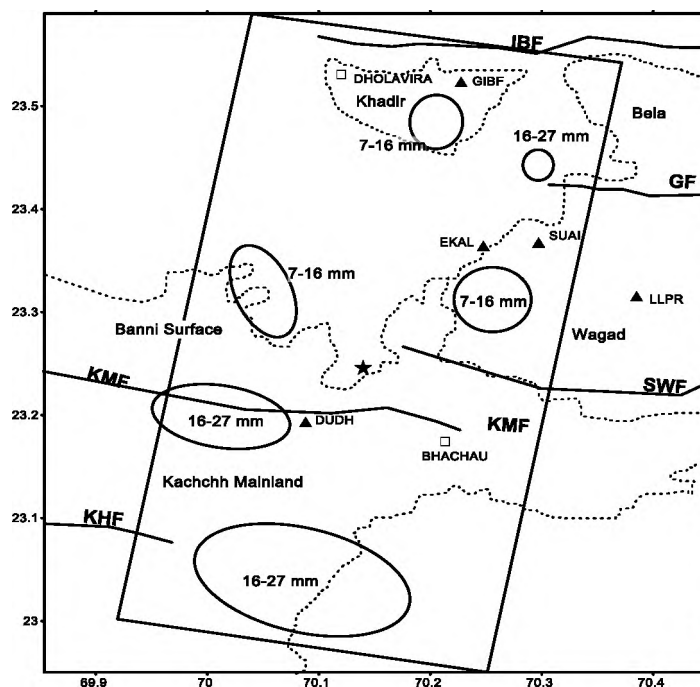


Fig. 4.5.1: Uplift/yr observed at Line of Site range-change generated from ENVISAT-ASAR interferogram. Positive values represent displacement towards the satellite (max. range change around 50mm during 1.5 yr corresponds to about 40 mm vertical in 1.5 yr or 27mm/yr). Interferogram fringes were identifiable in hilly-uplifted areas only but not in large low-lying areas. Star indicates the 2001 Bhuj earthquake. During 2004 to 2007 and 2007 to 2010 uplift of 10-20mm/yr is observed south of KMF and along extension of KHF (modified after ISR Annual Report 2012, [www.isr.gujarat.gov.in](http://www.isr.gujarat.gov.in))

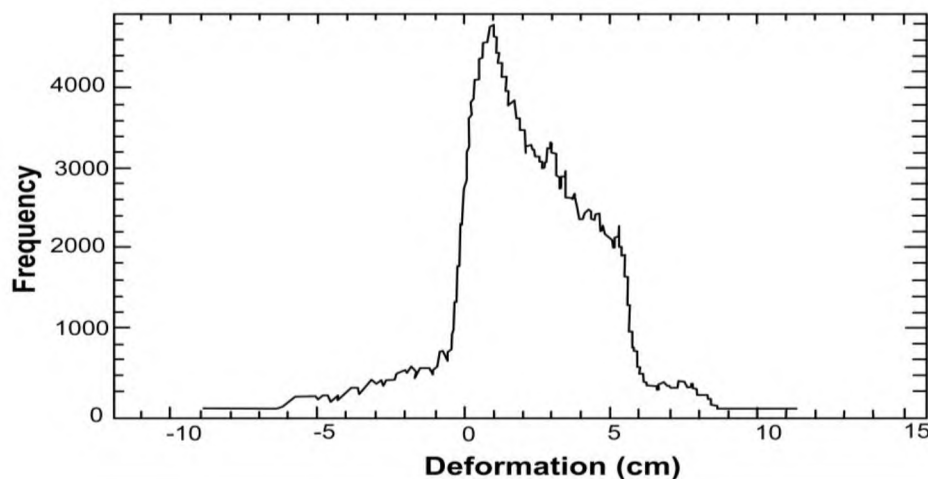
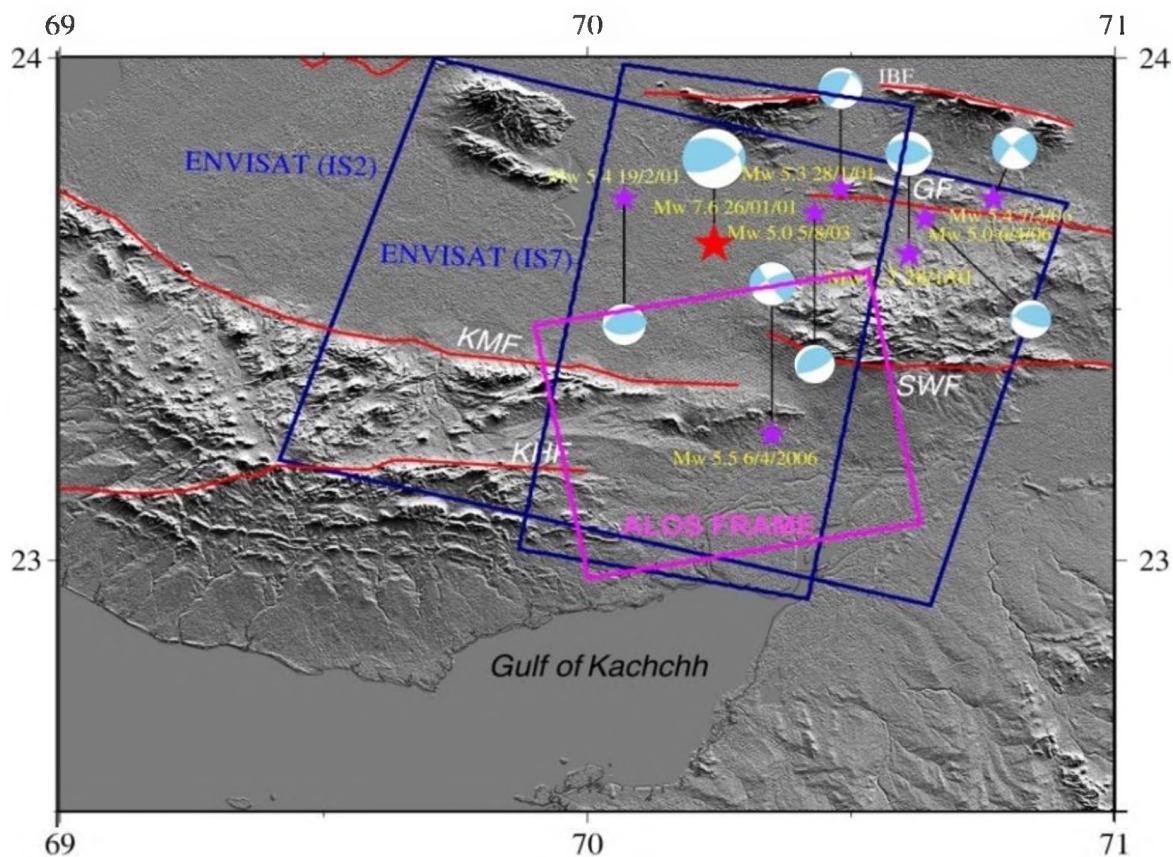


Fig. 4.5.2: Line of Site range change deformation by DInSAR is found to be high 1 to 5cm during 1.5 years (June 2008 and October 2009), ENVISAT data. Vertical deformation is reduced to 1-4 cm in 1.5 yr or 1 to 27mm/yr

## Satellite Data

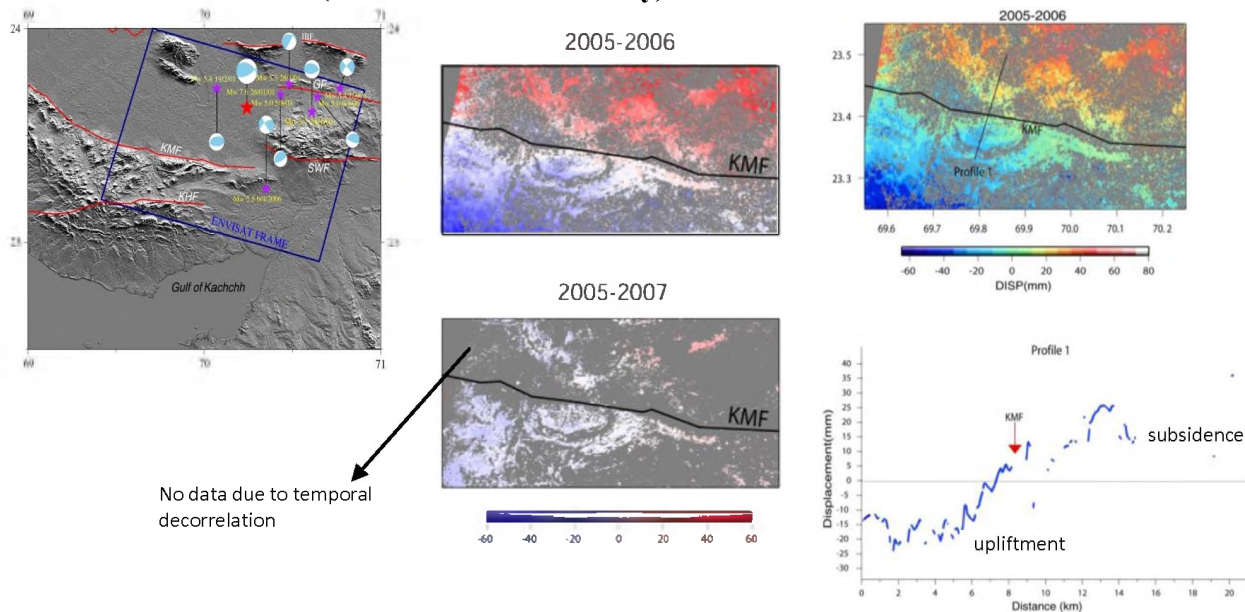
ENVISAT : 2004-2009

ALOS : 2007-2010



Study area with foot prints of ENVISAT and ALOS satellites

## Deformation 2004-2007 (ENVISAT Interferometry)



The displacement (along the line of sight of satellite) is negative ( $\sim 20$  mm) to the south of KMF indicating upliftment and positive ( $\sim 20$  mm) to the north indicating subsidence.



### Interferogram stacks showing LOS displacement rates (mm/yr) along KMF for time period 2007-2010

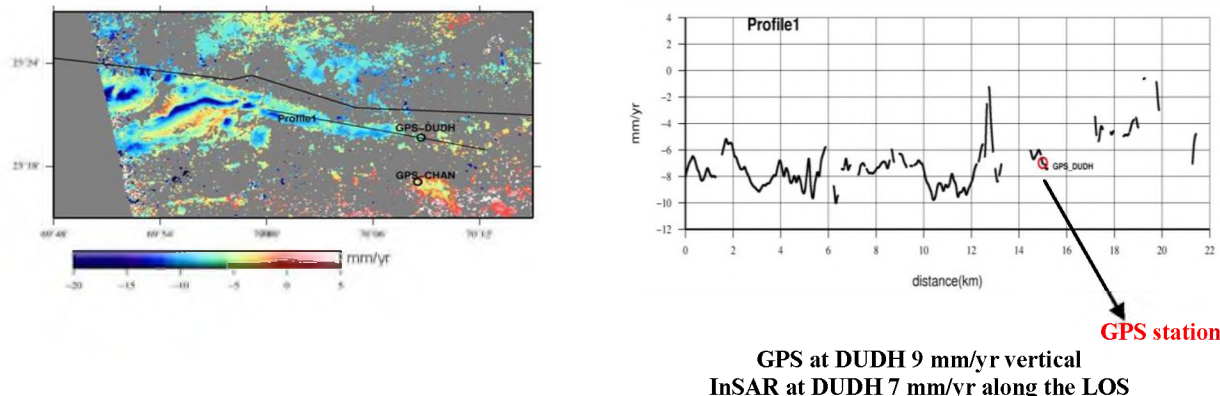


Fig. 4.5.3: Interferograms during 2004 to 2007 using ENVISAT data. Uplift of 10-20mm/y is indicated along KMF west of 2001 mainshock epicenter and eastern KHF.

#### Some points about InSAR study:

- ⇒ InSAR technique has been used to map surface deformation in Kachchh, India from 2004 to 2010 using ALOS PALSAR and ENVISAT ASAR data aided with DGPS based field measurements.
- ⇒ InSAR processing has been carried out using GMTSAR software (open source)
- ⇒ Crustal deformation rate were estimated from interferogram time series stacking
- ⇒ The InSAR analysis clearly suggests active deformation along the eastern part of the Kachchh Mainland Fault (KMF) or west of the epicenter of 2001 Bhuj earthquake. The Line of Sight (LOS) displacement is negative ( $\sim -20$  mm) to the south of KMF indicating upliftment.
- ⇒ The observed deformations seems to be long-term as the deformation signals were only detected in interferograms of SAR data pairs having temporal separations of  $> 10$  months.
- ⇒ DGPS data at Dudhai operating during 2007-2010 provided comparable deformation rates with satellite observation.
- ⇒ The analysis of the interefrograms time series and GPS data clearly suggests slow and continuous deformation along KMF.

## 4.6 TRIGGERED SEISMICITY IN KACHCHH AND SAURASHTRA

About 200 km x 300 km Kachchh region of Gujarat in western India is seismically one of the most active intraplate regions of the world. It has E-W trending six major faults of the failed Mesozoic rift which are getting reactivated by thrusting. Kachchh had earlier experienced earthquakes of  $M_w 7.8$  in 1819,  $M_w 6.3$  in 1845 and  $M_w 6$  in 1956, but small number of  $M < 6$  earthquakes.  $M_w 7.7$  great Bhuj earthquake of 2001 is followed by damaging aftershocks over a decade. The aftershock activity includes over 10,000 shocks of  $M$  1 to 2.9, 2401 shocks of  $M 3$  to 3.9, 357 shocks of  $M 4$  to 4.9 and 20 shocks of  $M \geq 5.0$ . In this region  $M_w 5$  or more level seismicity has continued until today, the latest being  $M_w 5$  on June 19, 2012. After  $M_w 7.7$  earthquake in 2001, besides the continuing high seismicity in the rupture zone of 20 km radius (Fig.4.6.1), several other faults within distances of 75 km away from the rupture zone and even after 12 years of the Bhuj earthquake are activated with earthquakes of  $M_w$  about 4-5.7 (Fig. 4.6.2). Initially the seismicity had spread eastward to SWF but to other faults from 2006. These faults include KMF, IBF, Gora Dungar F., SWF and Gedi F. Total no. of such mainshocks is at least 20 (Table 4.6.1). Many of these mainshocks are associated with foreshock-aftershock sequences. Moreover, the seismicity to  $M_w 3$ -5 level is triggered along small faults at twenty locations up to 120 km south since 2006 and up to 240km south since 2007 in the Saurashtra region (Figs. 4.6.2, 4.6.3). The three significant sequences which have continued for 5 years with hundreds of felt shocks are (i) near Jamnagar with  $M_w$  4.0 (ii) near

Surendranagar with  $M_w$  3.9 and (iii) at Talala with  $M_w$  5 in 2007,  $M_w$  5.1 in 2011 and several  $M_w$  4 to 4.8 tremors (Table 4.6.2). The shocks are usually shallow (focal depth <10km) and are accompanied by subterranean sounds. Generation of unusually large number of mainshocks is inferred to be due to triggering caused by migration of stress pulse generated by 20 MPa stress drop of M7.7 earthquake in 2001 to distances of 100-200 km and even 6-8 years after the great earthquake. The triggered seismicity may be because of increase in stress up to 1 bar in Kachchh and 0.1bar in Saurashtra as estimated by viscoelastic modeling. In mainland Gujarat, seismicity is not triggered or increased. Small no of shocks recorded are part of prevailing seismicity (Table 4.6.3).

**Table 4.6.1: Triggered Earthquakes in Kachchh after 2001Bhuj earthquake along different faults and other than aftershocks along the NWF.  $M_w$  until April 2006 from NGRI and subsequently from ISR. Many of these are associated with their own foreshocks and aftershocks. USGS magnitudes are usually mb.**

SN	Y	M	D	Lat	Long	Dep. km	Mag $M_w$	Mag USGS	Location	Mechanism
	2001	1	26	23.44	70.31	16.0	7.7	7.7	18km NW of Bhachau North Wagad F.	Thrust
1	2004	1	8	23.91	70.90	20.0	4.2		Gedi/Is. Belt F.	
2	2004	6	7	23.87	70.15	29.4	4.2		Dholavira/Is. Belt F.	
3	2005	3	8	23.85	69.74	11.6	4.3		Gora Dungar F.	
4	2005	10	8	23.35	70.69	24.0	4.5		South Wagad F.	
5	2005	10	9	23.74	69.93	6.6	4.3		Gora Dungar F.	
6	2006	2	03	23.92	70.44	28.0	5.0	4.5	Gedi F., foreshock	Thrust
7	2006	3	07	23.79	70.73	3.0	5.6	5.5	Tr. Bela F./Gedi F., ms	left lateral
8	2006	4	06	23.78	70.74	3.0	4.8	5.0	Gedi F., aftershock	Thrust
9	2006	4	06	23.34	70.39	29	5.6	5.5	Lakadia, SWF	
10	2006	4	10	23.51	70.06	4.9	4.9	4.9	*Banni	
11	2006	6	12	23.88	70.43	27.3	4.4		Gedi/Is. Belt F.	
12	2007	5	13	23.44	70.42	20.4	4.7		South Wagad F.	
13	2007	5	24	23.298	70.026	9.0	4.1		Kachchh Mainland F.	Thrust
14	2007	10	8	23.295	70.075	9.6	4.7	4.5	Kachchh Mainland F.	Left Lateral
15	2007	12	15	24.03	69.87	15.0	3.7		Allahbund F.	Right Lateral
16	2008	3	9	23.396	70.359	18.5	4.9	4.5	South Wagad F.	Left Lateral
17	2008	4	4	23.00	70.36	11.1	2.6		**Kandla	
18	2008	7	5	23.53	69.8	8.9	3.3		Banni F.	
19	2009	10	28	23.71	69.91	8.5	4.4	4.4	Gora Dungar F	Left Lateral
20	2011	1	18	23.27	70.51		3.8		Samkhiyali, SWF	
21	2011	5	17	23.55	70.57	18.2	4.2		E. of North Wagad F.	Thrust
22	2011	8	13	23.45	70.40	22.2	4.5	4.3	South Wagad F.	
23	2011	9	27	23.12	70.31	38.0	3.0		**Kandla	
24	2012	4	14	23.39	70.54	19	4.1	4.0	South Wagad F.	
25	2012	6	19	23.65	70.28	11	5.0	5.0	Khadir Tr. F.	
26	2012	12	8	23.13	70.42	21	4.5	4.1	20km SSE of Bhachau **Kandla	
27	2013	3	30	23.56	70.38	24	4.5		*Chobari	

\*May be aftershock of 2001 Bhuj earthquake \*\*May be Regional shock as it is single event.

**Table 4.6.2: Triggered Earthquakes in Saurashtra after 2001 Bhuj earthquake (\*May be regional shock).  
Many of these are associated with their own foreshock-aftershock sequences.**

SN	Y	M	D	Lat	Long	H	Mag.Mw	Location
1	2001			21.02	70.88		2.5	Tulsishyam, Junagadh
2	2003	1	13	22.30	70.93		2.0	*Rajkot
3	2003	1	29	21.46	70.51		3.1	Haripur, Talala
4	2003	8					3.0	Lalpur, Jamnagar
5	2004			21.00	70.50		3.0	Talala, Junagadh
6	2006	9	30	22.31	70.21	5.2	4.0	Khankotda, Jamnagar
7	2007	7	16	22.49	71.29	18.0	3.9	Paliyad, Surendranagar
8	2007	9	2	22.33	70.22	10.0	3.2	Khankotda, Jamnagar
9	2007	9	9	22.40	70.20	14.0	3.5	Vijrakhi, Jamnagar
10	2007	10	09	21.08	70.73	11	3.1	Ankolwadi, Junagadh
11	2007	11	06	21.12	70.51	8.5	M <sub>w</sub> 4.8 mb4.9	Hirenvel, Junagadh
12	2007	11	06	21.16	70.54	4.5	M <sub>w</sub> 5.0 mb5.0	Haripur, Junagadh
13	2007	11	11	21.93	69.82	10	2.9	Bhanwad
14	2007	12	10	21.05	70.66	7.4	3.1	Ankolwadi, Junagadh
15	2008	01	25	21.79	71.76	35	2.8	*Bhavnagar
16	2008	2	15	21.66	71.77	3.1	2.7	*Bhavnagar
17	2008	2	24	22.25	71.01	6.1	2.9	*Kotda, Rajkot
18	2008	3	3	22.45	71.50	12.8	3.4	Paliyad, Bhavnagar
19	2008	3	15	22.51	71.45	10.6	3.9	Chotila, Surendranagar
20	2008	4	2	22.82	70.78	18.6	2.7	*Morbi
21	2008	10	4	21.90	69.96	3.7	3.6	Bhanvad
22	2009	3	28	22.17	70.75	6.2	3.0	*Rajkot
23	2010	6	23	22.16	71.36	21.0	3.3	Botad
24	2010	9	6	22.20	70.37	15.0	2.8	Kalavad, Jamnagar
25	2010	9	23	21.90	69.7	3.1	3.0	Advana, Porbandar
26	2010	9	25	21.91	69.75	3.2	2.8	Bhanvad
27	2010	9	29	22.36	69.98	3.1	3.0	Motikhavadi, Jamnagar
28	2010	11	25	22.29	70.24	6.9	3.4	Khankotda, Jamnagar
29	2010	11	28	22.28	70.25	6.6	2.7	Khankotda (Sanala vil.)
30	2010	12	6	22.35	74.03	12	3.2	*Chota Udaipur
31	2011	4	18	22.45	71.51	6.1	2.4	*Sayla
32	2011	4	29	21.27	70.49	3.1	4.1	Talala
33	2011	5	23	21.1	70.53	3.9	4.0	Talala
34	2011	8	20	22.43	70.93	8.4	2.6	*Rajkot
35	2011	9	14	22.38	69.99	6.3	3.4	Lalpur, Jamnagar
36	2011	10	3	22.65	72.47	32.3	1.5	*Dholka, Ahmedabad
37	2011	10	18	21.26	71.19	7.9	3.1	*Visavadar
38	2011	10	20	21.09	70.45	5.8	5.1	Talala

\*May be regional earthquake as single event of low magnitude

**Table 4.6.3: Regional earthquakes in mainland since 2006 not triggered**

Y	M	D	Lat	Long	H	Mag ISR	Location
2008	05	20	21.16	73.05	7.4	M <sub>w</sub> 3.2	Surat
2008	11	5	21.95	73.89	8.5	M <sub>w</sub> 2.9	Kevadiya
2010	1	26	23.29	72.98	15	Mw 2.3	Gandhinagar
2010	3	30	23.61	72.57	11	Mw 3.2	Mehsana
2010	9	2	23.88	71.87	6.1	Mw4.4 mb4.0	Patan
2011	7	3	21.14	73.16	26	Mw 3.2	Bardoli
2011	11	7	24.38	72.66	13.7	Mw 3.1	Palanpur

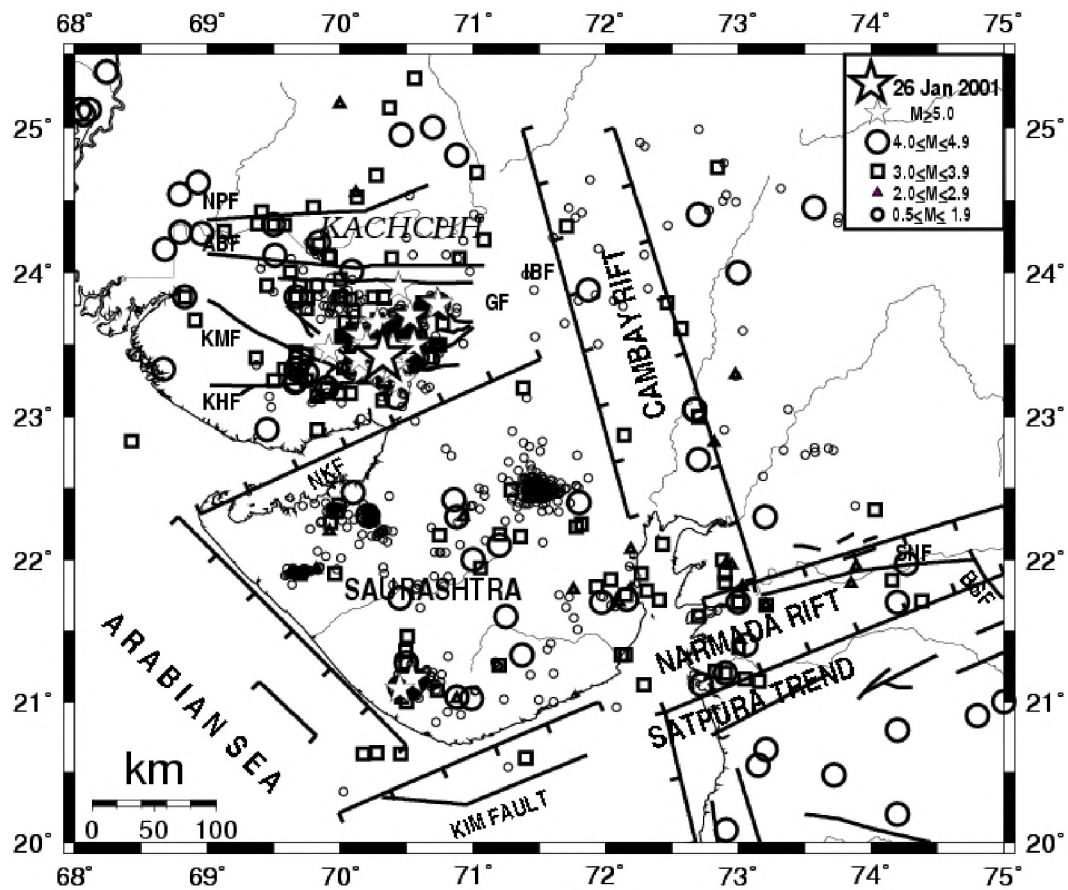


Fig. 4.6.1: Epicenters of M 0.5 to 5.1 during 2006-2012 in Gujarat. The big star shows epicenter of the 2001 Bhuj earthquake

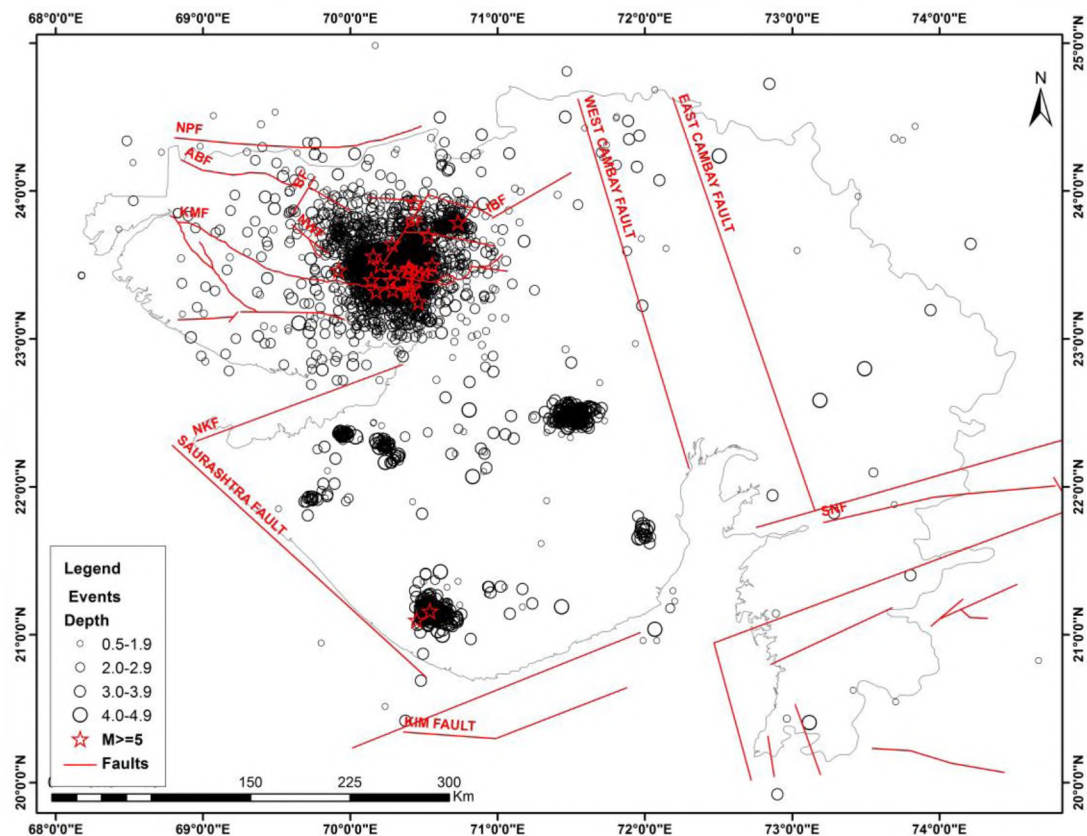


Fig. 4.6.1a: Epicentres during 2006 to 2012 in Gujarat and major faults. Epicentre of the 2001 Mw7.7 earthquake is shown as a big star.



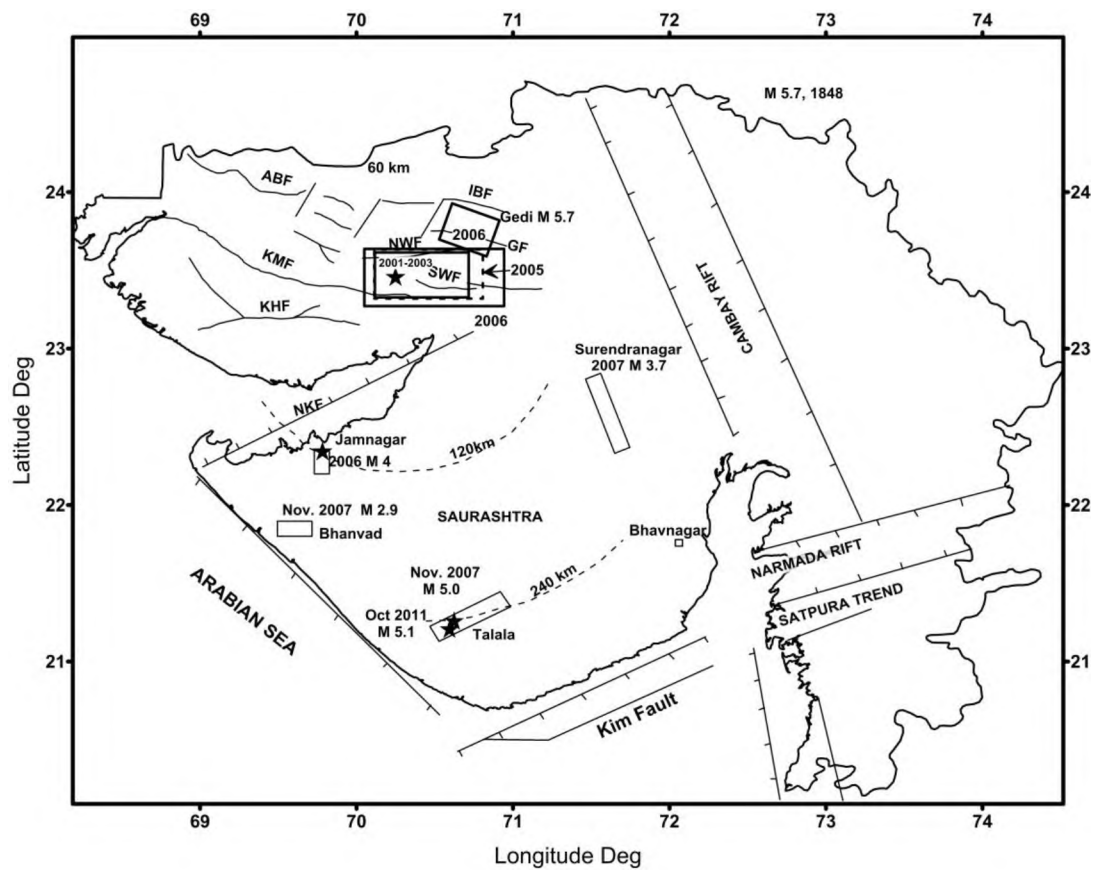


Fig. 4.6.2: Long-time and delayed triggering of seismicity in Gujarat from 2006 to 2011. Epicentral zones for significant sequences are marked by rectangles. The seismicity migrated to 120 km south to Jamnagar and Surendranagar area and to 240 km in Talala area of Saurashtra.

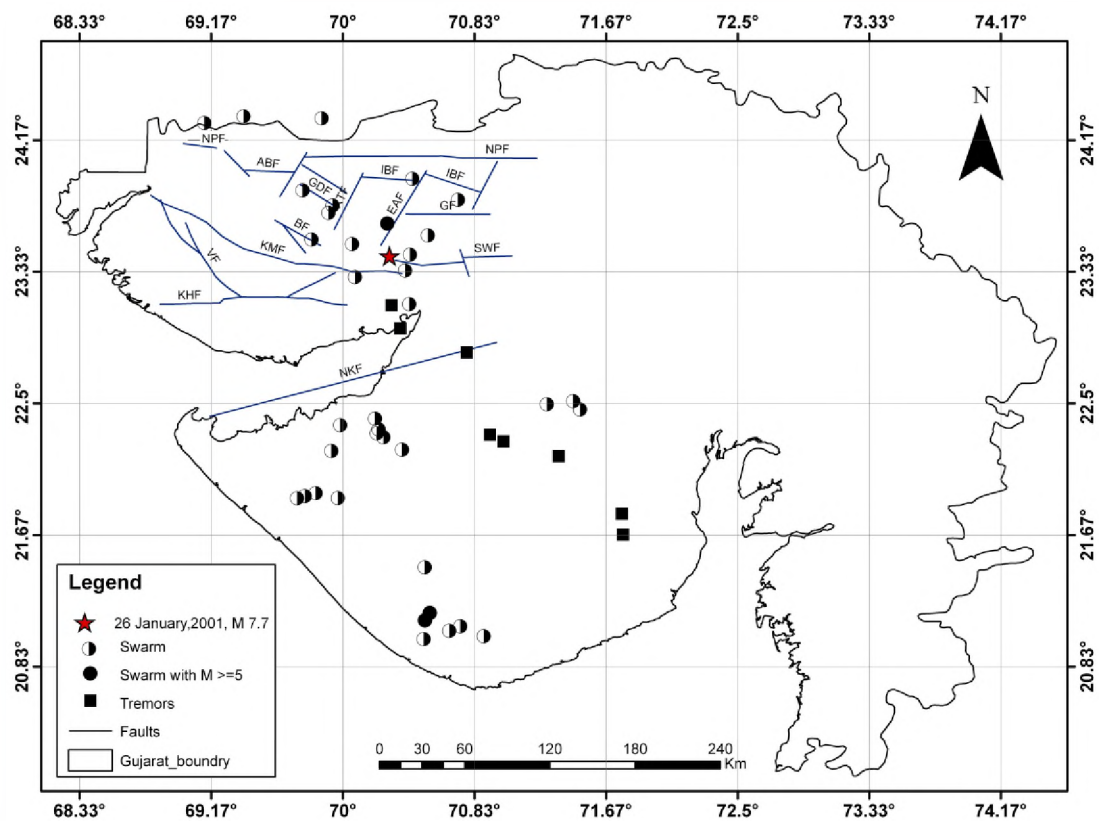


Fig. 4.6.3: Triggered seismicity (Tremors with or without swarms) in Kachchh and Saurashtra regions of Gujarat after the 2001 Bhuj Earthquake  $M_w 7.7$

## Cause of Triggering of Earthquakes

We propose, based on the seismological data, that the viscoelastic process / rheology change appears to be the plausible mechanism for long distance and delayed triggering of earthquakes with diffusion rates of 5-50 km/yr, which might have also facilitated by the migration of stress pulse of 20MPa stress drop caused by the 2001 Mw7.7 earthquake. Vertical deformation is observed to be high as measured up to 13 mm/yr by 6 years of GPS observations and 10-27 mm/yr by 10 years of InSAR observations. We feel that the stress transmission into the upper crust might have resulted in vertical deformation as observed in GPS measurements.

## 4.7 PALEOSEISMOLOGY AND ACTIVE FAULT INVESTIGATION IN KACHCHH BASIN

Active fault studies were carried out in Kachchh and Himalaya. Fig. 4.7.1 shows study areas in Kachchh which are, Gedi fault N. of Wagad, the Bharudia area of Wagad and Kachchh Mainland Fault

- Site 1 (GF Zone): Geological, GPR, RTK investigation in and around Gedi Fault zone. OSL sampling has been done.
- Site 2 (KMF zone): Geological, Gravity survey in and around KMF zone OSL sampling has been done
- Site 3 and 4 (KHF zone): Geological mapping and OSL sampling has been done
- Site 5 (Banas river section): Geological mapping and OSL sampling (Work under progress)

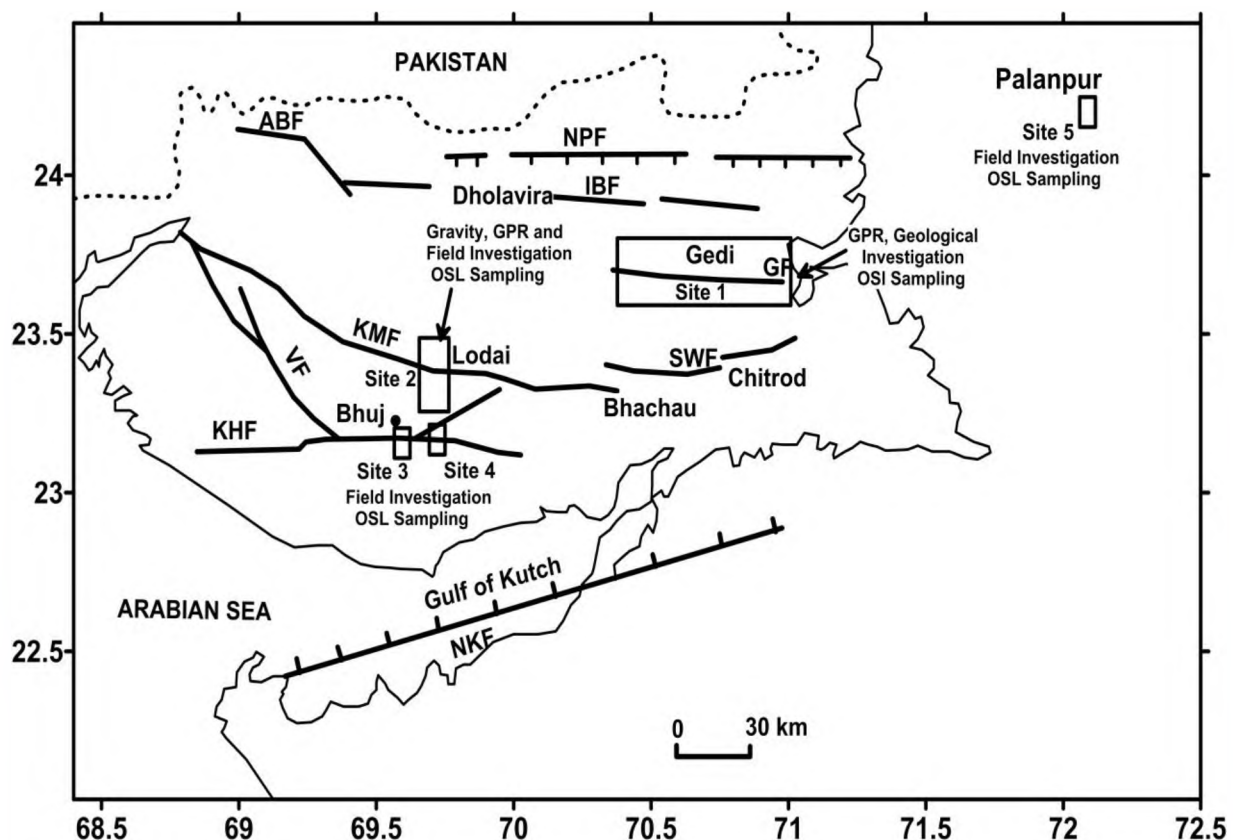


Fig. 4.7.1: Sites of Active Fault Studies

#### **4.7.1 Optically Stimulated luminescence Chronology and GPR Investigation along Gedi Fault; Eastern Kachchh**

*(Girish Ch. Kothiyari, B. K. Rastogi, R. K. Dumka, P. Morthekai)*

The Gedi fault area, about 60km NE from the 2001 Bhuj earthquake epicenter or 80km N of Bhachau or 25 km N. of Wagad uplift, witnessed a moderate earthquake of Mw5.6 and several large aftershocks from March 2006. The Gedi Fault (GF) trending nearly E-W shows thrust movement while a transverse NE trending fault crossing GF shows strike-slip. The March 7, 2006 mainshock of Mw5.6 showed Left-lateral strike slip along a NE trending fault while February 3, 2006 foreshock of Mw 5.0 and April 6, 2006 aftershock of Mw 4.8 showed thrusting with strike-slip component.

Geomorphological mapping in Desalpar-Gedi-Fatehghadh localities aided by Real-Time Kinematic (RTK) instrument for precise leveling and 2D GPR profiles has indicated (i) development of active fault scarp at along the Gedi Fault at Desalpar between Mesozoic and Tertiary rocks with slickensides

and fault propagating folds in Tertiaries, shifting and offsetting of river channels east and west of this scarp. Asymmetry of two basins of Karaswali and Malan rivers which flow northward from Wagad uplift and cross Gedi Fault is observed and inferred to be due to SE tilting of the ground. All these features indicate that the terrain is undergoing active deformation. Further the rate of deformation is estimated using the optical dating technique which shows an uplift rate of 3-7mm/yr during the last 8000 years. Ages of GF1, GF2, GF3 and GF4 from the sediments of Karaswali river shows homogeneity in age model. We used minimum age model (MAM) of Galbraith *et al.* (1999). We observed average dose rate using MAM for GF1, GF2, GF3 and GF4 is  $2.9 \pm 0.5\text{ka}$ ,  $1.2 \pm 0.4\text{ka}$ ,  $1.9 \pm 0.5\text{ka}$ ,  $1.9 \pm 0.5\text{ka}$ ,  $2.2 \pm 0.5\text{ka}$  respectively. We collected two samples from the hanging wall and two samples from footwall of fault zone. The GF1 is collected from the top unit of hanging wall deposited during  $4136 \pm 745$  years. The oldest sediment (GF2) collected from the hanging wall of GF shows  $8015 \pm 856$  years age. After deposition of sediments during  $4136 \pm 745$  years in the hanging wall of Gedi fault major tectonic activity took place due to growth of fault related folding of sediments. The sediments dated from footwall block show age of GF4 as  $1055 \pm 237$  years and for youngest sediment of  $75 \pm 27$  years. The stream offsetting and deformation of sediment is bracketed between offsetting of sediment  $1055 \pm 237$  years and  $4136 \pm 745$  years.

The Ground Penetrating Radar (GPR) survey was carried out to identify pattern of deformation and GF geometry. A 140m long 2D-GPR profile was acquired in the N-S direction after taking 4 test profiles to decide on the suitable survey parameters by 200MHz frequency antenna (SIR-3000) across the fault zone between (23.67282N-70.75430E and 23.67402N-70.75433E). The sampling rate of 512 sample/scans, 164 scans/unit, range 140ns and a dielectric constant for 7 were found suitable for survey with ground offset -5.76. We adopted different methods for processing the acquired image using RADAN 6.5 software. At 23.67381N-70.75430E up-warping of reflections are noticed along gently south dipping plane which is marked as GF. The GPR spectra images show weak reflection at many where radar waves have shown less penetration or absorption may be due to presence of tensional fractures through the radar waves might have escaped (Fig. 4.7.2). The continuous horizontal reflection above 2 m depth of all the profiles may be due to presence of loose soil and Quaternary alluvial sediments. The faulting observed in the GPR image is marked by folding of reflections towards north of fault. Within the fault zone the GPR image shows scattering in signals may be due to changes in dielectric constant of the medium or change in lithology.



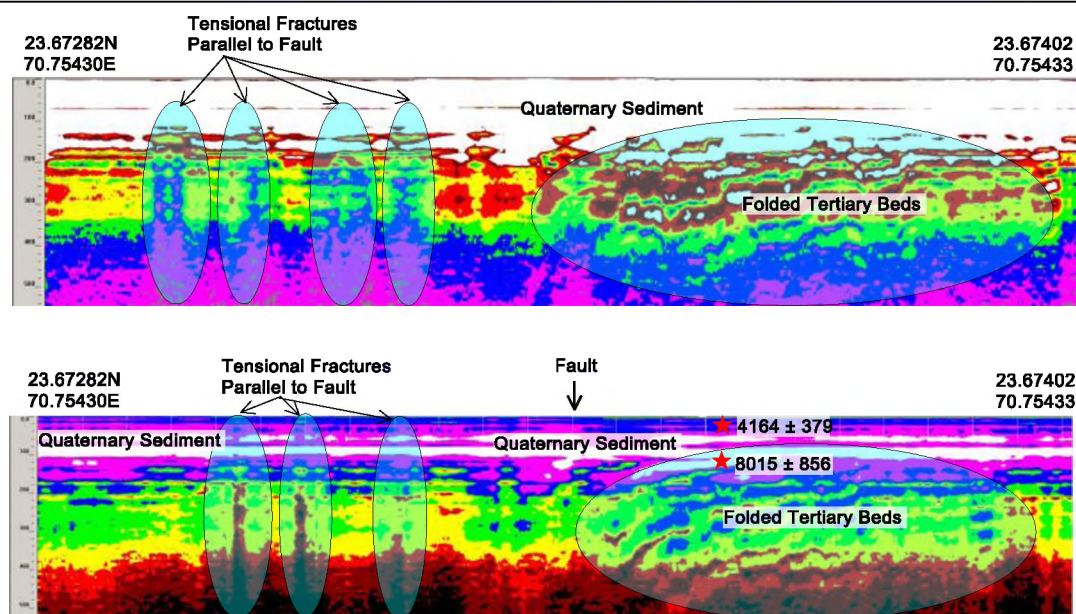


Fig: 4.7.2: 2D GPR image of Gedi Fault zone.

Table 4.7.1: Table showing optical ages and dose rates of samples.

Sample	U (ppm)	Th (ppm)	K (%)	WC (%)	CR rate (mGy/ka)	Dose rate (Gy/ka)	Palaeo dose (Gy)	OD(%)	Model	Age (years)
GF1	2.5 ± 0.4	15.8 ± 1.4	1.08 ± 0.09	1.5	193	2.9 ± 0.2	11.9 ± 0.7	31	MAM3	4164 ± 379
GF2	1.4 ± 0.2	4.8 ± 0.7	0.45 ± 0.05	7.8	174	1.2 ± 0.1	9.3 ± 0.7	46	MAM3	8015 ± 856
GF3	1.7 ± 0.4	13.3 ± 1.3	0.52 ± 0.06	5.2	194	1.9 ± 0.2	0.14 ± 0.03	133	MAM3	74 ± 16
GF4	2.2 ± 0.4	15.1 ± 1.3	0.61 ± 0.07	4.7	171	2.2 ± 0.2	2.3 ± 0.1	17	MAM3	1050 ± 93

#### 4.7.2 Identification of Monoclinial Flexure using 2D Gravity profile across Kachchh Mainland Fault (KMF) through Lodai

(Girish Ch. Kothiyari, Siddhartha Dimri, Rakesh K Dumka and B. K. Rastogi)

We have collected 36km long gravity data across the KMF, from Bhuj to Lodai using CG-5 auto gravimeter on average one kilometer interval. A number of bases have been established at 10 km spacing on permanent structures. The nearest base in the area was Bhuj which is tied with IGSN 1971 of Morelli et al., (1974). The tidal effect has been removed using Longman's (1959) algorithm. A geodetic survey in Real time Kinematic (RTK) mode has been used to achieve the accuracy of 1 mGal in Bouguer anomaly during elevation correction. The Kachchh region shows terrain effects upto 0.3 mGal (Chandrasekhar 2004), hence topographic effects has been calculated. The residual Bouguer anomaly along the profile (Fig. ) is obtained by subtracting the regional field from the observed field. The profile is passing over a gravity gradient may be a faulted basement. These gradients depend on the density contrast across these faults and their extents. The 2.5 D crustal model is prepared (Fig. ) using constraints from the 20 km long 2-D cross-section along Bhuj-Radhyampur-Habay-Lodai. The depth of the basement has been calculated using the bulk density of sediments. The residual gravity field of Quaternary, Mesozoic and basement rocks is computed with bulk densities of 2100, 2450 and 2700 kg/m<sup>3</sup> respectively using Geo-Soft oasis montaj 7.3. The gravity model shows an uplift of 3 to 4 km of basement across the gravity gradient (Fig). uplift is coincided with E-W trending KMF. The interpreted



model shows that the fault is dipping with 30-35° towards south. The gravity high at Lodai and adjacent area is caused by uplift of basement along KMF. This model section also shows that the thickness of Quaternary sediment is higher towards footwall of KMF. Towards the hanging wall of KMF the Mesozoic rocks are gently dipping towards south. The hanging wall movements towards north give rise gentle folding of Mesozoic rocks. The monoclonal flexure shear zone within the folded zone cause uplift and tilting of rocks in the footwall block. The KMF is well exposed in interpreted 2D gravity model indicated by abrupt folding of beds near northern margin.  
 ???

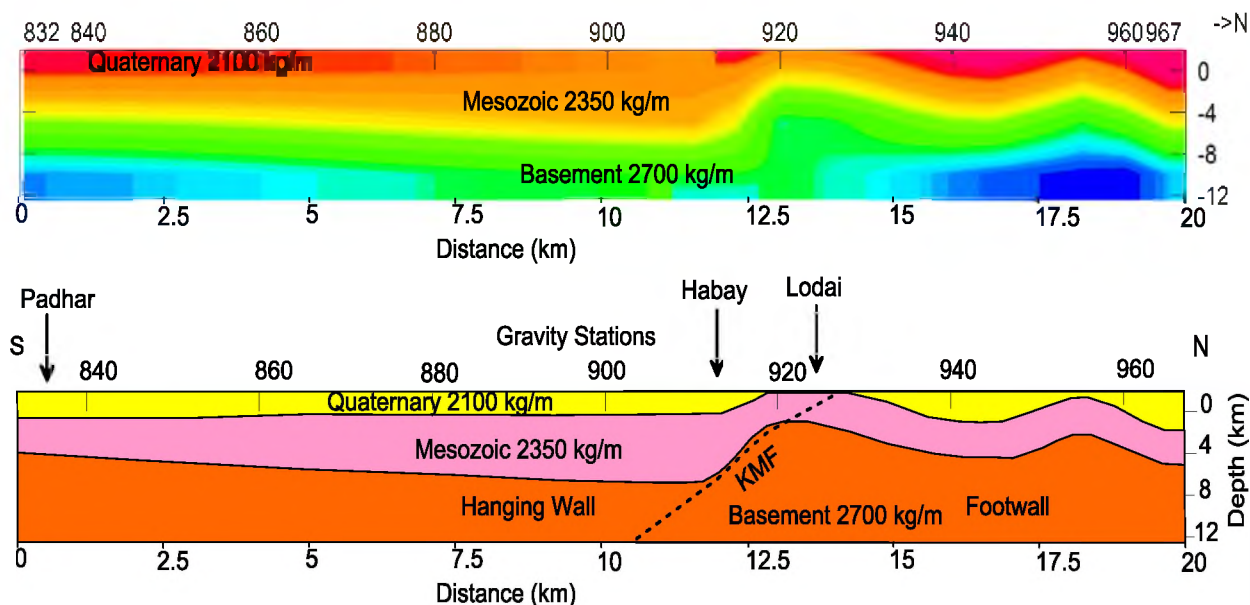


Fig. 4.7.3: 2D gravity picture across Kachchh Mainland Fault (KMF) showing development of monoclinial flexure towards footwall block

#### 4.7.3 Evidence of tectonic inversion along Kachchh Mainland Fault zone, Gujarat, India (Girish Ch. Kothyari, Rakesh Dumka and B. K. Rastogi)

The Kachchh Mainland Fault (KMF) is a major E–W trending seismically active fault of the Kachchh rift basin. The neotectonic investigation has been done south of KMF in its central part near Lodai, where the expression of north facing active fault scarp is visible. The fault trace is identified during our CORONA satellite photo interpretation and later verified in the field (Fig. 4.7.4). The scarp runs in E–W direction and dislocates major geomorphic units. The northward slope of KMF zone is controlled by north flowing streams shows rapid incision within the fault zone. The fluvial sediments were deposited toward the hanging wall as well as towards footwall of faulted blocks were streams become wider. These deposits comprises coarse as well as fine gravels, sand and aeolian deposits. Maurya et al, 2012 believe that the Quaternary sediments of the KMF zone show three major aggradation phases viz. (a) coarse and fine grained colluvio-fluvial sediments, (b) debris flows deposits and (c) alluvial fans. Alluvial fans associated with KMF are major geomorphic units witness to its active tectonism in the Late Quaternary (Fig. 4.7.4). These alluvial fans were probably formed due to sudden confinement of the river as they cross the KMF. These fans are composed of sub angular to rounded fragments of Mesozoic rocks with alternate bands of fine to medium sand. Towards the north, the alluvial fans are truncated due to neotectonic movement along the KMF. In the area the KMF is right laterally displaced by a NE–SW trending fault.

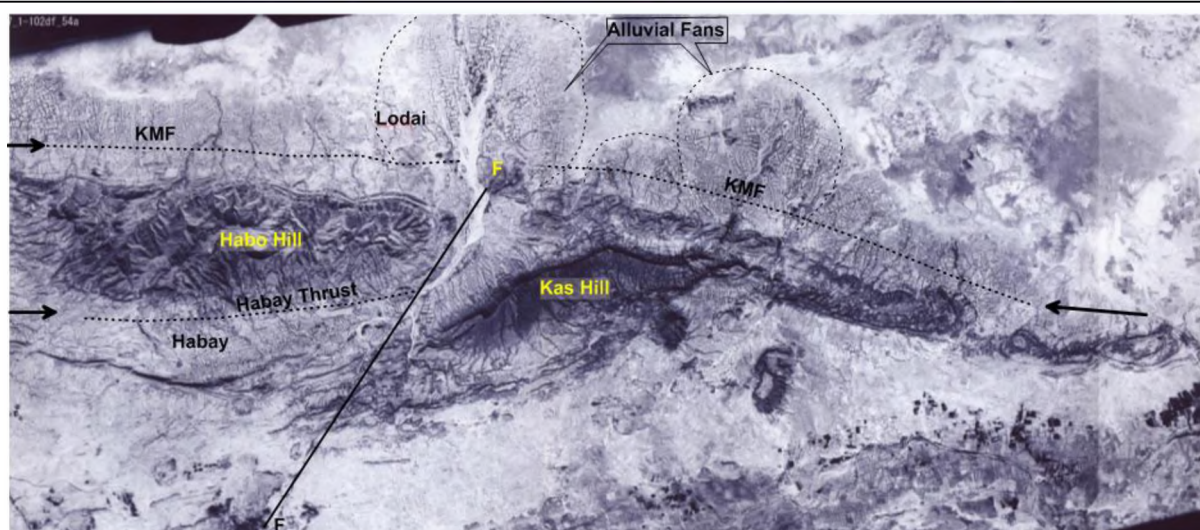


Fig. 4.7.4: CORONA satellite photograph of Lodai and adjacent areas in KMF zone. Arrows represent trace of active faults

From the examination of CORONA satellite stereo pair examination we identified an E-W scarp near Habay around 5 km south of Kachchh Mainland Fault (KMF). A section has been opened across the fault to show the nature of fault. In the exposed section three major formations have been identified. The oldest bed (unit 1) in the exposure is highly sheared and fractured shale of Jhumara Formation. The shale unit is overlain by unit 2 which is fine grained marl of Jhumara Formation. The unit 2 is finally overlain by Quaternary sediments. The geological formations in the area are gently dipping towards south. These units are broken by a E-W trending low angle  $10^{\circ}$ - $15^{\circ}$  south dipping thrust, we name this thrust as Habay thrust. We could identify two major phases of tectonic movements along this thrust. During First phase (F1) of tectonic movement, faulting has taken place within the rocks and unit 1 and unit 2 of Jhumara Fm. has been displaced. The Quaternary sedimentation starts after tectonic event (F1). After deposition of Quaternary sediments the second phase (F2) of tectonic activity takes place. During F2 activity the fine grained marl of Jhumara Fm is dragged over the Quaternary sediment.

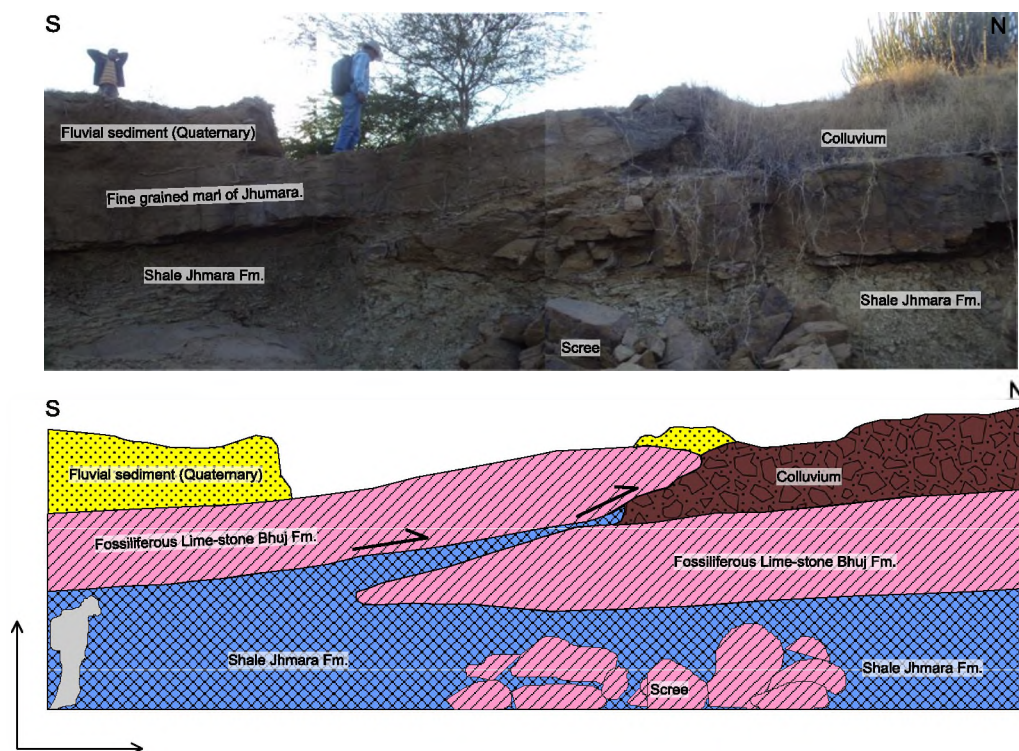


Fig. 4.7.5: Photomosaic of Habay thrust, below the sketch of active fault. The fault is dipping towards south by  $10^{\circ}$ - $15^{\circ}$  shows net 4.5 m displacement.



The trench investigation by Malik et al., (2008) also shows active nature of KMF during Holocene. They identified active fault scarp near Lodai Village just 5 km North of our site. Malik et al (2008) believe that the KMF zone has experience of major three phase of tectonic movement during Holocene. They found that during the latest phase of tectonic movement young sediments were deformed and displaced. In our study near Habay we observed that the cumulative displacement of Habay thrust is 4.5m. The older phase (Pre Quaternary) of tectonic movement F1 shows around 3 m displacement within the rocks of Jhumara Formations. The younger phase of tectonic movement shows net 1.5 m slip along the Habay thrust.

#### **4.7.4 Implications of Fossil Valleys and Associated Epigenetic Gorges in parts of the Central Himalaya**

*(Girish Ch. Kothiyari)*

Conventionally, epigenetic gorges in tectonically active orogen are attributed to the bedrock geometry and the original valley configuration. Since they are invariably associated with fossil valleys containing appreciable sediment succession, it is argued that the older river course was abandoned due to accelerated sedimentation (landslides or widespread fluvial aggradations) as a result of which rivers were forced to occupy the new course (epigenetic gorge). Thus it can be suggested that fossil valleys and the gorges are the outcome of the climate-tectonic interaction. The present study is therefore, undertaken in the monsoon dominated and tectonically active inner Lesser Central Himalaya to understand the role of climate and tectonics in their evolution. Preliminary observations in three river valleys indicate that their locations (epigenetic gorges) are structurally controlled (independent of lithology). However, the abandonment of old river course (fossil valleys) was caused due to the accelerated sedimentation (climatically induced). Chronology of the fill sediment indicates that old river course abandonment occurred during the early Holocene climatic optimum (15–9 ka) whereas the incision leading to the epigenetic gorge formation began after 9 ka.

In terms of processes point of view, (i) prior to valley fill aggradation (in the present day fossil valleys), the rivers were sediment limited, thus the ambient stream power was used to incise the channel. This probably happened prior to 15 ka (ii) when the rivers did not migrate laterally to its present course (epigenetic gorge), as observed in case of landslide dammed river courses. Had it been the case, the prominent rocky spur flanking the epigenetic gorges would have been eroded away. (iii) We hypothesize that while the present day fossil valleys being aggraded during 15 ka to 9 ka (Figure 4.7.6), there existed a subsidiary channel, as the valley began to clog with the sediments, and the hydrological condition dwindled, river was forced to occupy the subsidiary channel (least resistance path) from its upstream course after ~ 9 ka and since then it is continuously incising (Figure 4.3.6). The epigenetic gorges are 15 m to 43 m deep and are separated by a rocky spur. Assuming that rivers occupied the present course, after ~9 ka (discussed above) the estimated incision rate of these gorges are 1.66 mm/a for monsoon fed Kosi river. Which is significantly low when compared to the monsoon plus glacial fed Pindar river (4.77 mm/a) and the Alaknanda river (3.33 mm /a). The higher incision rates accord well with independent estimates obtained from the glacial and monsoon fed Alaknanda river catchment.

Finally the fact that epigenetic gorges are invariably associated with the sediment filled fossil valleys in the study area, it can be suggested that river's ability to incise the bed rock was not limited by the strength of the rock. This indicates that the rivers in which these kinds of epigenetic gorges forms are transport limited, as opposed to detachment limited, where incision into bedrock is regulated by a river's ability to detach and abrade the bedrock channel bed (Howard, 1994, Wipple and Tucker, E. G. 2002).

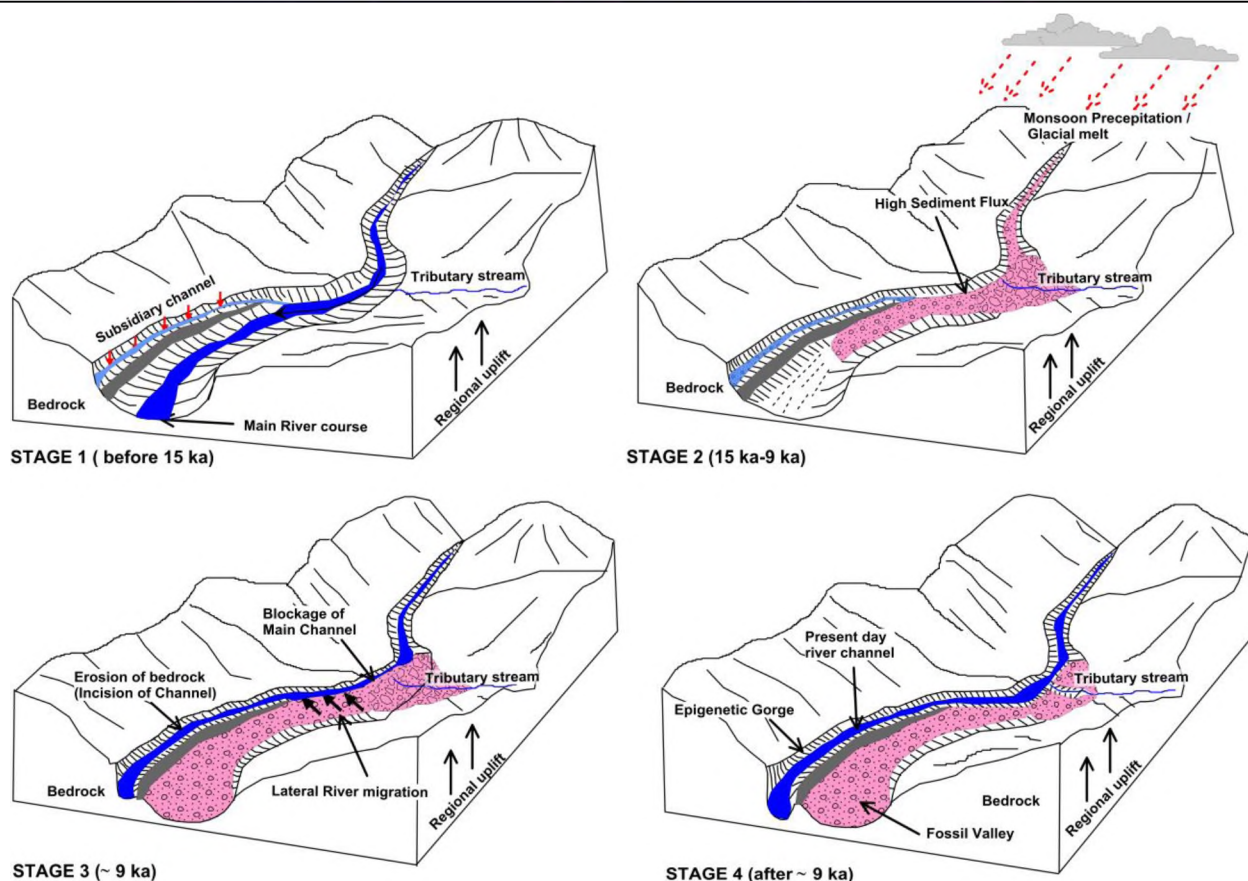


Fig. 4.7.6: Three dimensional block diagram showing evolutionary stages of fossil valleys and associated gorges in the study area. Stage 1 shows the position of river channel before 15 ka. Note the subsidiary channel towards the left bank of river. Stage-2 major valley fill aggradation occurred during early Holocene climatic optimum (15 ka - 9 ka). Stage-3 enhanced sedimentation led to the lateral river migration ~9 ka and occupied the subsidiary channel. Stage-4, present river course is flowing through the gorge section

### References:

1. Antolik, M., Dreger, D., 2003. Rupture process of the 26 January 2001 Mw7.6 Bhuj, India, earthquake from teleseismic broadband data. *Bull. Seismol. Soc. Am.* 93, 1235–1248.
2. Barnard, P. L., Owen, L. A., Sharma, M. C. and Finkel, R. C., Natural and human-induced landsliding in the Garhwal Himalaya of northern India *Geomorphology*, 2001, 40, 21–35.
3. Howard, A. D., A detachment-limited model of drainage basin evolution. *Water Resources Research*, 1994, 30, 2261–2285.
4. Juyal, N., Sundriyal, Y. P., Rana, N., Chaudhary, S. and Singhvi, A. K., Late Quaternary fluvial aggradation and incision in the monsoon dominated Alaknanda valley, Central Himalaya, Uttarakhand, India. *Journal of Quaternary Science*, 2010, 25, (9999), 1-13
5. Pollitz, F.F., 1997. Gravitational viscoelastic postseismic relaxation on a layered spherical Earth. *J. Geophys. Res.* 102, 17921–17941.
6. Ray, Y. and Srivastava, P., Widespread aggradation in the mountainous catchment of the Alaknanda Ganga River System: timescales and implications to Hinterland foreland relationships. *Quaternary Science Reviews*, 2010, 29, 2238-2260.
7. Whipple, K. X. and Tucker, G. E., Implications of sediment-flux dependent river incision models for landscape evolution. *J Geophysical Research*, 2002. 107 (B2). DOI: 10.1029/2000JB000044.



#### 4.7.5 Geochronological studies to reconstruct seismicity and climate along bedrock river of Katrol Hill Range, Kachchh.

*Falguni Bhattacharya and B.K. Rastogi in collaboration with Dr. Navin Juyal (PRL, Ahmedabad), M.G. Thakkar (K.S.K.V. Kachchh University, Bhuj) and R.C. Patel (Kurukshetra University)*

Bedrock rivers are particularly important to reconstruct tectonic and climatic interactions as incision into bedrock and transport of sediment is controlled by the rates at which (i) base-level signals (generated by tectonic, eustatic or climatic forcings) are transmitted through the landscape; and (ii) sediment is delivered from highlands to basins. Towards reconstructing tectonic and climate interactions, a channel-fill section along Khari river of Kachchh has been investigated. Khari River originates from Katrol Hill Range and debouching through the Banni Plains drains into the Rann (Fig.4.7.7). The tributary channel along which channel-fill section is investigated is perpendicular to the Khari River. The Khari River has incised ~6 m of the channel fill sediment and 3 m of the Mesozoic bedrock belonging to the Bhuj Formation.

Using the conventional sedimentological criteria (structure and texture), a total of six sedimentary units have been identified (Fig. 4.7.8). The erosional contact between the bedrock and the thin channel fill sediment (~6 m) suggests that sedimentation occurred on beveled Mesozoic bedrock. The deposition of unit-1 indicates that the initiation of channel fill sedimentation occurred under hyper-concentrated sediment gravity flow. The overlying parallel-laminated miliolite in unit-2 (both endurated and friable) suggest their deposition under aqueous condition. The overlying mm to cm thick parallel laminated friable miliolites along with desiccated clay lamina (unit-3) can be suggestive of low energy flood plain environment. A weakening of the hydrological condition can be suggested by the occurrence of angular ferruginous sandstone lithoclasts embedded in miliolite matrix (unit-4). The overlying weathered miliolite (unit-5) indicate prolonged sub-aerial exposure following their deposition, implying subdued water activity. The poorly sorted and platy clast dominated topmost gravels (unit-6) indicate their transportation by a combination of granular and fluid flow- a characteristics of debris.

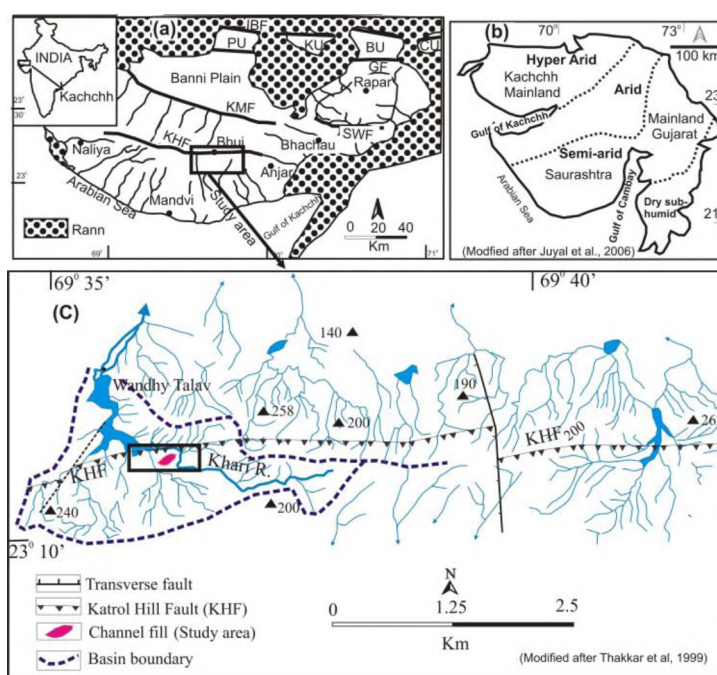


Fig. 4.7.7: (a) Map of Kachchh Mainland. Kachchh Mainland Fault (KMF), Katrol Hill Fault (KHF), South Wagad Fault (SWF), Island Belt Fault (IBF) and Gedi Fault (GF). Pachcham Uplift (PU), Khadir Uplift (KU), Bela Uplift (BU). Note that KHF act as drainage divide between the north and south flowing rivers. (b) The climatic zones of Mainland Gujarat, Saurashtra and Kachchh (c) The drainage map of the upper Khari basin, channel fill deposits lie on the hanging wall of the KHF.

Detailed sedimentology supported by optical chronology (Table-1a and 1b) suggests that the terrain witnessed two major events of enhanced seismicity. The older event which predates 20 ka was responsible for the channel incision under weak monsoon. This was followed by a phase of relative landscape stability during which the channel was aggraded by the sediments that were transported from the hinterland and were dominated by the fluviably reworked miliolites. Monsoon reconstruction based on the sedimentary structures and textural attributes of the fill sediment suggests gradual improvement of the southwest summer monsoon after 20 ka. This was followed by a phase of intensified monsoon during 9 to <7 ka. A gradual decline in monsoon strength and a renewed phase of seismicity after 7 ka was observed which seems to continue till present (Figs. 4.7.8 and 4.7.9).

These are the first chronologically constrained events of channel aggradation and incision from the upland reaches of the KHF implying that the channel aggradation occurred during the early Holocene strengthened monsoon whereas the incision was dominated by the tectonics during periods of reduced monsoon activity. The study demonstrates a close correspondence between the summer monsoon and channel aggradation. Most importantly, the present study has chronologically constrained two major events of enhanced seismicity (tectonic uplift). The older tectonic activity pre date 20 ka whereas the younger activity began sometime after 7 ka which probably continues till today.

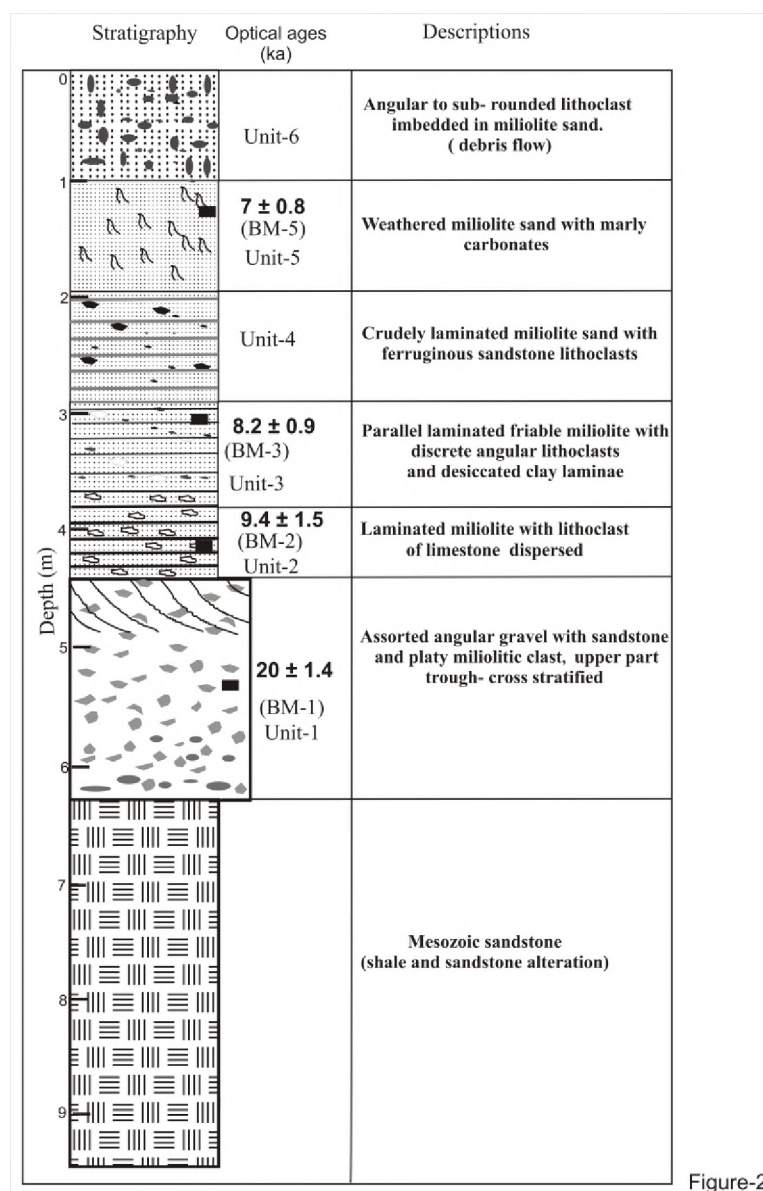


Fig. 4.7.8: Detail stratigraphy of the channel fill deposit. The ages obtained are using the minimum + 2\* sigma.

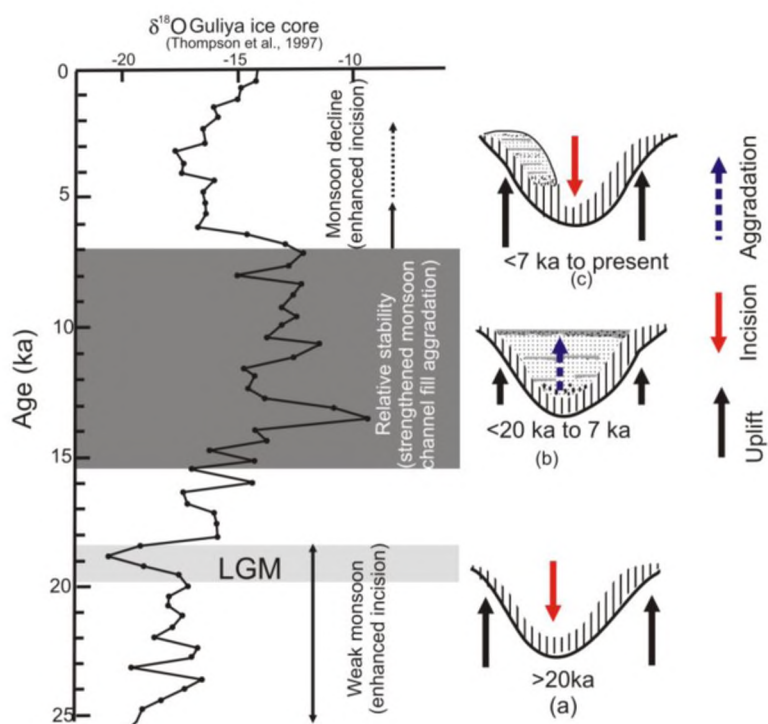


Fig. 4.7.9: Temporal changes in tectonic activity and channel fill aggradation during the last 20 ka. A close correspondence of the monsoon based on present study with that of the Guliya ice core data from Tibet (Thompson et al., 1997) indicate that fluvial processes of Kachchh region were intimately associated with the southwest summer monsoon variability.

Table 4.7.2: Details of uranium, thorium and potassium concentrations, cosmic ray dose rate and annual dose rate estimation of the samples analyzed in the present study. Water content used is  $10 \pm 2\%$

Sample No.	U (ppm)	Th (ppm)	K(%)	Cosmic Ray Dose Rate ( $\mu\text{Gy/a}$ )	Dose Rate (Gy/ka)
BM-1 (Unit-1)	$2.44 \pm 0.04$	$13.42 \pm 0.26$	$1.19 \pm 0.02$	$88 \pm 17.6$	$2.5 \pm 0.09$
BM-2 (Unit-2)	$2.53 \pm 0.05$	$14.81 \pm 0.29$	$0.77 \pm 0.01$	$103 \pm 20.6$	$2.2 \pm 0.08$
BM-3 (Unit-3)	$2.89 \pm 0.05$	$19.63 \pm 0.39$	$0.96 \pm 0.02$	$120 \pm 24.0$	$2.8 \pm 0.10$
BM-5 (Unit-5)	$3.18 \pm 0.06$	$18.12 \pm 0.36$	$1.83 \pm 0.04$	$169 \pm 33.8$	$3.6 \pm 0.10$

Table 4.7.3: Palaeodoses (De) obtained using the CAM, MAM and minimum plus two sigma and the ages obtained by these methods. In the discussion we have used the ages obtained by Minimum plus two sigma.

Sample No.	CAM (De in Gy)	MAM (De in Gy)	Min +2*sigma (De in Gy)	CAM (Age in ka)	MAM (Age in ka)	Min + 2*sigma (Age in ka)
BM-1 (Unit-1)	$69 \pm 2.83$	$63 \pm 1$	$49.35 \pm 2.83$	$27.8 \pm 1.5$	$25.4 \pm 1.03$	$19.9 \pm 1.4$
BM-2 (Unit-2)	$39 \pm 3.28$	$20 \pm 4$	$20.95 \pm 3.28$	$17.4 \pm 1.6$	$8.9 \pm 1.82$	$9.4 \pm 1.5$
BM-3 (Unit-3)	$35 \pm 2.52$	$19 \pm 1$	$23.00 \pm 2.52$	$12.5 \pm 1.0$	$6.8 \pm 0.4$	$8.2 \pm 0.9$
BM-5 (Unit-5)	$48 \pm 2.85$	$25 \pm 5$	$25.27 \pm 2.85$	$13.4 \pm 0.9$	$7.0 \pm 1.4$	$7.1 \pm 0.8$

(Reference cited: Falguni Bhattacharya, B.K. Rastogi, Mamata Ngangom, M.G. Thakkar, R.C. Patel (2013). Late Quaternary climate and seismicity in the Katrol Hill Range, Kachchh, Western India, Journal of Asian Earth Sciences, In Press. <http://dx.doi.org/10.1016/j.jseaes.2013.04.030>)



#### 4.7.6 Compared to the Gedi Fault, the North Wagad Fault seems to be more active

*Falguni Bhattacharya, B.K. Rastogi*

Recent studies suggest that the eastern Kachchh is a potential zone for major earthquakes in the near future. Particularly, the E-W trending faults are considered capable of generating large magnitude earthquakes is further indicated by the recent concentration of the earthquake shocks which show two prominent clustering around west and north of the Wagad upland. In view of this, the conventional morphometric analyses of a terrain bounded by the E-W trending North Wagad Fault (NWF) and the Gedi Fault (GF) has been undertaken to ascertain the influence of seismicity in the evolution of the drainage basin. The study suggests that the fifth order drainage basins responded to the seismicity associated with both the NWF and GF. However, compared to the GF, the NWF seems to be more active. In addition to this, based on the stream morphology, we could identify two lineaments trending N-S and E-W. The former appears to be associated with the activity along the Manfara Fault (MF) whereas the later seems to be the splays of the NWF. Further, a preferential westward shift of the streams suggests left lateral displacement of the E-W trending faults. Overall it can be suggested that the terrain is in juvenile stage implying tectonic instability.

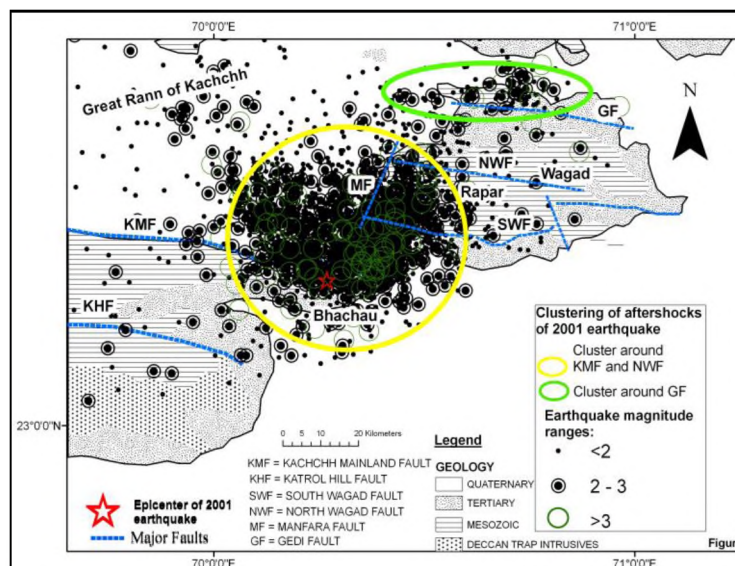


Fig. 4.7.10: Map showing the distribution of earthquake epicenters in the NE Kachchh. Note two major clustering between KMF and NWF and around GF. Source: Earthquake data obtained from ISR, Gandhinagar catalogue (2006-2010).

(Reference cited: Falguni Bhattacharya, B.K. Rastogi, Girish Kothiyari (2013). Morphometric evidence of seismicity around Wagad and Gedi Faults, eastern Kachchh, Gujarat, India, Journal of Geol Soc of India, vol 81, pp 113)

#### 4.7.7 Quaternary reactivation of South Tibetan Detachment System

*Falguni Bhattacharya (in collaboration with Naresh Rana (HNB Garhwal University), Dr. Navin Juyal (PRL, Ahmedabad)*

The present study is an attempt towards the suggestion that movement along the STDS did not end in the middle Miocene but persisted episodically or continuously into the Quaternary. Based on the occurrence of the Soft Sedimentary Deformation Structures (SSDS) in relict proglacial lake sediments and optical chronology, we demonstrated that the STDS was active during the late Quaternary (<20 ka). This study was undertaken in the Dhauli Ganga, Gori Ganga and Kali Ganga valleys of Uttarakhand Himalaya. Three lakes along these valleys have preserved the SSDS in the form of. *fragmented and convoluted laminae, water escape structures, flame structures, normal listric faults*) separated by undeformed layers. The optical chronology suggests that majority of the events in the three lakes occurred during 13.5 ka and 17 ka which implies that they were triggered by common earthquake. Based on a global data curve on known earthquake magnitudes and the distance of SSDS from the epicenter of shallow and deep-focused



earthquakes in various tectonic and sedimentary settings, the unknown earthquake magnitude is estimated in the present case to be between Mw 6.5 and >7 Mw having an epicenter in the vicinity of the STDS .

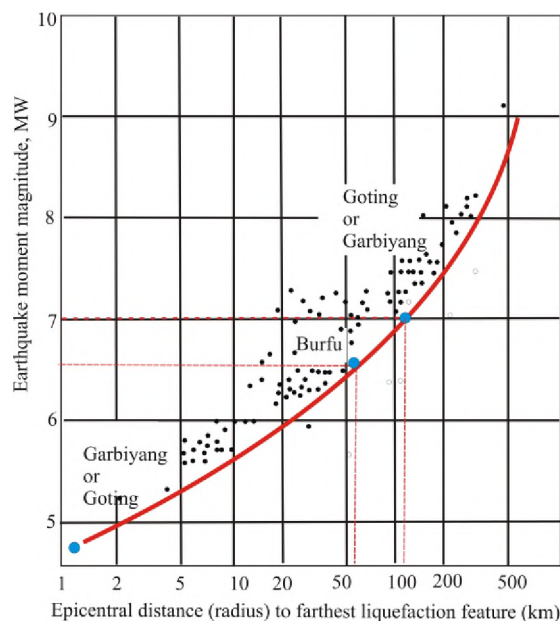


Figure 4.7.11.: Global data curve on known earthquake magnitudes and the distance of SSDS from the epicenter of shallow and deep-focused earthquakes in various tectonic and sedimentary settings

(Reference cited: Naresh Rana, Falguni Bhattacharya, N. Basavaiah, R.K. Pant, Navin Juyal (2013). Soft sediment deformation structures and their implications for Late Quaternary seismicity on the South Tibetan Detachment System, Central Himalaya (Uttarakhand), India, Tectonophysics 592,165–174)

#### 4.7.8 Early Holocene fluvial activity along the semi arid Mahi river basin, Guj.

(Falguni Bhattacharya in collaboration with Alpa Sridhar and L.S.Chamyal of M.S.Univ., Baroda and A.K.Singhvi of PRL, Ahmedabad)

Paleocompetence analysis and paleodischarge estimation techniques are applied to a late Pleistocene to early Holocene gravel terrace in the Mahi river basin, western India. Terrace sedimentology, comprising gravels overlain by sand lithofacies suggests a gradual change in paleohydrological conditions marking a switch from braided to meandering fluvial styles. The discharge values for the gravel bed-forms based on the clast size and the cross bed thickness are estimated between  $\sim 150\text{--}180 \text{ m}^3\text{s}^{-1}$  comparable with the present day observed values albeit with a much higher competence. Results indicate that fluvial aggradation occurred under low discharge conditions with intermittent high discharge events depositing longitudinal gravel bars. The incision of these gravels bars and the formation of terraces can be attributed to the higher discharge regime post 9.2 ka. The study further indicates that whereas the aggradation of the gravel terrace during the early Holocene was controlled by the large sediment flux, the incision that followed was in response to the increase in the discharge and competence of the river flow.

(Reference cited: Alpa Sridhar, L.S.Chamyal, Falguni Bhattacharya, A.K.Singhvi (2013) Early Holocene fluvial activity from the sedimentology and paleohydrology of gravel terrace in the semi arid Mahi river basin, India, Journal of Asian Earth Sciences 66, 240-248).

## CHAPTER 5

## EARTHQUAKE HAZARD ASSESSMENT

## 5.1 FREQUENCY CHARACTERIZATION MAP OF KACHCHH, GUJARAT

(A. P. Singh, Navaneeth Annam and Chinmayee Sahoo)

The Kachchh region is the second most seismically active regions in India after Himalaya. One of the disastrous Indian earthquakes of the new millennium was a Bhuj earthquake of 26 January 2001, which caused around 14,000 casualties. The main reason for such huge casualties is low earthquake awareness and poor construction practices. Hence, an increase in the knowledge and awareness of local authorities and decision makers for possible consequences of a large earthquake, based on improved seismic hazard assessment and realistic earthquake risk scenarios is required to mitigate the damage due to earthquake. The natural predominant ground frequency which is an important parameter to characterize local site effects has been determined from local earthquake data and the measurements of ambient vibrations at Kachchh in the state of Gujarat (Fig 5.1.1), a significantly active intra-plate earthquake region in India. The horizontal-to-vertical spectral ratio (HVSr) technique has been applied to detect the predominant frequency at the sites. The ambient vibration measurements were conducted at nearly 100 sites in Kachchh for 1 hour in the continuous mode of recording with a 100 samples per second. In order to maintain consistency we have validated the estimated predominant frequency of the ambient noise and the earthquake data recorded at 10 permanent/temporary BBS stations in the region. The resonance frequencies obtained in the experiments were related to the thickness of the sediments which are deduced by other geophysical and geological methods. It has been observed that geological time period has significant effect on predominant natural frequency of the ground. The predominant frequency of the measured ambient vibrations were found to vary at the sites belonging to Quaternary period from 0.2 to 0.8 Hz, Tertiary period 1.0 and 1.5 Hz, Cretaceous period 0.5 to 1.8 Hz, and Jurassic/Mesozoic period 1.3 and 2.0 Hz (Fig. 5.1.2). However, at the Deccan Trap sites it varies from 1.8 to 2.3 Hz. The difference of the predominant frequencies between the hard rocks and soft soil sites is distinct, and it depends heavily on the surface soil conditions. We have presented the detailed map of the predominant frequency distribution in the Kachchh region. The map shows important characteristics which need due consideration in studying seismic risk and a mitigation.

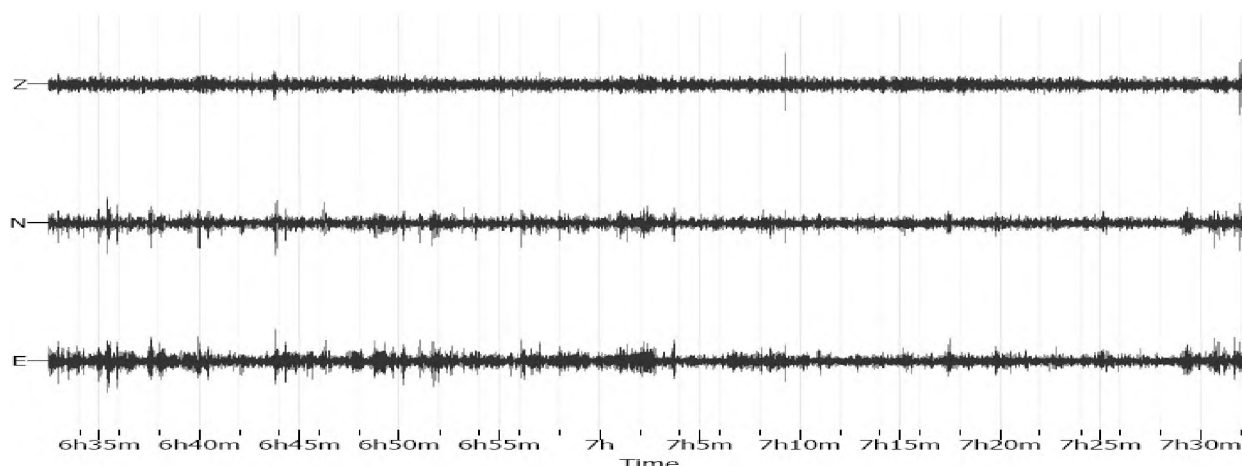


Fig. 5.1.1: A sample three-component (Z-Vertical, N-North and S-South) ambient vibration data record for 60 minutes at Bhuj site

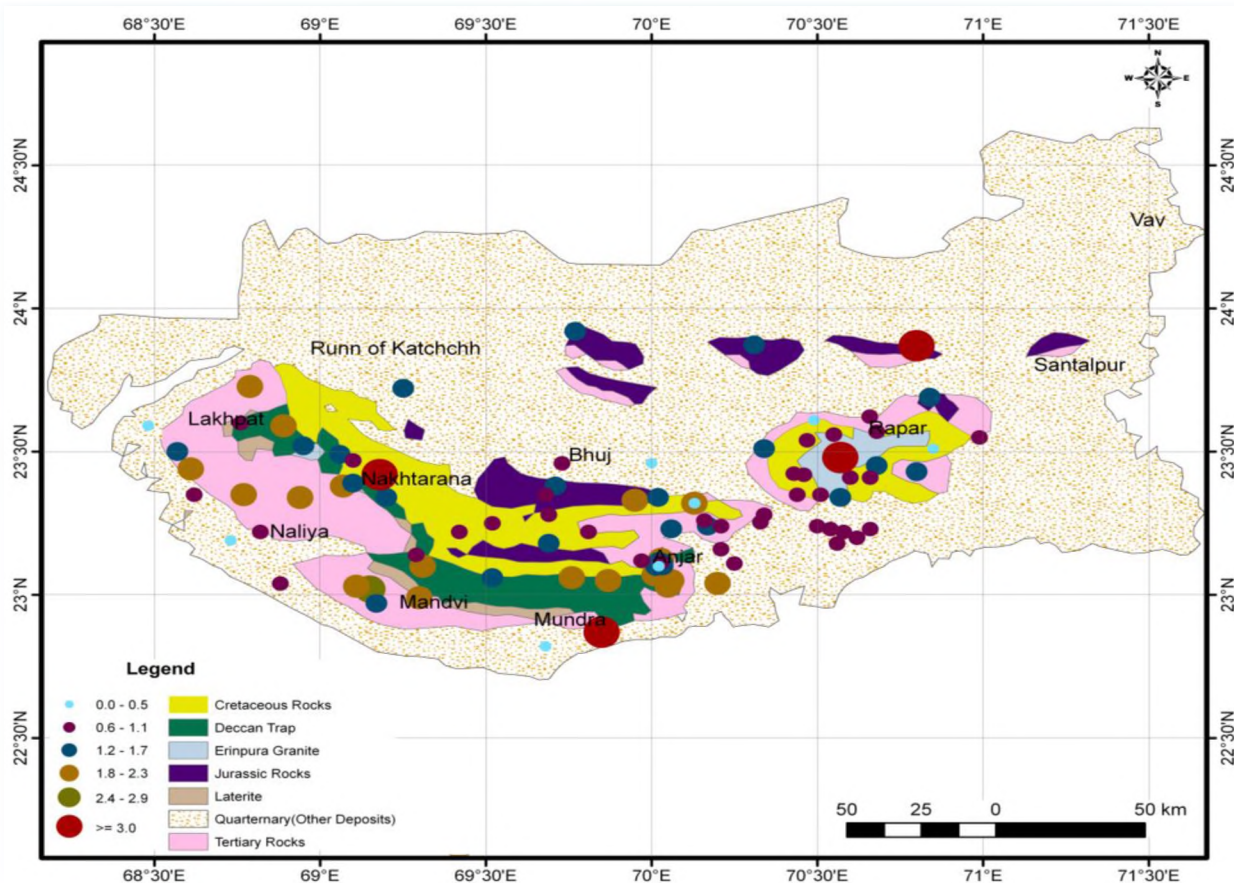


Fig. 5.1.2: Map of the predominant frequency over the subsurface geology in and around the Kachchh region

## 5.2 ASSESSMENT OF VULNERABILITY OF INSTALLATIONS NEAR GUJARAT COAST VIS-À- VIS SEISMIC DISTURBANCES

(B. K. Rastogi, A.P. Singh, Vasu Pancholi, Ashish Bhandari, Kapil Mohan, Collaboration with Prof. Ramancharla Pradeep Kumar, IIIT, Hyderabad)

### Work done during the period of 2012:

1. Site Response studies using earthquakes and ambient vibrations at *Dwarka, Mundra, Mandvi, Kandla, Jhagadia and Dholera Lakhpata, Jakhau and Sikka*
2. Soil Structure Interaction Studies for two types of buildings *namely rigid support and structure with actual soil base at Kandla port*
3. Inundation modeling for the coastal regions of Gujarat

INTRODUCTION: Gujarat has the longest coastline of 1640 km among the states of India. There are numerous ports, jetties, refineries, chemical industries and multistory buildings. Gujarat coasts are formed by faults which give occasional earthquakes of M6 to 8 (in seismic zones III to V) that can severely damage coastal installations. Any large earthquake can disrupt supplies of essential items like petroleum to whole India. Economic disruption in this region will also affect whole India. Hence, we carry out assessment of vulnerability of installations at the ports along Gujarat coast (Fig. 5.2.1) vis-à-vis seismic disturbances so that remedial measurements could be planned for preparedness.



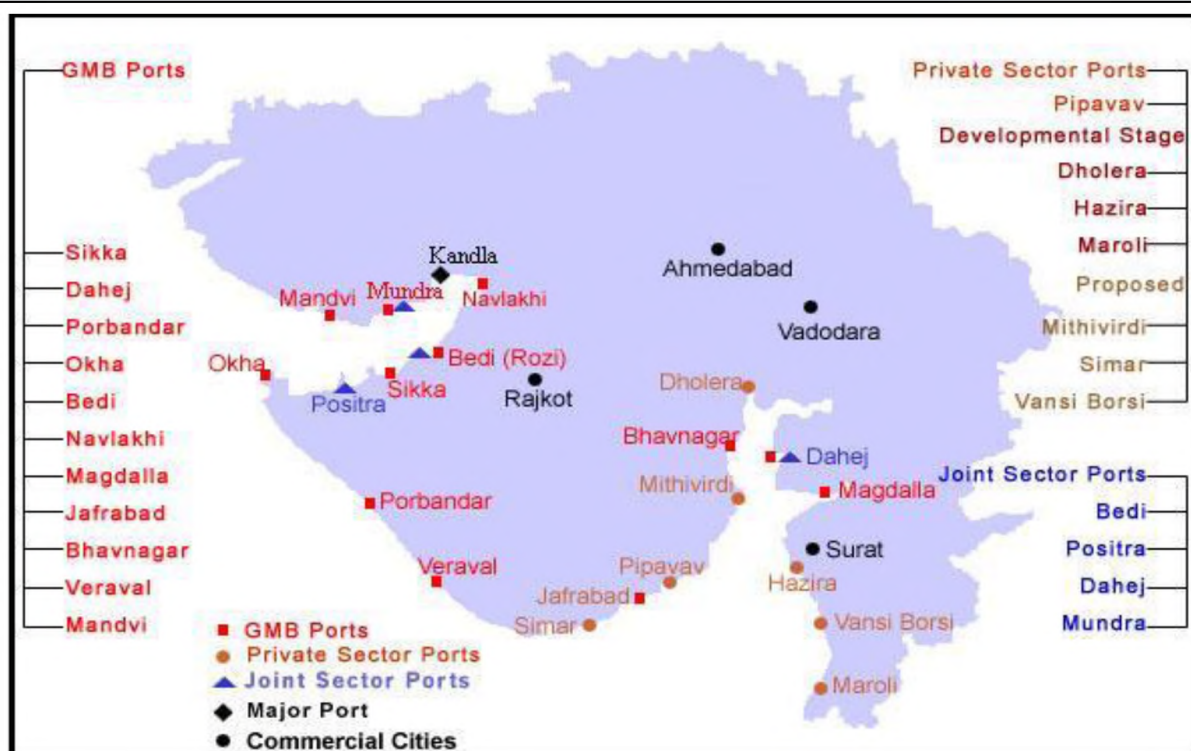


Fig. 5.2.1: Location of ports and jetties along Gujarat Coast

### Site Response in coastal regions of Gujarat

Using Earthquake data: The ISR deployed portable broadband seismographs at 6 sites in coastal regions namely, Dwarka, Mundra, Mandvi, Kandla, Jhagadia and Dholera for site response study. Using local earthquake data recorded at these sites the predominant periods and spectral amplifications are determined using Horizontal to Vertical Spectral Ratio (HVSr) technique (Fig. 5.2.2). Amplifications of 2-7 (max. at Kandla) and resonances frequencies of 2-4 Hz have been observed. For distant earthquakes the resonance frequencies of 0.2 to 0.4 Hz are estimated. The curve at Dwarka is almost flat as for hard rock with small amplification around 4 Hz. Dwarka is covered by Tertiary rocks. The predominant period at Mundra and Dholera is around 3 Hz. The maximum amplification is observed at Kandla of 6-7. At other sites it is 2-4.

### Site Response in and Around the Coastal Regions of Kachchh Using Micro-tremors:

At Dahej, Lakhpat, Jakhau and Sikka, the BBS were installed for few days but no earthquakes were recorded. In view of this, natural ambient vibrations (micro-tremor) data is used for the estimation of site response. Recording was done for 1 h with 100 samples per second using 5Hz seismometers. The horizontal-to-vertical spectral ratio technique has been applied to detect the predominant frequency at the sites (Fig. 5.2.3). The response at Lakhpat is almost flat as it is on Mesozoic rocks. The predominant frequency at Jakhau is 0.2 and 1.8 Hz may be as responses from Deccan Trap/Mesozoic and Quaternary/Tertiary boundaries. At Sikka a lower frequency resonance is at 0.04 Hz which may be from a deep layer or unreliable. The other resonance is at 1.8 Hz which may be from Quaternary/Tertiary boundary. The amplification estimates from micro-tremor are not reliable. Table 5.2.1 gives these results.



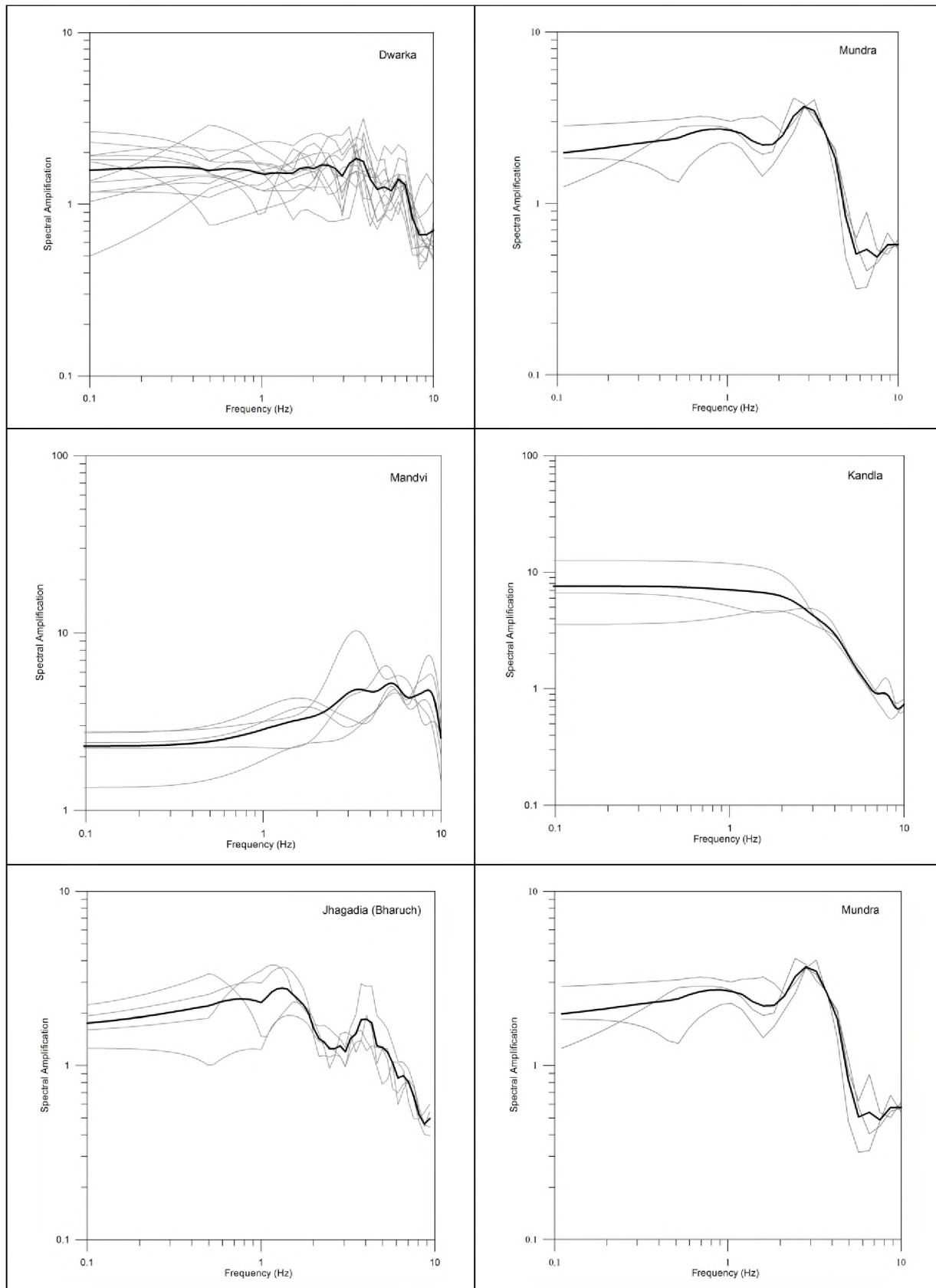


Fig. 5.2.2: Site response using HVSR technique and natural earthquakes at different coastal towns of Gujarat.

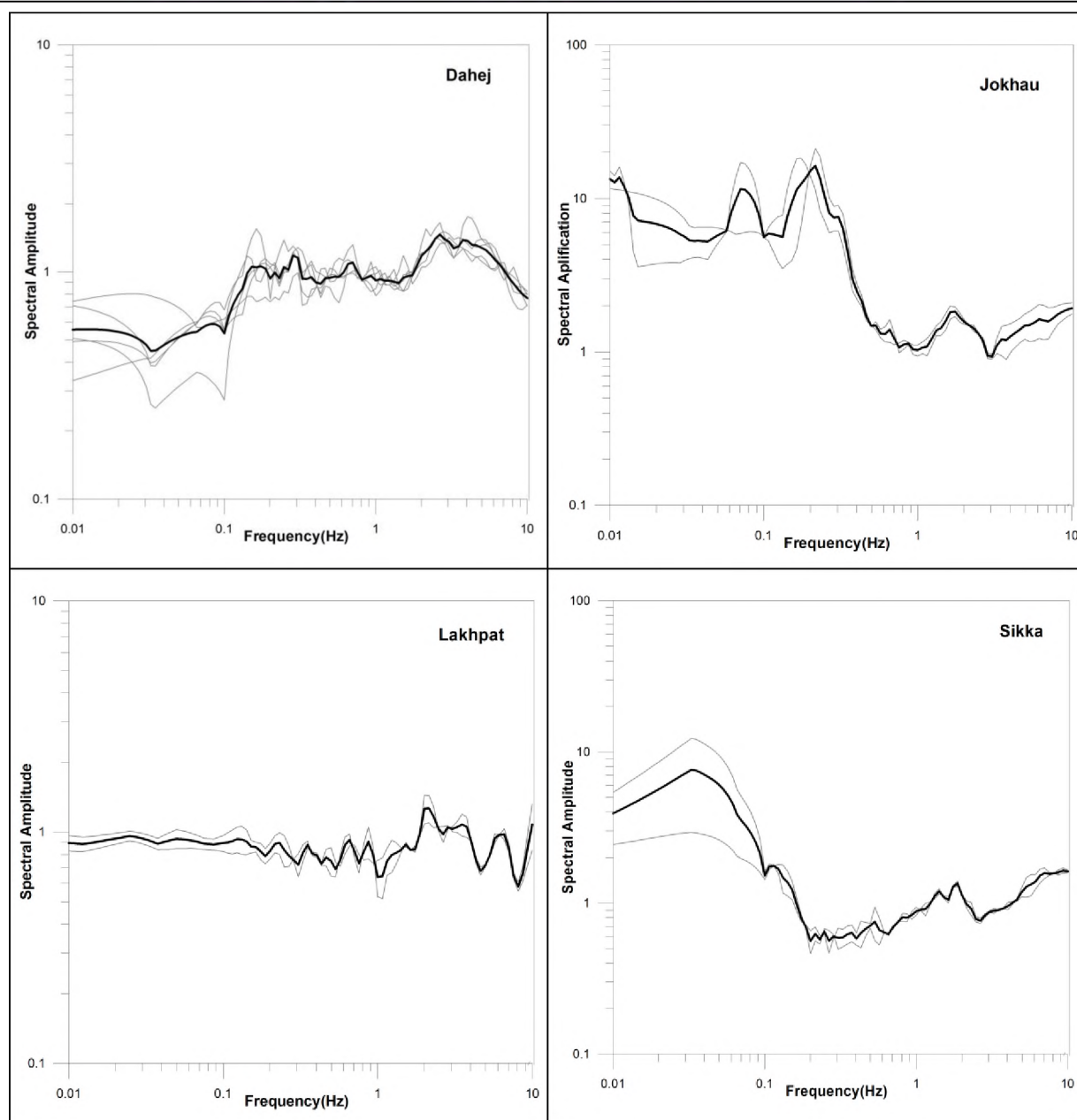


Fig. 5.2.3: Site response using HVSR technique and micro-tremors at different coastal towns of Gujarat.

Table 5.2.1: Geological boundaries from natural earthquakes and Ambient-vibrations at different coastal sites in Gujarat

Site name	Predominant frequency	Depth (m)	Geological Boundary	Source
Dwarka	4 Hz	60	Tertiary-Mesozoic	Earthquake
Mundra	3	80	Quaternary-Tertiary	Earthquake
Mandvi	2	125	Quaternary-Tertiary	Earthquake
Kandla	4	60	Quaternary-Tertiary	Earthquake
Jhagadia	2	125	Quaternary-Tertiary	Earthquake
Dholera	0.3	800	Deccan Trap/Mesozoic	Earthquake
Dahez	3	80	Quaternary-Tertiary	Ambient vibrations
Jakhau	1.8 0.2	150 1250	Quaternary-Tertiary Deccan Trap/Mesozoic	Ambient vibrations
Sikka	1.8	150	Quaternary-Tertiary	Ambient vibrations

Probabilistic Seismic Hazard to Coastal Regions of Gujarat by USGS program

The probabilistic hazard map of Gujarat was prepared from the earthquake catalog prepared by the ISR. The 2% and 10% probability of exceedance (PE) in 50 years which corresponds to 2500 years and 500 years of return period. It can be observed from Figure 5.2.4 that the expected PGA for 2% PE varies between 0.2 to 0.3 g in the western and central coastal belt of Kachchh (Lakhpur, Jakhau, Mandvi and Mundra). Near Kandla port it is between 0.3 to 0.5 g. In most of Saurashtra and south Gujarat coast it is around 0.1 g except at Saurashtra coast bordering Kachchh it is between 0.2 and 0.4 g. Also at Ghogha port and Dholera in Saurashtra and Bharuch and Dahej in mainland it is between 0.1 and 0.3 g.

The probabilistic analysis involves the evaluation of earthquake motion taking into consideration all possible seismic sources possible in and around the region in question. Probability of earthquake occurrence in each seismic source and the seismic motion are calculated and statistically accumulated. The probabilistic analysis of the Gujarat region was carried out using the code made by USGS for national seismic hazard maps. The code was written by Art Frankel (USGS OFR 96-532).

This program assumes that the annual frequencies of every earthquake sources are constant and independent on the time of occurrence of the previous event which is Poisson process. The seismic sources can be a fault source or an area source. In fault source location and magnitudes are known whereas in area source these are not known beforehand. Therefore probabilistic analysis can be carried out either by area source model or by fault source model or both. We have done preliminary analysis using area source model.

The area source model was based on the earthquake catalogue that was compiled by ISR. The data set includes some 200 earthquakes for 162 years (1845-2006). The completeness test of the catalogue of the region was carried out. The catalogue is complete after 1972 for earthquakes equal or larger than 3.0, after 1931 for earthquakes equal or larger than 4.0 and after 1912 for earthquakes equal or larger than 5.0.

The parameters 'a' and 'b' in the Gutenberg-Richter relation were computed using least square fitting method using earthquakes that have occurred in the Gujarat mainland region. The 'b' value for the region is found to be 0.58 and a value is 1.518. The b value was also estimated using the method of Weichert (1980). The 'a' and 'b' values from Weichert method are 1.534 and 0.49 respectively. However for probabilistic analysis 'b' value of 0.58 was taken which was determined by least square method. The background seismic activities are evaluated for each cell of a grid. The Gutenberg-Richter exponential magnitude recurrence model is assumed to govern the earthquake activity in these cells. The total number of earthquakes that are used in the analysis is 200. This means each cell of the grid does not have sufficient number of earthquakes for estimation of b value for individual cells; therefore the overall b value for the study area was used in every cell. The 'a' value of each cell was spatially smoothed using two-dimensional Gaussian filter with a decay distance of 10 km. The earthquake of Mw equal or less than 6.0 was treated and corresponded to background activity.

The annual rate of earthquake occurrence for each fault with magnitude M was presumed to be the difference of the accumulated number for M and M+0.1. This means that the activity is supposedly following a Poisson process. The annual rate for an earthquake of magnitude 6.0 or higher is found to be 0.00136.

The PGA distribution for 2% and 10% probability of exceedance in 50 years due to area sources is determined. This was calculated for base rock of shear wave velocity of 760 m/sec. The attenuation relationship used are Boore et al. (1997), Campbell (1997) and Sadigh et al. (1997) in equal proportion to estimate the PGA.

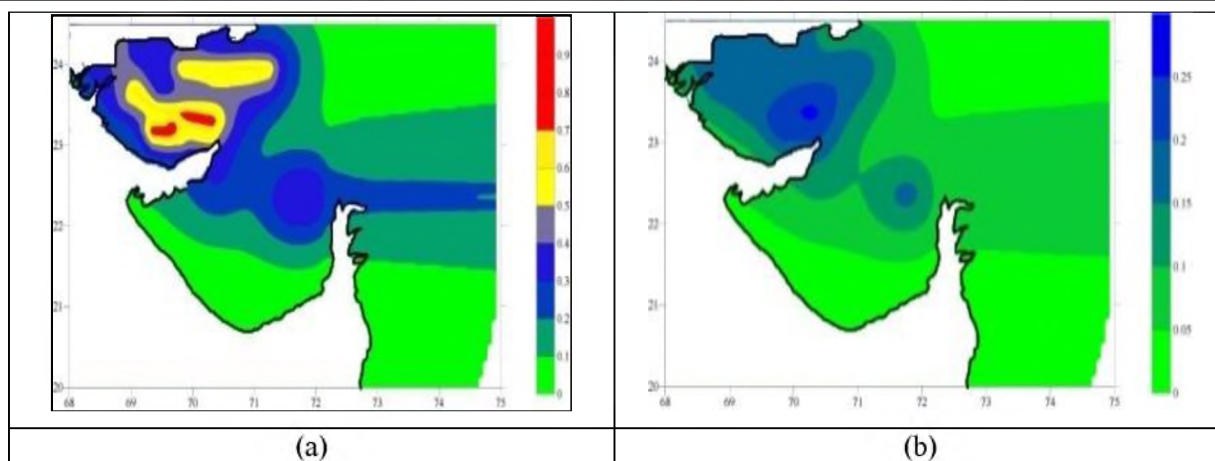


Fig. 5.2.4: Peak ground Acceleration (PGA) is estimated for 50yr return period at (a) 2% and (b) 10% probability in Gujarat taking into account the past seismicity

### PGA at base-rock level in Gujarat Coastal belt using Deterministic Method

The stochastic finite fault modeling technique is used to determine PGA at bed-rock level with  $V_s$  of 760 m/s. It has been observed from Figure 5.7 that in most of the coastal regions of Saurashtra and mainland the PGA is less than 100 gals. The coast near Bharuch can expect PGA between 100 and 150 gals due to proximity to Narmada fault. The Dwarka and Jamnagar coast in Saurashtra can expect between 100 and 200 gals due to proximity to large faults in Kachchh. The Mundra and Kandla in Kachchh can expect PGA of 200-400 gals whereas Lakhpat, Jakhau and Mundra can expect between 100 and 200 gals.

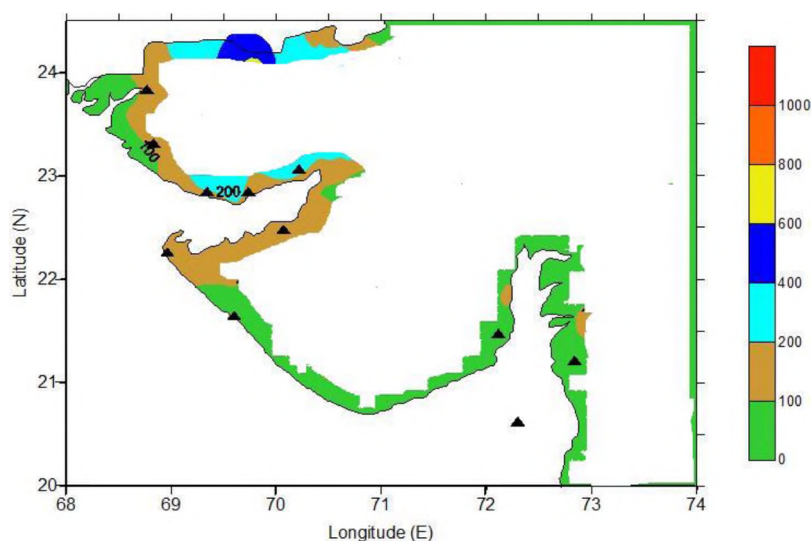


Fig. 5.2.5: PGA at bed-rock level in coastal regions of Gujarat for 2% probability in 50yr

### Structural Response Analysis of Port Buildings

Using the estimated PGA and amplification parameters and by physical observation at ports, structural responses at Mundra and Kandla are estimated. The Kandla port is one of the major ports in the Gujarat state, which is analyzed for eight ground motions using a finite element program. Building is analyzed for two cases namely structure with rigid support and structure with actual soil base. The seismic response results of both cases are compared. Due to soil-structure interaction (SSI), the structure is made more flexible, therefore increasing its natural period as compared to that for rigidly supported structure. Moreover, the SSI effect increases the effective damping ratio of the system. The smooth idealization of design spectrum suggests smaller seismic response with the increased natural periods and effective damping ratio due to SSI. Also non-linear analysis has been done and results obtained are compared with those of linear analysis. Push-over analysis of Kandla admin building is done and it is found to be safe.



We modelled all possible cases of pipelines and conveyor belts used in ports and performed non-linear analysis for estimated ground motions. Most of the cases were found to be safe but some unsafe.

Also the ground motion was estimated at eight sites considering the following occurrences:

Case I KMF=8 and KHF=7

Case II KMF=7.7 and KHF=7

Case III KMF=8

Case IV KMF=7.7

Case V KHF=7

In this work the strong ground motion has been simulated using Semi empirical approach along with the attenuation relationship of Joyner and Boore (1981). We observed that the values of peak ground acceleration are same for Case I and III. Hence, we can say that the effect of KHF can be ignored if we consider M8 at KMF. A sample time-history and its Fourier spectrum for M7 earthquake along KHF at Mandvi are shown in Fig. 5.8.

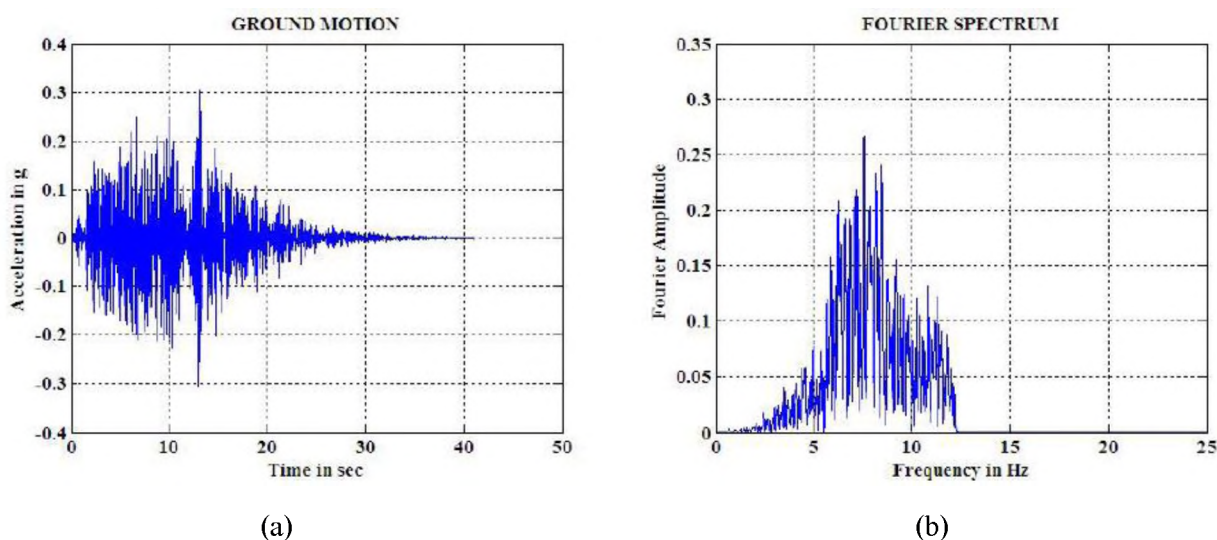


Fig. 5.2.6: Simulated ground motion due to M7 earthquake along KHF at Mandvi (a) Ground motion record (b) Fourier amplitude spectrum

### Response of structures

Basic data of port structures were collected during our visit to Mundra port site. The data of Navlakhi port was collected from GMB. Since it is difficult to get the details of structures of all other ports, we discussed with design consultants and took design basis report.

Response of jetty, port building, conveyor belt and buried pipe line was estimated for ground motions at 8 sites.

#### 1. Vulnerability Assessment of the Port Office Building at Kandla

The present study analyses the failure of the 22m high six-floor building called the Port and Customs Office Tower located very close to the waterfront (Figs. 5.2.7). The building was founded on 32 short cast-in-place concrete piles and each pile was 18m long. The piles were passing through 10m of clayey crust and then terminated in a sandy soil layer below.

The Port of Kandla is built on natural ground comprising recent unconsolidated deposits of inter bedded clays, silts and sands. The vertical profile of the region slopes downwards in the easterly direction towards

the coast line at about 12.5m/km. The water table is about 1.230 m below the ground. Fig. 5.2.1 shows the view of the natural grounds on which the Port of Kandla was built. The tower of the Port and Customs office considered for the present case study is located very close to Berths IV of the Kandla Port. The complete building details are given in Tables 5.2 and 5.3. The plan and elevation details and reinforcement details for members are shown in Figures 5.8. Reinforcement details are given in Fig. 5.9.

Table 5.2: Material & Soil Properties of the Kandla Port Office Building

Live load on floor =  $2 \text{ kN/m}^2$

Live load on roof =  $0.75 \text{ kN/m}^2$

Floor finishing =  $1 \text{ kN/m}^2$

Grade of concrete used = M<sub>25</sub> Poisson's ratio = 0.2



Figure 5.2.7: The Kandla Port Office Building

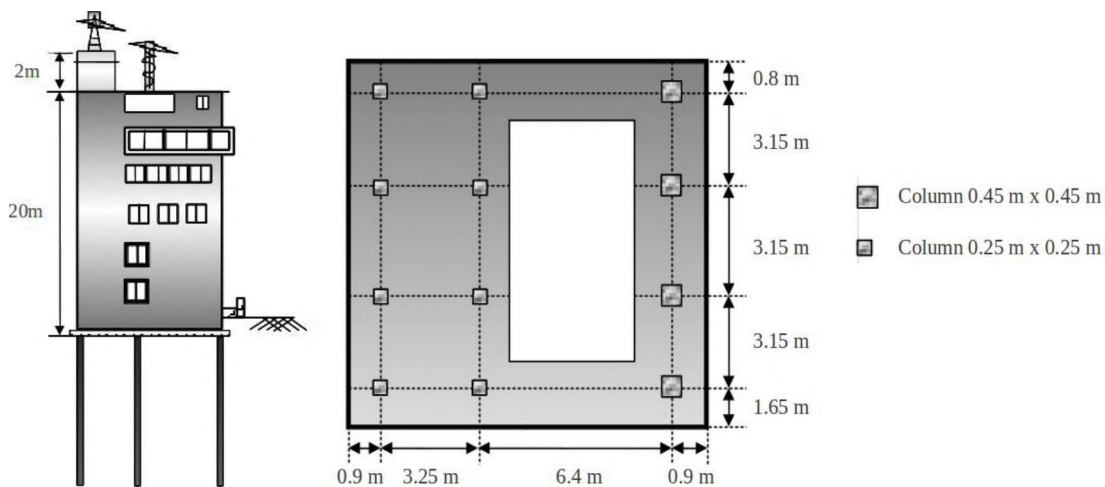


fig. 5.2.8: Elevation of port building, Dimensions of the Kandla Port Office Building and column details of port building

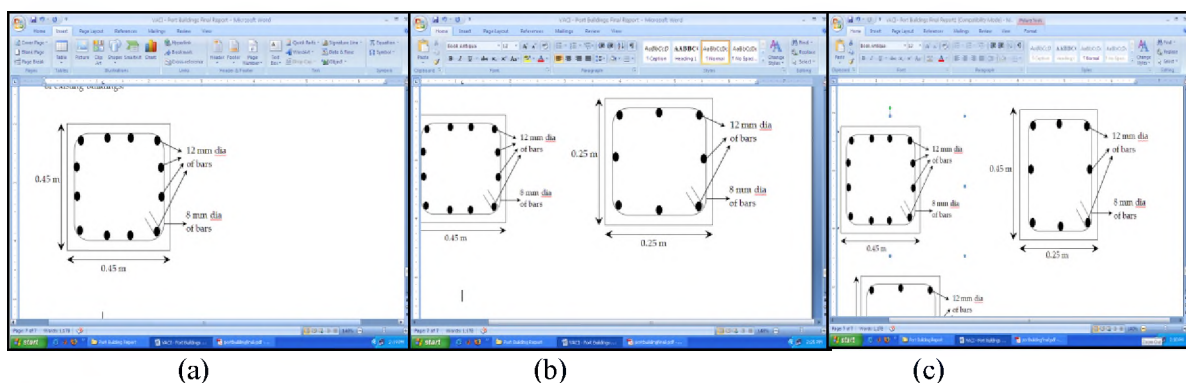







Fig. 5.2.10: Reinforcement details for members (a) column-1 (b) column-2 and (c) beam

**Table 5.3: Port building details**

Building Member	Dimension
Building height	22 m
Building plan at sill level	9.6 m x 9.8 m
Foundation raft	11.45 m x 11.90 m x 0.50 m
No. of columns	12
No. of piles	32
Length of pile	18 m
Diameter of concrete pile	0.4 m
Beam dimensions	0.25 m x 0.45 m
Slab thickness	0.15 m
Column-1 dimensions	0.45 m x 0.45 m
Column-2 dimensions	0.25 m x 0.25 m

**Soil Properties:** Properties of soil to depth of 42 m are shown. The water table is 5 m below the ground level. The Rayleigh  $\alpha$  and  $\beta$  values are taken as 0.01.

0 m		Soft clay with traces of fine sand, LL=62-68%, PL=26-28%, Su=10 kPa and $\gamma=16 \text{ kN/m}^3$
10 m		Fine sand, N<15 and $\gamma=17 \text{ kN/m}^3$
14 m		Coarse sand, N<15 and $\gamma=17 \text{ kN/m}^3$
22 m		Brown hard clay, LL=54-77%, PL=36-64%, Su=100 kPa and $\gamma=8 \text{ kN/m}^3$
32 m		Clayey sand, N<50 and $\gamma=18 \text{ kN/m}^3$
42 m		

The material model used in this analysis is Maekawa compression model (Tagel-Din Hatem, 1998). In this model, the tangent modulus is calculated according to the strain at the spring location. After peak stresses, spring stiffness is assumed as a minimum value to avoid having a singular matrix. The difference between spring stress and stress corresponding to strain at the spring location are redistributed in each increment in reverse direction. For concrete springs are subjected to tension, spring stiffness is assumed as the initial stiffness till it reaches crack point. After cracking, stiffness of the springs subjected to tension is assumed to be zero. For reinforcement, bi-linear stress strain relationship is assumed. After yield of reinforcement, steel spring stiffness is assumed as 0.01 of initial stiffness. After reaching 10% of strain, it is assumed that the reinforcement bar is cut. The force carried by the reinforcement bar is redistributed force to the corresponding elements in reverse direction. For cracking criteria (Hatem, 1998), principal stress based on failure criteria is adopted. The models for concrete, both in compression and tension and the reinforcement bi-linear model are shown in figure 5.2.10.

Kandla Port site was considered for the study purpose. Building is 6 storey and of height 22 m and it is located very close to the waterfront. The building was founded on 32 short cast-in-place concrete piles and each pile was 18m long. The piles were passing through 10m of clayey crust and then terminated in a sandy soil layer below. The Port of Kandla is built on natural ground comprising recent unconsolidated deposits of inter-bedded clays, silts and sands. The ground slopes in the easterly direction towards the coast at about 12.5m/km. The water table is about 1.2–3.0m below the ground. Initially structure is assumed to on the fixed base and linear and nonlinear response was calculated. For the considered ground motions the response of the structure is below the permissible limits. However, to get the complete collapse load of structure, structure was pushed until the yielding. This is done by pushover analysis which will create hinges at various locations. From the pushover curve we determined the stiffness degradation of structure. The stiffness degradation at different ports for given fault and magnitude has been estimated. Table 5.4 lists the amplitude, duration and frequency for different cases.

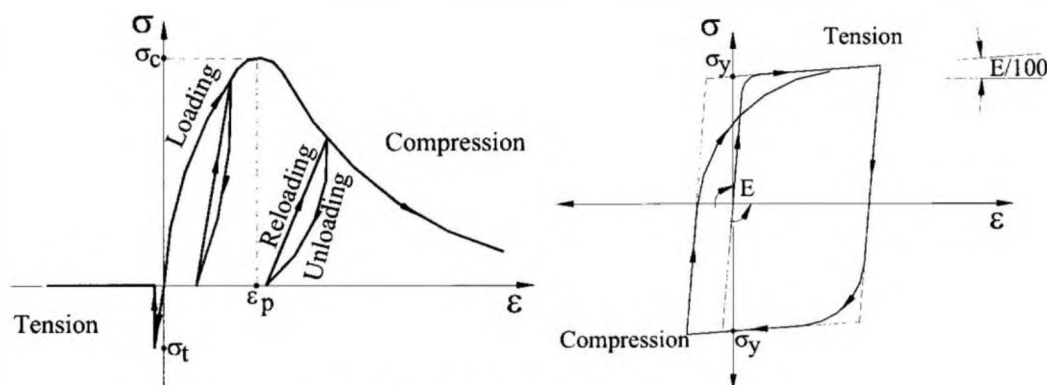


Figure 5.2.10: Material models for concrete and steel

**Table 5.4: Details of ground motions**

S.No	Ground Motion	Amplitude (g)	Duration (sec)	Frequency (Hz)
1	KHF Bharuch	0.012	-	7.0-9.0
2	KHF Mandvi	0.308	21.50	6.3-8.5
3	KHF Lalpur	0.091	8.48	6.2-9.5
4	KHF Dholera	0.013	-	5.8-7.1
5	KMF Bharuch	0.018	-	6.7-9.2
6	KMF Mandvi	0.122	14.80	5.5-8.5
7	KMF Lalpur	0.086	11.00	6.2-9.6
8	KMF Dholera	0.021	-	5.8-7.1



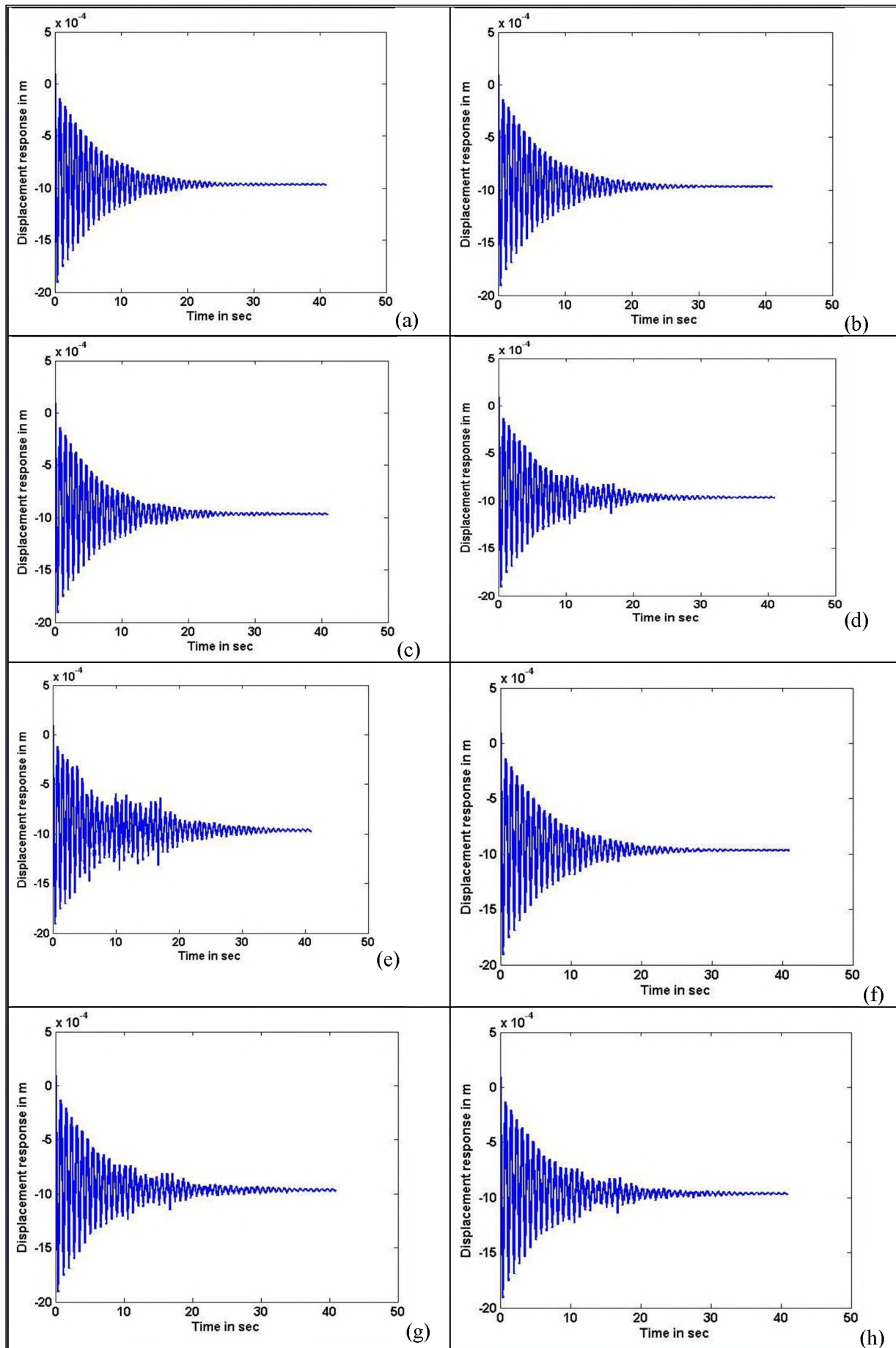


Figure 5.11: The displacement time histories for different port buildings for earthquakes along Katrol Hill Fault or Kachchh Mainland Fault (a)KHF-BRCH, (b)KHF-DHLRA, (c)KHF-LAL, (d)KHF-MAND, (e)KMF-BRCH, (f)KMF-DHLRA, (g)KMF-LAL and (h)KMF-MAND

### **Response of structure:**

Now the displacement response history of the structures (port buildings) is calculated from the selected ground motions. All the displacement response histories are showed in figure 5.2.11.

The fundamental frequency of the structure is not matched with the predominant frequency of all the ground motions and structure's fundamental frequency is very far away from the ground motion's frequency. Also the PGAs of ground motions have significantly less values.

### **Pushover analysis**

As per FEMA 356: 2000 and ATC 40, Pushover analysis is a static, nonlinear procedure using simplified nonlinear technique. It is an incremental static analysis used to determine the force-displacement relationship, or the capacity curve, for a structure. The analysis involves applying horizontal loads, in a prescribed pattern, to the structure incrementally; pushing the structure and plotting the total applied lateral force and associated lateral displacement at each increment, until the structure achieve collapse condition.

The static pushover analysis is becoming a popular tool for seismic performance evaluation of existing and new structures. The expectation is that the pushover analysis will provide adequate information on seismic demands imposed by the design ground motion on the structural system and its components. The pushover analysis of a structure is a static non-linear analysis under permanent vertical loads and gradually increasing lateral loads. The equivalent static lateral loads approximately represent earthquake induced forces. A plot of the total base shear versus roof displacement in a structure is obtained by this analysis that would indicate any premature failure or weakness.

The existing buildings can become seismically deficient since seismic design code requirements are constantly upgraded and advancement in engineering knowledge. Further, Indian buildings built over past two decades are seismically deficient because of lack of awareness regarding seismic behavior of structures. The widespread damage to buildings during earthquakes is exposed in the construction practices being adopted around the world, and generated a great demand for seismic evaluation and retrofitting of existing buildings.

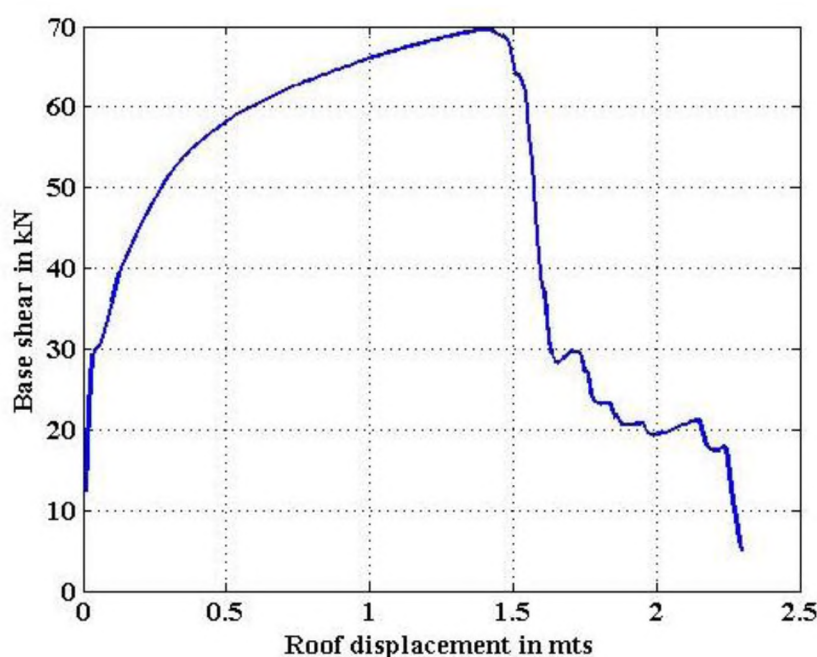


Figure 5.2.12: Base shear vs. Roof displacement plot for the port building

Now to get the load vs. displacement curve for a structure, the structure is pushed using either load control or displacement control. In this analysis we used displacement control till complete collapse of the structure. The load vs displacement plot is shown in figure 5.2.12. The stiffness of the structure getting reduced when the first crack starts or the first spring fails. The spring fails when the principle stress exceeds the limited value. Now the first spring fails at (4.75 m, 18.48 m) which causes crack in the structure. In this analysis, steel failure is also allowed. When the structure reaches the peak load value in the load vs. displacement curve, it starts coming down for further increase in the displacement.

### Fragility analysis

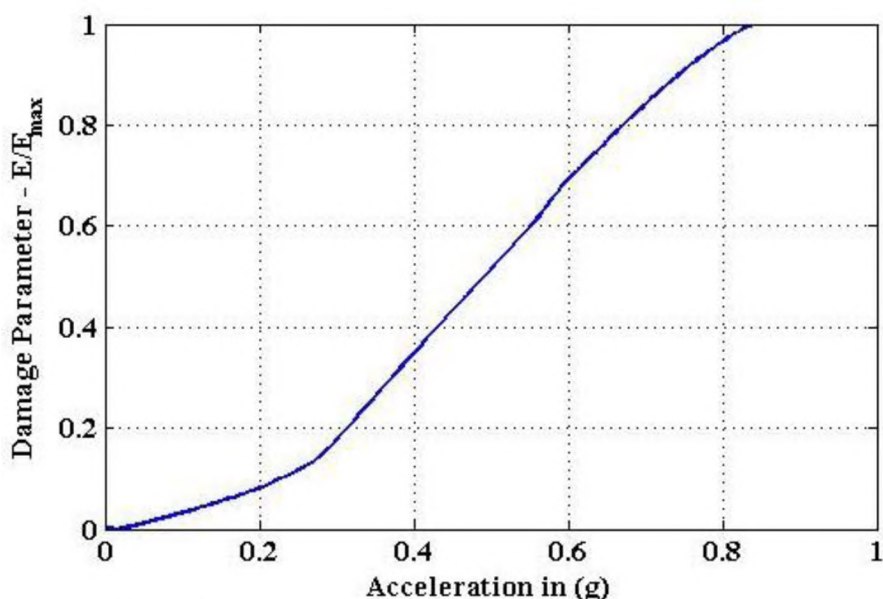


Figure 5.2.13 Damage curve for the port building for different PGA values

Now the area under the load vs. displacement curve is the total energy dissipated in the structure. We calculated elastic and inelastic energy of the structure at each and every displacement. The damage parameter is denoted as the ratio of inelastic energy to the total energy of the structure. The displacement values can be converted to spectral displacement and then converted to spectral acceleration values using  $4\Pi(SD)/T^2$ . Where  $SD$ =spectral displacement and  $T$ =time period. Figure 5.2.13 gives the damage curve for different PGA values of ground motion. From figure 5.2.14 we can estimate the amount of damage to the port building for the given ground motion PGA value.

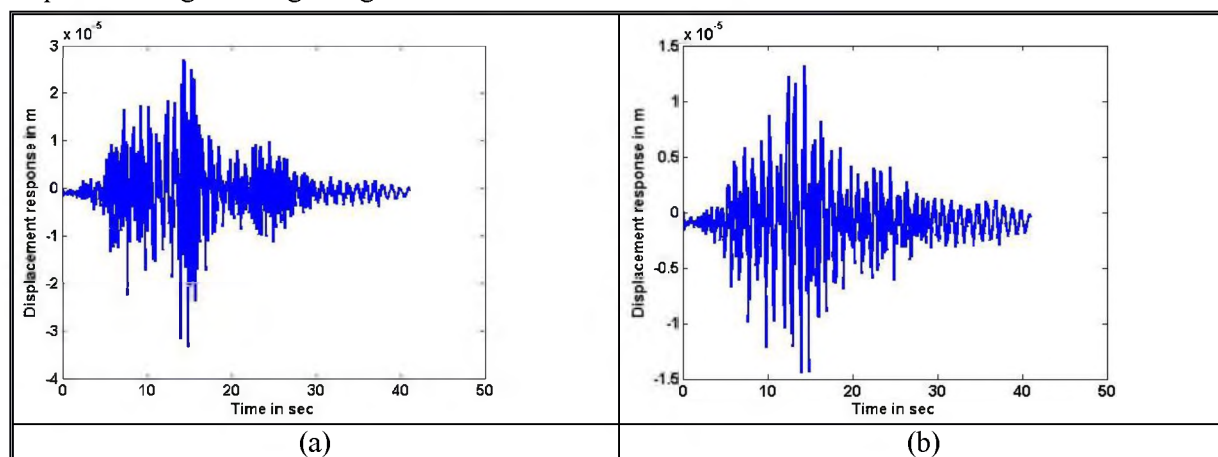


Fig. 5.2.14: Two sample response time histories of light houses for given input ground motions

**Vulnerability assessment of Light houses:** A study has been conducted to study the dynamic behavior of lighthouse. The dynamic properties of the lighthouse are as follows: The fundamental period of structure is 1.02 sec and the period of structure from mode-2 to mode-5 is 0.3 s, 0.143 s, 0.086 s and

0.060 s respectively. The procedure for finding out the response of the structure is already discussed in the earlier sections. Now the structure is subjected to several ground motions. Two sample response time histories of light houses for input ground motions as given above are shown in figure 5.2.14.

### **Tsunami inundation mapping along Okha & Dwarka Coast**

We have estimated possible arrival time and run-up of tsunami at various places along the coastal regions of Gujarat due to M8.0 Makran earthquake. The tsunami strikes Jakhau (23.500 N, 69.200 E), Dwarka (22.250 N, 69.050 E) & Mundra coast (22.820 N, 69.870 E) with wave heights of more than 1.8, 2.0 & 1.5 m, respectively.

West coast of India is affected by tsunami generated along Makran subduction zone. The most significant tsunamigenic earthquake in recent times was that of 28 November 1945, 21:56 UTC (03:26 IST) with a magnitude of 8.0 (Mw). Modeling of inundation has been made for the Dwarka coast from the Makran source using Tunami N2. The bathymetry data is taken from ETOPO1 and land topography data was collected using SRTM data. Makran, Fault strike 270°: The fault parameters of the earthquakes for the generation of tsunami are: fault area (200km length and 100km width), angle of strike, dip and slip (270°, 15° and 90°), focal-depth (10 km), magnitude (8.0). The simulated Arabian Sea tsunami propagation generated due to above mention tsunamigenic earthquake indicated that the first tsunami wave reached on the Dwarka coast in Gujarat region (Jaiswal, et al., 2009). At Dwarka, positive tsunami waves arrive within approximately 2 hours and 10 minutes. In this study the application of a numerical model to simulate tsunamigenic Makran event and an approach to estimate the extent of inundation along the coast of Dwarka. It is found that if the tsunami strikes during the low tide, 1.5m tide, and 3.0m tide are inundated 100-300m, 100-500m and 100-600 m, respectively along the Dwarka coast (Fig.5.2.15).

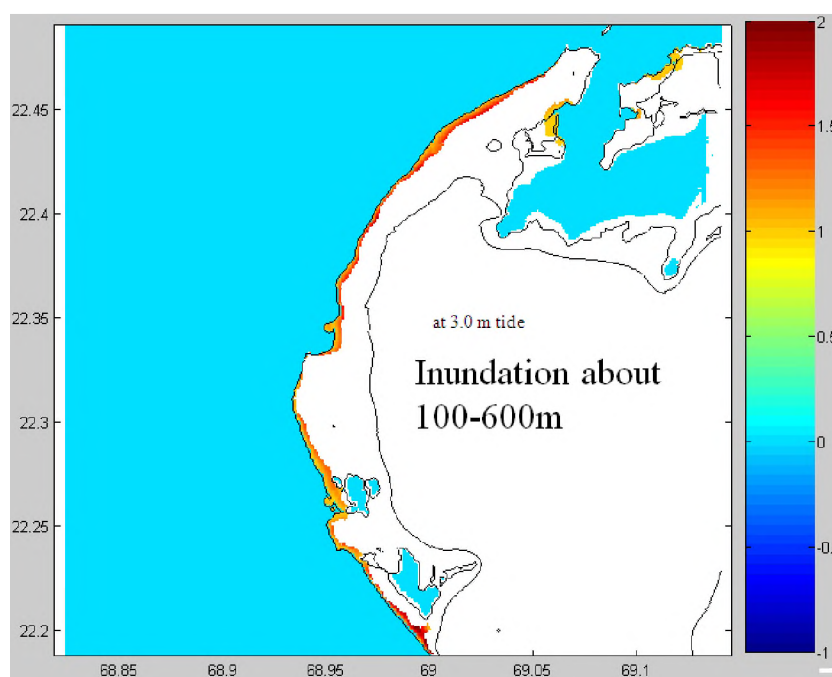


**Fig. 5.2.15: Tsunami inundation mapping during 3.0m tide along Okha & Dwarka coast**

**Drilling:** Drilling of ten boreholes has been done at the gulf of Kachchh region (Fig.5.2.16). The sites are Dwarka (22.244N°, 68.961E°); Jakhau (23.217N°, 68.715E°); Jangi (23.176N°, 70.599E°); Joiya (22.781N°, 70.329E°); Kandla (22.995N°, 70.156E°); Madhapar Bhunga (20.506N°, 70.030E°); Mandvi (22.833N°, 69.346E°); Okha (22.471N°, 69.079E°); Salya (22.308N°, 69.601E°); Sikaa (22.418N°, 69.855E°). From drillings data the soil and rock properties have been determined and used for geotechnical and strong motion analysis.



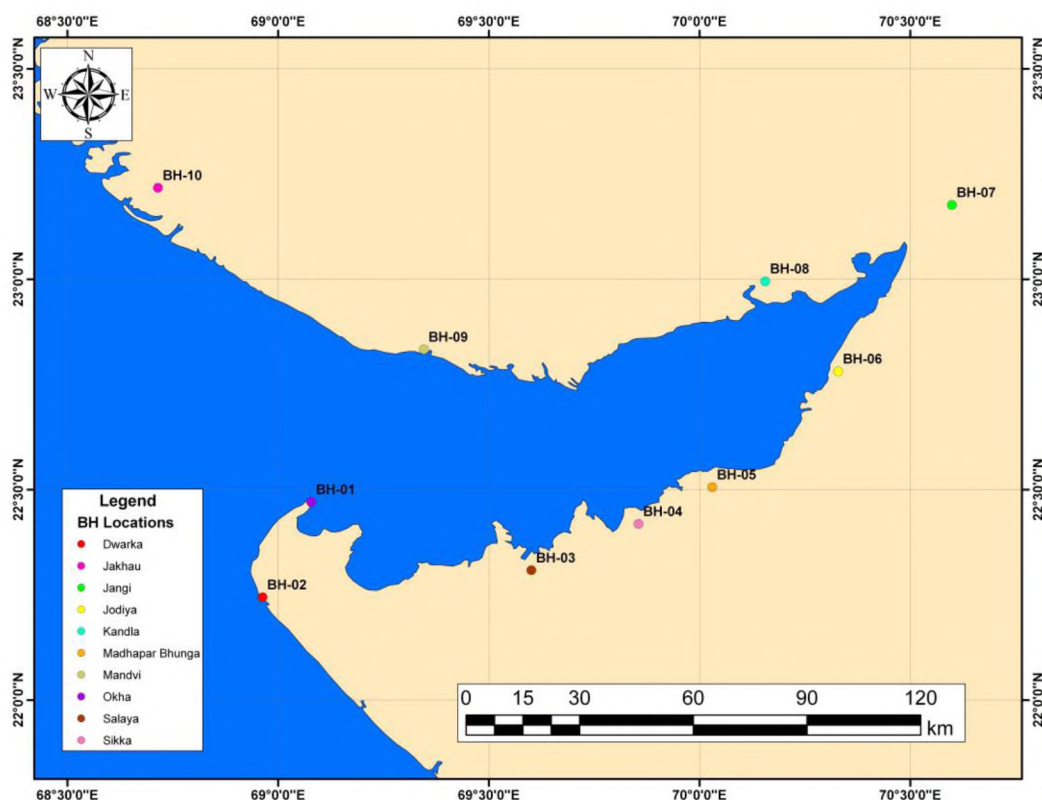


Fig. 5.2.16: Ten borehole locations along the Gulf of Kachchh made for our study

### 5.3 SHEAR-WAVE VELOCITY ESTIMATES IN DIFFERENT PARTS OF GUJARAT FROM MASW AND PS LOGGING

*B. Sairam, B. K. Rastogi, Vandana Patel and S. Venkateshwar*

During April 2012- March 2013,  $V_s$  profiles are obtained at 53 sites at various parts of Gujarat by MASW and PS-logging. So far, shear-wave velocity profiles are estimated at 366 locations in Gujarat.

MASW	Sites	PS-logging	Sites
VS- Hospital, Ahmadabad	4	VS- Hospital, Ahmadabad	1
Kachchh	22	Gandhinagar	2
Saurashtra	3	Surat	18
Total (MASW +PS-logging):		Coastal region of Kachchh and Saurashtra	3

### 5.4 PGA and $S_a$ MAPS FROM PSHA ANALYSIS CONSIDERING SITE CONDITIONS AT 2% PROBABILITY OF EXCEEDANCE IN 50 YEARS FOR THE GUJARAT REGION

*(B. Sairam, B. K. Rastogi and Prantik Mandal of NGRI)*

PSHA map is prepared for Gujarat region in western India (200000 sq. km) which is having high seismic hazard. For this purpose site condition map is prepared based on  $V_{s30}$  and geological rock formations. Shallow seismic surveys were carried out at 313 locations in different parts of Gujarat and the  $V_{s30}$  seismic velocities were assigned to different geological conditions in Gujarat.

In Gujarat and adjoining regions, there are three main seismic source zones (viz., along rifts of Kachchh, Cambay and Narmada). The earthquake hazard parameters viz., maximum magnitude ( $M_{max}$ ), a-value and b-value have been estimated for these zones. The hazard parameters are estimated using the earthquake catalogue compiled by ISR for the period 1668 to 2011 which is homogenized to  $M_w$

magnitude. As a reliable attenuation relation for Gujarat is not yet available, a New Generation Attenuation (NGA) relation of Boore and Atkinson (2008) is used in computing the seismic hazard for Gujarat. The Boore & Atkinson (2008) equations are applicable for  $MW = 5-8$  and  $VS30 = 180-1300$  m/s. PGA map was prepared for entire Gujarat for  $V_s$  of 760m/s which is generally considered suitable for assigning Engineering Bed Layer.  $VS30$  of 760m/s or more is found in the areas covered by Deccan Traps and Granitic firm rock in 1/3rd area. The 2/3rd area is covered by lower  $V_s$  30 of 500 in Mesozoic and Tertiary hard sediments as well as 300m/s in Quaternary stiff soils. PGA is estimated in these three types of areas. The PSHA maps at 760 m/s for firm rock site level and also at surface with three different site conditions are prepared. CRISIS2007 code is used to calculate PSHA maps for 2% probability of exceedance in 50 years (Figs. 2). Estimates have also been made for spectral accelerations at a few natural periods of buildings.

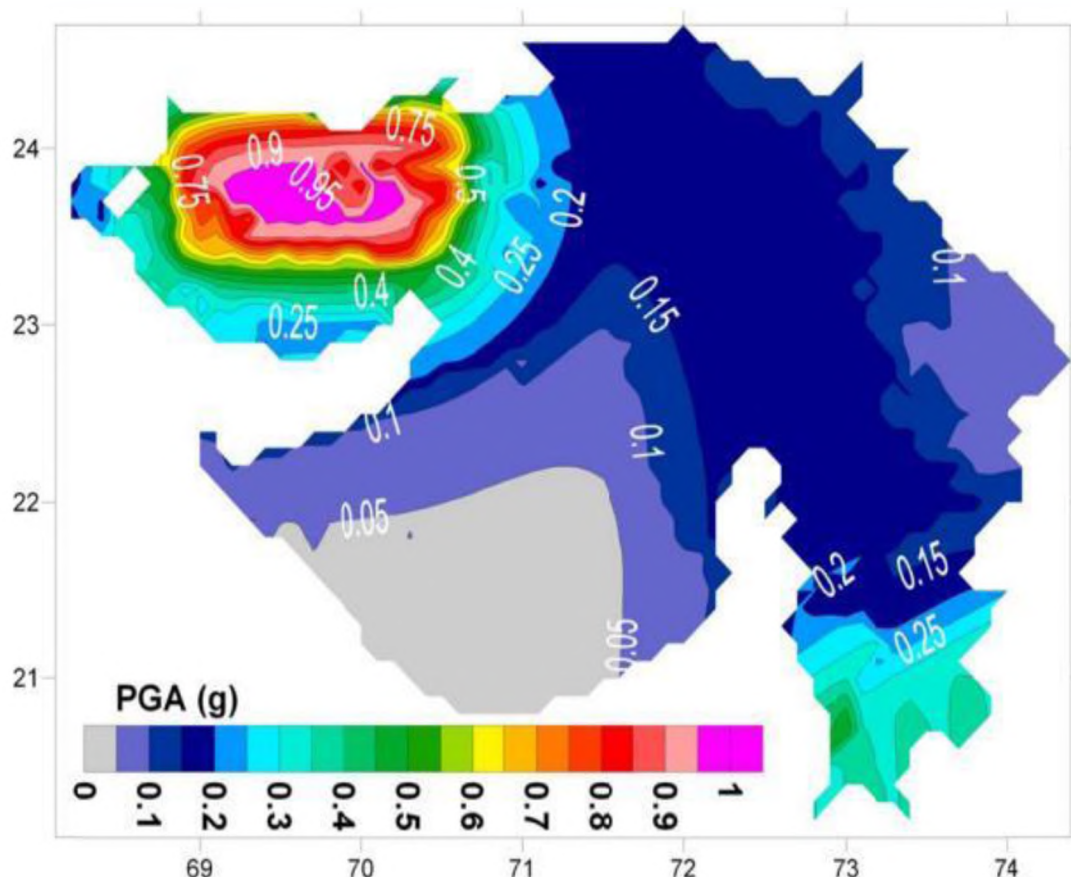


Fig. 5.4: PGA map at surface level considering site conditions ( $VS30 = 300, 500, 760$  m/s) for 2% probability exceedance in 50 years. New generation attenuation (NGA) relationship of Boore and Atkinson (2008) is used in estimation of PSHA. The CRISIS 2007 program is used in calculating PSHA

## 5.4 SEISMIC HAZARD ASSESSMENT OF NUCLEAR POWER PLANT SITES

### 5.4.1 Seismic hazard Assessment for Jaitapur Nuclear Power Plant site, Ratnagiri, Maharashtra (B.K. Rastogi)

The Jaitapur site ( $16^{\circ} 35'N$   $73^{\circ} 20'E$ ) is about 100km south of Koyna dam and 50 km south of Ratnagiri. Monitoring of seismicity since 2004 with five local seismograph stations or the Koyna network operating since 1962 with several stations at 50-100km distance have not recorded any shock within 50km of the site. The two earthquakes, Koyna 1967 ( $M_w$  6.3) and Ratnagiri 1965 ( $M$ 5) are likely to have caused intensity V at Jaitaur. The Latur earthquake of  $M_w$ 6.2 occurred about 200km east of the site. Koyna and Latur are in a Postulated “Koyna- Kurdwadi Rift” which is more than 50 km north of Jaitapur. Any

earthquake along this rift may cause intensity V at the site and hence will not cause any damage to the plant. The review of geological setting of the area indicates possibility of some coast parallel faults offshore and onshore which are of Tertiary age. However as will be described in the next session, no such fault could be found in the vicinity of the area by detail geological studies by the Geological Survey of India done for a number of years and also by ISR quick check up. No fault is observed near the coast or along the continental divide.

A review of geophysical studies of the area indicated that there are two deep Seismic profiles Koyna I (75 km north of Jaitapur) and Koyna II (150km north of Jaitapur) which are eastward from coast for about 150km length. These two profiles are south and north of Koyna reservoir. A NNW thrust fault dipping east was detected. This fault was not the causative fault for the Koyna earthquake as the Koyna earthquake was along a NNE trending strike-slip fault. Moreover, this fault does not extend further south as it is limited by a NW trending normal fault in Warna area.

#### **5.4.2 Geological Investigation by ISR at Jaitapur**

*(B.K. Rastogi, G.C. Kothiyari and Prabhin Sukumaran)*

A review of geology of the west coast region indicates existence of a series of offshore coast parallel faults which have been mapped by seismic survey which have formed grabens in Tertiary age accumulating Tertiary sediments. Though no such fault terrace or normal fault has been found onshore by seismic survey or geological investigations, possibility of such faults onshore has been expressed by geologists. Boreholes drilled on Jaitapur site indicate variation of several meters of Deccan Trap basement over which Miocene sediments were deposited. Possibility of such variation due to faulting has been expressed. However, such variations of Deccan Trap basement can be due to erosion as seen everywhere the Deccan Traps are exposed.

Roger Bilham has drawn our attention to one possible terrace or normal fault from Google image (Fig. ). This feature, a 50 km long NNW trending escarpment passing through west of Jaitapur was identified by Powar and Patil. The Geological Survey of India team investigated this lineament for 10 km length from Jaitapur southward for 3 years during 2003 to 2005. It did not find any evidence of fault in the area. During 2<sup>nd</sup> half of March 2012, a team of ISR geologists examined some ten areas along this lineament for a stretch of 50km where rivers/streams are shifted towards north on eastern side of the escarpment. During the last week of March 2012, a team of about 30 geologists / geophysicists of India thoroughly investigated the areas around Jaitapur and up to 8 km south of it. The team included experienced earth scientists from several agencies like GSI, ONGC, IIT Bombay and ISR etc. Top 20-25 m cover is found to be Tertiary laterite (post Miocene) in 80% area. Deccan basalts are seen in 20% area along slopes of hills and valleys. The hills have been formed in along a ridge which is about 50km in length and up to about 60m height. The ridge is formed in Tertiary times as there are no gullies or streams over the ridge which would be seen if formed in Quaternary time. The Quaternary deposits are along a few streams/rivers only. The Tertiary laterite is not found to be disturbed at any of the ten locations. The location near Girye, 8 km south of Jaitapur, was most thoroughly investigated as change in the river course appears to be most prominent. A E-W flowing tributary of Vagothan River suddenly changes its course to N-S direction, follows the escarpment for a length of about 3 km before merging with Vagothan river. This change of river course might have happened in Tertiary as there is no sign of tectonic disturbance in Holocene time. At Girye a escarpment of sand appears to have risen high near the coast. However, it appears to be started due to blocking of river due to anthropogenic reasons and further rising of the same due to Aeolian activity. The historical records indicate that the river was flowing to the sea at this location until a few centuries. The dating of soil samples at two heights from this escarpment indicates ages of about 300yr for the sample close to the ground and 200 yr for the sample at 3 m height

from the ground. Along this 3 km straight NNW trend of escarpment laterite was not disturbed. If a 50-100 km long fault is formed, it will have fractures, gouge material and sheared rocks. No such thing was found. Though shifting of river / stream courses and deposition of thin Miocene beds in small isolated basins indicates possibility of faulting in pre- Miocene time, no evidence could be found.

Numerous borelogs at different locations on both sides of the NNW lineament around Jaitapur and up to 8 km south of it do not show any material / anomaly that support the presence of fault (slicken sides, fault breccias etc.) within the laterite or sedimentary rocks overlying Deccan basalts.

Prof. R. Nagarajan of IITb has examined the history, historical naval hydrograph charts, old topographic sheets of Survey of India and aerial photographs of the area (personal communication). He believes that the change in river course in the coastal area is due to sediment deposition from the sea as well as from upstream side, aided by reclamation activities rather than any neotectonic activities. In most of the cases changes have happened in last 100 yr or less.

The Vijaydurg fort and several cannon – cum – watch towers built on hillocks nearby with laterite rocks without any mortar some 400-500 years ago are intact indicating absence of any severe earthquake at least in the past half millennium.

## **5.5 GENERATION OF SITE SPECIFIC GROUND MOTION (SPECTRA) WITH DUE CONSIDERATIONS OF SHEAR WAVE VELOCITIES AND SOIL CONDITIONS FOR INDUSTRIAL SITES OF THE BHUJ REGION**

*(Kapil Mohan, B. Sairam and B. K. Rastogi with Rajesh Mishra of BARC)*

### **5.5.1 Introduction to Generation of Site Specific Ground Motion (Spectra) for Industrial Sites of the Bhuj Region**

BRNS (Board of Research in Nuclear Sciences (BRNS) sponsored the work of generation of response spectra for industrial sites of the Bhuj region with due consideration of shear wave velocities and soil conditions. ISR carried out Vs30 shear-wave velocity measurements by Multichannel Analysis of Surface Waves (MASW) test at 16 sites near the industrial locations in Bhuj region. The average shear wave velocity (Vs30) is varying from 160 to 1137 m/s with varying geology at the selected industrial sites.

The Peak Ground Acceleration (PGA), Response spectra (Spectral acceleration) and design basis ground motion is computed in the present work at 16 industrial sites (Figs. 5.5.1 and 5.5.2) in the Kachchh region of Gujarat at the surface using Stochastic Finite Fault Modeling Technique. The estimates are made corresponding to the average shear wave velocity to 30 m depth (Vs30) of these sites. Kachchh is an intra plate seismically very active region where several faults are active and can generate earthquakes of magnitude up to 8. The industrial sites are situated close to Kachchh Mainland Fault (KMF) which is most active and can generate Bhuj 2001 like earthquake of Mw7.6 in its three segments. However analysis is conducted by simulating the scenario Bhuj earthquake of Mw7.6 & the same magnitude along the western and eastern portions of KMF (those are closest to industrial sites).

The average shear wave velocity (Vs30) is varying from 150m/sec to 580m/sec at the selected industrial sites. The maximum PGA of ~1.1g is calculated at Chobari due to 2001 Bhuj earthquake. The minimum PGA of ~ 0.065g is computed at KLTPS-1(with highest Vs30 = 580m/sec) site situated at western most part of Kachchh due to scenario earthquake of Magnitude Mw7.6 along Western segment of KMF (section-A). The spectral acceleration values are higher (200-3000 gals) in the period range of 0.1 to 0.4 sec period compared to higher periods.



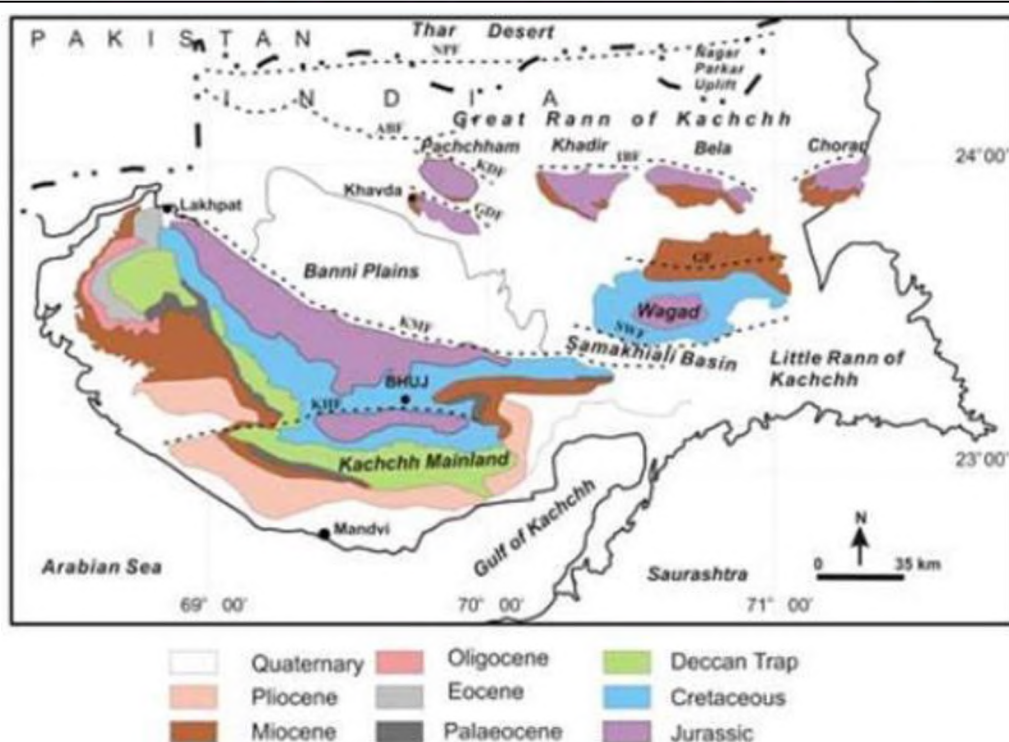


Fig. 5.5.1: Generalized geological map of Kachchh (Karanth, R. V. and Gadhavi, M. S. 2007). Broken line represents traces of major faults: Nagar Parkar Fault (NPF), Allah Bund Fault (ABF), Island Belt Fault (IBF), Kala Dongar Fault (KDF; a part of IBF), Gora Dongar Fault (GDF), Kachchh Mainland Fault (KMF), Katrol Hill Fault (KHF), Gedi Fault (GF) and South Wagad Fault (SWF).

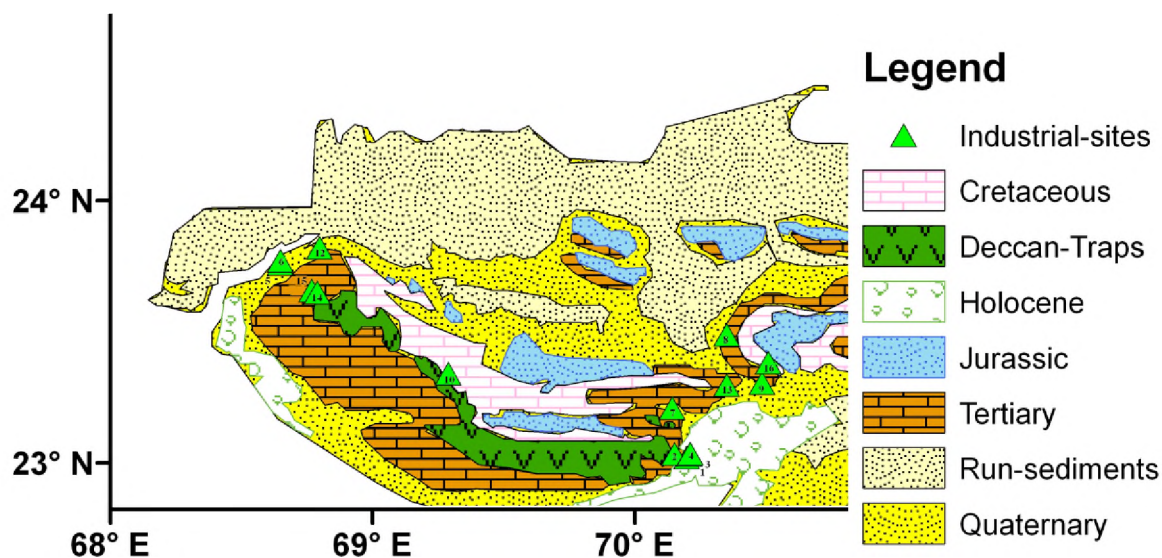


Fig. 5.5.2: Kachchh geology map (After Merh, 1995; GIS, 2001) with site locations of shear wave velocity estimations.

## 5.5.2 Rock Formations in Kachchh

The sediments are found younging southward as well as westward. But for some brief spells of hiatus, the Kachchh peninsula has recorded a nearly unbroken sequence of sediments from Late Triassic onwards (Table 5.5.1). Jurassic and early Cretaceous sedimentary formations are seen exposed in many parts of the rocky land mass. By and large, the Jhurio Formation is dominated by limestone and shale, the Jumara Formation by gypsaceous shale, the Jhuran Formation by sandstone and shale intercalations, and the Bhuj Formation by sandstone. Deccan Traps are seen exposed in the southern and western parts of the Kachchh Mainland. Tertiary sediments are distributed mainly in the western, southern and eastern parts of Kachchh (Karanth, R. V. and Gadhavi, M. S. 2007).

While Tertiary rocks are seen overlying the Deccan Traps in Kachchh Mainland, they are seen overlying the Mesozoic rocks in other uplifts. Of the Tertiary, only the sediments belonging to Miocene times are widespread. Vast areas of Banni Grassland, the Rann of Kachchh and the region between Mainland uplift and Wagad uplift, described as Samakhiali Basin, comprise unconsolidated soft sediments. The Precambrian basement rocks over which the Mesozoic sediments were deposited are not exposed in Kachchh. Intrusive bodies of igneous rocks that include coarse-to-fine-grained melanocratic alkaline basic rocks to oversaturated leucocratic granophyres are seen intruding into the Mesozoic sediments at many parts of Kachchh.

### 5.5.3 Shear wave velocity measurements by Multichannel Analysis of Surface Waves (MASW)

MASW is a geophysical method which generates a shear wave velocity ( $V_s$ ) profile (i.e.,  $V_s$  versus depth) by analyzing Raleigh-type surface waves on a multichannel record. The term “Multichannel record” indicates a seismic data set acquired by using a recording instrument with multiple channels. Forty eight channels Geode Seismograph and Seismodule Controller Software (SCS) of Geometrics Inc., USA has been used to acquire the data in this investigation. Data was acquired using standard CMP roll-along technique to achieve a continuous shot gather. Vertically stacked 20 impacts of a 30kg hammer on a metal plate were used as a source to generate seismic waves. These waves were recorded by twenty four vertical geophones/receivers of 4.5 Hz planted at a 2m interval along the profile line.

The MASW test was carried out at 16 locations for this study. The locations of the testing sites are shown in figure 5.5.2. An effective result of the MASW depends on signal to noise ratio (S/N) of surface waves. The optimum field parameters such as the source to the first and last receiver, receiver spacing and the spread length of survey lines are selected in such a way that the highest S/N ratio and required depth (more than 30 m depth) of information can be obtained.

The generation of a dispersion curve is an important step in MASW method. A dispersion curve is generally displayed as a function of phase velocity versus frequency. Each shot-gather generated one dispersion curve. Care has been taken to ensure that the spectral properties of the t-x (t is time & x is offset) data (shot gathers) were consistent with the maximum and minimum f- $V_c$  values (f is frequency &  $V_c$  is phase velocity of surface waves) contained in the dispersion curve. Each dispersion curve was individually inverted into an x- $V_s$  (z) trace [ $V_s$  (z) is shear wave velocity variation with depth]. Gathering all x-  $V_s$  (z) traces into shot station in sequential order results in a 2-D grid of the shear-wave velocity profile. Multi-channel records were analyzed with *SurfSeis* (a propriety software package of the Kansans Geological Survey, USA), which facilitates to use MASW with continuous profiling technique.

Average shear wave velocity to a depth 30 m ( $V_{s30}$ )

The shear wave velocity averaged from 0 to 30 m depth at each site has been computed using the following formula (eqn. 1)

$$V_{s30} = \frac{30}{\sum_{i=1, N} \frac{di}{V_{si}}} \quad (1)$$

Where  $di$  is the thickness of  $i^{\text{th}}$  layer (in meters),  $V_{si}$  is the shear wave velocity in  $i^{\text{th}}$  layer (in m/s).

Sites classification based on  $V_{s30}$  is given by the Federal Emergency Management Agency (FEMA, 1997), Uniform Building Code (UBC-19997), IBC2000 for National Earthquake Hazard Reduction Program (NEHRP) as given in the following Table 5.5.2.

Locations of Shear wave velocity measurements site are shown in Figure 5.5.2. Shear wave velocity profiles of different sites are shown in Figures 5.5.3. Vs30 values of Industrial/power plants/substation sites are shown in Table 5.5.3. Fig. 5.5.4 shows 1D Shear wave velocity models at Industrial sites of Kachchh, Gujarat.

**Table 5.5.2: NEHRP soil classification scheme.**

NEHRP Class	Vs30 m/s (Average shear wave velocity in the upper 30 m)	Description
A	>1500	Hard rock
B	760 – 1500	Rock
C	360 – 760	Very dense soil and soft rock
D	180 – 360	Stiff soil
E	< 180	Soft Soil
F	Special soil requiring	Site specific evaluation

**Table 5.5.3: Details of site locations, Vs30, NEHRP classes and Geology of each site.**

Category	Site Name	Vs30	NEHRP	Geology
(A). Quaternary				
	Kandla-1	171	E	Quaternary
	Kandla-2	357	D	Quaternary
	IFFCO-1	182	E	Quaternary
	IFFCO -2	160	E	Quaternary
	Akri-1	356	D	Quaternary
	Akri-2	405	C	Quaternary
	Bhimasar	462	C	Quaternary
	Chobari	273	D	Quaternary
	Samkhiali	423	C	Quaternary
(B). Cretaceous :				
	Nakhatrana	476	C	Cretaceous
	Dudai	560	C	Cretaceous
(C). Tertiary				
	Lakhpat	585	C	Tertiary
	Bhachau	547	C	Tertiary
(D). Deccan traps				
	KLTPS-1	611	C	Deccan traps
	KLTPS -2	1137	B	Deccan traps
(E). Jurassic				
	Adhoi	478	C	Jurassic

- IFFCO-Indian Farmers Fertilizer Cooperative limited, Gandhidham
- KLTPS- Kutch Lignite Thermal Power Station, Panandro

Shear wave velocities (Vs) profiles are obtained at 16 sites near to the Industries which are located at different geological formations. Nine sites are in Quaternary formations. The estimated Vs30 of Quaternary sites are in the range of 160-423 m/s. Two industrial site are in the Tertiary formations viz., Lakhpat (Vs30=585 m/s) and Bhachau (Vs30=547 m/s). Another two sites are in the Cretaceous formations which are showing Vs30 of 560 m/s for Dudai and 476 m/s for Nakhatrana. One site (Adhoi) is in Jurassic formation which has Vs30 of 478 m/s. Two sites which exist in Deccan traps formations have velocity of 611 and 1137 m/s at KLTPS-1 and KLTPS-2 sites respectively. There are two or three layers have seen at each site based on shear-wave velocity variation. It is evident from 2-D velocity models that the velocity generally increasing with depth. However, low shear wave velocity is inferred in between higher velocity layers.

(A) Sites of Quaternary sediments:

- (a) At Kandla-1 site top layer up to 11 m shows velocity in the range of 100-160 m/s and followed by second layer up to 32 m depth which has velocity 160-310 m/s.
- (b) Kandla-2 site shows two layers top layer is up to 5 m with velocity 100-270 m/s and followed by second layer up to 22 m depth Vs of second layer is in the range of 270-580 m/s.
- (c) IFFCO-1 sites shows two layers (Fig. 3 and 4), top layer is up to 11 m depth which has velocity of 100-155 m/s and second layer is up to 22 m depth with velocity of 150-250 m/s.
- (d) IFFCO-2 site is showing two layers first layer is up to 18 m depth ( $V_s=110-140$  m/s) and second layer is up to 22 m ( $V_s=140-230$  m/s).
- (e) At Akri-1 site, there are three layers first layer is up to depth of 23 m ( $V_s=250-450$  m/s) and second layer is up to a depth of 55 m ( $V_s=450-555$ ) and third layer is up to 64 m ( $V_s=500-840$  m/s).
- (f) At Akri-2 site  $V_s$  is obtained up to 26 m depth which shows two layers which is showing two layers top layer is up 12.5 m ( $V_s=200-360$  m/s) and second layer is up to 26 m depth ( $V_s=360-750$  m/s).
- (g) At Bhimasar site, there is top layer up to depth of 14 m ( $V_s=200-480$  m/s), followed by second layer up to depth of 44 m ( $V_s=482-654$  m/s) and then followed by third layer up to depth of 55 m ( $V_s=660-1020$  m/s).
- (h) At Chobari site  $V_s$  is in the range of 150 – 300 m/s up to 12 m depth.
- (i) At Samkhiali site top layer is up to 14 m ( $V_s=200-400$  m/s) and second layer is up to 80 m depth ( $V_s=400-1110$  m/s).

(B) Sites of Tertiary formations:

- (a) At Lakhpat site the top layer is up to 5 m ( $V_s=370-530$  m/s) and second layer is up to 65 m depth ( $V_s=530-600$  m/s).
- (b) At Bhachau site, there is top layer up to depth of 13 m ( $V_s=380-480$  m/s), followed by second layer up to depth of 23.4 m ( $V_s=380-480$  m/s) and third layer is up to 50 m depth ( $V_s=660-900$  m/s).

(C) Sites of Cretaceous formations:

- (a) Nakhatrana sites shows two layers, top layer is up to 20 m depth which has  $V_s$  of 400-550 m/s and second layer is up to 55 m depth with  $V_s$  of 400-850 m/s.
- (b) At Dudai site  $V_s$  is in the range of 400 – 700 m/s up to 10 m depth.

(D) Sites of Deccan traps formation:

- (a) Kltps-1 site shows two layers the top layer is up to 20 m depth ( $V_s=230-690$  m/s) followed by second layer to depth of 30 m ( $V_s=700-1000$  m/s).
- (b) Kltps-2 site is has two layers top layers is 26 m depth ( $V_s=370-1880$  m/s) and second layer is up to 42 m depth ( $V_s=1600-2170$  m/s).

(E) Site of Jurassic formation:

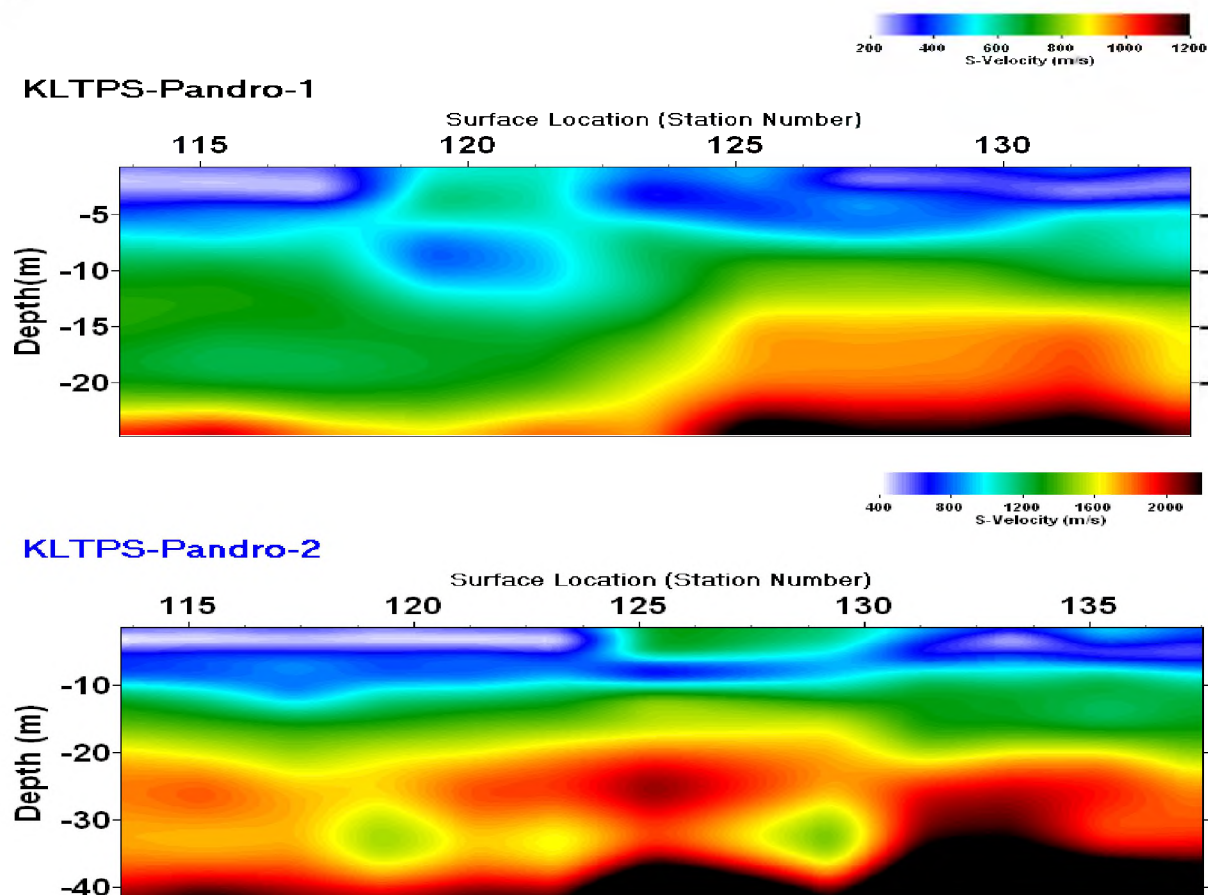
- (a) Adhoi site is in Jurassic formation which showing two layers top is up to 19 m depth ( $V_s=270-520$  m/s) and followed by second layer up to 50 m depth ( $V_s=520-1000$  m/s).



### Summary of the Results of MASW Measurements:

MASW test has been carried out at 16 sites near to industrial/power plants/substation sites. Shear wave velocity ( $V_s$ ) profiles have been obtained using the MASW technique. Average shear wave velocity ( $V_{s30}$ ) at each site has been computed. From the 2-D shear wave velocity profiles it is inferred that most of the power plants and industrial locations have been chosen at soft rock or rock sites except Kandla port area and IFFCO, Kandla site which have lowest shear wave velocity  $V_{s30}$  of about 200 m/s was found in. It is inferred that close to the Kandla coast there is loose soil. At a location about 4 km away from Kandla,  $V_{s30}$  is higher (about 360 m/s).

#### (D) Sites of Deccan transformations :



#### (E) Sites of Jurassic formations :

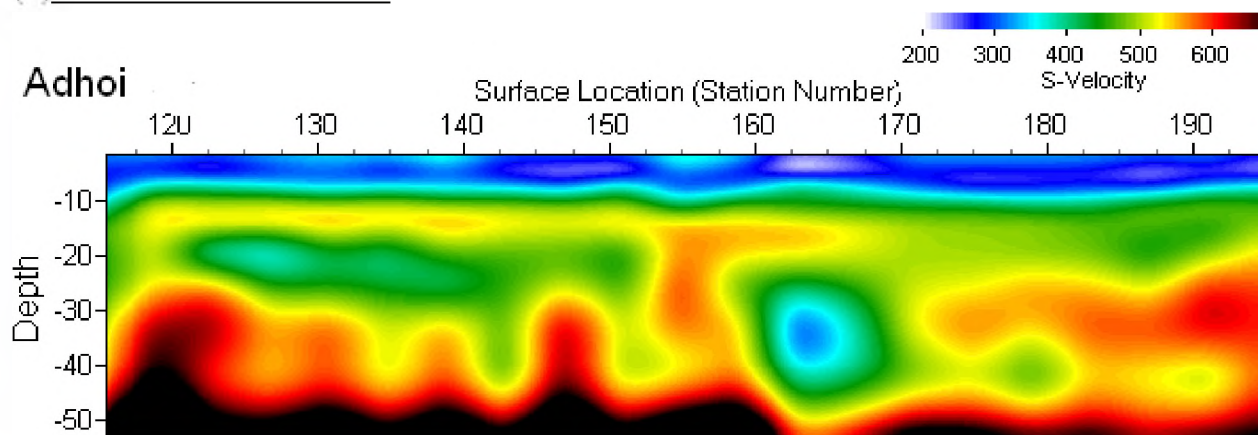
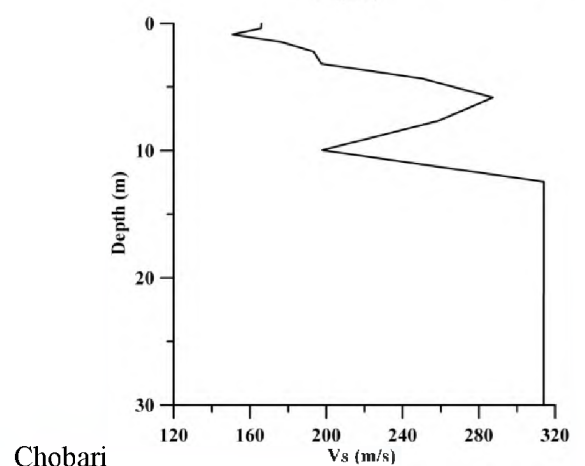
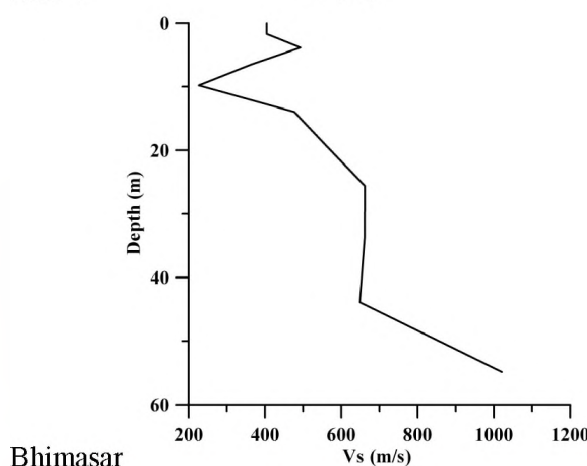
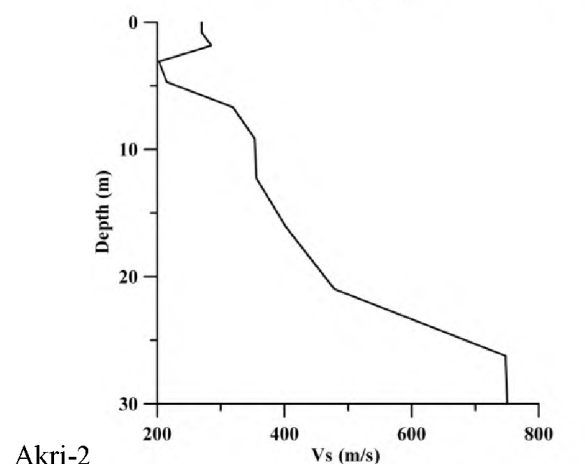
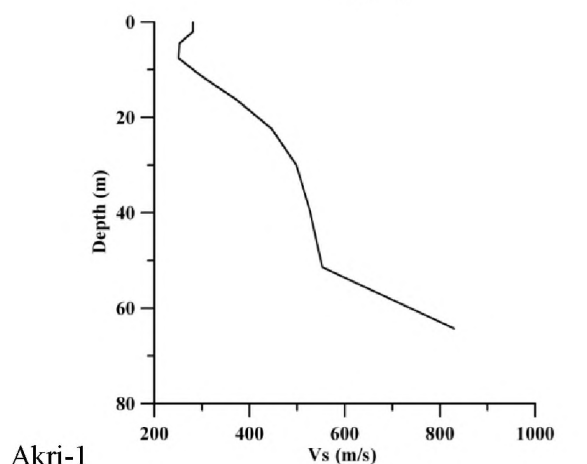
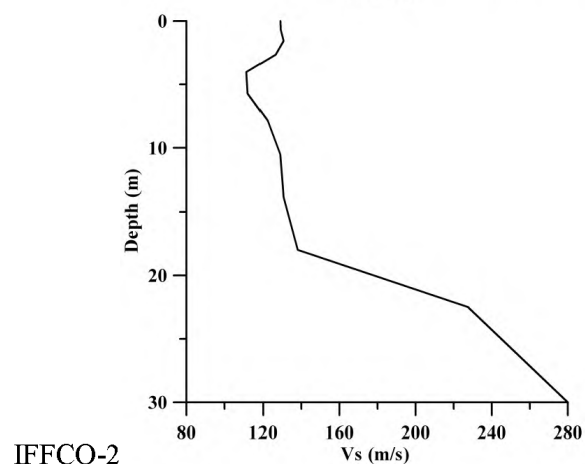
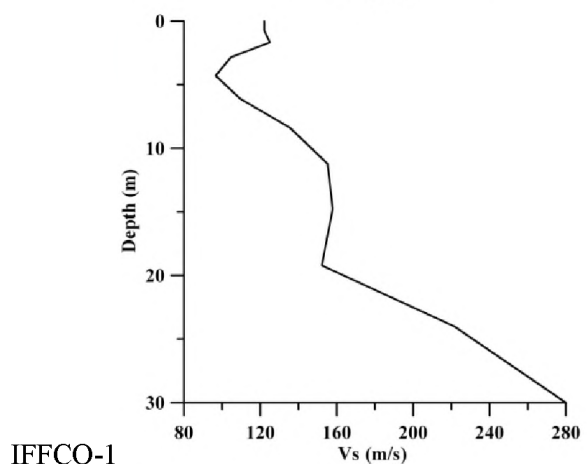
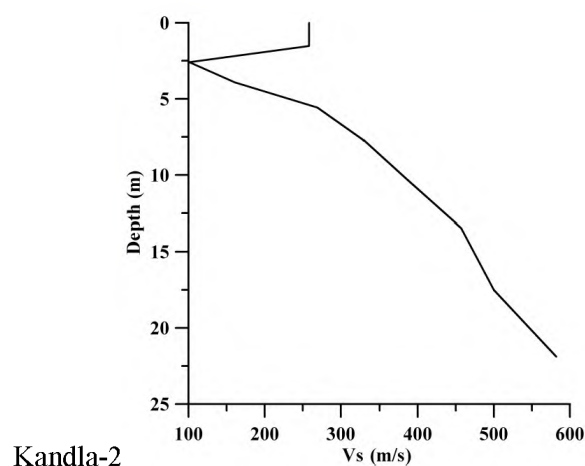
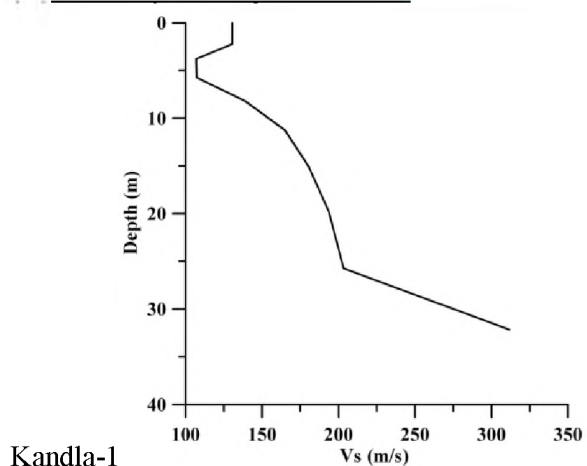


Fig. 5.5.3: Shear wave 2-D velocity profiles.

(A) Site of Quaternary formations:



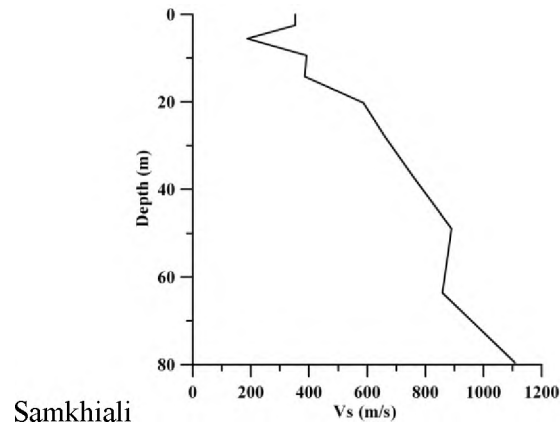
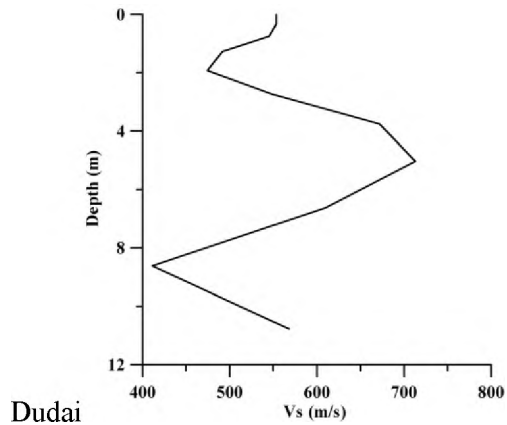
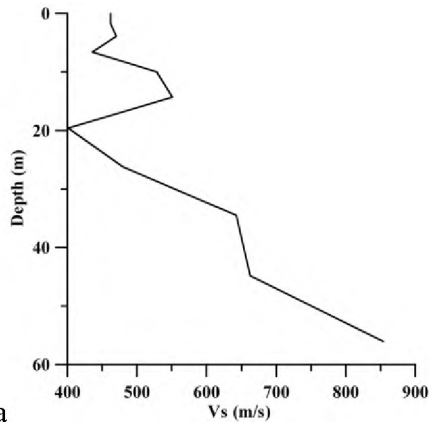
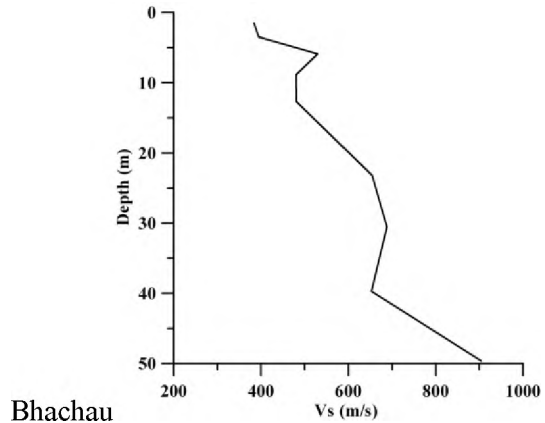
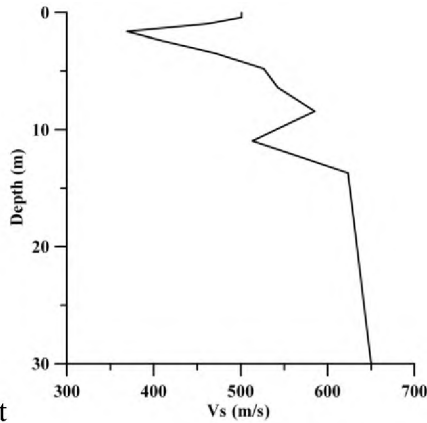


Fig 5.5.4: Shear wave 1-D velocity models

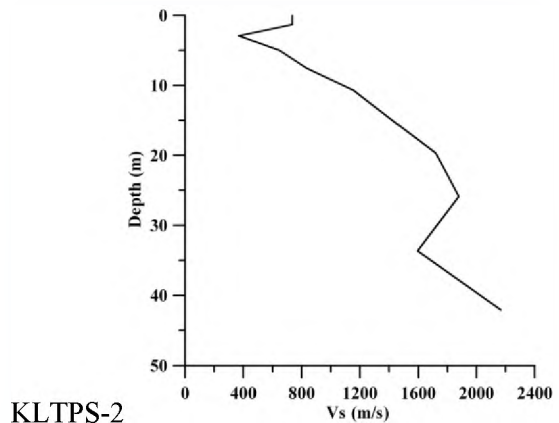
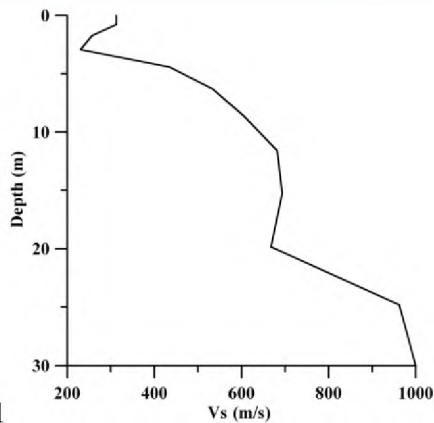
(B) Sites of Cretaceous formations:



(C) Sites of Tertiary formations:



(D) Sites of Deccan traps :



(E) Sites of Jurassic formations:

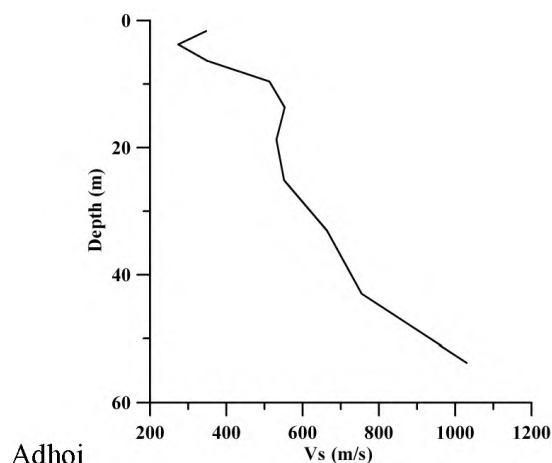


Fig 5.5.4: Shear wave 1-D velocity models at Industrial sites of Kachchh, Gujarat.

#### 5.5.4 Strong Motion Assessment at Industrial Sites in Kachchh

##### Methodology of Strong Motion Assessment:

The basis of the stochastic method is the observation made by Hanks and McGuire (1981) that the high frequency strong ground motion from earthquakes can be approximated by finite duration band limited white Gaussian noise. The band limitation is defined by spectral corner frequency and the highest frequency passed by the accelerograph or the Earth's attenuation. According to this method a site-specific shape of theoretical Fourier amplitude spectrum of the free field acceleration is estimated based on Brune (1970) model. Next a band limited white noise is windowed with a shaping function of prescribed duration (Boore, 1983). The windowed time series is transformed into frequency domain and scaled to the square root of the mean squared absolute spectra. The site specific theoretical Fourier amplitude spectrum generated above is multiplied with the scaled spectrum of windowed time series. The Fourier transformation back into the time domain generates the simulated acceleration time series.

This stochastic procedure described above has been applied successfully to simulate the ground motions by a number of investigators (e.g., Boore and Atkinson, 1987; Toro and McGuire, 1987; Ou and Herrmann, 1990; and Atkinson and Boore, 1995). Beresnev and Atkinson (1997) extended the stochastic procedure to large faults by subdividing a large fault into sub-faults each of which is then treated as a point source. The ground motions at a site can be obtained by summing the contributions over all sub-faults. Beresnev and Atkinson (1998) applied this finite fault radiation simulation technique to model strong motion acceleration data from the 1994 Northridge, California earthquake.

Motazedian and Atkinson (2005) introduced the concept of "dynamic corner frequency" by considering the corner frequency as function of time and presented the modifications to stochastic finite fault method. In the modified method the rupture history controls the frequency content of the simulated time series of each sub-fault. This modification takes care of the disadvantages recognized in the finite source stochastic method. Another advantage of the modified stochastic finite fault model is that it conserves moment with single triggering of each sub-fault as compared to multiple triggering in previous approaches (e.g. Silva and Darragh, 1995; Beresnev and Atkinson, 1998). This modified stochastic method based on dynamic corner frequency has been used successfully in modeling the ground motions for 1992 Landers earthquake (M 7.2), 1994 Northridge earthquake (M 6.7) and 2003 Bam, Iran earthquake (M 6.5) (Motazedian and Atkinson, 2005; Motazedian and Moinfar, 2006). Raghukanth et al. (2008) applied the same technique to estimate the ground motions for a great earthquake of magnitude



8.1 in the Shillong Plateau. In our modeling we have considered 45km rupture zones on hanging wall side of the KMF and 20km wide rupture zone on hanging wall side of North Wagad Fault (Fig. 5.5.5) which is a causative fault of 2001 Bhuj earthquake. The rupture lengths of about 135km are subdivided in 45 km sub-faults.

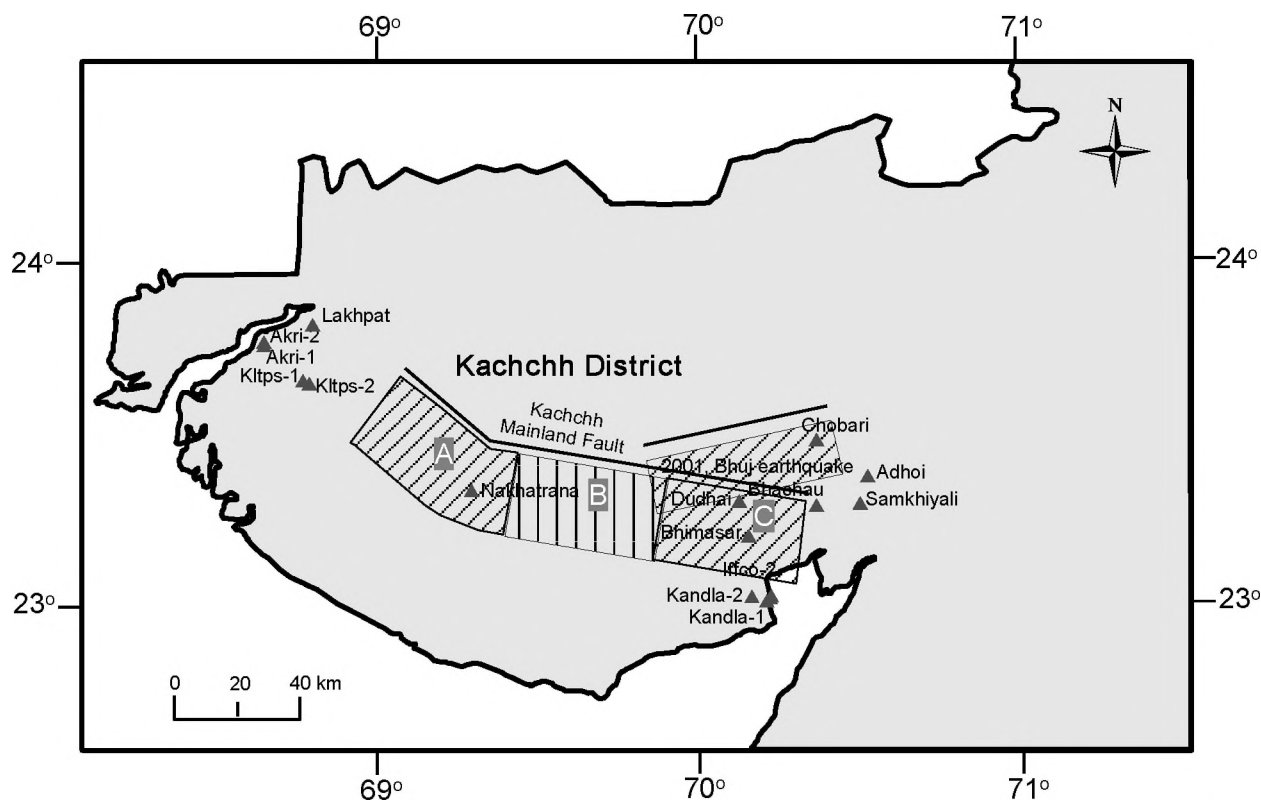


Fig. 5.5.5: Rupture zones (scenario earthquakes) and industrial stations considered in the study of seismic hazard at industrial sites in the Kachchh region.

Table 5.5.4: The Average Shear Wave Velocity ( $V_{s30}$ ) computed at selected industrial sites in Kachchh region.

Sr. No.	Station Name	$V_{s30}$
1	Bhachau	547
2	Nakhtarna	476
3	Lakhpat	585
4	Bhimasar	462
5	Adhoi	462
6	Akri-1	356
7	Akri-2	405
8	IFFCO-1	182
9	IFFCO-2	160
10	Kandla-1	171
11	Kandla-2	357
12	Chobari	273
13	KLTPS -1	611
14	Samkhiyali	423
15	Dudhai	560

**Table 5.5.5: Peak Ground Acceleration (PGA) values in cm/sec<sup>2</sup> computed from considering scenario earthquakes of Mw7.6 along Western portion (KMF-A), Eastern Portion (KMF-B) of KMF and due to 2001 Bhuj earthquake.**

1	Bhachau	788.5	124.0	937.3	937.3
2	Nakhtarna	170.4	931.6	141.5	931.6
3	Lakhpat	96.2	298.4	69.5	298.4
4	Bhimasar	576.4	140.0	938.0	938.0
5	Adhoi	538.8	104.8	637.9	637.9
6	Akri-1	85.5	244.4	64.6	244.4
7	Akri-2	85.7	245.8	70.0	245.7
8	IFFCO-1	457.5	163.3	715.7	715.7
9	IFFCO-2	459.2	154.0	719.2	719.2
10	Kandla-1	446.4	173.3	615.7	615.8
11	Kandla-2	419.6	151.6	609.6	609.6
12	Chobari	1077.7	137.4	657.8	1077.7
13	KLTPS -1	79.4	352.3	64.6	352.3
14	Samkhiyali	554.7	128.3	847.0	847.0
15	Dudhai	933.5	164.72	1030.3	1030.3

\*\* KLTPS- Kutch Lignite Thermal Power Station

\*IFFCO- Indian Farmers Fertiliser Cooperative Ltd.

**Table 5.5.6: The Peak Spectral Acceleration (PSA) computed at selected industrial sites in Kachchh region due to 2001, Bhuj Earthquake scenario.**

Sr. No.	Station Name	PSA(cm/sec <sup>2</sup> )	Predominant Period(sec)
1	Bhachau	1888.1	0.13
2	Nakhtarna	567.0	0.20
3	Lakhpat	240.0	0.42
4	Bhimasar	2151.0	0.22
5	Adhoi	1645.0	0.10
6	Akri-1	254.2	0.36
7	Akri-2	252.5	0.41
8	IFFCO-1	1336.4	0.16
9	IFFCO-2	1554.2	0.15
10	Kandla-1	1283.3	0.45
11	Kandla-2	1284.9	0.16
12	Chobari	3667.9	0.24
13	KLTPS -1	272.3	0.20
14	Samkhiyali	1937.6	0.25
15	Dudhai	2870.2	0.1

**Table 5.5.7: The Peak Spectral Acceleration (PSA) computed at selected industrial sites in Kachchh region due to scenario earthquake of Mw7.6 along western part of KMF (KMF-A).**

Sr. No.	Station Name	PSA(cm/sec <sup>2</sup> )	Period(sec)
1	Bhachau	382.0	0.18
2	Nakhtarna	2327.4	0.11
3	Lakhpat	855.6	0.10
4	Bhimasar	561.0	0.20
5	Adhoi	303.3	0.18
6	Akri-1	847.6	0.10

Sr. No.	Station Name	PSA(cm/sec <sup>2</sup> )	Period(sec)
7	Akri-2	777.7	0.16
8	IFFCO-1	434.5	0.35
9	IFFCO-2	432.2	0.59
10	Kandla-1	486.1	0.26
11	Kandla-2	587.6	0.17
12	Chobari	411.9	0.18
13	KLTPS -1	1190.1	0.14
14	Samkhiyali	345.0	0.22
15	Dudhai	570.5	0.16

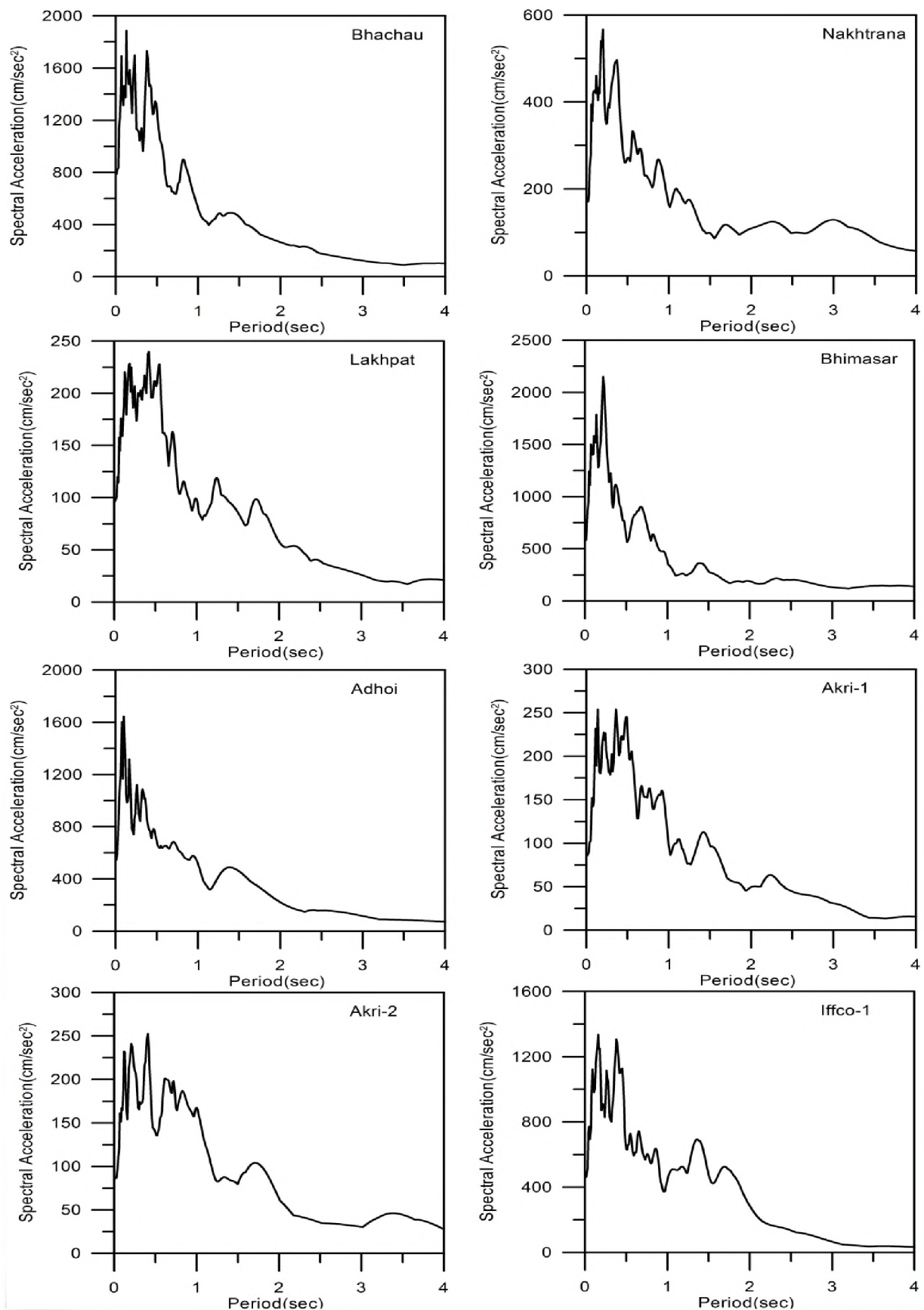
**Table 5.5.8: The Peak Spectral Acceleration (PSA) computed at selected industrial sites in Kachchh region due to scenario earthquake of Mw7.6 along eastern part of KMF (KMF-C).**

Sr. No.	Station Name	PSA(cm/sec <sup>2</sup> )	Predominant Period(sec)
1	Bhachau	2849.4	0.14
2	Nakhtarna	448.6	0.17
3	Lakhat	196.8	0.32
4	Bhimasar	3203.8	0.20
5	Adhoi	1958.2	0.10
6	Akri-1	224.4	0.24
7	Akri-2	209.4	0.38
8	IFFCO-1	2779.1	0.13
9	IFFCO-2	1974.3	0.16
10	Kandla-1	1642.1	0.16
11	Kandla-2	1692.1	0.09
12	Chobari	1716.0	0.14
13	KLTPS -1	210.0	0.09
14	Samkhiyali	2486.0	0.13
15	Dudhai	2811.9	0.25

### 5.5.5 Results and Discussion of Strong Motion Assessment at Industrial Sites in Kachchh:

The Peak Ground Acceleration (PGA), Response spectra (Spectral acceleration) and design basis ground motion is computed in the present work at 15 industrial sites in the Kachchh region of Gujarat considering three earthquake scenarios: (i) Due to 2001 Bhuj earthquake, (ii) An earthquake of magnitude Mw7.6 and western part of KMF (KMF-A) and (iii) An earthquake of magnitude Mw7.6 and eastern part of KMF (KMF-C). The PGA values computed due to all the three scenario earthquakes are given in Table 5.5.5. The maximum PGA value of 1.1g is computed at Chobari due to 2001 Bhuj earthquake. The PGA values are computed high at Dudhai (~1g), Bhachau and Bhimasar (~0.9g) due to KMF-C and at Nakhtarna (~0.9g) due to KMF-A as these sites are either falling near/on the rupture zone. The minimum PGA value (0.065g) is computed at KLTPS-1 site due to KMF-C may be due to higher Vs30 at the site and distance from the rupture zone.. The response spectra are also computed at all fifteen sites at 5% damping due to 2001 Bhuj earthquake scenario, KMF-A, KMF-C and are shown in Fig.5.5.6, Fig.5.5.7 and Fig.5.5.8, respectively. The maximum Peak Spectral Acceleration (PSA) due to 2001, Bhuj earthquake scenario is estimated at Chobari station (~3g) and minimum at Lakhat (0.24g) (Table 5.5.6). For KMF-A Lakhat shows a higher Vs30 and lower PSA compared to Akri-2 site which has higher Sa may be due to low Vs30 though Akri-2 is far from Lakhat. Due to scenario earthquake of Mw 7.6 along KMF-A, the maximum PSA is computed at Nakhtarna (~2g). Adhoi is showing low PSA (0.3g) (Table 5.5.7) because of distance from KMF-A. The maximum PSA of ~3g is computed at Bhimasar due to scenario earthquake of Mw7.6 along eastern portion of KMF (KMF-C) and the minimum at Lakhat

(0.2g) (Table 5.5.8). In all the three scenario earthquakes, the spectral acceleration values are found higher (200-3000 gals) in the period range of 0.1 to 0.4 sec period as compared to higher periods. The predominant periods in the response spectra are also given in Tables 5.5.6 to 5.5.8 along with the PSA. The response spectra due to the three earthquake scenarios at all fifteen station are shown in Fig.5.5.9.





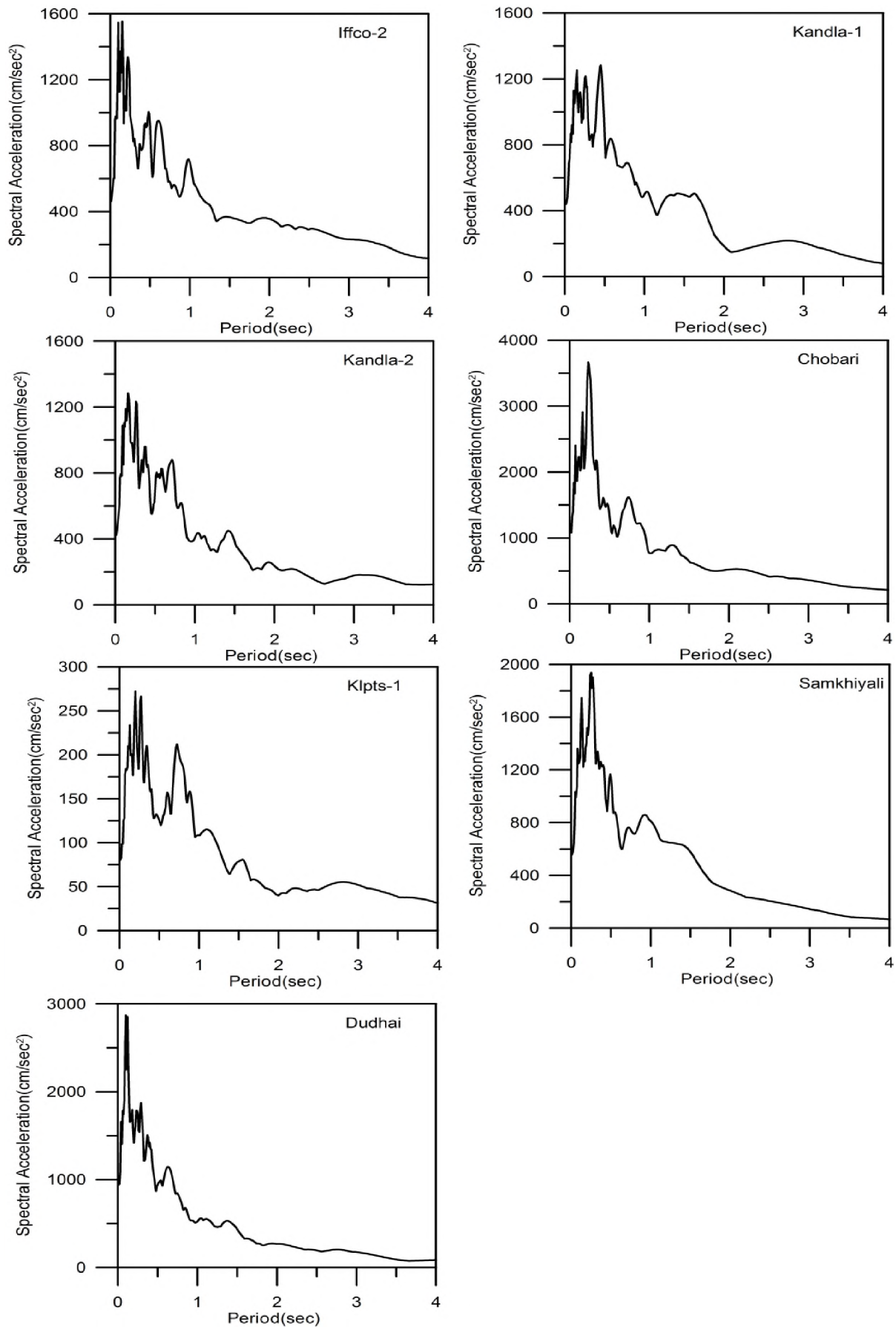
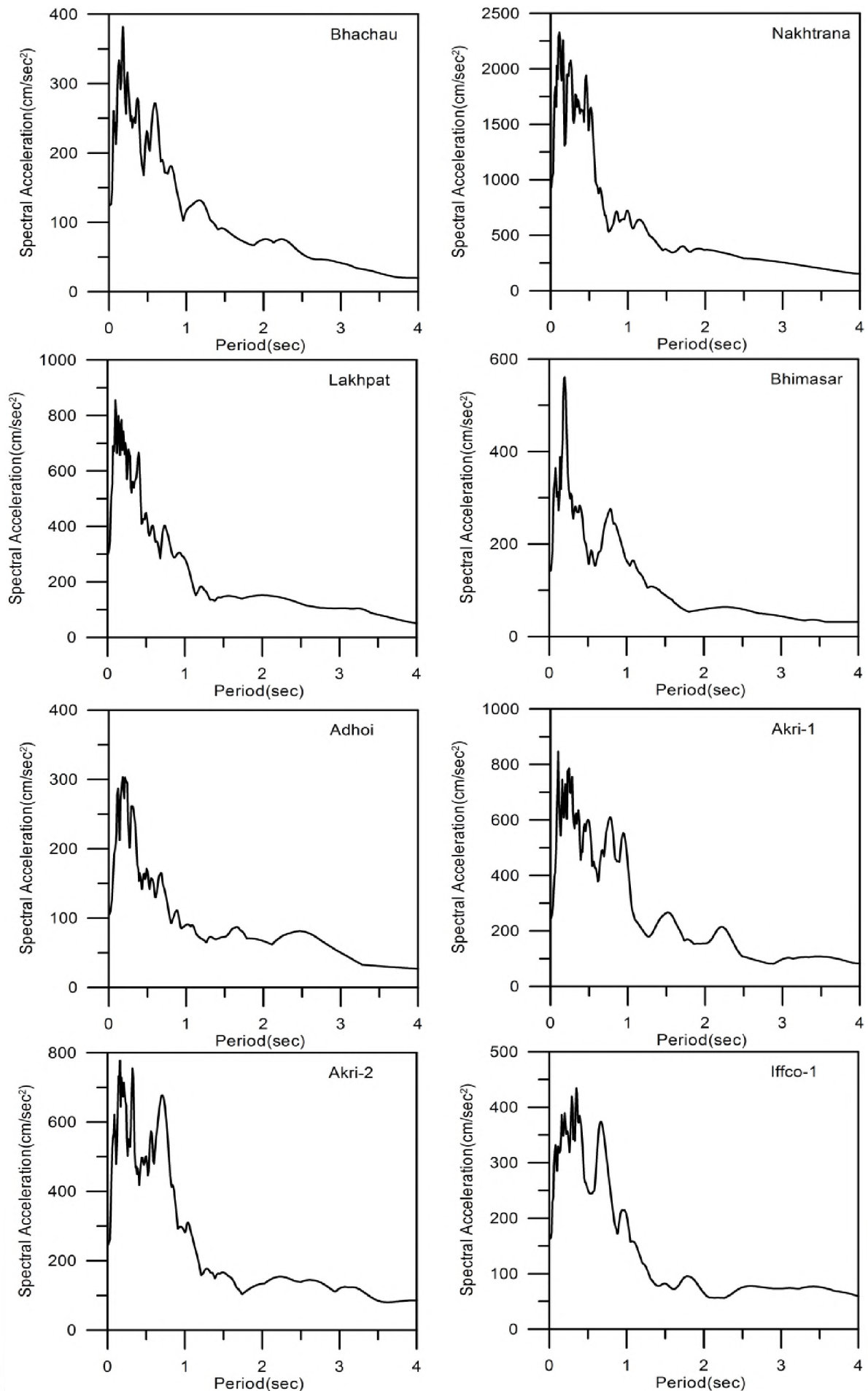


Fig.5.5.6: The response spectra at 5% damping computed for 2001 Bhuj earthquake scenario at stations mentioned in the upper right portions in the figures.



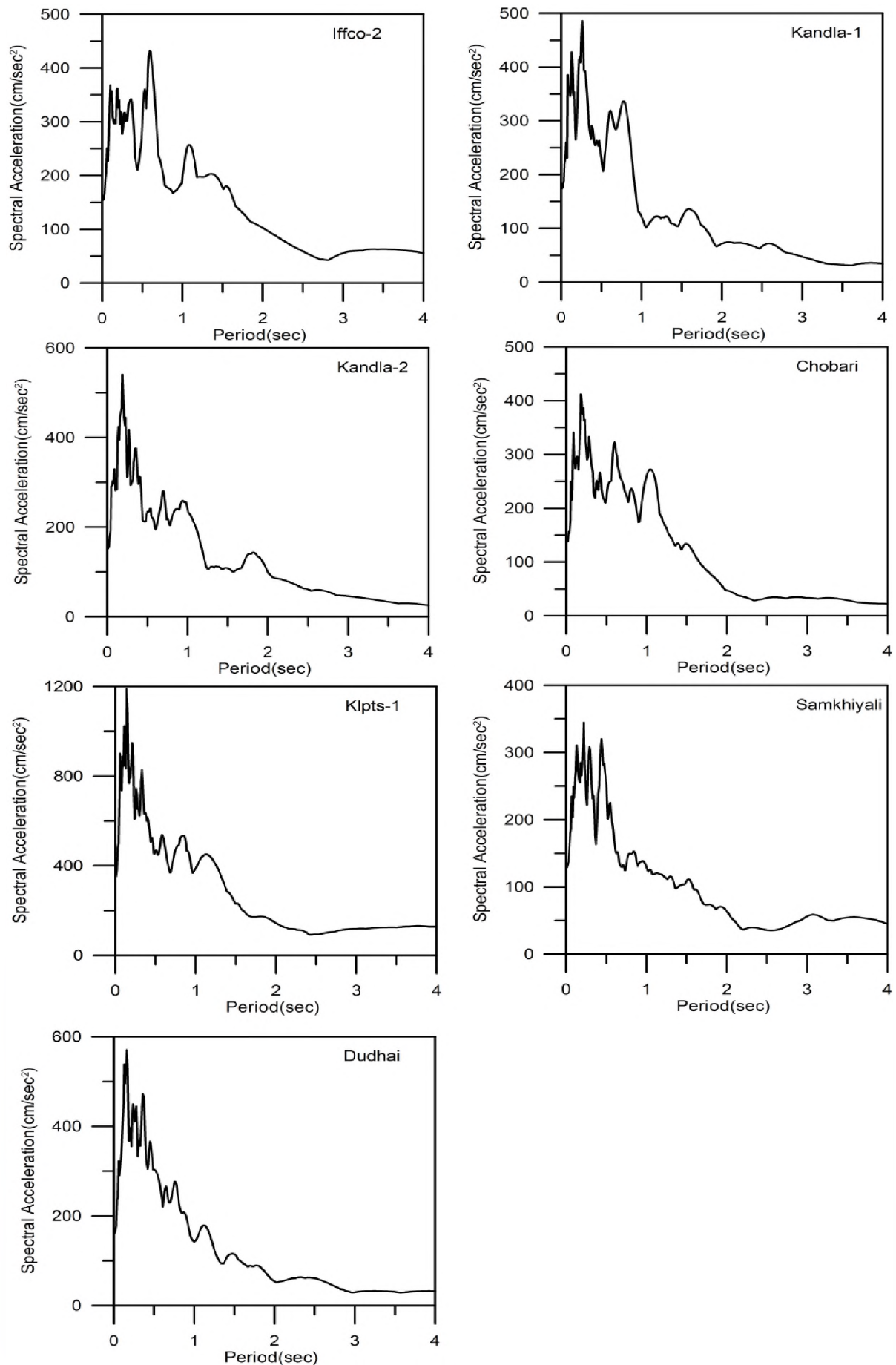
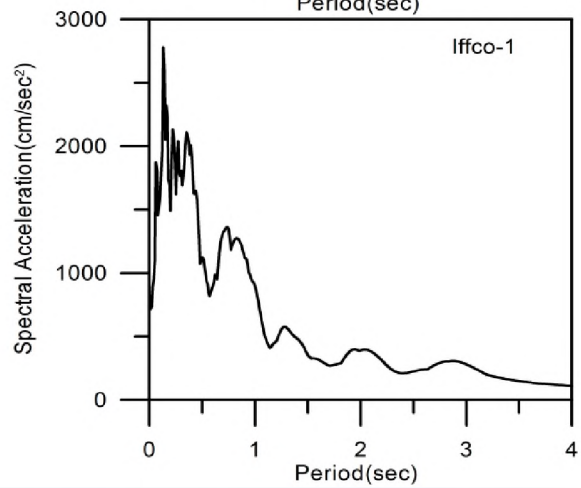
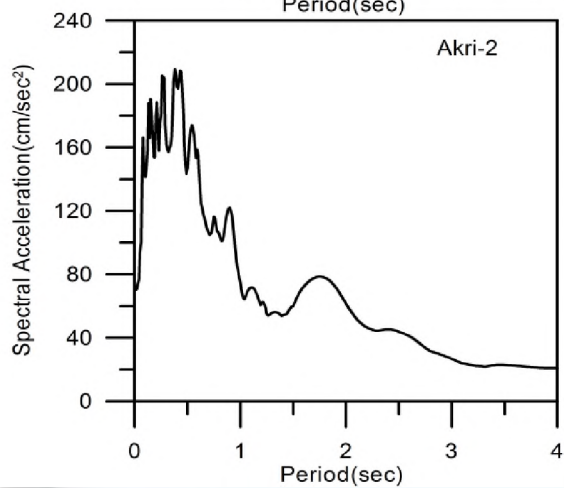
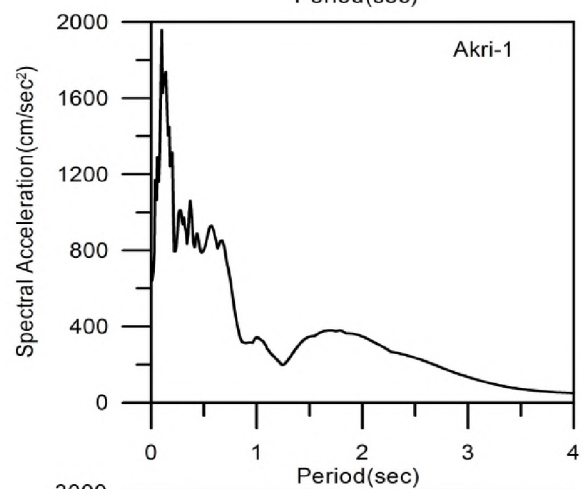
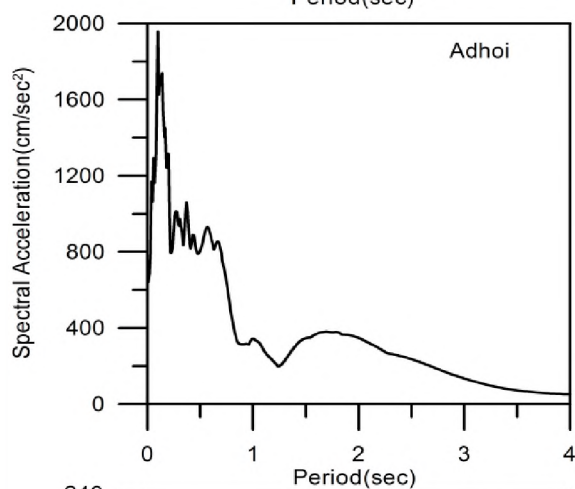
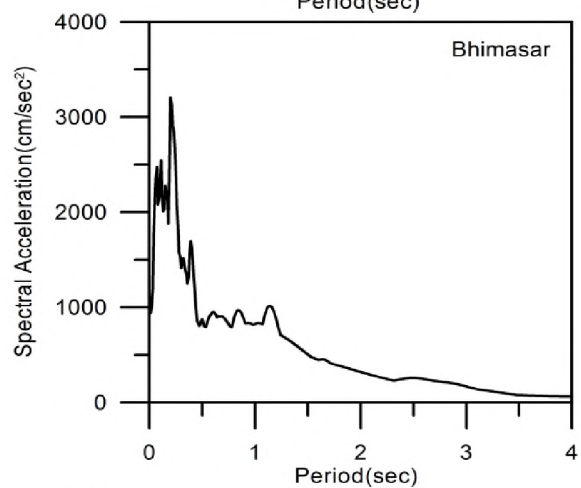
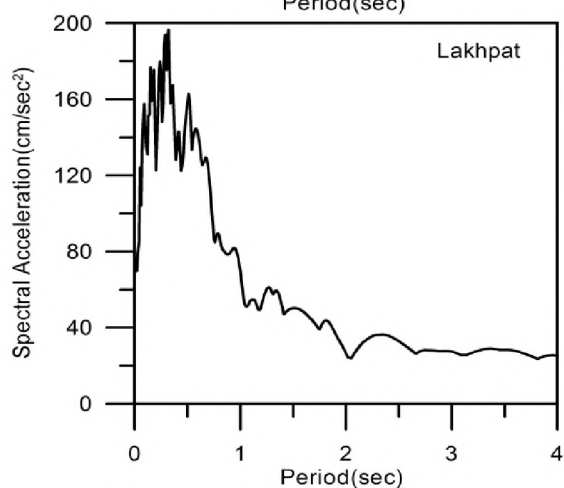
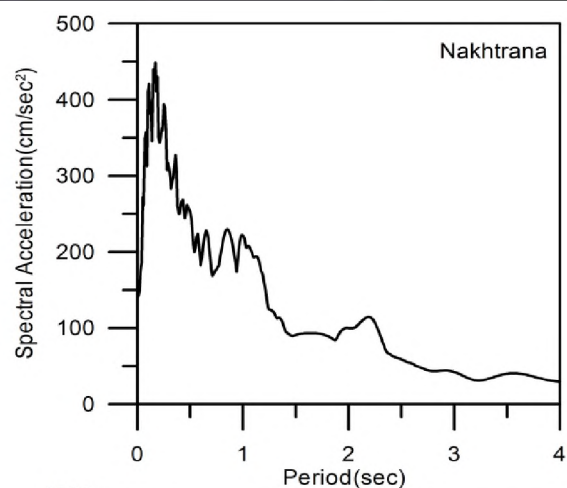
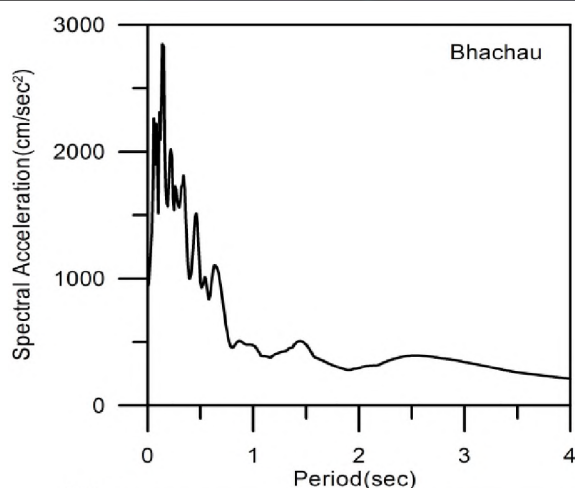


Fig.5.5.7: The response spectra at 5% damping computed for scenario earthquake along western part of KMF (KMF-A) at stations mentioned in the upper right portions in the figures.





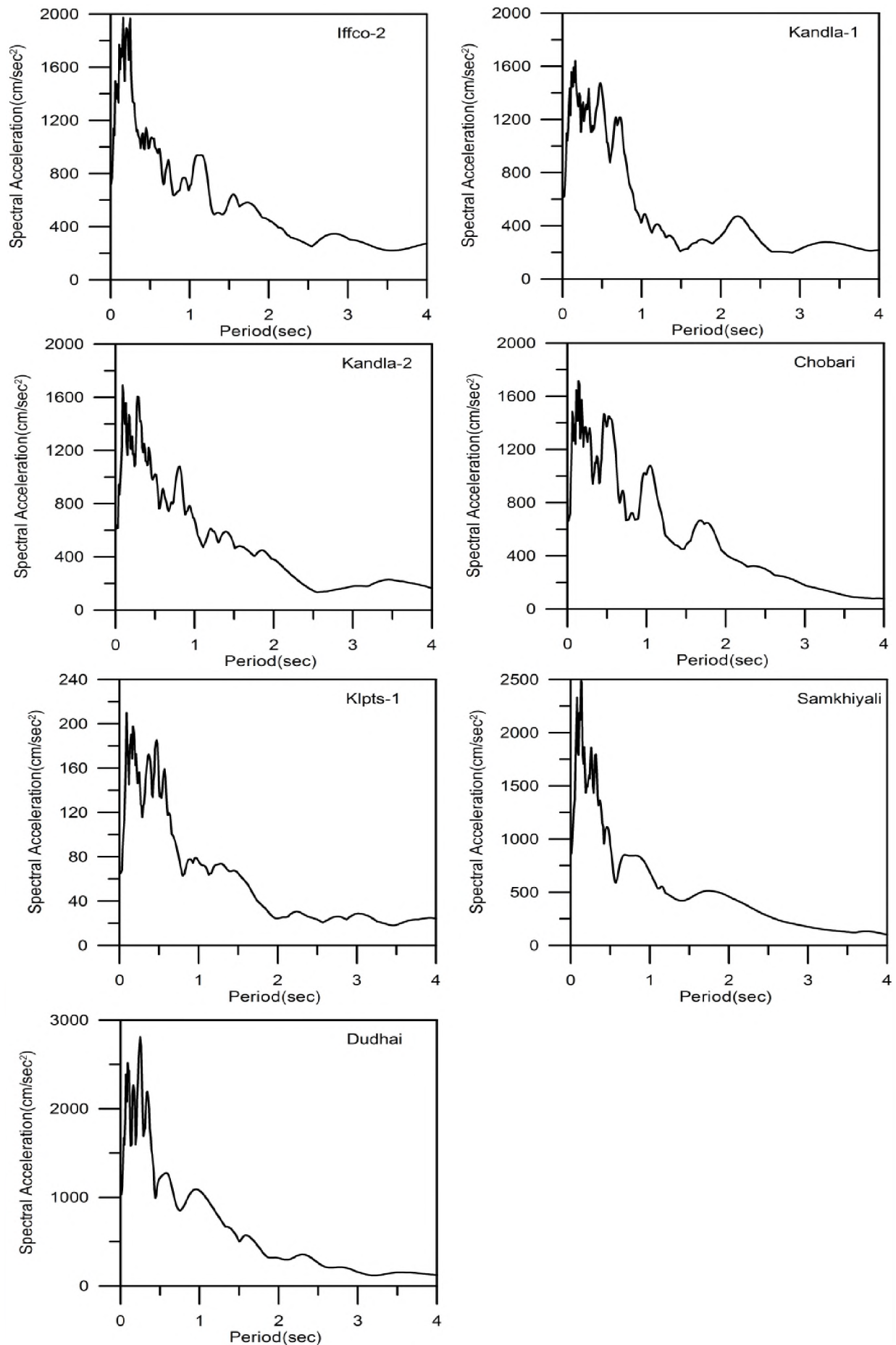
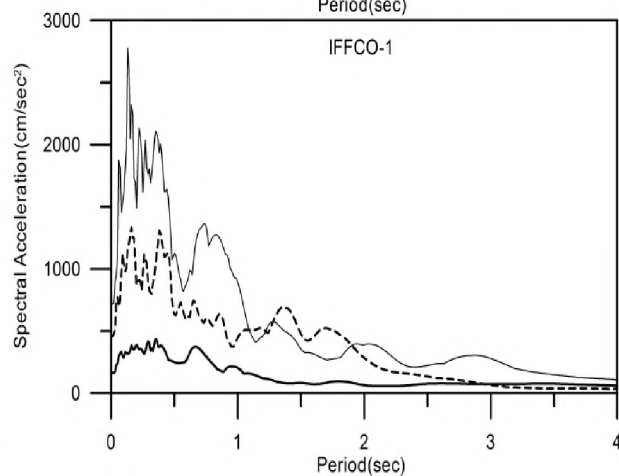
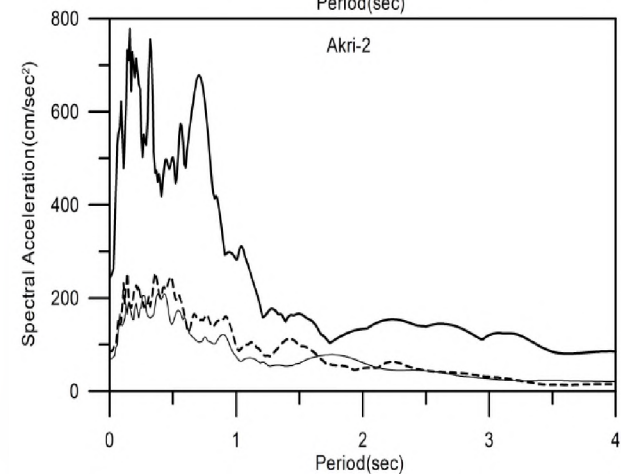
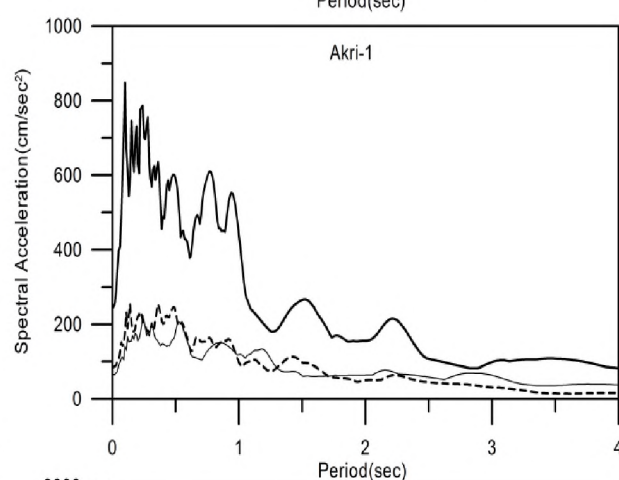
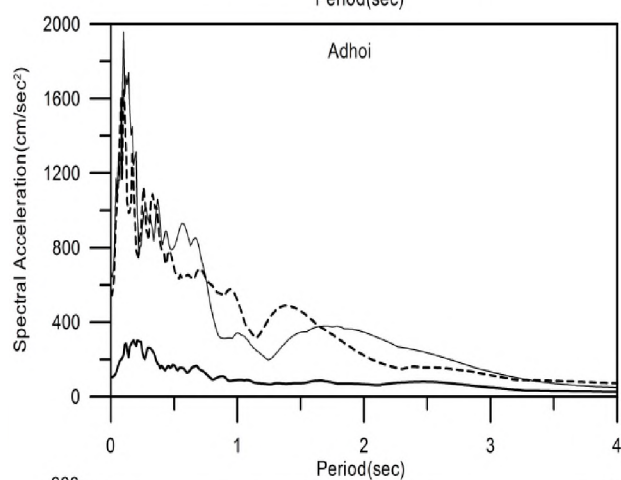
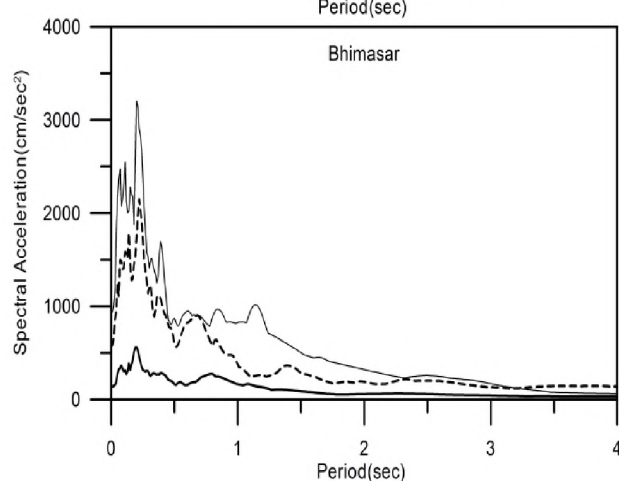
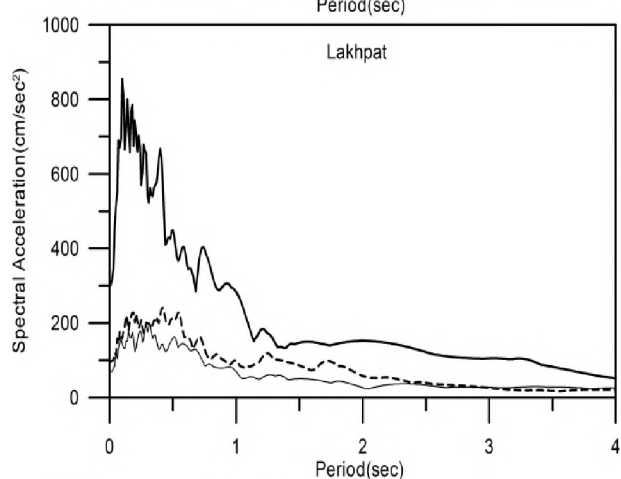
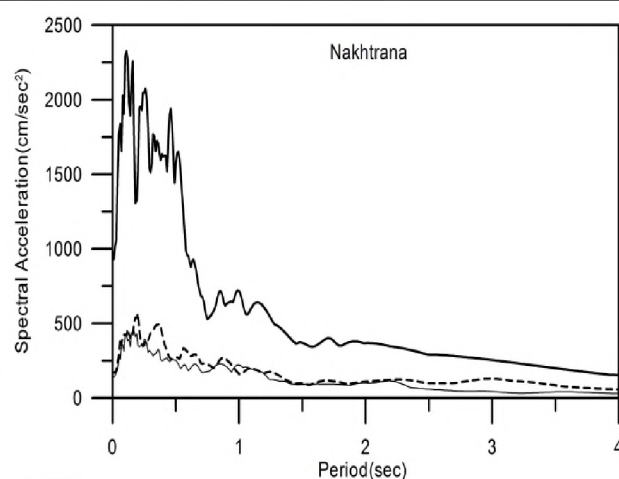
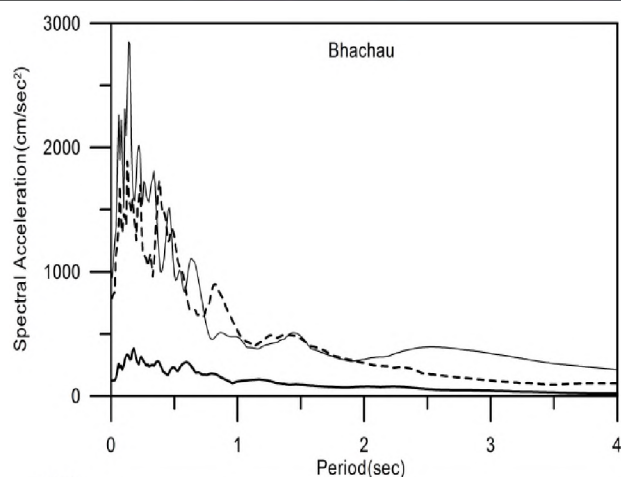


Fig. 5.5.8: The response spectra at 5% damping computed for scenario earthquake along eastern part of KMF (KMF-C) at stations mentioned in the upper right portions in the figures.



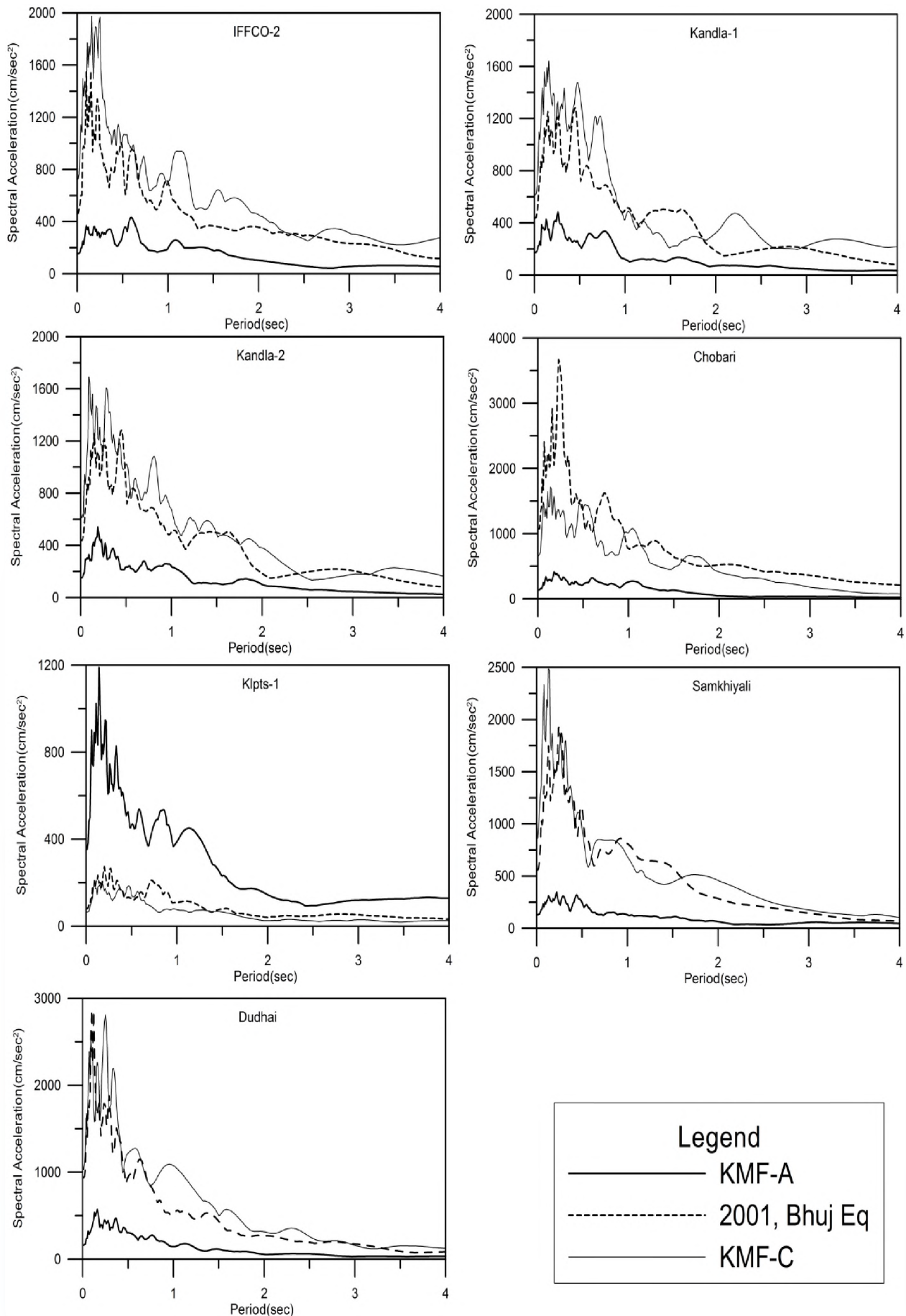


Fig. 5.5.9: The response spectra at 5% damping computed due to scenario earthquakes along western part of KMF (KMF-C), eastern part (KMF-A) and 2001 Bhuj earthquake at stations mentioned in the figures.

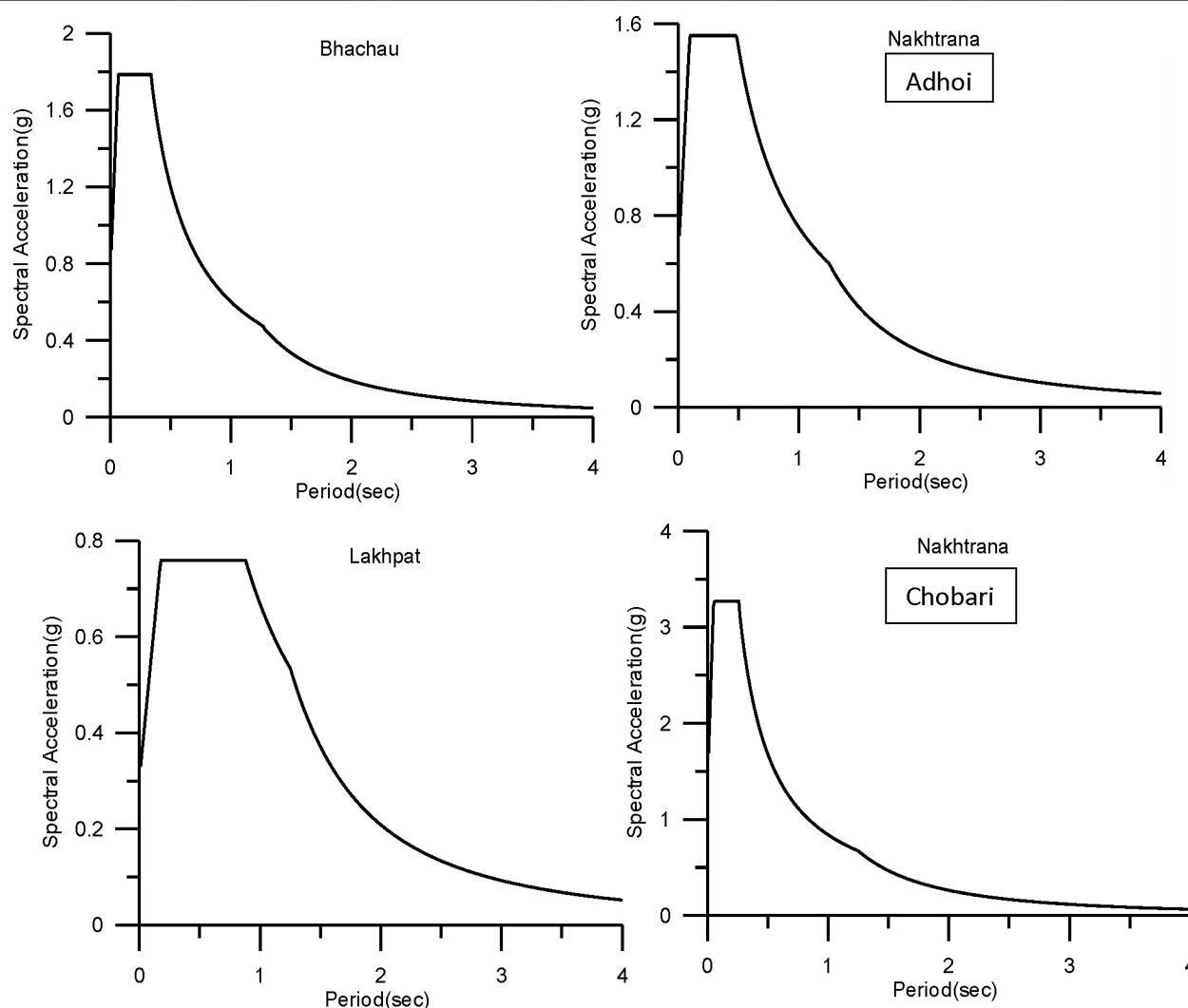


Fig. 5.5.10: The design response spectra calculated for the four industrial stations from NEHRP method. In this method the spectral acceleration at 0.2sec and 1sec are supplied as input with the soil type (A, B, C, D, E) from NEHRP classification.

## 5.6 DEFINITION OF SEISMIC AND TSUNAMI HAZARD SCENARIOS BY MEANS OF INDO-EUROPEAN E-INFRASTRUCTURES

*(Pallab Choudhury, B K Rastogi in Collaboration with A Peresan, F Vaccari and G F Panza, Trieste University, Italy)*

The Department of Geosciences, Trieste University has developed a new technique called neo-deterministic seismic hazard assessment (NDSHA) which gives a realistic output of the seismic ground motion due to an earthquake of given magnitude at a distance. The approach is based on modelling techniques that have been developed from a detailed knowledge of both the seismic source process and the propagation of seismic waves. The technique permits us to define a set of earthquake scenarios and to simulate the associated synthetic signals without having to wait for a strong event to occur. NDSHA can be applied at the regional scale, computing seismograms at the nodes of a grid with the desired spacing, or at the local scale, taking into account the source characteristics, the path and local geological and geotechnical conditions. Synthetic signals can be used as seismic input in subsequent engineering analyses aimed at the computation of the full non-linear seismic response of the structure or simply the earthquake damaging potential.



Under this joint project, the sites of Ahmedabad, Dholera and Gandhidham have been identified for the implementation of neo-deterministic method for the determination of seismic hazard and seismic microzonation and NDSHA has been carried out for Ahmedabad region for a local scenario.

A 1D sub-surface shallow profile is made for the Ahmedabad region using inputs from the receiver function analysis carried for the said region under a joint Indo-Taiwan research project on scenario strong motion studies in Gujarat region. The receiver function (RF) analysis was carried out beneath 32 seismic stations spread all over Gujarat including a station Gandhinagar, very close to Ahmedabad and in the same tectonic environ and two stations Surendernagar and Kadana on west and east side respectively of the Cambay rift. The averaged receiver functions obtained at each sites are then inverted using Genetic Algorithm (GA) to get the velocity structure beneath each site. A good 2D velocity structure is obtained for the Gujarat region including the Cambay basin in which Ahmedabad is located. An east-west section across Ahmedabad was prepared up to depth of 70m using velocity structure obtained from receiver function analysis for Gujarat region.

For 2D model, we have used velocities obtained from PS logging carried out in the Ahmedabad region by the ISR and made a 25 long profile. The path effect was compensated using data from published literature and work by ISR scientists in Gujarat region. The west Cambay marginal fault is capable of generating an earthquake of magnitude 6.0. For generation of ground motions, distance of the source from the profile is 20 km, depth is kept at 10 km, and orientation of the fault is kept such that strike=10, dip=60, and rake is taken as 90 as per prevailing tectonics. For computation of ground shaking of scenario earthquake in Ahmedabad region, we first generated the synthetic seismograms at the bedrock level. The ground motion at the surface is computed using 25km long and 70 m deep 2D cross section. The ground motions were then generated along the entire 25km long profile. We generated 99 realizations of source time functions for 0, 90 and 180 directivity angle. Finally the response spectra were generated for 99 realizations of source time functions for 0, 90 and 180 degree directivity angle for 2%, 5%, 10% and 20% damping.

An example of obtained ground motions and average response spectra are shown in Figures 5.6.1 and 5.6.2, respectively. The methodology will be used in the seismic microzonation of Ahmedabad region and subsequently at Dholera and Gandhidham and other parts of Gujarat. The initial results are encouraging and more realistic.

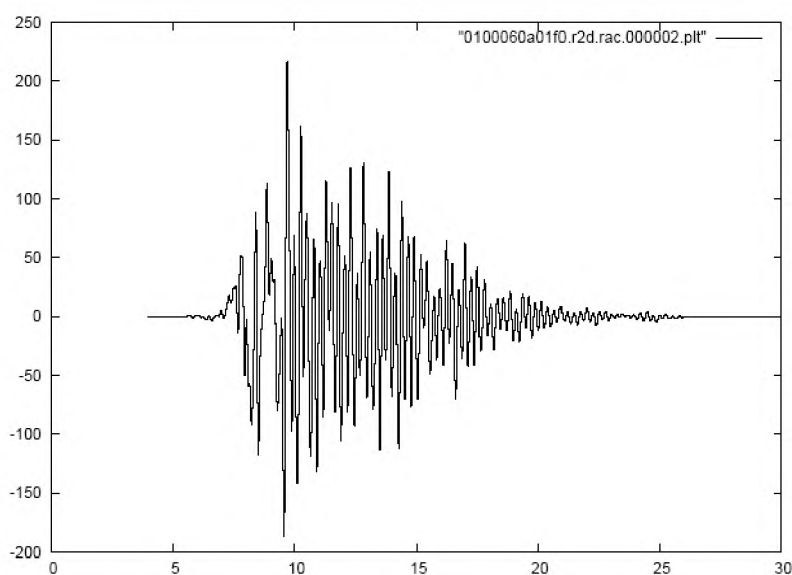


Fig. 5.6.1: Synthetic accelerogram for M6, focal depth 10km, epicentral distance 20 km derived for Ahmedabad region by NDSHA methodology.

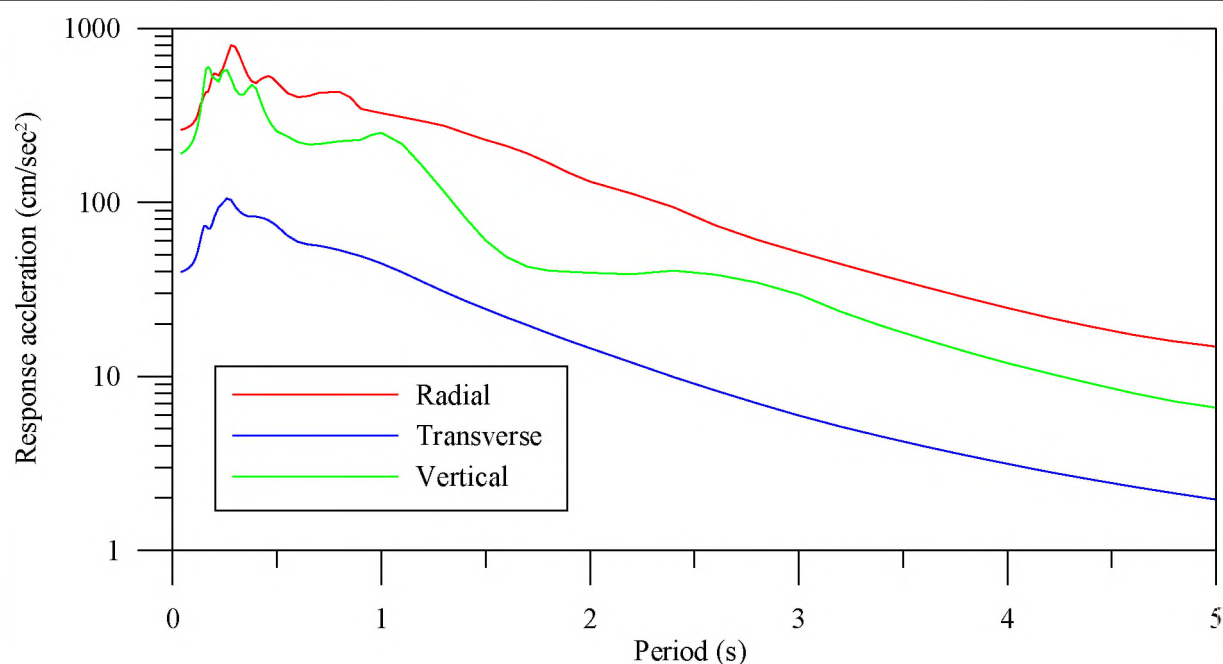


Fig 5.6.2: Average response spectra for 5% damping for M6, focal depth 10km, epicentral distance 20 km derived for Ahmedabad region by NDSHA methodology.

#### 5.7 A REVIEW OF STRONG MOTION STUDIES IN GUJARAT STATE OF WESTERN INDIA

*(Pallabee Choudhury, Ketan Singha Roy and B K Rastogi along with Sumer Chopra of Seismology Division, Ministry of Earth Sciences, Prithvi Bhawan, New Delhi)*

The work reviews the strong motion studies done in Gujarat state of Western India. The study has been carried out using actual acceleration data obtained from a dense network of 54 strong motion accelerographs as well as synthetic data generated using region specific ground motion parameters. The recorded data are used to obtain region specific ground motion parameters and ground motion prediction equation. The recorded acceleration time histories are also used as element earthquakes for generation of time histories for future large earthquakes using Empirical Green's Function approach. As Gujarat has three distinct regions having varied geological conditions, the recorded strong motion data gave an opportunity to study the effect of geological and local site conditions on the response spectra. This study for an intra-plate region like Gujarat is a pioneer work. Deterministic seismic hazard analysis (DSHA) has been carried out for the entire Gujarat region using modified stochastic finite fault modeling approach. The estimated PGA and MMI values obtained in the analysis have been used to estimate the vulnerability of the different types of buildings in 31 cities of Gujarat. The state of Gujarat is the most industrialized state of India with lots of new special investment regions and infrastructure projects are lined up. It is necessary that proper seismic hazard analysis is carried out at each site of interest. The recorded time histories play an important role in testing various models to constrain the parameters required for generating ground motions for a required magnitude at a site of interest. This is of much use in seismic microzonation of regions where actual recordings of large earthquakes are not available. The end result of all these studies would make the region safer from future earthquakes. Most of the active faults are in the Kachchh region where large earthquakes occurred. A lead time of few tens of seconds is available for cities like Ahmedabad, Gandhinagar, Surat and other industrial towns in south Gujarat. It is worth mentioning that for earthquake disaster mitigation, a successful early warning system can be a keystone. The success of such type of early warning will depend on the analysis of strong motion data recorded at various sites in Gujarat.

## 5.8 PROBABILISTIC SEISMIC HAZARD MAP OF INDIA

*(BK Rastogi, Pallabee Choudhury, Ketan Singharoy)*

The Bureau of Indian Standard (BIS) has given task to prepare a probabilistic seismic hazard map of India. As the large earthquakes in the neighboring countries also affect India, the study is conducted in the subcontinent region. The study region consists of India including Andaman-Nicobar islands and also Pakistan, Hindukush, Karakoram, Tibet and Burma bounded by  $5^{\circ}$  -  $40^{\circ}$  N and  $65^{\circ}$  -  $100^{\circ}$  E. A seismicity database has been prepared for the period AD 180 to 2008 containing 35302 earthquakes using all existing catalogues. The prepared seismicity database has been homogenized for moment magnitude ( $M_w$ ) with the help of various empirical relationships developed among different magnitude scales ( $M_L$ ,  $M_s$ ,  $m_b$  and  $M_w$ ). Around 50% dependent events (foreshocks and aftershocks) have been removed from the entire catalogue. The cut-off magnitude (threshold magnitude or magnitude of completeness,  $M_c$ ) for this seismicity database is estimated as  $M_w$  4.5 for interplate (Himalayan seismic belt) region and 4.1 for intraplate (Peninsular India) region. The completeness periods for different magnitude ranges are also estimated. It is observed that in Peninsular India, events with magnitude in the range 4.0-4.5 are complete for 80 years, while events for  $M_w > 4.5$  are complete for 200 years. Along Himalayan plate boundary regions, catalogue is complete for 40 years for magnitude between 4.0 and 5.0; 80 years for 5.0- 6.0; 100 years for 6.0-7.0; and 200 years for  $>7.0$ . The seismic source zones have been delineated based on earthquake epicenters distribution and active fault mapping. A total 32 main seismic source zones have been delineated in the study region. The seismotectonics characteristics of these source zones have been explained. The earthquake hazard parameters (maximum magnitude, earthquake activity rate, beta, b-value and return periods) have been estimated for all delineated seismic source zones. These hazard parameters have been used to prepare the probabilistic seismic hazard map of India for two levels of probability of exceedance in 50 yr (Figs. 5.8.1 and 5.8.2). Table 5.8.1 gives PGA values at ground with  $V_s$  610m/s at some locations. The analysis was carried out by using CRISIS 2003-CL, version 3.0.2 and all ground motions are computed for hard rock ( $V_s \geq 610$  m/s).

**Table 5.8.1: PGA values at ground with  $V_s$  610m/s at some locations**

Region	PGA in gals	
	10% PE	2% PE
Andaman	314	544
Arakan-Yoma	320	542
Himalayan Arc	326	571
Shillong Plateau	325	571
Trans-Himalaya	202	353
Tibet	151	268
Delhi	80	150
Cambay Region	86	152
Kachchh Region	150	340
Ahmedabad	47	100
Son-Narmada Region	65	140
Koyna region	99	192
Tamilnadu Region	30	65
Cuddapha Region	31	69
East Coast Region	23	54
Kerala region	34	75
Kolkata	26	61
Chennai	21	53
Guwahati	293	523
Hyderabad	30	68

475 years

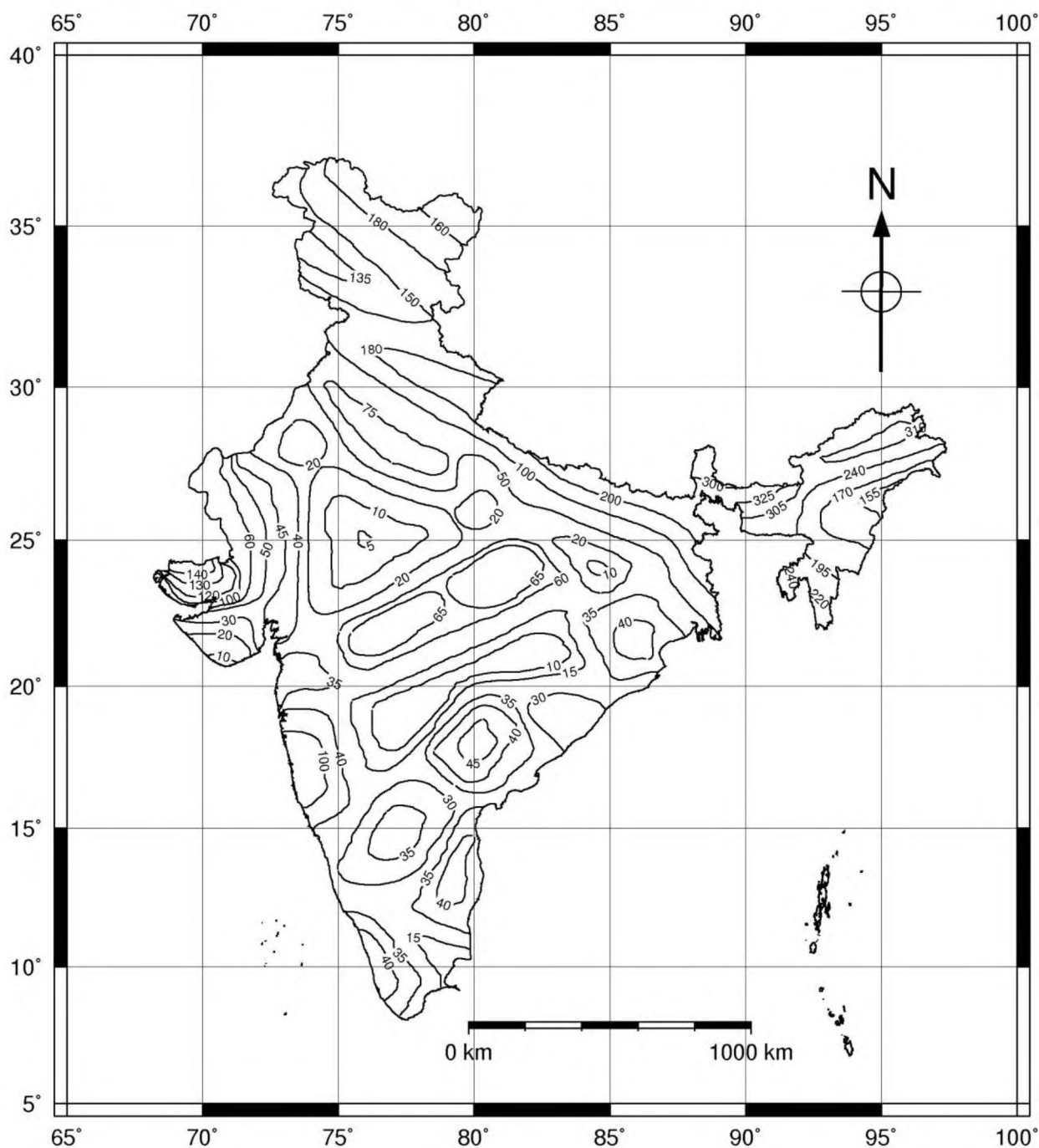
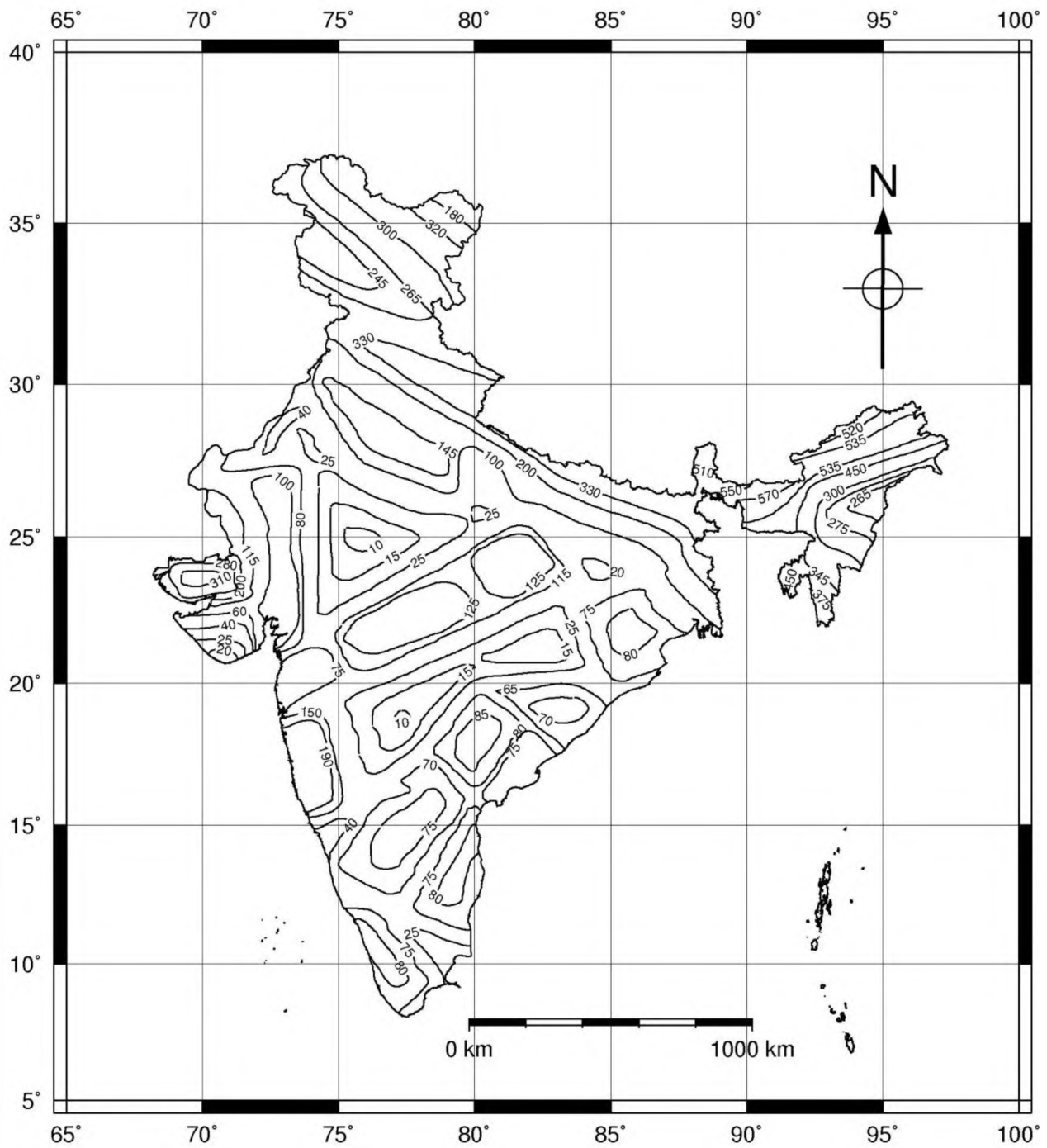


Fig. 5.8.1: PGA exceedance at ground with  $V_s$  610m/s at 10% probability in 50 years



2475 years



# CHAPTER 6

## SEISMIC MICROZONATION AND HAZARD ASSESSMENT OF INDIVIDUAL SITES

Seismic microzonation investigations were carried out for Ahmedabad, Gandhinagar, Dholera Special Investment Region and New VS Hospital building site in Ahmedabad. The quantity of different types of investigations in these areas is given in Table 6.1.

**Table 6.1: Quantity of boreholes, grid size, MASW, PS Logging and Array Microearthquake observations for different areas**

Location	Area,	Boreholes	Grid Size	MASW	PS Log	Array MicroTremor
Gandhidham	300 sq.km	80	500m	14	16	12
Dholera	900 sq.km	87	500m	41	16	23
GIFT City	1.5 sq.km	14 +126	500 m	7	7	5
Ahmedabad	625 sq.km	220	1.5 km	51	10	15
Gandhinagar	25 sq.km	12	1.5 km	61	6	10
VS Hospital	120mx60m	20	-	4	7	4

## 6.1 INVESTIGATIONS OF SEISMIC MICROZONATION OF AHMEDABAD CITY

### 6.1.1 Geotechnical Investigations in Ahmedabad

Borehole geotechnical data has been collected for around 500 bore holes of 10 m to 70 m depth range in Ahmedabad City (Fig.6.1.1 and 6.1.2). Location of Ahmedabad is shown in Fig. 6.1.3 on the Geology of Gujarat state. The litho-units are a mixed variety of clay with silt and sand units which form the flood plain deposits of Sabarmati River which divides the city into two parts one eastern and the other western. Also, the secondary geotechnical data was sorted for N-value corrections and mechanical properties of soil were determined as per the requirements for the microzonation. N-values are for about 300 or more boreholes. These boreholes are well distributed in Ahmedabad City. Around 87 boreholes of GSI are also included for SPT corrections ranging up to 50 m or so. Also, data collected by other geotechnical agencies are considered where SPT values are up to 20 m depth or so.

Drilling of 10 boreholes up to about 100m depth gave a regional picture of Engineering Bed Layer and act and provided controlling points regarding soil properties. The location of Ahmedabad on geological map of Gujarat is shown in Fig. 6.1.3.

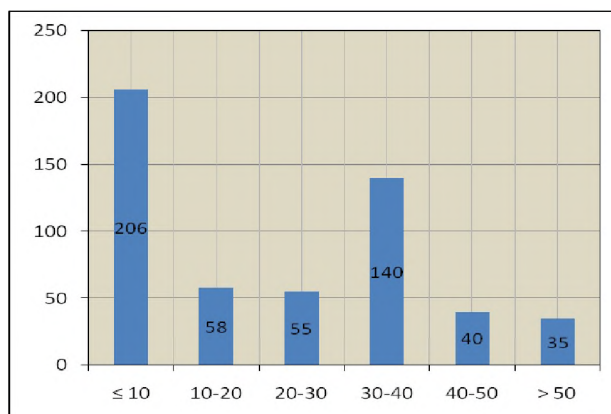


**Fig. 6.1.1: Depth (m) vs. Total no. of boreholes in Ahmedabad**

### 6.1.2 Details of Operation of Seismographs, Site Amplification Study Using Earthquake Records and Microtremors

In order to estimate site characteristics and to find geological structure, five broadband seismographs have been installed in Ahmedabad city, totally at 17 sites (Fig. 6.1.4 and Table 6.1.2). The seismographs are Guralp CMG 3T (50Hz to 120sec) velocity sensors with 24 bits REFTEK Digitizers.

The data of seismographs are periodically collected. The locations of the stations are changed after recording a few  $M \geq 4$  earthquakes. A total of 24 recorded earthquakes for two years observation are listed in Table 6.1.3, which are mostly from Kachchh, and a few from Rajasthan, Madhya Pradesh and Pakistan. Kachchh events are at epicentral distance around 220km, and almost once a month such an earthquake has been recorded. Only one local earthquake  $M$  2.3 about 38 km North-east of Bhat village Ahmedabad, seismic station has been recorded.

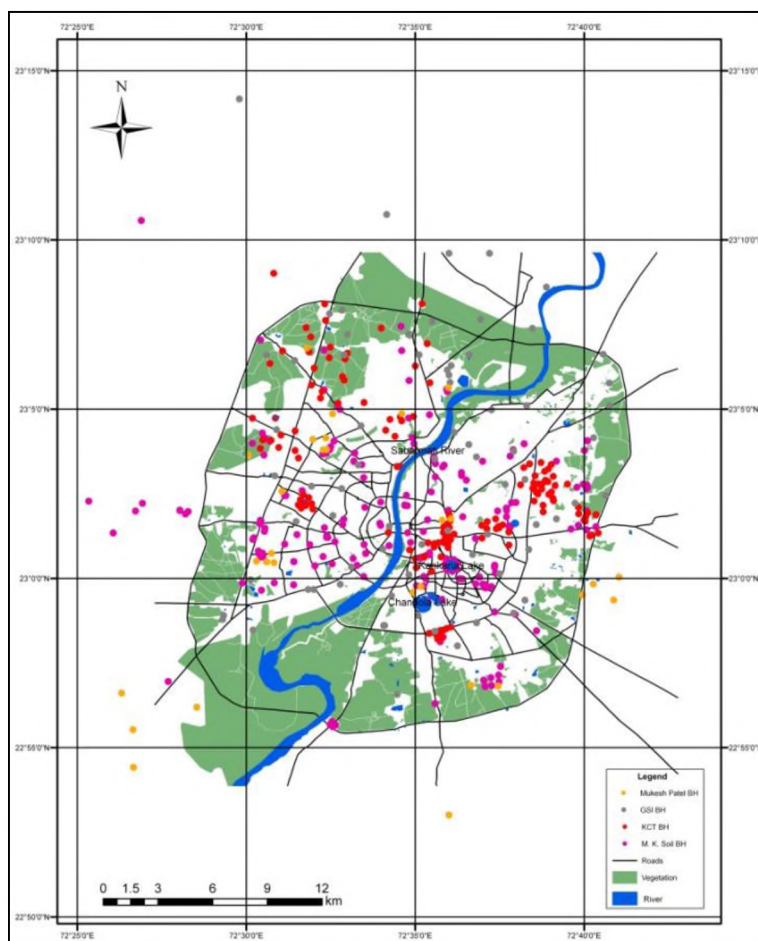


Fig. 6.1.2: Borehole Location Map of boreholes through secondary geotechnical data

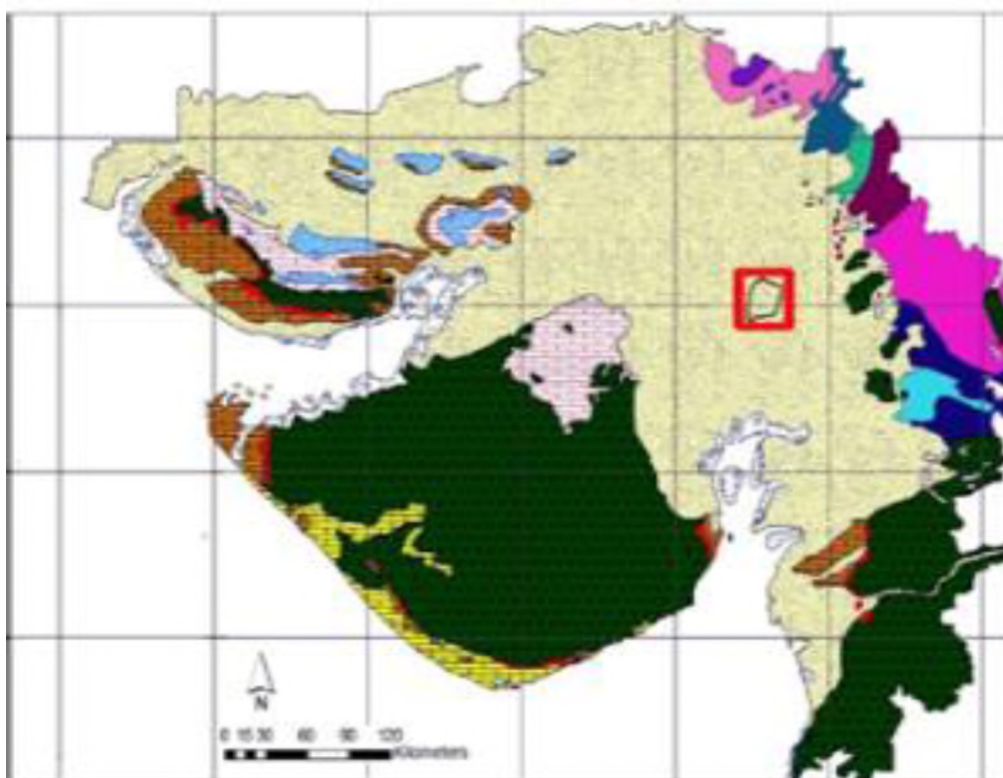


Fig. 6.1.3: Location of Ahmedabad on geological map of Gujarat

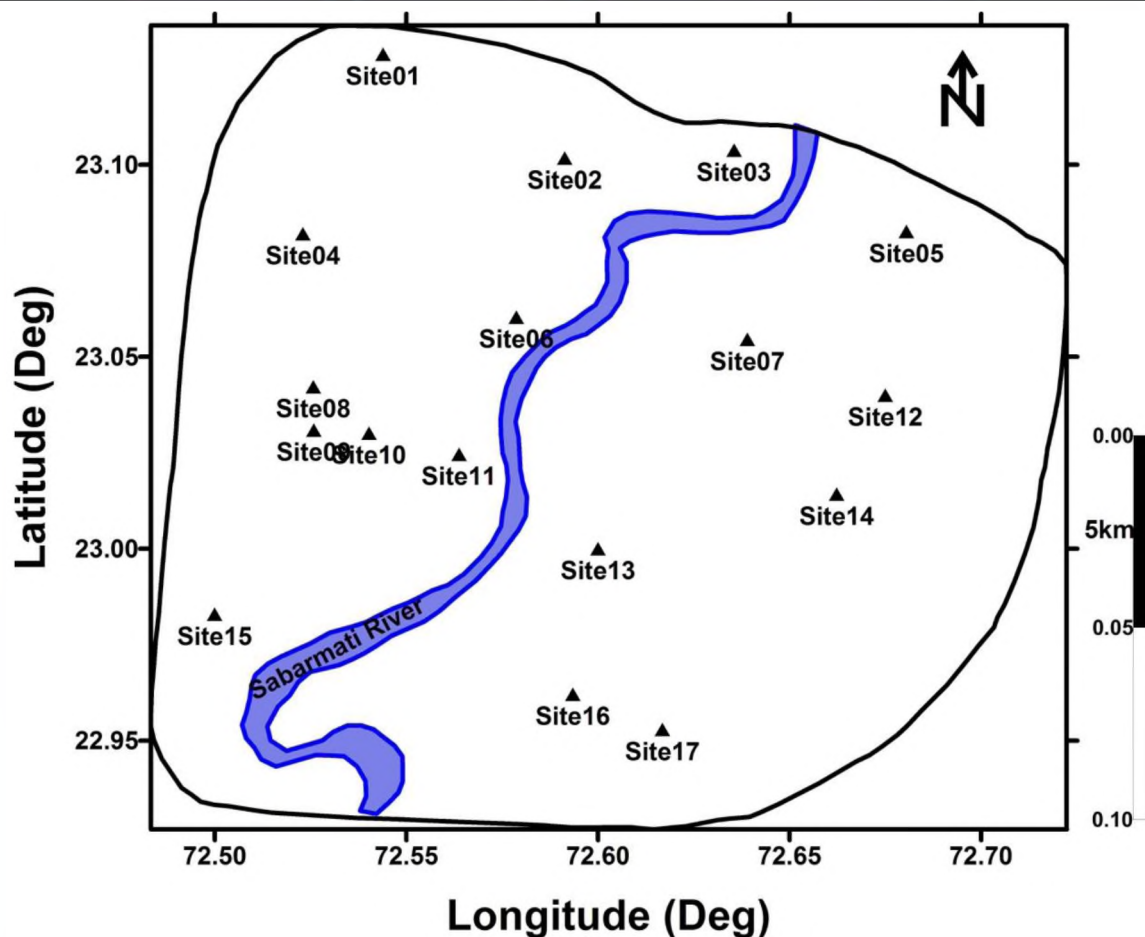


Fig. 6.1.4: BBS stations occupied in Ahmedabad city

Table 6.1.2: BBS stations deployed in Ahmedabad city

Site Sr. No.	Place Name in Ahm. city	Latitude (Deg)	Longitude (Deg)	Duration of Installation
Site01	Nirma University	23.1288	72.5439	07-05-2009 to 15-10-2009
Site02	D_Mart	23.10173	72.5913	Only two Hours Microtremor data
Site03	Bhat village	23.1038	72.6355	01-12-2009 to 26-07-2010
Site04	High court	23.08205	72.52295	08-11-2008 to 24-03-2009
Site05	Hanspura	23.0826	72.6805	Only two Hours Microtremor data
Site06	Gandhi-Ashram	23.06032	72.5787	Only two Hours Microtremor data
Site07	Krishannagar	23.0545	72.6390	15-10-2009 to 22-02-2010
Site08	Soham Tower	23.0422	72.5257	24-03-2009 to 28-11-2009
Site09	Sagar Tower	23.0309	72.5258	21-03-2009 to 07-12-2009
Site10	L.D.Eng.College	23.0301	72.5402	Only two Hours Microtremor data
Site11	Ellis-Bridge	23.0246	72.5637	04-10-2008 to 28-04-2009
Site12	Nicol	23.0400	72.6750	15-10-2009 to 14-05-2010
Site13	Maninagar	23.0000	72.6000	26-11-2009 to 26-10-2010
Site14	Adinathnagar	23.0142	72.6623	Only two Hours Microtremor data
Site15	Sarkhez	22.9829	72.4999	01-05-2009 to 16-01-2010
Site16	Narol	22.9621	72.5934	01-05-2009 to 18-05-2010
Site17	Vatwa	22.9529	72.6168	05-05-2009 to 25-11-2009



**Table 6.1.3: List of Earthquakes Records in BBS sites of Ahmedabad city**

Earthquakes			(SN) Serial Number, (S) Site, (NW) Not Working											
SN	Loc	Mag. Date	S04	S11	S9	S8	S15	S16	S17	S01	S07	S12	S13	S03
1	Kachchh 23.79 <sup>0</sup> N 70.70 <sup>0</sup> E	3.7 27/12/08	√	√								√		
2	Madhya .Pradesh 21.34 <sup>0</sup> N 75.28 <sup>0</sup> E	4.2 04/01/09	√	√										
3	Pakistan 35.56 <sup>0</sup> N 73.77 <sup>0</sup> E	5.3 20/02/09	√	√										
4	Kachchh 23.36 <sup>0</sup> N 70.39 <sup>0</sup> E	4.4 26/02/09	√	√										
5	Kachchh 23.36 <sup>0</sup> N 70.39 <sup>0</sup> E	3.7 10/03/09		N.W.										
6	Karachi 26.03 <sup>0</sup> N 66.50 <sup>0</sup> E	4.9 22/03/09		√										
7	Kachchh 23.36 <sup>0</sup> N 70.39 <sup>0</sup> E	3.7 31/03/09		N.W.	√	√								
8	Rajasthan 27.14 <sup>0</sup> N 70.70 <sup>0</sup> E	5.0 09/04/09		√	√	√								
9	Kachchh 23.42 <sup>0</sup> N 70.14 <sup>0</sup> E	4.1 12/04/09			√	√								
10	Kachchh 23.42 <sup>0</sup> N 70.14 <sup>0</sup> E	3.8 18/05/09			√	√	√	√	√	√				
11	Kachchh 23.42 <sup>0</sup> N 70.14 <sup>0</sup> E	3.8 26/05/09				√	√	√	√	√				
12	Kachchh 23.52 <sup>0</sup> N 70.40 <sup>0</sup> E	3.7 03/09/09			√	√	√		√	√				
13	Kachchh 23.39 <sup>0</sup> N 70.22 <sup>0</sup> E	4.3 05/09/09			√	√	√		√					
14	Kachchh 24.42 <sup>0</sup> N 69.27 <sup>0</sup> E	4.4 09/10/09			√		√	√	√					
15	Kachchh 23.52 <sup>0</sup> N 70.40 <sup>0</sup> E	3.7 10/10/09							√					
16	Kachchh 23.71 <sup>0</sup> N 69.91 <sup>0</sup> E	4.5 28/10/09			√				√		√	√		

Earthquakes			(SN) Serial Number,								(S) Site, (NW) Not Working			
SN	Loc	Mag. Date	S04	S11	S9	S8	S15	S16	S17	S01	S07	S12	S13	S03
17	Kachchh 23.42°N 70.14°E	3.8 29/12/09												
18	Gandhinagar 23.28°N 72.95°E	2.3 26/01/10										√	√	√
19	Kachchh 23.52°N 70.24°E	3.8 05/02/10						√			√	√	√	√
20	Kachchh 23.82°N 69.95°E	3.7 01/04/10										√	√	√
21	Kachchh 23.38°N 70.35°E	3.7 06/04/10						√				√	√	√
22	Kachchh 23.34°N 70.49°E	3.9 23/08/10											√	
23	Patan 23.84°N 71.87°E	4.4 02/09/10											√	
24	Kachchh 24.82°N 71.98°E	3.8 24/10/10											√	

### ***Acquisition Methods***

Currently Predominant frequency and site amplification for the region has been investigated using microtremor data by H/V method and using the earthquakes records is under progress. The digitizer was operated at 100Hz. The FFT is applied to the signal of three components (NS, EW and V) to obtain spectral amplitudes. The spectra are then smoothed by Konno and Ohmachi (1998), method.

For earthquake records, 10.5sec time window starting from 0.5 sec before S-wave phase arrival and covering main S wave phase was used for all components. This time window length was chosen to best contain most of the high amplitude of S-wave energy of earthquake records, as pointed out by Bonilla et al. (1997). Sometimes, longer duration will be better for estimation of site characteristics such as 20 seconds including surface waves in this case.

For microtremor data analysis, 5 dataset files of 20min have been observed and 7 to 10 Nos. 70sec multiple windows have been selected from each data set. Then, H/V spectral ratios are calculated for each sample. The average of each sample is again averaged and find out the site response curve at a particular site.

Amplification is noted from H/V plot. Depth (h) to a layer corresponding to dominant frequency (f) can be estimated using the following formula if shear-wave velocity (Vs) can be assumed:

$$h = \left[ \frac{V_s}{4f} \right]$$

### **Results of Seismograph Observations and Analysis**

An example of recorded Kachchh earthquake M4.5, Time History and its Fourier spectra at Ellis Bridge site Ahmedabad is shown in (Figure 6.1.5). In general, since the whole Fourier spectra show sudden decrease of amplitude at 10-20 Hz, this may be due to both the low magnitudes and site characteristics. And mostly all records have components of frequency between around 0.1 to 10 Hz.

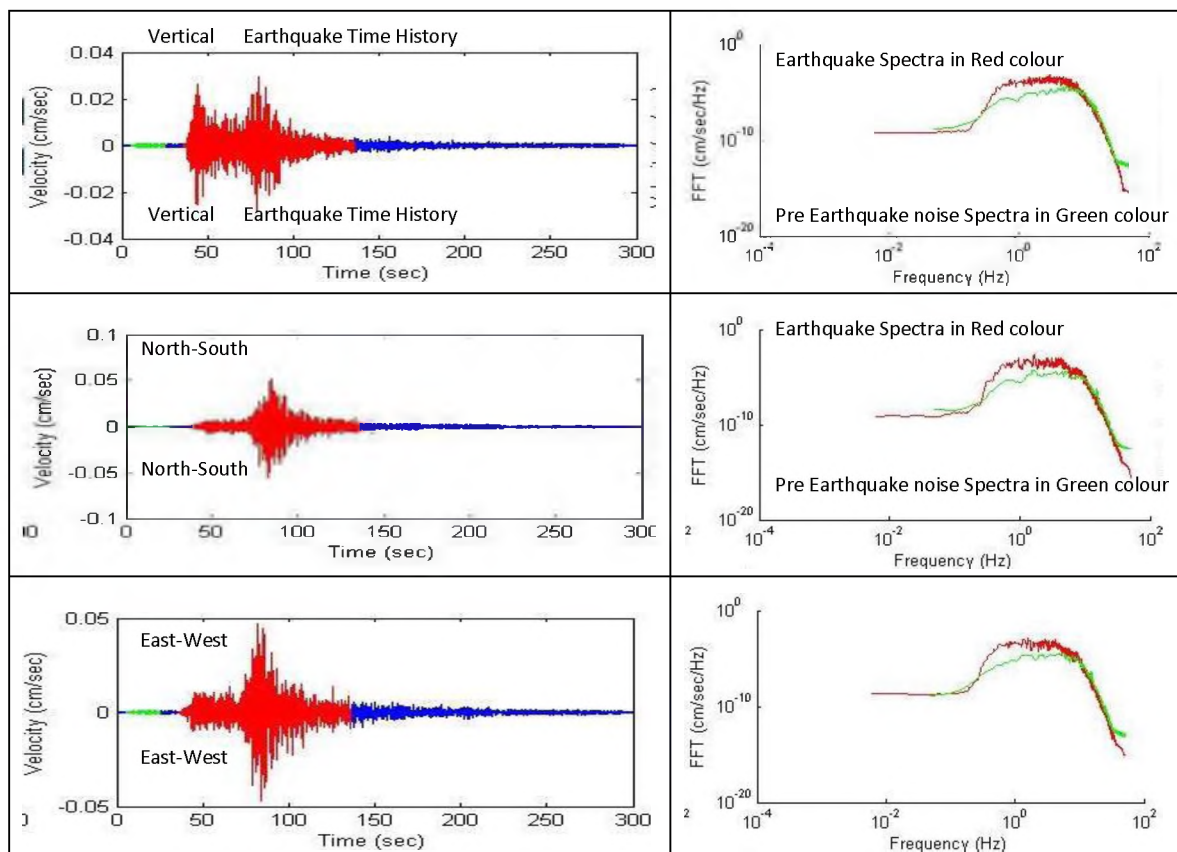


**Fig. 6.1.5: An Example of Earthquake records (Time History and Fourier Spectra), Kachchh Earthquake M 4.5 (28/10/2009)**

In regions with low seismicity but high seismic risk, such as Ahmedabad city, it is of high importance to derive the predominant frequency and amplification factor from the microtremor observation. The results estimate the resonance and dynamic behavior of multi-storey buildings or structure for assessment of damage due to local and regional earthquakes. In order to obtain the variations of these characteristics in the Ahmedabad city area, the systematic Broadband microtremor measurements, at 17 sites were carried out. Maps of predominant frequencies and amplifications factors were obtained. In the studied area the ground motion amplification factor is usually 1.3- 2.5 (in two locations about 6) over a frequency range of 0.2 to 10 Hz. The lower predominant frequency of resonance is 0.6 Hz which will correspond to Quaternary/Tertiary boundary at 333 m depth if  $A_v/V_s$  is taken as 800m/s. The higher frequency of resonance of 4 Hz may correspond to Holocene1/Holocene 2 boundary at 15-22 m depth for Average  $V_s$  250-350 m/s (Fig. 6.1.6, Table 6.1.4).

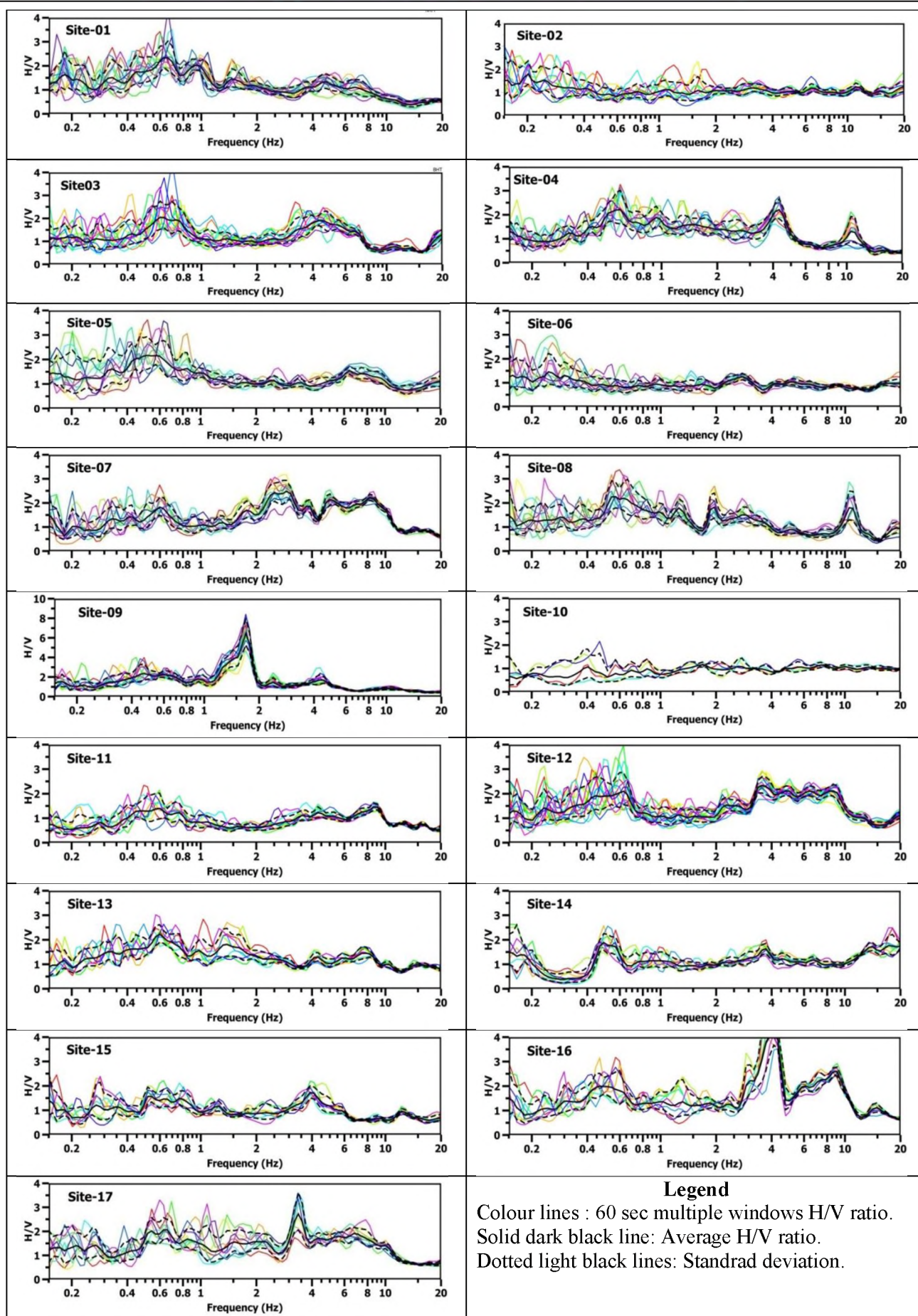
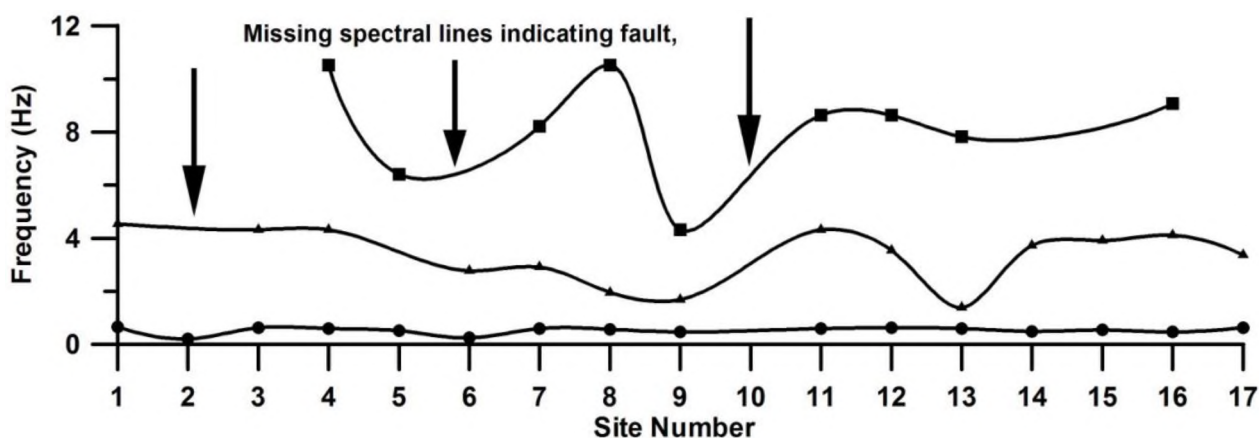


Fig. 6.1.6: H/V at different stations of seismograph operation using ambient vibrations



**Table 6.1.4: Peak frequency and Amplification factor using H/V spectral ratio of BBS Microtremor data**

Site	Place Name	F (Hz)	a	F (Hz)	A	F (Hz)	A
Site01	Nirma University	0.66	2.2	1.00	2.0	4.50	1.3
Site02	D_Mart near ONGC	0.20	2.0	Flat Response			
Site03	Bhat village	0.63	2.1	4.30	1.9	20	1.5
Site04	High court	0.60	2.2	4.32	2.2	10.52	1.3
Site05	Hanspura	0.52	2.2	6.42	1.5		
Site06	Gandhi-Ashram	0.25	1.5	2.77	1.3		
Site07	Krishannagar	0.60	1.8	2.91	2.5	8.22	2.2
Site08	Soham Tower	0.57	2.3	1.26	1.8	1.96	1.8
Site09	Sagar Tower	0.47	2.4	1.69	6.5	4.32	1.7
Site10	L.D.Eng.College	Flat Response					
Site11	Ellis-Bridge	0.60	1.4	4.32	1.2	8.63	1.5
Site12	Nicol	0.63	2.1	3.55	2.3	8.63	2.1
Site13	Maninagar	0.60	2.2	1.39	1.8	7.82	1.5
Site14	Adinathnagar	0.49	1.9	3.73	1.6	17.24	1.8
Site15	Sarkhez	0.54	1.6	3.91	1.7		
Site16	Narol	0.47	2.0	4.11	4.2	9.07	2.6
Site17	Vatwa	0.63	2.1	1.96	1.6	3.38	2.7



**Fig.6.1.7: H/V spectral frequency Vs Site plot, missing spectral frequency indicates fault.**

Peak frequency using Microtremor H/V spectral ratio Vs BBS sites depicts three main layers in Ahmedabad city (Figure 6.1.7). Uppermost soil layer is highly heterogeneous as compared to middle and bottom geological layer, because the high frequency amplification is varying drastically. The missing spectral frequency which mean flat response below one hertz also depict important information that there may be a local fault or fracture in that area.

## **6.2 GEOTECHNICAL INVESTIGATIONS FOR “SEISMIC MICROZONATION OF GANDHINAGAR, GUJARAT”**

*(Vasu Pancholi, Sarda Maibam, Meenakshi Rawat, Jaina Patel, Vinay Kumar Dwivedi, Darshit Modi)*

**Summary of the Geotechnical work done in Gandhinagar is as given below:**

1. There are 14 boreholes considered for soil investigation of the study area of about (8kmx4.km) 36 km<sup>2</sup>. Total 8 boreholes were got drilled by ISR to 50m depth with SPT measurements at every 3 m depth interval. While, one borehole data were collected from GERI & and for 5 boreholes from Mukesh Patel Consultancy.
2. The collected data was sorted and classified based on identified geotechnical units.
3. Data considered for soil modeling includes SPT N-values, Index properties of soil through Lab tests, Ground Water Level (GWL), Soil Type, etc.
4. Generation of 2D and 3D soil models using software applications like Rockworks, Surfer, ArcGIS, Global Mapper, etc.
5. A total of 200 SPT, 152 UDS and 50 DS were collected during drilling operations for soil properties estimation.
6. Determined soil index properties through lab tests like Grain Size Analysis (Sieve & Hydrometer), Atterberg's Limit, Specific Gravity, Moisture Content, Dry Density etc.
7. Determined shear parameters (Cohesion and Angle of Friction) by the help of lab tests like Dynamic Triaxial and Direct Shear Tests.
8. Correction of SPT N-values.
9. Developed N-Vs relation for Gandhinagar city.
10. Identified geotechnical soil units and generated 2D & 3D soil models in correlation with secondary models.
11. Ground Water Level measured in each borehole and Liquefaction Potential Index estimated for each borehole location.

The geophysical investigations include PS Logging of 8 boreholes, 61 MASW and 8 Micro-tremor profiles as shown in Fig. 6.2.1 and Table 6.2.1.

### **Lab Analysis:**

The laboratory soil tests were carried out in accordance with the relevant IS Codes and approved testing procedures for laboratory testing at K.C.T consultancy, Institute of Seismological Research (ISR). For undisturbed soil samples (UDS), mechanical analysis such as Direct Shear tests as well as Physical tests such as, Grain Size Analysis, Atterberg's Limit, Field Dry Density, Moisture Content, Specific Gravity, Free Swell Index tests have been conducted. The disturbed soil samples (DS) have undergone Physical tests only excepting Field Density and Water Content tests (see Table. 6.2.2).

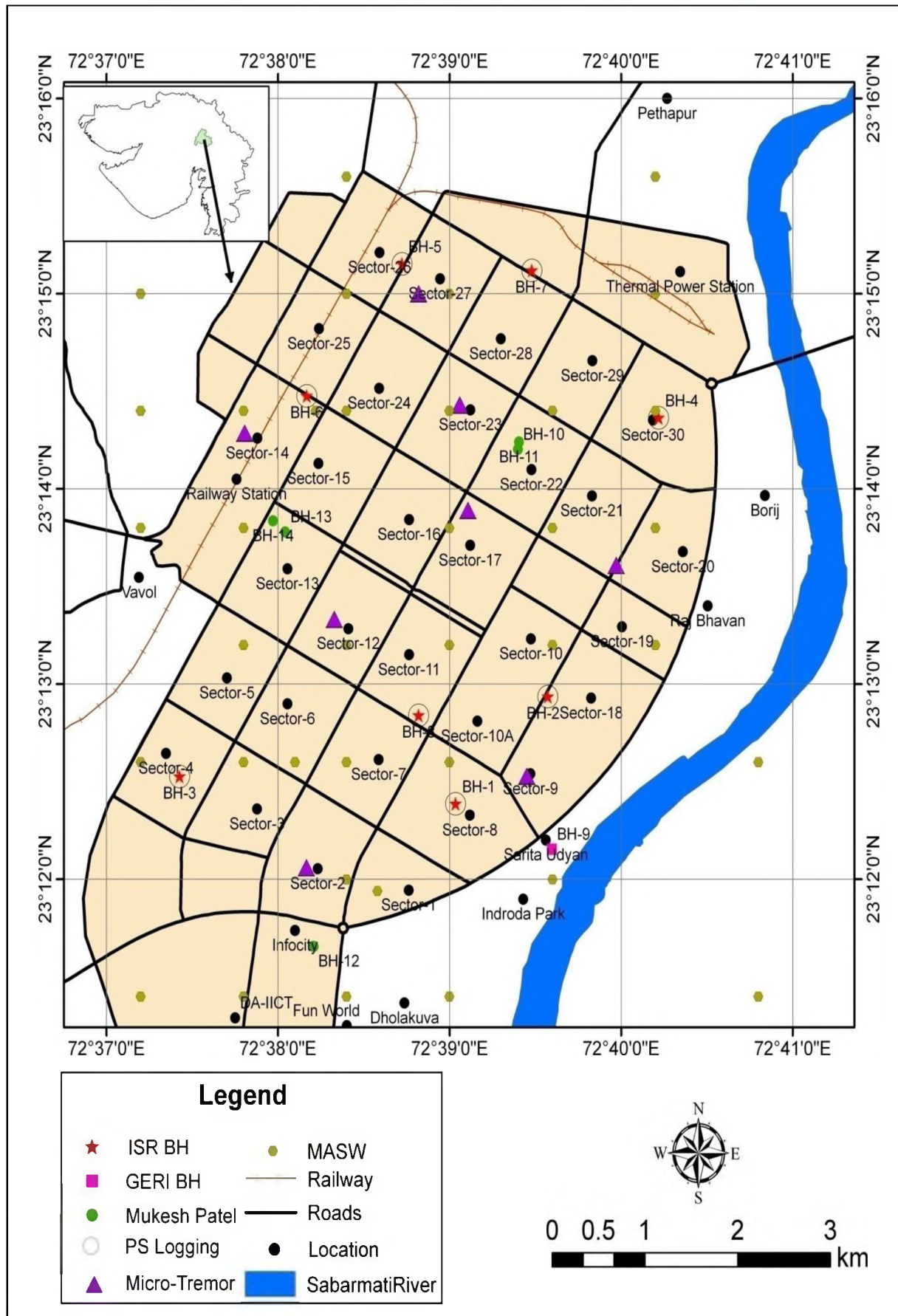


Fig. 6.2.1: Spread of drilled boreholes, MASW, Micro-Tremor & PS Logging in Gandhinagar

**Table 6.2.1: Details of Geotechnical survey**

Description		Total Depth (m)
Bore hole Drilling	14 Boreholes	502
PS Logging	8 surveys	250
Microtremor	8 surveys	Details till 100 to 200 m depth
MASW shallow seismic survey	61 profiles	120m each information obtained to

**Table 6.2.2: Total of Lab Tests done for seismic microzonation study of Gandhinagar city**

Lab Analysis		Total Samples	
		DS/SPT	UDS
Grain size Analysis	Sieve analysis	229	152
	Hydrometer	141	119
Atterberg's Limit		153	109
Field Dry Density		-	33
Field Moisture Content		178	133
Specific Gravity		32	133
Direct Shear Test		-	95
Free Swell Index		-	95

### ***Lithologs and Soil Classification***

Lithologs of all 14 boreholes were prepared with IS codes and SPT curve. For soil classification Indian standard (IS) criterion has been used shown in Table. 6.2.2.

A 3D model has been made based on Indian standard soil classification criterion which shows clear picture of the lithological subsurface details of the study area (Fig. 6.2.2). It clearly shows that most of the area is covered by silty & clayey sand while clay and silt is found as small patches.

Direction of the subsurface profile (Figs.6.2.3 and 6.2.4) is from North to South. A total of five boreholes are taken into consideration for the subsurface stratum. Majorly, the subsurface stratum comprises of Silty and Clayey sand with some patches of Clay. Maximum depth of the boreholes is around 50m. The present subsurface profile is developed considering the drilling results as per IS classification.

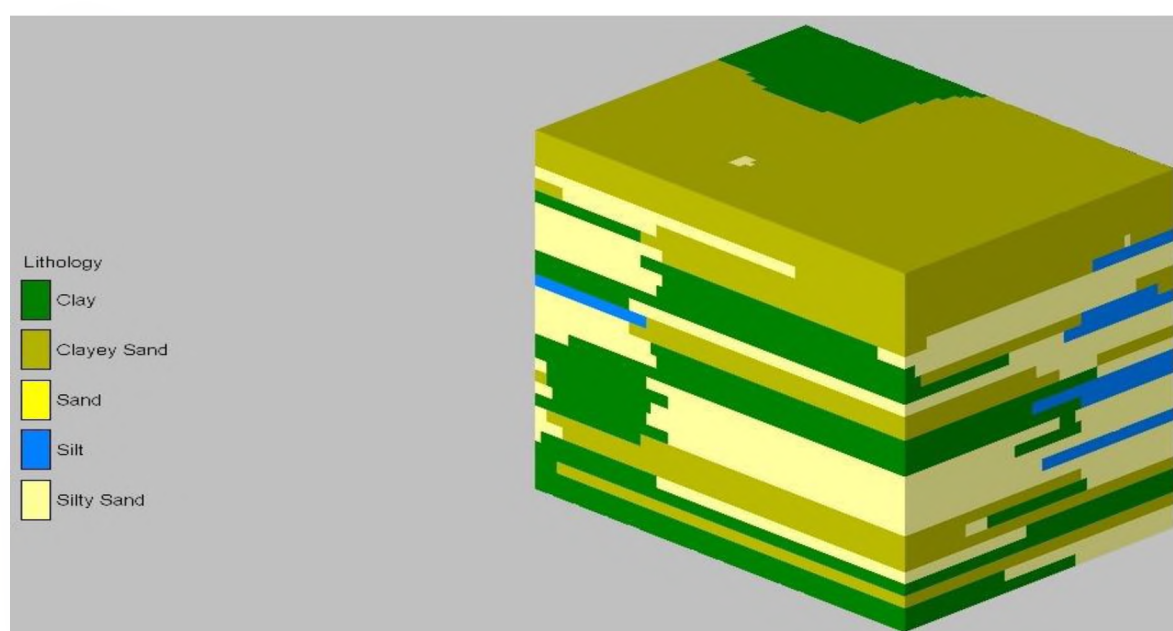


**Fig.6.2.2: 3D Geotechnical Unit Model from 14 boreholes**



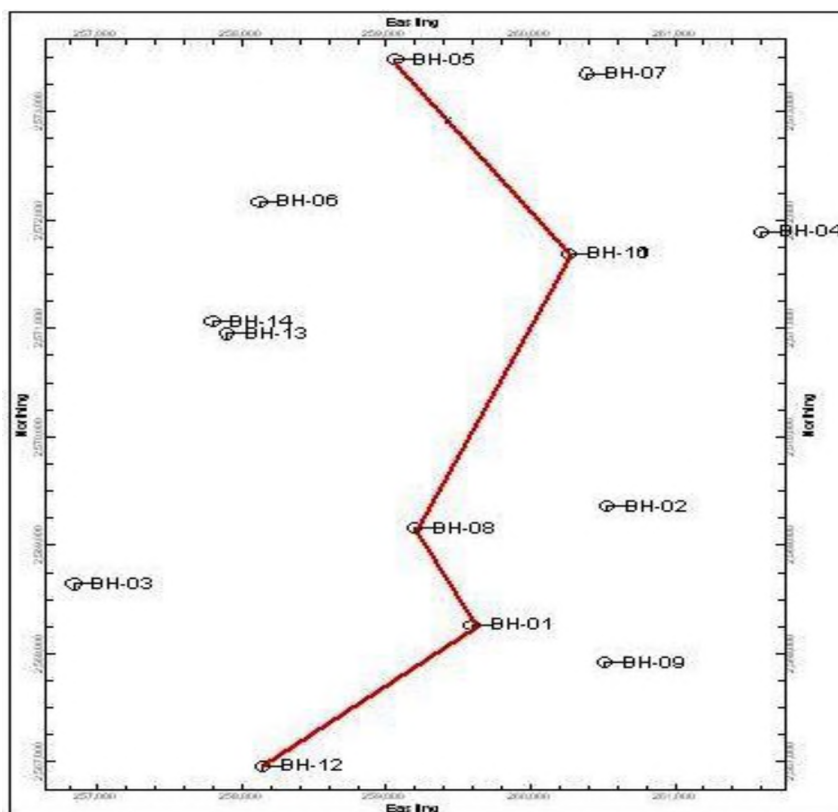


Fig.6.2.3: N-S Lithological section line of Gandhinagar

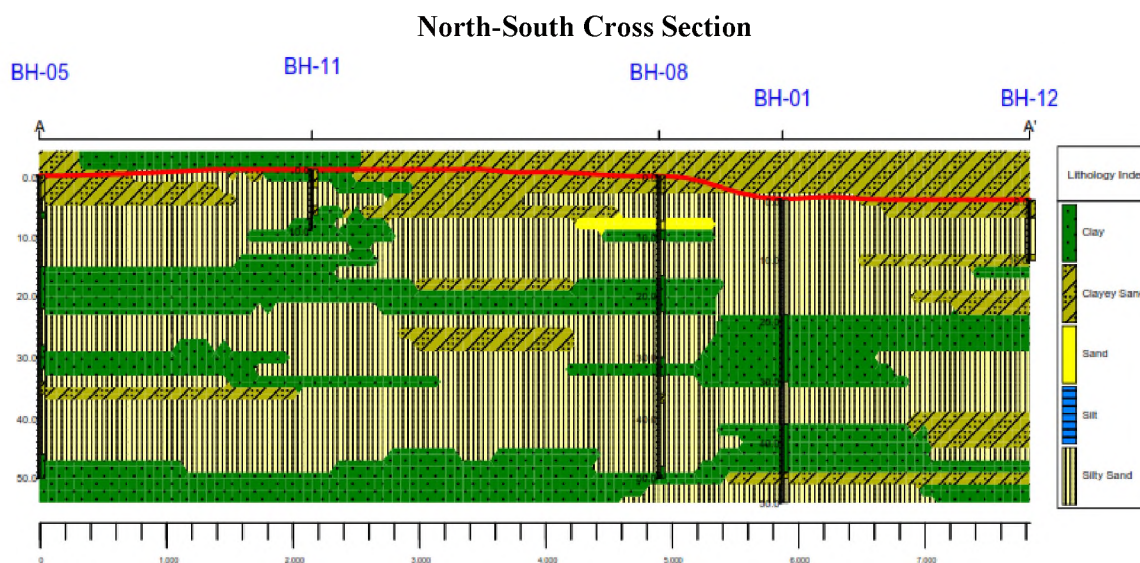


Fig. 6.2.4: N-S Lithological section of Gandhinagar

### Standard Penetration Test, N-Value:

SPT was conducted in accordance with IS: 2131 (1981) in bore holes at every change of strata or at an interval of 3.0 m depth in uniform strata. The test gives N-value; the blow counts of last 30 cm of penetration of the split spoon sampler with 65 kg hammer falling freely from 75 cm height. The rods to which the sampler is attached for driving are straight, tightly coupled and straight in alignment. There after the split spoon sampler is further driven by 30 cm. The number of blows required to drive each 15 cm penetration is recorded. The first 15 cm penetration is termed as a “Seating Value”, while the last 30

cm penetration is termed as the “N- Value”. Disturbed samples of soil are obtained from the split spoon sampler after completion of the tests.

### Field SPT Measurements:

As mentioned above, official N-value is the blow counts for the last 30 cm of penetration and 50 times is the maximum value. However, for harder soil penetration cases, there often happens that penetration depth does not reach 30 cm or counts need more than 50 times for 30 cm penetration.

For practical use of N-values for earthquake engineering purpose, the estimated N-value was defined in the following way:

- 1) P1, P2 and P3 exist, then follow original definition (SPT = N-value)
- 2) P1 and P2 only exist, then  $NSPT = (N2*30) / P2$
- 3) P1 only exists, then  $NSPT = (N1*30) / P1$

Further, N-values of each depth has been corrected for identification of true values based on correction factors as stated below and (N1)60 contour maps of different depths has been prepared for Gandhinagar city. Methodology used for Corrections is described in the next section of VS Hospital.

1. Overburden Pressure ( $C_N$ ), 2. Hammer Energy ( $C_E$ ), 3. Bore Hole Diameter ( $C_B$ ), 4. Presence or Absence of Liner ( $C_S$ ), 5. Rod Length ( $C_R$ ) and 6. Fine Content Correction

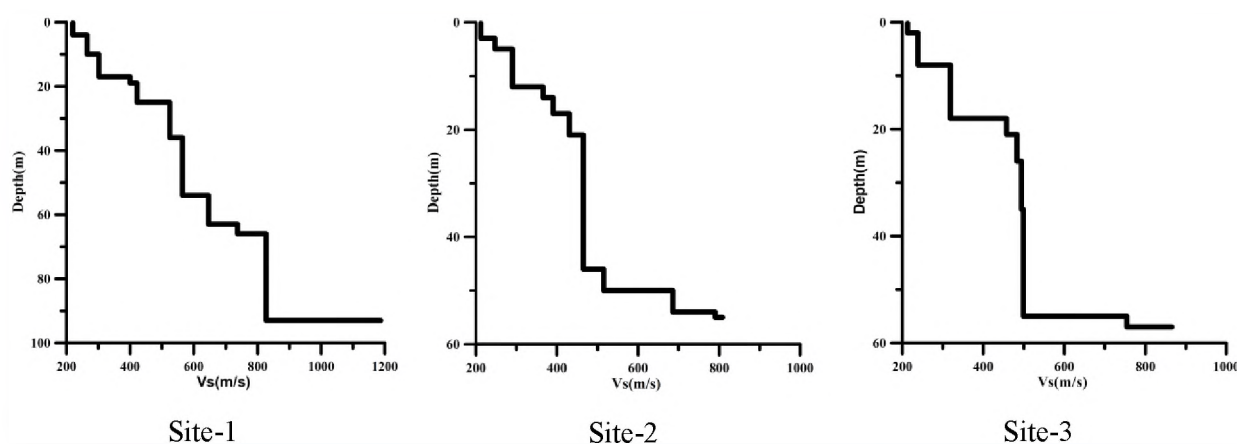
### Liquefaction Analysis:

Factor of Safety against liquefaction of soil layer has been evaluated based on the simplified procedure (Seed and Idriss, 1971) and subsequent revisions of the simplified procedures (Seed et al., 1983, 1985; Youd et al., 2001; Cetin et al., 2004). For Liquefaction calculation or estimations two variables, are defined based on Cyclic Stress Ratio (CSR) and Cyclic Resistance Ratio (CRR). Liquefaction resistance is estimated based on corrected SPT N value.

Liquefaction analysis has been done for all 14 boreholes of Gandhinagar city and Liquefaction Map has also been prepared for Gandhinagar city

**Safe Bearing Pressure (SBP) and Safe Bearing Capacity (SBC):** Safe Bearing Capacity and Safe Bearing Pressure are calculated as per IS 8900(Part-1)1976 for all 14 boreholes of Gandhinagar city by use of index properties and shear parameters of Soil.

**Shear-Wave velocity from Array Microtremor Measurements:** At 8 sites the array microtremor measurements have given shear-wave velocity to 100m depth (Fig. 6.2.5).



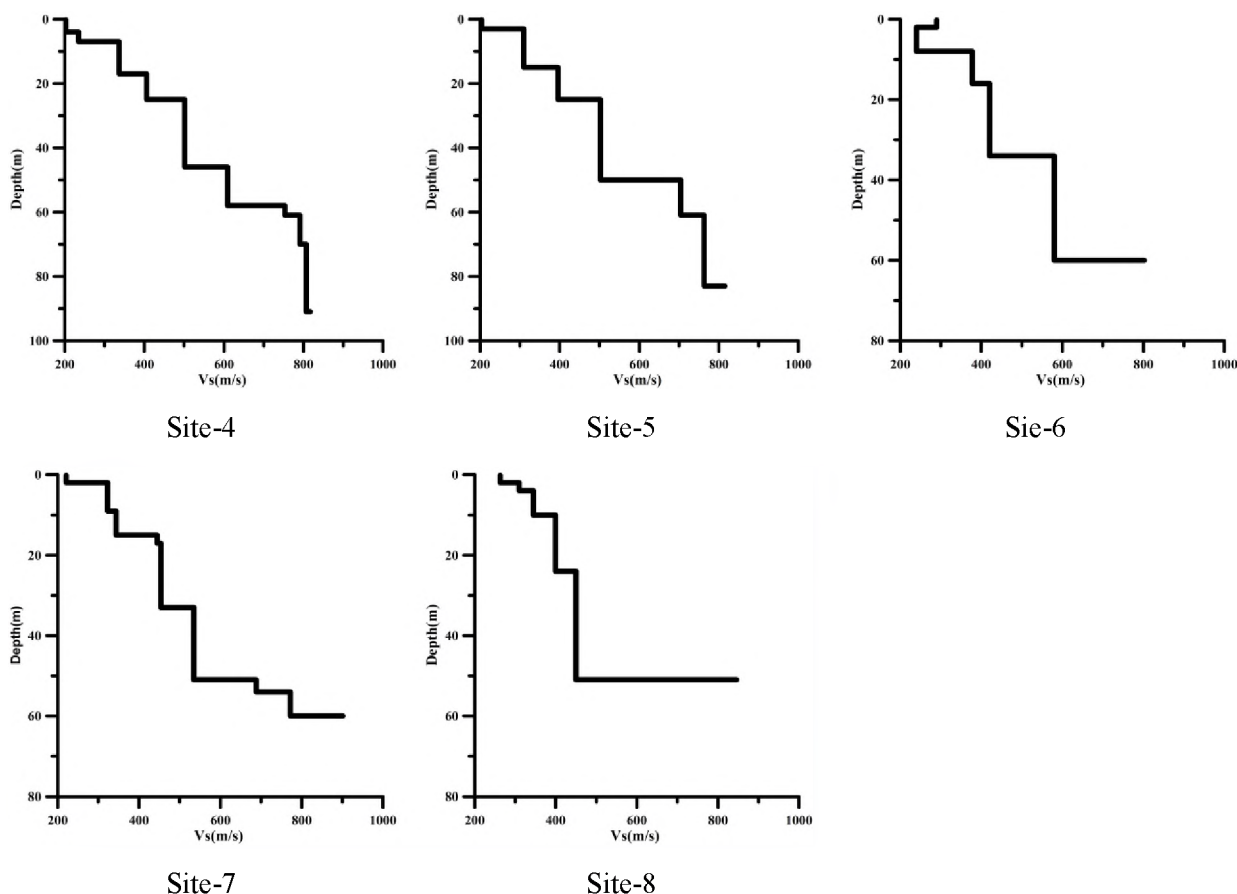


Fig. 6.2.5 : Shear wave velocity ( $V_s$ ) profile as a function of depth derived from inverting Rayleigh wave phase velocity at eight sites in Ahmadabad city from array microtremor study

### 6.3 GEOPHYSICAL & GEOTECHNICAL INVESTIGATIONS FOR SEISMIC HAZARD ASSESSMENT OF THE SITE FOR PROPOSED MULTI-STORIED BUILDING AT V. S. HOSPITAL, PALDI, AHMEDABAD CITY

#### EARTHQUAKE AND SEISMIC GROUND MOTION:

A Multi-Specialty Hospital is planned at Paldi, Ahmedabad city (Fig. 6.3.1). The proposed structural design is shown in Fig. 6.3.1a.

The V.S. Hospital site can be affected by the following two earthquakes: One is “Far Field Earthquake” with larger magnitude such as  $M_w 7.6$  in Kutch where seismicity is high and the epicenter is more than 200 km away. The other one is “near field earthquake”. The seismicity near V.S. Hospital site low and maximum magnitude will be  $M_w = 6.0$  along the East Cambay Margin Fault. According to the estimation in the project, near field earthquake and far field earthquake both can affect the site.

Detailed calculations are made at 80 m deep borehole drilled at the site. Estimates have been made on PGA at engineering bed layer and ground surface, and also response acceleration spectra. These data can be referred for anti seismic design of structures in the area.

The following assessments were made:

Due to near field earthquake, PGA's of 79 gals ( $\text{cm/sec}^2$ ) at ground surface is calculated corresponding to intensity VII in MSK or MMI seismic intensity scale and 49 gals ( $\text{cm/sec}^2$ ) due to far field earthquake. Also these values are within Zone factor  $Z=0.16g$  for Zone III of BIS (Bureau of Indian Standard) to which V.S. Hospital site belongs.



## **GEOLOGY, SOIL AND GEOMORPHOLOGY:**

In this project, existing literature on geology, soil and geomorphology are studied and deep soil investigation was conducted through drilling of 80 m deep borehole by ISR. Soil modeling for the ground response analysis was done considering BH-19. This borehole is also used for PS logging to get directly  $V_s$  (shear wave velocity) which is one of the most important dynamic soil properties.  $V_s$  was determined by geophysical prospecting like shallow seismic (MASW) and microtremor measurements. The necessary corrections to N-Values are also applied. Together with drilling and onsite tests, geophysical prospecting, the Engineering Bed Layer (EBL) was identified at the layer boundary of  $V_s$  around 460 m/s. The depth of EBL is fixed at 38.0 m based on N-Value,  $V_s$  and Wet Density.

AVs30 (Average Shear Wave velocity between 0 - 30 m depth) is one of the critical index of dynamic ground characteristics. AVs30 is 280 m/sec. At surface 200 - 220 m/s  $V_s$  is computed, which means relatively less amplification of seismic motion between EBL and surface.

The soils in the study area are showing alternative layers of Sandy and Clayey units with stiff to very stiff nature up to 20.0 m depth, while dense to very dense nature from 20.0 m onwards. At shallower depths of around 10.0 m, the corrected N-values reach  $> 50$ , while at deeper depths the values reach  $> 100$ . A total of 15 Direct Shear Tests were conducted on UDS for estimation of shearing values, which shows that the soils are of the order of Silty Sand and Sand (Shape: Round and Angular).



**Fig. 6.3.1: Map for the proposed multi-storied building at V. S. Hospital site, Paldi, Ahmedabad**

A total of 31 swell indexes were measured for BH-19. The values for BH-19 range between 6 – 43 %, describing less expansive nature of the encountered soils. The area is falling in the “Very Low” category of liquefaction hazard. Hence it can be said that the area is safe from liquefaction.



The spectral acceleration (Sa) values computed from both near field earthquake scenario and far field earthquake scenario in ground response analysis using SHAKE program shows  $215 \text{ cm/sec}^2$  and  $99 \text{ cm/sec}^2$ , respectively at 5% damping and  $315 \text{ cm/sec}^2$  and  $141 \text{ cm/sec}^2$ , respectively at 2 % damping . These values are lower than the BIS recommendation for ZONE III. Therefore BIS Sa values of Zone III are recommended to be on conservative side.

The project consists of two (2) Basements + Ground Floor + sixteen (16) floors with medical facilities + terrace with helipad. The structure shall be primarily framed in structural steel with RCC retaining walls in the basement areas.

#### Detail Description of Planned Building:

##### Floor Heights:

Basement - 1 & 2	: 4500 mm
Lower & Upper Ground Floor	: 4500 mm
1 <sup>st</sup> Floor to 3 <sup>rd</sup> Floor	: 4500 mm
4 <sup>th</sup> to 16 <sup>th</sup> Floor	: 3500 mm
Terrace/Helipad	: 3500 mm

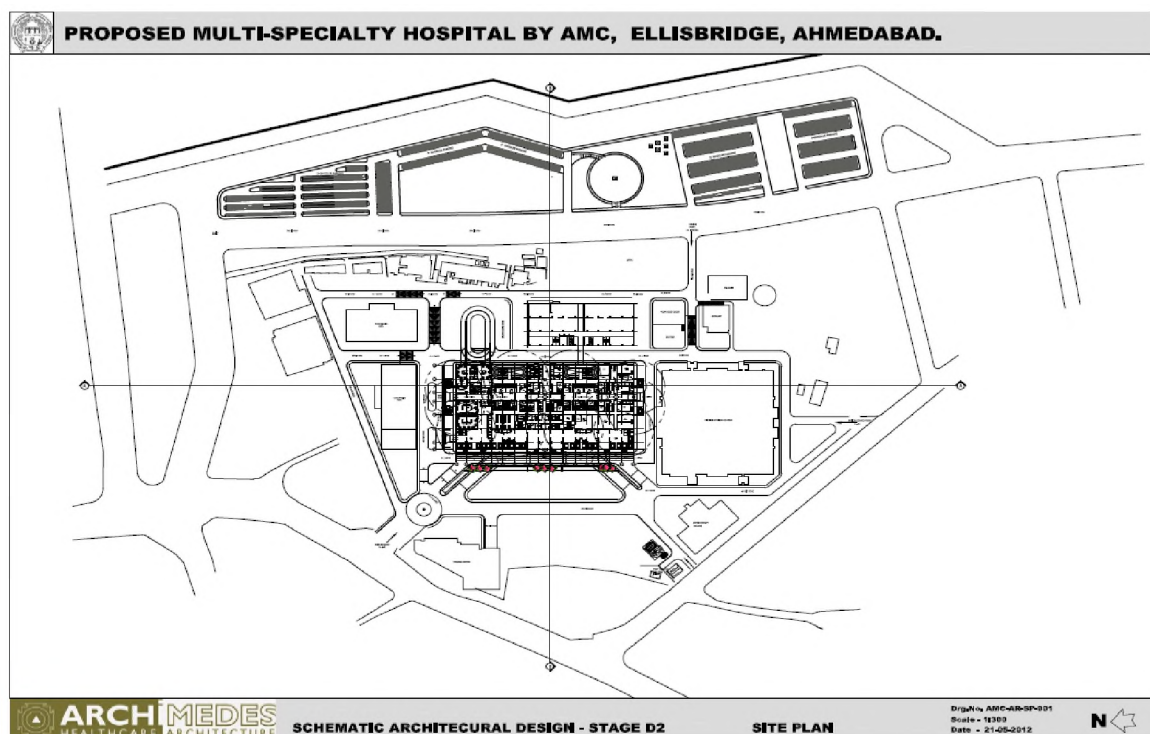


Fig. 6.3.1a: Schematic Architectural Design of proposed building at V. S. Hospital site, Paldi

**Reference:** Preliminary Concept Design report of Proposed Multi Specialty Hospital at Ellis bridge, Ahmadabad, Second Issue, April 2012 by Ramboll Engineering Consultancy Services India Pvt. Ltd.

### 6.3.1 Regional Geology and Seismotectonic Setup

#### Regional Tectonics and Geomorphology:

The site of present investigation is located on the right bank of Sabarmati River ( $23.01949^{\circ}\text{N}$  -  $72.5715^{\circ}\text{E}$ ). The Sabarmati River originates in the southwestern spurs of the Aravalli hills in Mewar region and meets the Gulf of Cambay. Over this distance it passes through three geomorphic zones, viz. the rocky upland, the middle alluvial plains and the lower estuarine zone (Tandon et al., 1997). Zeuner (1950) investigated the Sabarmati basin and suggested that the repeated dry and wet climate facilitated

the sedimentation in the basin, which shifted its course gradually to the east during the Quaternary. Based on lineament and drainage studies, Sareen et al. (1993) have shown that while the regional drainage in the Gujarat alluvial plain follows the NE-SW regional slope the Sabarmati River follows N-S to NNE-SSW trend. On the basis of sedimentological and geomorphological studies, Sridhar et al. (1994) suggested that the Quaternary sediments in the Sabarmati basin are unrelated to the present day river. The area has three major distinct geomorphic features viz. (a) upland terrace covered with fossilized dunes, (b) rivers incised into upland terraces and (c) scroll plains within the incised valleys. Morpho-stratigraphically, the upland terrace is the oldest feature. This is deeply incised by the Sabarmati River, giving rise to cliffed banks. The next youngest feature, the stabilized dunes are succeeded by the present day Sabarmati alluvium and scroll plains that occur along the modern meander bends (Fig. 6.3.2). The regional slope of the terrace is SW-SSW and its maximum elevation varies from 375 to 130 m ASL in the N-NE, to less than 20 m ASL in the S-SW. The alluvial plains extend to the Gulf of Cambay in the south and the Rann of Kachchh in the west, but are less extensive towards the north and northeast due to the presence of the Aravalli hills (Srivastava et al 2001). Tributaries emanating from the rocky terrain of the NE flow westward and meet the Sabarmati River. These tributaries have dissected the topography, which has given rise to a high drainage density. The tectonic structure of Cambay basin influenced sedimentation in the region during the Quaternary.

The Cambay basin is bounded by the East and the West margin Cambay Basin Faults that developed at the end of the Cretaceous (Biswas, 1982, 1987). NNE-SSW trending fractures (Fig. 6.3.3), which developed consequent to the formation of the Cambay graben and are responsible for the present day N-S course of the Sabarmati River (Sareen et al. 1993). The readjustment of river towards the N-S occurred sometime during the past 39 ka (Tandon et al. 1997). Stratigraphically the basin is divided into three major stratigraphic unit's viz. (a) Upper fluvial sequence, (b) Stabilized dunes and (c) Scroll plains.

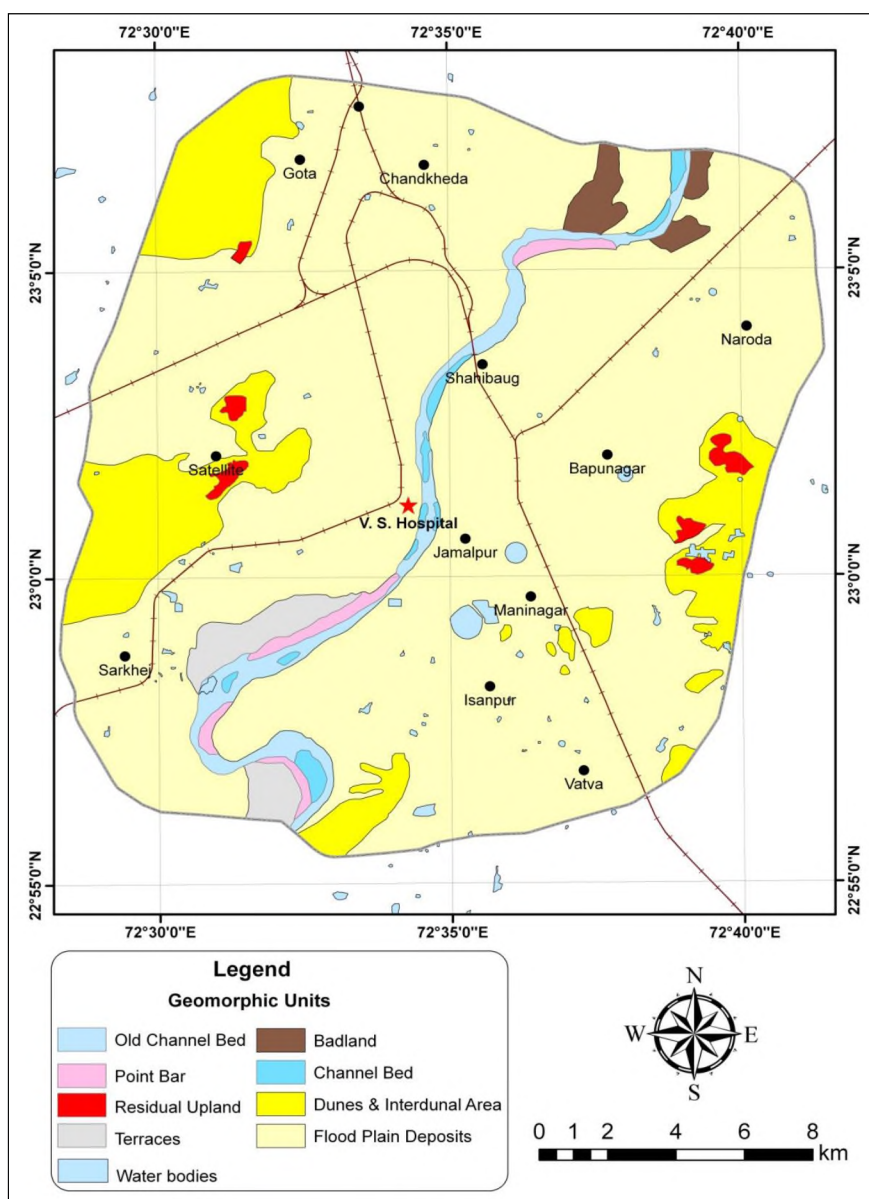


Fig. 6.3.2: Geo-morphological Map of V. S. Hospital site and surroundings

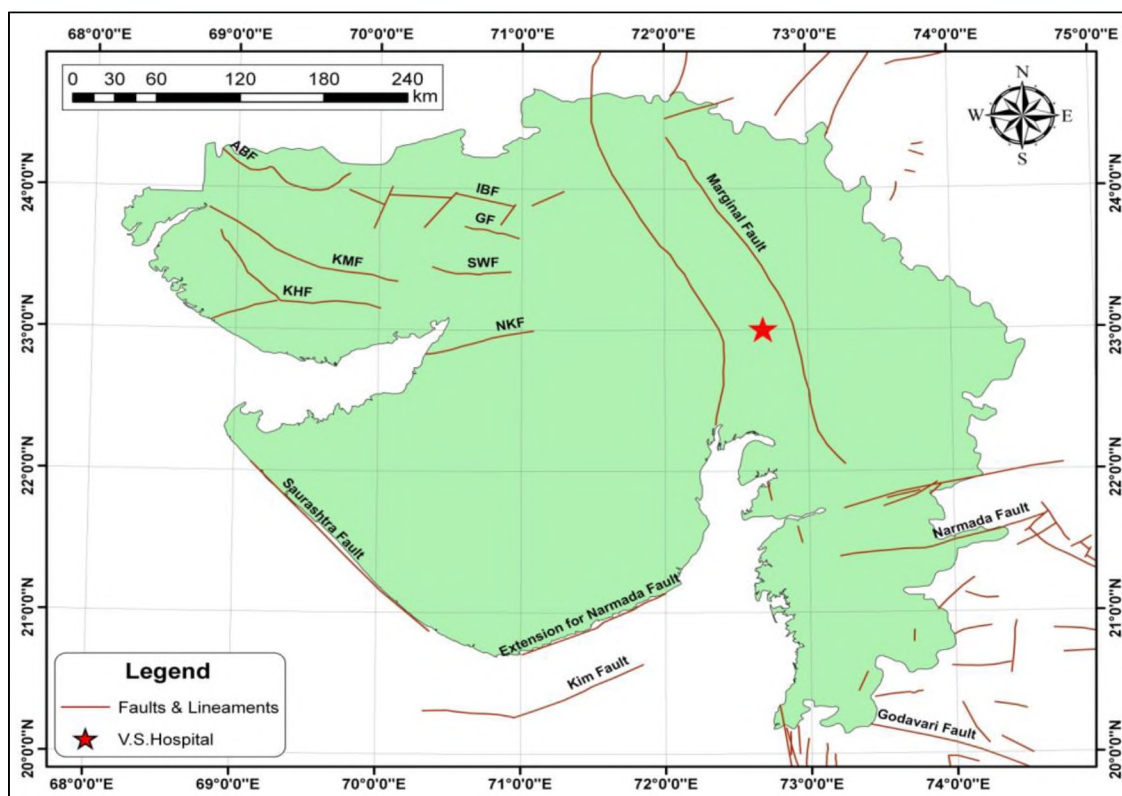


Fig. 6.3.3: Tectonic map of Gujarat (ABF: Allah Bund Fault, IBF: Island Belt Fault, KMF: Kachchh Mainland Fault & NKF: North Kathiawar Fault)

The upper fluvial sequence comprises grayish yellow fine sand and silt, overlying a red soil, with an erosional contact. This unit is overlain by frequent alternate bands of calcrete. The stabilized dune unit of linear and crescentic ridges on the terrace surface overlies the upper fluvial sequence and is readily identified in the field due to its pale grey colour and a friable nature. The scroll plains are present in the incised river valley occurring along the meander loops. Three generations shows trough and planar cross stratification overlain by fine sand.

The alluvial plain beginning at the foothills of the eastern Aravalli corridor extends WSW up to the Gulf of Cambay and Rann of Kachchh. Both, the alluvial plain and the lower estuarine zone have preserved extensive records of the Quaternary sediments. Overall, the slope of alluvial plain has a distinct bias towards W-SW (Sareen et al., 1993). Except for the rivers like Banas, Saraswati and Rupen the other major rivers viz. the Sabarmati, Orsang deviate from the regional slope with preferential flows towards SE. In the alluvial plain these rivers have deeply incised channels

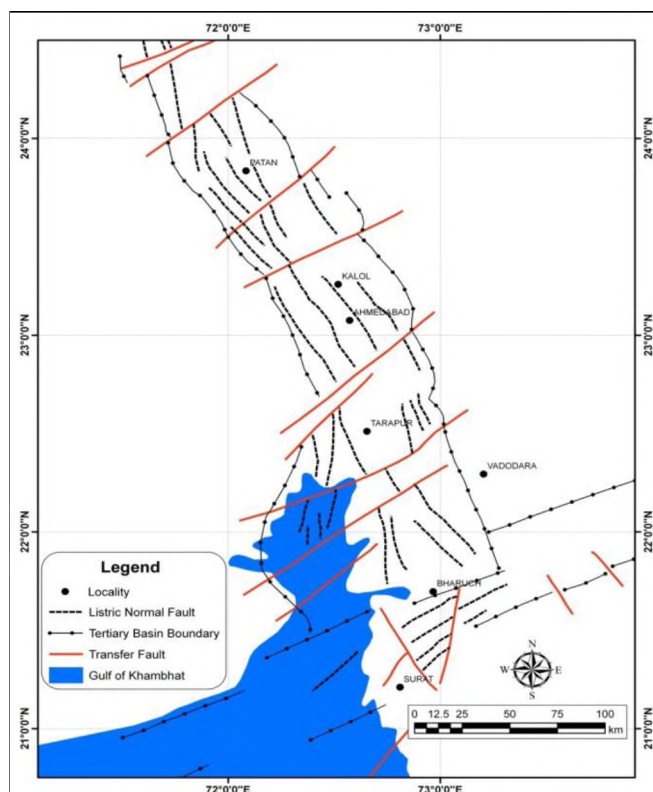


Fig.6.3.4: Structural & Tectonic Map of Cambay Basin, W. India (Wani & Kundu, 1995)



reaching a depth of ~40 m. Following this banks become less steep and river channel progressively widen towards the lower estuarine zone. Subsurface data indicate that the presence of pre-existing step faults (Fig. 6.3.4) parallel to the Eastern Cambay Basin Margin Fault acted as the depocenter for Late Pleistocene sedimentation (Maurya et al., 1995). A plot of subsurface lithology between Mehsana (NW) and Ankleshwar (S-SE) shows presence of horst and graben structures. Sabarmati River lie in a horst segment in which 200 - 300 m thick Quaternary sediment rest over the Tertiary basement (Maurya et al., 2000). Sediments were derived from the eastern upland made up of the Precambrian rocks and the Deccan volcanics. Partial Present day Sabarmati River flows parallel to the faults related to the Cambay graben. It has been suggested that the Sabarmati River used to flow towards SW and was draining into the Rupen River, which is also considered as palaeo-course of the Sabarmati River (Sridhar and Chamyal, 1996, Srivastava et al., 2001).

During Paleogene, the Cambay basin was bounded by faults on both sides namely East Cambay Fault (ECF) and West Cambay Fault (WCF). In between these marginal faults along which the Deccan Traps are down faulted by about 4 km, depositing thick Tertiary and Quaternary rocks. An area west of the Cambay Basin also subsided with a westerly dipping Deccan Traps towards the end of the Tertiary period over which formed a shallow 350 m deep basin of Miocene (Tertiary) and Quaternary beds deposited west of the main basin. In Neogene time the basin expanded. The western Neogene boundary fault follows the Trap-Quaternary boundary about 50-75 km west of the West Cambay Fault. Oil And Natural Gas Commission (Biswas, 1982, Wani and Kundu, 1995) inferred the faults and depth to different geological layers based on drill holes and detail seismic surveys (Fig. 6.3.4). In the area covered with alluvium, the faults can't be seen by geological mapping or satellite imagery or trenching. Due to the thick soil cover it is not possible to carry out active fault investigations in the study area. They can be detected by geophysical surveys only and Wani and Kundu (1995) investigation is the only work wherein they have mapped the faults by geophysical survey and confirmed them by detail drilling in the Cambay Basin. All other works are only inferences in a general sense, for example the work of GSI (2000). Inference about west Cambay fault by Bhattacharya et al. (2004) is based on the Deccan Traps / Quaternary boundary seen on the ground and for the Cambay-Dabhoi fault probably due to the shape of the coast line.

### Stratigraphy:

The Gandhinagar-Ahmedabad-Bavla-Dholka-Mehmdabad tract forms a part of the Cambay Basin and the general geological sequence given by the ONGC is given below (Table. 3.1).

Various litho-units have been identified in the area on the basis of colour, texture, degree of compaction and degree of oxidation. The Quaternary sequence hence has been divided into four formations viz: Varahi, Katpur, Akhaj and Rann Clay (Table 6.3.2). The Varahi and Katpur formations are fluvial in origin.

**Table 6.3.1: Geological sequence of Ahmedabad area**

	Age	Lithology	Thickness
Quaternary	Holocene	Alluvium	Maximum thickness about 700 m (400 m) near Ahmedabad
	Pleistocene		
Tertiary	Miocene	Sandstone and Shales	Maximum thickness about 900 m, near the margins of the basins
	UNCONFORMITY		
	Oligocene	Sandstone, Shales and Limestones	Maximum thickness 160 m
	Eocene	Shales and siltstones with minor sandstones/ and limestone intercalations	About 1000 m in center of the basin and thinning towards east and west
Mesozoic	Cretaceous	Deccan Trap	4000 m depth (ONGC)



**Table 6.3.2: Surface land forms and lithology of Ahmedabad city, Gujarat**

Surface Unit	Landforms	Lithology
T <sub>0</sub>	Present river channel and flood plain	Fluvial sediment, sand and silts
T <sub>1</sub> &T <sub>2</sub>	Fluvial terraces along present river channels	Silt, sand and clay
Katpur Formation	Low lying, flat, palaeodeltaic plain with buried old meandering channels	Grey silt and clay in mud flats, varieties of gray fine sand in palaeo-fluvial terrain
Varahi Formation	Mainly flat plain with isolated low lying undulations. Highly dissected, exhumed surface along river channels flat stable surface at places, higher than the younger fluvial surface	Fine to coarse highly oxidized sand. In low lying areas fine sand with little lime. It also occurs as fine to coarse, yellow to reddish grey sand with extensive lime concretions and concretionary conglomerate at base.
Akhaj Formation	Dunes, inter-dunes and flats	Aeolian and partly interdunal sediments, feebly oxidized sand
Rann Clay Formation	Flat plain with low lying undulations	Clay and silt

The Akhaj Formation is characterized by aeolian sediments and the Rann Clay Formation is mostly marine and consists of clay and silty sand. The Varahi Formation is fluvial in origin, exposed west of Sabarmati River along a linear belt, extending in Northeast-Southwest direction from Bhat in the North to Sarkhej in the South. East of Sabarmati this formation is exposed near S. V. P. Airport. It comprises of highly oxidized, red coloured, fine to coarse grained sand and clay. In southwestern portion, it is greyish black silty clay and in rest of the area, it is fine silt and sand. The lithounits of Varahi formation are highly dissected and eroded to form gullies and badlands along the river banks. Maximum thickness of this unit reaches 10 m as seen in a section north of Indroda. Geomorphic units of this formation are represented at places by detached buried channels, possibly remnants of old river course of Sabarmati aggraded with sand. The older Katpur Formation is exposed mostly east of Sabarmati River near Naroda, Kalupur, Jamalpur, Maninagar, Narol, Vatva, Lambha area. It consists of mainly grey silt and clays. It represents mud flats and palaeo-fluvial channels. The Akhaj Formation is represented by aeolian deposit occurring as parabolic dunes and sandy flats around Vadsar, Santej, Shilaj, Kamod, and east of LBS stadium. The formation consists of grey, yellowish grey, fine to medium grained sand (medium sand dominating) with dull white discoidal grains of calcareous material. The Formation occurs as an Aeolian cover over Varahi Formation (Tandon et al., 1997). The Rann Clay formations are exposed in limited area in southern part of the city and south east of Kamod village. It mostly consists of clay and sandy material of marine origin. The basement rock of Deccan Trap occurs at a depth of around 4000 m. The table below shows surface, landform and lithology (after Dasgupta and Jain, 1984).

#### **References for Geology:**

- Dasgupta A.K. & Jain K.C. (1984): A report on the environmental geoscientific appraisal of Ahmedabad Urban Complex, Ahmedabad district, Gujarat. Unpub. GSI report (FS 1979-80, 1980-81 and 1981-82)
- Maurya D. M., Chamyal L. S. and Merh, S. S. (1995): Tectonic evolution of the Central Gujarat Plain, Western India; *Current science* 69, 610-613
- Maurya D. M., Raj R. and Chamyal L. S., (2000): History of tectonic evolution of Gujarat Alluvial plain, western India during Quaternary: a review; *Journal of Geological society of India*, 55. 343-366
- Sareen B. K., Tandon S. K. and Bhola A. M. (1993): Slope deviatory alignment, stream network and lineament orientation of the Sabarmati river system: neotectonic activity in the mid-Late Quaternary; *Current Science* 64 827-836.
- Sridhar V and Chamyal L. S. (1996): Debris and sheet flow dominated gravels in the Sabarmati basin of western India; *Zeitschrift'ur Geomorphologie* 103 243-248
- Srivastava P, Juyal J, Singhvi A K, Wasson R J and Bateman M. D. (2001): Luminescence chronology of river adjustment and incision of Quaternary sediments in the alluvial plain of the Sabarmati river, North Gujarat, India; *Geomorphology* 36 217- 229.

Tandon S. K., Sareen B K, Rao M S and Singhvi A. K. (1997): Aggradation history and luminescence chronology of Late Quaternary semi-arid sequences of the Sabarmati basin, Gujarat, western India; *Palaeogeography Palaeoclimatology Palaeoecology* 128 339-357

Wani, M.R. and J. Kundu (1995): Tectonostratigraphic analysis in Cambay basin India: Leads for future exploration, Proc. Petrotech Conf., Technology Trends in Petroleum Industry, New Delhi, 147-164 pp.

Zeuner, F. E. (1950): Stone Age Pleistocene chronology of Gujarat; *Deccan College, Monograph* 6 46 pp.

### 6.3.2 SEISMICITY:

Ahmedabad city comes under Zone III of the seismic zoning map of India (BIS, 2002). From the catalogue of earthquakes prepared by ISR and the historical seismicity map of Ahmedabad city and surroundings, not much seismicity is observed in and around Ahmedabad city (Fig. 6.3.5). Eight shocks of magnitude 2.7 to 5.7 have been observed within 80 km radius of V. S. Hospital site (Table 6.3.3). In the historical past, Ahmedabad experienced 3 earthquakes in 1840, 1843 and 1864 of magnitudes 4.6, 3.7 and 5.7, respectively. Five other small shocks are cataloged. Moreover, a large earthquake in Kachchh region ( $M > 7$ ) can affect high rise buildings in Ahmedabad city, including V. S. Hospital building.

**Table 6.3.3: Catalog of earthquakes during 1668 to 2010 within 80km of Ahmedabad**

Year	Month	Date	Origin Time	Lat (N)	Long (E)	Depth	Magnitude	Intensity	Location	Ref.
1821	8	13		22.70	72.70		4.6		Kaira	USGS
1840	11	10		23.05	72.67		4.6		Ahmedabad	USGS
1843	2	8		23.00	72.70		3.7	IV	Ahmedabad	OLD
1864	4	29		22.30	72.80		5.7	VII	Ahmedabad	CHAN
1897	10	0		23.00	72.70		3.7		Ahmedabad	USGS
1898	10			23.05	72.67		4.3		Kheda	USGS
1962	9	1	22:01:30	24.00	73.00		4.6		Palanpur	IMD
1980	8	27	6:20:00	22.82	72.82		2.7		Chandraga	GERI

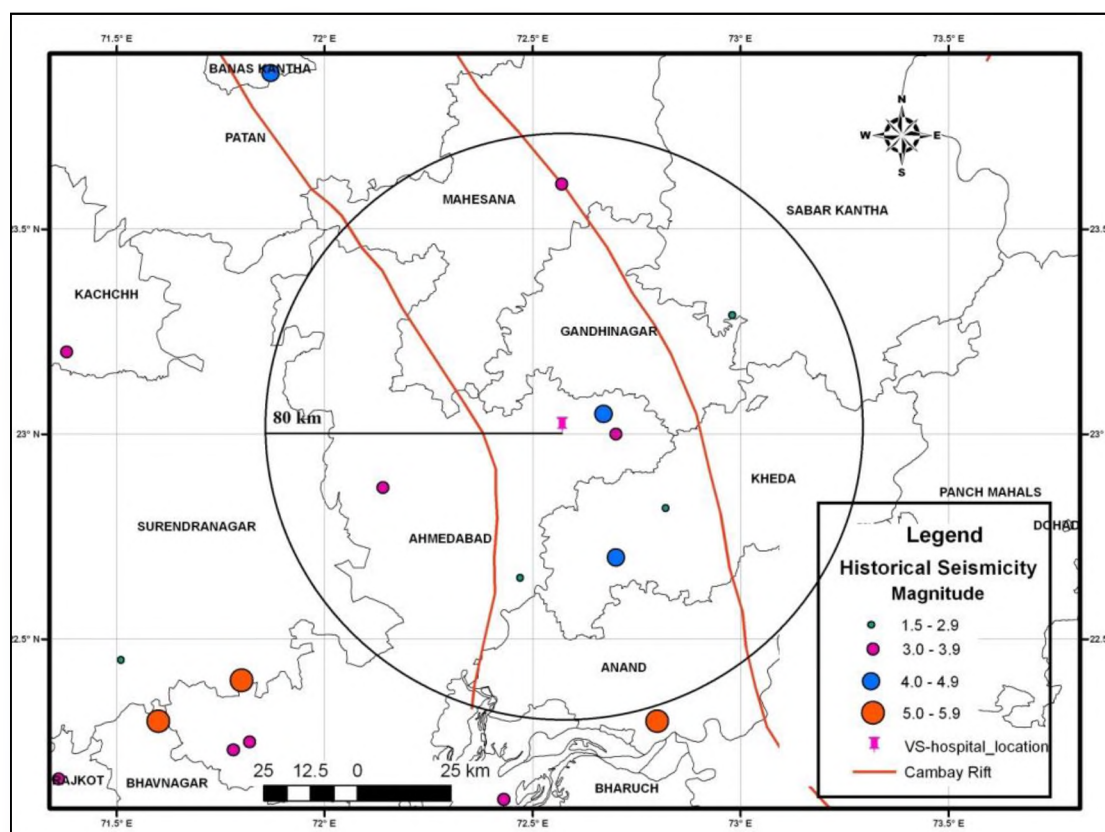


**Fig. 6.3.5: Epicenters of earthquakes  $M \geq 1.5$  occurring in the Ahmedabad and surrounding region during the period 1668 to March 2008**

### 6.3.3 Geophysical Investigations For Vs Hospital

The shear-wave velocity ( $V_s$ ) of near-surface geology is an important parameter in understanding the Dynamic soil properties of sites. MASW (Multi-Channel Analysis of Surface Waves), PS-logging and Micro-tremor Methods were conducted for estimation of shear wave velocity for V. S. Hospital site, Paldi.

#### **Vs Estimation by Multi-Channel Analysis of Surface Waves (Masw) Method:**

*B. Sairam, B. K. Rastogi, Vandana Patel and S. Venkateshwar*

During 2012,  $V_s$  profiles are obtained at 4 sites of VS Hospital by MASW and PS-logging of one borehole. Four shear-wave velocity profiles were obtained by MASW method close to the selected drilled 18 boreholes by M/s KCT, to get better and high resolution clarity on the sub-stratification of the V. S. Hospital site. Sample 2D- $V_s$  profiles are shown in Fig. 6.3.6. Shear-wave velocity was obtained up to 17.0 m depth, wherein top layer is ranging up to 4.0 m showing a very low velocity of about less than 200 m/s, while second layer is in between 4.0 m and 15.0 m depths, showing a velocity up to 250 m/s. Layer below 15.0 m depth shows a velocity of about 300 m/s.

This method is powerful, rapid and cost effective tool for estimation of shallow 1D  $V_s$  structures. The practical application of MASW provides reliable correlations to drill data. MASW technique is employed to utilize the dispersive properties of Rayleigh wave for imaging the subsurface layers. The entire process of the MASW consists of three major steps: (i) Acquisition of ground roll data of surface waves, (ii) Construction of a dispersion curve (a plot of phase velocity versus frequency) and (iii) Inversion of the shear wave velocity ( $V_s$ ) profile from the calculated dispersion curve. Integrating the MASW technique with CMP (Common Mid Point) style data acquisition permits the generation of laterally multiple cross sections of the  $V_s$ .

The MASW is a geophysical method which generates a shear wave velocity ( $V_s$ ) profile (i.e.,  $V_s$  v/s Depth) by analyzing Rayleigh-type surface waves on a multichannel record. The term “Multichannel record” indicates a seismic data set acquired by using a recording instrument with multiple channels. Forty eight (48) channels Geode Seismograph and Seismodule Controller Software (SCS) of Geometrics Inc., USA is used to acquire the data. The data acquired using standard CMP roll-along technique to achieve a continuous shot gather. Vertically stacked 20 impacts of a 30 kg hammer on a metal plate are used as a source to generate seismic waves. These waves were recorded by twenty four (24) vertical geophones/receivers of 4.5 Hz planted at a 1 m interval along the profile line. The geophone positions are shifted in steps to cover a total profile of 30 m. The information about sub-surface layers is obtained to depth of 17.0 m or more.

#### **Vs Estimation by Ps Logging Method**

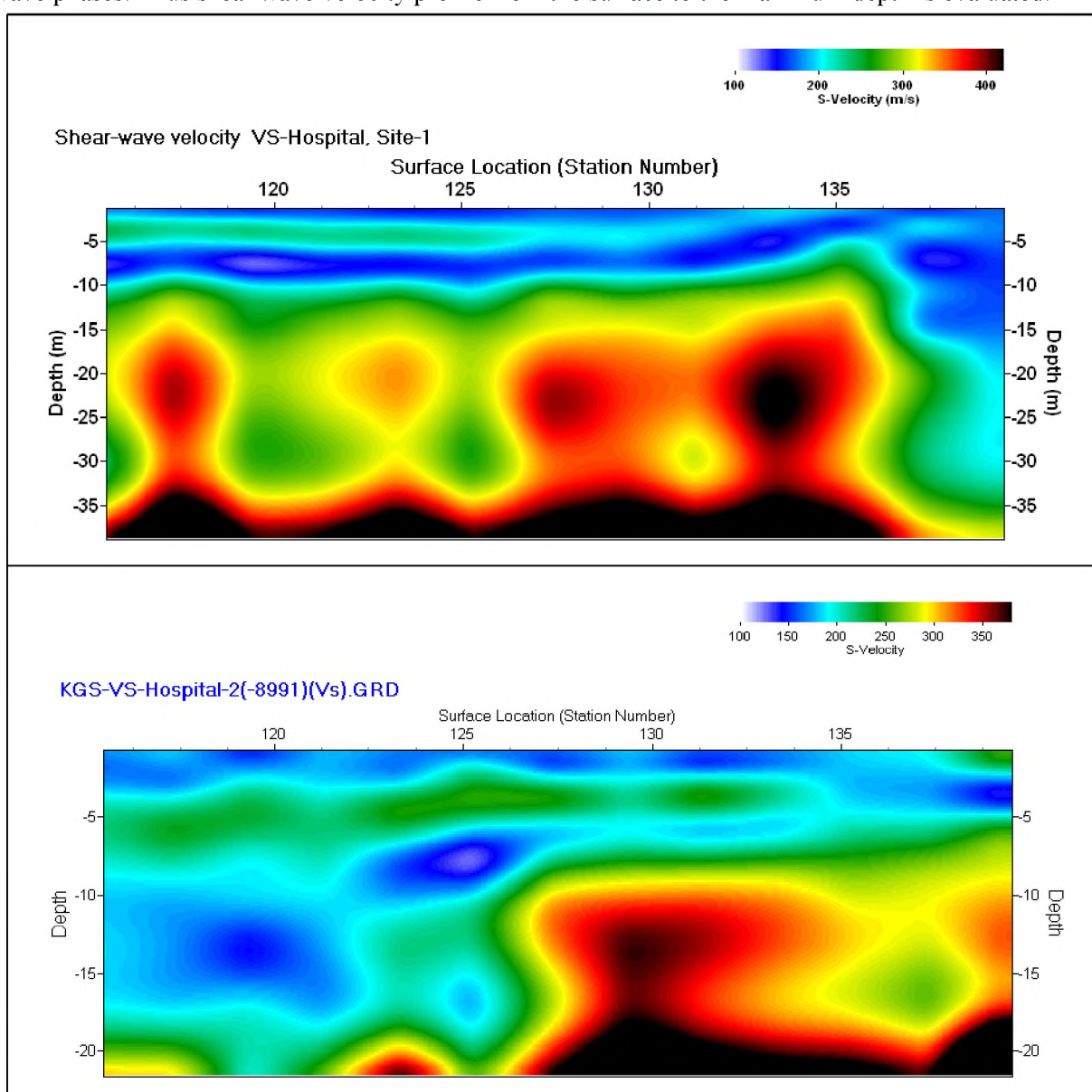
For estimation of shear-wave velocity, PS Logging test was carried out in BH-19 drilled by ISR. Data of PS-logging for  $V_s$  estimation was processed to a depth of 63 m and  $V_s$  variation with depth is given in Fig. 6.3.10 while comparing with other methods.

Suspension PS Logging is relatively recent technology in Geotechnical Engineering & Engineering Geophysics. Suspension PS Logging is one of the best methods for estimation of accurate 1D  $V_s$  profile. This method is used for assessment of site characterization for estimating earthquake ground motions. The measurements are done within the borehole as suggested above. Suspension PS Logger probe is about 8.0 m long, containing a weight, source driver, source, filter tube, lower and upper geophone, head reducer, cable head, 4-conductor cable, winch and logger/recorder.

The interval between upper and lower receiver is usually 1m, and distance from PS source to lower receiver is 4.0 m. Suspension PS Logging probe suspended by a cable through tripod, sheave and winch assemble. The probe is lowered into the borehole to a desired depth for measurement of shear wave velocity (Vs). For acquiring data in the field, suspension PS-Logging instrument and MCS SUS acquisition software built by OYO Inc, Japan are used.

Borehole in which Suspension PS Logger is lowered is completely filled with water. The data is acquired by giving a trigger command in the acquisition software. Three to nine stacks of triggers are used as an energy source. The source generates a pressure wave in the borehole fluid. The pressure wave is converted to P and S waves at the borehole wall. Along the wall at each receiver location, P and S waves are converted back to pressure waves in the fluid and received by the geophones, which send the data to the recorder on the surface.

Data is then processed using Glog-SUS processing software of OYO Inc, Japan. The elapsed time between arrivals of the waves at the receivers is used to determine the average velocity of a 1m high column of soil around the borehole. Processing of the data involves the accurate picking of P-wave and S-wave phases. Thus shear wave velocity profile from the surface to the maximum depth is evaluated.





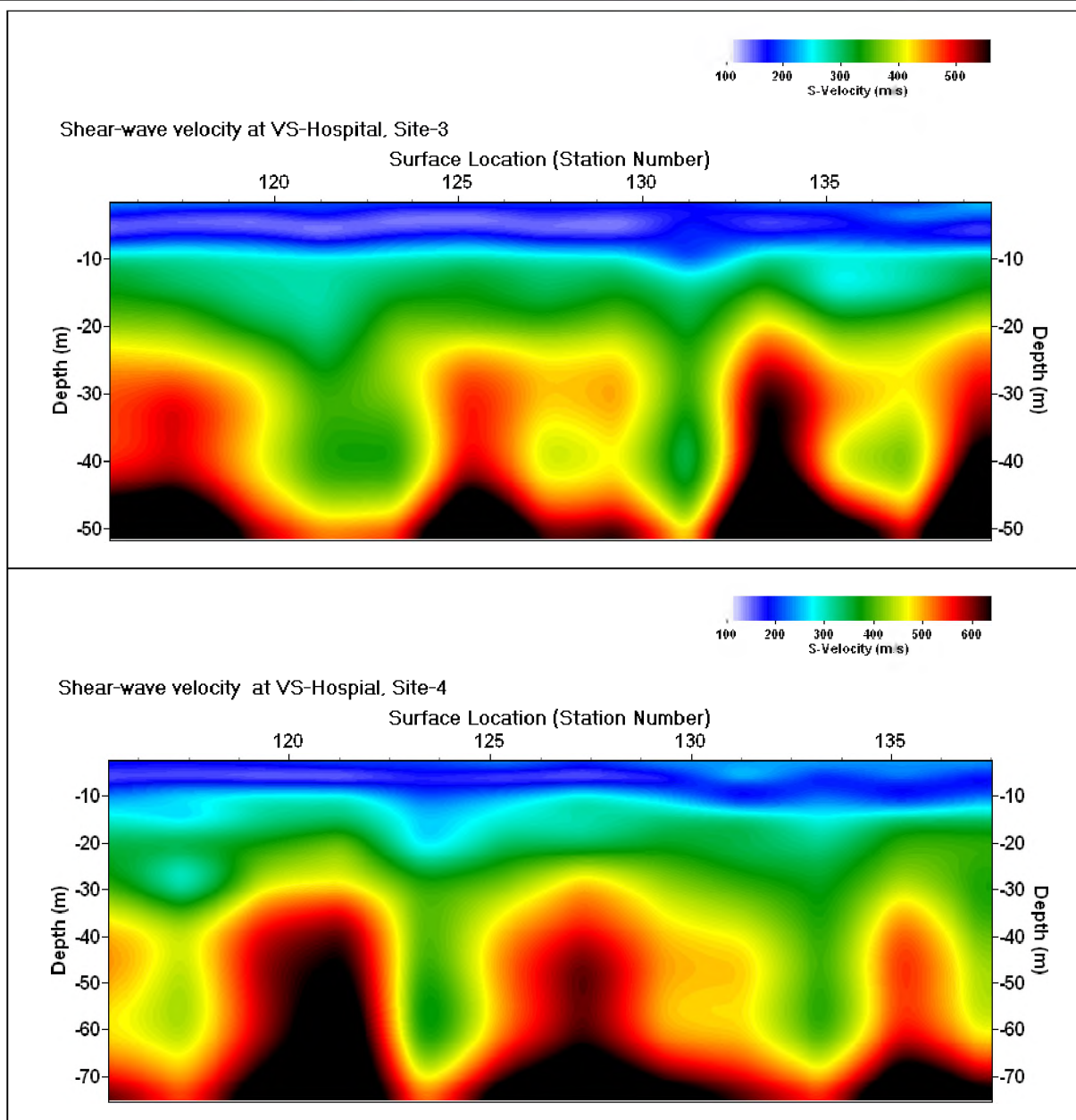


Fig. 6.3.6: Sample 2D-Vs profiles by MASW method

### Vs Estimation by Micro-Tremor Method

(A.P. Singh and Annam Navneeth)

The ambient vibration (micro-tremor) measurement is very inexpensive, non-destructive, non-invasive method and it can be applied in regions with low seismicity rates, a short time of acquisition is required in the field and low computational time and minimal computing resources are needed to analyze data. This technique uses low frequency ambient vibration generated due to ocean tides, winds and small and large scale meteorological phenomena, while local cultural noise is avoided (Fig. 6.3.7 (a) & (b)). The analysis of micro-tremor recording for site effect estimation has gained more interest in recent years and it is commonly thought that both single station horizontal-to-vertical spectral ratio's technique and multi-station (array) measurements may allow obtaining dynamic characteristics of the subsoil from ambient vibration measurements (Bard, 1999; Okada, 2003; Rastogi et al., 2011). Furthermore, in the earthquake engineering field, the shear wave velocity of the subsurface structure is considered key parameter for its major influence on local ground motion behavior. In this study, the purpose of the micro-tremor

measurements is to measure three parameters using ambient vibrations which are essential to quantify site effects namely, the fundamental resonance frequency of the deep soil basin, the relevant shear wave velocity profile and depth of the engineering seismic bedrock.

### Single and Array Micro-Tremor Measurement & Methodology:

Single station recordings have been carried out at three sites, while small aperture array measurement has been done at one site in and around V. S. Hospital site to determine the predominant frequencies and the relevant shear wave velocity profile of the deep soil basin. The observations were carried out for an hour at each site. For reliable experimental conditions we followed the guidelines proposed by Koller et al. (2004) in the framework of SESAME (WP02 of SESAME Project).

The measurements at site were taken using circular array which consists of three recording stations on the circumference of the inner circle, three of the outer circle and one in the center of the circle, shown in Fig. 6.3.7 (a). Seven sets of Lennartz LE-3D-5sec seismometers with City Shark-II digital recorders deployed in a circular array. It also has a master remote control which is used to trigger all the seven stations at a time in order to avoid any phase shift. For each array measurement two distances R, D was used for better resolution. R is the distance between the central and outer station and D is the distance between two outer stations.

In this campaign, D was chosen as 30 m for the array. The frequency-wave number method (f-k) is used for deriving the phase velocity dispersion curves from ambient vibration array measurements in the present report. The details of the methodology of single and array measurements are given in Capon, (1969); Nogoshi and Igarshi (1971); Nakamura (1989); Konno and Ohmachi (1998); Sambridge, (1999) as implemented by Wathelet et al. (2004).

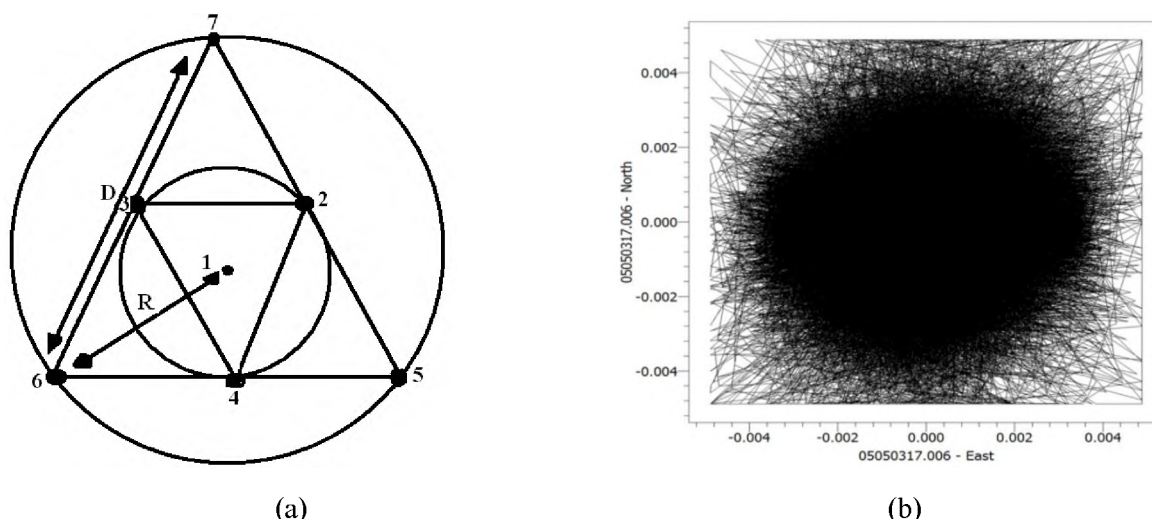
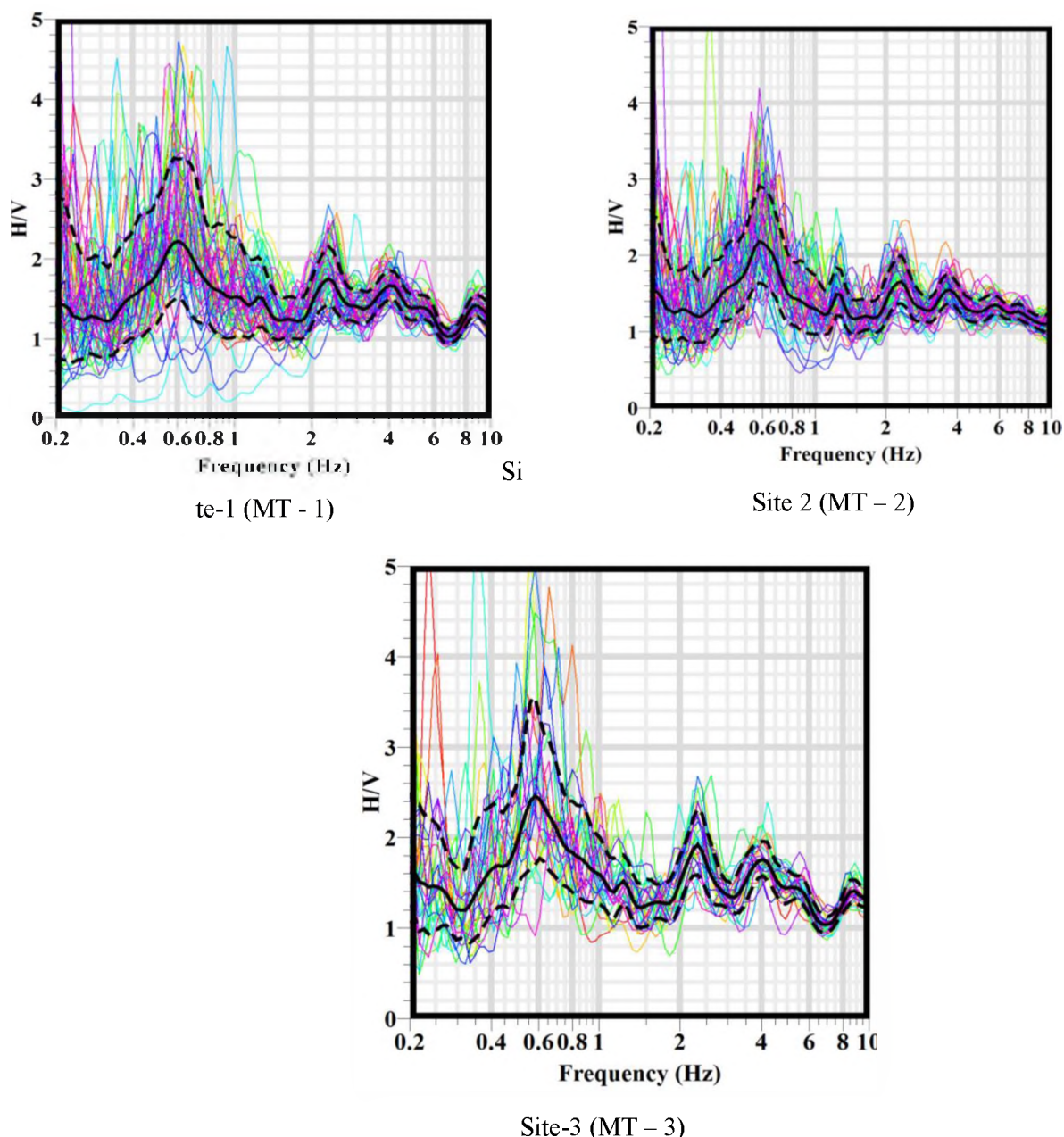


Fig. 6.3.7: (a) Geometry of the station used for micro-tremor array observations & (b) Particle motion from E-W and N-S during observation at the V. S. Hospital site, Paldi

### Results of Single Micro-Tremor Measurement:

The fundamental frequency obtained at three sites in and around the V. S. Hospital campus is shown in Fig. 6.3.8. From this figure it is found that the fundamental frequency range 0.59 - 0.60 Hz that means the thickness of the layer is about 416 m, if the thumb rule using the formula  $f = V_s/4H$  is applied for a shear wave velocity around 1000 m/s. The geological setting of Ahmedabad City which comprises very thick Quaternary sediments of about 400 m, H/V spectral ratio curve reflects almost same trend (Parvez and Madhukar, 2007; Mathur et al., 2009). This result indicates that the uppermost layer which varies

between 416 and 423 m of thickness is reasonably estimated in and around the V. S. Hospital campus. The peaks observed at about 0.6 Hz at each site are not sharp but more or less blunt which indicates that the impedance contrast between the top layer and the following layer is not high. This could interpret that the layer below 416 m is not bedrock but is some semi-consolidated layer. This layer is denser and where the geological and structural characteristics vary very gradually. This finding is supported by local geology.



**Fig. 6.3.8: Estimated Site amplification corresponding to the fundamental frequency (Hz) at three sites at V. S. Hospital site, Paldi**

The velocity profile after inversion has been illustrated in the Fig. 6.3.9 for V. S. Hospital site. First the dispersion curve calculated from ambient vibrations was inverted alone using the neighborhood algorithm. The measured phase velocity dispersion curve exhibits a regular shape and a five layer model (one soil layer with the power law variation of the velocity over the substratum) was used. The dispersion curve patterns at all sites may be nearly same. It is found that the uppermost layers up to 20 m has the low shear velocity varies between 200 - 400 m/sec, the second layer is 38 m and shear velocity has been estimated about 530 m/s. Thus, the third layer is at 75 m and shear velocity about 1100 m/s.



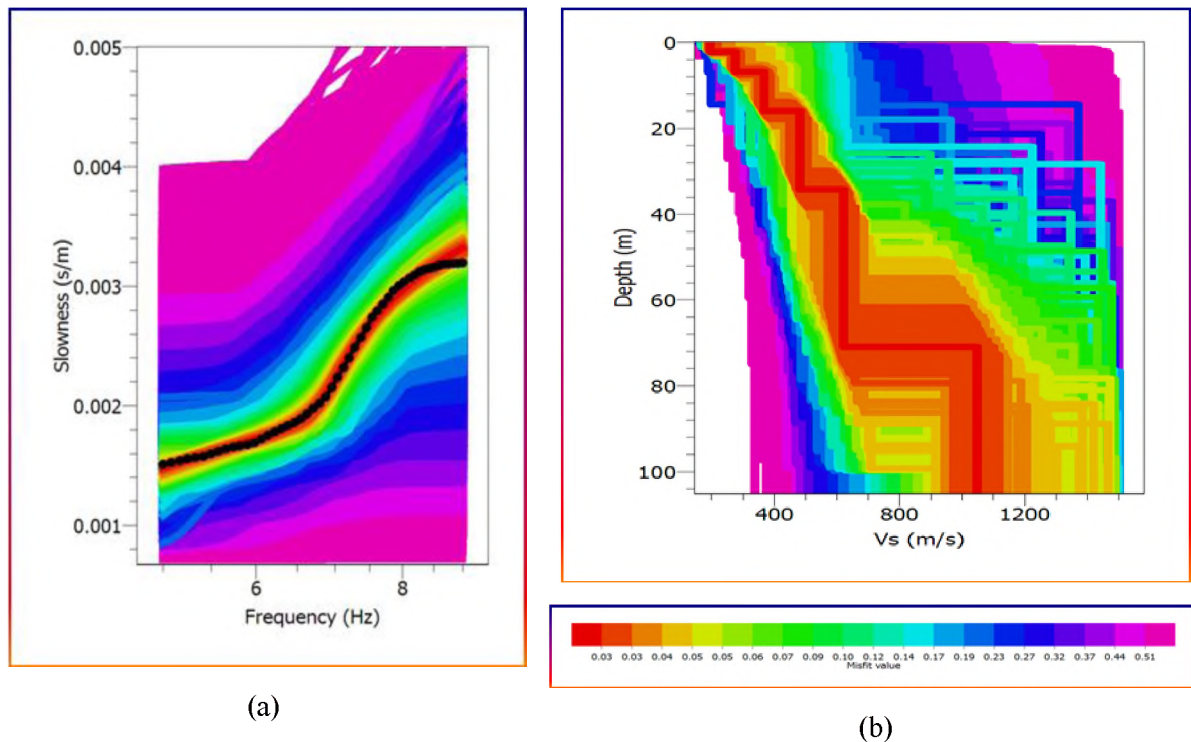


Fig. 6.3.9: (a) Inversion of the average dispersion curves & (b) Vs profile for array size 30 m at Site MT – 1

#### Conclusion from Micro-Tremor Survey:

1. H/V spectral ratio confirms that most of the sites are having fundamental frequency around 0.6 Hz without any sharp peak that means the thickness of the top layer is varying between 416 - 423 m. The micro-tremor results are also indicated that there is no high impedance contrast beneath the top layer. Micro-tremor survey also indicates layers at 38 m and 70 m. However, deepest depth of about 450 m may correspond to depth of soil.
2. An amplification of around 2.2 is observed at most of the sites between fundamental frequency ranges of 0.59 - 0.60 Hz using ambient vibrations. This corresponds to buildings of about 16 stories should be constructed with care, in and around V. S. Hospital site. However, the secondary peak in the H/V spectral ratio could be observed at about 1.5 Hz, which is not much clear as impedance contrast is less. Another clear peak is observed at about 2.1 Hz, which corresponds to 4-5 stories building. The response of this peak may be from the depth of 120 m.
3. The array analysis of micro-tremor shows low shear velocity zone up to 20 m and rapid variation between 60 and 100 m.

#### Comparison of Geophysical Surveys:

The comparative 1D-Vs model computed from micro-tremor, MASW and PS logging data along with N-values see Fig. 6.3.10. The Vs values computed from Micro-tremor and PS-logging are showing a gradual relationship with depth intervals. Also, the N-values, PS logging and Micro-tremor data shows a sharp correlation to the changes in stratification at depths of 10, 20, 40 m and so on.



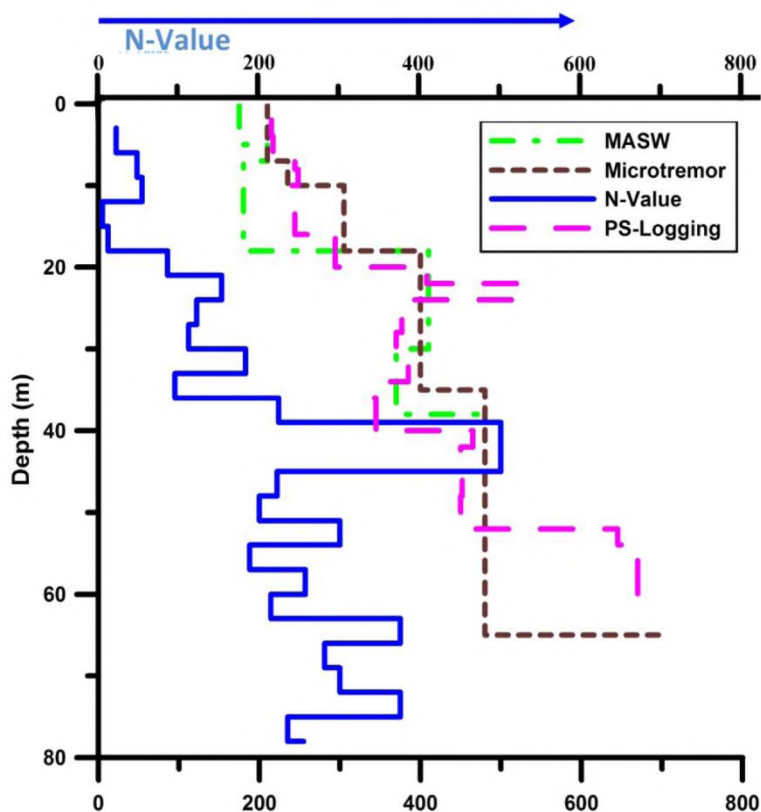


Fig. 6.3.10: Comparative 1D Vs Model for VS Hospital site from Geophysical Surveys

### References:

- Bard, PY (1999): Micro-tremor measurements: a tool for site effect estimation?, PROC. 2<sup>nd</sup> International Symposium. Effect of surface geology on Seismic Motion, Yokohoma, Japan. PP. 1251-1279.
- Capon, J (1969): High-resolution frequency-wave number spectrum analysis, *Proceedings of the IEEE* 57, 1408–1418.
- Koller, M, Chatelaine JL, B. Guillier, Duval A.M, Atakan K, Lacave C, BARD PY. and SESAME-Team (2004): Practical user guidelines and software for the implementation of the H/V ratio technique: measuring conditions, processing method and results interpretation. In proc. of 13<sup>th</sup> World conf .on Earthquake engineering, Vancouver, B.C., Canada, August 1-6, 2004.
- Konno, K, Ohmachi T (1998): Ground-Motion Characteristics Estimated from spectral Ratio between Horizontal and Vertical Components of Microtremor. *Bull. Seism. Soc. Am.*, 88(1), 228-241
- Nakamura, Y (1989): A Method for dynamic characteristics estimation of subsurface using microtremor on the ground surface. *Quarterly report of railway technical research institute, (RTRI)*, 30(1) 25-33.
- Nogoshi, M, Igarshi T (1971): On the Amplitude characteristics of Microtremor (part 2) (in Japanese with English abstract). *Jr. Seism. Soc. Japan* 24: 26-40.
- Okada, H (2003): *The Microseismic survey method: Society of exploration Geophysicists of Japan*. Translated by Koya Suto, Geophysical Monograph Series No.12. Society of exploration geophysicists.
- Parvez, IA and Madhukar K (2007): Site Response in Ahmedabad city using microtremor array observations: A preliminary report
- Rastogi, B. K., Singh, A. P., Sairam, B., Jain, S. K., Kaneko, F., Segawa, S. and Matsuo, J. (2011): The Possibility of Site Effects: the Anjar Case, Following the Past Earthquakes in the Gujarat, India. *Seismological Research Letters*, 82(1): 692-701; DOI 10.1785/gssrl.82.1.692.
- Sambridge, M (1999): Geophysical inversion with a neighborhood algorithm. I. Searching a parameter space. *Geophy. J. Int.*, 138:479-494.
- Wathelet, M, Jongmans D, Ohnberger M (2004): Surface wave inversion using a direct search algorithm and its application to ambient vibration measurements. *Near Surface Geophysics*, 2, 211-221.

### 6.3.4 Geotechnical Investigations for Vs Hospital

Site Characterization using Geotechnical Data: For the complete site response study, the subsurface material has to be characterized considering the local conditions. This chapter presents the subsurface soil properties using borehole drilling, geotechnical properties and SPT 'N' values with depth for site characterization. The geotechnical data was collected from the archives of M/s KCT Consultancy, Ahmedabad and drilling record of Institute of Seismological Research, Gandhinagar. GIS based model helps in data management, to develop geo-statistical functions, 3-dimensional (3-D) visualization of subsurface with geo-processing capability and future scope for web based subsurface mapping tool. The three major tasks carried out are as presented below: (1) Development of digitized map of V. S. Hospital site with several layers of information. (2) Development of GIS database for collating and synthesizing geotechnical data available with different sources (3) Development of 2D & 3D view of subsoil strata presenting various geotechnical properties such as location details, physical and mechanical properties, SPT 'N' values and strength properties for soil and rock along with depth in appropriate format.

#### Geotechnical Data Acquisition

Geotechnical data was basically collated from report of M/s KCT Consultancy and drilling record of Institute of Seismological Research (ISR) from geotechnical investigations carried out for V. S. Hospital site multi-storied building project at Paldi, Ahmedabad. The data was collected by geotechnical engineers during Feb – Mar' 2012. So far 19 borelog information (Table 6.3.4, see Fig. 6.3.11 & 6.3.12) has been keyed into the database, specifically for V. S. Hospital site. The database for 18 boreholes is to a depth of 30.0 m below the ground level at an interval of approximately 5.0 m. For 19<sup>th</sup> borehole drilled by ISR the depth is 80.0 m and data is collected at a depth interval of 1.5 m. The bar chart shown in Fig. 6.3.12 clearly gives the distribution of the boreholes classified based on the depth of borehole below ground level. No bedrock has been encountered in the considered boreholes. These boreholes spatially cover whole of the proposed area for the multi-storied building. Details of the total SPT tests conducted in each borehole are shown in Table. 5.2.

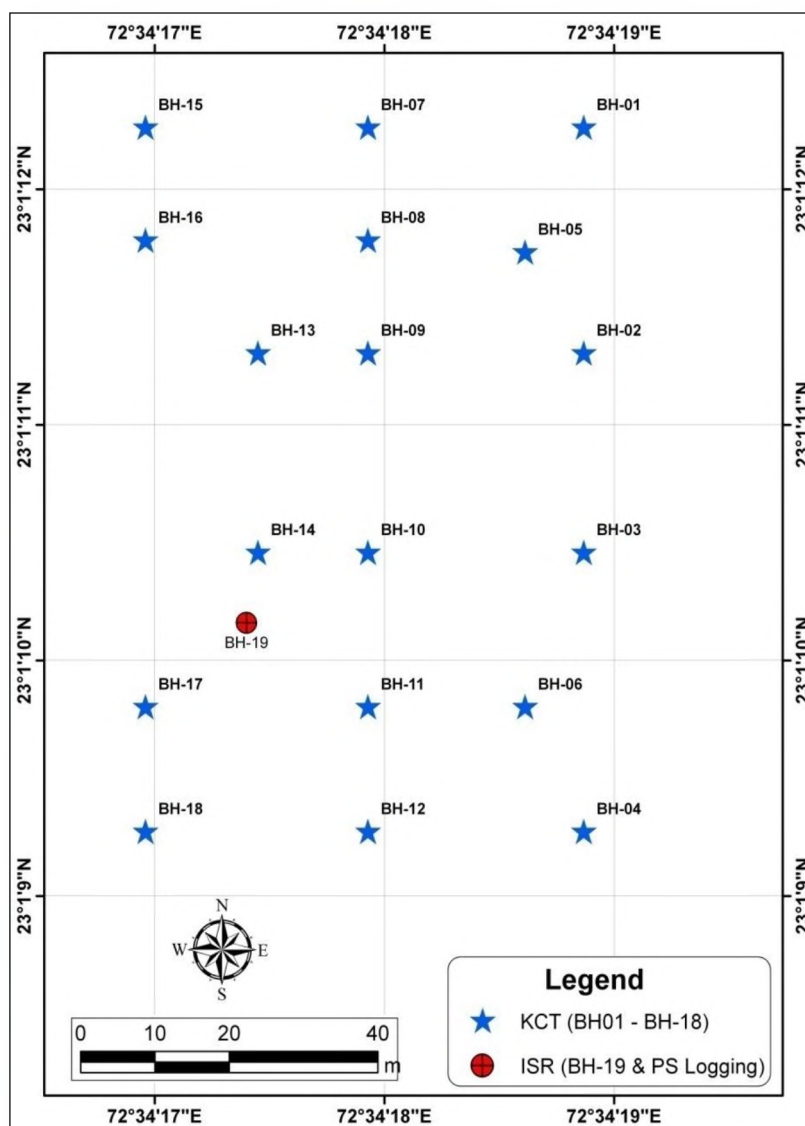
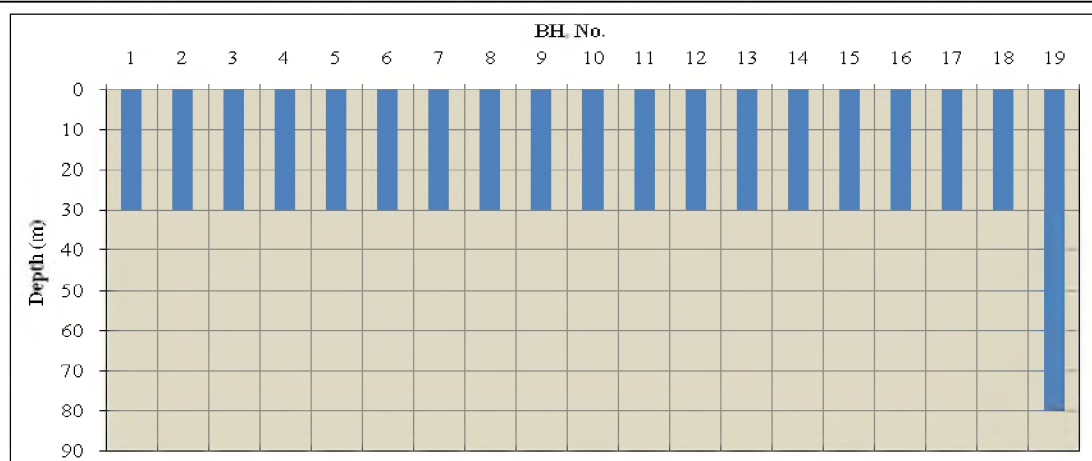


Fig. 6.3.11: Spread of 19 boreholes at V. S. Hospital site, Paldi



**Fig. 6.3.12: Distribution of boreholes based on depth (m)**

The split spoon sampler is lowered to the bottom of the hole and is then driven a distance of 450 mm in three 150 mm intervals, and the blows are counted for each 150 mm penetration. The penetration resistance (N) is the number of blows required to drive the split spoon for the last 300 mm of penetration. The penetration resistance during the first 150 mm of penetration is ignored, because the soil is considered to have been disturbed.

#### **Drilling of Boreholes:**

Soil investigation was carried out for 80.0 m borehole. Standard Penetration Tests (SPT) were carried out at every 3.0 m of borehole depth interval to know the strength and stiffness of the soil column. PS logging was carried out within the same borehole to determine P and S wave seismic velocities at every 1.0 m of borehole depth. Total borehole depth drilled by ISR was 80 m and the total undisturbed samples recovered were 15. The detail of collection of undisturbed samples and SPT samples within the borehole is as given in Table 6.3.4.

**Table 6.3.4: Details of samples collected from boreholes**

Type of Borehole	DS	SPT	UDS	Total	Depth (m)	PS Logging		Company Name
						(m)	BH #	
30m BH	136	179	63	378	540	-	-	KCT
80m BH	10	26	15	51	80	63	1	ISR
Total	146	205	78	429	620	63	1	-

Drilling of 80.0 m borehole (BH - 19) started on 18/07/2012 and completed on 26/07/2012. As one of the UDS Shelby fell in the borehole during drilling operations, the borehole was declared unsuitable for PS Logging and hence to avoid the chances of any sort of harm to the PS Logging instrument, it was decided to drill another borehole of same depth close to the previous borehole for Vs measurement. The drilling of other borehole started on 03/08/2012 at a distance of 15 feet from the previous borehole and was completed on 04/08/2012, while PS Logging was done on 05/08/2012 down to 63.0 m depth. Drilling was carried out to determine the stratification, SPT, soil sampling and suspension PS logging. Other than that, 18 boreholes were drilled by M/s KCT to depth of 30 m. Boreholes were drilled by rotary mechanical drilling, in accordance with IS: 1892. In this system, drilling is effected by the cutting action of a rotating bit which should be kept in firm contact with the bottom of the borehole (Fig. 6.3.13). The bit is carried at the end of hollow, jointed drill rods which are rotated by a suitable chuck. An M-laden fluid or grout is pumped continuously down the hollow drill rods and the fluid returns to the surface in the annular space between the rods and the side of the hole, and so the protective casing may not be generally necessary. In the case of rocks, core may be obtained by the use of coring tools, through this method.



**Fig. 6.3.13: Field Photograph of Mud Rotary Drilling Machine at V. S. Hospital site, Paldi**

#### **Disturbed Soil Samples:**

A total of 10 disturbed samples were collected during the drilling. The samples recovered were logged, labeled and placed in polythene bags and sent to laboratory for testing. The disturbed samples were collected, wherever UDS or SPT samples were not recovered, as per IS Standards.

#### **Undisturbed Soil Samples:**

A total of 15 undisturbed soil samples were collected by ISR as per IS: 2132 (1986), sealed, packed and sent for laboratory analysis. The 75 mm diameter Shelby tubes was used and the samplings were conducted at a depth interval of every 3.0 m. The samplers used for the sampling had smooth surface and appropriate area ratio and cutting edge angle thereby minimizing disturbance of soil during sampling by hammering penetration to soil. The samples were sealed with wax, on either side to avoid loss of moisture content. Sampler was coupled together with a sampler head to form a sampling assembly. The sampler head provides a non-flexible connection between the sampling tube and the drill rods. Vent holes are provided in the sampler head to allow escape of water from the top of sampler tub during penetration. Coating of oil is applied on both sides to obtain the undisturbed samples in best possible manner. The sampler was then lowered inside the borehole on a string of drill rods and was driven to pre-determined level. On completion of driving the sampler was first rotated within the borehole to shear the soil sample at bottom and then pulled out. The disturbed material in the upper end of the tube, if any, is completely



removed before applying wax for sealing. The soil at the lower end of the tube is trimmed to about 10 to 15 mm. After trimming, both ends are sealed with wax applied in such a way that will prevent the soil from giving up its sample. The polythene bags cover both the ends. The identification mark was then made on each sample.



**Fig. 6.3.14: Field Photographs of SPT and UDS sample**

### **SPT Soil Samples:**

A total of 26 SPT measurements were done in the drilled borehole, also the soil samples recovered through the SPT were sealed, labeled and packed in the polythene bags for determination of soil properties. Table 6.3.5 shows the details of 19 boreholes.

### **Lithologs and Soil Classification:**

Litholog profiles of all 19 boreholes (18 boreholes of 30.0 m depth by M/s KCT & 1 borehole of 80.0 m depth by ISR) were prepared as shown in Figs. 6.3.15 and 6.3.16. The lithologs includes two classifications one as that observed during drilling and second as identified from Soil properties measured in Lab and sample classified as per IS Classification of the Indian standards (IS) criterion as shown in Table. 6.3.6.

The lithological types from the two classifications are in many cases similar but also different in many cases. Especially silty soils in drilling observation are mostly clayey from IS classification, because grain size distribution often lack of clayey values. In most of the boreholes, top soils are rich in sand with less quantity fines down to depth of about 18 m. From both the soil classifications, gravel and soft rock are totally absent. As most of the boreholes have major sandy and silty layers within the depth range of 15 - 20 m, liquefaction analysis has to be considered.

**Table 6.3.5: Borehole Dimensions**

BH. No.	Latitude	Longitude	Elevation (m)	Total Depth (m)	GWL (m)	DS	SPT	UDS	PS Logging (m)
BH-01	23.01932	72.57192	54	30	15.5	7	10	4	-
BH-02	23.01927	72.57192	52	30	15.2	8	10	3	-
BH-03	23.01926	72.57192	51	30	15.0	7	10	4	-
BH-04	23.01921	72.57192	50	30	16.0	7	10	4	-
BH-05	23.01930	72.57192	53	30	15.0	6	10	5	-
BH-06	23.01923	72.57192	50	30	15.0	7	10	4	-
BH-07	23.01932	72.57190	54	30	15.0	8	10	3	-
BH-08	23.01930	72.57190	53	30	15.4	7	10	4	-
BH-09	23.01927	72.57190	52	30	15.2	9	10	2	-
BH-10	23.01926	72.57190	51	30	15.2	7	10	4	-
BH-11	23.01923	72.57190	51	30	17.0	7	10	4	-
BH-12	23.01921	72.57190	50	30	17.5	7	10	4	-

BH. No.	Latitude	Longitude	Elevation (m)	Total Depth (m)	GWL (m)	DS	SPT	UDS	PS Logging (m)
BH-13	23.01927	72.57188	53	30	15.2	7	10	4	-
BH-14	23.01926	72.57188	51	30	14.5	8	10	3	-
BH-15	23.01933	72.57187	54	30	15.5	10	9	2	-
BH-16	23.01930	72.57187	53	30	16.0	8	10	3	-
BH-17	23.01923	72.57187	51	30	15.5	8	10	3	-
BH-18	23.01921	72.57187	51	30	17.0	8	10	3	-
BH-19	23.01949	72.57150	51	80	17.0	10	26	15	63.0
Total						146	205	78	63

**Table 6.3.6: Indian Standard (IS) Soil Classification criterion for Litholog**

DIVISON	SUB-DIVISION		GROUP LETTER SYMBOL	MAPPING COLOUR	TYPICAL NAMES	FIELD IDENTIFICATION PROCEDURES (EXCLUDING PARTICLES LARGER THAN 80 MM AND BASING, FRACTIONS ON ESTIMATED WEIGHTS)
<b>COARSE-GRAINED SOILS</b> More than half of material is larger than 75 micron IS sieve size. (The smallest particle visible to naked eye)	Gravel More than half of the coarse fraction is smaller than 4.75 mm IS sieve size	Clean Gravels (Little or no fines)	GW	Red	Well graded sands, gravel-sand, mixtures: little or no fines	Wide range in grain sizes and substantial amounts of all intermediate particle sizes
			GP	Red	Poorly graded gravels or gravel-sand mixtures: little or no fines	Predominantly one size or a range of sizes with some intermediate sizes missing
		Gravels with fines (Appreciable amount of fines)	GM	Yellow	Silty gravels, poorly graded gravel-sand silt mixtures	Non-plastic fines or fines with low plasticity (For identification procedures, see ML and MI below)
			GC	Yellow	Wide range in grain size and substantial amounts of all intermediate particle sizes	Plastic fines (For identification procedures, see CL and CI below)
	Sands More than half of the coarse fraction is smaller than 4.75 mm IS sieve size	Clean Sands (Little or no fines)	SW	Red	Predominantly one size or a range or a range of sizes with some intermediate sizes missing	Wide range in grain sizes and substantial amounts of all intermediate particle sizes
			SP	Red	Non-Plastic fines or fines with low plasticity	Predominantly one size or a range of sizes with some intermediate sizes missing
		Sands with fines (Appreciable amount of fines)	SM	Yellow	Plastic fines (for identification procedures, see CL and CI below)	Non-plastic fines or fines with low plasticity
			SC	Yellow	Clayey Sands, poorly graded sand-clay mixture	Plastic fines (For identification procedures, see CL and CI below)

DIVISION	SUB-DIVISION	GROUP LETTER SYMBOL	MAPPING COLOUR	TYPICAL NAMES	FIELD IDENTIFICATION PROCEDURES (On fractions smaller than 425 micron IS sieve size)		
					Dry Strength	Dilatancy	Toughness
<b>FINE-GRAINED SOILS</b> More than half of material is smaller than 75 micron IS sieve size (The 75-micron IS sieve size is about the smallest particle visible to naked eye)	Silts and Clays with low compressibility and liquid limit less than 35	ML	Blue	Inorganic Silts and very fine sands, rock, lower, silty or clayey fine sand or clayey silts with none to low plasticity	None to low	Quick	None
		CL	Green	Inorganic Clays, gravelly clays, sandy clays, silty clays and clean clays of low plasticity	Medium	None to very slow	Medium
		OL	Brown	Organic Silts and organic silty clays of low plasticity	Low	Slow	Low
	Silts and Clays with medium compressibility and liquid limit greater than 35 and less than 50	MI	Blue	Inorganic Silts, silty or clayey fine sands or clayey silts of medium plasticity	Low	Quick to slow	None
		CI	Green	Inorganic Clays, gravelly clays, sandy clays, silty clays and clean clays of medium plasticity	Medium to High	None	Medium
		OI	Brown	Organic Silts and organic silty clays of medium plasticity	Low to Medium	Slow	Low
	Silts and Clays with high compressibility and liquid limit greater than 50	MH	Blue	Inorganic Silts of high compressibility, micaceous or diatomaceous fine sandy or silty soils, elastic silts.	Low to Medium	Slow to none	Low to medium
		CH	Green	Inorganic Clays of high plasticity, fat clays	High to very High	None	High
		OH	Brown	Organic Clays of medium to high plasticity	Medium to High	None to very slow	Low to medium



Fig. 6.3.15: Drill & IS Logs for 18 boreholes (\* Note: FM: Filled Up Material encountered during drilling of boreholes)

Depth (in m)	BH-01		BH-02		BH-03		BH-04		BH-05		BH-06		BH-07		BH-08		BH-09		BH-10	
	Drill	IS	Drill	IS	Drill	IS	Drill	IS	Drill	IS	Drill	IS	Drill	IS	Drill	IS	Drill	IS	Drill	IS
0.0	FM	FM	FM	FM	FM	FM	FM	FM	FM	FM	FM	FM	FM	FM	FM	FM	FM	FM	FM	FM
1.5	FM	FM	FM	FM	FM	FM			FM	FM	FM	FM	FM	FM	SM	SP	FM	FM	FM	FM
3.0					SC	SC							SC	SC	SC	SC				
4.5											SC	SC	SC	SC	SM	SP			SM	
6.0					MI	MI			SC	SP	SM	SP	SM		SM	SP	MI	CI		
7.5							SC	SC						SP						
9.0	SC	SC			CI	CI									SC	SC			SC	SC
10.5									SC		SC	SC							SC	
12.0			SC	SC	SC						SC	SC								
13.5													SC	SC			SC	SC		
15.0			SM	SP	ML	ML	CI	CI	MI	SP					SM	SP				
16.5	CI	CI							SC	SP	MI	MI			SM	SP	SM	SP	CI	MI
18.0	MI	MI	CI	CI	CI	CI	MI	MI	MI		SC	SC					CI	CI		CI
19.5	CI	CI			CH	CH	CH	CH	MI	MI	MI	MI	MI	MI			CH	CH	MI	CI
21.0							SC	SC			SC	SC	MI	CI						
22.5			SC	SC			SC	SC					CI	CI	CI	CI				
24.0	SM	SP							SM	SP	SM	SP							SM	SP
25.5					SM	SP	SM	SP					SM	SP			SM	SP		
27.0			SM	SP											SM	SP				
28.5	CI	CI					CI	CI	CH	CH	CI	CI	CH	CI					CH	MI
30.0			CH	CH																

Fig. 6.3.16: Drill & IS Logs for 18 boreholes (Contd.)

Depth (in m)	BH-11		BH-12		BH-13		BH-14		BH-15		BH-16		BH-17		BH-18	
	Drill	IS	Drill	IS	Drill	IS	Drill	IS	Drill	IS	Drill	IS	Drill	IS	Drill	IS
0.0	FM	FM	FM	FM	FM	FM	FM	FM	FM	FM	FM	FM	FM	FM	FM	FM
1.5			SC	SC									SC	SC		
3.0	MI	MI			SC	SC	SC	SC			SM	SC			SC	SC
4.5	CI	CI	MI	MI					MI	MI	SC	CI	MI	CI	MI	CI
6.0	SC	SC							SC	SC			SC	SC		
7.5					SM	SP			MI	MI						
9.0			SC	SC							SM	SP	SM	SP	SM	SP
10.5	SM	SP							SM	SP					SC	SC
12.0					SC	SC										
13.5	SC	SC					SC				CI	MI	SC	SC		
15.0					SM	SP	SM	SP			CI	MI	SC	SC		
16.5				CI				CI	SC	SC	SM	SP	MI	CI	MI	CI
18.0			CI	CI	CI	CI							CI	CI		
19.5	CH	CH	MI	MI					MI	MI	MI	CI			MI	CI
21.0	CI	CI			MI	MI	SM	SP			CI		SC	SC		CI
22.5	SM	SP			SC	SC			SM	SP			SM	SP	SM	SP
24.0			SM	SP	SM	SP					SM	SP				
25.5											SC	SC				
27.0											SM					
28.5																
30.0			CH	CH	CH	CH	CH	CH								



## Geotechnical Lab Analysis

Number of laboratory tests carried out are listed in Table 6.3.7. The laboratory soil tests were carried out in accordance with the relevant IS Codes and approved testing procedures for laboratory testing at NIRMA University, Ahmedabad. For undisturbed soil samples (UDS), mechanical analysis such as Direct Shear tests as well as Physical tests such as, Grain Size Analysis, Atterberg's Limit, Field Dry Density, Moisture Content, Specific Gravity, Free Swell Index tests have been conducted. The disturbed soil samples (DS) have undergone Physical tests only barring Field Density and Water Content tests.

PHYSICAL TESTS:

SPECIFIC GRAVITY:

The specific gravity was determined for soil samples in accordance with the method described in IS: 2720 (Part – III, Sec I & II, 1980). The 50 gm sample was ground to pass a 2.0 mm IS sieve and about 5 to 10 gm subsample was oven dried at 105 to 110°C and used for determination of G.

**Table 6.3.7: Lab tests carried out for the collected samples**

Laboratory Tests	No of Samples Tested			
	DS	SPT	UDS	Total
<b>Physical Tests</b>				
Specific Gravity	10	26	15	51
Field Dry Density	-	-	15	15
Natural Water Content	-	-	15	15
Sieve Analysis	10	26	15	51
Hydrometer Analysis	10	26	15	51
Atterberg's Limit	10	26	15	51
<b>Mechanical Tests</b>				
Direct Shear Test	-	-	15	15
Free Swell Index	-	-	15	15
<b>Note: DS: Disturbed Sample, UDS: Un-Disturbed Sample &amp; SPT: Standard Penetration Test</b>				

### Field Dry Density & Water Content:

Field dry density was carried out in accordance with IS: 2720 (Part – XXIX, 1975), while moisture content was determined in accordance with IS: 2720 (Part – II, Sec 1, 1973). The field density is found out by following equation:

Field Density (Bulk) = Weight of soil mass / Volume of soil mass, and

$$\text{Field Dry Density} = \frac{\text{Bulk Density}}{1 + \frac{w}{100}} \quad \text{where, } w \text{ is Water Content}$$

### Grain Size Analysis:

Grain size analysis was carried out in two parts, namely: Sieve Method & Hydrometer Method in accordance with IS: 2720 (Part – IV, 1985) to determine particle size distribution,  $D_{10}$  and  $D_{50}$  at the sampled depth.

### Sieve Method for Grain Size Analysis:

The sieve method was carried out for soil samples to determine coarser fraction in the soil sample. Compliance with the standard, with respect to minimum sample quantity is dependent on the maximum significant grain size and the method of sampling.

### **Hydrometer Analysis for Grain Size Analysis:**

Hydrometer analysis provides an estimate of the particle size distribution for the fine fraction ( $< 75 \mu\text{m}$ ) of a soil sample. The analysis is performed by monitoring the rate of settlement of soil particles initially suspended uniformly in distilled water. The rate of settlement, which is monitored by observing the change in fluid density with the hydrometer device, is theoretically related to the size of particles settling out of suspension.

### **D<sub>10</sub> & D<sub>50</sub> for Grain Size Analysis:**

The definition of D<sub>10</sub> is the equivalent diameter where 10 % mass (of the particles) of the powder has a smaller diameter (and hence the remaining 90 % is coarser). The average particle size, i.e. the average equivalent diameter, is defined as the diameter where 50 % mass (of the particles) of the powder have a larger equivalent diameter, while the other 50 % mass have a smaller equivalent diameter. Hence the average particle size is denoted as equivalent D<sub>50</sub>.

### **Atterberg's Limit:**

Liquid limit and Plastic limit tests were carried out on the soil samples in accordance with IS: 2720 (Part - V, 1985) by mechanical and cone penetrometer methods. Both Liquid limit and Plastic limit of soils depend upon the amount and type of clay in a soil and form the basis for the soil classification system for cohesive soils based on the Plasticity Index. The Liquid limit of the soil will correspond to the moisture content of a paste which would give 25 mm penetration of the cone in the Cone Penetrometer test, while in Mechanical test the number of blows required to cause the groove close is recorded and the test is repeated for 3 – 4 times with addition of varying amount to water to the soil sample. A graph is then generated with No. of Blows on the X-axis and Water Content (%) in the Y-axis and the cross-section of 25 numbers of blows is recorded as the Liquid Limit of the soil sample.

### **MECHANICAL TESTS:**

#### **Direct Shear Test (IS: 2720, Part – XIII, 1986):**

Direct shear test is performed to determine the shear strength of the soil with a maximum particle size of 4.75 mm. Shear strength is one of the most important engineering properties of a soil, because it is required whenever a structure is dependent on the soil's shearing resistance. The shear strength is needed for engineering situations such as determining the stability of slopes or cuts, finding the bearing capacity for foundations and calculating the pressure exerted by a soil on a retaining wall. Shear parameters determined by Direct Shear Test are Cohesion (c) and Angle of Friction ( $\phi$ ).

#### **Free Swell Index (IS: 2720, Part – XL, 1977)**

This test is performed to identify the potential of a soil to swell which might need further detailed investigation regarding swelling and swelling pressures under different field conditions. Two 10 g soil specimens of oven dry soil passing through 425 micron IS Sieve are taken and soil specimens are poured in each of the two glass graduated cylinders of 100 ml capacity. One cylinder is then filled with kerosene oil and the other with distilled water up to the 100 ml mark. After removal of entrapped air, the soils in both the cylinders are allowed to settle. Sufficient time (not less than 24 hrs) is allowed for the soil sample to attain the equilibrium state of volume without any further change in the volume of the soils. The final volume of soils in each of the cylinders is read out. The free swell index of the soil shall be calculated as follows:

$$\text{Free Swell Index, percent} = \frac{(V_d - V_k) * 100}{V_k}$$

where,  $V_d$  = Volume of soil specimen in the cylinder containing distilled water and  
 $V_k$  = Volume of soil specimen in the cylinder containing kerosene

### Standard Penetration Test, N-Value:

SPT was conducted in accordance with IS: 2131 (1981) in bore holes at every change of strata or at an interval of 3.0 m depth in uniform strata. The test gives N-value; the blow counts of last 30 cm of penetration of the split spoon sampler with 65 kg hammer falling freely from 75 cm height. The rods to which the sampler is attached for driving are straight, tightly coupled and straight in alignment. There after the split spoon sampler is further driven by 30 cm. The number of blows required to drive each 15 cm penetration is recorded. The first 15 cm penetration is termed as a “Seating Value”, while the last 30 cm penetration is termed as the “N- Value”. Respective tables mentioned below shows the details of N value and the penetration (in cm). Disturbed samples of soil are obtained from the split spoon sampler after completion of the tests.

### Field SPT Measurements:

As mentioned above, official N-value is the blow counts for the last 30 cm of penetration and 50 times is the maximum value. However, for harder soil penetration cases, there often happens that penetration depth does not reach 30 cm or counts need more than 50 times for 30 cm penetration. Table 6.3.8 shows a sample of field SPT log for BH-19.

For practical use of N-values for earthquake engineering purpose, the estimated N-value was defined in the following way:

- 1)  $P_1, P_2$  and  $P_3$  exist, then follow original definition ( $SPT = N\text{-value}$ )
- 2)  $P_1$  and  $P_2$  only exist, then  $NSPT = (N_2 * 30) / P_2$
- 3)  $P_1$  only exists, then  $NSPT = (N_1 * 30) / P_1$

Further, N-values are to be corrected for identification of true values based on correction factors as stated below.

1. Overburden Pressure ( $C_N$ ), 2. Hammer Energy ( $C_E$ ), 3. Bore Hole Diameter ( $C_B$ ), 4. Presence or Absence of Liner ( $C_S$ ), 5. Rod Length ( $C_R$ ) and 6. Fine Content Correction

**Table 6.3.8: Sample of field measured SPT N-values for BH-19 by ISR**

Depth	Standard Penetration Test				Penetration in cm.			$N_{SPT}$
	$N_1$	$N_2$	$N_3$	N-Value	$P_1$	$P_2$	$P_3$	
3.0	6	9	13	22	15	15	15	22
6.0	14	20	28	48	15	15	15	48
9.0	7	14	40	54	15	15	15	54
12.0	1	1	3	4	15	15	15	4
15.0	3	5	7	12	15	15	15	12
18.0	13	32	54	86	15	15	15	86
21.0	37	59	94	153	15	15	15	153
24.0	44	47	75	122	15	15	15	122
27.0	17	41	71	112	15	15	15	112
30.0	28	88	95	183	15	15	15	183

Depth	Standard Penetration Test				Penetration in cm.			N <sub>SPT</sub>
	N <sub>1</sub>	N <sub>2</sub>	N <sub>3</sub>	N-Value	P <sub>1</sub>	P <sub>2</sub>	P <sub>3</sub>	
33.0	23	48	47	95	15	15	15	95
36.0	68	92	50	142	15	15	4	224
39.0	102	50	-	50	15	3	-	500
42.0	50	-	-	0	3	-	-	500
45.0	100	-	-	0	13.5	-	-	222
48.0	31	83	50	133	15	15	5	200
51.0	55	50	-	50	15	5	-	300
54.0	50	-	-	0	8	-	-	188
57.0	45	60	-	60	15	7	-	257
60.0	50	-	-	-	7.0	-	-	214
63.0	90	50	-	-	15	4	-	375
66.0	47	75		75.0	15	8		281
69.0	80				8.0			300
72.0	50				4			375
75.0	102	50		50.0	13			235
78.0	85				10			255

### CORRECTIONS TO N-VALUES:

The SPT data collected is the field ‘N’ value without any applied corrections. Usually for engineering use site response study and liquefaction analysis the SPT “N” values need to be corrected with various corrections and a seismic borelog has to be obtained. The seismic borelog contains information about depth, observed SPT ‘N’ values, density of soil, fine content, correction factors for observed “N” values, and corrected “N” value. The ‘N’ values measured in the field using standard penetration test procedure have been corrected for various corrections, such as: (a) Overburden Pressure (C<sub>N</sub>), (b) Hammer energy (C<sub>E</sub>), (c) Borehole diameter (C<sub>B</sub>), (d) presence or absence of liner (C<sub>S</sub>), (e) Rod length (C<sub>R</sub>) and (f) Fine content (Seed et al., 1983, 1985; Youd et al., 2001; Cetin et al., 2004, Skempton; 1986 and Pearce and Baldwin, 2005). Corrected ‘N’ value i.e., (N<sub>1</sub>)<sub>60</sub> is obtained using the following equation:

$$(N_1)_{60} = N_{SPT} * C_N * C_E * C_B * C_S * C_R$$

### Overburden Pressure:

The effective use of SPT blow count for seismic study requires that the effects of soil density and effective confining stress on penetration resistance be separated. Consequently, Seed et al (1975) included the normalization of penetration resistance in sand to an equivalent  $\sigma'_{vo}$  of one atmosphere as part of the semi empirical procedure. SPT N-values recorded in the field increase with increasing effective overburden stress; hence overburden stress correction factor is applied (Seed and Idriss 1982). This factor is commonly calculated from equation developed by Liao and Whitman (1986). However Kayen et al. (1992) suggested the following equation, which limits the maximum C<sub>N</sub> value to 1.7, provides a better fit to the original curve specified by Seed and Idriss (1982):

$$C_N = \sqrt{\frac{P_a}{\sigma'_{vo}}} \leq 2.0$$

where  $\sigma'_{vo}$  is the vertical effective stress at the depth of N<sub>SPT</sub>  
and P<sub>a</sub> is one atmospheric pressure (101.325 kPa) in the same units as  $\sigma'_{vo}$ .

This empirical overburden correction factor is also recommended by Youd et al (2001). For high pressures (300 kPa), which are generally below the depth for which the simplified procedure has been verified, C<sub>N</sub> should be estimated by other means (Youd et al, 2001).



### Hammer Energy (see Table. 6.3.9):

The factor ( $C_E$ ) is used to correct the measured SPT blow count for the level of energy delivered by the SPT hammer. Using 60 % of the theoretical maximum energy as a standard, this correction is given by:

$$\frac{\text{actual energy delivered to top of drill rod}}{0.60 * \text{theoretical maximum SPT hammer energy}} = \frac{ER}{60}$$

where, ER is the energy ratio and the theoretical maximum SPT hammer energy is 4200 lb-in (from 140 weight dropping 30 inches in each blow). The energy ratio (ER) should be measured for the particular SPT equipment used. When such measurements are unavailable, the energy ratio and correction factor can be estimated from the average values given by Seed et al. (1985):

**Table. 6.3.9: Hammer Correction Factors (Robertson & Wride, 1998)**

Type of Hammers	Notation	Range of Correction
Donut Hammer	$C_E$	0.5 - 1.0
Safety Hammer	$C_E$	0.7 - 1.2
Automatic-trip Donut Hammer	$C_E$	0.8 - 1.3

### Bore Hole Diameter ( $C_B$ ) (see Table 6.3.10):

The third correction factor Borehole Diameter ( $C_B$ ), is for borehole diameters outside the recommended range. The following values are recommended:

**Table 6.3.10: Borehole Diameter Correction Factors (Robertson & Fear, 1996)**

Factor	Variables (in mm)	Correction
Borehole Diameter	65 – 115	1.00
Borehole Diameter	150	1.05
Borehole Diameter	200	1.15

### Presence or Absence of Liner ( $C_S$ )

The fourth correction factor, ( $C_S$ ) is for SPT samplers used without a sample liner. If the split spoon sampler is made to hold without a liner, the measured blow count should be corrected with  $C_S = 1.2$ , otherwise,  $C_S = 1.0$  for a Standard Sampler.

### Rod Length ( $C_R$ ) (see Table 6.3.11):

The last correction factor is ( $C_R$ ), which is used to correct for the loss of energy through reflection in short lengths of drill rod. In the NCEER recommendations, values of the correction factor  $C_R$  are given for ranges of rod length as shown in the below table.

**Table 6.3.11: Rod Length Correction Factors**

Factor	Variables (in m)	Correction
Rod Length	< 3	0.75
Rod Length	3 – 4	0.8
Rod Length	4 – 6	0.85
Rod Length	6 – 10	0.95
Rod Length	10 – 30	1.00

### Fine Content Correction:

The corrected N-Value “ $(N_1)_{60}$ ” is further corrected for fine content, based on the revised boundary curves as derived by Idriss and Boulanger (2004) for cohesion-less soils as described below:

$$(N_1)_{60CS} = (N_1)_{60} + \Delta(N_1)_{60}$$

$$\Delta(N_1)_{60} = \exp \left[ 1.63 + \frac{9.7}{FC + 0.001} - \left( \frac{15.7}{FC + 0.001} \right)^2 \right]$$

where, FC = percent fines content (percent dry weight finer than 0.074 mm)

The corrected N-value at every 3.0 m depth interval for BH-19 is enlisted in APPENDIX - C in tabular form.

### GEOTECHNICAL UNITS CLASSIFICATION:

The inferred preliminary geotechnical subsurface profile describing 5 geotechnical units across the site has been presented in a generalized way as shown in Table 6.3.12. This correlation of available boreholes reveals a better lithological inter-relationship between various geotechnical units; and such an evaluation can be really effective for the purpose of current study. A preliminary geotechnical model for the site is based on four directional cross-sections. With reference to the four considered cross-sections, the model indicates that the thickness of filled-up material within the study area typically varies between 1.5 to 4.5 m across the site. A summary description of the properties for each of the units is provided below:

- **Surface Fill (Unit - 1):**

Surface fill was encountered in all the boreholes ranging upto a maximum depth of 4.5 m below ground level, consisting of road material and concrete debris. The fill typically varies between 1.5 and 4.5 m thick but locally was encountered to depth of greater than 2.0 m. Fill in general was found to comprise of sandy and clayey soils mixed with gravel sized fragments including brick, concrete and other assorted materials. The fill is expected to be highly varying and unpredictable in its engineering properties in view of its age and range of placement methods during the demolition of old building and development of multi-storied building. In BH-19, surface fill was not encountered as the ground level was 3.0 m below EGL.

**Table 6.3.12: Generalized Geotechnical Model from 19 boreholes**

Unit No.	Generalized Descriptions	Lithological Attributes	Depth w.r.t each borehole
Unit – 1	Surface Fill	Filled Up Material	0.0 to 4.5 m
Unit – 2	Sands with minor quantity of fines	Sand – 1	1.5 to 21 m
Unit – 3	Clays & Silts	Clay – 1	4.5 to 22 m
Unit – 4	Poorly Graded Sands	Sand – 2	21 to 30 m
Unit – 5	Clays & Silts	Clay – 2	28.5 to 30 m

- **Sands with minor quantity of fines (Unit - 2):**

Sandy soils with minor percentage of fines (Silt and Clay) were encountered in most boreholes formed by fluvial processes of Sabarmati River. The percentage of coarser fraction is more compared to finer fraction. Majority of the soils are of non-plastic nature. These soils are yellowish brown in colour, loose to dense Silty Sands and Clayey Sands.

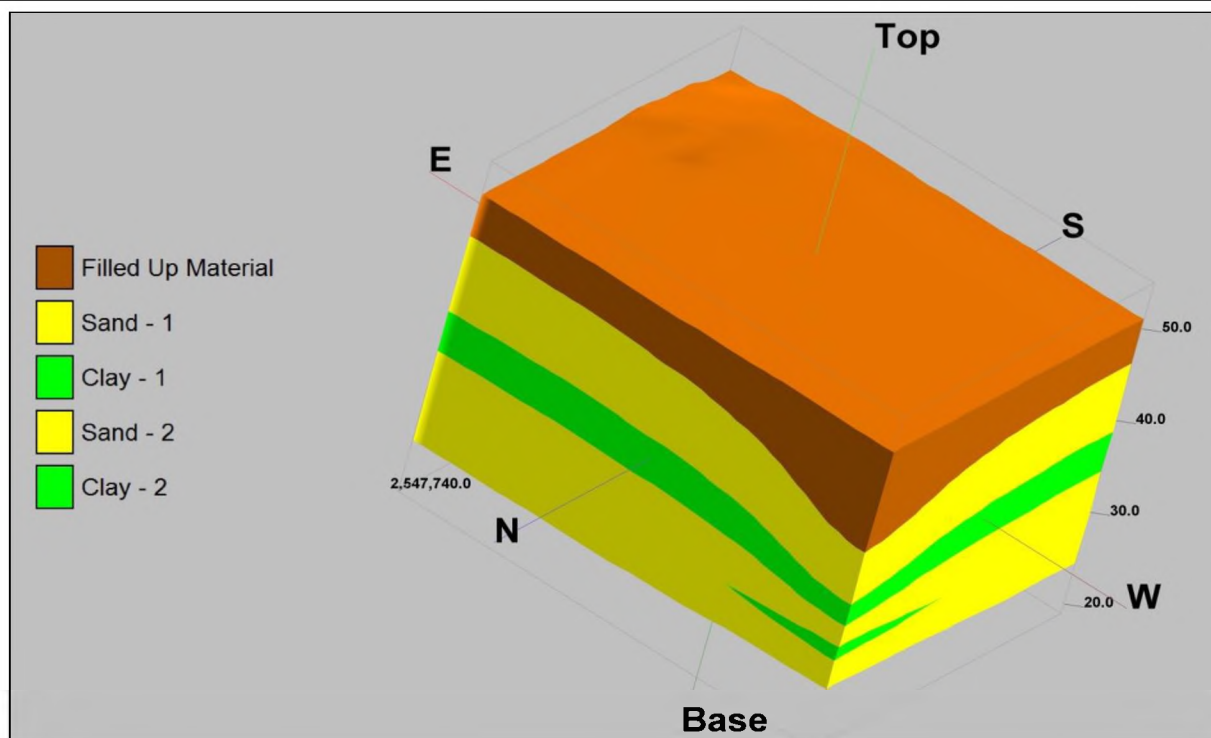


Fig. 6.3.17: 3D Geotechnical Unit Model from 19 boreholes

- **Clays & Silts (Unit - 3):**

Lensoidal Clays (Clay patches) present in Unit-3 are Clayey and Silty soil with minor percentage of coarser fraction. The lensoidal feature is exhibited as this zone is almost continuing within each and every borehole. The depth range varies from borehole to borehole. These soils are reddish brown in colour, stiff to very stiff Clays and Silts.

- **Poorly Graded Sands (Unit - 4):**

Sands are having minor percentage of fines and show the constituency of coarser, medium and finer sand. All the soils within this unit are purely non-plastic. These soils are yellowish brown in colour, dense to very dense sands.

- **Clays & Silts (Unit - 5):**

Clayey and Silty fractions are high, while coarser fraction is very less. All the layers within this unit are of intermediate to high plastic nature. These soils are yellowish grey in colour, stiff to very stiff Clays and Silts.

Fig. 6.3.17 depicts the 3D geotechnical unit model for 18 boreholes. The 5 layered model depicts top layer as Filled Up Material (FM), while the bottom layer as Sand – 3. But in borehole BH-19 drilled by ISR, Clay – 3 layer is encountered as the layer at 30.0 m depth, However, the preliminary geotechnical unit model is based on overall lithological analysis of all 19 boreholes.

### **Ground Water Information:**

Groundwater levels were measured in 18 boreholes by M/s KCT from Feb – Apr' 12 and in 1 borehole of 80.0 m by ISR during Jul' 12. Overall the area shows the ground water level in boreholes at a minimum level of 14.5 m (BH-14) to a maximum level of 17.5 m (BH-12) depth. The details of GWL are shown in Table. 5.10.

**Table 6.3.13: Details of GWL (m) in 19 boreholes**

BH. No.	Termination Depth (m)	Depth of GWL (m)	Elevation (m)	RWL (m)
BH-01	30	15.5	54	38.50
BH-02	30	15.2	52	36.80
BH-03	30	15.0	51	36.00
BH-04	30	16.0	50	34.00
BH-05	30	15.0	53	38.00
BH-06	30	15.0	50	35.00
BH-07	30	15.0	54	39.00
BH-08	30	15.4	53	37.60
BH-09	30	15.2	52	36.80
BH-10	30	15.2	51	35.80
BH-11	30	17.0	51	34.00
BH-12	30	17.5	50	32.50
BH-13	30	15.2	53	37.80
BH-14	30	14.5	51	36.50
BH-15	30	15.5	54	38.50
BH-16	30	16.0	53	37.00
BH-17	30	15.5	51	35.50
BH-18	30	17.0	51	34.00
BH-19	80	17.0	51	34.00

Based on lithological data and geotechnical unit model, it can be said that the water table level in the wells, is expected to be encountered within the loose to medium dense sands (Units – 2, 4 & 6). Also, these units enclose the major formation encompassing the lensoidal clayey layers. The occurrence of saturated water charged sands at varying depths, will have an important implications with regard to the design and construction of below ground structures.

#### **LIQUEFACTION ANALYSIS:**

The concept of liquefaction was first introduced by Casagrande in the late 1930's. Liquefaction may be defined as *"the transformation of a granular material from solid state to liquid state due to increase in pore pressure and reduced effective shear strength will behave more like a fluid"* (Marcuson 1978). The typical subsurface soil condition that is susceptible to liquefaction is loose sand, which has been newly deposited or placed, with a groundwater table near ground surface. During an earthquake, the upward propagation of shear waves through the ground generates shear stresses and strain that are cyclic in nature (Seed and Idriss, 1982). The application of cyclic shear stresses induced by the propagation of shear waves causes the loose sand to contract, resulting in an increase in pore water pressure. As the seismic shaking occurs quickly, the cohesionless soil is subjected to an undrained loading (total stress increase). The increase in pore water pressure causes an upward flow of water to the ground surface, where it emerges in the form of mud spots or sand boils. The development of high pore-water pressure due to the ground shaking and the upward flow of water may turn the sand into a liquefied condition, which has been termed as *Liquefaction*.

Structures on top of loose sand deposit liquefied during an earthquake will sink or fall over, while buried tanks will float to the surface where the loose sand liquefies (Seed, 1970). After the soil has been liquefied, the excess pore water pressure will start to dissipate. The length of time for the soil to remain in a liquefied state depends on two main factors:

- (1) The duration of the seismic shaking from an earthquake and
- (2) The drainage conditions for the liquefied soil.



Longer duration and stronger intensity of the cyclic shear stress application from an earthquake, results into a prolong state of liquefaction. Likewise, if the liquefied soil is confined by an upper and a lower clay layer, then it will need a longer duration for the excess pore water pressure to dissipate by the flow of water from the liquefied soil.

Parameters for estimation of Liquefaction Potential:

The liquefaction potential estimation depends on the following parameters:

- (A) Grain Size Distribution,
- (B) Duration of Earthquake,
- (C) Amplitude and Frequency of Shaking,
- (D) Distance from Epicenter,
- (E) Location of Water Table
- (F) Cohesion of the Soil,
- (G) Permeability of the layer

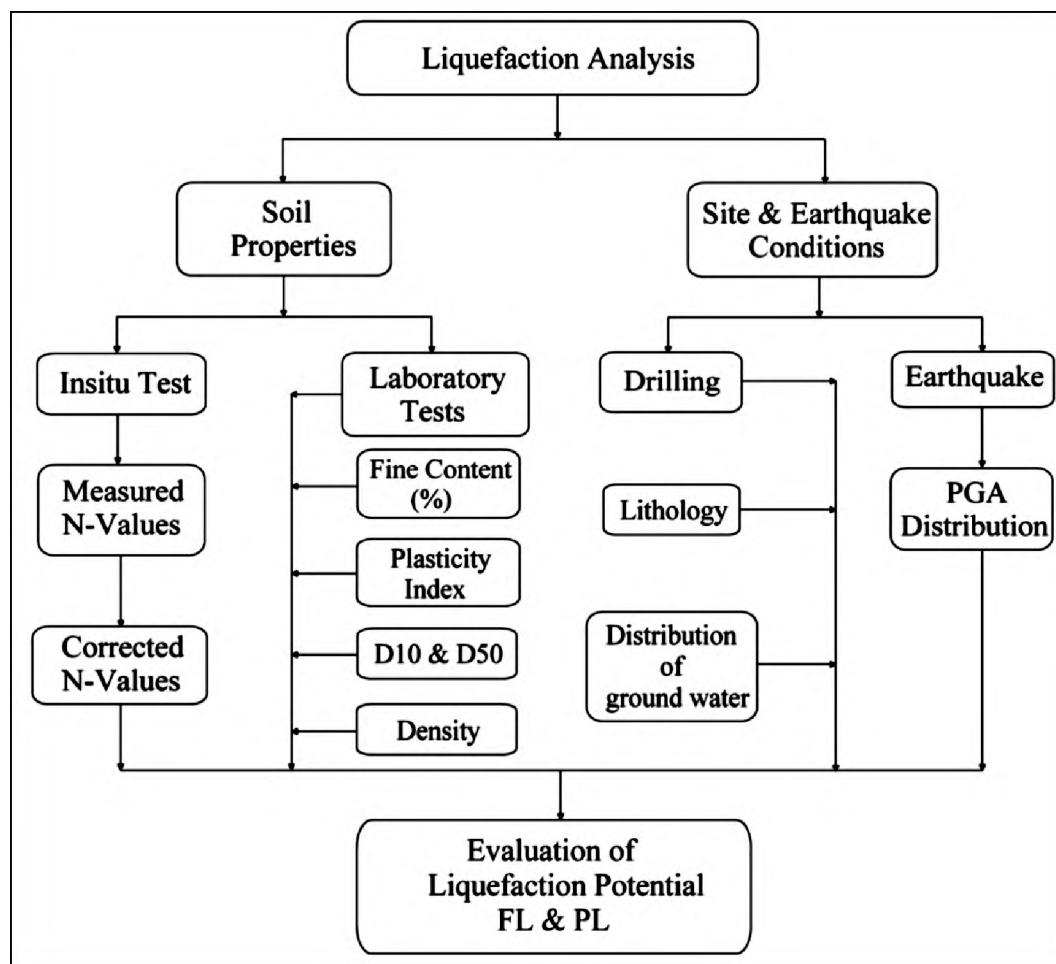


Fig. 6.3.18: Workflow for Liquefaction Potential Estimation

The first step for liquefaction analysis involves the identification of cohesionless soil layers, i.e. sandy horizons, present in the boreholes, as these layers are more prone to liquefy. For the present study of proposed multi-storied building at V. S. Hospital site, the Japan Road Association Method 2002 was

adopted for liquefaction analysis. The flowchart for the evaluation of liquefaction potential for the study area is shown in Fig. 6.3.18.

### **Methodology for Liquefaction Potential Estimation:**

Considering the available geo-technical field data and laboratory test results for all boreholes falling in the target area, the Japanese Road Association Method, 2002 was adopted to estimate the liquefaction potential of the deposit at each depth. In this particular method, two different steps are involved viz;

i)  $F_L$  Estimation &

ii)  $P_L$  Estimation

The liquefaction potential for individual layer was analyzed by the help of  $F_L$  Estimation, while the complete analysis for liquefaction potential estimation in each borehole was evaluated by the  $P_L$  Estimation based on the results of the  $F_L$  Estimation.

i)  $F_L$  Estimation:

The liquefaction potential for individual layers is analyzed by the  $F_L$  method. In this study, the earthquake type to decide the parameter  $C_w$  is adopted as "Type 2" according to the seismo-tectonic context of the scenario earthquakes.

Liquefaction Resistance factor,  $F_L = R / L$

$F_L \leq 1.0$ : Judged as liquefied

$F_L > 1.0$ : Judged as not liquefied

where,  $F_L$  = Liquefaction Resistance Factor

$R$  = Cyclic Shear resistance at effective overburden pressure

$$R = C_w * R_L$$

$C_w$  = Correlation coefficient for earthquake type

The parameter of  $C_w$  depends on the types of earthquakes

i.e Type 1 earthquake (plate boundary type, large scale),  $C_w = 1.0$

Type 2 earthquake (inland type),  $C_w = 1.0 (R_L \leq 0.1)$

$$C_w = 3.3 R_L + 0.67 (0.1 < R_L \leq 0.4)$$

$$C_w = 2.0 (0.4 < R_L)$$

where,  $R_L$  = Cyclic resistance ratio obtained by laboratory test

$$R_L = 0.0882(N_a/1.7)^{0.5}, \text{ when } N_a < 14$$

$$R_L = 0.0882(N_a/1.7)^{0.5} + 1.6 * 10^{-6} (N_a - 14)^{4.5}, \text{ when } N_a \geq 14$$

For Sandy Soil,  $N_a = c_1 N + c_2$

$$c_1 = 1 (0\% \leq FC < 10\%)$$

$$= (FC + 40) / 50, (10\% \leq FC < 60\%)$$

$$= FC/20 - 1, (60\% \leq FC)$$

$$c_2 = 0, (0\% \leq FC < 10\%)$$

$$= (FC - 10)/18, (10\% \leq FC)$$

where FC : Fine Particle Content (%)

For Gravelly Soil,  $N_a = \{1 - 0.36 \log_{10}(D_{50}/2.0)\} N_i$

N: SPT blow count

$N_g$ : N value correlated for grain size

$$N_f: 170N/(\sigma_v' + 70)$$

$D_{50}$ : Grain Diameter of 50% passing (mm)

$$\text{And, } L = \alpha / g \times \sigma_v / \sigma_v' \times r_d$$

$L$ : shear stress to the effective overburden pressure

$r_d$ : Stress Reduction Factor

$$r_d = 1.0 - 0.015x$$

$x$ : depth below the ground surface (m)

$\alpha$ : peak ground acceleration (gal)

$g$ : acceleration of gravity (= 980 gal)

$\sigma_v$ : total overburden pressure (kN/m<sup>2</sup>)

$\sigma_v'$ : effective overburden pressure (kN/m<sup>2</sup>)

$$F_L = (Cw * R_L) / \alpha / g \times \sigma_v / \sigma_v' \times r_d$$

## ii) $P_L$ Estimation:

The final liquefaction potential at each grid is evaluated by the  $P_L$  method based upon the results of the  $F_L$  method using past examples from Japan.

$$P_L = \int_0^{20} F * w(z) dz$$

$15 < P_L$ , Very high liquefaction potential

$5 < P_L \leq 15$ , Relatively high liquefaction potential

$0 < P_L \leq 5$ , Relatively low liquefaction potential

$P_L = 0$ , Very low liquefaction potential

where,  $F = 1.0 - F_L$  ( $F_L < 1.0$ )

$$= 0.0 \text{ } (F_L \geq 1.0)$$

$$w(z) = 10.0 - 0.5z$$

$P_L$ : Liquefaction Potential Index

$w(z)$ : Weight function for depth

$z$ : Depth below the ground surface (m)

$\sigma_v'$ : effective overburden pressure (kN/m<sup>2</sup>)

OR

$$FL = \tau_o / \tau_{av}$$

$\tau_o$  = Shear stress causing liquefaction

$\tau_{av}$  = Shear stress developed due to earthquake shaking

Note: If the shear stress developed due to earthquake shaking is greater than shear stress causing liquefaction then liquefaction will occur. i.e.  $\tau_o > \tau_{av}$ .

The different levels of liquefaction and care required for them is given in Table 6.3.14.

**Table. 6.3.14: Criterion for evaluation of Liquefaction Potential ( $P_L$ )**

$P_L$ value	Liquefaction Potential	Explanation
$15 < P_L$	Very High	Ground improvement is indispensable
$5 < P_L \leq 15$	Relatively High	Ground improvement is required
$0 < P_L \leq 5$	Relatively Low	Investigation for important facilities is indispensable
$P_L = 0$	Very Low	Investigation for important facilities is required
		No remedial estimation is required

Target Boreholes for Liquefaction Analysis:

According to the Japan Road Association (2002) method, the alluvial saturated sandy deposits, which satisfy the following three conditions at the same time, require liquefaction potential analysis:

- Saturated sandy layer above the depth of 20.0 m with groundwater level within a range of 10.0 m from the existing ground surface.
- Soil layer with fine particle content (FC %) less than 35%, or with plasticity index (Ip) less than 15% even with an FC of more than 35%.
- Soil layer with median grain size ( $D_{50}$ ) less than 10 mm, and with grain size of 10% passing ( $D_{10}$ ) less than 1 mm.

Liquefaction potential evaluation is recommended for alluvial deposits with a low N-value or showing a deformational history. Considering the above conditions, we have carried out liquefaction analysis for BH-19 (1 borehole of 80 m by ISR).

Details of liquefaction potential estimation for BH-19 for local and far type scenario based earthquakes is shown in the tabular form (see Table 6.3.15).

**Table. 6.3.15: Liquefaction potential for BH-19 (Local & Far EQ at Actual & Zero GWL)**

BH. No.	Water Level (m)	Earthquake Type I: Longer Duration (Inter-Plate) & II: Shorter Duration (Intra-Plate)	Horizontal Seismic Co-efficient $k_h$ (a/g)	Index ( $P_L$ )	Evaluation
Liquefaction Potential (EQ Local Field, GWL Actual)					
BH-19	17.00	Type II	0.07726	0.0	Very Low
Liquefaction Potential (EQ Far Field, GWL Actual)					
BH-19	17.00	Type II	0.05050	0.0	Very Low
Liquefaction Potential (EQ Local Field, GWL Zero)					
BH-19	0.00	Type II	0.07726	0.0	Very Low
Liquefaction Potential (EQ Far Field, GWL Zero)					
BH-19	0.00	Type II	0.05050	0.0	Very Low

#### Discussion about Liquefaction:

For the evaluation of liquefaction potential for the proposed multi-storied building at V. S. Hospital site, Japan Road Association (2002) method was used. Liquefaction potential analysis was carried out for BH-19 (borehole of 80 m by ISR) using two scenario based earthquakes, i.e., Local & Far type for pre-monsoon and monsoon periods (i.e., water level at surface). From the analysis done it is found that in all the four categories, BH-19 is falling under “Very Low” category.



### **Conclusions about Liquefaction:**

The soils in the study area are showing alternative layers of Sandy and Clayey units with stiff to very stiff nature up to 20.0 m depth, while dense to very dense nature from 20.0 m onwards. At shallower depths of around 10.0 m, the corrected N-values reach  $> 50$ , while at deeper depths the values reach  $> 100$ . A total of 15 Direct Shear Tests were conducted on UDS for estimation of shearing values, which shows that the soils are of the order of Silty Sand and Sand (Shape: Round and Angular).

Soils having free swell values greater than 100% are considered to be of potential problems, whereas soils with free swell values below 50% probably do not exhibit appreciable volume changes. A total of 31 swell indexes were measured for BH-19. The values for BH-19 range between 6 – 43 %, describing less expansive nature of the encountered soils.

The analysis for liquefaction potential assessment has been carried out purely based on the geology, sub-surface geology, seismic history and geotechnical characteristics of soil as collected. BH-19 soil properties and response analysis data was used for calculation of liquefaction potential of proposed multi-storied building at V. S. Hospital site. The results are presented into four sets ((i) Local EQ at Actual GWL, (ii) Local EQ at Zero GWL, (iii) Far EQ at Actual GWL and (iv) Far EQ at Zero GWL. BH-19 within the target area is falling in the “Very Low” category, describing least potential for liquefaction hazard. Hence it can be said that the area is safe from liquefaction.

### **References about Liquefaction:**

- Cetin, K. O., Seed, R. B., Kiureghian, A. D., Tokimatsu, K., Harder, L. F. Jr., Kayen, R. E. and Moss, R. E. S. (2004): Standard penetration test – based probabilistic and deterministic assessment of seismic soil liquefaction potential, *Journal of Geotechnical and Geoenvironmental Engineering*, Vol. 12, pp. 1314 - 1340
- IS: 1498 (1970): Classification and identification of soils for general engineering purposes (First Revision)
- IS: 1892 (1979): Code of practice for subsurface investigation for foundations (First Revision)
- IS: 2131 (1981): Method for standard penetration test for soils (First Revision)
- IS: 2132 (1986): Code of practice for thin-walled tube sampling of soils (Second Revision)
- IS: 2720 (Part II - 1973, Edition 3.1): Methods of test for soils - Determination of Water Content (Second Revision)
- IS: 2720 (Part III (Sec. I & Sec. II) – 1980): Methods of test for soils - Determination of Water Content (First Revision)
- IS: 2720 (Part IV (Part IV) – 1985): Method of test for soils – Grain Size Analysis (Second Revision)
- IS: 2720 (Part V – 1985): Method of test for soils – Determination of liquid and plastic limit (Second Revision)
- IS: 2720 (Part XIII - 1986): Methods of test for soils - Direct shear test (Second Revision)
- IS: 2720 (Part XXIX - 1975): Methods of test for soils – Determination of Dry Density of soils in-place by the core-cutter method (First Revision)
- Idriss I.M. and Boulanger R.W. (2004): Semi-empirical procedures for evaluating liquefaction potential during earthquakes. *Proc. of the 11<sup>th</sup> International Conference on Soil Dynamics & Earthquake engineering (ICSDEE) and 3<sup>rd</sup> International Conference on Earthquake Geotechnical Engineering (ICEGE)*, pp. 32 – 56
- Japan Road Association (1980, 1992 & 2002): Specifications for Highway Bridges, Part V Earthquake Resistant Design
- Liao, S. S. C. and Whitman, R. V. (1986): Catalogue of liquefaction and non-liquefaction occurrences during earthquakes, *Res. Rep., Dept. of Civ. Engrg., Massachusetts Institute of Technology, Cambridge, Mass*
- Marcuson, W. F. (1978): Definition of terms related to liquefaction, *J. Geotech. Engg. Div., ASCE*, Vol. 104 (9), pp 1197 – 1200
- Robertson P.K. and Wride C.E. (Fear) (1996): Cyclic liquefaction and its evaluation based on the SPT and CPT. *Proc. of the 1996 NCEER workshop on Evaluation of Liquefaction resistance of Soils, Report NCEER-97-0022*, pp. 41–87

- Robertson, P.K., and Wride (Fear), C.E. (1998): Evaluating cyclic liquefaction potential using the cone penetration test. *Canadian Geotechnical Journal*, 35: pp. 442–459
- Seed, H. B. and Idriss, I. M. (1970): Soil moduli and damping factors for dynamic response analysis, Report EERC 70 – 10, University of California, Earthquake Engineering Research Center, Berkeley, CA
- Seed, H. B. and Idriss, I. M. (1982): Ground motions and soil liquefaction during earthquakes, Earthquake Engineering Research Institute, Berkeley, CA, pp 134
- Seed, H. B., Idriss, I. M. and Arango I. (1983): Evaluation of liquefaction potential using field performance data, *J. Geotech. Engg. Div, ASCE* 1983; 109 (3), pp. 458 - 482
- Seed et al. (1985): Influence of SPT procedures in soil liquefaction resistance evaluations. *Journal of Geotechnical Engineering, ASCE*, 111 (12), pp. 1425 - 1445
- Skempton, A. W. (1986): Standard penetration test procedures and the effects in sands of overburden pressure, relative density, particle size, aging and overconsolidation, *Geotechnique* 1986; 36 (3), pp. 425 - 447
- Youd et al (2001): Liquefaction Resistance of soils: Summary from the 1996 NCEER and 1998, NCEER/NSF workshops on evaluation of liquefaction potential resistance of soils, *Journal of Geotechnical and Geoenvironmental Engineering*, pp. 817 - 833

### **6.3.5 Strong Motion Estimation & Ground Response Analysis for Vs Hospital**

#### **Introduction to Strong Motion Analysis:**

V.S. Hospital site falls in Zone III of the seismic zoning map of India (BIS) where maximum expected magnitude of an earthquake is 6.0. The seismic hazard analysis is done by Stochastic Finite Fault Source Modeling (SFFSM) method by taking magnitude 6.0 as scenario earthquake and East Marginal Fault as capable fault for generating near field earthquake. Since the structures proposed in V.S. Hospital site is of 16 floors, which may be affected by low frequency waves from a large earthquake in Kachchh region. Hence, a scenario earthquake of Mw7.6, 2001 earthquake along the eastern part of the Kachchh Mainland Fault (KMF) is also considered as far-field source for the hazard analysis.

#### **Soil Modeling and Engineering Bed Layer:**

The preliminary soil model for the V.S. Hospital area is prepared based on the following investigations and surveys:

- Drilling and Geotechnical investigation for soil properties
- PS logging for seismic wave velocities in boreholes
- Micro-tremor Array measurements for depth to different formations to estimate depth of Engineering Bed Layer
- Multichannel Analysis of Surface Waves (MASW)

A preliminary soil model was prepared considering results and analysis of various investigations. The 18 boreholes drilled by M/s KCT are of 30.0 m depth, while the data achieved by PS logging is upto 63.0 m, MASW and Micro-tremor survey results. The thickness of various layers, their densities and shear wave velocities are shown in Table 6.3.16. This data is very useful for dynamic response analysis.

#### **Soil Layering and Soil Properties:**

Lithology:

A systematic classification of lithology based on grain size analysis is adopted for soil modeling in order to analyze soil response. The procedure is shown below:

- (A) If Clay occupies more than 50%, then the soil is decided as Clay,
- (B) Else if Silt occupies more than 50%, then the soil is decided as Silt,

- (C) Else if Sand occupies more than 50%, then the soil is decided as Sand,
- (D) Else if Gravel occupies more than 50%, then the soil is decided as Gravel or
- (E) Else if every lithology occupies less than 50%, the lithology of maximum occupation is decided as the representative lithology.

**Table 6.3.16 Geological model for V.S. Hospital**

Layer	Width (m)	Depth from Surface (m)	Density (gm/cc)	Shear Wave Velocity (m/sec)	Source
1	3.0	3.0	1.89	216	Drilling Data, PS Logging, MASW & Micro-tremor Data
2	6.0	9.0	2.01	236	
3	7.5	16.5	1.96	256	
4	1.5	18.0	1.98	294	
5	3.0	21.0	1.98	351	
6	1.5	22.5	1.94	467	
7	3.0	25.5	2.00	377	
8	6.0	31.5	2.10	377	
9	1.5	33.0	2.10	364	
10	1.5	34.5	2.00	345	
11	1.5	36.0	1.94	344	
12	1.5	37.5	1.94	345	
13			2.00	465	EBL

Engineering Bed Layer (EBL) is considered at 38.0 m depth below EGL showing Vs more than 450 m/sec, identified by Multi Channel Analysis of Surface Waves (MASW) and PS Logging data.

#### **Density Estimation:**

Wet density as described in Geotechnical Section 6.4 has been considered.

#### **Estimation of Engineering Bed Layer:**

From the geotechnical investigations, MASW, PS logging and Array Micro-Tremor data, the engineering bed layer is adopted as the layer with N value more than 100 blow counts and Vs more than 450 m/s. The 18 boreholes drilled by M/S KCT are of only 30 m depth. The deeper borehole drilled by ISR has shown engineering bed layer in V.S. Hospital site at 38.0 m depth.

#### **Definition of Engineering Bed Layer:**

It is better to estimate seismic ground motion considering from earthquake source to ground surface in one go, but currently it is difficult to do so, because of the information shortage and preciseness or limitation of the theory and methodology to be used. Thus usually, the process is divided into number of parts. One is earthquake source, the second is earthquake source to base rock, and the third is base rock to engineering bed layer and the final portion will be engineering bed layer to ground surface. Sometimes first two or three portions are combined depends upon the strong ground motion simulation technique. In semi empirical technique first two portions are combined and in the Empirical Green Function (EGF) technique all four are combined. The usages of a particular technique depend upon the available input parameters and the source and site conditions. In the present case the first three portions are combined and the ground motion is estimated at Engineering Bed Layer considering a scenario earthquake of magnitude M6 along East Cambay Fault. The rupture parameters and attenuation characteristics of the ground motion are given for near field and far field earthquakes in Tables 6.3.17 and 6.3.18, respectively.

The definition of engineering bed layer is as follows: The layer should exist uniformly in the whole area. Below the layer, the variation of soil properties should be smaller than above. Above the layer, more

information of soil properties and structures should be available. Usually, the layer has Vs between 350 and 700 m/s. The investigations from Array micro-tremor measurements provided information about the geological structure in the area to 1100 m depth. MASW provided information to about 70 m depth. The geotechnical investigations and PS logging have provided information above subsurface layers to depths to 60 m. The following information is extracted from PS logging data, deep borehole (N value) and Micro-tremor:

- (i) At 38 m depth,  $V_s > 450$  m/sec is computed through PS logging.
- (ii) In 80 m borehole (done by ISR),  $N > 100$  is seen at 38 m (Although  $N > 100$  is seen at 28 m and 31.5 m also but in between, the lesser N values are observed and therefore these layers are not considered as EBL).
- (iii) KCT's 18 boreholes are of 30 m deep only. Below 30 m we can get information from ISR borehole only. Therefore, ISR Borehole data is used for response analysis.

#### **INPUT MOTION:**

The input motion is simulated using stochastic finite modeling technique with dynamic corner frequency approach, which is a new concept (Motazedian and Atkinson, 2005) at shear wave velocity of 520 m/sec.

#### **Methodology of Strong Motion Analysis**

We have used the dynamic corner frequency stochastic finite source simulation method (Motazedian and Atkinson, 2005). This method effectively models large earthquakes also. In this modified method the rupture history controls the frequency content of the simulated time series of each sub-fault. Raghukanth et al. (2008) applied the same technique to estimate the ground motions for a great earthquake of magnitude 8.1 in the Shillong Plateau. We have adopted this stochastic finite modeling technique to produce strong motion for a layer velocity of 520 m/sec because the shallow shear wave velocity structure calculated from different Geophysical Methods and Geotechnical data suggests an average shear wave velocity layer of ~450 m/sec. A minor difference of amplification is seen between layer with Vs of 520 m/sec and Vs of 450 m/sec.

The synthetic ground motions for both near field earthquake scenario (Magnitude Mw 6.0 along East Cambay Fault) and far field Earthquake scenario (Magnitude Mw7.6 along eastern part of Kachchh Mainland Fault) are generated using model parameters given in Tables 6.3.17 & 6.3.18, respectively and crustal amplifications determined for generic soils (Boore and Joyner 1997) of Vs30 (average shear wave velocity for upper 30 m) at 520 cm/sec (Table 6.3.19). The accelerogram thus computed for near field earthquake scenario and far field earthquake scenario is given in Fig. 6.1 (a) & (b).

**Table 6.3.17: Model Parameters for simulation of near-field ground motion**

Magnitude	6.0 (Mw)	
Fault Length and Width	13 km and 9 km	
Strike and Dip	135° and 60°	
Slip Distribution	Random	
Shear Wave Velocity	3.6 km/sec	
Density	2.8 gm/cm <sup>3</sup>	
Stress Drop	40 bars	
Kappa	0.03	
Anelastic Attenuation Q(f)	149f <sup>1.43</sup>	Chopra et al. (2010)



Geometric Spreading	$1/R$ ( $R \leq 40$ km) $1/R^{0.5}$ ( $40 \leq R \leq 80$ km) $1/R^{0.55}$ ( $R \geq 80$ km)	Bodin et al. (2004)
Duration Properties	$f_c^{-1}$ ( $R < 10$ km) $f_c^{-1} + 0.16R$ ( $10 \leq R \leq 70$ km) $f_c^{-1} - 0.03$ ( $70 < R \leq 130$ km) $f_c^{-1} + 0.04R$ ( $130 < R < 1000$ km)	Eastern North America Atkinson & Boore, (1995)
Pulsing Percent	50%	

**Table 6.3.18: Model Parameters for simulation of far-field ground motion**

Magnitude	7.6 (Mw)	
Fault Length and Width	45 km and 40 km	
Strike and Dip	100° and 50°	
Slip Distribution	Random	
Shear Wave Velocity	3.6 km/sec	
Density	2.8 gm/cm <sup>3</sup>	
Stress Drop	160 bars	
Kappa	0.03	Mandal & Johnston (2006)
Anelastic attenuation Q(f)	$339f^{0.61}$	Singh et al (2004)
Geometric Spreading	$1/R$ ( $R \leq 40$ km) $1/R^{0.5}$ ( $40 \leq R \leq 80$ km) $1/R^{0.55}$ ( $R \geq 80$ km)	Bodin et al. (2004)
Duration Properties	$f_c^{-1}$ ( $R < 10$ km) $f_c^{-1} + 0.16R$ ( $10 \leq R \leq 70$ km) $f_c^{-1} - 0.03$ ( $70 < R \leq 130$ km) $f_c^{-1} + 0.04R$ ( $130 < R < 1000$ km)	Eastern North America Atkinson & Boore (1995)
Pulsing Percent	50%	

**Table 6.3.19: Frequency dependent amplification characterized by Vs30 = 520m/s (Boore and Joyner 1997)**

Frequency (Hz)	Amplification
0.01	1
0.09	1.21
0.16	1.32
0.51	1.59
0.84	1.77
1.25	1.96
2.26	2.25
3.17	2.42
6.05	2.7
16.6	3.25
61.2	4.15

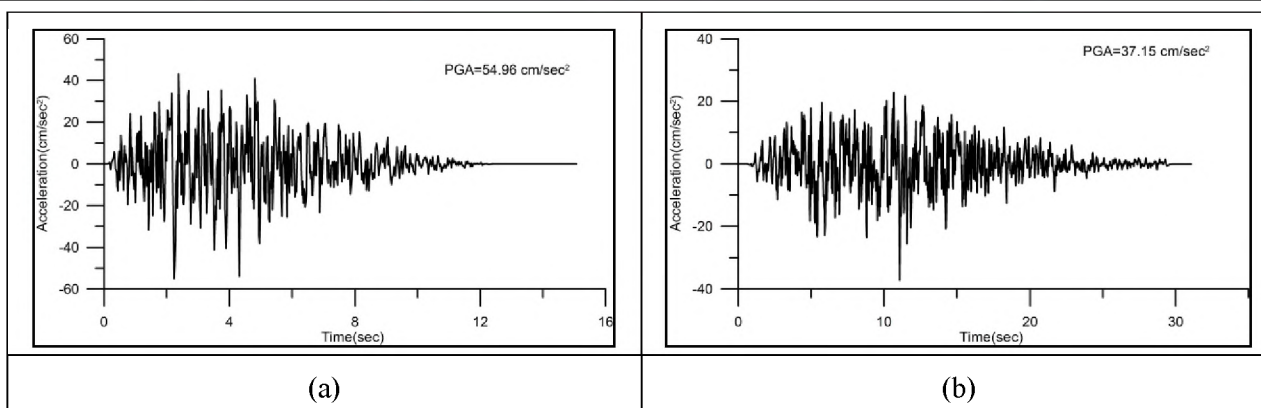


Fig. 6.3.19: Acceleration time history plot of (a) near field and (b) far field earthquake scenarios estimated from stochastic method at 520 m/sec.

The spectral acceleration at 5% damping and 2% damping are also computed and the input response spectra's for both (near field and far field) scenario earthquakes are given in Fig. 6.3.20. Below 0.5 sec, the near field input motion shows higher spectral acceleration. However at larger periods (more than 0.5 sec) the far field motion shows higher spectral acceleration than near field motion. The similar trend of input motion is seen in the Fourier spectra (Fig. 6.3.21). The Fourier amplitude of far field motion is higher than near field motion in low frequency (high period) and reverse scenario is observed at high frequency. This is the simple property of strong ground motion.

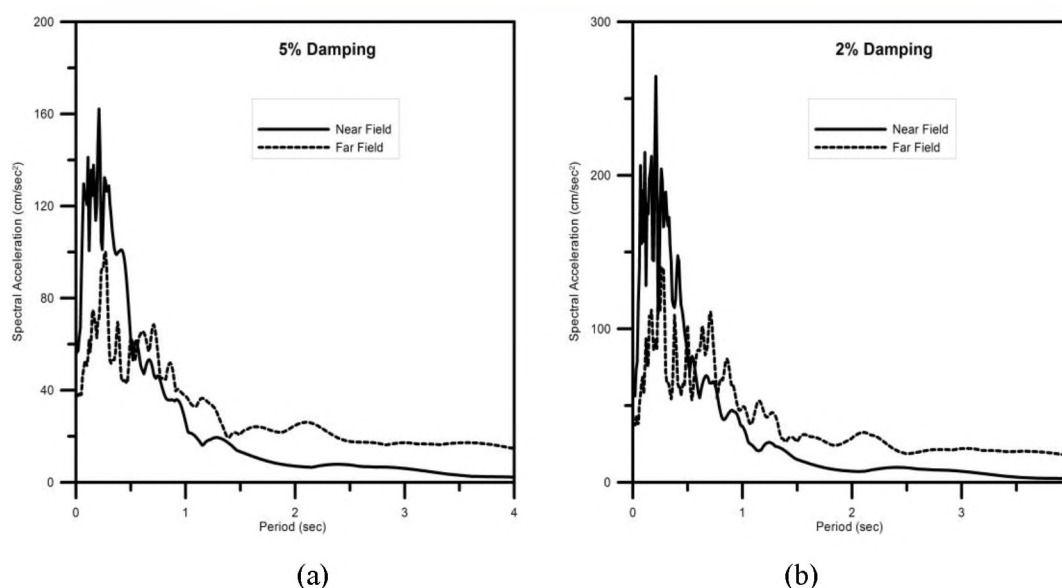


Fig. 6.3.20: (a) The spectral acceleration at 5% damping & (b) at 2% damping for both near field and far field earthquake scenarios supplied to EBL as input motion.

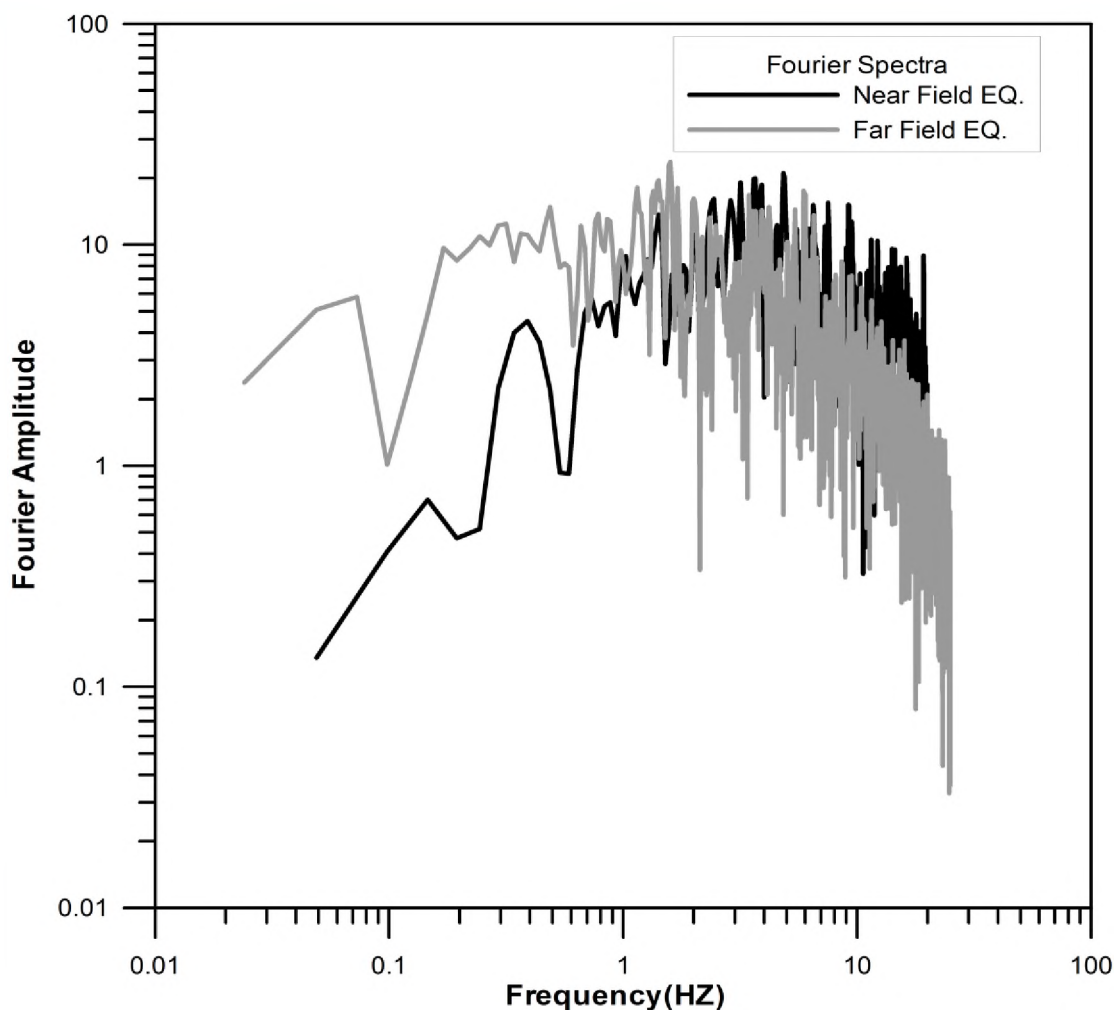


Fig. 6.3.21: The Fourier spectra for both near field and far field earthquake scenarios showing higher energy for far field scenario at lower frequency and low energy than near field scenario at high frequency

#### Ground Model for Response Analysis:

Based on soil investigation and geophysical exploration, soil model at BH-19 borehole in V. S. Hospital site is prepared to conduct the response analysis. The ground model is prepared for BH-19 in the following format:

- Number of Layers & Number of Layer Boundaries,
- Damping Factor (%),  $V_s$  (m/sec), Density ( $\text{g/cm}^3$ ), Thickness (m), Non-Linear Characteristic id (integer) for each layer &
- Upper Depth of each layer (m)

#### Modulus Reduction and Damping Curves:

The soil behavior under irregular cyclic loading due to an earthquake is modeled using modulus reduction ( $G/G_{\text{max}}$ ) and damping ratio ( $\beta$ ) vs. strain curves. The non-linearity of the shear modulus and damping is accounted for by the use of equivalent linear soil properties using an iterative procedure to obtain values for modulus and damping compatible with the effective strains in each layer. The degradation curves for sand, clay and rock used for the present work are those proposed by Seed and Idriss (1970), Sun et al. (1980) and Schnabel (1973) respectively. These curves are shown in Figs. 6.3.22 & 6.6.3.23. These curves are built-in the SHAKE database and used during calculations by selecting the options.

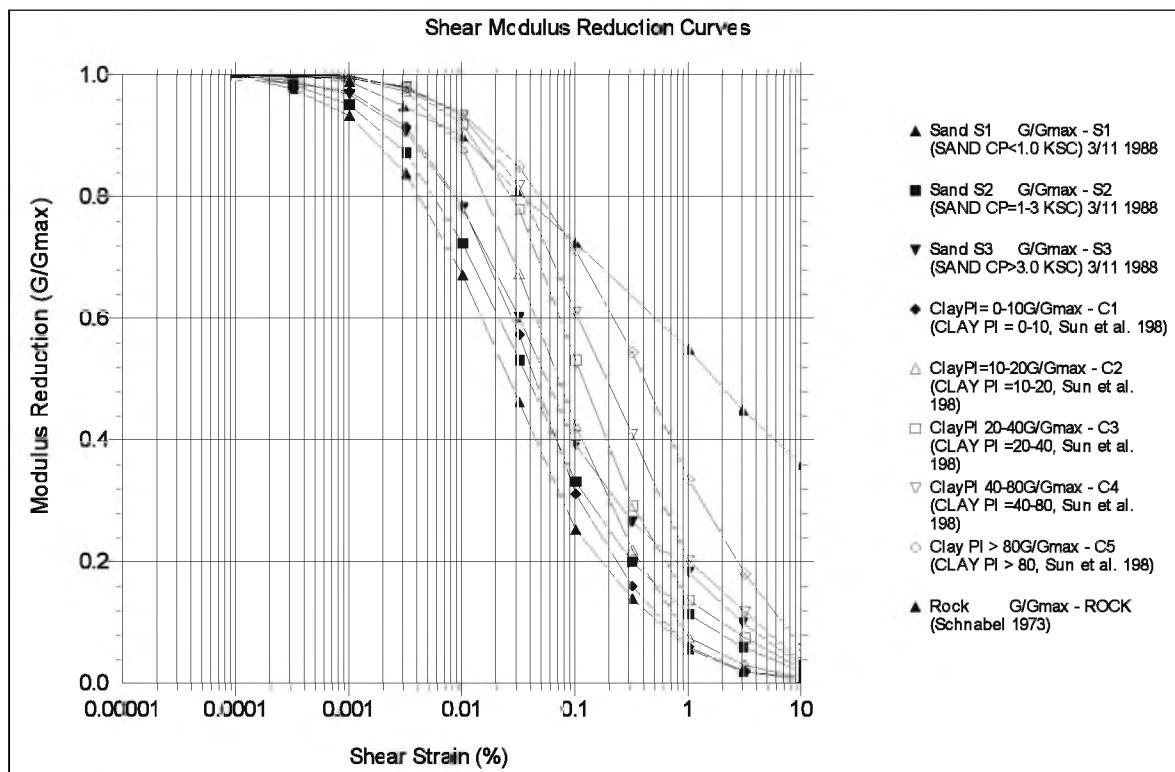


Fig. 6.3.22: Modulus Reduction v/s Shear Strain Curves for sand, clay and rock used in the analysis

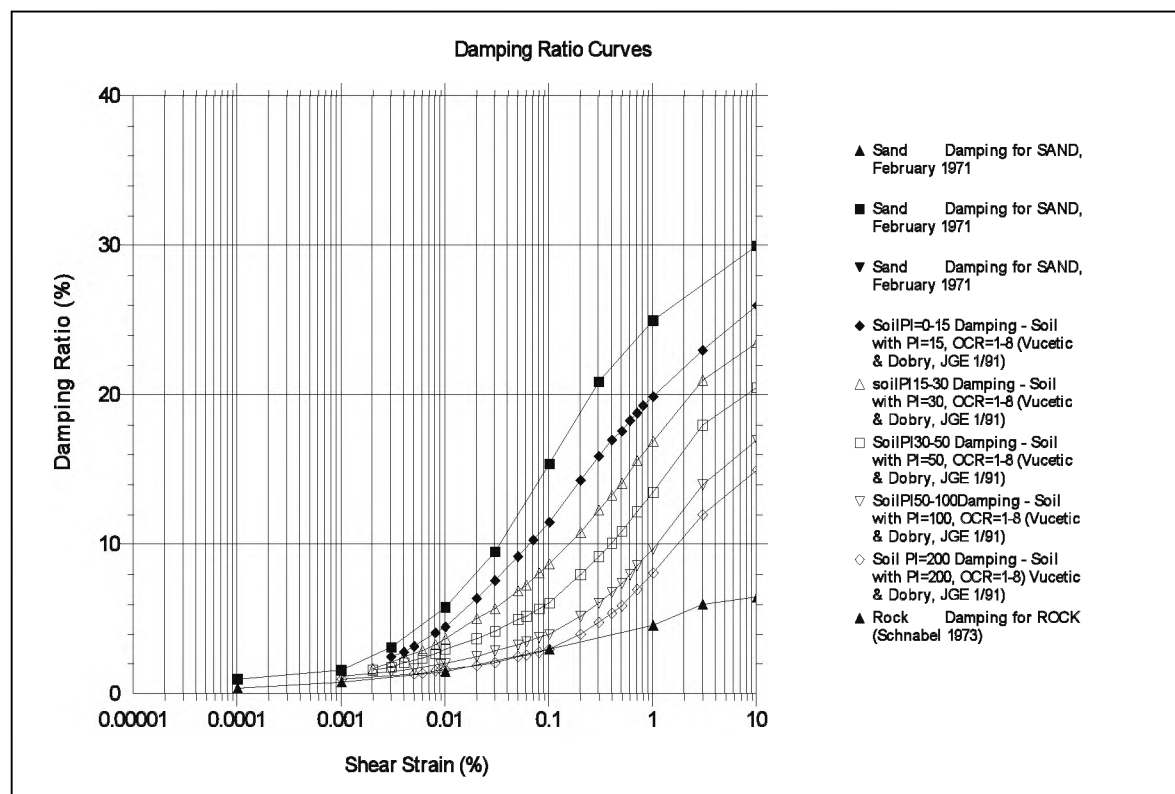


Fig. 6.3.23: Damping Ratio v/s Shear Strain for sand, clay and rock used in the analysis

## GROUND RESPONSE ANALYSIS:

### Strong Motion Analysis for Near Field Earthquake:

The ground response analysis is carried out at BH-19 borehole drilled up to 80 m depth. The soil model for the borehole above EBL is prepared and the natural period of the soil column is also computed and it is 0.43 sec that correspond to 4 - 5 storey building. The structures/buildings with natural period in this



range will suffer heavy damage if proper care is not taken while designing/construction. The input earthquake motion when applied at EBL and allowed to pass through the soil column either gets amplified or deamplified at the boundary of the layers. Finally, the response is observed at the surface in terms of PGA (from accelerogram) and spectral acceleration (from Response Spectra). This process is conducted using SHAKE program. The input motion of PGA  $54.96 \text{ cm/sec}^2$  is applied at EBL. In case of near-field earthquake, the PGA calculated at the surface is  $75.8 \text{ cm/sec}^2$  (Fig. 6.3.24). The PGA amplification factor is also calculated at the borehole and is 1.7. The ground motion is amplified maximum (almost 60%) from  $44 \text{ cm/sec}^2$  to  $75.8 \text{ cm/sec}^2$  in the top 3m layer of the soil column. The variation of acceleration with depth along the borehole (BH-19) is shown in Fig. 6.3.25.

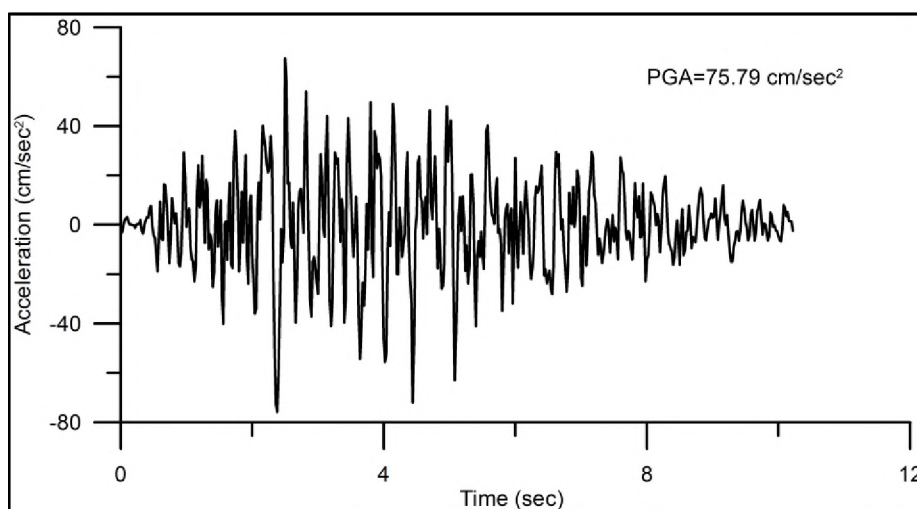


Fig. 6.3.24: The accelerogram of V.S. Hospital area for Near Field Earthquake Scenario computed using SHAKE program

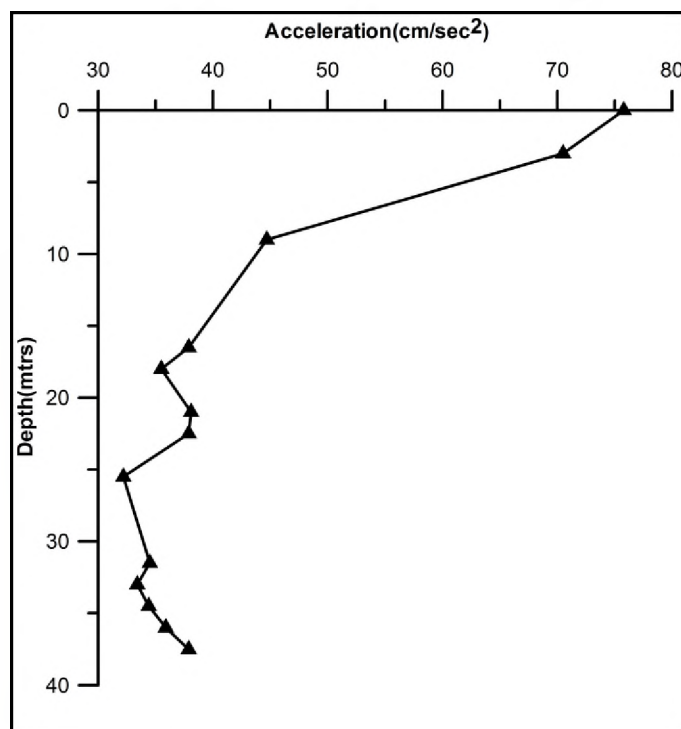


Fig. 6.3.25: PGA Amplification in the soil column for BH-19 at an earthquake of Mw 6.0 along East Cambay Fault

#### Strong Motion Analysis for Far-Field Earthquake:

In case of far-field earthquake, the input motion of PGA  $37 \text{ cm/sec}^2$  is applied at EBL. The PGA thus calculated at the surface when the motion is allowed to pass through the soil layers is  $49.5 \text{ cm/sec}^2$  (Fig. 6.3.26). PGA amplification factor is also calculated at the borehole and it is 1.7. The ground motion is

amplified maximum (almost 68%) from 34 cm/ sec<sup>2</sup> to 49.5 cm/ sec<sup>2</sup> in the top 3m layer of the soil column. The variation of acceleration with depth along the soil columns is shown in Fig. 6.3.27.

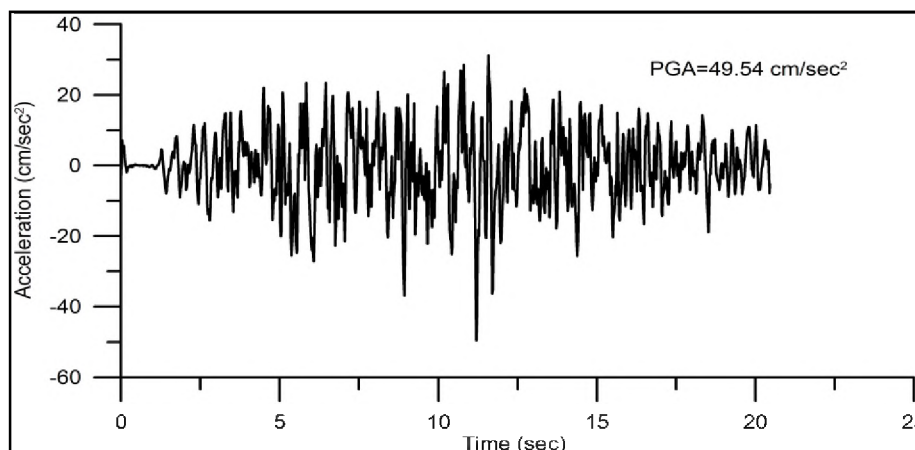


Fig. 6.3.26: The accelerogram of V.S. Hospital area for Far Field Earthquake Scenario computed using SHAKE program

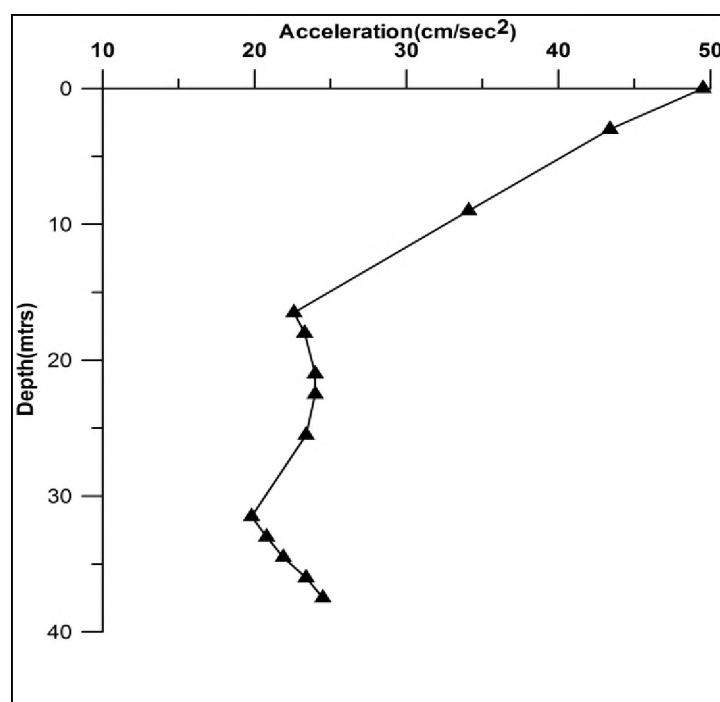


Fig. 6.3.27: PGA amplification in the soil column for different boreholes for an earthquake of Mw 7.6 along Eastern Part of Kachhh Mainland Fault (KMF)

## RESPONSE SPECTRA

The response spectra on the surface of the borehole (BH-19) for near-field as well as far-field earthquakes are shown in Fig. 6.3.28 (at 5% damping) and Fig. 6.3.29 (at 2% damping). The spectral acceleration values are calculated from 0.1 sec to 4.0 sec at an interval of 0.01 sec. For the near-field earthquake the maximum calculated spectral acceleration value is 215.3 cm/sec<sup>2</sup> for 5% damping (Fig. 6.3.28) and 315.2 cm/sec<sup>2</sup> for 2% damping (Fig. 6.3.29) at 0.2 sec (corresponding to 1 to 2 storey buildings).

For far field earthquake, spectral acceleration of 99 cm/sec<sup>2</sup> is observed at 0.2 sec (at 5% damping). High spectral acceleration in the range 83-87 cm/sec<sup>2</sup> is up to 0.7sec (corresponding to 6-7 storey buildings). For 2% damping the spectral acceleration is higher than that for 5% damping.

Comparison of near-field & far-field response spectra with BIS code

The response spectrum at the borehole (BH-19) site are compared with BIS recommended spectra (for 5% damping) for all three types of ground (Soft soil, Medium soil and Rock) for Zone III (Fig. 6.3.28).

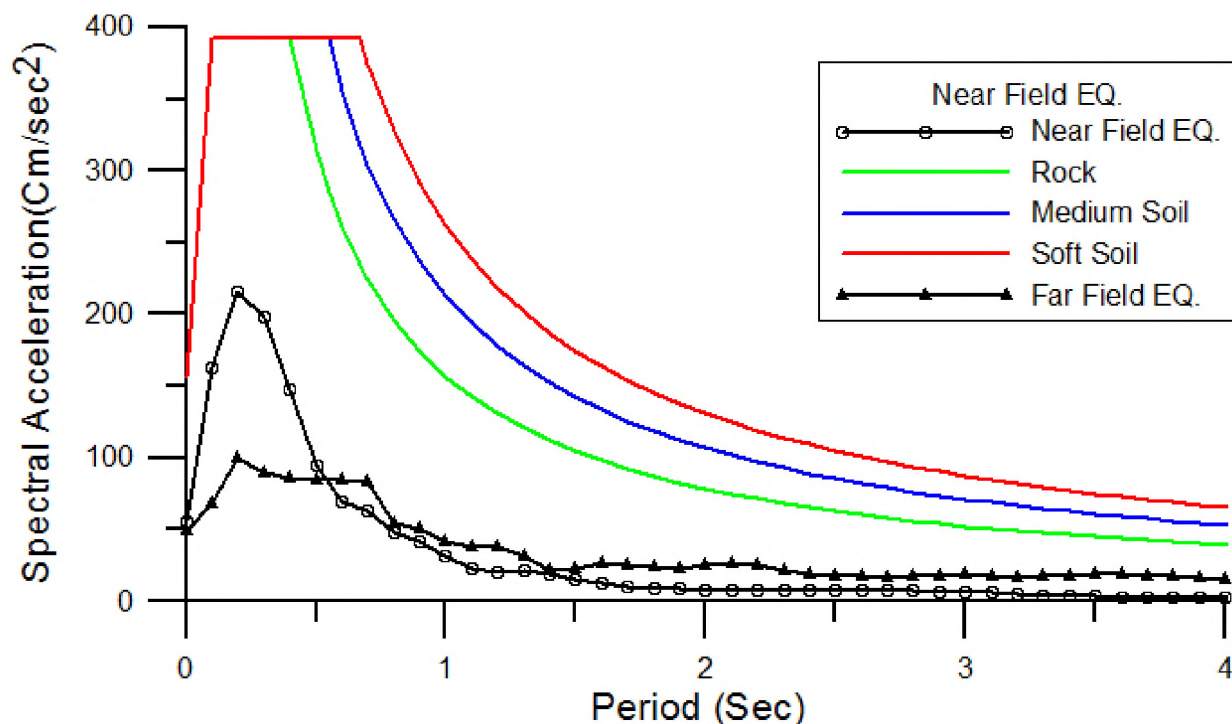


Fig 6.3.28: The spectral acceleration (Sa) curves at 5% damping for near field (with circle) and far field (with triangles) scenario earthquakes for borehole (BH-19) at around surface. The Sa curves are covered with BIS SA curves for Zone III

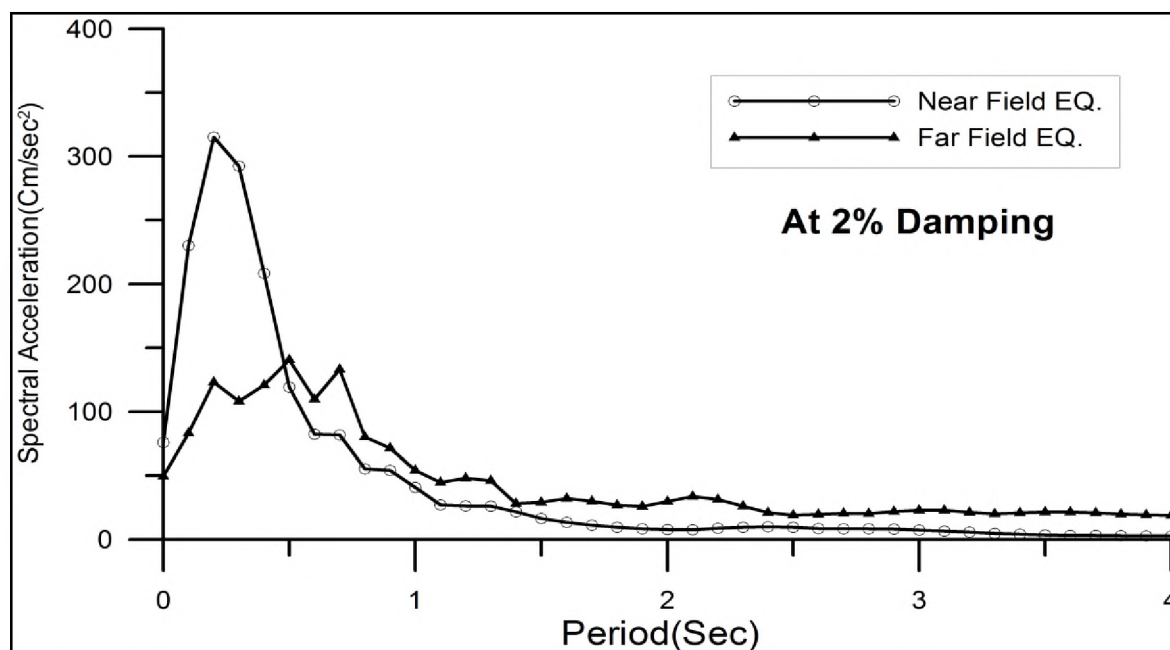


Fig 6.3.29: The spectral acceleration (Sa) curves at 2% damping for near field (with circle) and far field (with triangles) scenario earthquakes for borehole (BH-19) at ground surface

It has been observed that for near field earthquake, the maximum spectral acceleration is found at period of 0.2 sec ( $215.3 \text{ cm/sec}^2$ ) and for far field earthquake, it is found at 0.2 sec ( $99 \text{ cm/sec}^2$ ). At 2% damping, the maximum spectral acceleration of  $315.2 \text{ cm/sec}^2$  is computed for near field eq. and  $140.6 \text{ cm/sec}^2$  for far field eq. In both of the cases (near field and far field earthquakes), the spectral acceleration at 5% damping is found lesser than the values recommended by BIS (Fig. 6.3.28).

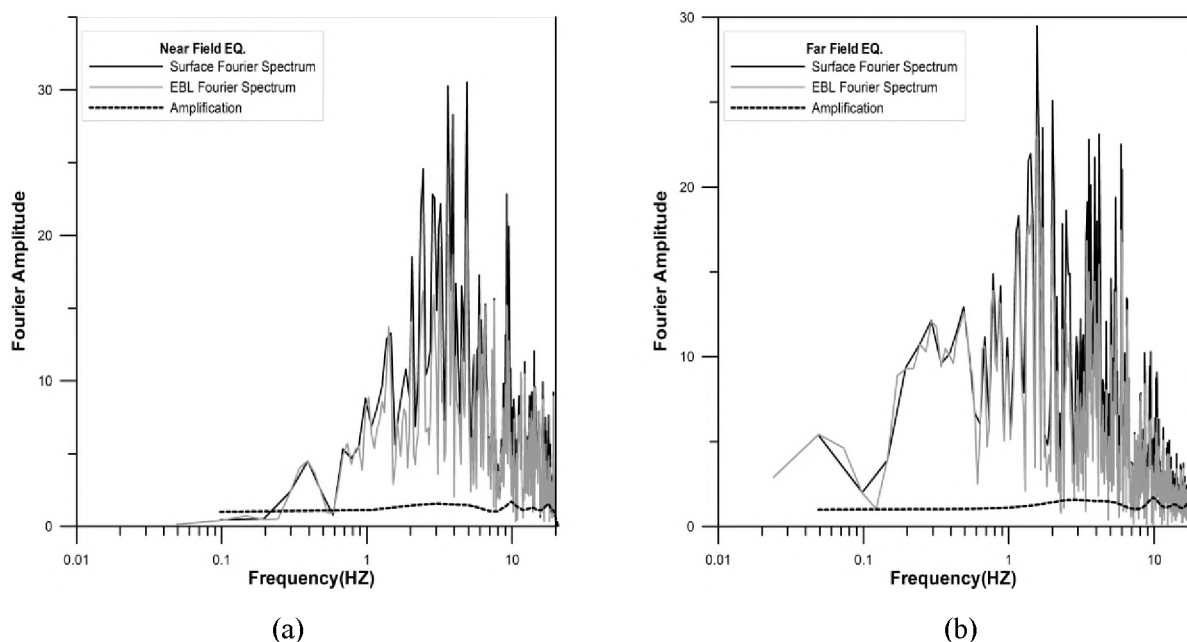


Fig 6.3.30: The Fourier spectra at EBL and surface with amplification curve for (a) near field earthquake and (b) far field earthquake

Fig 6.3.30 shows the Fourier spectra of input motion at EBL (light color lower values) and estimated strong motion at surface (dark color higher values) with amplification curve (lowermost continuous curve) for (a) near field earthquake and (b) far field earthquake. It indicates that far-field earthquake has large amplitudes at low frequencies. Amplification is about 2.

## References

- Atkinson, G. M. and Boore, D. M. (1995). Ground Motion Relations for Eastern North America, *Bull. Seismol. Soc. Am.*, 85, 17–30.
- Bodin, P., Malagnini, L. and Akinci, A. (2004). Ground-Motion Scaling in the Kachchh Basin, India, Deduced from Aftershocks of the 2001  $M_w$  7.6 Bhuj Earthquake, *Bull. Seismol. Soc. Am.*, 94, 1658-1669.
- Boore, D.M. and Joyner, 1997, Site amplification for Generic Rock Sites, *Bull. Seismol. Soc. Am.*, 87(2), 327-341.
- Mandal, P. and Johnston, A. (2006). Estimation of Source Parameters for the Aftershocks of the 2001  $M_w$  7.7 Bhuj Earthquake, India, *Pure Appl. Geophys.*, 163, 1537–1560.
- Motazedian D. and Atkinson G.M. (2005). Stochastic finite-fault modeling based on dynamic corner frequency, *Bull. Seismol. Soc. Am.*, 95, 995-1010.
- Raghukanth, S. T. G., Sreelatha, S. and Dash, Sujit Kumar (2008). Ground motion estimation at Guwahati city for an  $M_w$  8.1 earthquake in the Shillong plateau, *Tectonophysics*, 448, 98-114.
- Sumer Chopra, Dinesh Kumar and B.K.Rastogi (2010), Attenuation of high frequency P and S waves in the Gujarat Region, India, *PAGEOPH*, DoI 10.1007/s00024-010-0143-8.
- Seed, H. B., and Idriss, I. M., (1970). Soil Moduli and Damping Factors for Dynamic Response Analyses, Earthquake Engineering Research Center, University of California, Berkeley, California, Rep. No. EERC-70/10.
- Schnabel, P. B., (1973). Effects of Local Geology and Distance from Source on Earthquake Ground Motion, Ph.D. Thesis, University of California, Berkeley, California.
- Sun, J.I., Golesorkhi, R. and Seed, H.B. (1988). Dynamic Moduli and damping ratios of Cohesive soils. Report No. EERC 88-15, University of California, Berkeley.



## CHAPTER 7

**EARTHQUAKE PREDICTION RESEARCH**

*(K. M. Rao, M.S.B.S. Prasad, Dilip Kumar Halder, Prasanna Simha, Sushant Kumar Sahoo and Shikha S. Mishra)*

**7.1 Operation of Multi-Parametric Geophysical Observatories**

An earthquake research center at Bhachau and three Multiparametric Geophysical Observatories are operational since March 2009 in Kachchh region at Badargadh, Vamka and Desalpar for Earthquake Precursory Research. MPGO sites are east and northeast of the aftershock zone of 2001 Bhuj earthquake (Mw 7.6) where the activity has migrated from 2006 onwards. Magnitude 5 earthquakes are still occurring in Kachchh occasionally and 70 shocks of magnitude  $\geq 1$  are recorded on an average per month. Very Broadband Seismometer, Strong Motion Accelerograph, GPS and Radon recorders are installed at all the three sites. The radon sensors were only functional during Jan-June, 2012. As these are giving irregular/inconsistent results, we had shown these sensors to experts of Sarad Systems, Germany during Garhwal conference. As per their advice, these sensors were sent to Germany for repairs/re-calibration. Out of two Fluxgate magnetometers, one Fluxgate magnetometer has worked well at Desalpar and other one is showing fixed values initially and later higher values of Z-component which is now installed at Vamka. The Super Conducting Gravimeter which has been installed at Badargadh has worked smoothly. Only two water level recorders at Desalpar and Badargadh are installed at confined aquifer zone and all others are installed at shallow depth (below 5 m) & are not showing any variation in water level. Three Borehole Strain Meters have shortly been installed in Narmada region. Three Overhauser Magnetometers, three Declination/Inclination Magnetometers, three ULF Magnetometers are installed at MPGO's in December-2012. All these Magnetometers are working well. ISR in collaboration with ISRO has established the CALVAL site at Desalpar. This site is useful for Calibration of optical and microwave sensors and validation of Geo-physical data products which form an integral and vital component of any satellite programme. We observed some anomalies in the magnetic, radon and gravity measurements which can be correlated with micro earthquakes in the region.

**7.2 Installation of various new Magnetometers (3 ULF Magnetometers (LEMI-30), 3 Overhauser Magnetometers, 3 D/I Magnetometers) at MPGOs**

Recently we have installed three types of magnetometers namely Ultra Low Frequency Magnetometers (Lemi-30), Overhauser Magnetometers and Declination/Inclination Magnetometers to study electromagnetic precursors at Vamka, Desalpar and Badargadh. The Lemi-30 induction-coil ULF magnetometer is used for studying variations of magnetic field in the frequency range of 0-30 Hz, Overhauser Magnetometers for the total magnetic field and Declination/Inclination Magnetometer (dIdD) to detect the declination/inclination of magnetic field (orientation of field line). The description of these installations is given in this report. We have installed these Magnetometers in two months time during Nov-Dec, 2012 by making four field trips of 1-2 weeks duration of each trip at three sites simultaneously. Initially we have done noise survey throughout the site using ULF Magnetometer to select the proper place to get good signal with less noise. The criteria adopted for best site selection is to look for clear modes of Schumann resonance in the signal. Later, we made special pits for the sensor installation and made non magnetic huts for housing the Magnetometers. In the third trip we installed all the sensors in the pits and complete all constructions. Finally, we start getting the magnetic field time series in the middle of December 2012 onwards.



Fig.7.1 Specialised pits and non-magnetic huts for Magnetometers

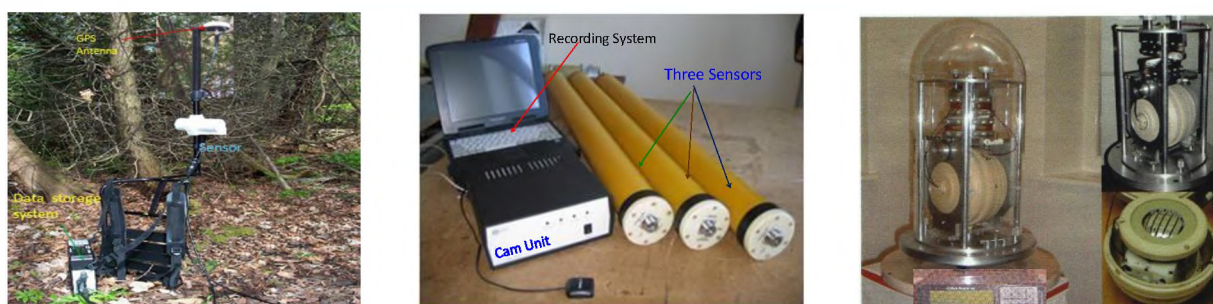


Fig.7.2 Overhauser, ULF and D/I Magnetometers

### 7.3 Development of a CAL-VAL site at Desalpar for Land and Atmosphere

Calibration of optical and microwave sensors and validation of Geo-physical data products form an integral and vital component of any satellite programme. A well calibrated sensor is essential to derive quantitative information from radiation reflected/scattered by various earth surface features as a function of space and time. Pre-launch calibration of optical sensors can be performed in laboratory controlled conditions to a high degree of accuracy ( $\sim 5\%$ ) using standardized radiation sources and an integrating sphere at different wavelengths. The output of detectors in a sensor to a known, standard illumination source is quantized to derive sensor calibration coefficients for each wavelength interval with a well characterized spectral response function. During and after satellite launch, the sensor on-board a satellite is subjected to different kinds of stresses which can lead to a possible degradation of sensor performance over a time period. Hence, it is essential to monitor the changes in sensor calibration periodically and



quantify its magnitude. This is achieved by vicarious calibration of sensors, where a well defined spatially and temporally homogeneous surface is chosen for in-situ radiance/ reflectance measurements. These are subsequently passed through an atmospheric correction code to predict top of atmosphere (TOA) at-satellite radiance/reflectance, which is then compared with satellite sensor radiance/reflectance to derive calibration coefficients. A temporal record of these coefficients indicates the variation of sensor response and its possible degradation over time.

Absolute calibration of Synthetic aperture Radar system is achieved through deployment of corner reflectors and active radar calibrator on uniform site and determining calibration constant through a well defined methodology. Validation of Geo-physical products e.g., surface reflectance, soil moisture, etc. is carried out by comparison with in-situ measurements carried out on the site. Also, it is planned to carry out monthly InSAR measurements on the site to give precise information about the ground deformation of the area, if any, specially the vertical movements. These measurements will be compared with periodical InSAR data of other parts of Kutch, Saurashtra and Narmada to study deformation across active faults of Gujarat. ISR in collaboration with ISRO is developing a CAL-VAL site at Desalpar in Rann of Kutch for Optical, Microwave RS sensors and InSAR measurements. We have completed all the civil works at the site and are taking campaign mode measurements at various parts of Gujarat. This site will be very useful for land and atmospheric Remote sensing applications. The site will be very useful for RESOURCESAT, OCEANSAT, MEGHATROPIKAUES, RISAT-1 SAR, CARTOSAT and future projects of ISRO/DOS.

#### **7.4 Monitoring of ULF (0-0.5 Hz) Geomagnetic field Variations in Kachchh region**

ULF Electro-Magnetic-Emissions (EME) is recognized as a promising precursory signature for earthquake prediction research. For earthquake precursory study, ISR continuously monitoring ULF geomagnetic field by Digital Fluxgate Magnetometer (DFM) which working in the range 0-0.5 Hz at Multi Parametric Geophysical Observatory (MPGO) site, Desalpar (Lat: 23.74568°N, Long: 70.68378°E). This site falls at the highly seismically active zone Kachchh and is near to Gedi fault. Electromagnetic emission phenomenon takes place in the ULF-ELF-VLF (0-30 kHz) frequency ranges prior to earthquakes. Basically there are two principal methods of observation of earthquake precursory signals. DFM is a tri-axial magnetometer manufactured by Magson GMBH, Germany. It measures the geomagnetic field variations along three components i.e., North-South (H), East-West (D) and Vertical (Z) in nano Tesla (nT). The detected signals are recorded through data acquisition system in the digital format. There are various processes to analyse the signal for detecting precursors like calculating polarising ratio, singular value decomposition method, fractal analysis, principal component analysis etc. Here, we have used temporal variations of H, D, Z components and polarization analysis to look for precursory signal. Monthly raw data plots of H, D, Z components for the whole year are shown in Figure-7.3. We observed high fluctuation in H-Comp 1-3 days before the occurrence of earthquakes; diurnal maximum values gradually decreases in the D-Comp from some days before the event; diurnal minimum value gradually increases in Z-Comp from some days before event. The increase of Z-comp is observed before earthquakes worldwide. Visual statistical analysis is given in the Table-7.1 for the entire year of 2012.

To know the impact of the events in our observations at Desalpar, we have calculated seismic indices using the formula  $10^{0.75M/10 \cdot D}$ , where M is magnitude and D is hypo central distance of the event. It is shown graphically in the fig-2b and found large seismic indices ( $>2$ ) for three  $\geq 4M_w$  events and for one event of 3.8 M. Natural ULF micro pulsations favourably arise during Kp and Dst index activity [Campbell, 2003]. To distinguish between the global and local effects towards the ULF emissions we

have taken the global planetary data (Kp & Dst indices) from world data centre (WDC) webpage and plotted in Fig.7.4(e),(f).

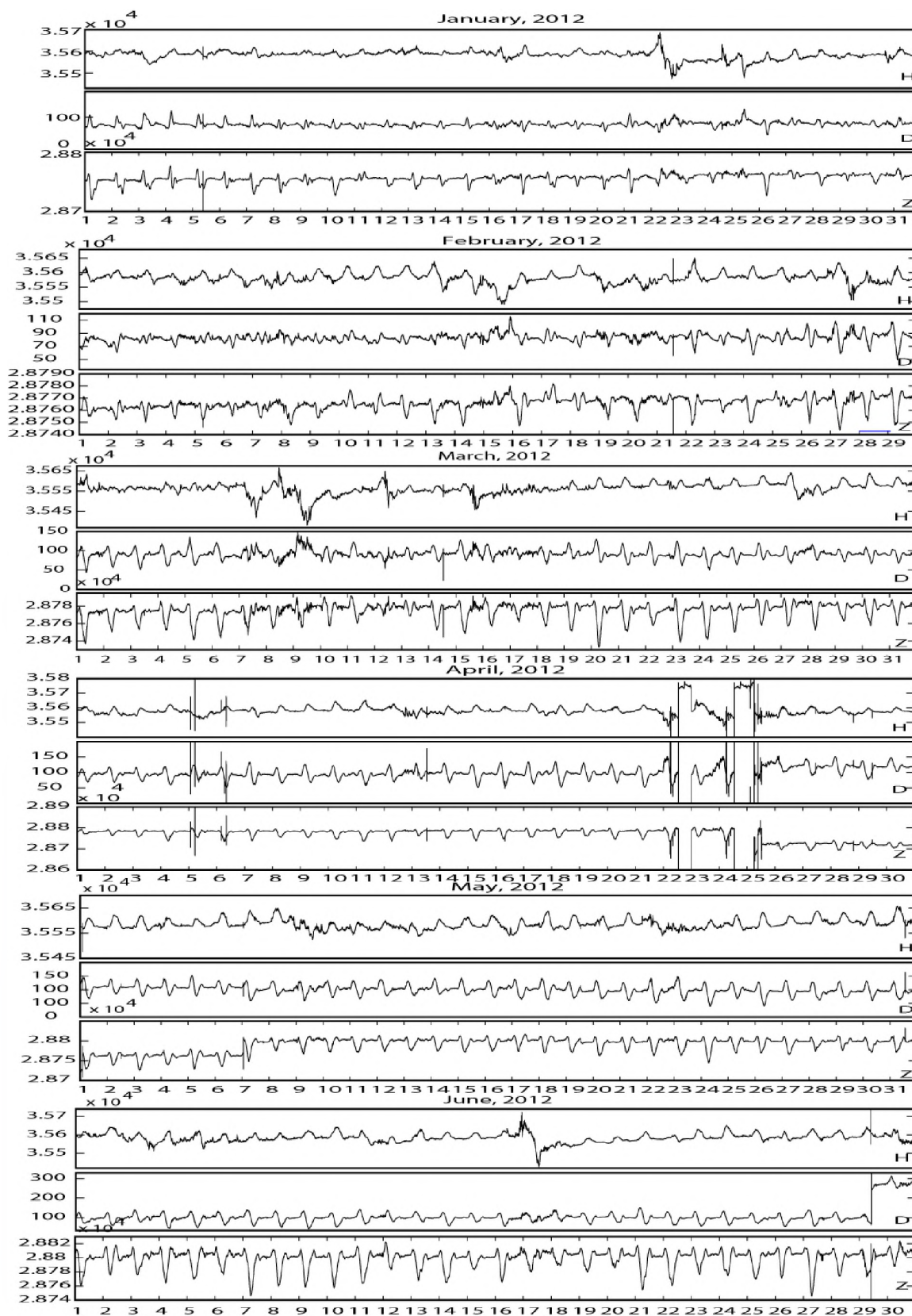


Fig. 7.3. Monthly intensity variations of the observed signals for the three components (H, D and Z), during the periods of January-June, 2012.



**Table-7.1: Statistical analysis of some typical observations for different components**

Observation of huge fluctuation in the H-Comp before some days			Gradual decrement of the peak value of the D-Comp			Gradual increment of the negative peak value of the Z-Comp		
Fluctuation before the events		No. of events fluctuation not observed	Decrement before the event		No. of event decrement not observed	Increment before the event		No. of events increment not observed
Days	No. of Event		Days	No. of Event		Days	No. of Event	
1 day	12	8	1 day	21	18	1 day	24	11
2 days	10		2 days	10		2 days	12	
3 days	10		3 days	4		3 days	6	
						4 days	2	

Percentage of anomalies:                      52% in H-Comp, 20% in D-Comp and 60% in Z-Comp

**Polarization ratio analysis:** We analyzed the signal by polarization ratio (Z/G) method only for the night time (18:00-21:00 hrs UT) geomagnetic field data to avoid diurnal variations and other day time cultural noise in five frequency bands  $f_1$  (0.001-0.005Hz),  $f_2$  (0.005-0.01Hz),  $f_3$  (0.01-0.05Hz),  $f_4$  (0.05-0.1Hz) and  $f_5$  (0.1-0.5Hz). We observed some typical variation in the polarization ratio before a local moderate shallow seismic event of magnitude 5.0 Mw at 20:14:00.4 UT on June 19, 2012, which was 46.3 Km away from the Desalpar observatory (Lat: 23.74568°N, Long: 70.68378°E) at a focal depth of about 10.5 Km, has been depicted in the Fig. 2. Few days prior to the event, we observed a raise in polarization ratio in all five frequency bands, which indicates that, the rise in conductivity before the event according to the theory of Dilatancy-Diffusion Model. In the observed study we have detected a remarkable change ( $>1$ ) in polarization ratio (Z/G) in  $f_4$  and  $f_5$  frequency bands. This kind of signal variations indicates some prominent EM emissions of lithospheric origin may be related to this particular earthquake.

In the fig 7.5 (c) & (d) we observed gradual small rise in all frequency bands before the 4.1Mw earthquake of 14<sup>th</sup> April, 2012 and 4.5 Mw earthquake of 8<sup>th</sup> December. And we observed a sudden large rise in  $f_4$  &  $f_5$  bands ( $Z/G > 1$ ) about 10 days before the 5.0 Mw seismic event of 19<sup>th</sup> June, 20.

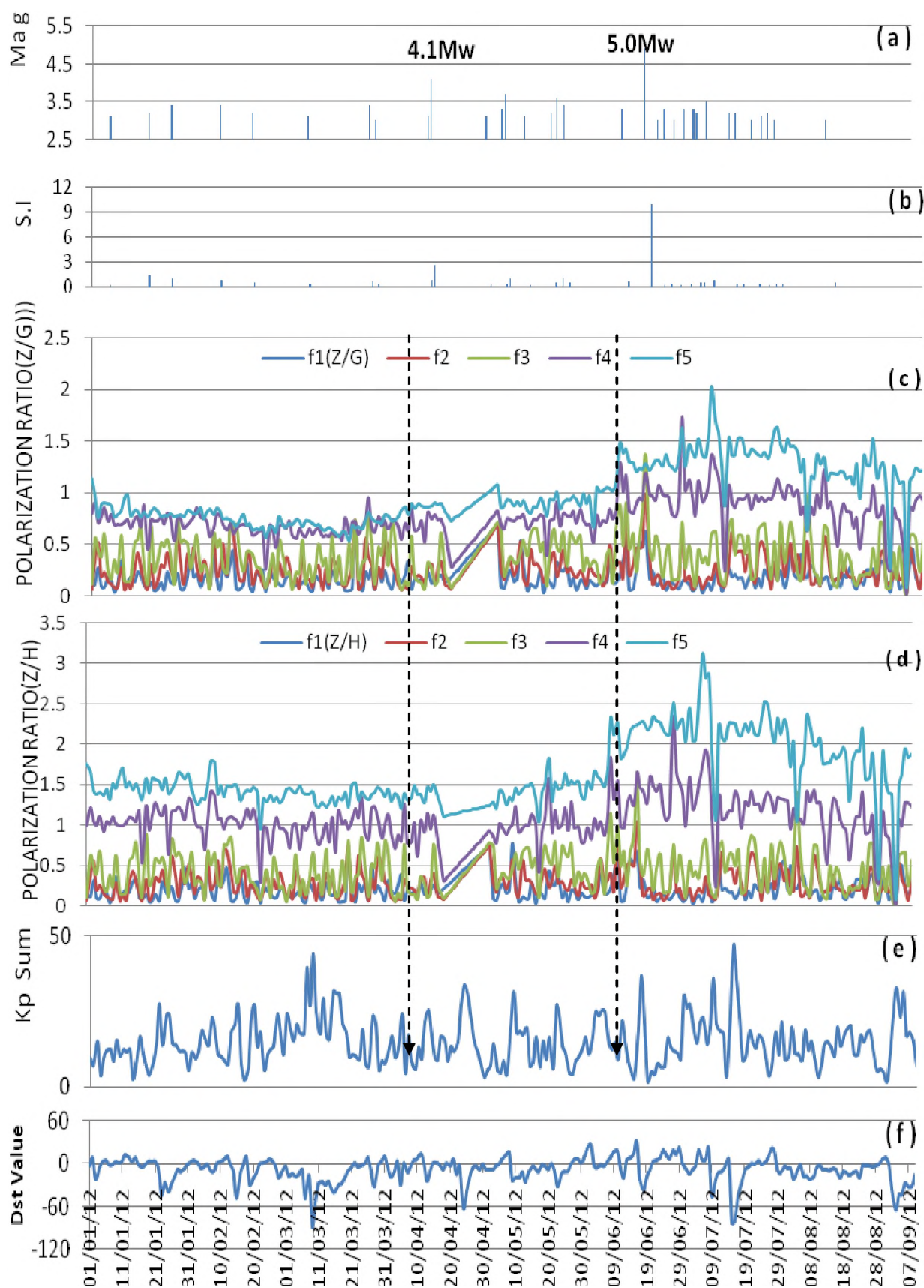
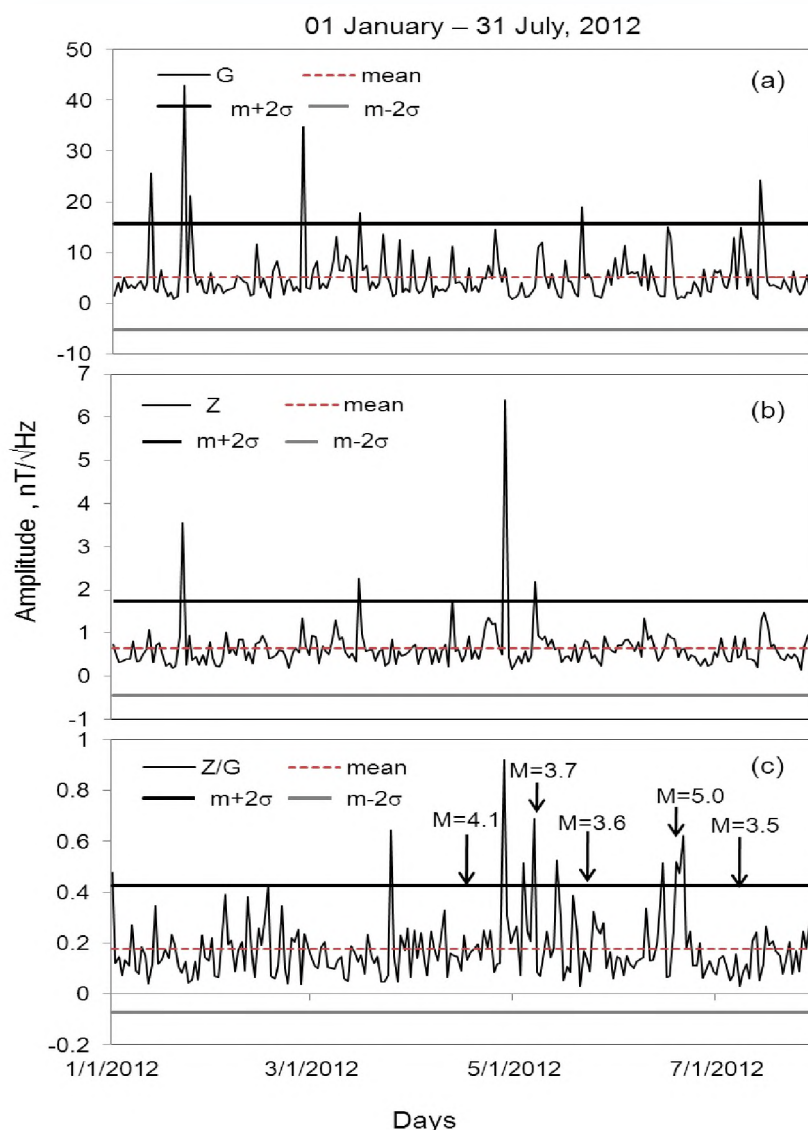


Fig 7.4: (a) Seismicity (>3 Mw ) in Kachchh region; (b): Seismic Indices; (c) & (d) : Desalpar DFM night time (18-21UT) data Polarization analysis in five frequency bands i.e.  $f_1$ ,  $f_5$  using Z/G & Z/H; (e) : Global Kp sum plot; (f) : Global Dst mean value plot

**Table 7.2. Seismic events of  $\geq 4M$  and  $\leq 100\text{Km}$  from Desalpar observatory.**

Date	Mag	Depth(km)	Location (Lat, Long)	Distance From the Stn (Km)
14 <sup>th</sup> April, 2012	4.1	19.1	23.394, 70.548	41
19 <sup>th</sup> June, 2012	5.0	7.4	23.629, 70.279	46
08 <sup>th</sup> Dec, 2012	4.5	16.3	23.126, 70.401	75



**Fig.7.5: (a) Amplitude variation of G-component, (b) Amplitude variation of Z-component along with  $m$  and  $m\pm 2\sigma$ , (c) variation of  $Z/G$  in first frequency band. The mean ( $m$ ) and standard deviation ( $m\pm 2\sigma$ ) are shown by dashed and straight lines**

### Results and Discussion

From the above figures we conclude that during our analysis we have got significant anomalous behaviour in Polarization ratio in all frequency bands, particularly in  $f_4$  and  $f_5$  bands ( $Z/G > 1$ ) before a moderate event of  $M=5.0$  (19<sup>th</sup> June, 2012) shows that some lithospheric originated ULF emissions may present which can be seen before moderate earthquakes as observed by other workers. But at the same time there was a storm shown by rise in both  $K_p$  and  $Dst$  values. At other times also large  $K_p$  sum values are present but no such Polarization ratio ( $Z/G > 1$ ) rise is observed. This polarization ratio rise ( $Z/G > 1$ ) before such a moderate shallow Kachchh earthquake ( $M=5.0$ ) for which the Seismic index also high may be considered as an earthquake precursor.

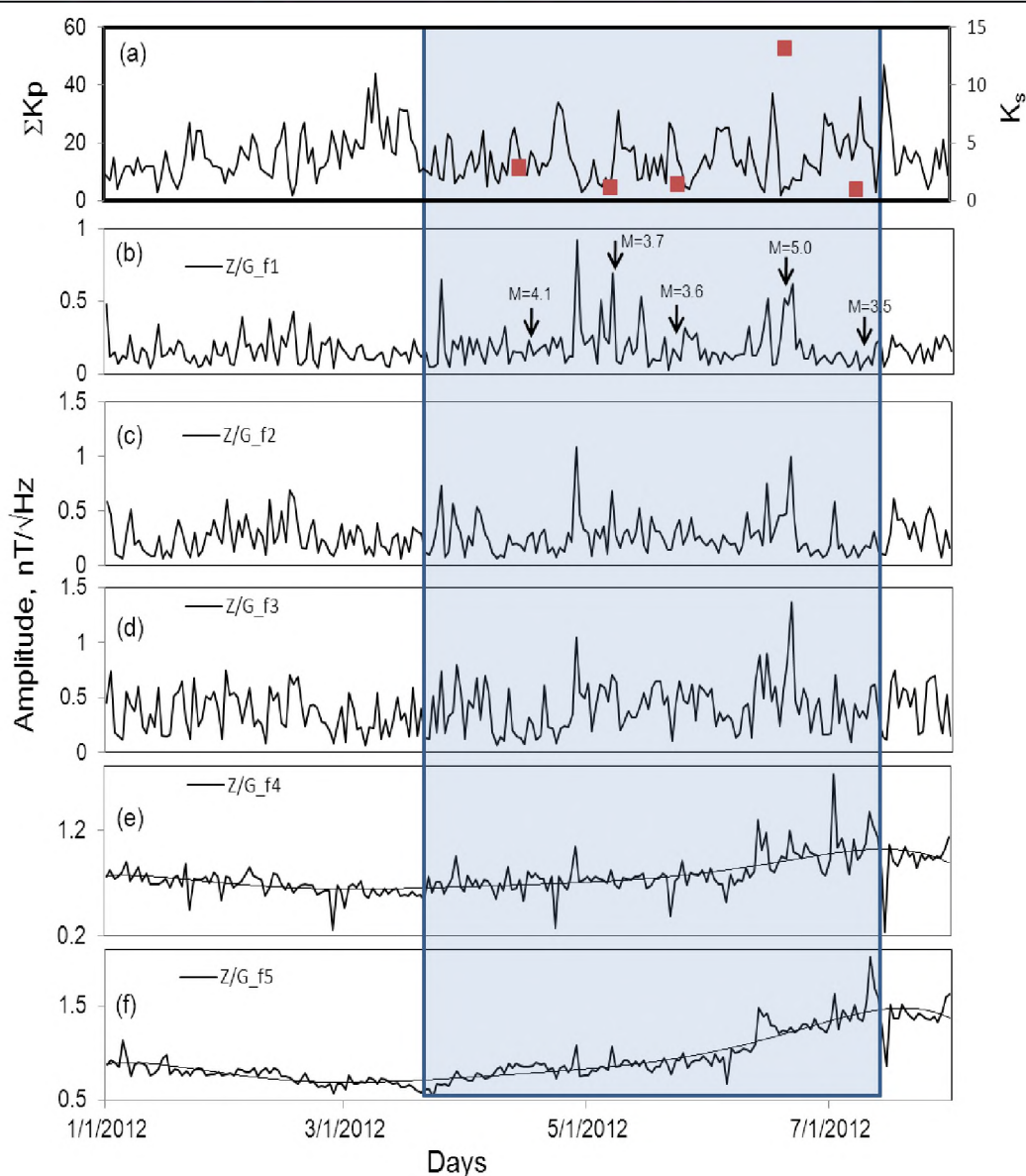


Fig 7.6: (a) Variation of  $\Sigma Kp$  and seismicity index  $K_s$ , (b) – (f) show the variation of Polarization ratio of all five frequency bands from f1 to f5 respectively

We study the EM emissions upto 0.5 Hz frequency by forming different-2 frequency bands in the light of local seismicity of the area, geomagnetic storms and lightning events. It can be seen from the figure-3 that amplitude variation of G crosses  $m+2\sigma$  line between 12 January, 2012 and 15 March, 2012. The values of amplitude of Z-component cross  $m+\sigma$  line only at four occasions, i.e. 22 January, 15 March, 28 April and 07 May, 2012. The polarization ratio plotted in Fig.7.5(c) is found to be enhanced over  $m+\sigma$  line between 25 March, 2012 and 21 June, 2012. During this period of enhanced Z/G ratio the seismic activity is also large which can be observed by indicated events of earthquakes marked with inverted arrows in the figure. To examine the DFM data in the light of geomagnetic storms and earthquakes, we plot variation of  $\Sigma Kp$  and seismicity index  $K_s$  in Fig.7.6 (a). Fig.7.6 (b) – Fig.7.6 (f) shows the variation of polarization ratio of all five frequency bands from f1 to f5 respectively. It can be seen clearly from the figure that when the values of  $\Sigma Kp$  are large the values of polarization ratio are found to be low in all frequency bands while clear enhancements can be seen in the polarization ratio of all frequency bands between 25 March and 11 July, 2012 when seismic activity is high. However, major enhancements appear in the first frequency band f1 but other frequency bands also show enhanced ratios during the same period with some reduced intensities. The last two frequency bands f4 and f5 show an increasing



trend till 11 July, 2012 with some peaks around 20 June, 2012. On the similar line we applied new improved polarization method on our data and presented the results in Fig.7.7.

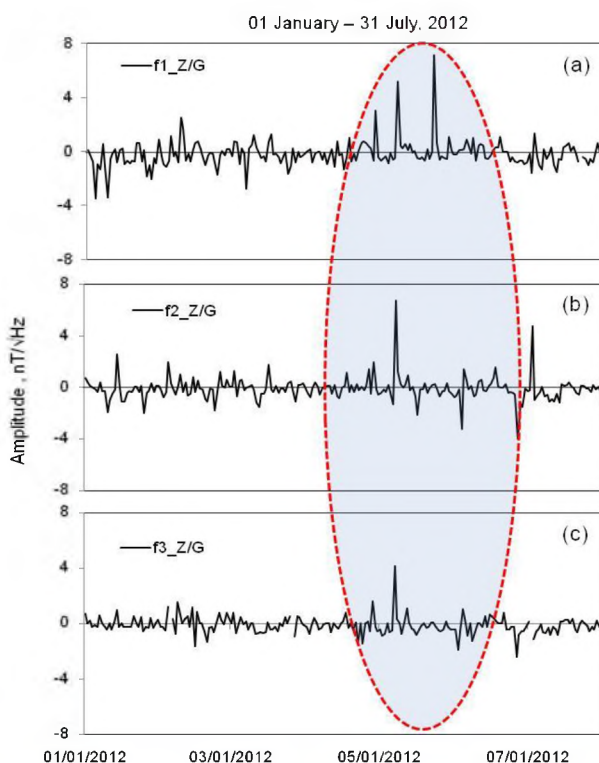


Fig 7.7: (a) to (c) are new improved Z/G ratio for three frequency bands of f1, f2 and f3

## 7.5 Radon Observations

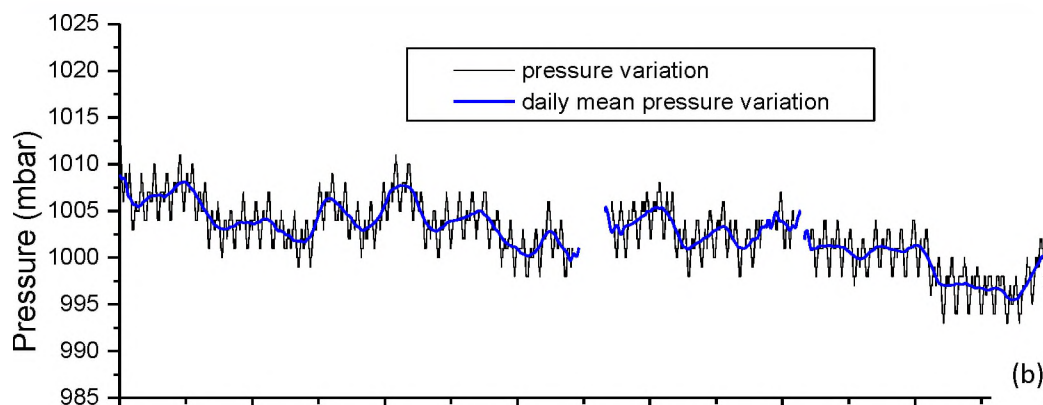
Radon is established as a useful geochemical precursor. Anomalous behavior of radon in soil and groundwater can be used as a reliable precursor for an impending earthquake. The first evidence of a correlation between radon and earthquake occurrence came from observation of radon concentration in well water prior to the Tashkent earthquake of 1966 (Ulomov and Mavashev 1967). This evidence stimulated research work in this area soon afterwards in many countries. Radon observations, both in soil-gas and in groundwater, revealed many precursory changes in its concentration before an earthquake. Radon is product of uranium decay series with a half life of 3.8 days. Radon displays poor intrinsic mobility due to its short half-life, and therefore in a diffusive system it obviously comes from a short distance below the measuring instrument. Deep origin signals can be observed only if convection/advection occurs, radon being carried upward to the subsurface by a rising gas/water column (e.g., Etiope and Lombardi 1995; Yang et al. 2003).

We are observing Radon emissions in the soil gas in Kachchh by RTM-1688 probe manufactured by SARAD instruments, Germany, which measures Radon concentration, Humidity, Temperature and Pressure of the soil-gas. In the Fig 7.8 we have presented radon raw data plot along with the pressure, Temperature and Humidity. The temperature increased from 30 - 37 °C and pressure decreased from 1008 - 995 mbar while Humidity gradually decreased from 97 - 91 (%) during this summer observation. Some minor periodicity is observed in the pressure curve. All parameters follow the same trend of our previous study of 2011 records. Mean value is 1.802 kBq/ m<sup>3</sup> with a standard deviation of .228 kBq/ m<sup>3</sup> the percentage variation is 12.65 % has been shown in Table 7.3.

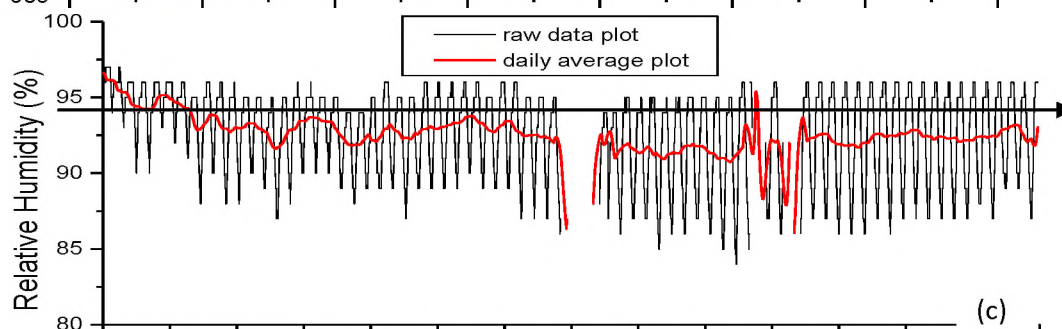
**Table 7.3: Average values of Radon and correlation coefficients with other parameters at Desalpar during the period of March- June, 2012**

Parameters	Average	Std.Dev	%Var.Coff(Average/Std.Dev)	Correlation coefficient
Radon (KBq/M <sup>3</sup> )	1.802	227.917	12.65	
Temp. (°C)	34.388	1.752	5.10	0.437
Humidity (%)	92.681	2.890	3.12	-0.318
Press. (mbar)	1002.553	3.350	0.33	-0.161

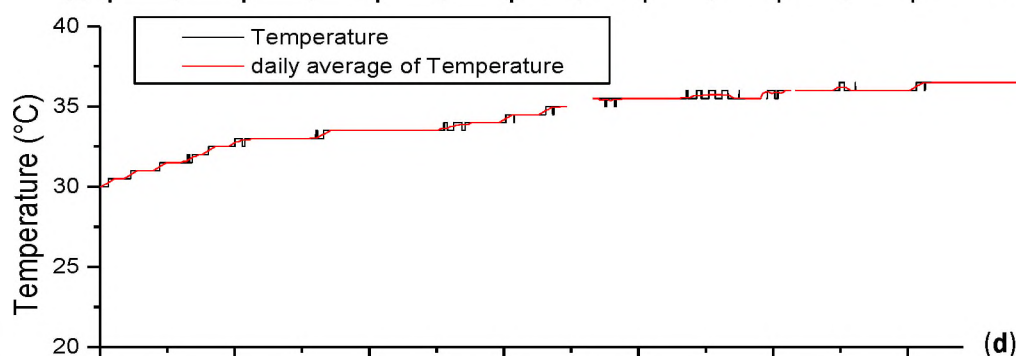
(a)



(b)



(c)



(d)

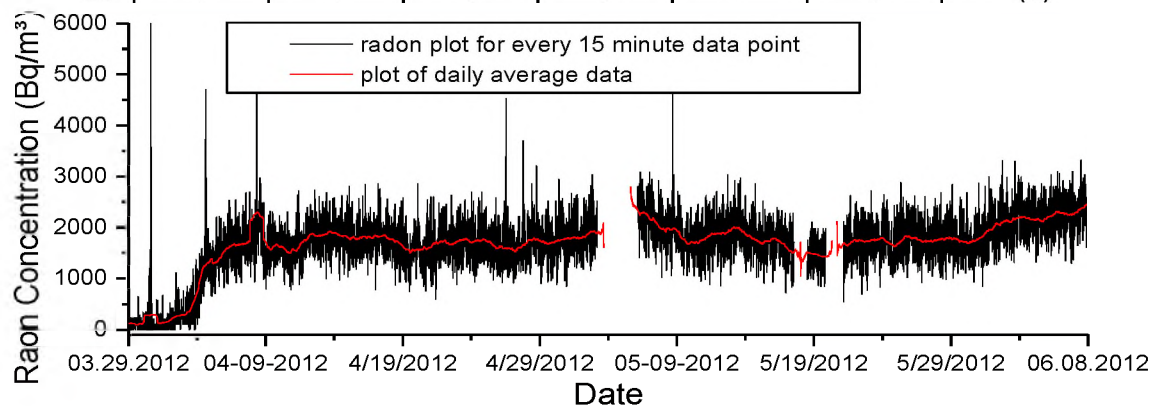


**Fig. 7.8** Variations of Radon concentration (15 minute sampling rate) along with Temperature, Humidity and Pressure at the Desalpar site for the period of March-June, 2012.

During our period of study we observe some seismic events of magnitude 3.0-4.0 Mw which are within 100 Km range. Here we detect huge fluctuation in the radon data, are indicated by circle. About seven days before the event of Magnitude 4.1 Mw, dated on 14th April, 2012 the Radon concentration reached up to the  $2\sigma$  level and again it decreased lower than the  $-\sigma$  level three days. For another minor event of magnitude 3.7Mw on 7th May, 2012 we got only positive anomaly which starts almost three days before earthquake. A negative anomaly has been detected four days before the event of Magnitude 3.6Mw on 23rd May, 2012 its value was lower than the  $-\sigma$  level and then gradually became normal. The further trend of enhancement (crossing  $2\sigma$ ) may be due to the event of 5Mw on 19th June, 2012 which was around 18 Km away from the site and depth was 9 Km (7.9). Thus continuous Radon study may be used a fruitful predictive tool for the Earthquakes precursor.

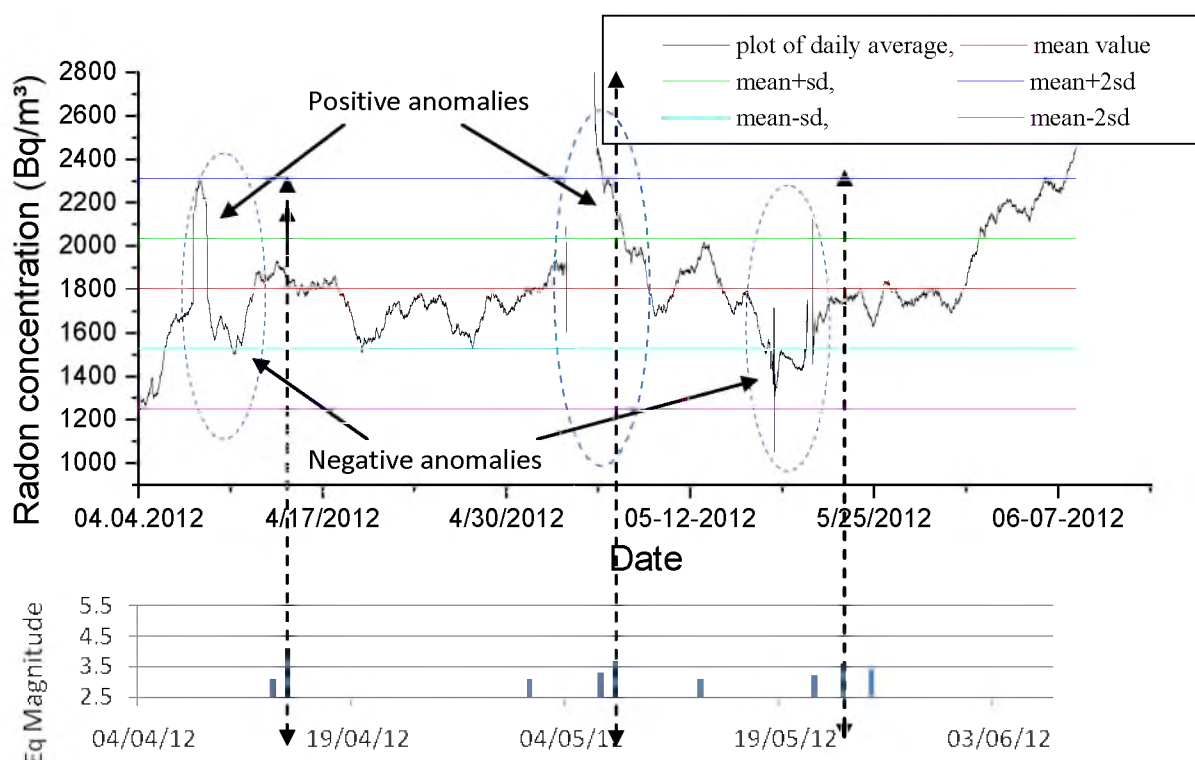


Fig. 7.9 In the first panel black colour curve depicts variation of daily average radon concentration along with mean (red), standard deviation  $\sigma$  (green and light blue) and 2-standard deviation  $2\sigma$  (blue and violet). And the second panel indicates local seismic events of <100 Km range for the same period.

## 7.6 Study of Schumann resonance by ULF Magnetometers (Lemi-30)

A number of electromagnetic emission phenomenon, originated from lightning discharges within the Earth-ionosphere waveguide, are occurring predominantly in the ULF, ELF and VLF (Ultra Low Frequency, Extremely Low Frequency and Very Low Frequency) frequency ranges. There occurs a resonance phenomenon within the spherical Earth-ionosphere cavity in the ULF bands. Winfried Otto Schumann first theoretically predicted this electromagnetic resonance phenomenon in 1952 and calculated their Eigen frequencies as 10.6, 18.4, etc...Hz. Thus, it is called as Schumann Resonance (SR). We have installed three induction coil magnetometers (Lemi-30) for the ULF signals (0-30 Hz) to study the electromagnetic precursory of the earthquake at the three MPGO sites namely Desalpar, Badargadh and Vamka. For the last two months, we recorded some data and analysed the signal intensity, spectral characteristics, and frequency as well as amplitude variations of different SR modes for the Desalpar (Lat: 23.74568° 70.68378°) station and the results are shown below.



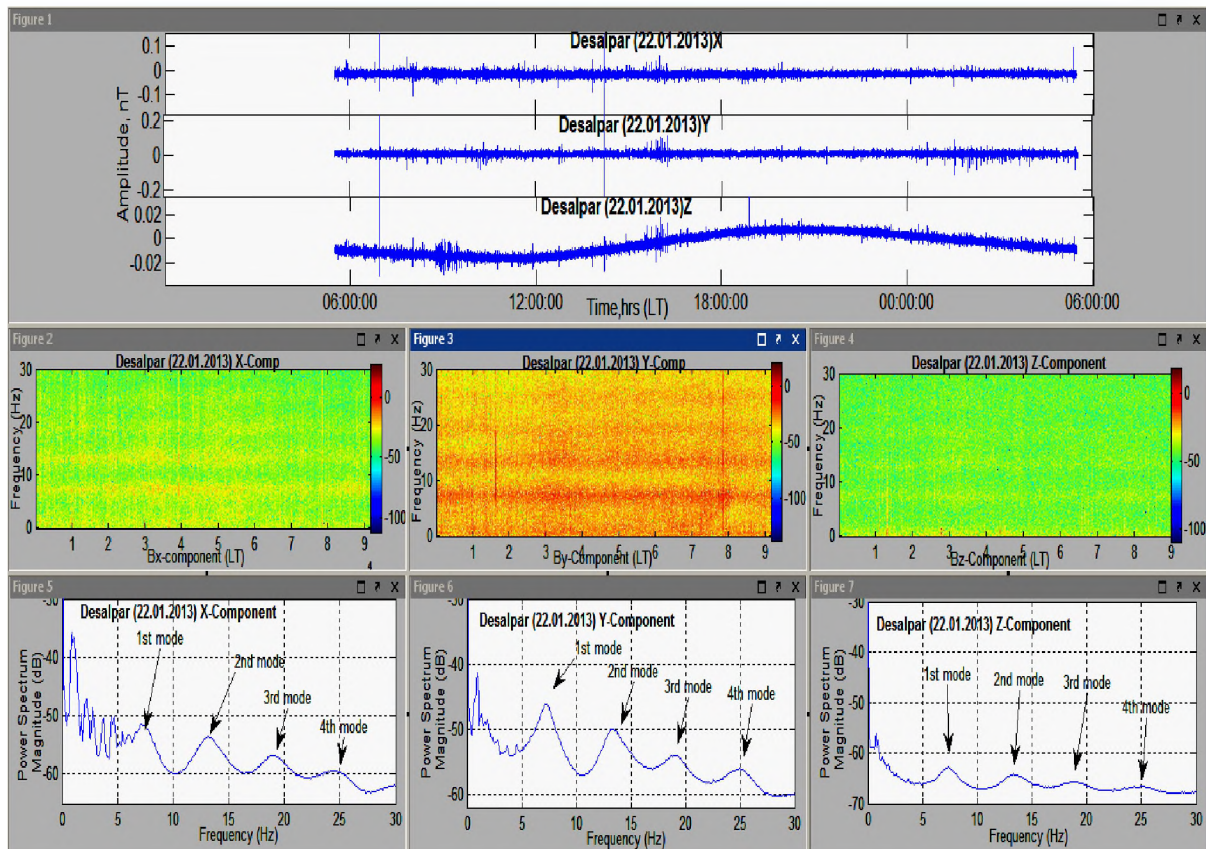
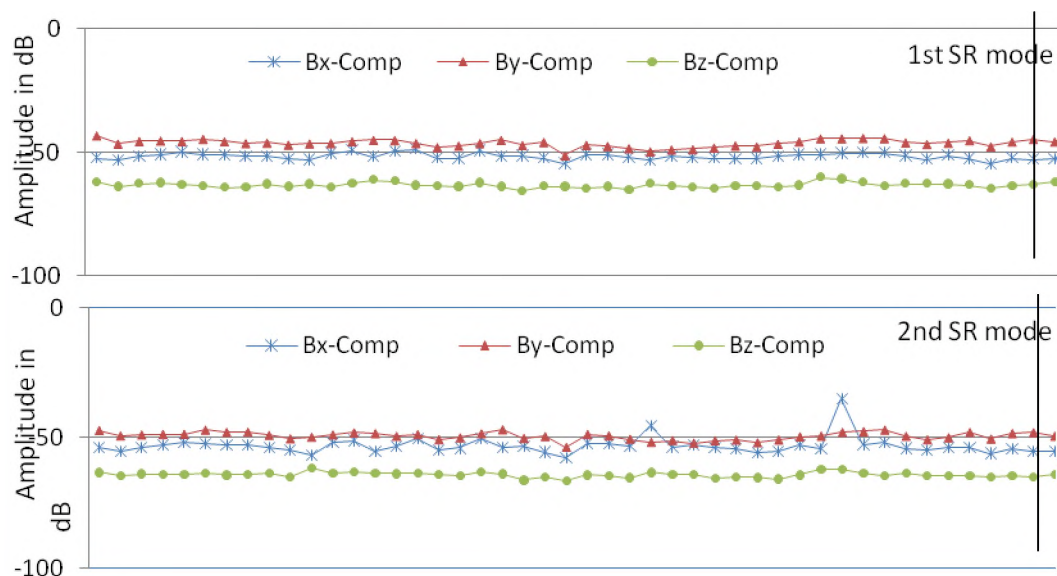


Fig. 7.10: (1) The diurnal variations of the signal amplitude in terms of nano Tesla (nT) in three components of the magnetic field of SR signal N-S ( $B_x$ ), E-W ( $B_y$ ), and vertical ( $B_z$ ). (2-4) indicates the power spectrum of three components, (5-7) showing the prominent Schumann resonance modes are indicated by the arrows as the 1<sup>st</sup>, 2<sup>nd</sup>, 3<sup>rd</sup> and 4<sup>th</sup> mode.

Figure 7.10 (2)-7.10 (4) shows the observed power spectrum for the three components, has been detected on 22.01.2013. Intensity of the E-W component is more than the other two components. It indicates that longitudinal distributions of the sources are more intense than the North-south direction. For the period of December-January along this longitude





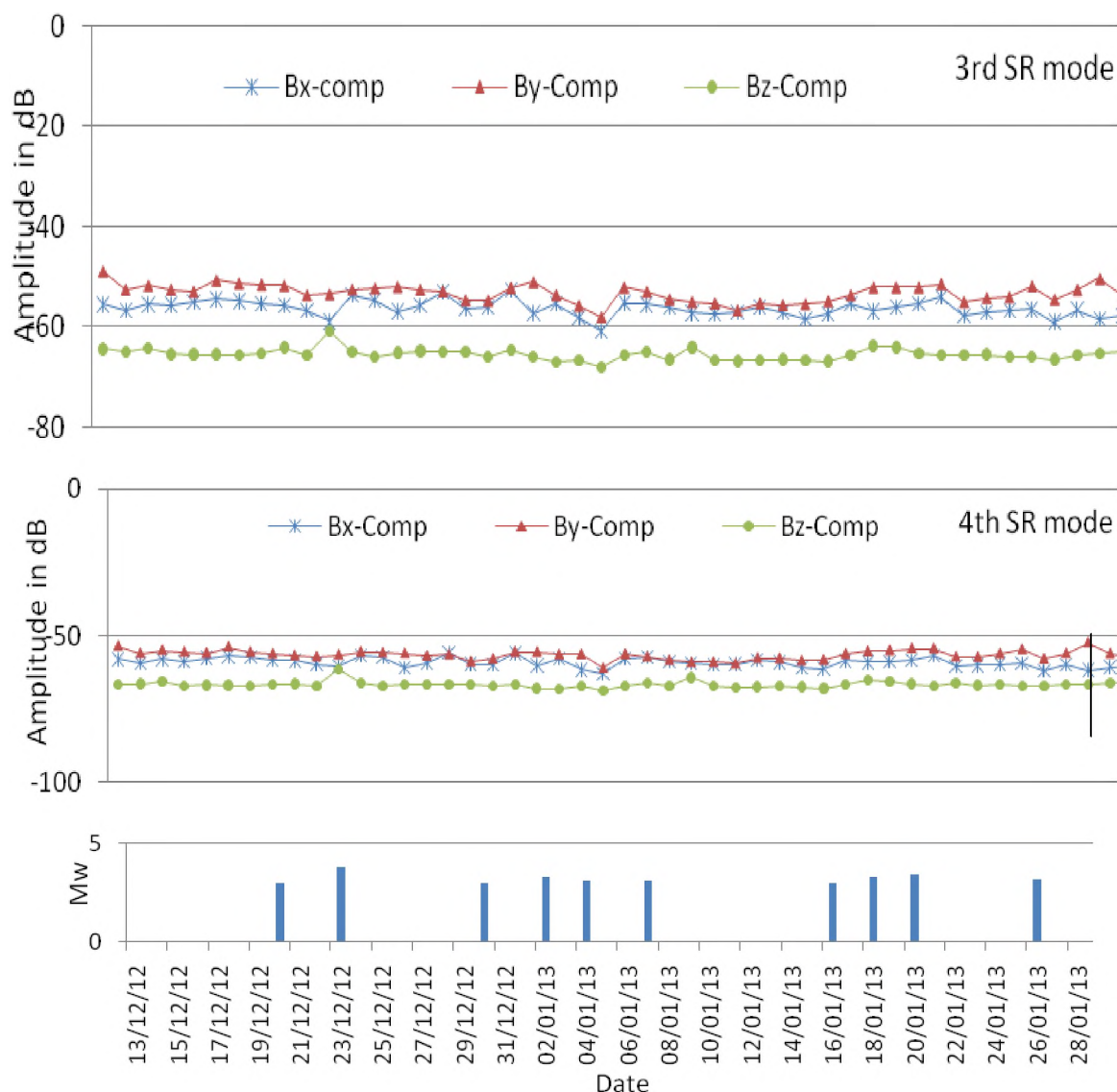


Fig. 7.11: The amplitude variations of first four Schumann resonance modes have been presented in upper four panels of this figure. Three different field components Bx, By and Bz are indicated by three different colours as blue, red and green. The bottom panel indicates the earthquake events for different dates in Kachchh region during this period of observation.

(longitude of observatory) occurrences of thunderstorms are very low because in the Northern hemisphere, it is winter and though it is summer for the Southern hemisphere but there are no continental parts to generate thunderclouds. This is the reason for low signal intensity. As the three thunderstorm centres (Asia-Australia, African and American thunderstorm centre) are distributed along the equatorial zone i.e., in the tropical region, the signal received from the E-W direction is larger, that is why, intensity of the  $B_Y$  component is much larger than the other two components. The spectral characteristics of Schumann Resonances for the three components have been presented in Figs. 7.10 (5)-7.10 (7), the prominent Schumann resonance modes are indicated by the arrows as the 1<sup>st</sup>, 2<sup>nd</sup>, 3<sup>rd</sup> and 4<sup>th</sup> mode. The monthly Amplitude and Frequency variations of the different modes have been present in Fig. 7.11.

In our observed signal there are no prominent amplitude variations. Main source of energy of this signal within the cavity is lightning discharges during the thunderstorm. In this observation period our place of observation belongs to winter season and there were no such winter showers. The Asia-Australia thunderstorm centre has been shifted towards Australia so, the distance from the three thunderstorm centre is very large. Thus the effect of three thunderstorm centres is minimum in our observed data. Thus the signal amplitude is low.

### Conclusions of initial results of analysis of ULF data:

Though some minor fluctuations are there in our observed SR signals both frequency as well and amplitude during some seismic events, indicated in the above figures, but we need further study with more data to interpret in the light of different geophysical events.

In the observed power spectrum Figures 7.10 (2)-7.10 (4) for the three components, it has been detected that the intensity of the E-W component is much intense than the other two components. It indicates that longitudinal distributions of the sources are larger than the North-south direction. For the period of December-January along this longitude (longitude of observatory) occurrences of thunderstorms is very low because in the Northern hemisphere it is winter and for the Southern hemisphere though it is summer but there are no continental parts to generate thunderclouds. This is the reason for low signal intensity. As the three thunderstorm centres (Asia-Australia, African and American thunderstorm centre) are distributed along the equatorial zone i. e., in the tropical region, the signal received from the E-W direction is larger, thus intensity of the  $B_y$  component is much larger than the other two components. The spectral characteristics of Schumann Resonances for the three components have been presented in Fig 7.10 (5)-7.10 (7), the prominent Schumann resonance modes are indicated by the arrows as the 1<sup>st</sup>, 2<sup>nd</sup>, 3<sup>rd</sup> and 4<sup>th</sup> modes.

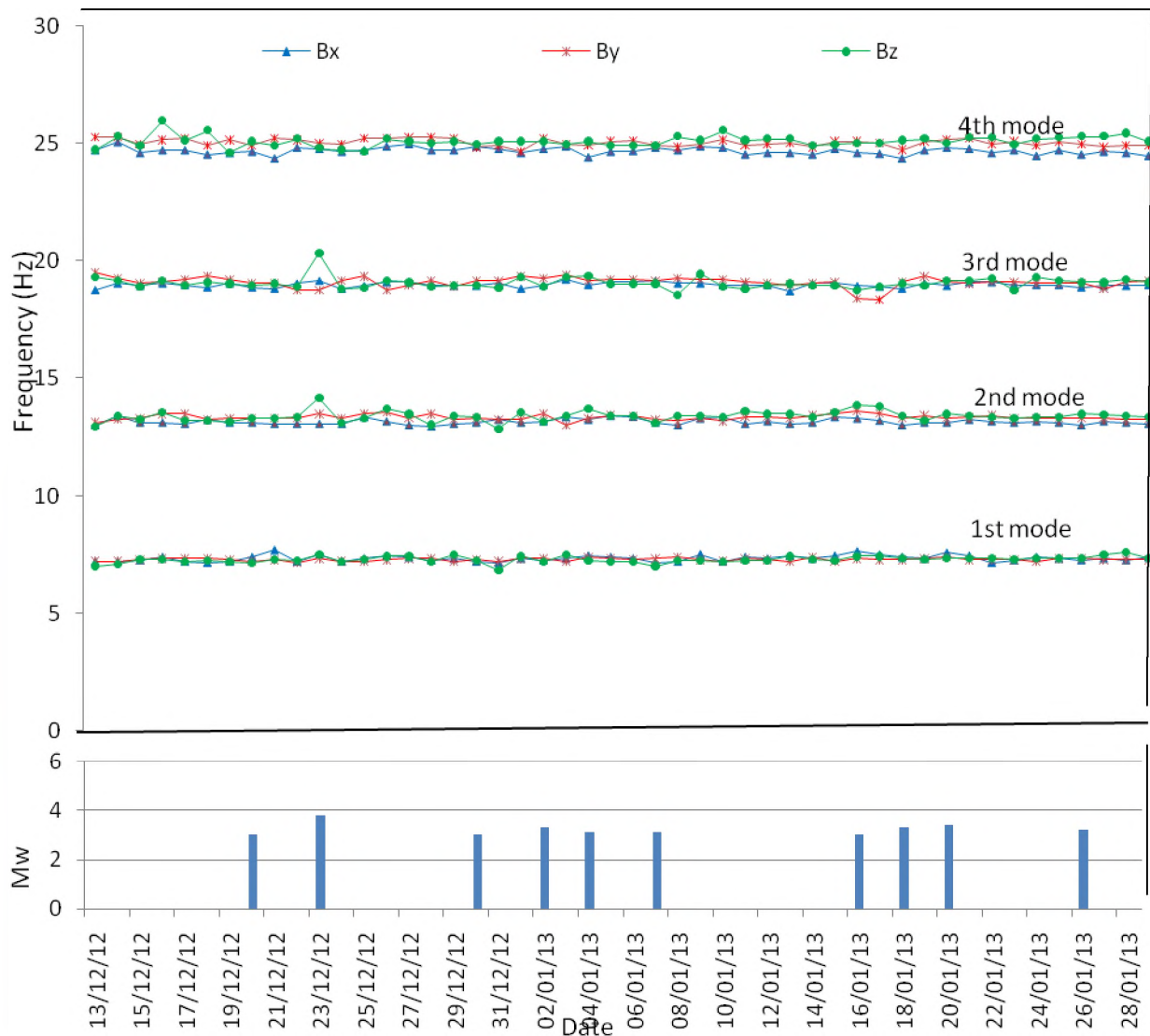


Fig. 7.12 Frequency variations of different SR modes are shown. Blue, red and green colours indicate  $B_x$ ,  $B_y$  and  $B_z$  components respectively. The seismic events during this period of observations have been shown by the bottom panel.

## 7.7 Total Electron Content, Outgoing Long wave Radiation and Surface Sea Temp

TEC is defined as the total number of electrons integrated along the path from the receiver to each GPS. The TEC as an indicator of ionosphere variability that derived by the modified GPS signal through free electrons. TEC is measured in units of  $10^{16}$  electrons/m<sup>2</sup> (1 TEC unit). The nominal range is 1016 to 1019 with minima and maxima occurring at midnight and mid afternoon approximately. Maximum TEC usually occurs in the early afternoon and minimum TEC usually occurs just before sunrise. Also daily TEC variations increase as one travels from north to south, as sunlight is more direct. The data types being currently practiced with global assimilative ionospheric model (GAIM) include line-of-sight TEC measurements made from ground-based GPS receiver networks and space-borne GPS receivers, satellite UV limb scans, and ionosonde. Intensive validation has also been conducted using various independent data sources, including vertical TEC measured using satellite ocean altimeter radar (such as those aboard TOPEX and Jason-1 missions), ionosonde, incoherent scatter radar.

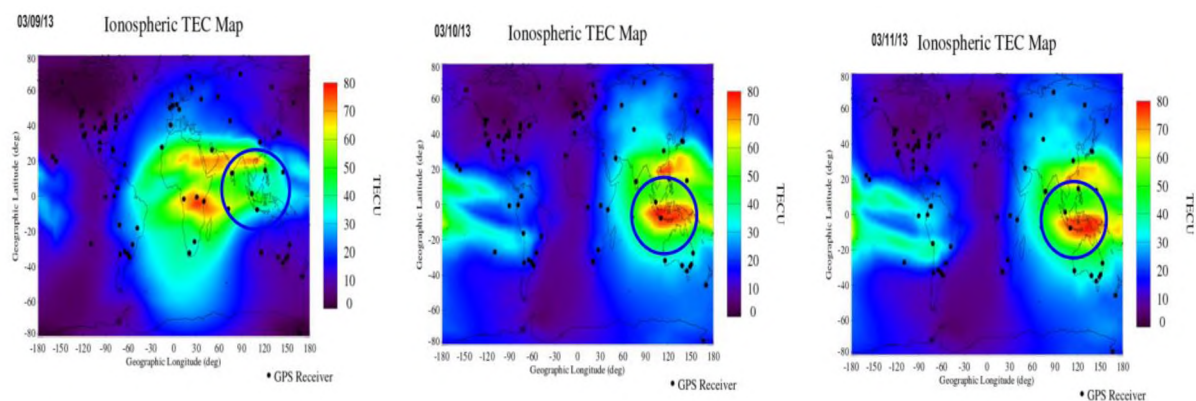


Fig 7.13: Ionospheric TEC map generated through GAIM

The TEC, OLR and SST during the significant recent earth quakes has been studied which occurred on 10<sup>th</sup> March 2013. The TEC had varied from 40 to 80 TECU over the three days where the earth quake had occurred with M=6.5 (as shown in fig.7.13), the TEC concentration had increased to 70 to 80 TECU, it persist for the next day also. The concerned one to one relationship clearly tells that whenever the earthquake have occurred there might be very good signature in the ionosphere. The Infrared emissions (OLR) anomalies prior to strong earthquakes can be noticed by satellite infrared Data. The total amount of the radiation that is emitted from the earth-atmosphere system to the outer space in 3 – 100  $\mu$ m wavelength bands is called Outgoing Long wave Radiation (OLR). OLR is an important value for the earth radiation budget. Sea surface temperature has been derived from a single thermal window channel (10.5-12.5  $\mu$ m) over cloud free oceanic regions. The most important part of the SST retrieval from IR observations is the atmospheric correction. Retrieval of sea surface temperature (SST) from thermal infrared window channels (10- 12  $\mu$ m) requires atmospheric corrections arising due to attenuation of signal by intervening moisture. This correction is more in tropics due to higher amount of atmospheric moisture.



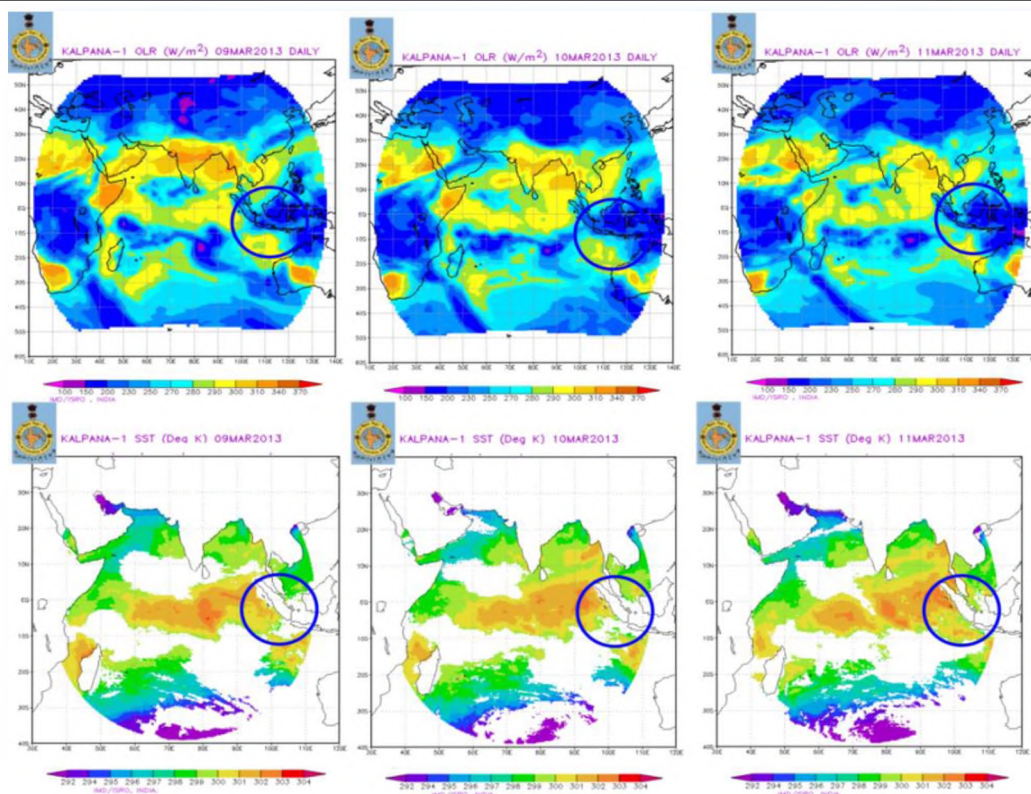


Fig 7.14: OLR and SST images generated through KALPANA (IMD)

The algorithm for SST retrieval using single thermal window channel of KALPANA and total water vapour content has been developed using transfer simulations for Indian tropical marine conditions. The three consecutive days of OLR, SST have been archived by Kalpana satellite (IMD) during the earthquake on 10<sup>th</sup> March 2013, the OLR is in the range of 150-200 Watts/m<sup>2</sup>, and SST is in the range of 301-304°K (fig 7.14). The OLR and SST values are not showing significant increase during this earthquake, its gradients are coming from the Indian subcontinent and Indian oceans. Hence we can conclude that TEC has shown significant variation before earthquake and found not much variation on OLR and SST.

## 7.8 Observations of Total Electron Content (TEC) at Desalpar

ISR established a network of 25 permanent GPS stations (Dual frequency receiver) network in Gujarat. GPS satellites transmit electromagnetic waves for positioning on two frequencies which are L1 (1575.42 MHz) and L2 (1227.60 MHz) allowing receivers equipped with dual frequency operation to be used. This enables us to extract the ionosphere TEC along the line of sight, from satellite to receiver. The ionosphere causes GPS signal delays to be proportional to TEC along the path from the GPS satellite to a receiver. TEC is defined by the integral of electron density in a 1 m<sup>2</sup> column along the signal transmission path. TEC is a key parameter in the mitigation of ionospheric effects on radio system. The TEC measurements obtained from dual frequency GPS receivers are one of the most important methods of investigating the Earth's ionosphere. The TEC itself is hard to accurately determine from the slant TEC because this depends on the sunspot activity, seasonal, diurnal and spatial variations and the line of sight which includes knowledge of the elevation and azimuth of the satellite. Owing to the importance of calculation of TEC from the permanent GPS stations, we have initiated calculating TEC from Desalpar GPS station. Here, we have taken the data of June 2012. A moderate earthquake of M 5.0 occurred on 19-06-2012. In Fig 7.15, red colour graph indicates hourly average ion-density during the period of June 9-28, 2012 and black colour graph depicts average diurnal variation through the whole period where we got minimum and maximum value around 25 and 73 with mean of 45.25 in TEC-Unit (slant TEC). Before seven days of occurrence of this earthquake, upper peak value of the curve got increased and it



becomes maximum on 14th June, 2012 about 83 TECU. Then it has shown normal TEC value during 14-16 June 2012. Four days before peak value increased during the event it was about normal. Thus we got regular fluctuating TEC value with high peak value. In our point of view these are a positive TEC anomaly due to earthquake. We will extend the method to other GPS stations for calculating the STEC and VTEC.

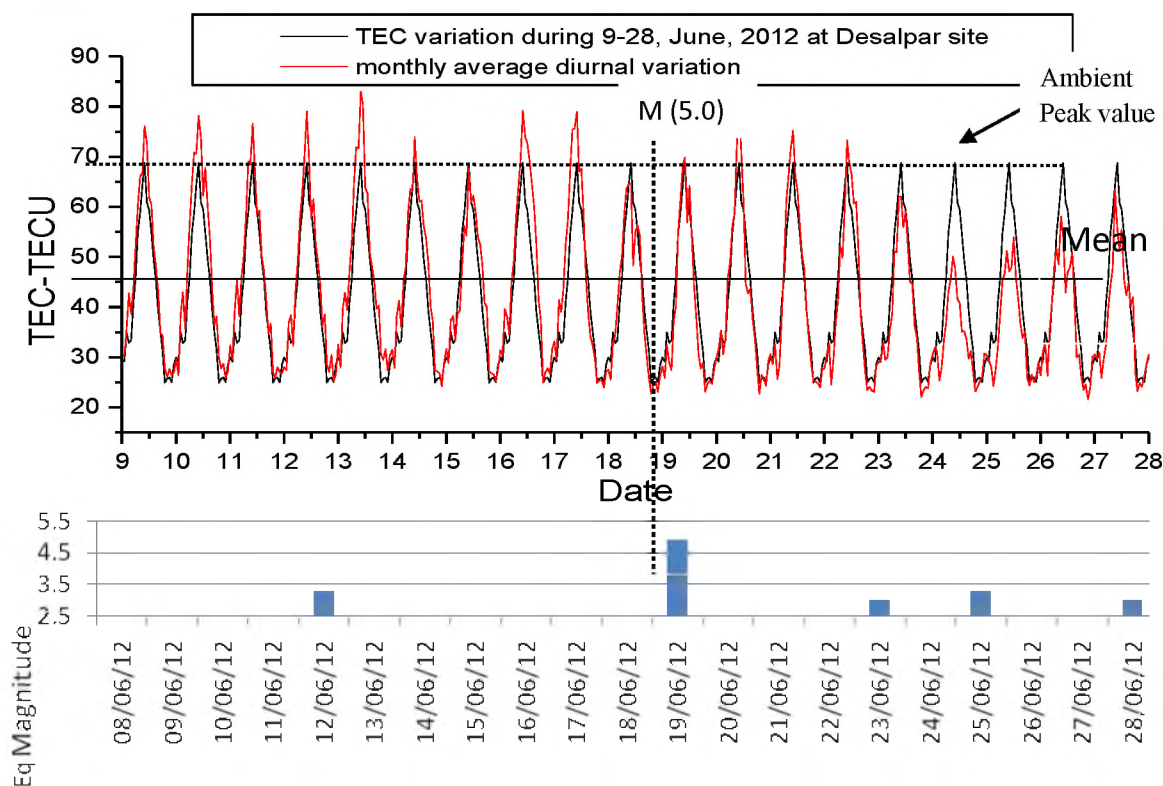


Fig. 7.15: Total Electron Content (TEC) variations at Desalpar during June 2012.

## 7.9 Observations of Ground Water level at Desalpar

Water level measurements are also useful tool for the earthquake prediction study earlier a number of research workers have studied on this subject and reported that rise of ground water level from few centimeters to meters before the earthquake. ISR has also started water level measurements using Madofil-II immersed data loggers with integrated sensors of pressure and temperature. We have not received good quality data from these sensors. In the recorded data of Desalpar, we got a seasonal variation i.e., gradual increasing value and there are also minor periodic fluctuation which may be due to moon positions but the occurrence of seismic events almost superposed on the peak value and also fluctuations are before and during the events (fig 7.16).

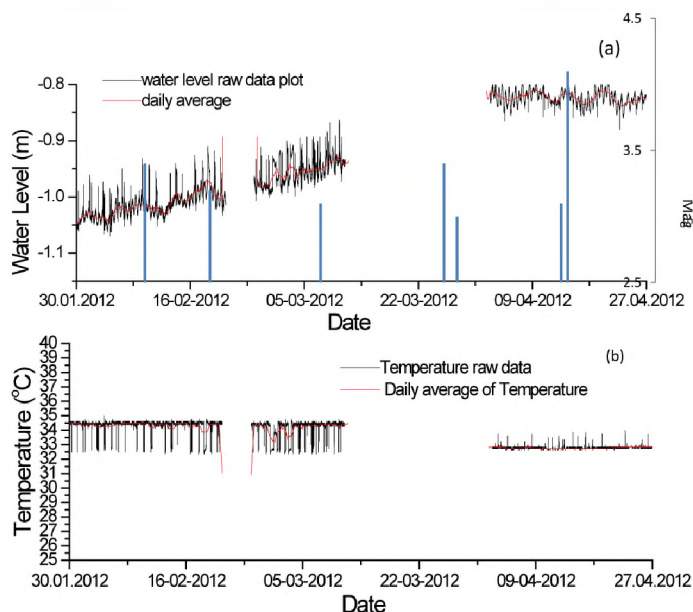


Fig. 7.16(a) Indicates water level variations in meters, black-curve shows the raw data plot and red-curve shows daily average data. (b) Depicts the temperature variations where the black and red curve indicates raw data and daily average plot respectively.

### **7.10 Processing of data of Super Conducting Gravimeter**

The raw gravity contains three parameters as Grav-1, Grav-2 and Atmospheric Pressure respectively. The gravity values are recorded in Volts while pressure data in hPa. Apart from this the raw data also contains details about Phase lag, Latitude, Longitude and the error in calculating these values, some of the information obtained from attached GPS sensor. For calculating the residual gravity, firstly the raw gravity data which was in voltage was converted into  $\text{nm/s}^2$  by multiplying the raw data with calibration coefficient  $-813 \pm 0.1$  for the Grav-1(channel-1) and  $-775.35 \pm 0.2$  for the Grav-2 (channel-2) obtained by calibration. The data or changes recorded in both the gravity values are similar, therefore, the data of only one (Grav-1) is used for further analysis. However, the data of Grav-2 was also utilized for obtaining appropriate value where there were gaps in the data. After this a phase shift correction of 8.4sec was applied to calibrated data followed by a subtraction of pressure effect (channel-3) and Earth tides induced gravity effect (channel-4). The final equation for residual gravity was obtained as-

$$g_{\text{res}} = g_{\text{raw}}(\text{calibrated, phase shift 8.4sec}) - (\text{theo\_earth\_tide}) + \text{ap\_adm} * (\text{atm. pressure})$$

Then the residual gravity time series was corrected for undesired artifacts such as spikes, earthquakes, steps and gaps using Tsoft software package, in order to reduce or eliminate the short-period impact on the residual gravity. Finally, the gravity records were recovered by adding the theoretical earth tide. The preprocessed gravity records were analyzed with ETERNA33 software package which was recommended by the International Center of Earth Tide (ICET). Having completed the above processing steps and corrections, we finally got the residual gravity series that represented unknowns including effects such as ocean currents, secular changes in elevation due to tectonics, gravity changes due to tectonics, gravity changes due to slow and silent earthquakes and hydrological changes (fig 7.17). Additionally, changes of atmospheric and hydrospheric parameters correlating to gravity variations such as atmospheric pressure, precipitation, groundwater table, soil moisture, or sea level variations have to be studied in detail. However, we can attribute the rise and fall in gravity values with the change of water level and the amount of rain precipitation.

### **7.11 Co-Seismic and Pre-Seismic Gravity changes**

An earthquake produces a discontinuous displacement along a fault plane within Earth and produces mass distribution around its focus as well as the propagation of seismic waves at distance points. This in turn results in a change in the gravity potential field of Earth in and around to its source. Viewed from a point fixed with respect to Earth, this should be observed as a small change in local gravity acceleration through two effects: apparent addition or subtraction of Earth's mass and a change in the distance to the centre of Earth. A theory has been developed to calculate co-seismic gravity changes for arbitrary fault geometries on the basis of the dislocation model of the earthquake source and has been shown to reproduce the observed values well. A careful scrutiny of residual gravity at Badargadh revealed unambiguous co-seismic jump of  $8.0 \mu\text{Gal}$  in relation to the moderate earthquake (M 5.0) on 19-06-2012 in Kachchh region (Fig 7.19). The raw gravity time series is shown as fig 7.18. The proximity of epicenter from the SG station is only about 30 km. Such gravity changes are a common feature in many parts of the world during local and regional earthquakes. Because co-seismic gravity changes depend on fault parameters, especially dislocation vectors, the observation of co-seismic change in gravity at multiple stations, if combined with other techniques such as global positioning system and strain-meters, should provide constraint on the nature of dislocations in the earthquake source region.

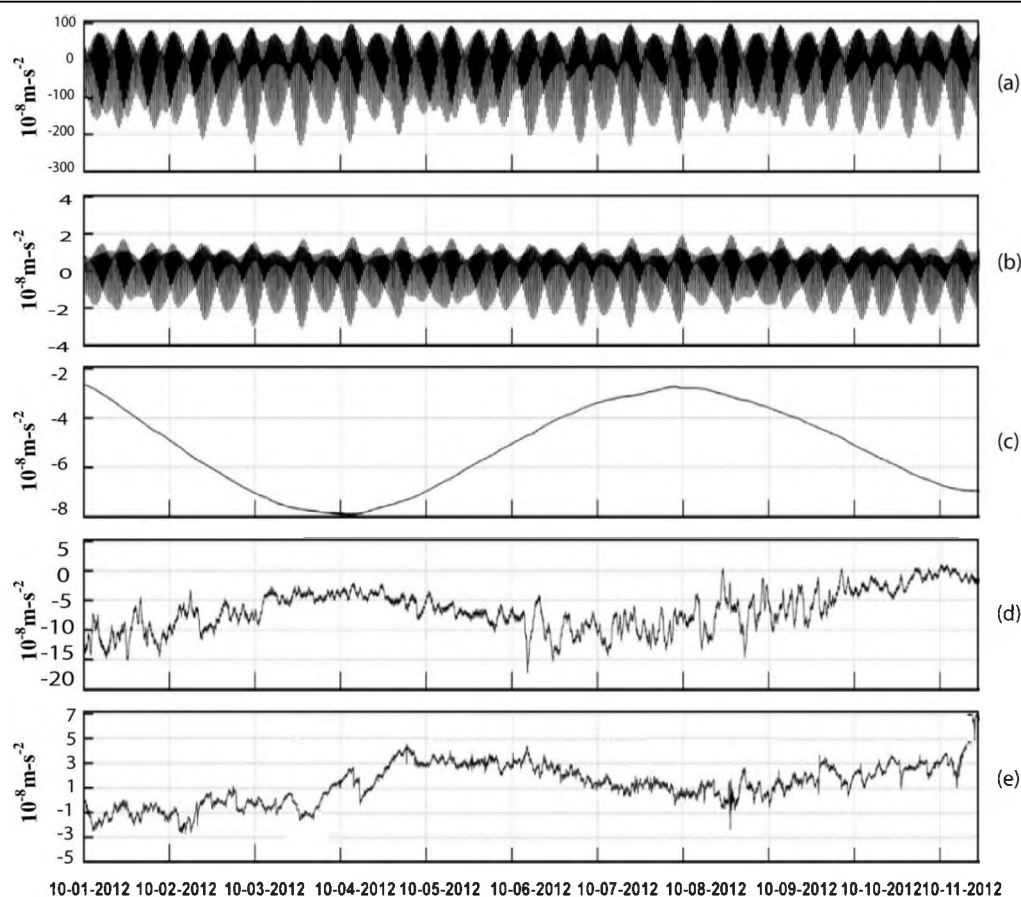


Fig. 7.17: (a) Preprocessed data of SG after removal of spikes, noise and filling the gaps; (b) Ocean loading by NAO99 ocean model (c) Polar tide; (d) Atmospheric loading effects; (e) Residual gravity corrected by solid earth tides, atmospheric loading effects and pole tide.

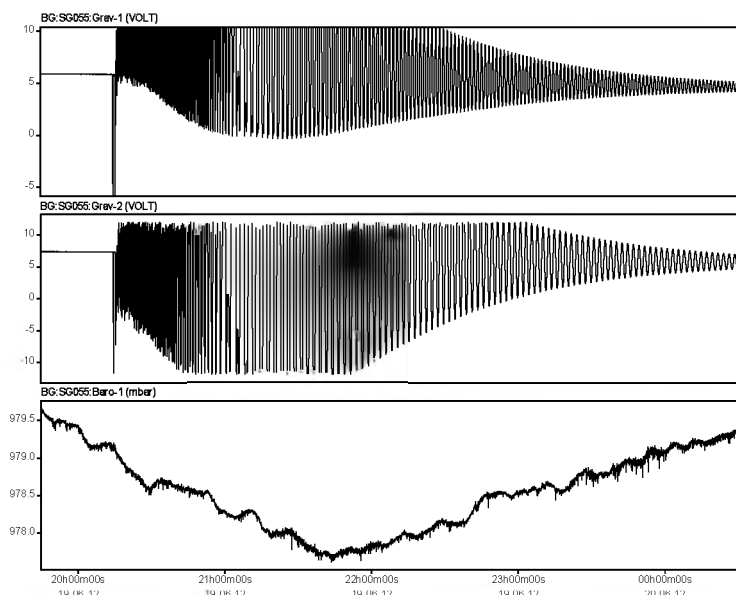


Fig. 7.18: Original 1 Hz SG (grav-1 and grav-2) and Barometric pressure records of Badargadh station during 19-20 June, 2012

A possible mechanism of the anomalous gravity signals prior to a large earthquake might be due to the ground (or tectonic) vibration that is caused by the slow slip of fault several days to several hours (or several minutes) prior to the earthquake event. The ground vibration due to the slow slip then results in accelerations as well as seismic waves (or gravity waves) that can be detected by SGs and broadband seismometers.



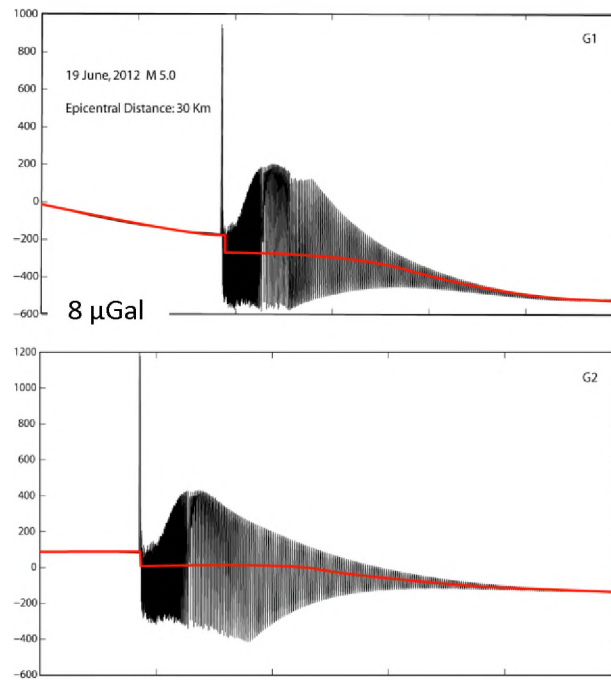


Fig. 7.19: Residual gravity series (grav-1 and grav-2) after removing barometric pressure and tides from records of Badargadh station on 19 June, 2012.

The dominant frequency of the anomalous signals we detected in this study ranges from 0.05 to 0.1 Hz (fig. 7.20). So the SG records as well as the broadband seismometers records might be significant information sources in detecting the anomalous signals prior to large earthquakes. In this study, the 1 Hz SG records show that there is a spectral band around 0.08 Hz, which is observed in the anomalous period just few hours prior to the earthquake occurrence but not in the quiet days. Hence, the spectral analyses gravity time series of SG suggest that there are anomalous signals prior to this moderate earthquake. However, the relationship between the source processes and the detected anomalous signals has not been yet established and needs further exploration.

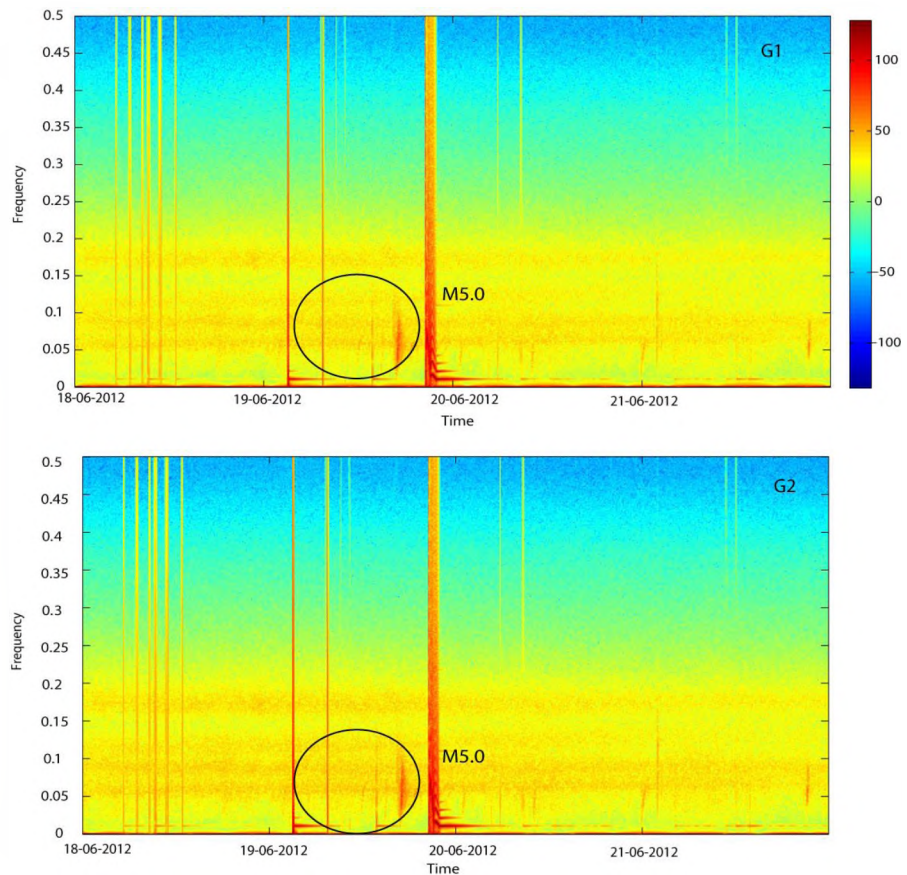


Fig 7.20: Spectrograph of residual SG data series that covers the period 18–21 June 2012 recorded and sampled at 1-s interval after removing the tidal effects



## CHAPTER 8

### PROJECTS OF SOCIETAL IMPORTANCE AND ADVICE TO IMPORTANT DEVELOPMENT ACTIVITIES

#### 8.1 PILOT PROJECT ON EXTRACTION OF URANIUM FROM NUCLEAR WASTE

*(Dr. R. M. Altekar of BARC and Dr. G. C. Kothiyari of ISR)*

Dr R. M. Altekar from Metallic Fuels Division of Bhabha Atomic Research Centre (BARC), Mumbai visited Institute of seismological Research (ISR) between 9-10-12 to 11-10-12 for magnetic separation of paramagnetic CuO (magnetic susceptibility  $242 \times 10^{-6}$  M<sup>3</sup>/Kg), and NiO (magnetic susceptibility  $740 \times 10^{-6}$  M<sup>3</sup>/Kg) mixed with graphite powder, and material between 200 to 1500  $\times 10^{-6}$  M<sup>3</sup>/Kg magnetic susceptibility from incinerator ash. Following experiments have been done in OSL lab.

1. Graphite powder have been separated from mixed iron oxide
2. Separated graphite was mixed with copper powder and finally copper has been separated using magnetic separator.
3. Nickel powder was mixed with Copper and the individual separation have been done
4. Graphite, Nickel and Copper powders were mixed together and Nickel and Copper has been separated

This was a pilot project which has been successfully completed. Now they can plan to procure bigger size magnetic separator to extract Uranium from nuclear waste.

#### 8.2 INVESTIGATION OF THE REPORTING OF CRACKS IN HOUSES IN FARADI VILLAGE OF MANDVI TALUKA IN KACHCHH BY MEANS OF RAPID VISUAL SCREENING WITH GEOLOGICAL & GPS SURVEY

*(Ashish Bhandari, Siddharth Prizomwala, Vasu Pancholi & Mohar Singh)*

It was reported to CM office of Gujarat that there is unusual number of cracks developed in houses of Faradi Village of Mandvi taluka in Kachchh. The report was sent to ISR for investigation. The villagers reported that even new houses develop cracks soon after construction. Rapid visual survey of a few hundred houses of the village was conducted and cracks in houses were compared with the cracks in nearby villages. The cracks are found to be normal plaster cracks or the cracks developed along joints of blocks of walls due to faulty construction practice. The somewhat wider cracks are those that developed due to 2001 Bhuj earthquake. The geological survey did not find any unusual settlement. However, GPS survey has been done and its repeat survey after 6 months or so may confirm the same or otherwise.

## CHAPTER 9

### NATIONAL AND INTERNATIONAL SCIENTIFIC COLLABORATION

#### 9.1 Indo-Italian Project on Earthquake Hazard Assessment

*(B.K. Rastogi, Pallabee Chaudhury and Ketan Singha Roy)*

The information about the basin structure, focal mechanism etc. has been assembled for applying the neo-deterministic method of seismic hazard assessment now favoured by the Italian group of Trieste.

#### 9.2 The 3D Magnetotelluric Survey in Kachchh along with NGRI and Ukrain Geophysicists

*(Kapil Mohan, Sunita Raika and K. Veeraswamy of NGRI)*

A 3D magnetotelluric survey was carried out in Kachchh for 2-months period during November – December 2011 along with NGRI and Ukrain geophysicists under an MoES project to depict the sub-surface nature of the South Wagad fault, hidden Samkhiali fault and the hidden North Wagad fault which caused 2001 earthquake. This 3D survey at close grid for upper crustal structure is pioneering in the World. Earlier studies were done for lower crust. About 40 sites were occupied with long-period and short-period instruments with 5 to 15 days deployment at each site.

# CHAPTER 10

## SOCIETAL OUTREACH

### 10.1 DISSEMINATION OF INFORMATION ABOUT EARTHQUAKES

#### 10.1.1 DATA CENTER AND WEBSITE

The ISR Data Center disseminates earthquake information round the clock. The ISR website is updated every day.

### 10.2 HELP TO THE UNIVERSITIES/INSTITUTES/ORGANISATIONS

10.2.1 M.Sc. Geophysics course has been started at Ganpat University, Mehsana. ISR designed the syllabus, Lecture Plan and has arranged 60 hours lectures for two Geophysics papers and field training of geophysical surveys.

10.2.2 Training of Sri S. N. Chowdhari, Geophysicist from Geological Survey of India, Central Geophysics Division, 27, J.L. Nehru Road, Kolkata – 700016, Contact No.: 09432014169 (M), (033) 24256078 (L) for conducting PS Logging of GSI instruments in boreholes drilled by ISR for Ahmedabad Microzonation and comparing it with the original data of ISR PS Logging as they have not been able to operate the instrument for last 3 years.

### 10.3 SEMINAR TALKS / LECTURES BY VISITORS

1. Distinguished lecture by Dr. Chandrakanth S. Desai on the topic “Finite element method for dynamic-earthquake analysis with realistic constitutive modeling” on 3rd February 2012.
2. Dr. Dhananjay Kumar from Chevron Oil Company, Houston, USA, lecture on “Seismic Wave Propagation in Earth” at ISR, Feb. 15, 2012.
3. National Science day lecture by Dr. T. J. Majumdar, Emeritus Scientist, SAC, ISRO, Ahmedabad on the topic “Remote sensing applications for geophysical exploration / hazard monitoring on 28th February, 2012.
4. A series of lectures was delivered by Dr. J. R. Kayal from 17-03-2012 to 23-03-2012 in ISR on following topics:
  1. Earthquakes & Seismic Waves : 17-03-2012.
  2. Earthquake Location : 17-03-2012 & 19-03-2012.
  3. Seismic Tomography : 19-03-2012.
  4. b-value & Fractal analysis/mapping : 20-03-2012.
  5. Fault plane solutions & Interpretations : 20-03-2012.
  6. Seismotectonics & Tectonic model of Himalaya and NE India : 21-03-2012.
  7. Earthquake precursor study in NE India : 22-03-2012.
  8. Seismotectonic of the Intraplate earthquakes of India : 23-03-2012.
  9. Seismic Hazard and Microzonation Studies in India: 23-03-2012.

All the Scientists, Geophysicists, Geologists, JRF attended the same.

5. Foundation Day lecture was delivered by Dr. Ajai, Group Director, Marine and Earth Sciences, SAC-ISRO entitled "Climate Change Studies: Role of Space Technology", 20/05/2012.
6. Prof. JR Kayal, of Jadavpur Univ. and former Addl. DG, Geol. Survey In., May 8-21, 2012, delivered 15 lectures on Seismology to ISR scientists and summer trainees and guided project work of trainees and scientists.
7. Prof. VC Thakur, former Director Wadia Inst. Himalayan Geology, Dehradun during May 28 to June 2, 2012 guided geological field work in Kachchh and delivered the following 3 lectures on Geology to ISR scientists and summer trainees:
  - i. Seismotectonics of Himalaya, 28.5.2012
  - ii. Lessons learnt from 2005 Kashmir earthquake: Extension of Balakote Bagh Fault, 28.5.2012
  - iii. Active Tectonics of Himalaya, 2.6.2012
8. Dr. SK Biswas, Visiting Prof. IITb and former Director KD Malaviya Inst. Petroleum Exploration, ONGC, Dehradun visited for discussions on Cambay and Kachchh Geology and delivered the following lecture:

Tectonic cycles stress dynamics & Active faults in Kachchh Graben, 8.6.2012
9. Sri RK Singh, Visiting Fellow, delivered 15 lectures on Gravity, magnetic, electrical and Seismic methods of geophysical exploration to ISR scientists and summer trainees and guided project work of trainees and scientists on gravity and electrical resistivity during May 7- 25 and June 4- 15, 2012.
10. Dr. S.K. Biswas, Former Director ONGC, Tectonic Cycles, Stress dynamics and Active fault in Kachchh Graben, 8 June 2012.
11. Navin Juyal of Physical Research Laboratory, "Holocene Evolution of Western Grater Rann during Last 5500 years", July 3rd 2012
12. Prof. Ajay Manglik, of NGRI, July 10-11, 2012, delivered 4 lectures on Mathematical Modeling in Solid Earth Geophysics to ISR scientists and summer trainees and guided project work of trainees and scientists.
  - Thermal geophysics: Structure and evolution of lithosphere
  - Geophysical fluid dynamics: Mantle convection
  - Geophysical fluid dynamics: Core convection
  - Inverse theory: Joint-inversion of geophysical data
13. Lectures delivered by Indrajit Ghosh Roy during July-August 2012:
  - Lectures on magnetotelluric method
  - Lectures on digital signal processing
  - Iteratively adaptive regularization with gradient based optimization: Applications on small and large scale geophysical inverse problems
  - From shallow to deep earth-geophysical insights.
14. Dr. Vasily K. Palamarchuk "Short-Term Earthquake Prediction", 15.9. 2012



#### **10.4 VISITORS**

1. Shri T. Nandakumar, IAS (Retd.), Hon'ble Member, NDMA, 15th Feb. 2012.
2. Dr. Imtiyaz A. Parvez, CMMACS, Bangaluru on 22.2.2012 and Dr. Franco Vaccari, University of Trieste, Italy, under Indo-Italy Collaborative Program, 22 to 26 Feb. 2012.
3. Mr. B. Bhattacharjee, Member NDMA along with CEO GSDMA visited on 13.3.2012
4. Mr. Arindam Majumdar and Mr. Akshay Anand came from Ahmedabad Urban Development Authority (AUDA) for discussion on revising the Draft Development Plan 2021 for Ahmedabad region and to understand the significance of fault lines and junctions from urban planning purposes, 2/4/2012.
5. Mr. Anup Mundvariya, CM Fellow, Social Justice Department visited ISR on 2.5.2012 for seeking help for mathematical modeling of the Empowerment Programs using MATLAB and Neural Network.
6. Prof. D. Behera, PDPU for Collaborative study on Geothermal Energy, 14.05.2012
7. Deepali gadkari of CEPT for help in her PhD, 15.5.2012
8. Dr. Indrajit Ghosh Roy, Geophysicist from Canberra Australia, Visiting Fellow, July 2 to Aug 25, 2012
9. Dr. Navin Juyal of Physical Research Laboratory, July 3rd 2012
10. Dr. Ranjit Bannerji, CEO, GSDMA and Dr. PK Mishra, Chairman, GERC (Guj. Electricity Regulatory Commission), July 7, 2012.
11. Dr. Ajai Manglik, of NGRI, Hyderabad, 09/07/2012 to 13/07/2012.
12. Dr. JR Kayal, Visiting Professor, July 10-30, 2012
13. Prof. Bharat Patel, Mehsana University, July 26, 2012.
14. Mr. Krishnani, Geol-I & Mr. R.R. Patel, Geol-II of SSNNL at 3.9.2012.
15. Sri Vishal Chauhan, Faculty of Engg. & Tech., RBS College, Bhichpuri, Agra, To install VLF system in MPGOs, 5/9/2012 to 11/9/2012.
16. Dr. N. Madhavan, Asst. Professor and Sunish Pathan, Security off., PDPU, Gandhinagar, To familiarizes with ISR, 17.9.2012
17. Dr. Vasily K. Palamarchuk (Hon. Prof. Harbin Engineering University, 1, Angliysky Prospect, 190121, St. Petersburg, Russia), The All-Russia Scientific Research Institute for Geology and Mineral Resources of the Oceans, Head of Multilevel Geophysical Monitoring Laboratory along with his student Miss Nadia, September 14-19, 2012
18. Prof. J.R. Kayal, Visiting Prof., ISR, gave lectures and their important guidance and to discussions with ISR Scientists, 3/10/2012 to 13/10/2012.
19. Dr. Sushil Gupta, General manager, RMSI, Noida
20. Dr. SK Biswas, for discussions on geology of Kachchh, Nov. 7-8, 2012
21. Dr. JR Kayal, for help in writing research papers to ISR scientists, Nov. 7-12, 2012
22. Ms. Alpa Sheth, Seismic Advisor to GSDMA and Mr. Birju Patel, Director GSDMA for discussions on Dholera seismic Microzonation, Nov. 7, 2012
23. Mr. S. Murugappan and his team for discussions on seismic data analysis of NHEP Subansiri Project for which they want to give us a sponsored project, Nov. 15, 2012

24. Dr. PM Nair, IPS, Director General of Police, National Disaster Response Force & Civil Defence, Government of India, New Delhi, visited ISR on 5-12-2012 for information on seismicity monitoring and discussions on how ISR work may be useful in quick response and readiness of NDRF in case of hazard due to earthquake.
25. Mr. GC Aggrawal, formerly with Atomic Energy Commission for discussions on Nuclear Plants, Dec 7-8, 2012

#### **10.5 VISITORS IN GROUPS**

1. Some 50 students from B.B.M. High School, Mandvi, Kachchh visited ISR along with principal Sh. Rajesh D. Sarathia and two teachers on 20th October 2011. A presentation was given by Sh. Santosh Kumar on basis of earthquakes and design of earthquake resistant houses.
2. 15 students of civil engineering department of L.D. Eng. College visited ISR on 9-03-2012.
3. 110 students from Dalia Institute of Diploma Studies, Kanera, Kheda visited ISR on 14-03-2012 of civil engineering, EC & IT (6th Semester) along with following faculty members:  
Pratik Shah (Lecturer in Civil Eng.), Girish B. Patel (lecturer in EC.), Harsh Patel (lecturer in EC.), Shailesh patel (lecturer in IT.), Kunal Megna (lecturer in IT.), Aasha Patel (lecturer in Civil Eng.)
4. 10 students of Civil Engg. Department of U.V. Patel college of Engineering, Ganpat University, Kherva, Mehsana visited ISR on 17-03-2012 alongwith Sh. Nirav Patel lecturer in civil eng. Department.
5. Mr. Arindam Majumdar and Mr. Akshay Anand came from Ahmedabad Urban Development Authority (AUDA) for discussion on revising the Draft Development Plan 2021 for Ahmedabad region and to understand the significance of fault lines and junctions from urban planning purposes, 2/4/2012.
6. A.K Shukla (26914375, 9898695101) and RP Prajapati (9427001159) of SAC, ISRO for discussions on CAL-VAL Project sponsored by SAC-ISRO, 4.5.2012
7. Shri H.J. Patel, S.E. Kevadia Colony and Shri N.T. Mathew Ex. Engg. Dam Div. Kevadia Colony for establishing strong motion instruments in different levels of Sardar Sarovar dam and Power House and for review of seismic monitoring done by ISR around Sardar Sarovar, 18/05/2012.
8. Mahesh Panchal and Pranav Gandhi, Architects from Archi Medes, Ahmedabad for enquiry whether ISR can do Seismotectonic Assessment for 22 storey hospital to be constructed by AMC in Paldi, 21.5.2012
9. Dr. Ajai, Dr. Rajawat and Ms. Sweta Sharma from SAC-ISRO for discussions on collaborative projects:
  - a. Vulnerability Modeling of Bhuj and
  - b. Earthquake Precursory study is Atmospheric ionization, satellite gravity and Geochemical precursors.
10. ISR and SAC-ISRO agreed to take up joint projects involving participation of some other agencies also as required, 06/06/2012.
11. 20-25 participants for GIDM training programme on "Earthquake Mitigation and management", Sep 12, 2012
12. 15-20 persons from Pune Municipal Corporation including Mayor, Councilors and Engineers accompanied by Tejas Bhandari, Asstt. Commissioner, AMC, and Apoorva Solanki, 8.6.2012

**Pune Municipal Corporation**

1.	Hon Mayor	Mrs. Vaishali S.Bankar
2.	Deputy Mayor	Mr. Deepak M.Mankar
3.	Municipal Commissioner	Mr. Mahesh Pathak
4.	General Body Leader / Party Leader (NCP)	Mr. Subhash Jagtap
5.	Party Leader (MNS) / Leader Opposition	Mr. Vasant More
6.	Chairman Standing Committee	Mr. Baburao D.Chandere
7.	Party Leader (Indian National Congress)	Mr. Arvind Shinde
8.	Party Leader (BJP)	Mr. Ashok Yanpure
9.	Party Leader (Shiv Sena)	Mr. Ashok Harnaval
10.	Party Leader (RPI)	Dr. Siddharth Dhende
11.	Councillor	Mr. Rajendra R. Wagaskar
12.	Councillor	Mr. Kishore N. Shinde
13.	Councillor	Mr. Balasaheb K. Bodke
14.	Councillor	Mr. Vishal V.Tambe
15.	Councillor	Mrs. Minal Sarvade + 1
16.	City Engineer	Mr. Prashant M. Vaghmare
17.	Add. City Engineer (Bldg Permission/ JnNURM)	Mr. Vivek Kharvadkar
18.	Add. City Engineer (Traffic)	Mr. Shrinivas Bonala
19.	Executive Engineer (Heritage Cell)	Mr. Shyaam Dhavalaey
officers from AMC		
Tejas Bhandari	Assistant Commissioner	9377409692 tejasbhandari@egovamc.com
Nilesh Patel	Assistant Manager	9327554903 nileshpatel@egovamc.com
Apoorva Solanki	Assistant Manager	9924851235

15. Mr. Panchal and Shrenik Shah of AMC for discussions on seismic hazard investigation of 13 story hospital near Civil Hospital, Ahmedabad, 20/06/2012.
16. Mr. A. K. Jha, Sr. Manager, SNT div., CMPDIL, Coal India Ltd., visited ISR on 22-25 June 2012 for discussion on possible future Projects and preliminary analysis of yield of explosives used.
17. Mike Allan (Chairman, Geothermal, New Zealand) Kunal Vatsyayan (Env. Planning, MT-GPCL), Neelesh Tripathi, Anjali Garg (Energy Specialist, Int. Fin. Corp., New Delhi) to discuss about Geothermal Energy in Cambay Basin.
18. Dr. Indrajit G. Roy, Geophy., Canberra, Australia, Lecture on “From Shallow to deep Earth-Geophysical Insights” 25/06/2012.
19. N.U. Chalpati Rao (Geol. BHU), Prashant Bhote (GSI) and Samrendra Sahoo (Ph.D student),for Visit of the ISR.
20. Group of 25 trainees of the GIDM Training Programme on “Earthquake Mitigation and Management” along with Dy. Director (I/C) Mr. Nisarg Dave, 13/9/2012.
21. 40 students of (M. Tech. final year), Civil and Applied Mechanics, accompanied by the following faculty members of L. D. College of Engineering, Ahmedabad on 15 Sep. 2012.  
Dr. R.K. Gajjar, H.O.D, Applied Mechanics Department, Dr. H.S. Patel (Appl. Mech.), Dr. B.J. Shah (Appl. Mech.), Prof. M.D. Doshi (Appl. Mech.), Prof. K.A. Parmar (Appl. Mech.), Prof. P.I. Modi (Appl. Mech.), Prof. C.S. Sangvi, Civil Engineering Department, Prof. P.G. Patel (Civil.Eng.), Prof. M.G. Vanza (Civil.Eng.)

Mr. Santosh Kumar gave a presentation on ISR studies.

22. Sri R. K. Singh, Visiting Prof. and Miss Payal Patel of Mehsana Urban Institute of Science, Ganpat University visited ISR along with the following seven students of M. Sc. Geophysics on 20 Sep. 2012:
- Miss Priyanka Patel, Miss Shital Patel, Miss Jignasha Modi, Mr. Pruthul Patel, Mr. Bhavesh Patel, Mr. Mehul Nagar, Mr. Dilip Singh
- The students visited different labs of ISR. Field demo was given on gravimeter and engineering seismograph
23. Some 24 students from Gujarat Institute of Technology, Vill. Moti Bhoyan, Khatraj- Kalol Road, Tq. Kalol, Dist. Gandhinagar visited ISR alongwith following 8 faculty members of civil engineering department on 06-10-2012:
- Prof. Priyanka Dalal, Prof. Madhu Trivedi, Prof. Vasudeo Chandhani, Prof. Sachin S. raval, Prof. Kapadiya Sandip Kumar V., Jay C. Parmar, Prof. Monika N. Shah and Prof. Komal S. Patel
24. Some 40 students from CEPT University of final semester, Ahmedabad visited ISR along with faculty members Prof. Anal Sheth, Prof. Komal Parikh and Prof. Parth Thakar of Department of Technology

## **10.6 TRAINING TO STUDENTS**

We are running two training / internship / dissertation programs named: “Summer of Applied Geology / Geophysics Experience (SAGE) Program of ISR” and “Winter of Applied Geology / Geophysics Experience (WAGE) Program of ISR”

These have become very popular and requests pour in from all over India and from IITs and prestigious universities. At a time we have 30-40 students and have to regret some requests due to want of accommodation.

- **The following 37 students were registered for summer training:**

Mr. Anil Rakholiya, M.Sc. Final year student, Faculty of Geomatics and Space Applications, CEPT University, Ahmedabad. “Generation of Soil Models using GIS Techniques”. (Feb. – May 2012).

Ms. Nisha Bakarania, M.Sc. Final year student, Faculty of Geomatics and Space Applications, CEPT University, Ahmedabad. “Morphotectonics of South East of Democratic Republic of Congo: A case study of Laupula River Basin”. (Feb. – May 2012).

Mr. Sandip Chatrola, M.Sc. Final year student, Faculty of Geomatics and Space Applications, CEPT University, Ahmedabad. “Seismic Vulnerability Assessment”. (Feb. – May 2012).

Mr. Priyank Rajpal, M.Sc. Final year student, Faculty of Science, M. G. Science Institute, Gujarat University, A’bad, Determination of index properties of soil for identification of sub-stratification in Ahmedabad city, Gujarat, W. India (Mar. – May 2012).

Ms. Drashti Gandhi, M.Sc. Final year student, Faculty of Science, M. G. Science Institute, Gujarat University, A’bad, Topographic studies Using RTK GPS of GIFT City, Gandhinagar. (Mar. – May 2012).

Ms. Parnavi Prajapati, M.Sc. Final year student, Faculty of Science, M. G. Science Institute, Gujarat University, A’bad, Age estimation of sediment using optically stimulated luminescence dating technique (Mar. – May 2012).



- Some 28 students from ISM Dhanbad, 1 from DU started their 8-10 weeks ISR summer training Internship Program
- Shashank Sangerwar of 3rd yr IITkh from 31 April to June 15, 2012
- Arun P. Jacob, final yr from Manomaniam Sundaranar Univ., Tirunelveli, 27 May to 30 June, 2012

Mr. Rajrishi Roy Chowdhury got training in OSL Laboratory during 7.1.2012 to 30.3.2012. He is a 5th year student of MS (Earth Sciences) in Indian Institute of Science Education and Research, Kolkata (IISER-K). His project is on palaeoclimate reconstruction in Eastern Himalaya in Bhutan.

Following students of 3rd year B.E. (Petroleum Technology) from Pandit Dindayal Petroleum University came to ISR for internship from 15.12.2011 to 2.1.2012:

Mr. Chintan Patel, Mr. Gunjan Vora, Mr. Gunjesh Patel, Mr. Kunal Rathod, Mr. Maulik Sutariya, Mr. Yogeshkumar Dalsania, Mr. Mohit Verma, Mr. Joy Modh and Mr. Vipul Keswani

Technical visit of students of 6th Semester, Civil Engg. Dept. of Bhagwan Mahavir College of Engineering and Technology, Surat – 395017 (Email: bmef\_1@rediffmail.com)

Following students of 3rd year Civil Engineering from Vel-Tech Technical University, Chennai, Tamilnadu came to ISR for internship from 15.12.2011 to 2.1.2012:

Students of M.G. Science Institute, Ahmedabad, studying in M.sc. Geology Sem-IV have started their dissertation in ISR from 26/3/2012 and will continue till 7/4/2012. They joined different laboratories as follows:

- 1) Gandhi Drasti N. - GPS Lab (RTK GPS)
- 2) Prajapati Parnavi D. - OSL Lab
- 3) Rajpal Priyank J. - Geotechnical Lab

Priyanka Nayak MSc Geology of Bundelkhand Univ., Jhansi: 3 months training on Geotechnical Investigations (3 Feb. to 25 April 2012)

### **Dissertations By Students**

Mr. Rahul P, Mr. Aghil T B, Mr. Robin Alby E, Mr. Jose Paul in Magneto-Telluric Lab for dissertation during 31.12.2011 to 15.02.2012. They are final semester students of (Msc. Applied Geophysics) M S University Tirunelveli, Tamil Nadu.

Vinay Kumar, Vinay Dwivedi, Shiv Kumar and Narendra Imalya- Four M.Sc. Geology final year students of Bundelkhand Univ., Jhansi: Dissertation on Geotechnical Investigations (3 Feb. to 25 April 2012)

### **Internship of Students**

Mr. Anil Rakholiya, M.Sc. Final year student, Faculty of Geomatics and Space Applications, CEPT University, Ahmedabad. "Generation of Soil Models using GIS Techniques". (Feb. – May 2012).

Ms. Nisha Bakarania, M.Sc. Final year student, Faculty of Geomatics and Space Applications, CEPT University, Ahmedabad. "Morphotectonics of South East of Democratic Republic of Congo: A case study of Laupula River Basin". (Feb. – May 2012).

Mr. Sandip Chatrola, M.Sc. Final year student, Faculty of Geomatics and Space Applications, CEPT University, Ahmedabad. "Seismic Vulnerability Assessment". (Feb. – May 2012).

# CHAPTER 11

## HUMAN RESOURCE AND DEVELOPMENT

### 11.1 Honors/ Recognitions/Awards to ISR scientists from Other Agencies

BK Rastogi is nominated as a Member Project Advisory Committee of DST, New Delhi

BK Rastogi awarded Golden Jubilee “Honorary Scientist” Award from International Institute of Seismology and Earthquake Engineering, Tokyo, Japan.

Dr. B.K. Rastogi nominated as member, CEPT University Review Committee of Professors

Dr. B.K. Rastogi acted as member selection committee for the post of Associate and Asst. Professors of IIT Bhuvaneshwar

Shri Santosh Kumar Sundariyal, Sc.D is nominated as Board of Directors in newly incorporated BISAG SATCOM Company.

BK Rastogi chaired a session of ‘Geosciences Area’ of Symposium on “Scientific Interventions for Societal Development” organized by North east Institute of Sc. & Tech., Jorhat, December 20, 2012.

BK Rastogi Chief Guest and Inaugurated the National Seminar on “Earthquake Hazards: Education, Preparedness and Management” organized by Environmental Watch and Management Institute, Guwahati, Dec 28-30, 2012.

Siddharth Prizomwala has been shortlisted for the ‘Young Scientist Award’ by the Indian Science Congress Association for ‘Earth Science’ Category for year 2012.

Siddharth Prizomwala has been awarded the Quaternary Conference Fund Award by the Quaternary Research Association (UK) to attend the 4<sup>th</sup> OSM PAGES Conference.

Siddharth Prizomwala submitted his PhD thesis entitled “Sediment Provenance, pathways and sink potential of the inner Gulf of Kachchh coast, Western India” to the M. S. University of Baroda.

B.K. Rastogi: Chairman Seminar Session “Current Scenario in area of earthquake resistant designing” and KEYNOTE ADDRESS “Seismic microzonation and earthquake hazard estimation for important structures” “Technical Workshop for Faculty and Academia” at SAL Inst. of Tech. & Engg. Research, Ahmedabad on 22.2.2013

B.K. Rastogi: KEYNOTE ADDRESS “Seismic Hazard” at NHPC North East Geologists’ conclave Subansiri Lower Hydro Electric Project. 11<sup>th</sup> March 2013

B.K. Rastogi: KEYNOTE ADDRESS “Engineering Seismology” at NHPC North East Geologists’ conclave Subansiri Lower Hydro Electric Project, 12<sup>th</sup> March 2013

### ISR SEMINAR TAKLS (INHOUSE SEMINARS)

Following 12 talks were delivered by ISR scientists on 12.12.12 for 12 minute duration each:

1. Santosh Kumar, Seismic Network, Seismicity, Seismic Background Noise of Gujarat Network at ISR, Dec. 12, 2012
2. A.P. Singh, 3-D Seismic Structure, Crack Attributes and b-Values of the Kachchh Gujarat, India and Its Implication for the Earthquake Hazard Mitigation, at ISR, Dec. 12, 2012
3. Girish Ch. Kothiyari, Neotectonic attribute of the Gedi Fault in Wagad area of Kachchh, Gujarat India, at ISR, Dec. 12, 2012

4. P. Mahesh, Seismotectonics of the Kumaun-Garhwal Himalaya, at ISR, Dec, 12, 2012
5. B. Sairam, probabilistic Seismic hazard assessment (PSHA) of Gujarat, at ISR, Dec. 12, 2012
6. S. P. Prizomwala, Is the southern coast of Kachchh uplifted? at ISR, Dec. 12, 2012
7. S. P. Prizomwala, Signatures of Tectonic Uplift Recorded by Marine Notches along Diu Coast, Western India, at ISR, Dec. 12, 2012
8. B.K. Rastogi, Delineation of Faults and Basement Structure in Kachchh Using High Resolution Gravity Survey, at ISR, Dec. 12, 2012
9. B.K. Rastogi, Seismicity of Gujarat From 2001 to 2012, at ISR, Dec. 12, 2012
10. B.K. Rastogi, Seismic Microzonation work in Gujarat by ISR, at ISR, Dec. 12, 2012
11. B.K. Rastogi, Seismic Hazard Assessment of the Industrial sites in Kachchh, at ISR, Dec. 12, 2012
12. B.K. Rastogi, Seismicity of Himalaya, at ISR, Dec. 12, 2012

#### **11.2 PhD Awarded:**

1. Babita Sharma (2007), Attenuation and Site Amplification Studies for Indian Regions using Coda Waves, Kurukshetra University, Kurukshetra, 161pp. Guide: Prof. S.S. Teotia.
2. R.B.S. Yadav (2009). Seismotectonic modeling of NW Himalaya: A perspective on future seismic hazard. Department of Earthquake Engineering, Indian Institute of Technology, Roorkee, Guide: Prof. Daya Shankar.
3. Kapil Mohan (2009). Seismic Hazard Assessment of Himalayan Regions (NE and Uttarakhand Himalayas) based on strong motion modeling of earthquake sources. Kurukshetra University. Guide: Prof. Anand Joshi
4. Rajeeva Kumar Jaiswal (2009) "Seismic characteristics of Earthquakes in India and Tsunami in the Indian Ocean" guides: Dr. B.K. Rastogi and Dr. V.P. Dimri
5. Sumer Chopra (2010). "Estimation of attenuation characteristics, site amplification functions and ground motions for the evaluation of seismic hazard in the Gujarat region, India", Kurukshetra University, guides: Dr. B.K. Rastogi and Prof. Dinesh Kumar.
6. Rakesh Kumar Dumka (2011) on the topic "Determination of Crustal Strain field in Kumaun Lesser to Tethys Himalaya using GPS geodesy" under the supervision of Prof V. K. Gaur and Prof. B. S. Kotlia from the Department of Geology Kumaun University, Nainital.
7. B. Sairam (2012) "Study of Source Parameters and Seismotectonics of the Gujarat, India: Implications towards the Seismic Hazard Mitigation, Osmania University, under the guidance of BK Rastogi and Prantik Mandal of NGRI.

#### **11.3 Deputations abroad:**

1. K.MADHUSUDHANA RAO, Training on Operation and Usage of ULF Magnetometers and its Analysis, LVIV Laboratory for Electromagnetic Investigations, 5-A Neukova Str, LVIV, Ukraine, October 22-31, 2012.
2. PALLABEE CHAUDHURY, Workshop on Geophysical Data Analysis and Assimilation, International Centre Theoretical Physics (ICTP), Trieste, Italy, 27th October- 2nd November, 2012 and Collaborative Research Work, Dept of Mathematics and Geosciences, Universita Degli Studi di Trieste, Italy, 3rd - 17nd November, 2012.
3. Prof. Dr. BK Rastogi and Dr. Kapil Mohan, to attend "Consultative South Asian Expert Meeting on Global Earthquake Model (GEMSAM)" in Kathmandu, Nepal, 28 Feb - 4 March, 2013.

#### **11.4 Workshops / Seminars Attended:**

1. G. C Kothiyari and Prabhin Sukumaran attended the International Geological correlation congress (IGCP) or now known as International Geoscience Program's annual meeting and conference on 'Tropical Rivers: Physical processes, Impact, Hazard and management' at IIT Kanpur, from 5th to 7th January 2012 and presented poster titled "The response of drainage basins to the late Quaternary tectonics in the Sabarmati River basin, Gujarat, Western India".
2. G. C Kothiyari and R.K. Dumka, National level Field workshop and Brain Storming Session on "Geology of Kachchh Basin, western India: Present Status and Future Perspectives", 26-29 January 2012.
3. B.K. Rastogi, Nainital to attend seminar, to present an invited paper and to chair a session, "Geology and Geo-resources of Himalaya and Cratonic Regions of India", Geology Dept., Kumaon Univ., Nainital, 10-12 March, 2012.
4. One Day Workshop on "Hydrological Data Management in Gujarat: Present State and Trends" held at Dept. of Civil Engg., Pandit Deendayal Petroleum University (PDPU), 21 April 2012.
5. Persons attended- Mr. K.M. Rao, Mr. Santosh Kumar, Dr. Kapil Mohan, Dr. Pallabee Choudhary, Mr. B.Sairam, Mr. Sandeep Aggrawal, Mr. R.K. Singh, Ms. Falguni Bhattacharya, Ms. Sunita Devi and Mr. Suresh.
6. B.K. Rastogi, Guest of Honor for Inaugural and Valedictory Function of "Refresher Course on Update on IPR" to held at ISR on 25th May 2012.
7. B.K. Rastogi, Guest of Honor, Inaugural Function of the Annual Review Meeting of Community Science Centers (CSC) of Gujarat, 1.6.2012

#### **11.5 Training of ISR staff outside**

1. Dr. Rakesh Dumka attended training on GPS data processing and interpretation with updated software at IIG, Mumbai during 7th March 2012 to 27th April 2012.
2. M.S.B.S. Prasad (Sc.B), Tarak Shah (Geophy.), Sushant Kumar Sahoo (JRF) and Sikha Mishra, attended training on Magnetic Observatory, Indian Institute of Geomagnetism (IIG), Rajkot during 6-8 June 2012.
3. Chirag Chavda (Librarian) attended National Workshop on "Open Access Software", at Parul Institute of Technology, Baroda, 15-16 June 2012.
6. Shikha Swarupa Mishra and Swagatika Dash attended SERC Course on "Application of GPS on atmospheric Constraints", at Osmania University, Hyderabad, 13 June to 3 July.
7. M.S.B.S. Prasad (Sc.B), Tarak Shah (Geophy.), Sushant Kumar Sahoo (JRF) and Jayashree Bennarjee (JRF), attended training on Geo Chemical Precursors, Variable Energy Cyclotron Centre (VECC), Dept. of Atomic Energy, Govt. of India, 1/AF Bidhan Nagar, Kolkata, 25 June to 3 July 2012.

Mr. Nagabhushan Rao did research work with Dr. N. Purnachandra Rao at NGRI, Hyderabad, August-September 2012.

Ms. Jyoti Sharma, attended the training regarding Moment Tensor Inversion and ambient Noise tomography under the guidance of Dr. N. Purnachandra Rao at NGRI, Hyderabad, Nov. 3-18, 2012.

Mr. Nagabhushan Rao finalized research papers with Dr. N. Purnachandra Rao at NGRI, Hyderabad, Nov. 9-30, 2012.



## 11.5 Lists of staff

### Scientific staff

Sn	Name	Post	PG	PG yr	Joining
1	K. Madhusudan Rao	Sc. D, GoG Plan	M.Sc. Tech. Geophys, OU	1995	01.02.2006
2	Santosh Kumar	Sc. D, GoG Plan	M.Tech in Applied Geophysics., KU	1996	01.04.2006
3	Dr. (Miss) Pallabee Choudhury	Sc. C, GoG Plan	M.Sc. Phys. Tezpur PhD Geophy. Tezpur	2001 2006	19.07.2007
4	Dr. Kapil Mohan	Sc. C, GoG Plan	M.Tech Geophys., KU Ph.D Geophys., KU	2001 2009	11.07.2007
5	Dr. B. Sairam	Sc. B, GoG Plan	M.Sc. Tech. Geophys. OU	2003	17.08.2006
6	A. P. Singh	Sc. B, GoG Plan	M.Sc. Tech. Geophy., BHU	2002	14.08.2006
7	Ms. Jyoti Sharma	Sc. B, GoG Plan	M.Sc. Phys., DU M.Tech, IITkh	2005 2008	01.12.2011
8	P. Mahesh	Sc. B, GoG Plan	M.Sc. Phys, AU	2005	29.12.2011
9	G. Pavankumar	Sc. B, GoG Plan	M.Sc. Phys. AU	2004	05.01.2012
10	Dr. Girish Chandra Kothiyari	Sc. B, Fast Track	M.Sc. Geol, Kumaun PhD, KU Nainital	2001 2009	13.4.2009
11	M.S. B. S. Prasad	Sc. B, SSNL	M.Sc. Tech. Geophys. AU	1989	11.6.2007
12	Dr. Rakesh Kumar Dumka	Sc. B, SSNL	M.Sc. Geol Kumaun Ph.D Kumaun	2003 2011	1.8.2007
13	Sandeep Kumar Aggarwal	Sc. B, SSNL	M.Tech Geophys., KU	2004	20.7.2007
14	Ms. Falguni Bhattacharjee	Sc. B, SSNNL	M.Sc. Geol, Jadavpur Uni	2004	13.2.2008
15	Vasu Pancholi	Sc. B, MoES-3	M.Sc. Geol., GU	2005	8.09.2011
16	Sidharth Dimri	Sr. Geologist	M.Sc. Geol., HNB Garhwal University	2002	15.1.2008
17	Vandana Patel	Geophysicist GoG Plan	M.Sc., Phys.	2006	06.9.2008
18	Nagabhushan Rao	Geophysicist GoG Plan	M.Sc. Phys.	2007	1.4.2010
19	Annam Navneeth	Geophysicist GoG Plan	M.Sc. Geophys. OU	2009	19.4.2010
20	Sunita Raika	Geophysicist GoG Plan	M.Tech. (Appl. Geoph.)	2010	03.09.2010 DoR 8.2.13
21	Siddharth Prizomwala	Geophysicist GoG Plan	M.Sc. Geol., MSU	2008	8.10.2012
22	Ketan Singha Roy	Geophys. Italian Proj	M.Tech Computational Seism., Tezpur	2009	30.7.2009
23	Ms. Sarda Maibam	Geophys. GoG Non Plan	M.Sc. Earth Sc. Manipur	2009	05.11.2009
24	Ms. Ranjana Naorem	Geophys. GoG Non Plan	M.Sc. Earth Sc, Manipur	2009	30.1.2010 DoR 14.3.13
25	Vishwa Joshi	Geophys. GoG Non Plan	M.Sc. Phys.	2007	20.05.2009
26	Manish Sharma	Hon. Sc.	M.Sc. Geol., MSU		30.07.2011
27	S. Venkateswara Rao	Senior Geophysicist	M.Sc. Geophysics Osmania University	2007	04.06.2012
28	Miss Meenakshi Rawat	Geologist	B.Tech. (Geosciences) Uni. of Petro. and Energy Stud., Dehradun	2011	04.07.2012
29	Miss Purnima Singh	Geologist	M.Sc. Geol., MSU	2011	20.08.2012
30	Mr. C. Prasanna Simha	Project Sc.	MSC Phys.,	2005	6.11.2012
31	Dilip Kumar Haldar	RA	M.Sc. Phys.	2007	1.10.2012

### List of JRFs

Sn	Name	Post	Qualifications	PG yr	Joined on
1	Jaina P. Patel	JRF, MoES-3	M.Sc. Env. Sc & Tech	2009	1.06.2009
2	*Ms. Jayashree Bannerjee	JRF, MoES-3	M.Sc. Geophy ISM, Dhanbad		10.6.201 DoR 20.2.13
3	*Gajendra Prasad	JRF, MoES-3	M.Sc. App. Geophy ISM, Dhanbad	2012	30.6.2012 DoR 1.5.13
4	Swagatika Dash	JRF, MoES-4	M.Sc. Geophy, Berhampur	2012	2.4.2012
5	*Mr. Kuntal Bhukta	JRF, MoES-4	M.Sc. App. Geophy., ISM Dhanbad	2012	3.9.2012 DoR 20.2.13
6	*Kavita Rani	JRF, MoES-4	M.Tech. Appl. Geophy Kurukshetra	2011	28.9.2011 DoR 1.5.13
7	Peush Chaudhary	JRF, MoES-5	M.Tech. Appl. Geophy Kurukshetra	2011	2.1.2012
8	*Monika Wadhawan	JRF, ISRO	M.Tech. Appl. Geophy, Kurukshetra	2011	28.9.2011 DoR22.12.212
9	Sushant Kumar Sahoo	JRF, ISRO	M.Sc. Geophy Berhampur	2012	2.4.2012
10	*Mohar Singh	JRF, GoG Plan	M.Tech. Remote Sensing	2010	29.9.2010 DoR 31.12.2012
11	Sunita Sahoo	JRF, GoG Plan	M.Sc. Geophy Berhampur	2012	2.4.2012
12	Sikha Swarupa Mishra	JRF, GoG Plan	M.Sc. Geophy Berhampur	2012	2.4.2012
13	Vinay Kumar Dwivedi	JRF, GoG Plan	M.Sc. Geol. Bundelkhand Uni.	2012	21.7.2012
14	Ms. Jayshri Solanki	JRF, GoG Plan	M.Sc. Geomatics, CEPT University	2012	4.9.2012
15	Ms. Drasti Gandhi	JRF, GoG Plan	M.Sc. Geology, M.G. Sci., A'bad	2012	18.9.2012
16	Ms. Parnavi Prajapati	JRF	M.Sc. Geology, M.G. Sci., A'bad	2012	18.9.2012

### Technical Officer

Name	Qualification	Joined on
Ganpat Parmar	BE (EC)	17.11.2007
Jignesh B. Patel	BE (Computer Science)	12.04. 2006

### Technical Assistant

Sn	Name	Qualification	Joined on
1	Jay Pandit	B.Com.	16.06.2007
2	Nirav Patel	Dipl. Electrical	18.10.2007
3	Dilip Chaudhari	Dipl. Electrical	30.10.2007
4	Sandip Prajapati	DEC	24.12.2007
6	Bharat D. Mevada	DEC	18.01.2008
7	Gaurav Parmar	DCE	10.03.2008
8	Tejendra Vaghela	Dipl. Electrical	03.10.2008
9	Dharmendra Solanki	B.Com.	01.12.2008 To July 2012
10	Mahesh Valekar	Dipl. Electrical	03.03.2009
11	Ankit Pandya	Dipl. Civil Engg.	01.04.2009
12	Bihari Darji	ITI Electronics	20.04.2009
13	Pritesh Chauhan	Dipl. Comp. Engg	01.05.2009
14	Jayesh Parmar	DEC	01.05.2009
15	Darshit Modi	DEC	04.05.2009
16	Suresh Thadani	BE (EC) 2012	13.7.2012
17	Pareesh A. Paradia	Dip. Electrical	16.10.2012

**Administrative Staff:**

1. Mr. P. H. Charan, Accounts Officer since 28.08.2010
2. Giriraj Chavda, Accountant
3. Utpal Bhatt, PA to DG
4. Chirag Chavda, Librarian since 21.05.2012
5. Jitendrasinh Chavda, Senior Clerk
6. Mitesh Lakhwara, Jr. Clerk since 1.8.2012
7. Mr. Ramnik Lal Suchak, Office Suptd. with Ind. Soc. Earthq. Sc.

**Distinguished Visiting Professor:**

1. Padmasri K.S. Valdiya, Hon. Prof., Jawaharlal Nehru Centre for Advanced Scientific Research, Bangalore

**Visiting Professor:**

1. Dr. JR Kayal, Former Addl. Director General Geological Survey of India
2. Prof. V.C. Thakur, Former Director Wadia Inst.Him.Geol., Dehradun
3. Dr. S.K. Biswas, Ex-Director KDMIPE, ONGC,

**Consultants:**

1. Dr. Sivram Sastry, Geophysicist, former Sc. NGRI, Hyd
2. Dr. TJ Majumdar, Geophysicist, Formerly Head, Earth Sciences & Hydrology Division, SAC-ISRO

**Staff Posted in Kachchh :**

Sr. No.	Name	Date of Birth	Educational Qualification	Date of Joining	Designation
1	Jayendra V. Jadeja, Vamka	14/01/1985	12 <sup>th</sup> passed, Computer Knowledge	12/02/2009	Lab Assistant
2	Vimal A.Parmar, Badargadh	26/05/1984	Diploma in Electrical, 2005	12/02/2009	TA
3	Shivrajsinh Jadeja, Bhachau	10/06/1975	8 <sup>th</sup> Pass	01/08/2007	Lab Assistant
4	Imran Ghanchi Desalpar	02/09/1986	B.Sc.(IT), 2008	12/02/2009	TA
5	Harpal Singh, Vamka	03/08/1981	B.A., LLB	2010	LA
6	Rajesh Gusai, Deshalpar	17/01/1992	SSC, ITI(Computers)	01/07/2011	LA
7.	Jayesh Kumar C. Darji Vamka	22/05/1990	SSC ITI (Welder)	1/8/2012	Lab Boy

**List of scientific staff that joined during 2012**

1. Gayatri Pawan Kumar (M.Sc. Phys, 2004, AU) Sc. B, 5.1.2012
2. Peush Chaudhary as JRF, M.Tech. (Applied Geophysics), K.U. Kurukshetra.
3. Sunita Sahoo as JRF (M.Sc. Geophys, Berhampur Uni., Odisha, 2012), D.o.J: 2.4.2012
4. Swagatika Dash, JRF (MSc.Geophysics, Berhampur Uni., Odisha, 2012), D.o.J: 2.4.2012
5. Sushant Kumar Sahoo, JRF (MSc.Geophys., Berhampur Uni., Odisha, 2012), D.o.J: 2.4.2012

6. Sikha Swarupa Mishra as JRF (MSc.Geophysics, Berhampur Uni., Odisha, 2012), D.o.J: 2.4.2012
12. S.Venkateswara rao, M.Sc. Geophysics from Osmania University, 2007. Did Seismic Surveys in Oil Industry for 5 yr (joined as Senior Geophysicist on 04/06/2012)
14. Miss Jayashree Bannerjee, M.Sc. Geoph, ISM, Dhanbad, JRF, 10.6.2012
15. Gajendra Prasad, M.Sc. Tech Applied Geophysics, ISM, Dhanbad, JRF, 30.06.2012
17. Miss Meenakshi Rawat, B.Tech. (Geosciences, 2011) University of Petroleum and Energy Studies, Dehradun, Geologist, joining date 4/7/2012.
19. Mr. Vinay Kumar Dwivedi, Bundelkhand University, M.Sc. Geol., JRF, 21.07.2012
20. Miss Purnima Singh, M.Sc. (Geol. 2011) MS Univ. Baroda, joined as Geologist on 20th Aug 2012.
21. Mr. Kuntal Bhukta, M.Sc. App. Geophy., ISM Dhanbad joined as JRF on 3.9.2012.
22. Ms. Jayshri Solanki M.Sc. (Geomatics, 2012) CEPT Univ. joined as JRF on 4.9.2012.
23. Ms. Drasti Gandhi, (M.Sc. Geology, 2012) M.G. Sci., A'bad as JRF on 18.9.2012
24. Ms. Parnavi Prajapati, M.Sc. (Geology, 2012) M.G. Sci., A'bad as JRF on 18.9.2012
25. Dilip Kumar Halder, As R.A. (M.Sc. Phys. 2007, Kolkata), 1.10.2012
26. Deepali Gadkari, As Visiting Fellow, 1.10.2012
27. Siddharth Prizomwala, (M.Sc. Geology 2008) M.S.U., Geophysicist, DOJ 8.10.12
28. Mr. C. Prasanna Simha, M.Sc. (Physics), 2005, First Class, Sri Venkateswara Uni., A.P. having 5 yrs experience in R&D in Indian Institute of Meteorology (IITM), Pune & ACRHEM, Uni. of Hyderabad joined ISR as Project Scientist (ISRO-II Project) with monthly remuneration of Rs.18,000/- on November 6, 2012 in CAL-VEL Project of ISRO-SAC.

#### **LIST OF STAFF THAT RESIGNED FROM ISR DURING 2012**

Geologist/Geophysicist who resigned

1. Mr. Srichand Prajapati, M.Sc. Geophy, BHU (resigned 9.5.2012), joined a US Univ.
2. Surya Prakash, M.Sc. Geol. Bundelkhand Univ. (joined 15.6.2010 resigned 5.4.2012)
3. Kiran Kumar Madari, M.Sc. Geophy, OU, 19.4.2010 to 11.5.2012
4. Mr. Kishansinh L. Zala, M. Sc. Physics, Bhavnagar Uni., 2006 (6.9.2008 to 4.6.2012) selected in Guj. Civil Service
5. Mr. Prabhin Sukumaran, M.Sc Applied Geology from ISM Dhanbad, 2006 (Joined 16.3. 2011 Resigned 19.7. 2012) Joined as Ass. Professor in Charusat Univ., Changa.
6. Tarak Shah Mr. Tarak Shah, M.Sc. Phys. 2006, JRF (Joined 2.3.2009 Resigned 25.7.2012)
7. Mr. V. Gopala Rao, Geophysicist (16.12.2009 to 23.11.2012), got regular job in Survey of India, Hyderabad.
8. Mr. Ashish Bhandari, M. Sc. Geology, MSU (joined 1.7.2010 resigned 29.11.2012) got Geologist post in GSI.



9. Monica Wadhawan, JRF, M.Sc. Tech Geophys., KU, DoJ 28.9.2011 DoR 22.12.2012, joined WIHG

**JRF who resigned**

1. Mr. Libu Jose, M. Sc. Geol. AU (joined 13.7.2011 resigned 26.1.2012). He is selected in ONGC
2. Miss Sachi Rana, M.Sc. Geomatics, CEPT Univ., JRF resigned from March 20, 2012
4. Mr. Suresh Kumar, M.Sc. Tech. Geophysics, Kurukshetra Univ. (Joined 2.1.2012 resigned 4.8.2012), joined Tojo-Vikas Exploration Co.
5. Sadanad Chaurasia, M.Sc. Geoph, ISM, Dhanbad,2011 JRF (Joined 10.6.2012 Resigned 6.11.2012)
6. Miss Chinmayee Sahoo MSc. Geophys. Berhampur Univ., 2012 (Joined 2.4.2012 resigned 7.11.2012) Got JRF at WIHG.
7. Mr. Mohar Singh, JRF, M.Sc. Remote Sensing and GIS (DoJ 29.9.2010 DoR 31.12.2012)

**Tech. Asstt. who resigned**

1. Sandip Parmar, DEC, (joined 16.1.2007 resigned 5.10.2012), got post of Sc. Asstt., in Guj. Irrigation Dept.

NOTE: There is large attrition as every year 15-20 no. scientific staff is leaving as ISR does not pay respectable salary. During 2012 no. of scientific staff members is 48 (30Sc. and 18 JRF), out of which 28 are employed during current year only. Hence, there is lack of experienced staff.

Year of joining	No. of Sc./ JRF still at ISR from that year of joining	Attritions during the year
2006	4	-
2007	5	4
2008	2	7
2009	4	19
2010	3	20
2011	4	13
2012	28	14

# CHAPTER 12

## PUBLICATIONS

### 12.1 Books/Chapters:

- i. Editing of special issue of the journal Natural Hazard (It is based on the papers presented in ISR Intl. Symp. held in Jan2011).
- ii. Structure and Tectonics of the Andaman Subduction Zone from modeling of Seismological and Gravity data (accepted in In Tech- Open Access Publisher) authors: Purnachandra Rao, Nagabhushana Rao, Pinki Hazarika, Virendra Tiwari, Ravi Kumar and Arun Singh. Book Titled: New Frontiers in Tectonic Research – General Problems, sedimentary Basins and Island Arcs.

### PUBLICATIONS OF ISR During 2006-2012 March

1	PhD	6
2	Chapters in Books	1
2	SCI Research Papers	67
3	Non-SCI Research Papers	15
3	Symp. Proceedings	17
4	Articles/Lecture Notes	6
4	Tech. Reports	67
5	Abstracts/Papers Presented in Sem.	113
6	Invited Lectures	31
7	Keynote Addresses	6
	Total	329

### PUBLICATIONS (Year wise)

Year	No of Papers Published		Reports	Abstracts	PhD	Total
	SCI	Others				
2006	4	5	5	9		23
2007	3	5	10	16	1	35
2008	7	11	15	7		40
2009	6	3	11	9	3	32
2010	9	5	19	33	1	67
2011	17	7	13	51		88
2012	18	6	9	60	1	97
2013 (part)	13					
Total	77	42	82	185	6	392

No. of SCI Papers Published by ISR Scientist. 1 <sup>st</sup> author (co-author)										
S N	Name	2006	2007	2008	2009	2010	2011	2012	2013	Total
1	B.K. Rastogi	2(1)		(5)	(3)	(6)	1(6)	7(7)	5	10(28)
2	Sumer Chopra			2(1)	(2)	2(2)	2(2)	2(3)	2	10(10)
3	RBS Yadav			1(1)	2	1(2)	4(1)	1(5)		9(9)
4	A.P.Singh		1		(1)	(2)	2(5)	3	1	7(10)

No. of SCI Papers Published by ISR Scientist. 1 <sup>st</sup> author (co-author)										
S N	Name	2006	2007	2008	2009	2010	2011	2012	2013	Total
5	Babita Sharma		1	1	1	1	1			5
6	G.C. Kothiyari					1(2)	(1)	1(2)		3(5)
7	RK Jaiswal			1	1		1	1		4
8	Falguni Bhattacharya								2	2
8	Srichand Prajapati						2(1)			2(1)
9	Prabhin Sukumaran							2		2
10	Pallabee Choudhury						(2)	1(6)		1(7)
11	B. Sairam			(1)			1(1)			1(2)
12	Kapil Mohan			(1)	(1)		1			1(2)
13	K.M. Bhatt			1						1
14	F. Bhattacharya								2	2
15	Santosh Kumar			(3)		(1)	(1)	1(4)		(9)
16	Sandeep Aggarwal						(1)	(2)		(3)
17	K.M. Rao			(2)						(2)
18	MS Gadhavi		(1)	(1)						(2)
19	Arun K. Gupta					1		1		2
20	Prabhin Sukumaran							2		2
21	Nagabhushan Rao								1	1

First author (coauthor)

#### IMPACT FACTOR OF SCIENTIFIC CITATION INDEX (SCI) PAPERS BY ISR

Journal		IF	Total IF
Bull. Seism.Soc.Am.	3	2.313	6.939
Current Sc. India	5	0.897	4.485
Geophys. J. Intl.	1	2.353	2.353
Gondwana Res.	1	5.503	5.503
Intl. J. Remote Sensing	2	1.182	2.364
J. Asian Earth Sc.	6	2.215	6.645
J. Geol. Soc. In.	9	0.673	4.038
J Earth System Sc (Proc. Ind. Ac. Sc.)	1	0.941	0.941
J. Seismol.	3	0.673	1.919
Marine Geodesy	1	1.053	1.053
Marine Geophy Res	1	0.729	0.729
Marine Geol.	1	0.702	0.702
Natural Hazards	16	1.398	22.268
Pure & Appl. Geophys	9	0.938	8.442
Seismo. Res. Letters	5	1.826	9.130
Soil Dynamics and Eq. Engg.	1	1.01	1.01
Tectonophysics	4	2.509	10.036
Zeitschrift fur Geomorphologie	2	0.477	0.477
Total	71		98.175

## 12.2 Papers Published in Scientific Citation Index (SCI) Journals

SN	Authors	Year	Title	Details
1	Naveenchandra N. Srivastava, Rita U. Thakor, Sejal V. Patel, Sejal G. Viroja, Urvi S. Chetta and Shashikant A. Sharma.	2006	Construction of Beachball Diagram using Java-based Software Application "Dishansh 2005".	Seismological Res. Letts., 77 (5), 550-554. [Impact Factor 1.826]
2	Rastogi, B.K.	2006	Seminar on Paleoseismology and Active Faults in Gujarat (Notes).	J. Geol. Soc. In., 68, 1116-1118. [Impact Factor 0.673]
3	Rastogi, B.K.	2006	Seminar on "Seismology in India (Notes).	J. Geol. Soc. In.69, 1375-1376. [Impact Factor 0.673]
4	Ugalde, A., J.N. Tripathi, M. Hoshiba and B.K. Rastogi.	2006	Intrinsic and scattering attenuation in western India from aftershocks of the 26 January, Kachchh earthquake.	Tectonophysics, 429(1-2), 111-123. [Impact Factor 2.509]
5	Karanth R. V., and Gadhavi M. S.	2007	Structural Intricacies: Emergent Thrusts and Blind Thrusts of Central Kachchh, Western India.	Current Science, 93(9), 1271-1280. [Impact Factor 0.897]
6	Sharma, B., S. S. Teotia and Dinesh Kumar.	2007	Attenuation of P, S, and coda waves in Koyna Region, India.	J. Seism., 11, 327-344. [Impact Factor 0.673]
7	Singh, A. P., U. C. Mohanty, M. Mandal, and P. Sinha.	2007	Impact of different land surface processes on Indian summer monsoon circulations.	Natural Hazards, 42(2), 423-438. [Impact Factor 1.398]
8	Bhatt, Kaushalendra Mangal, Andreas Hordt and Santosh Kumar.	2008	Seismicity analysis of the Kachchh aftershock zone and tectonic implication for 26 Jan 2001 Bhuj earthquake.	Tectonophysics, 465, 75-83. [Impact Factor 2.509]
9	Chopra, Sumer, K. Madhusudhan Rao, B. Sairam, Santosh Kumar, A.K. Gupta, Hardik Patel, M.S. Gadhavi and B.K.Rastogi.	2008	Earthquake Swarm Activities after Rains in Peninsular India and a Case Study from Jamnagar.	J. Geol. Soc. In., 72, 245-252. [Impact Factor 0.673]
10	Chopra, Sumer, R. B. S. Yadav, Hardik Patel, Santosh Kumar, K. M. Rao, and B. K. Rastogi, Abdul Hameed and Sanjay Srivastava.	2008	The Gujarat (India) Seismic Network.	Seismological Research Letters (79) 6, 806-815. [Impact Factor 1.826]
11	Jaiswal, R.K., B.K. Rastogi, Tad Murthy.	2008	Tsunamigenic sources in the Indian Ocean.	J. Science of Tsunami Hazards, 27(2), 32-50.
12	Joshi, A., and K. Mohan.	2008	Simulation of accelerograms from simplified deterministic approach for the 23 <sup>rd</sup> October 2004 Niigata-ken Chuetsu, Japan earthquake.	J. Seismology., 12, No.1, 35-51. [Impact Factor 0.673]
13	Sharma, B, Arun K Gupta, Kameswari Devi, Dinesh Kumar, SS Teotia and BK Rastogi	2008	Attenuation of high frequency seismic waves in Kachchh Region, Gujarat, India	Bull. Seism. Soc. Am., 98 (5), 2325-2340 [Impact Factor 2.027]
14	Yadav R.B.S., J.N. Tripathi, B.K. Rastogi and S. Chopra.	2008	Probabilistic assessment of earthquake hazard in Gujarat and adjoining region, India.	Pure and Applied Geophysics, 165, 1813 – 1833. [Impact Factor 0.938]



SN	Authors	Year	Title	Details
15	Jaiswal, R.K., A. P. Singh and B. K. Rastogi.	2009	Simulation of the Arabian Sea Tsunami propagation generated due to 1945 Makran Earthquake and its effect on Western parts of Gujarat (India).	Natural Hazards, 48(2), 245-258. [Impact Factor 1.398]
16	Joshi, A. and Mohan, K.	2009	Expected peak ground acceleration in Uttarakhand Himalaya, India region from a deterministic hazard model.	Natural Hazards, 52, 299-317. [Impact Factor 1.398]
17	Rajesh S. and Majumdar T.J.	2009	Geoid height versus topography of the northern Ninetyeast Ridge: implications on crustal compensation.	Mar Geophy Res, 30(4), 251-264. [Impact Factor 0.729]
18	Sharma, Babita, S. S. Teotia, Dinesh Kumar and P.S.Raju.	2009	Attenuation of P and S waves in the Chamoli region, Himalaya, India.	Pure and Applied Geophysics, 166, 1949-1966 [Impact Factor 0.938]
19	Yadav, R.B.S., P. Bormann, B.K. Rastogi, M.C. Das and S. Chopra	2009	A homogeneous and complete earthquake catalogue for northeast India and the adjoining region.	Seismological Research Letters, 80(4), 609-627. [Impact Factor 1.826]
20	Yadav R.B.S., J. N. Tripathi, B. K. Rastogi, M. C. Das and S. Chopra.	2009	Probabilistic assessment of earthquake recurrence in Northeast India and adjoining region.	Pure and Applied Geophysics, 167(11), 1331-1342. [Impact Factor 0.938]
21	Bormann, P. and R. B. S. Yadav	2010	Reply to Comments of R. Das and H. R. Wason on "A Homogeneous and Complete Earthquake Catalog for Northeast India and the Adjoining Region.	Seismological Research Letters, 81 (2), 215 – 220. [Impact Factor 1.826]
22	Chopra, Sumer, K.M. Rao and B.K. Rastogi	2010	Estimation of Sedimentary Thickness in Kachchh Region by Converted Phases	Pure and Applied Geophys. 167 (2010), 1247–1257 [Impact Factor 0.938]
23	Chopra Sumer, Dinesh Kumar and B.K. Rastogi.	2010	Estimation of Strong Ground Motions for 2001 Bhuj (Mw 7.6), India Earthquake.	Pure and Applied Geophysics, 167(11), 1317-1330. [Impact Factor 0.938]
24	Gupta, Arun.	2010	A note on 2 <sup>nd</sup> Asia Workshop on Superconducting Gravimetry.	J. Geol. Soc. In., 76, 301. [Impact Factor 0.673]
25	Joshi, M., Kothiyari, G. C., Ahluwalia, A. D. and Pant. P. D	2010	Neotectonic Evidences of Rejuvenation in Kaurik Change Fault zone, Northwestern Himalaya.	Journal of Geog. Infor. Syst. 2, 176-183
26	Joshi, M. and Kothiyari, G. C	2010	Assessment of Tectonic activity in a seismically locked segment of Himachal Himalaya,	International journal of Remote Sensing, 31 (3), 681-689. [Impact Factor 1.182]
27	Kothiyari, Girish Ch., P. D. Pant, Moulisree Joshi, Khayingshing Luirei and Jawed N Malik.	2010	Active Faulting and Deformation of Quaternary Landforms, Sub-Himalaya, India.	Geochronometica, 37, 63-71.
28	Srikanth, T., R. Pradeep Kumar, A.P. Singh, B.K. Rastogi and Santosh Kumar.	2010	Earthquake Vulnerability Assessment of Existing Buildings in Gandhidham and Adipur Cities Kachchh, Gujarat (India).	European Journal of Scientific Research, 41(3), 336-353.

SN	Authors	Year	Title	Details
29	Yadav R.B.S., D. Shanker, S. Chopra, and A. P. Singh.	2010	An application of regional time and magnitude predictable model for long-term earthquake prediction in the vicinity of October 8, 2005 Kashmir Himalaya earthquake.	Natural Hazard, 54(3), 985-1014. [Impact Factor 1.398]
30	Aier, I., Luirei, K., Bhakuni, S. S., Thong, G. T., and Kothiyari, G. C.	2011	Geomorphic evolution of Medziphema intermontane basin and Quaternary deformation in the schuppen belt, Nagaland, NE India.	Zeitschrf fur Geomorphologie, 55, 247-265. [Impact Factor 0.477]
31	Chopra Sumer, Dinesh Kumar and B.K.Rastogi.	2011	Attenuation of high frequency P and S waves in the Gujarat Region, India.	Pure and Applied Geophysics, 168 (5), 797-813. [Impact Factor0.938]
32	Chopra, S. and Choudhury, P.	2011	A study of response spectra for different geological conditions in Gujarat, India.	Soil Dynamics and Earthquake Engineering, 3, 1551-5164. [Impact Factor 1.01]
33	Jaiswal, R. K., Singh, A.P., Rastogi, B. K., and Murty, T.	2011	Aftershock sequences of two great Sumatran earthquakes of 2004 and 2005 and simulation of the minor tsunami generated on September 12, 2007 in the Indian Ocean and its effect.	Natural Hazards, 57(1), 7-26. [Impact Factor 1.398]
34	Mohan,K. and Joshi, A.	2011	Role of attenuation relationship in shaping the seismic hazard.	Natural Hazards 60, 649-670. [Impact Factor 1.398]
35	Patel, V.M., H.S Patel and A.P Singh.	2011	Comparative Study of Earthquake and Tsunami Loading on Vertical Evacuation Structure at Dwaraka.	International Journal of Earth Science and Engineering, 4(4), 659-668
36	Prajapati, S., Chauhan, M., Gupta, A. K., Pradhan, R., Suresh, G., and Bhattacharya, S. N.	2011	Shield-Like Lithosphere of the Lower Indus Basin Evaluated from Observations of Surface-Wave Dispersion.	Bull. Seism. Soc. Am, 101, 859-865. [Impact Factor 2.313]
37	Prajapati, S., Suresh, G., and Bhattacharya, S. N.	2011	Crustal Structure of the northwestern deccan Volcanic Provinces, India and Adjoining Continental Shelf through Inversion of Observed Surface Wave Dispersion.	Bulletin of the Seismological Society of America, 101(4), p 1106-1113. [Impact Factor 2.027]
38	Rastogi, B. K., Singh, A. P., Sairam, B., Jain, S. K., Kaneko, F., Segawa, S., and Matsuo, J.	2011	The Possibility of Site Effects: The Anjar Case, following Past Earthquakes in Gujarat, India.	Seismological Research Letters 82, 59-68. [Impact Factor 2.317] [Impact Factor 1.826]
39	Sairam,B, Rastogi, B.K., Aggarwal,S.,Chauhan,M., and Bhonde, U.	2011	Seismic site characterization using Vs30 and site amplification in Gandhinagar region, Gujarat, India.	Current Science, 100(5), 754-761. [Impact Factor 0.897]
40	Sharma, Babita, Dinesh Kumar, S. S. Teotia, B. K. Rastogi, Arun K. Gupta and Srichand Prajapati.	2011	Attenuation of Coda Wave in the Saurashtra Region, Gujarat India.	Pure Appl. Geophys, 169, 89-100. [Impact Factor0.938]
41	Singh, A. P., Mishra, O., Rastogi, B. K., and Kumar, D.	2011	3-D seismic structure of the Kachchh, Gujarat, and its implications for the earthquake hazard mitigation	Natural Hazards 57(1), 1-23. [Impact Factor 1.398]

SN	Authors	Year	Title	Details
42	Singh, A. P., R. P. Singh, P.V. S. Raju and R. Bhatla.	2011	The impact of three different cumulus parameterization schemes on the Indian summer monsoon circulation.	International Journal of Ocean and Climate Systems, 21(1), 27-44.
43	Yadav, R. B. S., E. E. Papadimitriou, V. G. Karakostas, D. Shanker, B. K. Rastogi, S. Chopra, A.P. Singh and Santosh Kumar.	2011	The 2007 Talala, Saurashtra, western India earthquake sequence: Tectonic implications and seismicity triggering.	Journal of Asian Earth Sciences, 40(1), 303-314. [Impact Factor 2.215]
44	Yadav, R. B. S., Bayrak, Y., Tripathi, J. N., Chopra, S, Singh, A. P and Bayrak, E.	2011	A Probabilistic Assessment of Earthquake Hazard Parameters in NW Himalaya 2 and the Adjoining Regions.	Pure and Applied Geophysics, 169(2), 1619-1639, DOI 10.1007/s00024-011-0434-8. [Impact Factor 0.938]
45	Yadav, RBS, V.K. Gahalaut, Sumer Chopra and Bin Shan	2011	Tectonic Implications and Seismicity Triggering During the 2008 Baluchistan, Pakistan Earthquake Sequence	Journal of Asian Earth Science, 45, 167-178, DOI 10.1016/j.jseas.2011.10.003 [Impact Factor 2.215]
46	Yadav, R.B.S., J.N.Tripathi, B.K.Rastogi, M.C.Das and Sumer Chopra	2011	Probabilistic assessment of earthquake recurrence in northeast India and adjoining regions	Pure and Applied Geophysics, DOI 10.1007/s00024-010-0105-1, 56, 145-167 [Impact Factor 0.938]
47	Chopra, Sumer, Dinesh Kumar, Pallabee Choudhury and R.B.S.Yadav.	2012	Stochastic Finite Fault Modeling of Mw 4.8 Earthquake in Kachchh, Gujarat, India.	J. Seismology, 16(3), 435-449. [Impact Factor 0.673]
48	Chopra S, Kumar D, Rastogi B.K., Choudhury P, Yadav RBS.	2012	Deterministic seismic scenario in Gujarat, India.	Natural Hazards, DOI: 10.1007/s11069-011-0027-y 60(2), 517-540 [Impact Factor 1.398]
49	Gupta, Arun, Anup Sutar, Sumer Chopra, Santosh Kumar and B K Rastogi.	2012	Attenuation Characteristics of coda waves in Mainland Gujarat (India).	Tectonophys., 530, 264-271. [Impact Factor 2.509]
50	Gupta., Sandeep P. Mahesh, K. sivaram & S. S. Rai	2012	Active fault beneath the Tehri dam, Garhwal Himalaya-seismological evidence	Current Science, 103(11) [Impact Factor 0.897]
51	Jaiswal, R.K. and B.K. Rastogi	2012	Next Tsunami in India in the Arabian Sea?	J. Geophysics, 33(4), 111 - 115 [Impact Factor: 0.133]
52	Kothyari, G. C., Pant. P. D and Luirei. K.	2012	Landslides and Neotectonic Activities in the Main Boundary Thrust (MBT) zone: Southeastern Kumaun, Uttarakhand	J. Geol. Soc. In. 79, 1-10. [Impact Factor 0.673]
53	Kumar, Santosh, Sumer Chopra, Pallabee Choudhury, A.P.Singh, R.B.S. Yadav and B.K. Rastogi	2012	Ambient noise levels in Gujarat state (India) seismic network	Natural Hazards and Risk, 1-13.
54	Mahesh, P. et al. including Choudhury, P.	2012	Rigid Indian plate: constraints from GPS measurements	Gondwana Research, doi: 10.1016/j.gr.2012.01.011, 22 (3), 1068-1072 [Impact Factor 5.503]
55	Mahesh, P., Sandeep Gupta, S. S. Rai & Rajagopala Sarma	2012	Fluid driven earthquakes in the Chamoli region, Garhwal Himalaya: evidence from local earthquake tomography	Geophy.J.Int., 191, 1295-1304 doi: 10.1111/j.1365-246x.2012.05672.x [Impact Factor 2.353]

SN	Authors	Year	Title	Details
56	Phartiyal, B. and Kothiyari, G. C.	2012	Impact of Neotectonics on drainage network evolution reconstructed from morphometric indices: case study from NW Indian Himalaya	Zeitschrift für Geomorphologie, 56(1), 121-140 [Impact Factor 0.477]
57	Rastogi, BK	2012	Indo-US Workshop on Intraplate Seismicity	J. Geol. Soc. In. (NEWS AND NOTES), 79, 316-317 [Impact Factor 0.673].
58	Rastogi, BK	2012	Comments on the paper by Bilham and Gaur	Current Science Vol. 103(2), 1-2 [Impact Factor 0.897].
59	Singh A. P., O. P. Mishra, R. B. S. Yadav, and Dinesh Kumar	2012	A new Insight into Crustal Heterogeneity beneath the 2001 Bhuj Earthquake Region of Northwest India and its Implications for Rupture Initiations.	Journal of Asian Earth sciences, 48, 31-42. [Impact Factor 2.215]
60	Singh, A.P., T. S. Murty, B. K. Rastogi, and R. B. S. Yadav	2012	Earthquake generated tsunami in the Indian Ocean and probable vulnerability assessment for the east coast of India.	Journal of Marine Geodesy, 35 (1), 49-65. [Impact Factor 1.053]
61	Singh A. P., Mishra, O. P., Santosh Kumar, Dinesh Kumar, R. B. S. Yadav.	2012	Spatial Variation of the Aftershock Activity across the Kachchh Rift Basin and Its Seismotectonic Implications.	Journal of Earth System Science, 121(2), 439-451. [Impact Factor 0.941]
62	Sukumaran, Prabhin, DA Sant, K.Krishnan and Govindan Rangarajan.	2012	High resolution facies record on Late Holocene Flood plain sediments from Lower Reaches of Narmada Valley, Western India.	Journal of Geological Society of India, 79, 41-52. [Impact Factor 0.673]
63	Sukumaran, Prabhin, C. Rajshekhar, Dhananjay A. Sant and K. Krishnan	2012	Late Holocene Storm Records from Lower Reaches of Narmada Valley, western India.	J. Geol. Soc. In., 80: 403-408 [Impact Factor 0.673]. .
64	Yadav, RBS, Yusuf Bayrak, J. N. Tripathi and Sumer Chopra and E Bayrak	2012	Regional Variation of the $\omega$ -Upper Bound Magnitude of GIII Distribution in Hindukush-Pamir Himalaya and the Adjoining Regions: A Perspective on Earthquake Hazard	Tectonophysics, doi:10.1016/j.tecto.2012.03.015 [Impact Factor 2.509]
65	Bhattarchya F, Rastogi, B. K. and Kothiyari G. C.	2013	Morphometric evidences of Seismicity around Wagad and Gedi Faults. Eastern Kachchh. Gujarat.	J. Geol. Soc. In. DI-11-001891R. 81 (1), 113-121, [Impact Factor 0.673]
66	Bhattacharya, Falguni, B.K. Rastogi, Mamata Mgangom, M.G.Thakkar and R.C.Patel	2013	Late Quaternary climate and seismicity in the Katrol Hill Range, Kachchh, Western India	J Asian Earth Sciences, Vol 73 (2013) 114-120, DOI: 10.1016/j.jseaes.2013.04.030 [Impact Factor 2.215]
67	Chopra S., Kumar D., Rastogi B.K., Choudhury P., Yadav R.B.S.	2013	Estimation of site amplification functions in Gujarat region, India.	Natural Hazards, DOI: 10.1007/s11069-012-0116-6. (2013) vol. 65 (2) 1135-1155 [Impact Factor 1.398]



SN	Authors	Year	Title	Details
68	Chopra, Sumer, Dinesh Kumar, B.K.Rastogi, Pallabee Choudhury and R.B.S.Yadav	2013	Estimation of seismic hazard in Gujarat region, India	Nat Haz, DoI: 10.1007/s11069-012-0117-5 vol. 65 (2), 1157-1178 [Impact Factor 1.398].
69	Choudhury, P., Catherine, J.K., Gahalaut, V. K., Chopra, S., Dumka, R. and Roy, K. S.	2013	Post Seismic deformation associated with the 2001 Bhuj earthquake	Natural Hazard Doi: 10.1007/S11069-012-0191-8 1.398, vol 65 (2), 1109-1118. [Impact Factor 1.398]
70	Kothyari, G. C. and Juyal, N.	2013	Implication of Fossil Valleys and Associated Epigenetic Gorge in part of the Central Himalaya	<i>Current Science (U740)</i> [Impact Factor 0.79]
71	Nagabhushan Rao, Ch., Purnachandra Rao, N., Rastogi, B.K.	2013	Evidence for Right-Lateral Strike-Slip Environment in the Kutch basin of Northwestern India from Moment Tensor Inversion studies	J. Asian Earth Science, doi.org/10.1016/j.jseaes.2012.12.012, 64, 158-167 [Impact factor: 2.215]
72	Rastogi, BK	2013	Report on 2 <sup>nd</sup> International Symp. "Advances in Earthquake Sc." (AES-2013) and Intl. School on "Use of e-infrastructures for Advanced Seismic Hazard Assessment in Indian Sub-continent	J. Geol. Soc. In, 81 (5), 724-726. [Impact Factor 0.673]
73	Rastogi, B.K., J.R. Kayal and T. Harinaryana	2013	Introduction to the special volume on Bhuj earthquake	Nat Hazards, Doi10.1007/s11060-012-0431-y, vol 65 (2), 1023-1025 [Impact Factor 1.398]
74	Rastogi, B.K., Santosh Kumar, and Sandeep Kumar Aggrawal.	2013	Seismicity of Gujarat	Natural Hazard, DOI 10.1007/s11069-011-0077-1. (2013) vol 65 (2), 1027-1044. [Impact Factor 1.398]
75	Rastogi, B. K., Sandeep Kumar Aggrawal, Nagabhushan Rao and Pallabee Choudhury.	2013	Triggered/migrated seismicity due to the 2001 M <sub>w</sub> 7.6 Bhuj earthquake, Western India	Nat. Hazard, DOI 10.1007/s11069-011-0083-3, (2013) vol 65 (2), 1085-1107. [Impact Factor 1.398]
76	Rastogi B.K., Santosh Kumar, Sandeep Kumar Aggrawal, Kapil Mohan, Nagabhushan Rao, N. Purnachandra Rao and Girish Chandra Kothyari	2013	The October 20, 2011 Mw 5.1 Talala Earthquake in the Stable Continental Region of India	Nat. Haz. DOI: 10.1007/s11069-012-0226-1, (2013) vol 65 (2), 1197-1216.[Impact Factor 1.398]
77	Singh, A.P., O.P. Mishra, B. K. Rastogi & Santosh Kumar	2013	Crustal heterogeneities beneath the 2011 Talala, Saurashtra earthquake, Gujarat, India source zone: Seismological evidence for neo-tectonics	<i>Journal of Asian Earth sciences, DOI:10.1016/j.jseaes.2012.11.017.</i> 62, 672 – 684 [Impact Factor 2.215]

### Research Papers Published in SCI Journals during 2012-13 (in list form):

Note: Some papers published during 2012 were listed in 2011-12 Annual report. However, these are again given here to make a complete calendar-year list.

1. Chopra, Sumer, Dinesh Kumar, Pallabee Choudhury and R.B.S.Yadav (2012), Stochastic Finite Fault Modeling of Mw 4.8 Earthquake in Kachchh, Gujarat, India, *Journal of Seismology*, DOI 10.1007/s10950-012-9280-0, **16**(3), 435-449 [Impact Factor 0.673].
2. Chopra S, Kumar D, Rastogi BK, Choudhury P, Yadav RBS, (2012), Deterministic seismic scenario in Gujarat, India. *Natural Hazards*, DOI: 10.1007/s11069-011-0027-y. **60** (2), 517- 540 [Impact Factor 1.398]
3. Gupta, Arun, Anup Sutar, Sumer Chopra, Santosh Kumar and B K Rastogi (2012), Attenuation Characteristics of coda waves in Mainland Gujarat (India), *Tectonophysics*, **530**, 264-271 [Impact Factor 2.509].
4. Gupta, Sandeep, P. Mahesh, K. Sivaram and S. S. Rai (2012). Active fault beneath the Tehri dam, Garhwal Himalaya- First seismological evidence, *Current Science* Vol. **103**(11).
5. Jaiswal, R.K. and B.K. Rastogi (2012) Next Tsunami in India in the Arabian Sea? *Jour. of Geophysics*, Oct. 2012, Vol.**33**(4), 111 - 115, [Impact Factor: 0.133]
6. Kothiyari, G. C. Pant P.D., and Luirei, K. (2012). Landslides and Neotectonic activity in Main Boundary Thrust (MBT) zone, Southern Kumaun Himalaya. *J. Geol. Soc. In. DI-10-60165R2*, V. **79**, PP1-10 [Impact Factor 0.673].
7. Kumar, Santosh, Sumer Chopra, Pallabee Choudhury, A.P.Singh, R.B.S. Yadav and B.K. Rastogi (2012). Ambient noise levels in Gujarat state (India) seismic network, *Natural Hazards and Risk*, I.1-13, **3**, 342-354.
8. Mahesh, P., J.K. Catherine, V.K. Gahalaut, Bhaskar Kundu, A. Ambikapathy, Amit Bansal, L. Premkishore, M. Narsaiah, Sapna Ghavri, R.K. Chadha, Pallabee Choudhary, D.K. Singh, S.K. Singh, Subhash Kumar, B. Nagarajan, B.C. Bhatt, R.P. Tiwari, Arun Kumar, Ashok Kumar, Harsh Bhu and S. Kalita (2012) Rigid Indian plate: Constraints from GPS measurements, *Gondwana Research*, doi:10.1016/j.gr.2012.01.011 **22** (3), 1068-1072 [Impact factor 5.503].
9. Mahesh, P., Sandeep Gupta, S. S. Rai & Rajagopala Sarma (2012). Fluid driven earthquakes in the Chamoli region, Garhwal Himalaya: evidence from local earthquake tomography, *Geophy. J. Int*, doi: 10.1111/j.1365-246x.2012.05672.x, **191**, 1295-1304 [Impact factor 2.353].
10. Phartiyal, B., Kothiyari, G.C., (2012). Impact of Neotectonics on drainage network evolution reconstruction from morphometric indeces: case study from NW Indian Himalaya. *Zeitschrift fur Geomorphologie* Vol **56**(1), 121-140.
11. Rastogi, BK (2012). Indo-US Workshop on Intraplate Seismicity, *J. Geol. Soc. In. (NEWS AND NOTES)*, **79**, 316-317 [Impact Factor 0.673].
12. Rastogi, BK (2012) Comments on the paper by Bilham and Gaur, *Current Science* Vol. **103**(2), 1-2 [Impact Factor 0.897].
13. Singh A. P., O. P. Mishra, R. B. S. Yadav, Dinesh Kumar (2012) A New Insight into Crustal Heterogeneity beneath the 2001 Bhuj Earthquake Region of Northwest India and its Implications for Rupture Initiations, *Journal of Asian Earth sciences*, **48**, 31-42 [Impact Factor 2.215]

14. Singh, A.P., T. S. Murty, B. K. Rastogi, and R. B. S. Yadav (2012) Earthquake generated tsunami in the Indian Ocean and probable vulnerability assessment for the east coast of India. *Journal of Marine Geodesy*, **35** (1), 49-65
15. Singh, A.P., Mishra, O. P. and Santosh Kumar (2012). Spatial variation of aftershocks activity across the Kachchh rift Basin and its Seismotectonic Implications. *Jr. Earth System Sciences*, **121**(2), 439-451 [Impact Factor 0.941]
16. Sukumaran, Prabhin, D.A Sant, K.Krishnan and Govindan Rangarajan (2012), High resolution facies record on Late Holocene Flood plain sediments from Lower Reaches of Narmada Valley, Western India. *Journal of Geological Society of India*, **79**, 41-52 [Impact Factor 0.673]
17. Sukumaran, Prabhin, C. Rajshekhar, Dhananjay A. Sant and K. Krishnan (2012) Late Holocene Storm Records from Lower Reaches of Narmada Valley, western India. *Journal of Geological Society of India*, **80**: 403-408 [Impact Factor 0.673].
18. Yadav, R. B. S., Bayrak, Y., Tripathi, J. N., Chopra, S, Singh, A. P. and Bayrak, E. (2012) A Probabilistic Assessment of Earthquake Hazard Parameters in NW Himalaya 2 and the Adjoining Regions. *Pure and Applied Geophysics* DOI 10.1007/s00024-011-0434-8, vol. **169**, 1619-1639 [Impact Factor 0.938]
19. Bhattacharya F., Rastogi, B. K. and Kothiyari G. C. (2013) Morphometric evidences of Seismicity around Wagad and Gedi Faults. Eastern Kachchh. Gujarat. J. Geol. Soc. In., DI-11-001891R., **81** (1), 113-121, [Impact Factor 0.673]
20. Bhattacharya, Falguni, B.K. Rastogi, Mamata Mgangom, M.G.Thakkar and R.C.Patel (2013) Late Quaternary climate and seismicity in the Katrol Hill Range, Kachchh, Western India", *J Asian Earth Sciences*, Vol. **73** (2013)114-120, DOI: 10.1016/j.jseaes.2013.04.030.
21. Chopra, Sumer, Dinesh Kumar, B.K.Rastogi, Pallabee Choudhury and R.B.S.Yadav (2013), Estimation of site amplification functions in Gujarat region, India, *Nat Haz*, DOI: 10.1007/s11069-012-0116-6 (2013) vol. **65** (2) 1135-1155 [Impact Factor 1.398].
22. Chopra, Sumer, Dinesh Kumar, B.K.Rastogi, Pallabee Choudhury and R.B.S.Yadav (2013), Estimation of seismic hazard in Gujarat region, India, *Nat Haz*, DoI: 10.1007/s11069-012-0117-5 (2013) vol. **65** (2), 1157-1178 [Impact Factor 1.398].
23. Choudhury, Pallabee, J. K. Catherine, V. K. Gahalaut, Sumer Chopra, Rakesh Dumka, Ketan S. Roy (2013). Post-seismic deformation associated with the 2001 Bhuj earthquake *Natural Hazards*, doi:10.1007/s11069-012-0191-8, vol **65** (2), 1109-1118 [Impact Factor 1.398].
24. Kothiyari G. C. and Juyal N. (2013). Implication of Fossil Valleys and Associated Epigenetic Gorge in Parts of the Central Himalaya. *Current Science (U740)* [Impact Factor 0.79].
25. Nagabhushana Rao, Ch., Purnachandra Rao, N., Rastogi, B.K. (2013). Evidence for Right-Lateral Strike-Slip Environment in the Kutch basin of Northwestern India from Moment Tensor Inversion studies. *J Asian Earth Science*, doi.org/10.1016/j.jseaes.2012.12.012, **64**, 158-167 [Impact factor: 2.215]
26. Rastogi, B.K. (2013). Report on 2<sup>nd</sup> International Symp. "Advances in Earthquake Sc." (AES-2013) and Intl. School on "Use of e-infrastructures for Advanced Seismic Hazard Assessment in Indian Sub-continent", *J. Geol. Soc. In*, **81** (5), 724-726.

27. Rastogi, B.K., J.R. Kayal and T. Harinaryana, (2013) Introduction to the special volume on Bhuj earthquake, *Nat Hazards*, Doi10.1007/s11060-012-0431-y (2013) vol **65** (2), 1023-1025 [Impact Factor 1.398]
28. Rastogi B.K., Santosh Kumar, Sandeep Kumar Aggrawal, (2013), Seismicity of Gujarat, *Natural Hazard*, DOI 10.1007/s 11069-011-0077-1, **65**(2), 1027-1044 [Impact Factor 1.398]
29. Rastogi, B. K., Sandeep Kumar Aggrawal, Nagabhushan Rao and Pallabee Choudhury (2013), Triggered/migrated seismicity due to the 2001  $M_w$ 7.6 Bhuj earthquake, Western India, *Natural Hazards*, DOI 10.1007/s11069-011-0083-3, **65** (2), 1085-1107 [Impact Factor 1.398].
30. Rastogi B.K., Santosh Kumar, Sandeep Kumar Aggrawal, Kapil Mohan, Nagabhushan Rao, N. Purnachandra Rao and Girish Chandra Kothyari (2013) The October 20, 2011  $M_w$  5.1 Talala Earthquake in the Stable Continental Region of India. *Nat. Haz.* DOI: 10.1007/s11069-012-0226-1, **65**(2), 1197-1216 [Impact Factor 1.39]
31. Singh, A.P., Mishra, O. P. B. K. Rastogi & Santosh Kumar (2013).Crustal heterogeneities beneath the 2011 Talala, Saurashtra earthquake, Gujarat, India source zone: Seismological evidence for neo-tectonics. *Journal of Asian Earth sciences*, DOI: 10.1016/j.jseaes.2012.11.017. volume **62**, year, pp. 672 – 684 [Impact Factor 2.215].

#### SCI Accepted

1. Pavankumar, G and Manglik, A. (2012)Electrical anisotropy in Main Central Thrust Zone of Sikkim Himalaya: Inferences from anomalous MT phases, *J. A. Earth Sci.* (Accepted)
2. Prajapati, Srichand, G. Suresh and S. N. Bhattacharya (2012), The Himalayan foreland basin crust (*accepted-BSSA*)
3. Manglik, A , Pavankumar, G and S.Thiagarajan (2012) Transverse tectonic features in the Sikkim Himalaya : a magnetotelluirc (MT) study (accepted in tectonophysics)

#### SCI Communicated

1. Bhattacharya, Falguni, B.K. Rastogi, Mamata Mgangom, Mahesh Thakkar, R.C. Patel “Late Quaternary climate & tectonic reconstruction based on channel fill deposits in the Katrol Hill Range, Kachchh, Western India. (JAES).
2. Dumka, R.K., B.S. Kotlia, Sridevi Jade, Kireet Kumar and L. M. Joshi, “GPS (Global Positioning System) derived Crustal Deformation study in Kumaun Himalaya, India, *Journal of Mountain Sciences*.
3. Joshi, Vishwa, Sandeep Aggarwal, Ombehari Srivastav, B. K. Rastogi (2012) Evaluation and comparison of the crustal structure of the Indus block up to Kutch region and Saurashtra region using GA inversion of surface-wave dispersion, *J. Seismo*
4. Kothyari et al. Surface Deformation Zone of Active North Wagad Fault in Kachchh Rift Basin, Gujarat: Constraints from Geological and Geophysical observations, which has been submitted for possible publication in BSSA.
5. Kothyari, G.C. and Navin Juyal, “Implications of Fossil Valleys and Associated Epigenetic Gorges in parts of the Central Himalaya, *Current Science*.



6. Kumar, Santosh, Dinesh Kumar and B.K. Rastogi “Source Parameters and Scaling Relations for small earthquakes in the Kachchh Region of Gujarat, India.” Natural Hazard.
7. Pavankumar, G., Manglik, A. and Thiagarajan, S. (2012) Crustal Geoelectric structure of Sikkim and adjoin Ganga Foreland basin using magnetotellurics , *Geophy. J. Int.* (under review)
8. Rana, Naresh, Falguni Bhattacharya, N. Basavaiah, R.K. Pant and Navin Juyal, “ Soft sediment deformation structures and their implications towards the Late Quaternary seismicity around the South Tibetan Detachment System, Uttarakhand, Himalaya” . Tectonophys
9. Rao, K.M., M. Ravikumar, Arun Singh and B.K.Rastogi “Shear wave splitting beneath the Northwestern Deccan Volcanic Province: Evidences for lithospheric and APM related strain”, (Under Review, Journal of Geophysical Research (JGR)).

### 12.3 RESEARCH PAPERS IN NON-SCI JOURNALS

1. A. Magrin, A. Peresan, F. Vicari, S. Kozzini, B.K. Rastogi, I.A. Parvez, G.F. Panza (2012) Definition of seismic and tsunami hazardscenarios by exploiting EU-Indo Grid e-infrastructures, Proceedings of Science, The International Symposium on Grids and Clouds (ISGC), Feb 26-March 2, 2012, Paper No. 030, pp., 1-12.
2. Rastogi, B. K., Choudhury, R. Dumka, K. M. Sreejith, and T. J. Majumdar (2012), Stress pulse migration by viscoelastic process for long-distance delayed triggering of shocks in Gujarat, India, after the 2001  $M_w$  7.7 Bhuj earthquake, in *Extreme Events and Natural hazards: The Complexity Perspective*, Geophys. Monogr. Ser., vol. 196, edited by A.S. Sharma et al. 63-73, AGU, Wahington, D. C., DOI: 10. 1029/2011GM001061.
3. Rastogi, BK (2012). Earthquake mechanism, seismic waves, parameters, strong motion, effects, and hazards, DST-SERC School on Seismo-Electromagnetics, RBS College, Bhichpuri, Agra, Lecture Notes Vol. I, 244-275.
4. Rastogi, BK (2012). Research on short and medium-term earthquake forecasts in India, DST-SERC School on Seismo-Electromagnetics, RBS College, Bhichpuri, Agra, Lecture Notes Vol. I, 276-291.
5. Rastogi, BK (2012). Seismicity of Indian stable continental region, DST-SERC School on Seismo-Electromagnetics, RBS College, Bhichpuri, Agra, Lecture Notes Vol. I, 292-309.
6. Ajay Manglik and G. Pavan Kumar (2012), Current channeling and Electrical anisotropy in the Main Central Thrust Zone, Sikkim Himalaya, DST Newsletter, 2-5

### 12.4 RESEARCH PAPERS COMMUNICATED IN NON-SCI JOURNALS

1. Choudhury, Pallabee Sumer Chopra and B.K. Rastogi (2012) Strong Motion Studies in Gujarat, for Jaikrishna Vol. IITr,
2. Rastogi, B.K (2012), Earthquake Hazard Assessment: Macro to micro level, paper No.: A012, Proceedings of ISET Golden jubilee Symposium.

### 12.4 Technical Reports

1. Dumka, R.K. and Mohar Singh. Preliminary report on rolling down of vehicles at Tulshi Shyam of Junagadh District, Jan. 2012, ISR Technical Report No. 63, pp.1-6.

2. Rao, K.M., Dr. Kapil Mohan, Ashish Bhandari and Prabhin Sukumaran. Proposed Pipeline of HDNPL from Hazira to Dahej, W. Gujarat, India (Punjab Loids), An Abridged Report on Seismological and Geological/ Geomorphologic Setup, May 2012, ISR Technical Report No. 64, pp.1-13.
3. Rastogi, B. K., Sumer Chopra, Kapil Mohan, B.Sairam, A. P Singh, Sandeep Aggrawal, Ashish Bhandari and Pallabee Choudhury (2012) Final Report on Seismic Hazard Assessment of Gujarat International Finance Tec-City (GIFT) Area, ISR Tech. Report No. 65, 169 pp.
4. Rastogi, B.K. et al. (2012) Final Report on "Seismic Study of Dholera Special Investment Region, ISR Technical Report No. 66, pp.315. [RESTRICTED]
5. Rastogi, B.K. et al. (2012). GIS-Based Maps of Sector/Ward Wise Different Attributes: Rapid Visual Survey for Seismic Evaluation of Existing Buildings in Gandhidham and Adipur Cities- Vol. III, ISR Technical Report No. 67, pp.42.
6. Rastogi, B.K. et al. (2012) Progress Report on "Geotechnical & Geophysical Investigations for Multi-Storied Building at V. S. Hospital, Paldi, Ahmedabad city, ISR Tech. Report No. 68,
7. Rastogi, B.K. et al. (2012) Draft Report on "Geotechnical & Geophysical Investigations for Multi-Storied Building at V. S. Hospital, Paldi, Ahmedabad city, ISR Tech. Report No. 69, pp.81
8. Rastogi, B.K. et al. (2012) Report on "Geotechnical & Geophysical Investigations for Multi-Storied Building at V. S. Hospital, Paldi, Ahmedabad city, ISR Tech. Report No. 70, pp.81.
9. Bhandari Ashish et al. (2012) Report on Rapid Visual Screening with Geological & GPS Survey in FARADI Village, Mandvi, Kachchh, Gujarat, ISR Tech. Report No. 71, pp.1-15.
10. Madella, M., Ajithprasad, P., Balbo, A., Saiz, J. C., Cecilia, F., Fos, J. J. G.-G., Lancelotti, C., Rondelli, B., Rajesh, S. V., Ruiz, J., Mateos, J. L., Gadekar, C. S., Dumka, R. K., Kothiyari, G. C., Mortekhai, P., and Sukumaran, P.(2012) "The 2011 Excavation Campaign of North Gujarat Archaeological Project (Nogap) Interdisciplinary Approach to the Study Socio-Ecological Contexts in the Holocene (In Spanish)" In Reports and work excavations abroad 2011, edited by Isabel Argerich, Felix Benito, Ana Carrasson, Soledad Diaz, Mana Domingo, Guillermo Enriquez de Salamanca, Adolfo Garcia, et al., 261-72. Ministry of Education Culture and Sports, Spain.

#### **12.5 Invited Lectures / Keynote Address / Inaugural Speech**

1. B.K. Rastogi, "Gujarat Earthquake Studies and Hazard Assessment", Guj Sc. Academy Annual Meeting, S.P. Uni., Vallabh Vidya Nagar, Jan 8, 2012
2. B.K. Rastogi, "Monitoring Earthquake hazard in Gujarat", SPIPA, Ahmedabad Jan 21,2012 The DoI of the Tectonophysics paper of Gupta et al is "Attenuation Characteristics of coda waves in Mainland Gujarat (India) by Arun Gupta, Anup Sutar, Sumer Chopra, Santosh Kumar and B K Rastogi (2012) DoI 10.1016/j.tecto.2012.01.002
3. B.K. Rastogi, deliver 4 lectures on Seismology in India at SERC School on Seismo-Electromagnetics at R.B.S. College, Bichpuri, Agra, 4.2.2012 to 10.2.2012
4. B.K. Rastogi, gave Invited Lecture on Earthquake Hazard Assessment in India, Geological Survey of India, Northern Region headquarter, Lucknow, Feb 2012.

4. B.K. Rastogi, Lead Lecture on “Earthquake and Tsunami Hazard in Gujarat”, Gujarat Science Congress, M.S. University, Baroda, Feb 26, 2012.
5. BK Rastogi, Guest Faculty to conduct an interactive session on Excitement in Earth Science on 1st May 2012 in the “Vacation Training Programme on Bioresources for School Children”, four-week long training programme from 20th April to 18th May 2012 organized by Gujarat Council of Science City, working under the aegis of Department of Science & Technology, Government of Gujarat,

*This training programme was been designed for meritorious students of Std. X who appeared the SSC Board examination this year. The programme is catalyzed and supported by the Department of Biotechnology, Government of India. The programme aims to provide proper awareness and understanding about the importance of bio resources, their sustainable use and conservation. It will also provide an opportunity to the young students to interact with leading scientists and experts from the field. About 30 students are selected from 26 districts of the state for this programme, who are the toppers of their districts. As a part of the programme, we have arranged for education trip to various eco-regions and wildlife sanctuary in Gujarat.*

6. B.K. Rastogi, Lecture on “Seismicity of NE India and Scientific Microzonation” and chaired a session of ‘Geosciences Area’ of Symposium on “Scientific Interventions for Societal Development”, Jorhat, December 19-21, 2012.
7. B.K. Rastogi, Lecture on “Earthquake Hazard Assessment of Gujarat” at National Seminar on “Earthquake Hazards: Education, Preparedness and Management” at Environmental Watch and Management Institute under the aegis of MOES. Hyderabad and Guwahati, December 28, 2012.
8. B.K. Rastogi (2012) Invited lecture entitled “Seismicity of NE India and Scientific Microzonation” and chair a session of ‘Geosciences Area’ of Symposium on “Scientific Interventions for Societal Development” organized by North east Institute of Sc. & Tech., Jorhat. December 20, 2012
9. B.K. Rastogi (2012) Inaugural Speech “Earthquake Risk Mitigation for Sustainable Development of NE India” at the National Seminar on “Earthquake Hazards: Education, Preparedness and Management” organized by Environmental Watch and Management Institute, Guwahati, Dec 28, 2012.

#### **12.6 Lectures in Training Courses**

1. B.K. Rastogi “Geological Hazards (Tsunami and Storm Surges)”, in training programme on “Coastal Hazard Risk Management” at GIDM, SPIPA Campus, A’bad on 22/05/2012.
2. B.K.Rastogi, “ISR Initiative for Disaster Mitigation”, in the program on “Interaction Studio of Geomatics Department”, CEPT University, Ahmedabad, 04/07/2012.
3. B.K. Rastogi, Earthquake hazard assessment (I & II), GIDM, 12 Sep 2012
4. B.K. Rastogi, Case Studies: Earthquake Disaster Management, I-Latur 1993 earthquake, II- Bhuj 2001 earthquake, GIDM, 13 Sep 2012
5. B.K.Rastogi, Introduction to Geodynamics (Plate Tectonics), Ganpat Univ., Mehsana, 14 Sep2012
6. B.K.Rastogi, Introduction to Seismology, Ganpat Univ., Mehsana, 14 Sep2012
7. B.K.Rastogi, Applications of Seismology, Ganpat Univ., Mehsana, 14 Sep2012

8. B.K.Rastogi, Earthquake parameters, magnitude, intensity, energy, effects, hazard, Ganpat Univ., Mehsana, 21 Sep. 2012
9. B.K.Rastogi, Seismicity of India, Ganpat Univ., Mehsana, 21 Sep. 2012
10. B.K.Rastogi, Tectonics of India, Ganpat Univ., Mehsana, 21 Sep. 2012
11. B.K.Rastogi, "Earthquake monitoring and Prediction" at Refresher training course for Teachers at Department of Environmental Science, Guwahati University, December 29, 2012.
12. BK Rastogi (2012) "Seismic Microzonation and Risk Mitigation at the Refresher training course for Teachers at Department of Environmental Science, Guwahati University on Dec.29, 2012:

## 12.7 ABSTRACTS

Indo-US workshop on "Intraplate Seismicity", ISR, Jan 15-18, 2012 (Also reported in the previous Annual Report ut reported here also for a total no. of 2012)

### Oral Presentations

1. BK Rastogi (ISR), Prantik Mandal (NGRI), Mechanism of Intraplate Earthquakes, S1.4, p.5.
2. Javed N. Malik (IITk) , Michio Morino (OYO Int.), Mahendra S. Gadhavi (LD Engg.), Khalid Ansari (IITk), Chiranjeeb Banerjee(IITk), BK Rastogi (ISR), Fumio Kaneko (OYO Int.), F Bhattacharjee (ISR), AK Singhvi (PRL,A'bad).Active fault and paleoseismic evidence: Implication towards seismic hazard in Kachchh region, western Gujarat, S4.2, p.27.
3. BK Rastogi (ISR), Sandeep K Aggrawal(ISR), Nagabhushan Rao (ISR), and Pallabee Choudhury (ISR)Triggered Seismicity due to the 2001  $M_w$ 7.6 Bhuj Earthquake, Western India, S6.1, p.67.
4. Pallabee Choudhury, Rakesh K Dumka and B K Rastogi, Crustal deformation studies by DGPS in Kachchh, S7.4, p.81.
5. K. M. Sreejith, T. J. Majumdar, A. S. Rajawat and Ajai (*Geosciences Division, Marine, Geo and Planetary Sciences Group, EPSA, SAC(ISRO)*); B.K. Rastogi, Pallabee Choudhury, and Rakesh K Dumka (ISR)InSAR and GPS evidences for crustal deformation in Kachchh, India, S7.5, p.82..
6. Pallabee Choudhury (ISR), Crustal deformatuion studies in Gujarat

### Poster Presentations

7. Santosh Kumar, Sandeep Kumar Aggrawal and BK Rastogi, ISR;Seismicity of Gujarat state, Western India, S1-P2, p.13.
8. B. Sairam(ISR), BK Rastogi(ISR) and Prantik Mandal (NGRI); Study of Source Parameters and Focal mechanism solutions of earthquakes occurring in the Gujarat region, India.S2-P1, p.18.
9. BK Rastogi, Santosh Kumar, Sandeep Aggrawal, Kapil Mohan, Nagabhushan Rao (ISR), Sumer Chopra (MoES); Source Parameters and effects of Talala, Saurashtra M5 earthquake of Oct 20, 2011 and aftershock study, S2-P4, p.21.
10. Santosh Kumar, Dinesh Kumar and B.K.Rastogi, ISR; Source Parameters and Scaling relation for the Earthquakes in Jamnagar region of Gujarat, S2-P5, p.22.
11. Rastogi BK (ISR), M. S. Gadhavi (ISR, Now LD Engg.), J. N. Malik (IITk) , AK Singhvi (PRL) and M. Morino (OYO Int.); Paleoseismic and Active Fault Studies in Kachchh, S4-P1, p.38.



12. Falguni Bhattacharya, BK Rastogi, GC Kothiyari (ISR), Ascertaining the seismicity using morphometric indices in the vicinity of Wagad and Gedi Faults, eastern Kachchh, Gujarat, India, S4-P2, p.39.
13. Kothiyari, GC, BK Rastogi and Rakesh K Dumka, ISR; Surface deformation zone of the North Wagad Fault and neotectonic evidences in the Gedi Fault area of Kachchh, S4-P3,
14. Sumer Chopra (MoES), Tao-Ming Chang (NCREE, Taiwan), B.K.Rastogi (ISR) and RBS Yadav (INCOIS); Crustal Structure beneath Gujarat region, S5-P1, p.59
15. K.Madhusudhana Rao (ISR), M. Ravi Kumar (NGRI) and B.K.Rastogi (ISR); Seismic constraints on anisotropy and structure beneath Northwestern Deccan Volcanic Province of India, S5-P4, p.60.
16. A.P. Singh, O.P. Mishra (Disaster Cell, SARC, New Delhi), Navaneeth Annam, Libu Jose, and Santosh Kumar (ISR); 3-D Rayleigh Wave Group Velocity Tomography of Gujarat, India, S5-P5, p.62.
17. Babita Sharma (MoES) and B.K.Rastogi (ISR); Attenuation of Seismic Waves in Kachchh and Saurashtra Regions, Gujarat, India, S5-P7, p.64.
18. Kapil Mohan, Sunita Devi, (ISR) K. Veeraswamy and T. Harinarayana (NGRI); 2D-Geoelectric Subsurface structure in the surroundings of the Epicenter Zone of 2001, Bhuj Earthquake Using Magnetotelluric Studies, S5-P8, p.64.
19. Srichand Prajapati (ISR) and S. N. Bhattacharya (IISER-K, Mohanpur); Lithospheric Structure of the Lower Indus Basin as well as Onshore and Offshore Western India Evaluated from Surface-Wave Data, S5-P9, p.65.
20. G.Swetha (NGRI), G. Pavankumar (ISR) and A. Manglik (NGRI); Intraplate Stress Analysis by COMSOL Multiphysics, S5-P11
21. R.K. Singh, B.K. Rastogi, Gopal Rao, Om Behari, Sidharth Dimri and M Kiran Kumar (ISR); Preparation of 1 m.gal Interval Bouguer Anomaly Contour map of Kachchh and identification of Faults, S6-P1, p.74.
22. A.P. Singh, O.P. Mishra and B.K. Rastogi, ISR; New Model for Crack density, Saturation rate and Porosity at the 2001 Bhuj earthquake Hypocenter: Vindicating fluid driven earthquake, S6-P3, p.75.
23. A.P. Singh, RBS Yadav, Santosh Kumar and BK Rastogi, ISR; Coulomb stress changes and Seismogenesis beneath Kachchh region due to 2001 Bhuj earthquake, S6-P4, p.76. 26<sup>th</sup> Gujarat Science Congress, M.S. University, Baroda, Feb. 26, 2012
24. Rastogi, B.K. (2012) Invited Lecture "Earthquake and Tsunami Hazard in Gujarat", Proc. , 87-88. Nat. Sem. "Geology and Geo-resources of Himalaya and Cratonic Regions of India", Geology Dept., Kumaon Univ., Nainital, 10-12 March, 2012.
25. B.K. Rastogi (2012). Invited Lecture "Seismotectonics of Himalaya: Some new Findings", Abstract Vol., p.18.
26. Kothiyari, GC, RK Dumka, PD Pant, BS Kotlia and Ketan Singha Roy (2012). Evaluation of neotectonic Deformation in Kumaon Himalaya: India, Abstract Vol. p 35

27. PD Pant, GC Kothiyari, Ritu Chauhan (2012). Tertiary fault kinematics and Quaternary reactivation in North Almora Thrust (NAT), Lesser Himalaya Kumaun. Abstract Vol. p 69  
3<sup>rd</sup> Intl. Geohazards Research Symp., *Department of Physics, H.N.B. Garhwal University* Tehri Garhwal, June 10-14, 2012
28. Rastogi, BK (2012) Earthquake risk mitigation in Himaya, , *Abstract Volume Page no.5*.
29. Singh, A.P., B.K. Rastogi, Sandeep Aggrawal and Santosh Kumar (2012)Assessment of site response using earthquake and ambient vibration measurements: A case study of Dholera, Special Investment Region in Gujarat, India,
30. Santosh Kumar, Dinesh Kumar and B.K. Rastogi, Scaling Law and Kappa (K) for the Kachchh Region of Gujarat, Abstract Volume Page No. 63.  
Regional Science Congress, M. S. University Baroda, 15<sup>th</sup>-16<sup>th</sup> September, 2012
31. Kothiyari G. C, Rastogi, B.K., Dumka R. K and Mukesh Chauhan (2012) Surface Deformation of North Wagad Fault in Kachchh Rift Basin, Gujarat. Presented Poster, 15<sup>th</sup> Sept. 2012.  
3<sup>rd</sup> Intl. Geohazards Research Symp., *Department of Physics, H.N.B. Garhwal University* Tehri Garhwal, June 10-14, 2012
32. Rastogi, BK (2012) Earthquake risk mitigation in Himalaya, , *Abstract Volume Page no.5*.
33. A.P. Singh, B.K. Rastogi, Sandeep Aggrawal and Santosh Kumar (2012)Assessment of site response using earthquake and ambient vibration measurements: A case study of Dholera, Special Investment Region in Gujarat, India,  
ISET Golden Jubilee Symp., IITr, Roorkee, October 20-21, 2012
34. Rastogi, BK (2012) Earthquake hazard Assessment: Macro to Micro level,
35. Patel, VM, M. B. Dholakia, A. P. Singh (2012) Tsunami risk 3D visualization: the Okha Coast of Gujarat, India, Paper No. B001  
49<sup>th</sup> Annual Convention of the Indian Geophysical Union “Towards the Energy Security- Exploration and New Strategies”, Ahmedabad, October 29-31, 2012
36. Falguni Bhattacharya, B.K. Rastogi, Mamata Mgamgom, Mahesh Thakkar , R.C. Patel, Late Quaternary climate and tectonic reconstruction based on channel fill deposits in the Katrol Hill Range, Kachchh, Western India.
37. Choudhury, Pallabee, Sumer Chopra and B K Rastogi, Estimation of Seismic Hazard in Gujarat Region
38. Choudhury, Pallabee, Sumer Chopra and B K Rastogi, Study of Response Spectra for Different Geological Conditions in Gujarat.
39. Choudhury, Pallabee, Sumer Chopra and B K Rastogi, Deterministic Seismic Hazard Assessment for Gujarat Region. (Page No. 35)
40. Girish Ch. Kothiyari, A. K. Gupta, Sandeep Agrawal, Sanjay Prajapati and Rakesh K., A Felt Earthquake Mw 5.0 on June 20, 2012, in Kachchh region of Western India (Page No. 32).
41. Kumar, Santosh, Sandeep Kumar, A.P. Singh, P. Mahesh, Ketan S. Roy, Vandana Patel, and B.K. Rastogi, Seismic Network and Seismicity of Gujarat State. (Page No. 40)

42. Kapil Mohan, Deterministic Seismic Hazard Assessment in Kachchh (Gujarat), Using Semi-empirical approach. (Page no. 43)
43. Rastogi, B.K., Girish Ch. Kothiyari, Sandeep K. Aggrawal and S. K. Biswas, Seismicity and Tectonic Model of Cambay Basin. (Page No. 31)
44. Rastogi, B.K. and Jyoti Sharma, Temporal Pattern of Global Seismicity. (Page no. 34)
45. Rastogi, B.K., Kapil Mohan, Ashish Bhandari, Vasu Pancholi, B. Sairam, A. P. Singh, Girish Ch. Kothiyari, Sandeep K. Aggrawal, Seismic Microzonation of Different Parts Of Gujarat. (Page No. 33)
46. Sairam, B. and B. K. Rastogi, Preparation Of The Probabilistic Seismic Hazard Analysis Maps And Structural Response Maps Of Gujarat. (Page No. 34)
47. Sharma, Jyoti and Sumer Chopra, Source, path and site characteristics using accelerograms for Garhwal-Kumaon and Sikkim Himalaya region. (Page No. 39)
48. Singh, A.P. and O. P. Mishra, Crustal heterogeneities beneath the 2011 Talala, Saurashtra earthquake, Gujarat, India source zone and its Seismotectonic Implications. (Page No. 37)
49. Veeraswamy K., K.K. Abdul Azeez, Kapil Mohan, A.K. Gupta, T. Harinarayana and B.K. Rastogi, Upper crustal faults in the Bhuj earthquake region as imaged by Magnetotellurics. (Page No. 42)

Poster presentations:

50. Annam, Navaneeth, A. P. Singh and Chinmayee Sahoo, Local Site Effects Estimated From Earthquake and Ambient Vibration Measurements at Kachchh, Gujarat, India. (Page No. 47)
51. Choudhury, Pallabee, Rakesh Dumka, Monika Wadhawan, Swagatika Das and B K Rastogi, Estimation of Plate Velocity and Crustal Deformation in the Gujarat Region, Western India Using GPS Measurements. (Page No. 45)
52. Choudhury, Pallabee, Sumer Chopra and B K Rastogi, Site dependent response spectra derived from ground motions record in Gujarat, India. (Page No. 45)
53. Gupta, Sandeep, P. Mahesh, K. Sivaram, S. S. Rai, Seismicity near the Tehri dam, Garhwal Himalaya. (Page No. 48)
54. Gupta Arun K., Anup K. Sutar, Sumer Chopra, Santosh Kumar and B.K. Rastogi, Coda waves attenuation in Mainland Gujarat. (Page no. 46)
55. Kumar, Pavan G. and A. Manglik, Localized Enhancement In Magnetic Field At The Northern Boundary Of The Main Central Thrust Zone, Sikkim Himalaya. (Page No. 103)
56. Kapil Mohan, Peush Chaudhary, Pavan Kumar, Sunita Devi and B.K. Rastogi, Magnetotelluric study to delineate the subsurface geo-electrical structure in the Western most part of the Cambay Basin (Page No. 118).
57. Kapil Mohan, B.Sairam, Vandana Patel and B.K.Rastogi, Deterministic Seismic Hazard Assessment in the Wagad area of Kachchh. (Page No.51)
58. Roy, Ketan Singha, Jyoti Sharma and B.K.Rastogi, Estimation of the site response characteristics by using different techniques for the Gujarat region. (Page No.48)

59. Sairam, B. and B. K. Rastogi, Ketan Roy and Vandana Patel, Preparation of the Site Characteristic Map of Gujarat. (Page No. 44)
60. Singh, AP., Indrajit G. Roy and J. R. Kayal, Appraisal of seismic characteristics of the 2001 Bhuj and the 2007 Talala earthquakes in Gujarat: Fractal and b-value studies. (Page no. 46)  
National Conference on "NATURAL HAZARDS AND ITS MITIGATION" organized by Eshan College of Engineering, Farah, Mathura, Dec 04-05, 2012
61. Sushanta Kumar Sahoo, M.S.B.S. Prasad, K.M. Rao and B.K. Rastogi (2012) Detection of ULF Electromagnetic emissions as a precursor to the Earthquake (M=5.0) at Kutch, Gujarat with Polarization analysis  
American Geophysical Un. Fall meeting abstracts 2012, San Francisco
62. Purnachandra Rao, N., Rao, C.N., Hazarika, P., Tiwari, V.M., Ravi Kumar, M., Singh, A., 2012. Structure and Tectonics of the Andaman Subduction Zone from modeling of Seismological and Gravity data, Dec. 15, 2012.

#### **ISR SEMINAR TAKLS (INHOUSE SEMINARS)**

Following 12 talks were delivered by ISR scientists on 12.12.12 for 12 minute duration each:

1. Santosh Kumar, Seismic Network, Seismicity, Seismic Background Noise of Gujarat Network at ISR, Dec. 12, 2012
2. A.P. Singh, 3-D Seismic Structure, Crack Attributes and b-Values of the Kachchh Gujarat, India and Its Implication for the Earthquake Hazard Mitigation, at ISR, Dec. 12, 2012
3. Girish Ch. Kothiyari, Neotectonic attribute of the Gedi Fault in Wagad area of Kachchh, Gujarat India, at ISR, Dec. 12, 2012
4. P. Mahesh, Seismotectonics of the Kumaun-Garhwal Himalaya, at ISR, Dec, 12, 2012
5. B. Sairam, probabilistic Seismic hazard assessment (PSHA) of Gujarat, at ISR, Dec. 12, 2012
6. S. P. Prizomwala, Is the southern coast of Kachchh uplifted? at ISR, Dec. 12, 2012
7. S. P. Prizomwala, Signatures of Tectonic Uplift Recorded by Marine Notches along Diu Coast, Western India, at ISR, Dec. 12, 2012
8. B.K. Rastogi, Delineation of Faults and Basement Structure in Kachchh Using High Resolution Gravity Survey, at ISR, Dec. 12, 2012
9. B.K. Rastogi, Seismicity of Gujarat From 2001 to 2012, at ISR, Dec. 12, 2012
10. B.K. Rastogi, Seismic Microzonation work in Gujarat by ISR, at ISR, Dec. 12, 2012
11. B.K. Rastogi, Seismic Hazard Assessment of the Industrial sites in Kachchh, at ISR, Dec. 12, 2012
12. B.K. Rastogi, Seismicity of Himalaya, at ISR, Dec. 12, 2012



# CHAPTER 13

## PROJECTS

SN	Project	Sponsoring Agency	Period	Value Rs. L
1	Paleoseismology in Kutch	GoG	Apr.2007-Continuing	100.00/yr
2	Microzonation in Gujarat	GoG	Apr.2007-Continuing	100.00/yr
3	Seismic Study for Dholera Special Investment Region	GIDB	Dec. 2008-Jul 2013	200.00
4	Seismotectonic Study around Mundra	GSPC	Oct 2008-Sep 2012	138.94
5	Seismic Microzonation of Guj. Intl. Finance Tech City	GIFT	May 2009-June 2012	27.00
6	Active fault investigation in Kachchh	GSDMA	Apr 2009-Aug. 2013	5.00
7	Crustal Deformation in Kutch and Narmada	MoES-2	Apr 2007-Sep 2012	77.88
8	Assessment of Vulnerability of Installations near Gujarat Coast vis-à-vis Seismic Disturbances	MoES-3 Coastal Vul	April 2009 – Aug 2013	153.84
9	Seismic Microzonation of Ahmedabad, Gujarat	MoES-4 Ahmedabad	April 2010- Sep 2013	37.68
10	Imaging of 3D Geoelectric subsurface structure of the Source Zone of 2001, Bhuj earthquake with Magnetotellurics	MoES-5 MT	June 2011-Aug 2013	10.00
11	Surface deformation mapping using SAR interferometry in Kachchh	SAC, ISRO	Apr. 2008-Feb 2013	19.00
12	Generation of site specific ground motion (spectra) with due considerations of measure shear wave velocities and soil conditions for industrial sites of Bhuj region	BRNS, Atomic Energy	Apr 2011- March 2012	7.40
13	*Tsunami Studies	GPCL	Jan 2012-March 2012	1.80
14	Morphotectonic and geological Investigation of Kumaun Lesser Himalaya	DST, SERC Fast Track	September 2011- September 2014	19.95
15	*Calibration & Valuation of satellite signals	SAC, ISRO	Apr 2012 Mar 2017	81.50
16	*GPR, RTK and seismic surveys at Archeological Survey: (			2.00
			Total	1381.99

\*NEW PROJECTS

**GRANTS RECEIVED:**

	Agency	Funds, Rs.	Date
1	GoG Plan	3,82,00,000	
2	GoG Non-Plan	1,15,00,000	
3	Corpus Fund Interest	1,45,60,000	
4	GICC-GIDB, Dholera SIR	39,11,400	7.4.2012
5	GSDMA, Active Fault Study	2,93,500	16.4.2012
6	Punj Loyed	1,00,000	5.5.2012
7	SAC-ISRO, CAL-VAL	17,50,000	30.5.2012
8	SAC-ISRO, Loss Assessment	4,60,000	3.8.2012
9	SAC-ISRO, Precursory study	1,50,000	11.2.2013
10	Univ. Geosc., Italy	6,14,582 7,21,827	8.6.2012 5.12.2013
11	Ahmedabad Municipal Corp.	8,50,000	12.7.2012
12	GoI, Fast Track	5,00,000	1.8.2012
13	SAC-ISRO-3, Loss Assessment	4,60,000	3.8.2012
14	GSPC LNG, Mundra	10,78,200	5.10.2012
15	Assam State Disaster Management Authority	2,50,000	31.12.12
16	Archeology Department	3,10,000	4.2.2013
17	GUJCOST	1,00,000	6.2.2013
	Total	7,56,49,509	

# CHAPTER 14

## INSTRUMENTS PROCURED

### List of Instrument Purchased during year 2012

Party Name	Instrument Description	Qty	Foreign Currency	INR + Custom +Shipping chrgs.	Total	Project
M/s. Emeral power Systems, Ahmedabad	Solar System set	20	-	-	28,37,100/-	Corpus Fund
M/s.Hughes Communication In.	Five years Total Cost.		-	-	34,22,030/-	
M/s.LEMI Ukraine	3 complete sets induction magnetometer LEMI-30	3	45,990/- Euro	32,67,750/- Inst.cost. 1,68,289/- Custom duty 24,130/- Shipping chrg	34,60,169/-	Corpus Fund
M/s GEM Systems Canada	Magnetometers Overhauser D/1 Magnetometers	3	1,38,795/- Cad \$	70,37,184/- Inst.cost. 2,471/- custom duty 59,249/- Shipping chrg.	70,98,904/-	Corpus Fund
M/s.Nanometrics Canada	Broad Band Seismograph.	4	80,330/- USD	40,09,981/- Inst.cost. 3,75,174/- custom duty 21,294/- Shipping charges.	44,06,449/-	

## COMPUTERS / SOFTWARES PROCURED DURING 2012

Sr.no	Name	Supplier	Qty	Price	Project
1	HP Laptop	Shree Saikrupa Commercial Enterprise	01	42,450/-	Fast Track
2	HP 6200 Desktop System	Data Tech computers	06	2,01,915/-	GOG – Non Plan
3	Trend Micro Enterprise Security Endpoint – Standard	Wellmark IT Consultant	101	1,22,137/-	GOG-PLAN
4	Cisco C1905 Router	Wellmark IT Consultant	01	36,750/-	GOG – Non Plan

## CHAPTER 15

### SPECIAL EVENTS

#### 15.1 FOUNDATION DAY CELEBRATION

Foundation Day was celebrated on 20th May. ISR Foundation Stone was laid by Sri Narendra Modi, Honorable CM on 20th May 2007. Foundation Day lecture was delivered by Dr. Ajai, Group Director, Marine and Earth Sciences, SAC-ISRO entitled "Climate Change Studies: Role of Space Technology".

The lecture was followed by remarks from Sri Ravi Saxena and Dr. SK Biswas and dinner for families and guests







## **15.2 Cultural Evening and dinner for the summer trainees**

A Cultural Evening and dinner for the summer trainees was organised on 7.6.2012. Dr. B.K. Rastogi welcomed the students, ISR staff and guests for the function. He said that besides dissertations of M.Sc. / M. Tech. Students for periods of a few months to a year, ISR has two programs of structured summer and winter training programs called Summer of Applied Geophysics Experience (SAGE) and Winter of Applied Geophysics Experience (WAGE). These training programs consist of lectures by ISR scientists and invited faculty, field training of different types of geophysical surveys and their processing and interpretation of acquired data. The sightseeing and excursion visits are also arranged. The Chief Guest: was Dr. S.K. Biswas, Former Director ONGC. He remarked that students need to learn the subjects to acquire knowledge and not merely to pass the exams. He then recalled how with hard work and great insights he discovered several oil fields in Assam and Gujarat. The students at the end expressed their utmost satisfaction of the rich experience and Gujarat hospitality.

## **15.3 Seminars/Symposia/Workshops Organised**

15.3.1 Co-hosted with GERMI and PDPU the 49th Annual Convention of the Indian Geophysical Union “Towards the Energy Security-Exploration and New Strategies”, Ahmedabad, October 29-31, 2012

Responsibilities S&T Dept. and ISR:

\*GUJCOST provided fund of Rs. 1.00 lakh

\*Housed 75 delegates at ISR Campus

\*Rastogi, BK: Convenor 49th IGU Convention, Chairman of the session on (i) “Inter and Intraplate seismicity” and (ii) the part of the Invited Talks by: Dr. Rasik Ravindra and Dr. Surjalal Sharma in the session on Atmospheric & Planetary Sciences and released Technical Program at the Inaugural Function

\*Dr. Kapil Mohan: Chairman Session V- Solid Earth Geosciences (Poster Session) of the 49th Annual Convention of the Indian Geophysical Union.

### **INAUGURAL PROGRAM AT PDPU**

Dr. Omkar Jani, Sc. GERMI: Inviting dignitaries to the dias.

Dr. Hari Narayana, Director GERMI: Welcome Address

Dr. P. Koteswar Rao: Report of Secretary IGU

Dr. VP Dimri: Presidential Address and presentation of Awards

Sri D.J. Pandian, Chief Guest: Release of Abstract Volume and Inaugural Address

Dr. B.K. Rastogi: Release of Technical Program and Remarks

Prof. P.K. Banik, Director General PDPU: Remarks and Vote of Thanks

Remarks by BK Rastogi during the Inaugural Function of the 49th Convention of Indian Geophysical Union

Sri D.J. Pandian, Principal Secy. Energy & Petrochemicals Dept. Govt. of Gujarat and Chief Guest, Padmasri Dr. VP Dimri, President Ind. Geophys. Un., Prof. Hari Narayana, Convener, IGU and members have been helping ISR for its development since its inception. Now it is the age of multifaceted research. Ind. Soc. Earthq. Sc. has been started to foster synergy between different branches of Seismology as well as between Seismology and Earthquake Engineering. Towards this ISR had held an Intl. Symp. on Earthq. Sc. in the year 2011 and same is planned bi-annually. Hence, the next International Symposium



on Advances in Earthquake Science is to be organized during February 1-2, 2013 followed by Intl. School on Earthquake Hazard Assessment named as “Use of e-infrastructures for advanced seismic hazard assessment in Indian Subcontinent”

In future we plan to hold joint Conventions of IGU and ISES.

It is my great pleasure to release the Technical Program.

High lights of the Seminar on “Towards the Energy Security-Exploration, Exploitation and New Strategies”

About 50 oral and 50 papers were presented in 3 days seminar in the following sessions:

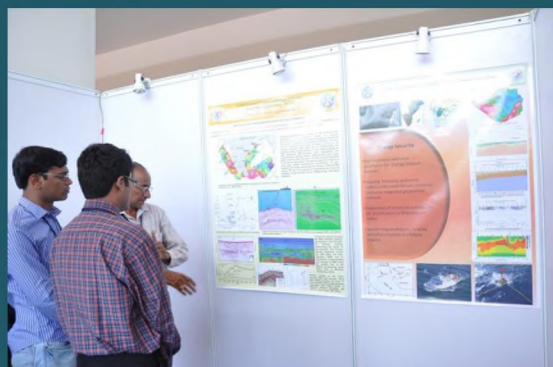
Towards the Energy Security-Exploration, Exploitation and New Strategies

- I. Inter and Intra Plate Seismicity
- II. Marine Geoscience
- III. Atmospheric & Planetary Sc.
- IV. Solid Earth Geosciences

Highlights: About 300 delegates attended the seminar in which 50 oral and 50 poster papers were presented. ISR scientists and JRFs presented 20 papers in sessions II and V. The Co-Chairman of Session II Dr. Dipankar Sarkar remarked that highlight of the session was papers presented by ISR scientists. ISR has made a complete study of seismic hazard of Gujarat and other states need to emulate that.









**15.3.2. ISR Co-hosted with GERMI the 2nd Indo-German Workshop on “Magnetotelluric Data Acquisition, Processing and Modeling”, Gandhinagar, November 1- 3, 2012.**

**Responsibilities:**

Sri Ravi Saxena: Chief Guest and inaugurated the Workshop.

Dr. BK Rastogi: delivered Welcome Address as Coordinator 2<sup>nd</sup> Indo-German Workshop on “Magnetotelluric Data Acquisition, Processing and Modeling”

Dr. Kapil Mohan: Convener from ISR.

Hosted about 45 trainees and 20 Resource persons in ISR Campus

Arranged field demonstration of two types of geophysical surveys at GIFT City and IITg site

WELCOME ADDRESS BY DG-ISR DURING THE INDO-GERMAN WORKSHOP ON MAGNETOTELLURICS DATA ACQUISITION, PROCESSING AND MODELING” November 1, 2012

Chief Guest Mr. Ravi Saxena, Addl. Chief Secretary, S & T Dept. Govt. of Gujarat , President In. Geophys. Un. Padmasri Dr. VP Dimri, and Guest of Honor, Dr. Sudhakar, Advisor MoES, coordinators Prof. Heinrich Brasse, from Free Univ., Berlin and Prof. Hari Narayana, other dignitaries on the dias, it is heartening to welcome you all in the Second Indo-German workshop on “Magnetotelluric Data Acquisition, Processing and Modeling” jointly organized by Institute of Seismological Research (ISR), GERMI and NGRI. I welcome conveners Dr. Kapil Mohan, from ISR and Dr. Ajay Manglik of NGRI.

I welcome some 20 Indian resource persons some of whom have already arrived:

NGRI: Nandini Nagarajan, Ajay Manglik, B.P.K. Patro, S.P Sharma, S.K Verma, K.K Abdul Azeez

Wadia Institute of Himalayan Geology: B.R. Arora,

SN Bose National Centre for Basic Science, Kolkata: BB Bhattacharya

IIT Roorkee: Dr. Md. Israil, Sri Niwas, PK Gupta

IIT Bombay: E. Chandrasekhar,

Indian Institute of Geomagnetism (IIG): S.G. Gokarn

.....

I specially welcome the German resource persons:

Prof. Michael Becken of University of Münster,

Prof. Bulent Tezkan of University of Cologne,

Dr Katrin Schwalenberg of Bundesanstalt für Geowissenschaften und Rohstoffe (BGR),

Dr. Friedrichs Bernhard of Metronix

and Dr. Ulrich Matzander also of Metronix

ISR has carried out considerable amount of Geophysical Investigations related to earthquake studies. In Magnetotellurics, ISR along with NGRI has pioneered 3-D survey method for upper crust. ISR has done

detail survey for detection of subsurface faults in India. I have not seen in literature such clear indications of faults as inferred in Kachchh as well as Cambay.

Lately MT method of geophysical exploration is emerging as an inexpensive alternative to seismic methods and in some cases like Deccan trap country the only successful method. Moreover, it is the only reliable method for deeper structure to 30-40km. It has been used for oil exploration, geothermal exploration and the study of lithospheric structure. It has been used in land as well as ocean. It is also good to note that extensive expertise has been developed within India in recent times. As the expertise of interpretation is fast developing, the young researchers are keen to learn the same from the experts. It is evident from the overwhelming response from the participants and resource persons. More than 40 participants are from 12 organizations including four IITs (Kanpur, Roorkee, Kharagpur, Bombay), ONGC, Hindustan Zinc, Atomic Minerals Division (AMD), NGRI, Ind. Inst. of Geomagnetism, Nat. Remote Sensing Center, Hyderabad..

The training consists of lectures; hand on experience, field training, numerical modeling and data interpretation making it a complete package.

I am sure that the workshop will act as an excellent tool to disseminate the advance knowledge in the Electromagnetics and the participants will utilize it in their individual organization for Nation building in terms of oil and mineral exploration, seismic hazard assessment (identification of faults) etc.

Remarks of the German Coordinator: The German Coordinator Prof. Heinrich Brasse, from Free Univ., Berlin remarked that the Magnetotelluric data coming out from India is now of high quality and Indian Group may become largest magnetotelluric group in the World.

Remarks by the Guest of Honour Dr. M. Sudhakar, Advisor MoES: The present century may be the Earth Science Century because of resources and energy crunch. Hence, the students and researchers have great responsibility in the coming years.

Remarks by President IGU Dr. VP Dimri: Several types of studies and geophysical surveys are being done by ISR for earthquake studies. In record short time ISR has become Centre of Excellence.

Remarks by the Coordinator Dr. T. Hari Narayana, Director GERMI: Expressed that ISR should have at least 5 more MT units for effective and faster surveys.

#### **Inaugural Address by Chief Guest Sri Ravi Saxena:**

1. Students have to prepare for the greater need of work in Earth science in this century of Earth Science.
2. Gandhinagar is becoming knowledge hub as earlier it was Hyderabad. It is apparent from the fact that carnival of Geophysics is organised by GERMI, PDPU and ISR by way of holding 49th Convention of Indian Geophysical Union and the Indo-German Workshop on “Magnetotelluric Data Acquisition, Processing and Modelling” in which the S&T Dept of GoG is associated with.
3. The Honourable CM sends good wishes for the workshop. He is always happy to meet the Scientists, but could not do so due to busy schedule.

4. The GoG uses e-Technology for administration. It has five departments. Under GSBTM the lion genome sequencing has been done. GUJCOST is popularizing science. Enrolment in Science stream has increased.

Gujarat had 2000 yr of microcosm and population was busy in trading. Now the task is instilling the Science culture.

5. Six years back focusing on earthquake studies an institute of this nature was established which is fully dedicated to earthquake study. Dr. Rastogi has brought it a long way. The Institute is now well recognised all over the world. It has also partnered with the engineering community. Work on intra-plate seismicity was recognised as best data sets and valuable assets for future research. The Institute has 3 major Schemes of work: Study of Physics of the Earthquake Process, Earthquake Hazard Assessment and Earthquake Forecasting.

Now MT Method will be used with vigour as I agree for buying of 10 more MT Units as suggested by Experts present in the inaugural function.

In fact, country as a whole and Gujarat also is planning to increase the investment in R&D to 1% or more.

Highlights of the 2<sup>nd</sup> Indo-German Workshop on “Magnetotelluric Data Acquisition, Processing and Modelling” – Concluding Session

Remarks by Dr. B.K. Rastogi, Chairman:

Dr. Heinrich Brasse, Resource Persons, Participants, I am sure you had two days of intensive crack course on magnetotellurics. One more day is for training on Field deployment, recording and Processing experience on two methods of MT & TEM. Some 36 participants and 22 resource persons attended from a dozen different organizations from different parts of India and Germany.

TWO DAYS Lectures Covered (i) Fundamentals (ii) New and improved instrumentation including Radio MT and VLF for shallow sub-surface (iii) Improved interpretation techniques for 2D and Exposure to 3D interpretation (iv) Tutorial on software

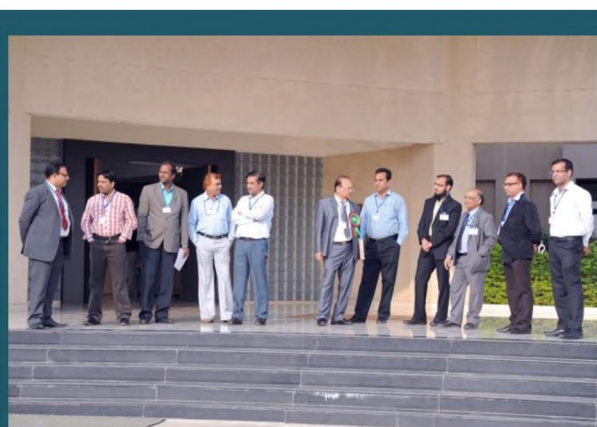
I talked to some of the participants. They are happy to know so many aspects of MT Survey and many new advances directly from renowned experts.

This is all good but in future you can plan one week Training course focussing more on field deployment, processing and interpretation. That should not have many theoretical development and case studies. The suggestion was supported by several resource persons and students.

Remarks of Prof. Heinrich Brasse:

The students should do their own programming. Learn what available software is doing. The suggestion was supported by several delegates and students. Inversion in Seismology is similar to MT. Hence, Seismological developments can be brought for MT. This is needed for 3D inversion of MT data. He informed that an International Symposium on MT will be held in Germany August end of 2014 and the Next Indo-German workshop may be held in 2016.











**ISR Stall at Vibrant Gujarat Global Trade Show 2013,  
During 3-11 Jan. 2013 at Mahatma Mandir, Gandhinagar.**







**A Report on 2<sup>nd</sup> International Symposium on “Advances in Earthquake Science” (AES-2013), February 1-2, 2013**

An International Symposium on “Advances in Earthquake Science (AES-2013)” was held during February 1-2, 2013 at Institute of Seismological Research, Gandhinagar.

The Symposium was sponsored by Ministry of Earth Science and Nuclear Power Corporation and was organized to take stock of research in India in the field of Seismology and plan future research directions. It was to promote exchange of ideas amongst the seismologists, geologists, earthquake engineers and geotechnical engineers by discussion on subjects of interests in the field of Earthquake Science.

In the Symposium, 8 foreign and 150 Indian delegates participated including 65% young researchers. Foreign delegates were from Italy, Germany and Taiwan. Indian delegates were from different parts of the country from Uttarakhand in the northwest; Delhi and UP in the north; Assam, Arunachal Pradesh and Mizoram in the northeast, West Bengal in the east, Andhra Pradesh, Karnataka and Tamilnadu in the south and Maharashtra as well as Gujarat in the west.

- Some 80 oral and 20 poster papers were presented. Lectures were at three levels. Sr. Scientists delivered Key Note Lectures reviewing status of different themes. Cutting edge state of the art lectures were by experienced scientists and new research by young scientists.

**DETAILS OF DIFFERENT SESSIONS**

**1. Earthquake Precursors and Prediction Studies, Convener: BR Arora, UCOST, Dehradun):**

Recognizing that earthquake precursory research hold key to earthquake prediction, search for precursors and their documentation has continued in different parts of the globe. Accumulated evidences bring forth variety of precursory signals including seismological, atmospheric/ionospheric, geodetic/geomagnetic, electrical resistivity/hydrological as well as geochemical anomalies. Despite certain definite success cases, scepticism prevails as noted changes are not observed at all earthquakes sites or even for different earthquakes in the same region. The dilatancy-diffusion model based on behaviour of rocks under stresses in laboratory conditions has some success in explaining some of the noted precursory signals. Induction of con-current multi-sensor measurements and availability of satellite data have begun to demonstrate the promising role of non-seismological parameters in earthquake forecasting programs. Papers in the session reviewed the advances in earthquake precursory programs and devised road map for future planning and practical application of earthquake precursory research. Papers dealing with several aspects of earthquake precursory research were presented. Papers focused on modern mathematical tools to isolate precursory signature in real time, establishing their space-time relation to earthquake cycle and highlighting strategies for integrating multi-sensor data.

**2. Seismic /Tsunami Hazard Assessment, Convener: A. Peresan, Trieste, Italy**

Purpose of the seismic hazard assessment (SHA) is to provide a scientifically consistent estimate of seismic hazard for engineering design and other considerations. Session included papers on the advanced methods for seismic hazard assessment and seismic microzonation utilizing up-to date earthquake science principles to derive the seismic hazard in terms of a ground motion or related quantity and its occurrence frequency at a site, as well as the associated uncertainty. The Italian scientists presented three papers on Neo-Deterministic methodology and results from Italy.

Chairperson A. Peresan remarked that regarding Hazard Studies and Engg. Seismology amazing amount of data of high quality has been generated by ISR and different types of analysis have been carried out. India is a good place to carry out new research and check/validate new models. I am going back with positive feeling.



East coast of India is affected by tsunami generated along Andaman-Sumatra subduction zone and west coast from Makran subduction zone. Numerical modelling to determine the tsunami propagation, potential run-ups and inundation from tsunamigenic sources is recognized as useful and important tool, since data from past tsunami are usually insufficient to plan future disaster mitigation and management plans. Models can be initialized with potential worst case scenarios for the tsunami sources or for the waves just offshore to determine corresponding impact on nearby coast. Models can be initialized with smaller sources to understand the severity of the hazard for the less extreme but more frequent events and also far taking into account the shape of the coast line and shelf. Paleotsunami study is important to decipher pre-historic tsunamis. All this information then forms the basis for creating tsunami evacuation maps and procedures. Papers were presented on these topics regarding tsunami and seismic hazard assessment studies.

### **3. Neotectonics, Convener: VC Thakur, WIHG, Dehradun**

Neotectonics is the study of young tectonic events which have occurred or are still occurring in a given region after its orogeny or after its last significant tectonic set-up. The tectonic events are recent enough to permit a detailed analysis by differentiated and specific methods, while their results are directly compatible with seismological observations. This approach has been accepted by many researchers. It is also defined as the study of geologically recent motions of the Earth's crust, particularly those produced by earthquakes, with the goals of understanding the physics of earthquake recurrence, the growth of mountains, and the seismic hazard embodied in these processes. Another source of different interpretations for a region is that changes in different tectonic plates of the region may occur at different times, giving rise to the notion of the "transitional time", during which both palaeotectonic and neotectonic features coexist. For example, for central/northern Europe, the transitional period stretches from the middle early Miocene to the Miocene-Pliocene boundary. This session included papers on the problems of recent tectonic movements that occurred in the upper part of Tertiary (Neogene) and in the Quaternary, which played an essential role in the origin of the contemporary topography.

### **4. Real- time seismology, Convener: JR Kayal, Visiting Professor, ISR, Gandhinagar**

Aim of the real-time seismology is to collect and analyze seismological data rapidly during a seismic crisis and utilize them for developing information on hazard, potential damage of large events, actual damage, and aftershock risk, with the aim of mitigating the earthquake impact on human society. Before a main shock the focus is on providing indications for an impending event by time-dependent assessment of hazard and risk. During a shock an alert and shake maps of ground shaking allow rapid assessment of the damage in affected area for relief work; in many cases several seconds to a minute might be available for early warning of strong shaking with options to shut down critical facilities, secure industrial facilities, and issue alarms where appropriate. After the main shock the rapid damage estimates based on seismological information and on a modeled ground conditions can be delivered to the agencies handling emergency. Also, the risks associated with aftershocks can be assessed. Operational systems covering some of the aspects mentioned above are being attempted in the country. Papers were presented dealing with the state-of-the-art of this evolving technology.

Chairman J.R. Kayal complimented ISR for organizing the symposium on annual basis and this will help in disseminating new ideas/research and will certainly help young scientists/researchers. Presentation of online data analysis and different types of analyses with state of the art methods in this Seminar made me so happy. The results from Antarctica which were presented in the symposium were fascinating.

### **5. Lithospheric structure, Convener: M Ravi Kumar NGRI, Hyderabad**

Our understanding of the Earth as a dynamic system has primarily evolved owing to development of new incisive tools to probe the Earth's interior from the crust to core, tremendous strides in acquisition of

high quality data from dense observational networks coupled with enhanced computational power. Multidisciplinary knowledge accrued from high resolution studies of the continental lithosphere, nature and deformation of subducting slabs, physical and thermal state of the mantle transition zone, the lowermost mantle region and the inner core in conjunction with mineral physics experiments is continually refining the forefront of knowledge thereby unveiling the fundamental global and regional scale dynamic processes of our planetary interior. Papers were presented on our current knowledge of the deep structure, evolution and dynamics of the stable continental interiors and actively deforming plate boundary regions in diverse tectonic settings covering research from a wide variety of disciplines from active and passive seismology, geodynamics and Magnetotellurics. Papers were presented on evolution of the Indian shield and its plate boundary regions like the Himalaya, Burma and Andaman arc.

Chairman M. Ravi Kumar remarked that it was heartening to have seen new and very interesting results being presented by young scientists. Hence, there is hope for future. There was amazing length of discussion after each talk. It necessitated the session chairmen to reduce the presentation time and increase the discussion time. The sessions were learning experience for even Senior Scientists. He opined that the present research in the field of Crustal Structure is more tool based. It should be more process based. He stressed a need for a regional crustal model of India as lots of tomographic studies are carried out by various researchers which can be used to develop regional model. It needs to be prepared as it will be useful for hazard modeling also.

6. Engineering seismology: advanced approaches and practical implementation, Conveners: Antonella Peresan (University of Trieste and ICTP-SAND group, Italy) and Imtiyaz Parvez (CSIR-CMMACS, Bangalore, India).

Lessons learnt from recent destructive earthquakes show that a single hazard map cannot meet all the requirements from different end-users. Nowadays it is recognized by the engineering community that peak ground acceleration (PGA) estimates alone are not sufficient for the adequate design of special buildings and infrastructures, since displacements may play a critical role and the dynamical analysis of the structure response requires reliable time series of ground motion. A reliable characterization of the maximum displacement at different periods is essential, for example, to the design of seismically isolated structures and other special infrastructures. Moreover for structures of considerable linear dimensions (e.g. bridges and also some buildings), it is necessary to account for the possible asynchronous ground motion along the base of the structure.

When dealing with the protection of cultural heritage and critical structures (e.g. nuclear power plants), where it is necessary to cope with hazard for extremely long time intervals, the standard probabilistic approach to seismic hazard assessment (PSHA) is by far unsuitable, due to its basic heuristic limitations. Extrapolating ground motion with an infinitely long return period from a few hundred years of the available earthquake catalogues, in fact, may turn out to be a purely numerical exercise with no connection with reality. Another major problem in classical methods for seismic hazard assessment consisted so far in the adequate characterization of the attenuation models, which may be unable to account for the complexity of the medium and of the seismic sources, and are often weakly constrained by the available observations. The recent introduction of the Next Generation Attenuation (NGA) approach may not be able to remove the problem in that NGA reduces the product of earthquake source tensor with the Green function of the medium, i.e. the tensor product routinely used to formally represent a seismogram, to a scalar (peak value) and such a strong simplification can be totally inadequate, in particular when dealing with the complex geological structures which are present, as a rule, in active deformation areas. Therefore the need for an appropriate estimate of the seismic hazard, capable of properly accounting for the local amplifications of ground shaking (with respect to bedrock), as well as for the fault properties (e.g. directivity) and the near-fault effects is a pressing concern for seismic

engineers. Such problems are expected to be overcome in the Neo-Deterministic modeling proposed by the Italian group. Contributions were on advanced tools for seismic hazard assessment, particularly on the following topics:

- Ground motion modeling
- Site effects characterization
- Source characterization and simulation
- Seismic input definition for special infrastructures
- Interdisciplinary studies about the response of structures to seismic input
- Applications, practical problems and requirements in earthquake engineering

#### **ANNOUNCEMENT OF FORMATION OF WORKING GROUPS**

BK Rastogi informed that as the delegates have expressed need for forums for frequent in depth discussions and collaboration on various aspects it is proposed to form Working Groups on various aspects like Earthquake Precursors, Active Faults, Crustal Deformation, Seismic Microzonation, Seismic Hazard, Earthquake Catalogs and Real-Time Seismology, Networks and Digital Data processing under the aegis of ISES.

Indo-Italian Int. School on "Use of e-infrastructures for advanced seismic hazard assessment in Indian Subcontinent", during February 4-7, 2013 at Institute of Seismological Research (ISR), Raisan, Gandhinagar.

The International School provided training on advanced tools for seismic hazard estimation. About 40 trainees from different earthquake affected parts of India took part in the International School.

The International School was organized under a project funded by Friuli Venezia Giulia Region Service for International Relations and European Integration with the following Partners:

- (i) CSIR Centre for Mathematical Modeling and Computer Simulation (C-MMACS) [council of Scientific & Industrial Research]
- (ii) International Centre for Theoretical Physics (ICTP)
- (iii) Democritos Modeling Centre for Research in Atomistic Simulation (Democritos)
- (iv) Università Degli Studi Di Trieste (Department of Mathematics and Geosciences)

Besides the basic lectures on seismology and strong motion processing, the lectures covered the following topics:

- i. Probabilistic and Deterministic methods of seismic hazard analysis and the neo deterministic method devised by the Italian group.
- ii. Advanced tools of Seismic Hazard Assessment, and
- iii. Use of Worldwide e-infrastructure for GRID or CLOUD computation for new models enabling more computational power than even a 'Super Computer'.

There were more computational exercises with some new Programs developed in Italy.

- The faculty consisted of six from Univ. of Trieste, Italy: Ms. Antonella Peresan, Franco Vaccari, Stefano Cozzini, Andrea Magrin, Fabio Romanelli, Francesco De Giorgi and five from India: (i) Imtiaz Parvez of C-MMACS, Bangalore, (ii) ID Gupta, Director CWPRS, Pune, (iii) Prof. J.R. Kayal, (iv) Dr. Sushil Gupta of RMSI and (v) Dr. B.K. Rastogi
- Prof. BK Rastogi coordinated the International School from Indian side and Prof. Antonella Peresan, University of Trieste, Italy coordinated the Int. School from the Italian side.

















**Appendix 1: CATALOGUE OF EARTHQUAKES IN GUJARAT REGION FROM EARLIEST  
TIME TO Dec2012**

Year	MM	DD	O.T.	Lat (N)	Long (E)	Dep.	Mag.	MMI Mag.	Location	Ref.
1668	05	06		25.00	68.00		7.8	X	Samaji Indus	IMD
1684				21.20	72.90		3.7		Surat	USGS
1819	06	16		24.00	69.00		M <sub>w</sub> 7.8	X	Kachchh	IMD
1820	01	27		23.20	69.90		3.7		Kachchh	USGS
1820	11	13		23.20	69.90		3.7		Kachchh	USGS
1821	08	13		22.70	72.70		4.6		Kaira	USGS
1828	07	20		23.24	69.66		4.4		Kachchh	USGS
1840	11	10		23.05	72.67		4.6		Ahmedabad	USGS
1842	10	09		22.30	73.20		4.3	V	Baroda	OLD
1843	02	08		23.00	72.70		3.7	IV	Ahmedabad	OLD
1844				24.33	69.50		4.3		Lakhpat	USGS
1845	04	19		23.80	68.90		6.3	VIII	Lakhpat	OLD
1845	06	19		23.80	68.90		5.7	VII	Lakhpat	OLD
1848	04	26		24.40	72.70		5.7	VII	Mount Abu	OLD
1856	11	02		23.20	69.90		4.6		Anjar	USGS
1856	12	25		20.00	73.00		5.7	VII	Surat	CHAN
1858	12	31		21.00	75.00		4.3	V	Khandeish	OLD
1863	11	18		22.00	75.00		5.0	VI	Barwani	IMD
1864	04	29		22.30	72.80		5.7	VII	Ahmedabad	CHAN
1869	07	04		20.20	74.20		4.3	V	Nasik	OLD
1869	07	12		20.90	74.80		4.3	V	Dhulia	OLD
1871	01	03		21.20	72.90		4.3	V	Surat	OLD
1871	01	31		21.20	72.90		5.0		Surat	USGS
1872	04	14		21.75	72.15		5.0	VI	Bhavnagar	CHAN
1882	06	10		23.20	71.38		3.5		Bhachau	MALIK
1882	06	28		23.35	70.58		5.0		Lakadia	MALIK
1882	06	29		23.35	70.58		5.0		Bhachau	MALIK
1883	10	20		21.70	71.97		4.4		Bhavnagar	USGS
1886	04	14		22.47	70.10		4.4		Jamnagar	USGS
1887	11	11		22.30	70.88		4.4		Rajkot	USGS
1888	08	20		23.83	70.00		3.5		Khavda	MALIK
1890	06	01		23.83	68.83		4.0		Lakhpat	MALIK
1891	07	27		21.33	71.37		4.4		Amreli	USGS
1892	01	11		23.83	70.00		3.5		Lakhpat	MALIK
1892	07	09		23.50	70.72		3.5		Rapar	MALIK
1893	11	04		23.83	68.83		3.5		Lakhpat	MALIK
1896	02	26		23.83	69.67		3.5		Lakhpat	MALIK
1897	10	00		23.00	72.70		3.7		Ahmedabad	USGS
1898	01	30		23.16	70.08		3.5		Anjar	MALIK
1898	04	01		23.25	69.67		4.0		Bhuj	MALIK
1898	09	13		23.30	69.75		4.0		Bhuj	MALIK
1898	10			23.05	72.67		4.3		Kheda	USGS
1898	10	15		23.33	69.67		4.0		Bhuj	MALIK
1900	12	21		23.50	70.67		3.5		Rapar	MALIK
1903	01	14		24.00	70.00		5.6		Kachchh	IMD
1904	04	09		23.33	68.67		4.0		Bhuj	IMD
1904	04	28		23.50	70.16		4.0		Anjar	MALIK
1904	07	30		23.83	70.33		3.5		Khadir	MALIK
1904	11	30		24.33	69.58		3.5		Lakhpat	MALIK



Year	MM	DD	O.T.	Lat (N)	Long (E)	Dep.	Mag.	MMI Mag.	Location	Ref.
1905	07	10		23.33	69.67		3.5		Bhuj	MALIK
1906	01	11		23.83	70.33		3.5		Khadir	MALIK
1906	06	30		23.83	69.75		3.5		Khavda	MALIK
1906	08	15		24.40	72.70		4.3	V	Mt. Abu	USGS
1907	03	12		23.83	69.75		3.5		Khavda	MALIK
1907	07	12		22.91	69.83		3.5		Mundra	MALIK
1907	10	09		23.83	69.75		3.5		Khavda	MALIK
1907	10	21		23.25	70.33		3.5		Bhachau	MALIK
1908	09	29		23.83	69.75		3.5		Khavda	MALIK
1908	10	21		23.83	69.75		3.5		Khavda	MALIK
1909	02	07		23.83	69.75		3.5		Khavda	MALIK
1909	04	09		23.25	70.33		3.5		Bhachau	MALIK
1910	03	24		23.25	69.75		3.5		Bhuj	MALIK
1910	08	01		23.83	69.67		3.5		Khavda	MALIK
1910	12	13		23.41	70.58		4.0		Lakadia	MALIK
1910	12	16		23.25	70.33		3.5		Bhachau	MALIK
1911	01	23		23.41	70.58		3.5		Lakadia	MALIK
1911	10	11		24.33	69.50		3.5		Lakhpatt	MALIK
1912	10	01		23.83	69.75		3.5		Khavda	MALIK
1912	11	07		23.83	70.33		3.5		Khadir	MALIK
1913	06	26		23.75	69.75		3.5		Khavda	MALIK
1918	06	10		23.50	70.41		3.5		Bhachau	MALIK
1919	04	21		21.70	72.25		5.7	VII	Ghogha (Bhavnagar)	CHAN
1920	10	18		23.50	70.75		3.5		Rapar	MALIK
1920	11	13		23.33	69.58		3.5		Bhuj	MALIK
1921	02	11		25.00	70.70		4.2		Thar Pakistan	ISC
1921	10	26		25.00	68.00		5.5		Indus Kachchh	IMD
1921	10	27		23.83	69.67		4.0		Narayan Sarovar	MALIK
1922	02	09		23.41	70.67		3.5		Chitrod	MALIK
1922	03	13		23.41	69.37		3.5		Mandvi	MALIK
1922	03	13		22.00	71.00		4.3	V	Jhalavad	CHAN
1923	08	07		22.91	69.45		4.0		Bhuj	MALIK
1924	03	05		23.91	69.83		3.5		Khavda	MALIK
1924	10	25		23.67	68.91		3.5		Khavda	MALIK
1925	10	01		23.83	69.67		3.5		Khavda	MALIK
1925	10	13		23.33	70.28		3.5		Shikra	MALIK
1926	12	26		23.91	69.70		3.5		Khavda	MALIK
1927	11	18		23.45	69.67		3.5		Bhuj	MALIK
1930				22.40	71.80		4.3	V	Paliyad	CHAN
1930	12	30		23.91	69.45		3.5		Khavda	MALIK
1932	03	06		23.83	70.33		3.5		Khadir	MALIK
1935	01	25		23.75	70.67		3.5		Rapar	MALIK
1935	07	20		21.00	72.40		5.7		Surat	IMD
1935	07	23		23.25	69.50		3.5		Bhuj	MALIK
1938	06			22.30	71.60		5.0		Botad	TAN
1938	07	19		22.40	71.80		5.0		Paliyad	CHAN
1938	07	23		22.40	71.80		5.7	VII	Paliyad	CHAN
1940	10	31	10 03	22.50	70.40		5.0	VI	Jamuanathali Jamnagar	CHAN
1940	11	13		23.57	70.33		4.0		Anjar	MALIK
1941	01	30		23.83	70.25		3.0		Khadir	MALIK
1950	06	14	04 24	24.00	71.20		5.3		Kachchh	CHAN
1956	07	21	15 32	23.30	70.00	35	M <sub>w</sub> 6.0	VIII	Kachchh	IMD

Year	MM	DD	O.T.	Lat (N)	Long (E)	Dep.	Mag.	MMI Mag.	Location	Ref.
1956	07	22		23.16	70.00		3.0		Anjar	MALIK
1962	03	12		24.10	70.90		3.0		Kachchh	MALIK
1962	09	01	22 01	24.00	73.00		4.6		Palanpur	IMD
1963	07	13	19 08	24.90	70.30	35	5.3		Thar, Pakistan	IMD
1965	03	26	10 04	24.40	70.00	33	5.1		Kachchh	IMD
1966	05	27	22 14	24.46	68.69	5.0	5.0		Thar, Pakistan	ISC
1966	11	12	12 16	25.12	68.04	33.	4.8		Kachchh	ISC
1967	01	06	11 41	21.97	74.27		4.5		Tankhala	IMD
1968				21.60	71.25		4.3	V	Amreli	GSI
1968				21.73	70.45		4.3	V	Dhoraji	GSI
1969	03	23	04 21	24.54	68.79	19	4.4		Kachchh	ISC
1969	10	24	11 45	24.76	72.54	31	5.5		Mount Abu	IMD
1970	02	13	15 05	24.60	68.61	33	5.2		Kachchh	USGS
1970	03	23	01 53	21.60	72.96	8	5.4		Bharuch	USGS
1970	08	09		21.70	73.00		3.5		Bharuch	USGS
1970	08	30		21.70	73.00		4.1		Bharuch	USGS
1970	09	10		21.60	72.70		3.4		Bharuch	USGS
1971	05	14	17 14	25.12	68.11	57	4.5		Thar Pakistan	USGS
1971	06	18		21.70	73.00		3.4		Bharuch	IMD
1973	06	05	01 19	25.09	68.07	33	4.8		Thar Pakistan	USGS
1974	10	20		21.70	74.20		4.6		Narmada	USGS
1975				22.10	71.20		4.3	V	Jasdan	GSI
1975	09	19	16 49	24.69	71.03	33	3.7		Kachchh	USGS
1975	09	25		20.80	74.20		4.2		Gujarat	USGS
1976	06	04	00 43	24.51	68.45	18	5.1		Allah Band Pakistan	ISC
1977	09	26	19 48	25.38	68.24	33	4.5		Kachchh	ISC
1978	04	10	09 10	21.84	72.90		3.0		Amod	IMD
1978	11	25	10 09	21.97	72.91		2.8		Amod	IMD
1979	02	22	22 11	21.33	72.15		3.3		Bhavnagar	GERI
1979	06	09	22 43	21.83	73.85		2.6		Rajpipla	GERI
1979	08	24	01 13	22.11	72.43		3.1		Khambhat	GERI
1979	09	05	10 08	21.33	72.12		3.6		Bhavnagar	GERI
1979	09	22	22 48	21.75	72.15		3.3		Bhavnagar	GERI
1979	12	10	22 19	21.90	72.90		3.2		Amod	GERI
1980	01	06	00 42	22.23	71.78		3.2		Botad	GERI
1980	03	18	18 22	21.81	73.03		2.9		Nabipur	GERI
1980	06	04	11 16	21.68	73.21		2.6		Nartrang	GERI
1980	06	04	11 17	21.68	73.21		3.1		Nartrang	GERI
1980	07	21	04 08	22.87	72.14		3.1		Nartrang	GERI
1980	08	27	06 20	22.82	72.82		2.7		Chandraga	GERI
1980	10	20	11 40	21.96	72.95		2.6		Kevadia	GERI
1981	04	26	18 12	24.12	69.51	33	4.3		Bhuj	ISC
1982	01	31	16 48	24.21	69.84	33	4.8		Kachchh	ISC
1982	03	10	03 45	21.38	73.00		3.1		Bharuch	GERI
1982	04	09	09 00	22.07	72.19		2.9		Khadi	GERI
1982	05	10	01 00	21.90	72.27		3.2		Bhavnagar	GERI
1982	06	24	01 27	22.00	72.88		3.6		Amod	GERI
1982	06	26	18 48	22.25	71.82		3.1		Dhandhuka	GERI
1982	07	02	16 30	21.86	72.04		3.5		Bhavnagar	GERI
1982	07	18	15 46	23.40	70.66	33	4.8		Bhuj	ISC
1984	09	13	04 48	24.95	70.46	33	4.2		Allah Band Pakistan	ISC
1985	04	07	21 10	24.36	69.74	33	5.0		Kachchh	ISC

Year	MM	DD	O.T.	Lat (N)	Long (E)	Dep.	Mag.	MMI Mag.	Location	Ref.
1985	04	27	04 59	20.66	73.21		4.6		Dharampur	GERI
1985	09	03		21.03	70.88		4.3		Visavadar, Junagadh	GERI
1986	02	26	12 47	20.48	73.72	33	4.3		Gujarat	USGS
1986	09	16		20.60	71.40		3.8		Rajula	GERI
1986	11	15	00 25	24.45	73.57	22	4.1		Near Mount Abu	ISC
1987	02	10	22 02	24.10	70.39	10	3.9		Kachchh	ISC
1987	04	10		24.55	70.12	10	2.0		Kachchh	IMD
1987	12	31		21.71	74.38		3.5		Narmada	GERI
1988	07	17		25.16	70.00	33	2.0		Kachchh	IMD
1989	03	21	00 57	24.27	68.96	33	4.0		Bhuj	ISC
1989	06	21	15 35	20.09	72.91	33	4.1		Valsad	ISC
1989	12	10	11 58	24.81	70.88	33	4.7		Kachchh	ISC
1991	01	20		23.13	69.83	35	2.0		Kachchh	IMD
1991	01	20	19 44	23.40	69.71	33	4.9		Bhuj	USGS
1991	01	30	10 44	20.55	73.15		4.6		Anklach	GERI
1991	09	10	06 54	24.16	68.68	35	4.7		Kachchh	ISC
1991	09	10	07 20	24.28	68.80	26	4.7		Kachchh	ISC
1992	05	04	11 20	24.52	70.13	33	3.4		Allah Band, Pakistan	ISC
1993	02	09	20 51	24.62	68.93	36	4.3		Allah Band, Pakistan	ISC
1993	08	09		20.60	71.40		3.1		Rajula	GERI
1993	08	24	23 18	20.60	71.40	29	5.0		Rajula	IMD
1993	12	31	13 32	21.12	72.72	35	4.1		Rajula	ISC
1996	02	17		23.33	69.67	33	4.5		Bhuj	IMD
1996	08	05	22 15	22.83	68.43	23	3.8		Bhuj	ISC
1996	11	17	18 12	21.40	73.06	10	4.0		Gujarat	ISC
1998	07	19		22.42	70.86		4.4		Rajkot	IMD
1998	09	21	06 23	21.81	71.93		3.0		Bhavnagar	GERI
1998	10	08	15 01	24.45	69.80	33	3.7		Bhuj	ISC
1998	11	28	16 59	21.94	71.06		3.2		Gondal	GERI
1999	09	21	11 00	21.70	72.10		2.5		Bhavnagar	GERI
2000	08	10	13 30	21.78	72.31		3.6		Bhavnagar	GERI
2000	08	13	13 28	21.02	70.99	7	4.6		Tulsi Shyam, Junagadh	ISC
2000	09	12	00 53	21.72	72.16	10	4.2		Bhavnagar	IMD
2000	12	24	11 22	24.01	70.09	43	4.7		Bhuj	ISC
2001	01	26	03 16	23.44	70.31	16	M <sub>w</sub> 7.7	X	Kachchh	ISC
2001				21.02	70.88		2.5		Tulsi Shyam, Junagadh	GERI
2003	01	13		22.30	70.93		2.0		Rajkot	GERI
2003	01	29		21.46	70.51		3.1		Haripur, Junagadh	IMD
2003	08			22.20	69.92		2.5		LalpurTq. Jamnagar	GERI
2004	1	8		23.91	70.90	20.0	4.2		Gedi/Is. Belt F.	
2004	6	7		23.87	70.15	29.4	4.2		Dholavira/Is. BeltF	
2004				21.00	70.50		3.0		Talala Junagadh	GERI
2005	3	8		23.85	69.74	11.6	4.3		Gora Dungar F.	ISR
2005	10	8		23.35	70.69	24.0	4.5		South Wagad F.	ISR
2005	10	9		23.74	69.93	6.6	4.3		Gora Dungar F.	ISR
2006	02	03	00 54	23.92	70.44	28	M <sub>w</sub> 5.0	m <sub>b</sub> 4.5	Gedi, Rapar	NGRI
2006	03	07	18 20	23.79	70.73	3	M <sub>w</sub> 5.6	M <sub>w</sub> 5.5	Gedi, Rapar	NGRI
2006	04	06	12 02	23.78	70.74	3	M <sub>w</sub> 4.8	m <sub>b</sub> 4.9	Gedi, Rapar	NGRI
2006	04	06	17 59	23.34	70.39	29	M <sub>w</sub> 5.6	m <sub>b</sub> 5.5	Lakadia	NGRI
2006	04	10	22 05	23.51	70.06	4.9	M <sub>w</sub> 4.9	m <sub>b</sub> 4.9	Banni, Kachchh	NGRI
2006	6	12	23.88	70.43	27.3	4.4			Gedi/IBF Tr.	NGRI
2006	09	30	00 16	22.31	70.21	10	M <sub>w</sub> 4.0	V	Khankotda, Jamnagar	ISR

Year	MM	DD	O.T.	Lat (N)	Long (E)	Dep.	Mag.	MMI Mag.	Location	Ref.
2007	5	13		23.44	70.42	20.4	4.7		South Wagad F.	
2007	5	24		23.298	70.026	9.0	4.1		KMF	
2007	07	16	21 21	22.49	71.29	18	M <sub>w</sub> 3.9		Paliyad	ISR
2007	09	02	16 38	22.33	70.22	10	M <sub>w</sub> 3.2		Khankotda, Jamnagar	ISR
2007	10	8	23.295	70.075	9.6	4.7	4.5		KMF	ISR
2007	10	09	03 49	21.08	70.73	11	M <sub>w</sub> 3.1		Ankolwadi, Junagadh	ISR
2007	11	06	00 27	21.12	70.51	8.5	M <sub>w</sub> 4.8	m <sub>b</sub> 4.9	Hirenvel, Junagadh	ISR
2007	11	06	09 38	21.16	70.54	4.5	M <sub>w</sub> 5.0	m <sub>b</sub> 5.0	Haripur, Junagadh	ISR
2007	11	11	13 03	21.93	69.82	10	M <sub>w</sub> 2.9		Verad, Bhanwad	ISR
2007	12	10		21.05	70.66	7.4	3.1		Ankolwadi	ISR
2007	12	15		24.03	69.87	15.0	3.7		ABF	ISR
2008	01	25	23 36	21.79	71.76	35	M <sub>w</sub> 2.8		Bhavnagar	ISR
2008	2	15		21.66	71.77	3.1	2.7		Bhavnagar	ISR
2008	2	24		22.25	71.01	6.1	2.9		Kotda, Rajkot	ISR
2008	03	09		23.39	70.33	30	M <sub>w</sub> 4.9	m <sub>b</sub> 4.5	Chobari, Kachchh	ISR
2008	4	4		23.00	70.36	11.1	2.6		Kandla	ISR
2008	05	20	08 57	21.16	73.05	7.4	M <sub>w</sub> 3.2		Surat	ISR
2008	7	5		23.53	69.8	8.9	3.3		Banni F.	ISR
2008	11	5	03:53	21.95	73.89	8.5	M <sub>w</sub> 2.9		Kevadiya	ISR
2008	10	4	05:29	21.90	69.96	3.7	M <sub>w</sub> 3.6		Bhanvad	ISR
2009	3	28	05:57	22.17	70.75	6.2	M <sub>w</sub> 3.0		Rajkot	ISR
2009	10	28		23.71	69.91	8.5	4.4	4.4	Gora Dungar F	
2010	1	26	01:22	23.29	72.98	15	M <sub>w</sub> 2.3		Gandhinagar	ISR
2010	3	30	19:57	23.61	72.57	11	M <sub>w</sub> 3.2		Mehsana	ISR
2010	9	2	08:39	23.88	71.87	6.1	M <sub>w</sub> 4.4		Patan	ISR
2010	6	23	16:54	22.16	71.36	21	M <sub>w</sub> 3.3		Botad	ISR
2010	9	23	23:44	21.90	69.7	3.1	M <sub>w</sub> 3.0		Advana	ISR
2010	11	28	07:04	22.28	70.25	6.6	M <sub>w</sub> 2.7		Sanala	ISR
2010	12	6	23:35	22.35	74.03	12	M <sub>w</sub> 3.2		Chota Udaipur	ISR
2011	01	18	20:26	23.27	70.51		M <sub>w</sub> 3.8		Samkhyali	
2011	4	18	07:36	22.45	71.51	6.1	M <sub>w</sub> 2.4		Sayla	ISR
2011	4	29	02:47	21.27	70.49	3.1	M <sub>w</sub> 4.1		Talala	ISR
2011	5	17	16:00	23.55	70.57	18.2	M <sub>w</sub> 4.2		E of North Wagad, Kachchh	ISR
2011	5	23	23:43	21.1	70.53	3.9	M <sub>w</sub> 4.0		Talala	ISR
2011	7	3	00:26	21.14	73.16	26	M <sub>w</sub> 3.2		Bardoli	ISR
2011	9	27		23.12	70.31	38	3.0		Kandla	ISR
2011	8	13	02:59	23.45	70.40	22.2	M <sub>w</sub> 4.5		South Wagad, Kachchh	ISR
2011	8	20	18:20	22.43	70.93	8.4	M <sub>w</sub> 2.6		Rajkot	ISR
2011	9	14	23:16	22.38	69.99	6.3	M <sub>w</sub> 3.4		Lalpur, Jamnagar	ISR
2011	10	3	06:35	22.65	72.47	32.3	M <sub>L</sub> 1.5		Dholka, Ahmedabad	ISR
2011	10	18	05:50	21.26	71.19	7.9	M <sub>w</sub> 3.1		Visavadar	ISR
2011	10	20	17:18	21.09	70.45	5.8	M <sub>w</sub> 5.1		Talala	ISR
2011	11	7	03:05	24.38	72.66	13.7	M <sub>w</sub> 3.1		Palanpur	ISR
2012	4	14	03:22	23.391	70.537	18.9	4.1		SWF	ISR
2012	6	19	20:14	23.645	70.283	11.1	5.0		N of NWF	ISR
2012	12	8	07:06	23.134	70.422	21	4.5		Kandla	ISR
2013	3	30		23.56	70.38	24	4.5		Chobari	ISR



**Appendix 2:**

**List of earthquakes recorded on single station, mostly at SMA station in Hirevel, Talala.**

<b>Year</b>	<b>MON</b>	<b>DD</b>	<b>HR</b>	<b>MM</b>	<b>Sec</b>	<b>LAT</b>	<b>LONG</b>	<b>Depth</b>	<b>M</b>
2012	6	19	20	14	0.4	23.638	70.281	10.5	5.0
2012	6	19	20	19	55.6	23.617	70.261	8	2.2
2012	6	19	20	26	47.6	23.651	70.277	11.3	2.6
2012	6	19	20	32	38.5	23.649	70.283	8.8	2.3
2012	6	19	20	37	40.5	23.644	70.274	11.5	1.7
2012	6	19	20	42	12.4	23.632	70.274	13.8	3.0
2012	6	19	20	45	36.9	23.644	70.28	11.7	2.9
2012	6	19	21	3	2.2	23.654	70.279	12.3	2.5
2012	6	19	21	8	52.1	23.664	70.284	18.6	1.5
2012	6	19	21	11	7.8	23.622	70.264	8.3	2.8
2012	6	19	21	15	56.6	23.639	70.259	12.8	2.8
2012	6	19	21	26	1.3	23.641	70.286	14	1.7
2012	6	19	21	44	17.2	23.622	70.266	11.3	1.9
2012	6	19	21	46	22.9	23.644	70.262	8.6	2.0
2012	6	19	23	26	39.6	23.646	70.278	10.6	1.8
2012	6	19	23	47	3.6	23.653	70.292	9.1	2.5
2012	6	20	0	11	53.2	23.645	70.268	6.7	1.8
2012	6	20	0	28	58	23.68	70.283	3.9	2.3
2012	6	20	1	27	55.5	23.644	70.276	9.9	1.8
2012	6	20	2	28	27	23.637	70.303	15.2	2.3
2012	6	20	7	20	50.5	23.639	70.285	7.1	2.6
2012	6	20	8	15	32.8	23.647	70.281	9.8	1.7
2012	6	20	8	40	45	23.645	70.291	9.7	2.3
2012	6	20	14	8	22.8	23.625	70.27	6.8	2.2
2012	6	20	14	39	59.1	23.639	70.261	6.3	1.7
2012	6	20	18	3	53.3	23.624	70.269	6.1	1.7
2012	6	20	20	1	57.8	23.649	70.27	18.5	1.7
2012	6	20	20	48	31.9	23.656	70.28	15.1	1.6
2012	6	21	4	53	57.3	23.624	70.264	6.8	2.7
2012	6	21	11	33	2.7	23.664	70.283	6.5	1.8
2012	6	21	20	5	20.5	23.647	70.287	12.7	2.6
2012	6	23	0	18	51.3	23.639	70.291	12.7	1.5
2012	6	23	18	46	52.1	23.647	70.284	12.4	1.5
2012	6	23	21	38	13.6	23.66	70.296	7.9	1.8
2012	6	24	19	24	37.1	23.636	70.275	6.2	1.6
2012	6	25	9	17	50.6	23.615	70.266	8.4	1.6
2012	6	25	10	24	21.6	23.624	70.279	6.9	1.9
2012	6	25	11	30	33.7	23.644	70.266	6.1	1.9
2012	6	25	12	31	17.5	23.645	70.261	6.3	1.7
2012	6	25	21	1	33.1	23.67	70.281	9.8	3.0
2012	6	27	7	56	22.1	23.646	70.273	9.1	2.5
2012	6	28	23	6	1.1	23.633	70.299	15.3	1.7
2012	6	29	14	5	20.7	23.628	70.293	15.1	2.0
2012	6	29	15	29	53.3	23.627	70.27	14.7	1.9
2012	7	1	6	26	0.5	23.633	70.273	11	1.9
2012	7	1	14	49	34.9	23.625	70.274	6.1	2.5
2012	7	1	18	7	58.8	23.653	70.292	10.5	1.9
2012	7	1	6	26	0.5	23.633	70.273	11	1.9

Year	MON	DD	HR	MM	Sec	LAT	LONG	Depth	M
2012	7	1	14	49	34.9	23.625	70.274	6.1	2.5
2012	7	1	18	7	58.8	23.653	70.292	10.5	1.9
2012	7	2	12	0	44.1	23.615	70.284	10	1.5
2012	7	2	12	19	21.8	23.627	70.278	9.5	2.5
2012	7	2	13	56	33	23.634	70.291	22.2	1.7
2012	7	2	12	0	44.1	23.615	70.284	10	1.5
2012	7	2	12	19	21.8	23.627	70.278	9.5	2.5
2012	7	2	13	56	33	23.634	70.291	22.2	1.7
2012	7	3	8	28	19.3	23.631	70.275	7.5	1.7
2012	7	3	8	28	19.3	23.631	70.275	7.5	1.7
2012	7	6	8	41	16.4	23.615	70.259	6.9	1.5
2012	7	6	8	41	16.4	23.615	70.259	6.9	1.5
2012	7	8	8	58	25.4	23.632	70.283	10.7	3.5
2012	7	8	8	58	25.4	23.632	70.283	10.7	3.5
2012	7	9	16	42	50.1	23.635	70.281	6.3	1.9
2012	7	9	16	42	50.1	23.635	70.281	6.3	1.9
2012	7	10	0	45	41.7	23.619	70.283	12.3	1.5
2012	7	10	0	45	41.7	23.619	70.283	12.3	1.5
2012	7	11	11	41	30.8	23.615	70.278	6.1	1.9
2012	7	11	11	41	30.8	23.615	70.278	6.1	1.9
2012	7	16	10	55	11.8	23.63	70.277	6.1	2.8
2012	7	16	10	55	11.8	23.63	70.277	6.1	2.8
2012	7	20	5	32	14.8	23.613	70.276	16.8	1.9
2012	7	20	5	32	14.8	23.613	70.276	16.8	1.9
2012	7	21	5	9	51.8	23.632	70.287	16.1	1.5
2012	7	21	5	9	51.8	23.632	70.287	16.1	1.5
2012	7	25	8	23	35.3	23.611	70.267	13.1	1.9
2012	7	25	8	23	35.3	23.611	70.267	13.1	1.9
2012	7	26	6	9	6.5	23.614	70.286	14.2	2.8
2012	7	26	12	26	49.5	23.603	70.264	8.2	1.6
2012	7	26	6	9	6.5	23.614	70.286	14.2	2.8
2012	7	26	12	26	49.5	23.603	70.264	8.2	1.6
2012	7	27	7	50	33.5	23.633	70.3	11.7	1.5
2012	7	27	7	50	33.5	23.633	70.3	11.7	1.5
2012	8	2	23	2	12.3	23.605	70.316	20.6	2.2
2012	8	7	15	38	33.9	23.621	70.267	14.4	1.7
2012	9	2	23	29	20.3	23.624	70.286	10	2.6
2012	9	4	0	36	54.3	23.612	70.28	6.1	3.1
2012	9	10	8	0	57	23.62	70.282	6.7	1.7
2012	10	2	3	39	29.8	23.622	70.271	6.1	1.7
2012	10	18	8	6	6.1	23.62	70.264	9	1.5
2012	10	30	14	38	49.3	23.626	70.306	6.1	3.1
2012	11	4	14	52	0.4	23.626	70.306	9.7	1.8
2012	11	9	23	49	29.7	23.622	70.279	10.2	1.5
2012	11	13	7	11	56.5	23.605	70.292	15	2
2012	11	20	23	12	27.1	23.618	70.301	14.5	1.6
2012	11	25	0	8	54.6	23.616	70.271	6.2	1.6

-----